Copper induced functional and structural modulations in *Ricinus communis* L. and stress amelioration by exogenous application of cytokinins

Thesis submitted to
the University of Calicut in partial fulfillment of
the requirements for the degree of

DOCTOR OF PHILOSOPHY IN BOTANY

By

SAMEENA P. P.

PLANT PHYSIOLOGY AND BIOCHEMISTRY DIVISION
DEPARTMENT OF BOTANY
UNIVERSITY OF CALICUT
MARCH 2022

UNIVERSITY OF CALICUT
DEPARTMENT OF BOTANY
CALICUT UNIVERSITY P.O., KERALA

Dr. Jos T. Puthur
Professor & Head

Plant Physiology and Biochemistry Division
Email: jtputhur@yahoo.com
Mob: 9447507845

CERTIFICATE

This is to certify that the thesis entitled **"Copper induced functional and structural modulations in *Ricinus communis* L. and stress amelioration by exogenous application of cytokinins"** submitted by **SAMEENA P. P.** in partial fulfillment of the requirements for the degree of **Doctor of Philosophy** in **Botany** of the **University of Calicut,** is a *bona fide* record of the research work undertaken by her in this department under my supervision and guidance and no part thereof has been submitted for the award of any other degree.

C.U. Campus
Date:

Prof. (Dr.) Jos T. Puthur

DECLARATION

I, **Sameena P.P.,** do hereby declare that the Ph.D. thesis entitled **"Copper induced functional and structural modulations in *Ricinus communis* L. and stress amelioration by exogenous application of cytokinins"** is a research work accomplished by me under the supervision of **Dr. Jos T. Puthur, Professor & Head, Plant Physiology and Biochemistry Division, Department of Botany, University of Calicut,** in partial fulfillment of the requirements for the award of **Doctor of Philosophy** in **Botany, University of Calicut**. I also declare that this has not been submitted by me for the award of any other degree or diploma, and it represents original work done by me.

C.U. Campus **Sameena P. P.**
Date:

Acknowledgement

A word of thanks to God, The Almighty for providing me the opportunity to step in the excellent world of science and for giving me the strength to undertake this research and complete it successfully.

I would like to express my heartfelt gratitude to my mentor and supervisor **Dr. Jos T. Puthur**, **Professor and Head**, Department of Botany, University of Calicut,for always creating invaluable space for me, to develop myself as a researcher and to find my own path. I am highly indebted to you sir, for your excellent guidance, priceless advices, friendly discussions, constant encouragement and support throughout this journey. You convincingly encouraged me to be professional and do the right thing even when the situation got tough. Our association dates back to my post-graduation days, and my master's dissertation was also ascribed to your encouragement and effort. Without you, this entire journey and thesis too would not have been materialized.

I am so blessed to have **Dr. K. Azeez**, Principal, PSMO College, Tirurangadi, Malappuram, as my mentor and a wonderful teacher. You have been a source of comfort and courage to face the toughest times of my life, whether it is personal or academic. Your continued and unfailing support, motivation, love and care helped in the completion of this thesis. Thank you sir, for understanding and believing in me, as well as for guiding my journey down the right path.

I record my profound gratitude to **Rtd. Prof. (Dr.) E. Nabeesa Salim,** Department of Botany, University of Calicut, for the valuable suggestions, extensive discussions, constant support and care throughout this research journey.

I am extremely indebted to **Prof. V. V. Radhakrishnan, Prof. Santhosh Nampy, Prof. John E. Thoppil,** former Heads, Department of Botany, University of Calicut, for

providing necessary facilities to carry out this work. I also wish to express my deep gratitude to the entire teaching and non teaching faculties of the department for their support during this period. Special mention must be given to **Prof. Santhosh Nampy** and **Prof. C. C. Harilal,** for providing the system microscope and AAS facilities.

I am thankful to **Dr. Om Parkash Dhankher,** Professor in Crop Biotechnology, Stockbridge School of Agriculture, University of Massachusetts, United States, who has increased the horizon of my knowledge in the field of phytoremediation. I would like to thank **Dr. Hazem M. Kalaji,** Associate Professor, Department of Plant Physiology, Institute of Biology, Warsaw University of Life Sciences SGGW, Warsaw, Poland, for the timely suggestions, expert guidance and criticisms in my work.

I am grateful for the financial support provided by the **University Grants Commission**, New Delhi, India, in the form of **Junior & Senior Research Fellowships**, which enabled me to undertake this research programme to the next level.

I do acknowledge the **Tapioca and Castor Research Station (TCRS), Tamil Nadu Agricultural University, Salem**, for providing me the seeds of castor to carry out this work.I take a lot of pride in praising the services provided by **Central Sophisticated Instrumentation Facility (CSIF), University of Calicut; Department of Chemistry, University of Calicut; Kerala Forest Research Institute (KFRI), Peechi;** and **College of Agriculture, Padannakkad, Kasaragod,** for providing SEM-EDX, ICPMS, FTIR, GCMS and AAS facilities essential for the Work.

A word of gratitude to **Dr. L. Resmi**, Assistant Professor, Dept. of Botany, University of Calicut, and **Mr. Ayyoob**, Research Scholar, Dept. of Commerce and Management Studies, University of Calicut, for the help in carrying out the statistical analysis. I express my heartfelt thanks to **Dr. Muhammed Noufal**, Assistant Professor in English, CKGM Govt. College, Calicut, for his valuable suggestions that improved my

writing skills. I am thankful to **Dr. K. V. Ajayan,** UGC Kothari Post Doctoral Fellow, Dept. of Botany, University of Calicut, for his timely help. I am thankfully remember the scholarly atmosphere maintained by **Mrs. Sony Krishnan** and **Dr. P. M. Prakasan**, present and former Librarians of this Department, and helping me in searching the relevant books and articles essential for this research. I also extend my sincere thanks to **Mr. Rajesh & crew,** Bina Photostat, for their timely help in materializing this work in to a presentable format.

Sisters always need not to be by blood, sometimes actions and affections leads to sisterhood. I would like to remember the loving care, timely advice and constant support rendered by **Mrs. Anusha K. C.,** my best ever companion. I extent my sincere thanks to my M.Sc. classmates, **Dr. Soumya P.**, **Mrs. Aswathi P.**, **Mrs. Farhad V. P.**, **Dr. Neethu K.**, **Dr. Surekha Y. Pawar**, and other colleagues in the Department **Dr. SyamRadh S.**, **Dr. Archana E. R.**, **Dr. Rubeena M.**, **Dr. Arunkumar P. G.**, **Mrs. Shahina A. S.**, **Ms. Drisya, V.**, **Mr. Vishnu Mohan**, **Ms. Divya K.**, **Mr. Muhammed Irfan T. K.** and **Mr. Prasanth Prabhu** for their cheering presence in this journey. I will thankfully remember this beautiful campus through these people: **Mr. Afsal**, **Mr. Jamsheed Ali**, **Mr. Shamjith**, **Mrs. Meghna**, **Ms. Greeshma**, **Mr. Habeeb Rahman** and **Mr. Yunus**, whose companionship turned my journey into a pleasure.

I have great pleasure in acknowledging my gratitude to my lab-mates, **Mr. Sarath G. Nair, Dr. Akhila Sen, Mr. Jeyaraj S., Ms. Aswathi Raj K. P., Mrs. Veena Mathew, Ms. Riya Johnson, Ms. Anjitha K. S., Ms. Sherin George, Mrs. Rincy P., Mrs. Musfira , Mrs. Anjana Ajith, Mrs. NavyaPatrik and Mrs. Sruthi P.,** for the support and active discussions. Special thanks must be given to **Dr. Janeeshma E., Ms. Amritha M. S.** and **Mr. Noble Louis**, for their generous care, concern and love. Your presence has always been very important in this journey, which often feels like a great relief during the

toughest times, and I am so lucky to have you all with me in the last few years. I find myself short of words in expressing my sincere thanks to all my seniors, **Dr. Swapna K. S.**, **Dr. Jisha K. C.**, **Dr. Vijayakumari K.**, **Dr. Shackira A. M.**, **Dr. Mirshad P. P.**, **Dr. Pravisya P.**, **Dr.Faseela P.**, **Dr. Sinisha A. K.**, **Dr. Sruthi P**. and **Dr. Dhanya Thomas T. T.** for their encouragement, moral and emotional supports.

My acknowledgement would be incomplete without thanking the biggest source of my strength, **my family**. I will forever be grateful to God for giving me such an amazing family. Words are insufficient to say how much they mean to me and their endless love, prayers and continuous support made me to achieve this. Words will be insufficient to thank my loving parents **Mr. Ahammed** and **Mrs. Aysha**, for the affection and concern shown to me. I consider myself the luckiest in the world to share an amazing siblinghood. I thank God for sending **Mrs. Sajeena, Mr. Shuhaib, Mrs. Sumayya**, and **Mr. Sufaid**, beside me with their love, unconditional support and vise counsel. Special thanks should be given to my Nieces and Nephews; **Mr. Ajmal**, **Shadi, Ninu, Munna, Innoos, Minnu, Vava, Nasha** and **Ponnu**, whose presence always been a positive energy and helped to find the pleasure inside me. I would also like to remember and thank my brother in laws **Mr. Shafeek** and **Mr. Latheef**, and sister in law **Mrs. Sakkiya**, for always being with me.

Finally, I would like to thank everybody who has been there until the successful realization of my thesis, as well as expressing my apology that I could not mention all personally one by one. Once again remembering the supreme power for guiding me throughout.....

Sameena P. P.

I will forever be grateful to God for bestowing me with valuable people:
The source of my happiness and comfort....
This work is dedicated to them....

Copper induced functional and structural modulations in *Ricinus communis* L. and stress amelioration by exogenous application of cytokinins

Sameena P. P.

Abstract

The present study was carried out to investigate the copper (Cu) induced stress and tolerance potential of a non-edible bioenergy plant – *Ricinus communis* L. (castor oil plant). Various analyses were performed in the roots, cotyledonary and primary leaves of *R. communis* to evaluate the functional and structural modulations in the plants exposed to Cu stress. Furthermore, the stress amelioration potential of two cytokinins - kinetin (KIN) and 6-benzylaminopurine (BAP), was evaluated by their exogenous application to the $CuSO_4$ treated *R. communis* seedlings, and the variations in the functional and structural aspects in the cotyledonary leaves were analyzed. As per the findings, *R. communis* can withstand higher levels of Cu by modulating the antioxidation machinery and osmotic adjustment, and allocating the translocated Cu^{2+} more into the cotyledonary leaves, thereby favourably modulating the photosynthetic efficiency in the primary leaves. The integrated networking of antioxidant system could successfully scavenge the ROS molecules, leading to reduced oxidative damage in the primary leaves. The enhanced synthesis of cell wall polysaccharides and pectic compounds play vital role in efficient sequestration of toxic levels of Cu^{2+} in the cell wall, thereby preventing the presence of toxic ions in the cytoplasm and enhancing Cu stress tolerance in *R. communis*. Moreover, the plants were able to overcome Cu-induced oxidative stress by the exogenous application of cytokinins, which assisted in the restoration of cellular redox status in the cotyledonary leaves. This resulted in improved photosynthetic efficiency supported by effective stomatal responses which would ensure the

amelioration of Cu toxicity in these leaves due to cytokinin application. The antisenescing function of cytokinins helps in the establishment of seedlings under adverse environmental conditions. It was also observed that BAP was found to be more efficient than KIN in preventing Cu-induced early abscission of the cotyledonary leaves and keeping them photosynthetically active. Resultantly, the exogenous application of BAP is found to be an effective strategy to increase the tolerance potential with comparatively fewer toxicity symptoms in *R. communis*. Furthermore, the utilization of the molecular mechanisms associated with Cu-stress amelioration by BAP will lead to develop transgenic plants with the potential to overproduce cytokinins, which might be a more effective technique in ameliorating Cu stress.

CONTENTS

3.5.5. Chlorophyll *a* fluorescence analysis
3.5.6. Chlorophyll stability index (CSI)
3.5.7. Osmolality
3.6. Analysis of reactive oxygen species
3.6.1. Superoxide ($^{\bullet}O_2^-$) content
3.6.2. Hydrogen peroxide (H_2O_2) content
3.7. ROS induced membrane damage
3.7.1. Lipid peroxidation
3.7.2. Membrane stability index (MSI)
3.7.3. Electrolyte leakage (EL%)
3.8. Estimation of primary metabolites
3.8.1. Total soluble sugars content
3.8.2. Total proteins content
3.8.3. Total free amino acids content
3.8.4. Proline content
3.9. Free radical scavenging mechanism
3.9.1. Enzymatic antioxidants
3.9.1.1. Glutathione reductase (GR, EC 1.6.4.2)
3.9.1.2. Monodehydroascorbate reductase (MDHAR, EC 1.6.5.4)
3.9.1.3. Dehydroascorbate reductase (DHAR, EC 1.8.5.1)
3.9.1.4. Catalase (CAT, EC 1.11.1.6)
3.9.1.5. Guaiacol peroxidase (POD, EC 1.11.1.7)
3.9.1.6. Ascorbate peroxidase (APX, EC 1.11.1.11)
3.9.1.7. Superoxide dismutase (SOD, EC 1.15.1.1)
3.9.2. Non-enzymatic antioxidants
3.9.2.1. Ascorbate (AsA) content
3.9.2.2. Glutathione (GSH) content
3.9.2.3. Total phenolics content
3.9.2.4. Flavonoids content
3.9.2.5. Anthocyanins content
3.10. Bioaccumulation and distributional pattern of elements
3.10.1. Bioaccumulation and translocation of Cu
3.10.2. Subcellular distribution pattern of Cu
3.11. Leaf micromorphological characters
3.12. Anatomical studies

5.2. Analysis of tissue water status
    5.2.1. Cu induced reduction in tissue water status
    5.2.2. Effect of cytokinins on maintaining tissue water status
5.3. Photosynthesis and JIP parameters
    5.3.1. Effects of Cu on photosynthesis and JIP parameters
    5.3.2. Modulation of photosynthesis by application of cytokinins
5.4. ROS accumulation and oxidative stress
    5.4.1. Cu-induced ROS accumulation and oxidative stress
    5.4.2. Cytokinin mediated alleviation of ROS accumulation and oxidative stress
5.5. Metabolic dynamisms and osmotic adjustment
    5.5.1. Cu-induced alterations in primary metabolites and osmolality
    5.5.2. Modulation of primary metabolites and osmolality by cytokinin application
5.6. Antioxidant defence mechanisms
    5.6.1. Cu stress mediated elicitation of antioxidant defence mechanisms
    5.6.2. Cytokinin mediated modulation of antioxidant defence mechanisms
5.7. Bioaccumulation of Cu and distributional patterns
    5.7.1. Enhanced Cu bioaccumulation and cellular as well as subcellular distribution patterns
    5.7.2. Influence of cytokinins on Cu bioaccumulation and distribution
5.8. Distribution of essential elements in the xylem tissues
    5.8.1. Influence of Cu on distribution of essential elements
    5.8.2. Cytokinin mediated modulation of essential elemental distribution
5.9. Leaf micromorphological characters
    5.9.1. Effect of Cu on leaf micromorphological characters
    5.9.2. Impact of cytokinin on leaf micromorphological characters
5.10. Anatomical modifications

LIST OF TABLES

14. Bioaccumulation of copper (Cu) in the root, stem, cotyledonary and primary leaves, and translocation factor (TF) in the cotyledonary and primary leaves of *R. communis* seedlings subjected to increasing concentrations of $CuSO_4$ (Control, 40, 80, 120, 160 and 200 µM) on 6 and 10 d.
15. Bioaccumulation of Cu (µg/g DW) in the root, stem, cotyledonary leaves and primary leaves and translocation factor (TF) in *R. communis* seedlings on 6 d of exposure to $CuSO_4$ (80 and 160 µM) and cytokinins (KIN and BAP).
16. SEM-EDX data showing the distribution of various macro and micro-elements (weight %) in the xylem tissues of root, stem, cotyledonary and primary leaves of *R. communis* seedlings on 6 d of $CuSO_4$ (control and 200 µM) treatments
17. SEM-EDX data showing the macro and micro-elements (weight %) in the cotyledonary leaves of *R. communis* seedlings on 6 d of $CuSO_4$ (160 µM) and cytokinins (KIN and BAP) treatments.
18. Subcellular distribution of copper (Cu) in the root, stem, cotyledonary and primary leaves of *R. communis* seedlings subjected to $CuSO_4$ treatment (control and 200 µM) on 6 d. Values are the mean ± SE of three independent experiments.
19. Xylem wall thickening in the root, stem, cotyledonary and primary leaves of *R. communis* seedlings subjected to $CuSO_4$ treatments (control and 200 µM) on 6 d.
20. Bioactive compounds detected in the methanolic extracts of cotyledonary leaf, primary leaf and roots of *R. communis* seedlings on 6 d of $CuSO_4$ (control and 200 µM) treatments.
21. Bioactive compounds detected in the methanolic extracts of cotyledonary leaves of *R. communis* seedlings on 6 d of $CuSO_4$ (80 and 160 µM) and cytokinins (KIN and BAP) treatments.
22. Pearson's correlation coefficients between various parameters related to photosynthesis in the cotyledonary leaves of *R. communis* seedlings exposed to $CuSO_4$.
23. Pearson's correlation coefficients between various parameters related to photosynthesis in the primary leaves of *R. communis* seedlings exposed to $CuSO_4$.
24. Pearson's correlation coefficients between various parameters related to photosynthesis in the cotyledonary leaves of *R. communis* seedlings exposed to $CuSO_4$ along with kinetin (KIN).
25. Pearson's correlation coefficients between various parameters related to photosynthesis in the cotyledonary leaves of *R. communis* seedlings exposed to $CuSO_4$ along with 6-benzylaminopurine (BAP).

LIST OF FIGURES

24. Malondialdehyde (MDA) content in the cotyledonary leaves (A), primary leaves (B), roots (C), and cotyledonary leaves (exposed to cytokinins for 6 d) (D) of *R. communis* seedlings subjected to increasing concentrations of $CuSO_4$.

25. Membrane stability index (MSI) in the cotyledonary leaves (A), primary leaves (B), roots (C), and cotyledonary leaves (exposed to cytokinins for 6 d) (D) of *R. communis* seedlings subjected to increasing concentrations of $CuSO_4$.

26. Electrolyte leakage (EL%) in the cotyledonary leaves (A), primary leaves (B), roots (C), and cotyledonary leaves (exposed to cytokinins for 6 d) (D) of *R. communis* seedlings subjected to increasing concentrations of $CuSO_4$.

27. Total soluble sugars content in the cotyledonary leaves (A), primary leaves (B), roots (C), and cotyledonary leaves (exposed to cytokinins for 6 d) (D) of *R. communis* seedlings subjected to increasing concentrations of $CuSO_4$.

28. Total proteins content in the cotyledonary leaves (A), primary leaves (B), roots (C), and cotyledonary leaves (exposed to cytokinins for 6 d) (D) of *R. communis* seedlings subjected to increasing concentrations of $CuSO_4$.

29. Total free amino acids content in the cotyledonary leaves (A), primary leaves (B), roots (C), and cotyledonary leaves (exposed to cytokinins for 6 d) (D) of *R. communis* seedlings subjected to increasing concentrations of $CuSO_4$.

30. Proline content in the cotyledonary leaves (A), primary leaves (B), roots (C), and cotyledonary leaves (exposed to cytokinins for 6 d) (D) of *R. communis* seedlings subjected to increasing concentrations of $CuSO_4$.

31. Glutathione reductase (GR) activity in the cotyledonary leaves (A), primary leaves (B), roots (C), and cotyledonary leaves (exposed to cytokinins for 6 d) (D) of *R. communis* seedlings subjected to increasing concentrations of $CuSO_4$.

32. Monodehydroascorbate reductase (MDHAR) activity in the cotyledonary leaves (A), primary leaves (B), roots (C), and cotyledonary leaves (exposed to cytokinins for 6 d) (D) of *R. communis* seedlings subjected to increasing concentrations of $CuSO_4$.

33. Dehydroascorbate reductase (DHAR) activity in the cotyledonary leaves (A), primary leaves (B), roots (C), and cotyledonary leaves (exposed to cytokinins for 6 d) (D) of *R. communis* seedlings subjected to increasing concentrations of $CuSO_4$.

ABBREVIATIONS

ABA	-	Abscisic acid
ABS	-	Absorption flux
APX	-	Ascorbate peroxidase
AsA	-	Ascorbate
BAP	-	6-benzylaminopurine
CAT	-	Catalase
Chl	-	Chlorophyll
CK	-	Cytokinin
CSI	-	Chlorophyll stability index
CSm	-	Cross section related to Fm
Cu	-	Copper
DCMU	-	3(3,4dichlorophenyl)-1,1-dimethyl urea
DCPIP	-	2,6-dicholrophenolindophenol
DHA	-	Dehydroascorbate (oxidized ascorbate)
DHAR	-	Dehydroascorbate reductase
DIo	-	Dissipated energy flux
DTNB	-	5-dithio-bis-2-nitrobenzoic acid
DW	-	Dry weight
EDX	-	Energy dispersive X-ray analysis
EDTA	-	Ethylenediaminetetraacetic acid
EL%	-	Electrolyte leakage %
ETo	-	Electron transport flux
Fm	-	Maximum chl *a* fluorescence
F_O	-	Initial chl *a* fluorescence
FTIR	-	Fourier Transform Infrared
Fv	-	Variable chl *a* fluorescence
FW	-	Fresh weight
GCMS	-	Gas chromatography and mass spectrometry
GR	-	Glutathione reductase
GSH	-	Reduced glutathione
GSSG	-	Oxidized glutathione

H_2O_2	-	Hydrogen peroxide
HEPES	-	N-(2-Hydroxyethyl)piperazine-N-(2-Ethanesulphonic acid)
KBr	-	Potassium bromide
KIN	-	Kinetin
LHC	-	Light harvesting complex
MC%	-	Moisture content %
MDA	-	Malondialdehyde
MDHA	-	Monodehydroascorbate
MDHAR	-	Monodehydroascorbate reductase
MSI	-	Membrane stability index
MT	-	Metallothionein
MV	-	Methyl viologen
NaN_3	-	Sodium azide
NBT	-	Nitroblue tetrazolium
$^{\bullet}O_2^-$	-	Superoxide
PBQ	-	para-Benzoquinone
PCs	-	Phytochelatins
PI	-	Performance index
POD	-	Guaiacol peroxidase
PSI	-	Photosystem I
PSII	-	Photosystem II
r	-	Pearson’s correlation coefficient
RC	-	Reaction center
ROS	-	Reactive oxygen species
RWC	-	Relative water content
SEM	-	ScanningElectron Microscope
SOD	-	Superoxidedismutase
TBA	-	Thiobarbituricacid
TCA	-	Trichloroaceticacid
TF	-	Translocation factor
TRo	-	Trapping energy flux

INTRODUCTION

Contamination of lands by toxic heavy metals has become a severe environmental concern, particularly with the rapid growth of industrialization and urbanization. The presence of heavy metals has a detrimental impact on environmental stability, and it also poses threat to the biological systems on the earth. Originally, heavy metals have derived from natural processes occurring on the earth's crust; however, anthropogenic activities such as mining and smelting of ores, agricultural activities such as the application of chemical pesticides and fertilizers, sewage sludge, industrial effluents, urban runoff, and burning of liquid and solid fuels are all contributing to the heavy metal contamination of soil and water bodies (Abdelsalam *et al.*, 2019). Because of the long-term persistence, non-degradability, penetration into the food chain and biological toxicity, heavy metal pollution has emerged as the most significant threat to the environmental and agricultural systems (Sall *et al.*, 2020).

Heavy metals are a group of elements exhibiting metallic characteristics, including transition metals, metalloids, lanthanides and actinides (Ali and Khan, 2018). They are either essential or non-essential for the normal functioning of a living cell. The essential elements such as cobalt (Co), copper (Cu), iron (Fe), manganese (Mn), molybdenum (Mo), nickel (Ni), selenium (Se) and zinc (Zn) are essential for carrying out the fundamental processes of growth, metabolism and development of the living organisms. At optimum concentrations, they may act as cofactors, which are structurally and functionally vital for the enzymes and proteins (Arif *et al.*, 2016). But, the range of optimal concentration remains highly varied among the organisms including plants. Therefore, the essential elements become a

stress factor in the plants above the threshold concentrations. In contrast, the non-essential heavy metals such as aluminium (Al), arsenic (As), cadmium (Cd), chromium (Cr), lead (Pb) and mercury (Hg) impart severe toxicity in plants even in trace amounts and are often regarded as the greatest threat to life forms (Henao and Ghneim-Herrera, 2021).

1.1. Significance of copper in plants

Copper (Cu) is an essential trace element required for normal growth and development and is involved in a variety of physiological processes of plants. It is a structural and functional component of many macromolecules and is an important cofactor for many metalloproteins. It participates in a variety of electron transport events in photosynthesis and respiration and plays a role in redox reaction catalysis in plant cells (Yruela, 2009). Copper deficiency in plants resulted in alterations of gene expressions, which triggered morphological changes including leaf and root architecture. It was also observed that, Cu deficiency first appeared in the younger leaves, causing distortion, chlorosis, or even necrosis occurs (Yruela, 2005).

Yet, excess Cu in cells can cause toxicity problems. Though the redox property of Cu makes it an essential element, the same property contributes to its toxicity also. Because Cu is both an essential cofactor and a toxic element with a complicated network of metal trafficking routes, plants have developed multiple techniques to regulate their cellular homeostasis. These strategies prevent the metal from accumulating in its freely reactive state (metal detoxification pathways) and ensure their proper targeting to the specific metalloproteins (Yruela, 2005). Redox cycling between Cu^{+} and Cu^{2+} may produce extremely toxic hydroxyl radicals, causing significant lipid peroxidation and membrane denaturation (Burkhead *et al.*, 2009).

1.2. Land degradation and remediation mechanisms

Land degradation is the downward trend in land conditions caused by direct or indirect human-induced processes, reflected as a long-term decline or loss of biological production or ecological sustainability. These complex ecological processes resulted in the progressive reduction of soil fertility (Halbac-Cotoara-Zamfir *et al.*, 2020). According to reports of Milman (2015), one-third of the arable land has been lost in the last 40 years due to soil erosion and/or pollution, posing a threat to food security. From both the ecological and economic standpoint, land degradation may lead to an irreversible state of desertification and a loss of agricultural productivity if remedial actions are not taken (Briassoulis, 2019). Therefore, it is vital to rehabilitate these areas to effectively cultivate food crops, which necessitates the identification and remediation of contaminants (Javaid *et al.*, 2020).

Nowadays, various heavy metal remediation procedures have been employed in the field, including physico-chemical and biological methods (Liu *et al.*, 2018a). Chemical precipitation, flotation, adsorption and soil washing, flushing, landfilling, and ion exchange are less cost-effective physico-chemical remediation procedures that might cause irreversible changes in soil properties (Akhtar *et al.*, 2020). On the other hand, phytoremediation is a plant-based, environment-friendly, economically feasible, cost-effective, and widely accepted approach for immobilizing or deactivating pollutants such as heavy metals and metalloids from soil and water.

1.3. Bioenergy producing non-edible hyperaccumulators for phytoremediation

Because of population growth and industrialization, the dependence on fossil fuels for energy purposes is on the increase. These non-renewable fuels,

including coal, oil, and natural gas, generate power and transportation energy and supply approximately 88% of the world's energy demands. Fossil fuels produce alarmingly high CO_2 and other greenhouse gas emissions, causing global warming and climate change. As a result, renewable energy sources, particularly bioenergy, appear to be one of the most efficient energy sources (Scarlat *et al.,* 2015). Bioenergy accounts for around 14% of worldwide energy consumption, and photosynthesis is the major source of bioenergy production, which may be extracted by utilizing modern technologies (Ale *et al.*, 2019). In this context, the cultivation of bioenergy plants for the phytoremediation of polluted lands is a better option to counter both the pollution problem and the energy crisis.

Furthermore, due to the risk of toxic metal ions entry to the food chain, the utilization of non-edible plants is a better option for effective and efficient phytoremediation processes. Therefore, the non-edible bioenergy plants having higher heavy metal tolerance potential, including *Arundo donax*, *Brassica juncea*, *Jatropha curcas*, *Ricinus communis*, *Thlaspi caerulescens* and various species of *Salix* and *Miscanthus,* seems to be of high importance (Jha *et al.*, 2017). Morover, these plants cultivated on heavy metal polluted soils can also be utilized to generate bioenergy. In this regard, coupling of bioenergy production with heavy metal phytoremediation using metal hyper-accumulating, non-edible bioenergy plants can resolve two critical environmental problems, i.e., soil contamination with heavy metals and temperature rise due to fossil fuel combustion (Lima *et al.*, 2019).

1.4. Heavy metal toxicity and tolerance mechanisms in plants

Although most plants can accumulate and bio-concentrate the toxic heavy metals in small quantities, severe toxicity symptoms may develop when the concentration exceeds the standard toxicity thresholds. Heavy metals cause serious negative consequences in the organisms once they enter the

food chain, including alterations in the metabolic and developmental processes or even damage the genetic makeup (Ali *et al.*, 2019). Plants respond to these environmental stimuli through a series of phases, which include (a) recognizing external stress stimuli, (b) signal transduction and transmission into the cell, and (c) initiating appropriate responses to counteract the detrimental effects of stress stimuli by modifying the physiological, biochemical and molecular status of the cell (Viehweger, 2014). It is possible to monitor the early responses, such as the extent of oxidative stress and the tolerance strategies covering the functions of transcription factors (transcriptomics), metabolites (metabolomics), stress-inducible proteins (proteomics), trace elements (ionomics) and phytohormones for studying the sensing and signal transduction cascades that occur in plants during stress exposure (Singh *et al.*, 2016). Heavy metals cause toxicity in plants in a wide range of methods, including (i) competition for absorption at the root surface due to mimicking with nutrient ions, (ii) deactivation of protein due to the interaction of metals with the sulfhydryl groups, (iii) functional loss of proteins due to the displacement of essential ions from specific binding sites, and (iv) damage to DNA, RNA, proteins and lipids due to over-production of ROS (Singh *et al.*, 2017a).

The stress tolerance mechanisms should be well-developed in plants used for the dual purpose of phytoremediation and bioenergy generation. These plants manage heavy metals in different ways, including removal, transfer, degradation, and immobilization (Usman *et al.*, 2013). These plants perform phytostabilization or phytoextraction mechanisms to handle and reduce the metal toxicity in the cells. Therefore, it is essential to understand how these non-edible metallophytes respond to heavy metal stress, so that plants with appropriate agronomic features for heavy metal tolerance can be developed.

The regulation and maintenance of osmotic and ionic homeostasis is a fundamental cellular and physiological condition for the sustainable growth of the plant (Rai *et al.*, 2021a). Plants grown in heavy metal stressed environments must acclimatize to escape the severe impacts of metal-induced toxicity at physiological, biochemical and molecular levels. Plants have innate defensive mechanisms for heavy metal detoxification, which include blocking and trafficking of metal ion uptake, synthesis of osmolytes and activation of enzymatic and non-enzymatic antioxidant systems (Viehweger, 2014; Sidhu *et al.*, 2016; Khan *et al.*, 2018). The structural modifications, including the development of trichomes, the formation of thick cuticles and effective exclusion or sequestration of metals, also indicate the effective innate defence mechanisms. The functional groups associated with the cell wall materials can bind with metal ions, preventing further transportation across the plasma membrane. The binding of the metal ions with transporter proteins such as phytochelatins and metallothioneins, and further sequestration of the protein-metal complex into the vacuole is yet another important detoxification mechanism.

1.5. Role of phytohormones in heavy metal stress tolerance

Phytohormones are regulatory compounds synthesized in low concentrations that act as chemical messengers to control various physiological and developmental processes in plants. They also control internal and external stimuli and play an important role in signal transduction pathways during the stress response (Kazan, 2015). Auxins (IAAs), cytokinins (CKs), abscisic acid (ABA), gibberellins (GAs), and ethylene are the five principal categories of phytohormones, and salicylic acid (SA), brassinosteroids (BRs), jasmonic acid (JA), strigolactones (SLs), and polyamines contribute to the new families of phytohormones. Traditionally, plant defenceis connected with ethylene, SAs and JAs, whereas plant growth

is associated with GAs, IAAs, CKs and BRs. ABA modulates plant responses to abiotic stressors. However, it is becoming increasingly clear that all plant hormones can affect various plant processes, including biotic and abiotic stress tolerance directly or indirectly (Santino *et al.*, 2013; Colebrook *et al.*, 2014; Wani *et al.*, 2016).

Since the amount of ABA in plants normally increases during abiotic stress situations, and this higher ABA can facilitate plant adaptation to diverse abiotic stressors, ABA is regarded as the principal hormone that mediates plant responses to adverse environmental conditions (Aslam *et al.*, 2022). The extensive review made by Li *et al.* (2021a) revealed that ABA and SA help plants to cope with the harmful consequences of stresses by minimizing oxidative damage and preserving photosynthesis. Similarly, CKs promote the antioxidant enzyme activity, and BRs improve stress tolerance by boosting the rate of photosynthesis and enhancing the expression levels of HSP. These hormones can interact with other biomolecules and develop defensive mechanisms that modulate the main metabolic processes in plants under stress (Ahmad *et al.*, 2016a,b). However, abiotic stressors alter the production of endogenous growth regulating phytohormones such as auxins and cytokinins in plant cells, which in turn disrupt plant development under severe stress situations (Atici *et al.*, 2005; Khan *et al.*, 2011; Peleg and Blumwald, 2011; Asaf *et al.*, 2017).

In this context, exogenous supplementation of phytohormones either in the growing medium or as the foliar spray has been recently examined as a potential strategy for easing and establishing tolerance as well as promoting growth and metabolism in plants under abiotic stress conditions (Wang and Zhang 2017; Acidri *et al.* 2020; Li *et al.*, 2021a). However, little is known about the relationships and the underlying mechanisms between exogenous applications of phytohormones in modulating the endogenous hormone levels

during stress. According to Cai *et al.* (2018), exogenous application of cytokinins enhanced the accumulation of endogenous cytokinins in *Triticum aestivum* and therefore reduced the ABA to cytokinin ratio, which in turn enhances the growth of the plants under stress. Though the physiological and biochemical responses are known, the evidence for this relationship at the molecular level is meagre.

Endogenous cytokinins have been shown to protect the plants against heavy metal stress, which may be due to the direct influence of cytokinins on the regulation of the metallothionein-like gene (MT-L2) or from the indirect effect of cytokinin-mediated antioxidant activity (Thomas *et al.*, 2005). By scavenging reactive oxygen species (ROS), they can delay metal-induced leaf senescence in plants (Zhang *et al.*, 2021a). Researchers have recently established that cytokinins such as 6-benzylaminopurine, kinetin and zeatin supplementation improves plant tolerance to abiotic stress conditions such as heavy metals, drought, salinity and temperature (Gurmani *et al.*, 2011; Aldesuquy *et al.*, 2014; Nawaz *et al.*, 2016; Kumari *et al.*, 2018; Gujjar *et al.*, 2020; Piotrowska-Niczyporuk *et al.*, 2020; Yu *et al.*, 2020). According to Singh *et al.* (2018), kinetin supplementation significantly reduced metal toxicity in tomato seedlings exposed to Cd stress by enhancing physiological functioning and detoxifying potential *via* modulation of the ascorbate-glutathione cycle. Similarly, the application of 6-benzylaminopurine decreased Co uptake, translocation, and bioaccumulation in tomato plants (Kamran *et al.*, 2021).

1.6. *Ricinus communis* L. as a potential weed in landfills

Ricinus communis L. (castor oil plant) is a fast growing, high biomass producing, non-edible, heavy metal-hyperaccumulating plant, grouped under Euphorbiaceae family of flowering plants. Because of its potential to grow luxuriantly on contaminated soils and bio-concentrate heavy metals, castor

has recently been accepted as a value-added plant for phytoremediation of polluted lands as well as for economic and ecological services (Gajić *et al.*, 2018). It can be found abundantly in disturbed or wastelands, as well as roadsides under adverse environmental conditions, and therefore used for coupled action of phytoremediation and bioenergy generation (Abdelsalam *et al.*, 2019; Palanivel *et al.*, 2020). The earlier studies have shown that the *R. communis* plant is tolerant to Cd, Co, Ni, Pb and Zn, and it has been employed as an indicator plant that grows luxuriantly in these metal polluted soils without displaying any morphological and anatomical alterations (Wang *et al.*, 2016a; Yashim *et al.*, 2016; Sun *et al.*, 2018; He *et al.*, 2020a; Yeboah *et al.*, 2020).

Based on the facts presented above, the removal of heavy metals from contaminated lands using biomass-producing hyperaccumulator plants is receiving greater attention nowadays. Understanding the mechanisms of heavy metal uptake and accumulation by these plants will aid in the successful elucidation of phytoremediation purposes coupled with bioenergy production. Furthermore, these plants are helpful to figure out and manage the positive adaptations in non-edible non-accumulator plants in order to improve stress tolerance and heavy metal bioaccumulation potential. Keeping in view of these facts, *R. communis*, which is grown luxuriantly on the polluted roadsides and wastelands, was selected for the investigation of heavy metal (copper) tolerance potential and elucidation of the underlying phytotechnology. Furthermore, a comparative analysis of the role of exogenous application of two cytokinins, kinetin (KIN) and 6-benzylaminopurine (BAP), on the metal bioaccumulation and amelioration of Cu toxicity in *R. communis* has also been carried out. Therefore, the present study was designed with the following objectives.

1. Preliminary screening of soil and plant samples for heavy metal concentrations collected from the polluted lands, where *R. communis* grows luxuriantly.
2. Evaluation of the tolerance level of *R. communis* towards Cu by conducting simulated experiments in Hoagland nutrient medium artificially contaminated with known concentrations of $CuSO_4$.
3. Evaluation of the differential responses in the photosynthetic efficiency of cotyledonary and primary leaves of *R. communis* exposed to Cu stress.
4. Validation of the metabolomics in the leaves and roots of *R. communis* on exposure to Cu stress.
5. Analysis of the oxidative stress intensity induced by excess Cu and antioxidative mechanisms developed in the leaves and roots of *R. communis* to counter the stress.
6. Evaluation of the influence of Cu on the uptake and distribution of essential elements in *R. communis*.
7. Evaluation of the anatomical re-modulations and differential subcellular distributions of Cu in the leaves and roots of *R. communis* exposed to Cu stress.
8. Comparative analysis of the stress amelioration potential of kinetin and 6-benzylaminopurine in the cotyledonary leaves of *R. communis* exposed to Cu stress.

REVIEW OF LITERATURE

2.1. Land degradation and heavy metal pollution

Land degradation refers to a wide range of land conditions, including desertification, salinization, heavy metal pollution, erosion, and the encroachment of invasive species (Gibbs and Salmon, 2015; Kumar and Sharma, 2020). This situation may reduce the productivity of the land and render it unsuitable for cultivation (Noojipady *et al.*, 2015). Land degradation is on the rise and spreading over the globe, including cultivated areas (20%), broadleaved forests (24%), needle-leaved forests (19%), and rangelands (20–25%) (Bai *et al.*, 2008). Approximately 3 million locations in the European Economic Area and the West Balkans are potentially contaminated due to industrial operations such as mining and smelting, domestic and municipal wastes, fertilizers and chemicals used in agriculture, petroleum-derived products, and traffic emissions (FAO, 2018). According to Mythili and Geodecke (2016), approximately 44% of the land area is degraded in India, and unscientific farming practices and natural hazards are the primary reasons for these degradations.

In India, approximately 60% of the total geographic area is cultivable/arable lands (175 Mha), of which around 80% (141 Mha) is used for growing crops, 6% (10 Mha) is rangelands. The remaining 14% (24 Mha) are not cultivated (Mythili and Geodecke, 2016). According to the reports of Bhattacharya *et al.* (2015) and Mythili and Geodecke (2016), about 147 Mha of land is affected with different types of soil degradations, which includes, water erosion (94 Mha), salinity/acidification/alkalinity (23 Mha), flooding (14 Mha), wind erosion (9 Mha), and combination of these factors (7 Mha).

Land degradation can be divided into three categories: physical, chemical, and biological (Katyal and Vlek, 2000; Xie *et al.*, 2020). Physical land degradation is caused by erosion, soil organic carbon loss, and changes in the physical structure of the soil, such as compaction, crusting, and surface sealing. Chemical land degradation is caused by acidification, fertility depletion, leaching, nutrient imbalances, salinization, and the presence of excess heavy metals. Deforestation, biodiversity loss, and catastrophic floods are the main causes of biological land degradation (Tóth *et al.*, 2018). Poor agricultural practices and monoculture have also been deleterious impacts on soil nutrients, lowering the soil quality and productivity (Paz-Ferreiro and Fu, 2016). Land degradation negatively affects the activity of beneficial microorganisms in the soil, resulting in a drop in soil fertility and production and water quality (Karlen and Rice, 2015). As a result of these land degradations, the soil organic matter and the flora and fauna populations in the soil are reduced, culminating in the loss of biodiversity. Land degradation develops gradually and steadily, bringing about long-term consequences for the entire biological species.

Among all the land degradation processes, chemical degradation attracts special attention these days. The usage of agricultural chemicals, improper waste disposal, and industrial activities contribute to the chemical degradation of land, either individually or in combination (Osman, 2013a). The xenobiotic chemicals used on the land can contain heavy metals and metalloids, which turn out to be the most widespread soil contaminants. According to the reports of Osman (2013a,b), approximately 240 Mha of land is undergoing chemical degradation, which includes loss of nutrients (136 Mha); salinization (77 Mha); persistent organic compounds [trichloroethylene (TCE), tetrachloroethene (PCE), polycyclic aromatic hydrocarbons (PAHs) and polychlorinated biphenyls (PCBs)] and inorganic heavy metals (11 Mha); and acidification (6 Mha).

Of the 10 million sites of soil pollution documented worldwide, more than 50% are contaminated with heavy metals and/or metalloids (He *et al.*, 2015). The rate of soil degradation caused by the accumulation of heavy metals is growing at a high pace (Liu *et al.*, 2014a). Heavy metal pollution has emerged due to anthropogenic activities, primarily due to metal mining, smelting, and other metal-based industries, as well as metal leaching from various sources such as landfills, waste dumps, runoffs, automobiles, and road works (Ali *et al.*, 2019). The use of pesticides, insecticides, fertilizers, and other heavy metals in agriculture has been a secondary source of heavy metal contamination (Wu *et al.*, 2018). Volcanic activity, metal corrosion, metal evaporation from soil and water, sediment re-suspension, soil erosion, and geological weathering are natural factors that might increase heavy metal pollution (Briffa *et al.*, 2020).

2.2. Impacts of heavy metal pollution

Environmental pollution has been a severe problem since the industrial revolution and anthropological activities. Among the various contaminants in the soil and water, heavy metals are the most detrimental one, which negatively affects a wide range of soil enzymes and the functional diversity of microorganisms (Fazekašová and Fazekaš, 2020). Heavy metals are hazardous environmental pollutants due to their chronic toxicity, non-biodegradability, and environmental bioaccumulation (Zaynab *et al.*, 2022). They can be transported and biomagnified through food chains, posing a major health risk to humans (Liu *et al.*, 2018b). Heavy metal concentrations and their impacts, distribution, and environmental origin are causing difficulties at the local, regional and national levels (Kumar *et al.*, 2019).

Heavy metals are naturally occurring elements with a density greater than 5 g cm^{-3}, including essential and non-essential elements. According to the United States Environmental Protection Agency reports, Ag, Al, As, Be,

Cd, Cr, Cu, Fe, Hg, Ni, Pb, Se and Zn are primary contaminant metals (Patniak, 2010). In addition, the Agency for Toxic Substances and Disease Registry (ATSDR) has considered heavy metals as the priority chemicals because of their potential threat and toxicity to human health (ATSDR, 2020). The essential heavy metals such as Cu, Fe, Mn, Mo, Se and Zn have diverse roles in the physiological and metabolic activities in living organisms at minimal concentrations; however, higher concentrations can lead to toxicity symptoms. In contrast, some metals like As, Cd, Cr, Hg and Pb are non-essential, causing detrimental effects even in minute concentrations. Because of their non-degradable and accumulative qualities in environmental compartments, heavy metals have a harmful impact on the environment. They adversely affect the growth, development, and metabolism of plants, microbes and animals (Ali *et al.*, 2019).

Heavy metal pollution resulted in alterations in various environmental factors such as alkalinity, turbidity, pH, temperature, hardness, dissolved oxygen, *etc*., and nutritional status of the soil and water. Heavy metals once have entered into the environment, will remain in the soil for a longer period, adversely affecting the growth of crop plants, quality of water, soil microorganisms and human health (Du *et al.*, 2013; Kaddour *et al.*, 2017). Heavy metal toxicity is the ability of a metal to affect the survival, growth, and reproduction of an organism. They exert toxicity effects in the soil biota by altering the soil microbial activities and inhibiting the metabolism of plants even at low concentrations. Plants uptake these heavy metals and bio-concentrate in their tissues and get transferred through the food chain, becoming a potential threat to the ecosystem. Therefore, the introduction of these toxic metal ions leads to instability of the ecosystem and poses a severe risk for human health as mutagens and carcinogenic agents (Mahar *et al.*, 2016).

Considering the higher level of metal concentration on cultivable lands due to irrigation from bore-wells, mining, and other industrial activities, effective remediation of these lands is important for sustainable development (Hou *et al.*, 2020). The toxicity symptoms produced by plants, animals and humans due to heavy metal exposure include imbalances in the nutrient uptake, production of reactive oxygen species (ROS), and associated membrane damage (Tarekegn *et al.*, 2020). Since plants are sessile, they cannot move out of the contaminated environment. Therefore, developing defence mechanisms and tolerant genotypes is the only option to survive under harsh environmental conditions.

2.3. Sources and bioavailability of copper in the environment

Copper exists naturally in the soil environment, with a mean concentration of 30-35 mg/kg dry soil, although the average Cu content in the earth's crust is 60 mg/kg (Kupiec *et al.*, 2019). It is confined to distinct fractions in soil due to cation exchange, precipitation, or adsorption, but its stability is determined by pH (Young, 2013). Copper enters the environment *via* both natural and anthropogenic activities. Volcanic eruptions, wind-blown dust, and forest fires contribute to natural sources of Cu pollution. Mining, metal and electrical manufacture, agricultural and domestic use of pesticide and fungicides, leather processing, and particles from car brakes are all anthropogenic sources of Cu in the environment (Panagos *et al.*, 2018; Altaf *et al.*, 2021). From the 21st century onwards, automotive emissions are one of the primary sources of heavy metal pollution in the natural environment, most significantly along the roadsides, which is directly linked with the significant increase in the number of motor vehicles. According to the studies conducted by Skorbiłowicz *et al.* (2021), roadside topsoil is rich in Cu, and the average amount of Cu was higher than the geochemical background values.

Increased copper concentrations in municipal wastewaters and sewage sludge result from copper pipes, copper roofs, and other domestic copper installations (Boller and Steiner, 2002). Sewage sludge is a source of organic matter that contains a high concentration of plant-available nutrients, with a significantly higher amount of Cu (Fjällborg and Dave, 2003). According to the reports of Milieu (2008), the amount of Cu in the sewage sludge (on dry solids) ranges between 100-500 mg/kg. It is well established that sludge may enhance soil qualities, and it is commonly applied to depleted agricultural fields (Roig *et al.*, 2012). Therefore, Cu concentrations in agricultural fields are closely related to unmanaged solid and liquid wastes discharged by agricultural enterprises and households (Romic and Romic, 2003).

The speciation of Cu determines the level of Cu in the environment, their bioavailability and range of toxicity (Montenegro *et al.*, 2015). Furthermore, there is a direct correlation between Cu levels and its bioavailability in the soil, implying that Cu directly impacts bulk speciation and ecotoxicology (Cuypers *et al.*, 2013). Through cation exchange, biosorption, adsorption or precipitation, Cu may form complexes with organic and inorganic ligands in the soil (manganese and iron oxides) to limit the magnitude of free metal ions (Cui *et al.*, 2017). Therefore, soil organic matter with a larger negative charge and cation exchange capacity significantly influences the elemental distribution of Cu in the soil profile (Zhang *et al.*, 2020). It was reported that Cu bioavailability has been linked to physical, chemical, and biological properties at the soil-root interface in the rhizosphere (Kumar *et al.*, 2021).

2.4. Phytoremediation of heavy metals

Plants having the ability to accumulate exceedingly higher concentrations of the heavy metals in their biomass and also with the bioenergy potential have been commonly used for the coupled

phytoremediation and bioenergy production (Barbosa *et al.*, 2015). *Arundo donax*, *Ricinus communis*, *Jatropha curcas*, *Helianthus annuus*, *Salix alba*, *Panicum virgatum*, *Miscanthus fuscus* and *Populus deltoides* have been identified as potential species for heavy metal hyperaccumulation and biofuel production (Bauddh *et al.*, 2017). In the majority of the bioenergy plants, the heavy metals accumulated in the shoot biomass were below the standard toxicity levels (Bauddh *et al.*, 2015a; Palanivel *et al.*, 2020). As a result, the shoot biomass of bioenergy plants used for phytoremediation may be employed safely for bioenergy extraction. In contrast to these findings, certain bioenergy plants accumulate significantly more toxic metal ions in their shoot system than in their root system, which is potentially hazardous, and hence their disposal is crucial with respect to phytoremediation (Chang *et al.*, 2014; Mohanty, 2016). As a result, the bio-accumulated metals must be retrieved without interfering with the generation of bioenergy to establish a successful phytoremediation procedure (Kidd *et al.*, 2018). Bioenergy is often created from plant biomass by direct combustion, thermo-chemical processes such as pyrolysis, gasification, and catalytic liquefaction, or biological processes such as fermentation/anaerobic digestion employing appropriate microbial systems (Singh *et al.*, 2014; Srivastava, 2019). After bioenergy generation, the leftover fraction is subjected to extraction processes to separate the metals, known as phytomining (Jiang *et al.*, 2015).

Heavy metals must be removed from the environment, which necessitates rehabilitation of polluted and/or degraded soil. On the other hand, metal remediation is quite challenging and complex. Traditional treatments, including extraction or immobilization by physico-chemical methods such as electro-kinetic treatment, ion exchange, chemical oxidation or reduction, pollutant stabilization, precipitation, excavation, and incineration, can harm soil structure and potentially damage natural ecosystems (Singh *et al.*, 2017a). Furthermore, many procedures are not completely successful and are also

quite expensive. An environmentally benign technology known as phytoremediation has gained attention as an alternative to these traditional approaches, demonstrating that it can restore polluted areas at a low cost with few collateral effects (Muthusaravanan *et al.*, 2018).

Phytoremediation is a green engineering approach that uses the heavy metal tolerance potential of a plant and its associated rhizospheric microorganisms to immobilize, degrade or sequester metal contaminants in the soil or water (Pilon-Smits, 2005; Ibañez *et al.*, 2016). Majority of the plants have a pronounced ability to metabolize and degrade many recalcitrant xenobiotic chemicals and can be considered as "green livers", functioning as a major sink for harmful chemicals in the environment. These metal tolerant plants either stabilize them in their root systems or transform them into less toxic forms. The degradation, uptake and accumulation mechanisms of heavy metals vary from plant to plant. Plants with phytoremediation capabilities that can produce useful biomass even in the presence of heavy metals in the soil are the most effective. They can maintain a higher growth rate and biomass, along with enhanced root penetration (Oh *et al.*, 2013).

Recently, a new strategy of integrating phytoremediation with oil crop production has been adopted and tested to accomplish low-cost soil decontamination techniques along with biofuel production (Bauddh *et al.*, 2015b). For this purpose, selecting suitable energy crops with exceedingly higher heavy metal tolerance potential is essential. Cultivating bioenergy crops in degraded areas might provide an additional economic incentive, and also, these areas do not compete with agricultural fields (Hunce *et al.*, 2019). Greater knowledge of the underlying processes in plants that allow them to handle toxins safely can aid us in developing ways for plants to remove metal pollutants from the soil and water efficiently. The capacity of a plant to withstand high concentrations of heavy metals within its tissues and their

absorption and translocation efficiency into shoots and subsequent sequestration in vacuoles and specialized tissues determines its phytoextraction capability (Gupta and Sandiolo, 2012).

Different plant species can be utilized to restore soil fertility by implementing effective remediation. For the feasibility and efficiency of phytoremediation, the plant species should be non-edible and grow luxuriantly in contaminated lands. Even though several reports regarding the potential of edible plants for phytoremediation purposes are coming into focus, it is better to use non-edible plants to avoid the risks of heavy metal entry into the food chain (Abdelsalam *et al.*, 2019). In China, about 64 plant species are being introduced as potential bioenergy plants, but their growth and development largely depend on the biological and environmental suitability of the growing region and climate conditions (Li *et al.*, 2010).

The most popular biodiesel plant, *Jatropha curcas*, is a perennial oil yielding plant growing abundantly in tropical and subtropical regions. This plant is widely used for the decontamination of wetland ecosystems and the re-vegetation of the mining dump sites and coal fly ash landfills (Abioye *et al.*, 2017). Approximately 2.6 million hectares of land in India and China are used to cultivate *Jatropha* for bioenergy production (Fairless, 2007). *Ricinus communis* is an oilseed plant growing luxuriantly in marginal lands with approximately 50% of seed oil content and oil productivity of 1414 kg/ha, with a wide range of industrial and pharmaceutical uses (Kaur and Bhaskar, 2020). Castor oil has high lubricity characteristics such as viscosity, density and thermal conductivity compared to the standard lubricants (Patel *et al.*, 2016). *Helianthus annuus*, an ornamental and biofuel crop, can stabilize, absorb and accumulate heavy metals at higher concentrations from industrial effluents (Chauhan and Mathur, 2020). The study conducted concerning biogas production from plant biomass, which was collected from metal-

contaminated and non-contaminated lands, indicates that *H. annuus* produces 134-154 mL g^{-1} biogas with insignificant differences in the contaminated and non-contaminated lands (Hunce *et al.*, 2019).

For the removal of Cd and Zn from contaminated soils, a comparative study was conducted using eight energy crops: *Cannabis sativa* (hemp), *Linumusitatissimum* (flax), *Ricinus communis* (castor), *Brassica rapa* (rapeseed), *Carthamus tinctorius* (safflower), *Arachis hypogea* (peanut), *Glycine max* (soybean) and *Helianthus annuus* (sunflower) (Shi and Cai, 2009a, 2010). The results showed that three of them, hemp, flax and castor, were more tolerant towards both the metals than the other five energy crops, which were moderately tolerant. The findings of this study proved that hemp, flax and castor are excellent candidates for phytoremediation of Cd and Zn from polluted lands and that they may also create additional revenue through bioenergy generation (Shi and Cai, 2009a, 2010). The promising non-edible bioenergy plants with heavy metal phytoremediation potential have been listed in Table 1.

2.5. Mechanisms of phytoremediation

Plants have a variety of ways to remove heavy metals, depending on their inherent abilities. Phytoremediation is an *in situ* remediation technology utilizing the innate heavy metal accumulation potential of plants and their mechanisms. The efficiency of phytoremediation depends on the nature of the pollutant, bioavailability and soil properties (Rai *et al.*, 2019). Phytoremediation mechanisms may be broadly divided into five categories: phytostabilization, phytoextraction, phytovolatilization, phytodegradation/ phytotransformation and rhizodegradation/phytostimulation. Of these, phytoextraction and phytostabilization are most important concerning heavy metal absorption and the associated processing of plant biomass. They are the

most acceptable strategies for phytoremediation of heavy metal polluted areas (Clemente *et al.*, 2015).

Understanding the underlying principles involved in removing contaminants can help us develop techniques for removing pollutants more efficiently. Because metals are immutable, some of the low-cost phytoremediation techniques available for organic pollutants, such as phytodegradation and rhizodegradation, are ineffective in metal-contaminated soils (Vangronsveld *et al.*, 2009). Furthermore, phytovolatilization is limited to certain metals such as As, Hg and Se (Ali *et al.*, 2013). Similarly, the effectiveness of the land clean-up relies on the survival of plants on metalliferous soil. However, phytoextraction is the only method that can efficiently remove pollutants from contaminated soils through hyperaccumulation, and it is the most promising for commercial use (Sun *et al.*, 2011).

2.5.1. Phytostabilization

Phytostabilization is a method of immobilizing heavy metals by precipitation or absorption in the root system, thereby preventing the leaching of the metals to the groundwater and reducing the shoot translocation of the metal. Unlike other phytoremediation mechanisms, in phytostabilization, the metals are not removed from the soil permanently; but get stabilized in the root system or soil, reducing the mobility and bioavailability of the metal into the food chain (Lan *et al.*, 2020). Because of the root immobilization and reduced translocation, phytostabilization becomes significant in cultivating food crops in contaminated lands (Janeeshma and Puthur, 2020). To achieve phytostabilization potential, a plant must have a fast growth rate, deep root system, and reduced translocation factor. Generally, phytostabilization has the advantages of effective and rapid immobilization of pollutants, and there is no need for biomass removal. The major drawback of phytostabilization is that

contaminants remain in the soil or the root system, primarily in the rhizosphere (Zgorelec *et al.*, 2020).

Phytostabilization is a technique involved in the Gentle Remediation Options (GROs are cost-effective and eco-friendly solutions for the clean-up of soils simultaneously polluted with organic and inorganic contaminants), which are, among other things, safer and less disruptive to the environment (Radziemska *et al.*, 2017). An excellent example for the plants with phytostabilization potential is the grasses from the fescue family, frequently used in post-mining regions and slag heaps, to generate a vegetation cover. From the fescue family, *Festuca rubra* (red fescue) was commonly used in the phytostabilization of heavy metal contaminated soils (Gołda and Korzeniowska, 2016; Touceda-Gonzalez *et al.*, 2017).

Phytostabilization associated with soil amendments is termed aided phytostabilization (Bolan *et al.*, 2011; Touceda-Gonzalez *et al.*, 2017). Biochar and ethylenediaminetetraacetic acid (EDTA) are used in soil amendments to induce and promote phytostabilization, which aids in immobilizing metals/metalloids (Rathika *et al.*, 2021). Soil amendments such as liming agents, phosphates, Fe, Al and Mn (oxyhydr)oxides, organic amendments, and industrial waste products have been extensively used for phytostabilization experiments. It was reported that the P and Fe-rich composts could effectively immobilize the heavy metals in the polluted lands (Li *et al.*, 2021b). The effect of organic amendments on the bioavailability of heavy metals differs depending on the degree of decomposition of organic matter. The electrostatic complexation between the metal and soil organic matter influences the oxidizable fraction of heavy metals, affecting the toxicity of metals in contaminated soils (Xia *et al.*, 2019). The chief ligands for toxic metals in humic compounds are the hydroxyl and phenolic groups, which form insoluble complexes with metals and reduce the bioavailability

and pollution risks (Zhang *et al.*, 2017a; Yang *et al.*, 2021). Therefore, these techniques can be an effective tool to reduce the environmental risk of heavy metals. Recent advances in the enhanced heavy metal tolerance of plants using soil amendments have been described in section 2.10.

2.5.2. Phytoextraction

Phytoextraction is the process in which plants absorb organic or inorganic compounds, including heavy metals, from the soil or water through their roots and transport them to the shoots, where they are eventually accumulated. The presence of hazardous metals in excess causes very little damage or does not influence the normal metabolic processes in the case of plants with phytoextraction potential (Nedjimi, 2021). The characteristics of the plants used for phytoextraction purposes include a well-developed root system, a higher rate of biomass production, and an enhanced level of metal accumulation and translocation. Such plants with increased accumulation and bio-concentration of metals in their shoot system are termed hyperaccumulators or metallophytes (Chandra *et al.*, 2016). When sufficient biomass has been attained, they are harvested and removed from the field. Hence the metal concentration in the soil is reduced to acceptable levels (Lu *et al.*, 2019). After harvesting the biomass, they are exposed to combustion or incinerator burning, which is used for bioenergy production. After the complete burning, the bottom ash becomes a rich source of metals termed the bio-ore, used for extracting and recycling the metal (Li *et al.*, 2020a). Metal contaminants such as nickel (Ni), zinc (Zn), copper (Cu), lead (Pb), chromium (Cr) and cadmium (Cd) are commonly removed from the contaminated sites *via* phytoextraction techniques (Babu *et al.*, 2021).

The absorbed metals are transported and distributed in leaves through apoplast or symplast, where the ions are sequestered in extracellular compartments (cell walls) or vacuoles, avoiding the accumulation of free

metal ions in the cytoplasm. Therefore, the detoxification of metals inside the plants is mainly achieved by the long-term storage of metals inside the vacuoles of leaf mesophyll tissues or by sequestration in the cell walls (Yan *et al.*, 2020). Plants have spatially distributed transporters and complexing agents that contribute to the absorption, translocation, and redistribution of metals for intercellular and inter-organellar metal transport (Jogawat *et al.*, 2021). The specialized transporters (channel proteins) or H^+-coupled carrier proteins located in the root cell plasma membrane are actively involved in the metal ion absorption from the soil. They can transport specific metals across cellular membranes and facilitate metal translocation from roots to shoots by mediating influx-efflux (DalCorso *et al.*, 2019). Metal transporters discovered so far have been grouped into various families based on their sequence homology. They include zinc-regulated, iron-regulated transporter-like proteins (ZIP), heavy metal ATPases (HMAs), metal tolerance proteins (MTPs), and natural resistance-associated macrophage proteins (NRAMPs) (Yan *et al.*, 2020). These are the integral membrane proteins involved in the uptake and transport of heavy metal cations from root to shoot, which play significant roles in metal homeostasis and tolerance in plants (Nevo and Nelson, 2006; Smith *et al.*, 2014; Krishna *et al.*, 2020). MTPs are involved in the translocation of metals to the extracellular space and internal compartments such as vacuole (Gustin *et al.*, 2011).

2.5.3. Phytovolatilization

Phytovolatilization is the technique in which plants absorb toxins from the soil, convert to their volatile state, and then release them into the atmosphere through their aerial parts.The process of phytovolatilization is used to eliminate organic compounds and inorganic contaminants of Hg, As and Se (Tagmount *et al.*, 2002; Sakakibara *et al.*, 2010; Chen *et al.*, 2012; Tiodar *et al.*, 2021). In the case of Hg, the mercuric ion (Hg^{2+}) is transformed

into less toxic elemental mercury (Hg^0) (Tiodar *et al.*, 2021). In concomitant with the absorption from the soil, the speciation of Hg^{2+} to Hg^0 facilitates in plants, and the volatile Hg^0 diffuse into the xylem or outside the cells, eventually escaping either directly or by stomatal transpiration (Khalid *et al.*, 2017). Similarly, the absorption and transformation of toxic selenium compounds into comparatively less toxic dimethyl selenide was observed in *Astragalus bisulcatus* and *Brassica oleracea* (Hasanuzzaman *et al.*, 2020a). According to Sakakibara *et al.* (2010), *Pteris vitatta* can volatilize 90% of the uptaken arsenic in the form of arsenite and arsenate.

Phytovolatilization exists in two different forms, direct and indirect phytovolatilization, of which, direct phytovolatilization is the more intuitive and well-studied method. In other words, direct phytovolatilization indicates the contaminant absorption and transport by plants and subsequent volatilization through the above-ground tissues (Limmer and Burken, 2016). Due to the plant root activities, the organic contaminants may be volatilized from the subsurface of the soil, termed as indirect phytovolatilization (Grzegórska *et al.*, 2020). The plants involved in the phytovolatilization of organic compounds include the deciduous trees such as *Salix* and *Poplar* and coniferous trees like *Pinus* (Arnold *et al.*, 2007; Ferro *et al.*, 2013; Peter *et al.*, 2017).

2.5.4. Phytodegradation/phytotransformation

Phytodegradation comprises the breakdown of organic pollutants such as TCE (trichloroethane), herbicides, *etc*., with the help of root exudates or enzymes, and the degraded products are integrated into plant development (Nedjimi, 2021). Various plant enzymes involved in phytodegradation include phosphatases (transformation of organophosphates), nitroreductases (for the reduction of the aromatic nitro group), oxidases (for detoxification of TNT (2,4,6-trinitrotoluene)), and nitrilases (transformation of nitrile group into

carboxylic acid) (Susarla *et al.*, 2002; Jabeen *et al.*, 2009; Surriya *et al.*, 2015). Das *et al.* (2010) observed that *Vetiveria zizanioides* removed 97% of TNT from the soil. Similarly, Hannink *et al.* (2007) found that the roots of *Nicotiana tabacum* exude the *NfsI*nitroreductase enzyme, which can degrade TNTs.

2.5.5. Rhizodegradation/phytostimulation

Phytostabilization in association with microbes, known as rhizodegradation or phytostimulation, promotes the immobilization of metals and the breakdown of organic pollutants into non-toxic forms (Janeeshma and Puthur, 2020; Fagnano *et al.*, 2020). The agronomic practices that increase root development and efficiency can positively contribute to rhizodegradation. Therefore, organic fertilization and inoculation with mycorrhizal fungi and endophytic bacteria have minimized pollutant-induced stress in plants (Abhilash *et al.*, 2012). Bacteria such as *Bacillus*, *Burkholderia*, *Pseudomonas*, *Agrobacterium*, *Alcaligenes*, *Arthrobactor*, *Micrococcus*, *etc*., and mycorrhizal fungi such as *Glomus* are actively involved in rhizodegradation (Ojuederie and Babalola, 2017; Allamin *et al.*, 2020; Li *et al.*, 2020a; Saleem *et al.*, 2021). Organic contaminants such as pesticides and hydrocarbons are degraded into non-toxic forms *via* rhizodegradation.

2.6. Growth and phytoremediation potential of *R. communis*

Ricinus communis L. (the castor oil plant) is a species of perennial flowering plant in the family Euphorbiaceae (spurge family) and is the only species of the monotypic genus. In spite of its name, the castor bean, the seed of the plant, is not actually a bean. The *R. communis* plant is native to the Southern Mediterranean Basin, Eastern Africa, and India. However, it is found all across the tropical regions. Castor seed yields castor oil, which has a

wide range of applications, including its most popular therapeutic usage as an efficient laxative (Kamal and Joshi, 2006). The seed contains 40-60% of the oil, which is rich in triglycerides. Therefore, *R. communis* is a significant oil crop for the industry but not edible for humans or animals. Ricine is a water-soluble toxin found in lesser amounts throughout the plant. *Ricinus communis* is a widespread weed in landfills, and ecologically, it is often considered as an excellent colonizer of wastelands (Mehmood *et al.*, 2011). According to Guinness World Records, castor is the world's most poisonous common plant.

Generally, castor plants grow on marginal lands that are usually unsuitable for food crop cultivation. This plant has received considerable attention because of its ability to flourish in extremely contaminated soil, together with its capacity for metal ion accumulation. It has a strong root system and produces a large amount of biomass. As a result, castor can be cultivated for phytoremediation and for bioenergy generation, addressing two significant global issues: growing energy demands and the remediation of heavy metal contaminated lands.

According to the studies conducted by Bauddh *et al.* (2015a,b) and Mendes *et al.* (2015), *R. communis* has an immense potential for phytoremediation of heavy metal contaminated soil. Because of its rapid growth and large leaves, which have a vast surface area of contact with the air and the pollutants therein, *R. communis* plants have the potential to be utilized as bioindicator plants (Mendes *et al.*, 2015). This plant can rehabilitate areas contaminated with mine tailings, including higher concentrations of Cd, Cu, Mn, Pb and Zn, making it a highly valuable, renewable resource (Olivares *et al.*, 2013). It can bioaccumulate Cd concentrations exceeding 200 mg/kg along with extremely higher tolerance potential, and therefore *R. communis* plants can very well be considered as a potential phytoremediator (Shi and Cai, 2009; Bauddh and Singh, 2012a,b).Yashim *et al.* (2016) stated that *R.*

communis could perform phytoremediation in the field based on its bioaccumulation and translocation factors for Cd, Co, Ni, and Pb. Table 2 summarizes earlier reports on the potential of *R. communis* for heavy metal phytoremediation.

2.7. Heavy metal toxicity and tolerance mechanisms in plants

Plants grown in metalliferous soils are characterized by a variety of morphological, physiological, biochemical, and anatomical adaptations to help them to tolerate metal toxicity (Hodson, 2012; Sameena and Puthur, 2021a). Generally, these responses are triggered by a cascade of events that begin with the perception of environmental changes and culminate in expressing a broad spectrum of genes. Metal tolerance in plants is achieved through two primary strategies: metal exclusion and metal accumulation. Metal excluders are non-hyperaccumulator plants that resist metal ion translocation to the above-ground parts through both external and internal detoxifying processes. On the other hand, accumulators are plants that absorb and concentrate toxic metal ions in the above-ground tissues. Metal hyperaccumulators, for example, absorb and bio-concentrate a far larger number of harmful metal ions in the shoot system, maybe hundreds of times more than in the rhizospheric zone (Reeves *et al.*, 2018). The plants in all three situations have a complex and interconnected network of defensive systems for avoiding or tolerating heavy metal-induced phytotoxicity (Emamverdian *et al.*, 2015). The mitogen-activated protein kinase (MAPK) cascade is the basis of cell signaling, which was reported to be involved in the stress-related signaling pathways (Lin *et al.*, 2021). According to the studies conducted by Liu *et al.* (2018c), Cu^{2+} stress caused by oxidative stress activates the antioxidant defence mechanisms *via* the MAPK pathway in maize leaves, and thus the signaling pathway is represented as Cu^{2+}-H_2O_2-*ZmMPK3*-antioxidant enzymes.

2.7.1. Effect of heavy metals on photosynthesis

The inhibition of cytoplasmic enzymes and oxidative stress damage to cell structures are some of the direct harmful consequences of toxic metal concentrations. The replacement of essential nutrients from the active sites of various enzymes is an indirect effect of heavy metal toxicity in plants (Riyazuddin *et al.*, 2022). Heavy metals interact with the photosynthetic apparatus at multiple levels of organization and architecture, including (i) metal accumulation in the leaf, (ii) partitioning in leaf tissues and cells such as mesophyll, stomata and bundle sheath, (iii) interaction of metals with cytosolic enzymes, (iv) alterations in chloroplast membranes and photosystems (Souri *et al.*, 2019). Plants may experience changes in some physiological processes as a result of disturbances in photosynthesis processes, such as disturbances in nutrient and water uptake as well as transport, alterations in nitrogen metabolism, damages to ATPase activity, interferences with plant growth and closing of stomata, which ultimately results in the dysfunction of plant photosynthetic machinery (Shahid *et al.*, 2014; Khalid *et al.*, 2017).

Photosynthetic inhibition is one of the most common responses in plants to Cu stress because they invariably affect the photosynthetic apparatus and its functions, reducing chlorophyll synthesis and inhibiting Calvin cycle activities, either directly or indirectly, by inhibiting both light and dark reactions of photosynthesis (Küpper *et al.*, 2003). Heavy metals increase the chlorophyllase activity and replace the central Mg ion in the porphyrin ring of the chlorophyll molecule, causing chlorophyll molecules to degrade (Riyazuddin *et al.*, 2022). Likewise, the interactions of heavy metals with the enzyme involved in chlorophyll synthesis, protochlorophyllide reductase, and δ-aminolevulinic acid dehydratase, resulted in the reduction of chlorophyll molecules, which directly affects the photosynthesis (Chandra and Kang,

2016; Jain *et al.*, 2018; Yang *et al.*, 2020). According to the studies conducted by Mallick and Mohn (2003), heavy metals such as Cd, Cr, Cu, Ni and Zn have a severe negative impact on the water-splitting complex, as these heavy metals can replace Mn ions from the water-splitting complex of the oxidizing side.

The chlorophyll fluorescence analysis revealed that the inactivation of photosystem II reaction centers and their transformation into excitation quenching and the blockage of electron transport in the oxygen-evolving complex were the negative effects of heavy metal toxicity (Paunov *et al.*, 2018). Giannakoula *et al.* (2021) revealed that Cu toxicity leads to the reduction in capturing and conversion efficiency of harvested light energy by photosystems, represented as Fv/Fm, which have been resulted from the increase in initial fluorescence (Fo) and decrease in maximal fluorescence (Fm). As indicated by earlier studies, the increase in Fo during Cu excess was probably due to the reduced plastoquinone acceptor (Q_A) being unable to be oxidized completely, and the decrease in Fm was associated with the reduced activity of the water-splitting enzyme complex (Ouzounidou *et al.*, 1997).

2.7.2. Accumulation of metabolites to counter the heavy metal stress

Plants use osmoregulation or osmoprotection to defend themselves from numerous abiotic stressors, including heavy metals, by accumulating osmoprotectants or osmolytes. Osmolytes are low molecular weight organic solutes, such as polysaccharides, sugar alcohols, amino acids, betaines and tertiary sulphonium compounds (Rhodes *et al.*, 2002; Ashraf and Foolad, 2007; Slama *et al.*, 2015). Therefore, plant stress tolerance is always linked to increased accumulation of compatible solutes (Anjum *et al.*, 2016a). Osmolytes are accumulated to maintain the osmotic potential of cells, and they do not interfere with cellular functions but at the same time assist in maintaining the cell activities. They also safeguard macromolecular

subcellular structures and minimize the impact of ROS formed in response to abiotic stressors (Szabados and Savoure, 2010; Slama *et al.*, 2015).

Heavy metals limit the upward flow of water and have a detrimental impact on the water supply to the shoot by slowing down the short and long-distance water transport through symplast and apoplast. This is caused by changes in aquaporins and plasmodesmata, reductions in the number and size of xylem vessels, reduced stomatal conductance, and obstructions generated by metals in the xylem, such as metal depositions and cellular debris (Rucińska-Sobkowiak, 2016). Therefore, plants accumulate compatible solutes that lessen the osmotic potential through a process known as osmotic adjustment to survive the heavy metal-induced water deficit (Blum, 2011; Vezza*et al.*, 2018). According to the observations of Yadav *et al.* (2021), abiotic stress resulted in the accumulation of metabolites such as sugars, amino acids, organic acids, and some antioxidants such as kaempferol, melatonin and quininic acid, which significantly contributes towards the stress tolerance *via* osmotic adjustment and antioxidant activity. Similarly, Merewitz *et al.* (2012) reported that the enhanced stress tolerance was associated with the accumulation of metabolites such as sugars (sucrose, maltose, fructose and ribose), amino acids (proline, alanine, glycine and γ-aminobutyric acid) and organic acids, which are primarily involved in the citric acid cycle. These metabolites act as stress signaling molecules, participate in osmotic adjustment, and assist in respiration and energy production.

Carbohydrates are structural and storage substances, respiratory substrates, and intermediate metabolites of many biochemical processes and are also involved in stress tolerance as modulators of gene expression, acting as osmoprotectants or signaling molecules in both abiotic and biotic stress tolerance (Gangola *et al.*, 2018). Sucrose, the product of photosynthesis in

majority of the plants, is a significant carbon and energy source. It is carried from the source to the sink in the phloem, where it is used in physiological processes that aid the plant growth and development as well as stress response (Patrick *et al.*, 2013). Sucrose and its derivatives act as signal molecules, modulating plant responses to stress directly or through interactions with hormone and redox signal molecules (Ruan, 2014). They also act as osmotic protectants of biomolecules and membranes in plants and resulting in the increase of plant tolerance to abiotic stresses (Thomas *et al.*, 2012).

Several enzymes aid the metabolism of sucrose. For example, sucrose-phosphate synthase catalyzes the biosynthesis of sucrose, invertases (including acid invertase and neutral invertase) hydrolyzes sucrose into glucose and fructose, and sucrose synthase is a glycosyl transferase enzyme that plays a key role primarily in the sink tissues that catalyzes the reversible cleavage of sucrose into fructose and either adenosine diphosphate glucose or uridine diphosphate glucose (Obenland, 1993; Roitsch and González, 2004; Stein and Granot, 2019; Li *et al.*, 2020b). The changes in activities of these enzymes involved in sucrose metabolisms as well as the expressions in sugar transporter genes were observed in plants during stress situations (Ruan, 2014; Hir *et al.*, 2015; Durand *et al.*, 2016). The elevated accumulation of sugars is utilized for energy production, maintenance of membrane integrity, turgor and signaling, all of which confer heavy metal tolerance to plants (Gurrieri *et al.*, 2020).

Plants respond to toxic metals in the environment by stimulating the expression of genes that encode stress-related proteins. These metal ions significantly impact cellular protein homeostasis by disrupting the folding process and aggregation of nascent or non-native proteins, resulting in reduced cell viability (Hasan *et al.*, 2017). However, plants are characterized by a variety of ubiquitous cellular monitoring systems that allow them to

efficiently detoxify heavy metals and increase their tolerance to metal stress (Li *et al.*, 2020b). As proteins are the main workhorses of living cells, chelation of metal ions in the cytosol with phytochelatins and metallothioneins and sequestration to the vacuoles, as well as the removal and destruction of proteins that fail to achieve their native conformations, are all important for plant tolerance to heavy metal stress (Hall, 2002). The mechanisms of metal transport and sequestration by specific proteins are detailed in the following sections. In addition to the usual transport and sequestration functions of proteins, the enhanced production of these stress-related proteins could also contribute towards the osmotic adjustment in plant cells (Neto *et al.*, 2009).

Amino acids are the precursors and components of proteins, which play a vital role in the metabolism and development of plants. During exposure to abiotic stresses, including heavy metal stress, plants accumulate particular amino acids, which may be involved in stress tolerance, including the role played as osmolytes, signaling molecules, modulation of ion transport and involvement in metal ion detoxification, regulation of pH and stomatal opening (Rai, 2002; Xu *et al.*, 2012a; Zemanová *et al.*, 2013). Joshi *et al.* (2010) observed that the branched-chain amino acids valine, leucine and isoleucine play an essential role in plants during osmotic stress by accumulating compatible osmolytes. Polypeptides and proteins rich in glycine, proline, hydroxyproline, leucine, cysteine and methionine play a vital role in forming plant cell walls and stress adaption (Pavlíková *et al.*, 2008; Zemanová *et al.*, 2017). In addition to de novo synthesis, the higher amino acid pools might result from decreased protein synthesis or overall protein degradation during abiotic stresses (Joshi *et al.*, 2010). According to Xu *et al.* (2012b), Cd stress enhanced the expression of eight genes involved in the metabolism, biosynthesis, and transportation of serine, threonine, and aspartate in *Solanum* plants. Glycine betaine, a well-known osmolyte

accumulated during heavy metal stress, was synthesized with the help of glycine in plants.

Proline is a key variable amino acid in defining protein and membrane structures, as well as scavenging reactive oxygen species (ROS), and act as a strong osmoprotectant in stressed cells (Ashraf and Foolad, 2007; El-Beltagi *et al.*, 2020). In addition to its function as an osmolyte or compatible solute, proline serves as a molecular chaperone, protecting protein integrity and maintaining the enzyme activity (Chattopadhyay *et al.*, 2004). It is also regarded as a non-enzymatic antioxidant due to its capacity to scavenge ROS and quench singlet oxygen (Suprasanna *et al.*, 2015). Proline accumulation occurs primarily due to the up-regulation of cytosolic proline biosynthesis and down-regulation of mitochondrial proline degradation. Changes in the expression or activity levels of the two enzymes performing the initial reactions in proline synthesis pathways, pyrroline-5-carboxylate synthetase and proline dehydrogenase, are frequently used to characterize the stress responses in plants (Lebreton *et al.*, 2020).

2.7.3. Accumulation of ROS molecules and antioxidant defence mechanism

One of the principal responses of plants to heavy metal stress is the oxidative burst, which generates enormous amounts of reactive oxygen species (ROS) such as superoxide anion ($^{\bullet}O_2^-$), hydroxyl radical ($^{\bullet}OH$), singlet oxygen ($^1O_2$) and hydrogen peroxide (H_2O_2). The generation of ROS is an inherent property of plant cells, and it contributes to the oxidative damage that leads to cell death (Kohli *et al.*, 2017). In plants, the generation of ROS is limited to mitochondria, chloroplasts and peroxisomes, compared to other cellular compartments (Hasanuzzaman *et al.*, 2020b). ROS is an essential component of the chloroplast signaling system, which transmits vital information concerning redox pressure within the electron transport chain to

the nucleus (Foyer, 2018). The generation of ROS alters several physiological processes, including degradation of enzymes, proteins and amino acids, and causes changes in cell structure. ROS also act as secondary messengers, involved in a range of cellular functions, including cell acclimation to stress, and they are interconnected with several other signaling pathways (Hasanuzzaman *et al.*, 2020c).

ROS scavenging in plants is generally moderated by two antioxidant defence systems: primarily the enzymatic antioxidants and secondarily the non-enzymatic antioxidants. The enzymatic antioxidant system includes guaiacol peroxidase (POD), glutathione peroxidase (GSH), catalase (CAT), superoxide dismutase (SOD), and the enzymes involved in the ascorbate-glutathione (AsA-GSH) pathway such as ascorbate peroxidase (APX), monodehydroascorbate reductase (MDHAR), dehydroascorbate reductase (DHAR) and glutathione reductase (GR). Ascorbate (AsA), glutathione (GSH), carotenoids, tocopherols, proline, anthocyanins, flavonoids, and other phenolic compounds constitute the non-enzymatic antioxidant system (Yap *et al.*, 2021). Both these systems are functionally interconnected, and they can protect plant cells from ROS-induced oxidative damages by detoxifying the ROS molecules.

The scavenging of superoxide anion ($^{\bullet}O_2^-$) by SOD and decomposition of H_2O_2 by APX, POD and CAT are primarily related to the maintenance of cellular redox stability during heavy metal stress, including Cu toxicity (Sgherri *et al.*, 2007; Liu *et al.*, 2018c). Therefore, rapid enhancement in the antioxidant activities occurred concomitantly with ROS generation in plants (Sgherri *et al.*, 2007). SOD prevents damage to the electron transport system and structural components by removing superoxide radicals from chloroplasts and mitochondria (Soliman *et al.*, 2018; Elkelish *et al.*, 2019). According to Lwalaba *et al.* (2020), Cu toxicity resulted in an up-regulation of the SOD

isozymes in barley genotypes. A concentration-dependent enhancement in CAT activity was recorded in *Abutilon indicum* subjected to Cu stress, which will efficiently decompose H_2O_2, produced by the activity of SOD, into H_2O and O_2 (Rout *et al.*, 2017).

The AsA-GSH pathway comprises four enzymatic antioxidants: APX, MDHAR, DHAR and GR, and two non-enzymatic antioxidants, AsA and GSH. APX, the first enzyme of the cycle, consumes two molecules of AsA, reduces H_2O_2 and produces two monodehydroascorbate (MDHA), a radical with a short life span (Pandey *et al.*, 2015). This MDHA was reduced to AsA, utilizing NAD(P)H as an electron donor by the action of MDHAR. If the conversion of MDHA does not occur rapidly, MDHA will spontaneously disproportionate to AsA and DHA (oxidized ascorbate). DHA is regenerated to AsA by the action of the enzyme DHAR, using GSH as a reductant, which converts reduced glutathione (GSH) to oxidized glutathione (GSSG). Similarly, GSH is regenerated from GSSG through GR (Shin *et al.*, 2013). Because DHA is readily hydrolyzed to 2,3-L-diketogulonate, the rapid reduction of MDHA and DHA by MDHAR and DHAR is essential for maintaining the ascorbate pool. Therefore, the enzymes MDHAR and DHAR are necessary for the generation of AsA, which is critical for the efficient scavenging of the ROS (Shin *et al.*, 2013).

In addition to the enzymes of the AsA-GSH cycle, phenolic compounds and lipophilic compounds such as carotenoids and tocopherols constitute the major antioxidative systems in plants. Phenolics are a diverse category of secondary metabolites found in plant tissues and include flavonoids, tannins, hydroxycinnamate esters, lignins, *etc*. (Sakakibara *et al.*, 2003). The methylation pattern and frequency of methyl groups attached to the polar head of the phenolic ring are ideal for trapping free radicals and determining the relative antioxidant activity of the isomers in vivo

(Dumanović *et al.*, 2021). Similarly, α-tocopherol has the highest antioxidant activity due to its three methyl substituents. Phenolics have a strong capability to donate an electron or hydrogen atom, quickly stabilize generated phenol radicals, and have stronger activity in an in vitro system when compared to AsA and α-tocopherol (Dumanović *et al.*, 2021).

Anthocyanins are the natural pigments in the flavonoid family and are found in various plant parts, including flowers, fruits, stems, roots, and leaves (Naing and Kim, 2018). During extreme stress effects, the over-production of ROS and oxidative damage to the plants resulted in the production of anthocyanins after ROS signaling *via* the up-regulation of anthocyanin biosynthesis genes (Altangerel *et al.*, 2017; Xu *et al.*, 2017). These anthocyanins can help in antioxidant activities by scavenging excess ROS. Due to their antioxidant characteristics, anthocyanins protect plants against growth inhibition and cell death by lowering oxidative stress, allowing plants to cope with abiotic stresses (Naing and Kim, 2021). According to the studies conducted by Vidal *et al.* (2020), the phenolic compounds, including flavonoids and anthocyanins, were prominently accumulated in *Imperata cylindrica* plants exposed to Cu stress, which significantly contributed to the efficient antioxidation mechanisms.

2.7.4. Uptake and translocation of heavy metals

The uptake of metals by the roots is dependent on the availability of metals in the soil solution, which in turn depends on a number of factors, including pH and density of the soil, water-holding capacity, degree of complexation with ligands, type of charge in soil colloids, the surface area of soil particles and presence of hydrous ferric oxides (Chibuike and Obiora, 2014; Balkhair and Ashraf, 2016). Vamerali *et al.* (2009) reported that Cu is said to have a strong affinity for soil organic materials and a high root retention rate. Heavy metals will be localized in the roots, and their

translocation into the shoots will be limited, allowing the plants to carry out their normal metabolic processes in the shoot without being hampered by metals (Shackira *et al.,* 2017). Though heavy metal translocation to the shoot is limited, Cu and Zn accumulated at higher levels as compared to many other heavy metals in the soil, indicating the enhanced uptake and translocation of these two metals than other heavy metals (Romdhane *et al.,* 2021).

For the enhanced tolerance towards the toxic metal ions, plants have evolved homeostatic mechanisms such as prevention of root metal ion absorption and lowering long-distance metal ion transport (Clemens *et al.*, 2002). In response to heavy metal exposure, plants activate multiple signaling pathways and defence systems that synthesize stress-related proteins (Mourato *et al.*, 2015). Heavy metal-associated proteins (HMPs) have a heavy metal-associated domain, which plays a principal role in heavy metal translocation and detoxification in the cells (Zhang *et al.*, 2018).

Casparian strips on the endodermis and exodermis, the specific structure deposited in anticlinal walls, are distinguished by impregnating the primary wall pores with lignin and suberin, often preventing the apoplastic translocation of metals and other contaminants from root to shoot (Chen *et al.*, 2011). In order to escape this barrier, metals travel symplastically to reach the xylem. Besides this, endodermis also has 'passage cells' for metal entry, which include (i) the region of root apex where the casparian band is not fully developed and (ii) basal regions of the root where the endodermis is ruptured due to the emergence of lateral roots from the pericycle *via* cortex (Huang and Van Steveninck, 1989; Marschner, 1995).

The cellular localization of Cu in the roots of *Erica australis* using cryo-scanning electron microscopy along with energy-dispersive X-ray analysis (cryo-SEM/EDX) revealed that Cu was uniformly localized in the epidermis, cortex and vascular tissues (Trigueros and Rossini-Oliva, 2021).

However, Cu also remained compartmentalized in cell walls, vacuoles and/or cytoplasmic vesicles of these tissues (Liu and Kottake, 2004; Sharma *et al.*, 2016a; Kumar *et al.*, 2021). On the contrary, cellular localization of Zn in *Populus deltoides* roots by cryo-SEM/EDX revealed that Zn is accumulated primarily in root peripheral tissues, with concentrations decreasing towards the central cylinder due to the protection of vascular tissues by the suberized endodermis (Stoláriková *et al.*, 2015).

2.7.5. Biomass accumulation and abscission of older plant organs

One of the major strategies adopted by the plants during heavy metal stress is the accumulation of biomass in order to dilute the presence of heavy metals by spreading the metal out into every region of their enhanced biomass. The same accumulated biomass may be used to generate renewable energy also. According to Tian *et al.* (2012), *Zea mays* can produce larger biomass during phytoremediation of Cd contaminated soil. When the quantity of this metal in the soil was 45mg/kg, this plant accumulated about 1 μg of Cd in a single plant. Mukhtar *et al.* (2010) discovered that when *Helianthus annuus* was cultivated in Ni and Pb polluted water, the bioaccumulation of the metal and biomass production were comparatively higher. Lima *et al.* (2019) reported that sorghum plants produce large biomass under higher Cu toxicity because of their enhanced tolerance and excellent phytostabilization potential.

Though the organ age of a plant controls the onset of senescence, it can also be influenced or accelerated by a range of environmental conditions, including heavy metal stress (Zhang *et al.*, 2011). The sequestration of toxic metal ions to the older organs has been considered as one of the stress tolerance mechanisms in plants, thereby avoiding the influence of these metal ions in actively metabolizing younger organs (Almehdi *et al.*, 2019). The abscission of the older leaves occurred after the effective translocation of metal, which also ensured that the accumulated metal did not remobilize into

the growing regions (Sameena and Puthur, 2021b). According to Ahmad and Guo (2019), almost all phytohormones have a role in the senescence signaling pathways of both age-dependent and stress-induced leaf senescence. Therefore, the senescence-related genes act as the integrators of various signaling pathways that regulate the stress responses in plants (Jibran *et al.*, 2013). The involvement of the *R2R3 MYB* gene family (genes related to abscission zone separation) in the early abscission of leaves of *Manihot esculenta* exposed to diverse stress conditions was observed by Liao *et al.* (2016).

2.7.6. Structural modifications and changes in cellular architecture

Metal accumulation in plants resulted in alterations of the root, stem and leaf anatomy (Adejumo *et al.*, 2021). The studies conducted by Fu *et al.* (2015) in Cu accumulator and excluder plants revealed that heavy metal accumulators show substantially higher leaf stomatal density, numerous and longer epidermal hairs, and thick cuticle covered on the guard cells than metal excluder plants. The presence of druse crystals, formed as the mineral structures with calcium oxalate (CaOx) depositions in the cells, contribute a significant role in the detoxification of heavy metals (Mazen, 2004; Jáuregui-Zùñiga *et al.*, 2005). The co-precipitation of Cu and CaOx crystals in the plant cells selectively isolate the toxic Cu, and therefore these highly insoluble salts no longer osmotically or physiologically become active (McBride *et al.*, 2019; Martins *et al.*, 2020). A similar type of druse crystal formation was observed in the idioblast cells of stem and leaves of *Alternanthera tenella* in response to excess Cu (Martins *et al.*, 2020)

The leaves of Zn-treated *Populus deltoids* were thinner, with shrunken cells and greater intercellular spaces in the mesophyll cells (Stoláriková *et al.*, 2015). In contrast, heavy metal accumulation causes *Arachis hypogea* to develop xerophytic characteristics such as smaller leaflets, thicker epidermis

and mesophyll cells, and a large number of tiny stomata (Shi and Cai, 2009b). The ultrastructural studies of chloroplasts in Zn-treated mesophyll cells revealed that Zn accumulation leads to the enhancement in the number of plastoglobuli and thylakoids and also lowered the number of grana (Azzarello *et al.*, 2012). Similarly, Zn stress reduces the number and size of starch grains within the chloroplasts of *Populus alba* (Todeschini *et al.*, 2011).

To deal with heavy metal stress, hyperaccumulator plants use two major physiological strategies: compartmentalization and excretion (Choi *et al.*, 2001). Heavy metal complexation with ligands and compartmentalization of these complex forms in metabolically inactive regions such as cell walls or vacuoles are the mechanisms of compartmentalization/sequestration in these plants (Rascio and Navari-Izzo, 2011). These complexes are also sequestered to epidermis, trichomes or cuticles, where they do the least damage to the cell machinery (Ma *et al.*, 2005; Asemaneh *et al.*, 2006; Freeman *et al.*, 2006). Some plants excrete heavy metal complexes to the outside of the plant body *via* salt glands, trichomes, or subsidiary and guard cells of stomata, all of which protect plant cells from heavy metal toxicity (Neumann *et al.*, 1995; Choi *et al.*, 2001; Broadhurst *et al.*, 2004; Cosio *et al.*, 2005; Rascio and Navari-Izzo, 2011). Although the methods outlined above are common, different metal hyperaccumulator plants have exhibited different mechanisms for minimizing the harmful effects of heavy metals, and even different plant parts within the same plant respond to different heavy metals in different ways (Asad *et al.*, 2019).

2.7.6.1. Deposition in the cell wall

Plant cell walls are mostly made up of celluloses, hemicelluloses, pectins, and proteins with carboxyl, hydroxyl, amino, and aldehyde groups. These functional groups can bind metal ions, thereby preventing their transportation across the plasma membrane (Wang *et al.*, 2008). According to

Zornoza *et al.* (2002), when white lupin (*Lupinus sp*.) was exposed to Cd stress, about 60% of total up-taken Cd was bound to the cell walls. Lignins and lamellar suberins, the major constituents of the cell wall, control the entry of metal ions into the roots (Lux *et al.*, 2011). Unmethylated pectin residues in the cell wall are negatively charged at apoplastic pH, which can ionically interact with cations including Cu, thereby immobilizing the metal in the cell wall (Printz *et al.*, 2016). In some plants, complex changes such as callose deposition occur between the cell wall and the plasma membrane and act as a barrier for metal transport (Krzesłowska, 2011).

The drawback of this barrier is that it can also prevent essential nutrients from being transported as reported by Fahr *et al.* (2013). The authors discovered that when *Glycine max* was exposed to Pb stress, these callose depositions restrict the entrance of Pb into plants and can also prevent the transfer of other beneficial molecules/elements by impeding cell to cell transport.

2.7.6.2. Accumulation and secretion through trichomes

Plant trichomes are superficial, protective, and highly dynamic tissue that may respond to a wide range of environmental stimuli (Karabourniotis *et al.*, 2020). One of the key processes in plant resistance to heavy metal toxicity is the accumulation of heavy metal complexes in trichomes, and the proximity of trichomes to the leaf periphery makes them good locations for heavy metal deposition (Cosio *et al.*, 2006). Moreover, trichomes serve as the site for the secretion of the metal substituted Ca crystals (Sarret *et al.*, 2006; Emamverdian *et al.*, 2015). The increased frequency of highly lignified trichomes in the stem and leaves of *Alternanthera tenella* plants subjected to Cu stress indicated the tolerance potential of the plant towards the toxic levels of Cu and also the role of Cu as the modulator of lignin biosynthesis (Nair and Chung, 2015; Martins *et al.*, 2020).

It was reported that Cd was accumulated preferentially in the leaf trichomes in *Brassica juncea*, a well-known metal hyperaccumulator plant (Salt *et al.*, 1995). Choi *et al.* (2001) discovered that plants exposed to Cd exclude the metal in the form of crystals through their trichomes. Many annual plants, such as *Arabidopsis thaliana* and *Alyssum lesbiacum* exposed to heavy metal stress, have shown similar results (Krämer *et al.*, 1997; Ager *et al.*, 2002). The energy-dispersive X-ray (EDX) analysis in combination with proton-induced X-ray emission (PIXE) microanalysis revealed that the amount of Cd deposited inside the trichome was 10 times greater than in the epidermis, with preferential accumulation near the base underneath the branching point (Domínguez-Solís *et al.*, 2004). The SEM-EDX analysis of the leaf tissues of *Erica australis* plants exposed to Cu stress revealed that Cu was preferentially accumulated in the abaxial trichomes, thereby restricting the accumulation of Cu in the mesophyll cells (Trigueros and Rossini-Oliva, 2021).

2.7.7. Chelation and sequestration of heavy metals in the vacuole

Chelation of the metal and subsequent sequestration of the chelated complex into the vacuole is one of the general methods developed by plants for heavy metal detoxification (Cobbett, 2000). It is dependent on two vacuolar pumps [vacuolar-type ATPase (V-ATPase) and membrane-bound proton-pumping pyrophosphatase (V-PPase)] as well as a group of tonoplast transporters that are driven directly by proton motive force and primary ATP-dependent pumps (Sharma *et al.*, 2016a). In the case of non-hyperaccumulator plants, the heavy metals largely sequester in the root vacuoles, whereas hyperaccumulators sequester them mainly in the leaf vacuoles after efficient long-distance translocation. The long-distance transport of metals is primarily contributed by cytosolic metal chelators and tonoplast-localized transporters, or the interplay between them (Peng and Gong, 2014). This technique reduces

the toxicity and interference of heavy metals with cell organelles (Wang *et al.*, 2008).

The genes such as *VIT2* (*Vacuolar Iron Transporter 2*), *MTP3* (*Metal Transporter 3*), *CAX4* (*Cation Exchanger 4*) and *ZIF1* (*Zinc-Induced Facilitator 1*) regulate the sequestration of metal ions to the vacuole, which gets up-regulated in the presence of the excess amount of heavy metals in the environment and the enhanced expression results in the increase of vacuolar sequestration capacity and metal accumulation (Peng and Gong, 2014). Sulfur-rich peptides (phytochelatins) and organic acids are also the major contributors for the transport and storage of metals into the vacuoles (Stolt *et al.*, 2003). The sequestered metal in the vacuole is inactivated by precipitation as metal-phytates or by binding with low molecular weight organic acids (Salt *et al.*, 1999). The major transporters involved in the sequestration of toxic metal ions, especially to the vacuole, are detailed in the following section.

Similar to the direct vacuolar sequestration, there are few reports on the role of vesicle trafficking in heavy metal transport to the vacuole (Sharma *et al.*, 2016a). For example, Leitenmaier and Küpper (2011) identified Cd-rich vesicle-like structures in the leaf cell protoplasts of the *Thlaspi caerulescens*, and they are thought to play a role in vacuolar sequestration of Cd. But the exact origin or fate of these vesicles is unknown. Similarly, Zn-rich vesicular structures were observed in the root protoplasm of Zn stress affected *Arabidopsis thaliana* seedlings (Kawachi *et al.*, 2009).

2.7.8. Metal-binding molecules

Among the various metal-binding molecules, the metal transporters/ proteins are contributing a major role in the chelation of metals than the organic acids, phenolic compounds or other secondary metabolites (Hasan *et al.*, 2017; Jogawat *et al.*, 2021). Several metal chelators have been identified

in plants, of which the enzymatically synthesized phytochelatins and gene-encoded metallothioneins are the best characterized peptides. These peptides bind with metal cations, thereby inhibiting their activity and reducing the transport of free metal ions to aerial parts (Cobbett and Goldsbrough, 2002).

2.7.8.1. Phytochelatins (PCs)

Phytochelatins are cysteine-rich oligopeptides, with $(\gamma\text{-Glu-Cys})_n\text{-Gly}$ structure, where n = 2-11, which chelate metal ions through their sulphydryl groups (Cobbett and Goldsbrough, 2002; Roncarati *et al.*, 2015). They are synthesized enzymatically in the cytosol from GSH by phytochelatin synthase (PCS), a γ-glutamylcysteine dipeptidyl transpeptidase enzyme and the expression of the PCS gene was activated in plants upon exposure to heavy metal stress (Grill *et al.*, 1989; Tennstedt *et al.*, 2009; Uraguchi *et al.*, 2021). Therefore, PCs are used as biomarkers for the early detection of heavy metal stress in plants (Keltjens and Van Beusichem, 1998; Saba *et al.*, 2013). Increased heavy metal concentrations activate the PCS enzyme in the cytoplasm along with the presence of reduced glutathione (GSH). PCs form complexed with heavy metals, and the metal–PC complex is subsequently carried to the vacuoles, where it can be detoxified (Song *et al.*, 2014).

The extent of PC synthesis is specific to plant as well as metals. It was reported that Ag, As, Cd and Hg are strong inducers of PCs, whereas Cu and Ni are moderate inducers and Pb and Zn are weak inducers (Anjum *et al.*, 2015). Modern techniques such as HPLC-MS, LC-MS/MS and X-ray absorption spectroscopy revealed the binding of metal ions with PCs (Mou *et al.*, 2016; Dennis *et al.*, 2021). Copper stress-induced accumulation of PC2 to PC5 was observed in the *Colobanthus quitensis*, of which the extent of accumulation of PC2 and PC4 were dependent on the concentration of Cu, whereas PC3 and PC5 were accumulated in the concentration-independent manner (Contreras *et al.*, 2018).

2.7.8.2. Metallothioneins (MTs)

Metallothioneins (MTs) are gene encoding small cysteine-rich proteins that bind to metals using cysteine residues *via* mercaptide bonds, and the arrangement of these residues determines the metal-binding ability of the MTs (Grennan, 2011). They perform a key function in reducing metal toxicity and regulating metal metabolism. MTs impart metal stress tolerance in plants through degeneration of ROS, activation of genes involved in the transcription of metalloenzymes and sequestration of metals into the vacuoles (Hassinen *et al.*, 2011; Sharma *et al.*, 2016b). Based on the arrangement of cysteine residues, plant MTs are classified into four subfamilies: MT1, MT2, MT3 and MT4 (Cobbett and Goldsbrough, 2002; Leszczyszyn *et al.*, 2013).

Kim and Kang (2018) reported the up-regulation of Type 1 MT genes and down-regulation of Type 2 MT genes in rice plants exposed to Cu stress. Similar results were also observed in *Eleocharis montevidensis* growing in Cu mine areas. These observations suggest that the isoforms of Type 1 MTs could be playing a specific role during Cu stress tolerance in monocots than Type 2 MTs (Llerena *et al.*, 2021). Although there was down-regulation of Type 2 MTs in the earlier case, there was up-regulation of the same observed in *Arabidopsis thaliana* exposed to Cu stress (Kim and Kang, 2018). Similarly, the enhanced transcription of Type 1 MTs was observed in transgenic *Arabidopsis* exposed to As, Cd and Cr, thereby reducing the accumulation of stress markers such as thiobarbituric acid reactive substances and H_2O_2, increased accumulation of antioxidant molecules, and improved metal tolerance (Dubey *et al.*, 2021).

2.8. Copper toxicity in plants

Copper (Cu) is an essential redox-active transition metal that plays a key role in a variety of functions in plant development and growth, including

CO_2 absorption, electron transport, cellular transportation, mitochondrial respiration and ATP generation, protein trafficking and hormone signaling (Demirevska-Kepova *et al.*, 2004; Ferreira *et al.*, 2015). It is essential for the activity of various proteins and enzymes involved in photosynthesis and respiration, including plastocyanin, cytochrome c oxidase, Cu/Zn superoxide dismutase (SOD), polyphenol oxidase, laccase, and ascorbate oxidase (Burkhead *et al.*, 2009). Though Cu is essential for proper plant growth and development at lower concentrations, higher concentrations result in toxicity symptoms, visualized by chlorosis and necrosis, as well as stunting and inhibition of root and shoot growth (Yruela, 2009; Chen *et al.*, 2015; Jung *et al.*, 2015). Cu-mediated leaf chlorosis resulted from the retardation of pigment accumulation and deceleration of chlorophyll integration into photosystems. Excessive Cu buildup causes nutritional deficits and interferes with cellular respiration, nitrate reductase activity and the catalytic cycle of peroxidase in plants (Martins *et al.*, 2016). Copper-induced root abnormalities range from the disruption of root cuticle, decreased root hair proliferation to severe root deformation (Sheldon and Menzies, 2005; Kumar *et al.*, 2021). Moreover, the reduced root surface area due to Cu stress negatively affects nutrient absorption. According to Liu *et al.* (2014b), Cu-induced inhibition of root activities in maize seedlings may be developed as a result of cell membrane damages to the roots.

It was reported that Cu forms stable complexes with amino acids in the xylem sap, facilitating the transport of metals from root to shoot in hyperaccumulator plants (Shabbir *et al.*, 2020). At higher concentrations, cupric (Cu^{2+}) and cuprous (Cu^{+}) ions can take part in redox reactions affecting organisms at the cellular level, primarily through three well-established mechanisms: (i) direct inactivation of protein through undesired amino acid-metal interactions due to the high affinity of Cu^{2+} towards carboxyl-, imidazole-, and thiol- groups, (ii) Cu^{2+} can be reduced to Cu^{+} in the presence

of superoxide or other reducing agents, which can catalyze the generation of hydroxyl radicals *via* the non-enzymatic Fenton's reaction, and (iii) displacement of essential cations from the specific binding sites of enzymes (Ritter *et al.*, 2014; Sağlam *et al.*, 2016).

Copper excess in photosynthetic organisms can cause the replacement of magnesium in chlorophylls, preventing energy transfer from chlorophylls to PSII in low light, or it can directly block the PSII reaction center during high light (Küpper *et al.*, 2002; Laporte *et al.*, 2020). According to experiments conducted by Küpper *et al.* (2009), Cu-induced inhibition of photosynthesis in *Crassula helmsii* plants was due to the negative impact of Cu on PSII reaction centers. There has been a significant decrease in photosynthetic gas exchange and chlorophyll fluorescence characteristics observed in the leaves of *Avicennia germinans* and *Bruguiera cylindrica* during Cu stress (Gonzalez-Mendoza *et al.*, 2013; Sruthi and Puthur, 2019). The loss of leaf area during the excess of Cu resulted in lignin accumulation in the xylem, which leads to cell wall thickening and hardness, which has a negative impact on cell development and leaf expansion by reducing its elasticity. Moreover, Cu toxicity resulted in oxidative stress in plants, owing to an increase in the generation of extremely toxic oxygen free radicals (Kumar *et al.*, 2021).

2.9. Role of phytohormones in heavy metal stress tolerance

Phytohormones are chemical messengers produced by plants in very low concentrations, which can regulate a wide range of growth and developmental processes (Jiang and Asami, 2018). In response to diverse biotic and abiotic stresses, they can trigger various signal transduction pathways (Rhaman *et al.*, 2021). According to the observations of Sytar *et al.* (2019), the endogenous phytohormone levels were enhanced upon exposure to heavy metal stress, which modulates the stress-responsive characters of the

plant. In order to identify and characterize diverse molecular pathways involved in phytohormones-mediated heavy metal stress tolerance in plants, numerous research approaches like expression profiling, microarray, mutant screening, proteomics, and bioinformatics have been experimented (Singh *et al.*, 2016; Saini *et al.*, 2021). Though the exogenous application of phytohormones has been successfully used to enhance the metal stress tolerance in plants, the specific role of phytohormones in modulating heavy metal stress response signaling is still lacking (Nguyen *et al.*, 2021). Previous studies related to the functions of various phytohormones in heavy metal stress tolerance have been briefly discussed below.

2.9.1. Roles in alleviating growth inhibition

According to recent research, phytohormones may control and integrate growth responses in plants to diverse environmental stimuli to sustain life. They allow the plants to maintain growth flexibility during development and are likely the primary way by which plants adapt to abiotic and biotic stressors (Colebrook *et al.*, 2014; Xu *et al.*, 2016). The complex interactions between the endogenous phytohormones activate the defence and response mechanisms in plants during exposure to heavy metals (Piotrowska-Niczyporuk *et al.*, 2020). During metal exposure, the synthesis and accumulation of defence-related hormones (abscisic acid, ethylene, brassinosteroids, salicylic acid and jasmonate) have been enhanced, and the growth-promoting hormones (auxin, cytokinins and gibberellins) have been decreased in plants (Montero-Palmero *et al.*, 2014a,b). This would result in the inhibition of growth and acceleration of stress responses in plants to sustain adverse situations. Moreover, this would ensure the plant to prepare for the revival of growth once the toxicity is reduced in the environment (Nguyen *et al.*, 2020).

According to Wang *et al.* (2015a), heavy metal exposure resulted in alterations in the expression levels in auxin homeostasis genes of *Arabidopsis thaliana* seedlings, and these differential transcriptional changes can adjust the location and effective accumulation of auxin within the plant for improved adaptation and survival in a hostile environment. The antagonistic effects of cytokinin and abscisic acid during stress exposure resulted in the enhanced tolerance to stress by regulating the stomatal aperture and increasing the apical dominance (O'Brien and Benková, 2013; Fahad *et al.*, 2015). Khan *et al.* (2016) reported that ethylene could potentiate the sulfur mediated reversal of heavy metal-induced inhibited growth responses in *Brassica juncea* exposed to Cd, which was resulted from the efficient production of thiols and the thiol-mediated protection of photosynthetic apparatus.

2.9.2. Roles in photosynthesis

Phytohormones play crucial roles in the photoprotection of photosynthetic apparatus during stress situations. Reduced photosynthesis during metal stress resulted in the excess excitation energy in chloroplasts (Asada, 2006). However, plants have several innate photoprotection mechanisms such as production and scavenging of singlet oxygen, excess energy dissipation through xanthophylls cycle, activation of the water-water cycle and enhanced photorespiration, which enable them to respond to stresses and protect the photosynthetic apparatus (Triantaphylidès and Havaux, 2009; García-Plazaola *et al.*, 2012; Huang *et al.*, 2019; Shi *et al.*, 2022). The crosstalk between this redox signaling with phytohormones in the modulation of photosynthesis and photoprotection and regulation of production and scavenging of ROS during various abiotic stresses has been reviewed in detail by Müller and Munné-Bosch (2021).

Though research related to endogenous phytohormone-mediated alleviation of drought and salinity stress-induced photosynthetic damages is

available, only limited works have been focused on the direct role of endogenous phytohormones in alleviating the heavy metal mediated photosynthetic damages. But, the roles of various phytohormones in alleviating the photosynthetic damages induced by heavy metals have been studied in detail by exogenous application of phytohormones or by transgenic approaches. Exogenous application of various phytohormones such as cytokinins, auxins, ethylene, ABA, brassinosteroids and jasmonic acid effectively modulated the heavy metal-induced photosynthetic damages in plants (Maksymiec and Krupa, 2002; Janeczko *et al.*, 2005; Ouzounidou and Ilias, 2005; Hayat *et al.*, 2007; Ali *et al.*, 2008; Masood *et al.*, 2012; Ahammed *et al.*, 2013; Khan and Khan, 2014; Gururani *et al.*, 2015; Khan *et al.*, 2019). According to the observations of Khan and Khan (2014) and Khan *et al.* (2019), exogenous application of ethylene restored the photosynthesis and improved the net photosynthetic rate in *Brassica juncea* exposed to Zn stress through enhanced Rubisco, APX and GR activities, photosynthetic nitrogen use efficiency, efficient PSII activity, improved proline and glyoxylase system and nutrient homeostasis. The high-throughput microarray hybridization of miRNAs in As treated roots revealed that the complex networking of phytohormones, miRNAs and S in the plant system regulate the developmental and photosynthetic processes, uptake and assimilation of mineral elements, and phytohormone biosynthesis and functions in *Brassica juncea* under As toxicity (Srivastava *et al.*, 2013).

2.9.3. Roles in oxidative stress response

Heavy metal stress leads to disturbances in the cellular homeostasis and accumulation of ROS, which in turn results in enhanced oxidative stress in plants (AbdElgawad *et al.*, 2020). Therefore, the signal processes involved in the perception and homeostatic adjustment of plants to heavy metals may be mediated through hormone signaling (Hernández *et al.*, 2012; Bucker-Neto

et al., 2017). The crosstalk between ethylene and cellular redox signaling alleviates oxidative stress in plants has been reviewed in detail by Keunen *et al.* (2016). Zhang *et al.* (2014) revealed that ethylene and salicylic acid have been involved in heavy metal stress responses of *Arabidopsis*. Similarly, ABA treatment alleviated Cd toxicity in *Brassica campestris*, by modulating effective scavenging of ROS through activation of antioxidant enzymes (Shen *et al.*, 2017). The activation of the antioxidant defence system in *Acutodesmus obliquus* exposed to Pb stress was observed by exogenous application of auxin and cytokinins, which helps the cells in reducing Pb-induced oxidative stress (Piotrowska-Niczyporuk *et al.*, 2018).

The early transcriptional analysis of *Medicago sativa* towards Hg stress using oligonucleotide microarrays revealed that a large number of ethylene-responsive genes were differentially expressed, which were complementary to the stress indices such as accumulation of MDA and H_2O_2, root growth inhibition and activity of NADPH-oxidase activity (Montero-Palmero *et al.*, 2014a,b). Krishnamurthy and Rathinasabapathi (2013) reported that auxin transporter mutants of *Arabidopsis thaliana* were much more sensitive to As stress than the wild type due to elevated accumulation of ROS. Similarly, the application of auxin transport inhibitors significantly reduced the As tolerance in wild type *A. thaliana*. However, exogenous application of indole-3-acetic acid (IAA) improved the As tolerance in these mutant plants, suggesting the role played by auxin in stress-induced ROS signaling.

2.9.4. Roles in heavy metal accumulation

Along with the activation of antioxidative defence mechanisms, the application of phytohormones to plants alleviate the heavy metal toxicity by reducing the root metal uptake and translocation *via* the modulation of the expression and activities of heavy metal transporters (Koç *et al.*, 2013; Rizwan *et al.*, 2017). Fan *et al.* (2014) reported the ABA-mediated reduction of Cd uptake by the roots of *Arabidopsis* plants. The authors observed that exogenous ABA inhibited the gene expression of iron-regulated transporter 1

(IRT1, a broad spectrum divalent transporter) in the roots, which in turn resulted in the reduced uptake of Cd in wild type *Arabidopsis* roots. It was also noticed that Cd uptake in *irt1* mutants was least affected on the application of ABA (Fan *et al.*, 2014). Similarly, Kamran *et al.* (2021) observed that application of BAP alone or in combination with ABA reduced the Co phytotoxicity in *Solanum lycopersicum* by minimizing the uptake, translocation and bioaccumulation of Co.

In contrast to the above observations, the involvement of phytohormones in the activation of heavy metal transporters was observed by various authors (Chen *et al.*, 2020a; Piotrowska-Niczyporuk *et al.*, 2020). Zhou *et al.* (2019) reported that application of *trans*-zeatin riboside (a cytokinin) increased the resistance of *Kosteletzkya pentacarpos* towards the Cd and Zn by increasing the accumulation of endogenous hormones such as cytokinin, auxin and salicylic acid, reducing the accumulation of ABA and jasmonic acid, enhancing the activities of antioxidant system and accumulation of phytochelatins. And all of these contribute towards the enhanced uptake and accumulation of Cd and Zn. ABA-mediated enhanced uptake, vascular loading and translocation of Pb was observed in *Populus* × *canescens*, by stimulating the transcription of genes involved in metal uptake such as natural resistance-associated macrophage protein 1.4 (*NRAMP1.4*), ATP-binding cassette transporters (*ABCG40* and *ABCC1.1*), ferric reductase defective protein 3.1 (*FRD3.1*), and phytochelatin synthetase 1.1 (*PCS1.1*) (Shi *et al.*, 2019).

2.10. Strategies for the enhancement of metal bioavailability and stress tolerance in plants

The uptake of metal ions by the roots is a highly complex process involving the transfer of metal from soil sap into the root cells. There are different strategies in use to enhance the heavy metal stress tolerance potential

of the plants or to enhance the bioavailability of the metals. Some of them are detailed below.

2.10.1. Application of soil amendments

For solubilizing the complex metal ions present in the soil, several soil amendment practices are applied, which will contribute to the increased phytoremediation potential of the plants. Recently, the applications of citric acid and EDTA, as well as the inoculation of plant growth-promoting rhizobacteria (PGPR) and endophytes, have been efficiently utilized to improve phytoremediation (Zhang *et al.*, 2015; Saxena *et al.*, 2020). The use of biodegradable metal chelating agents and micronutrients to the polluted lands can help the plants to enhance the root metal uptake. Citric acid-mediated enhancement in the phytoremediation potential of the biofuel plant *Salix* by increasing metal bioavailability and mobility was observed by Arsenov *et al.* (2020). Therefore, the metal accumulation potential of the non-accumulating bioenergy plants can be increased by using soil amendment practices. PGPR also promotes the growth of accumulator plants and is a cost-effective strategy for environmental clean-up (He *et al.*, 2020b). The PGPR produces siderophores, amino acids, proteins and 1-aminocyclopropane-1-carboxylate (ACC) deaminase, which improves the metal phytoextraction potential (He *et al.*, 2013; Sharma and Archana, 2016; Rosier *et al.*, 2018). The inoculation of PGPR has recently been demonstrated to improve heavy metal accumulation potential in accumulator plants, including bioenergy plants (Asad *et al.*, 2019).

Exogenous application of citric acid, oxalic acid and ethylenediamine disuccinate to the soils polluted with Cd and uranium improves the mobilization of these metals to the plant system (Chen *et al.*, 2020b). Similarly, the use of abscisic acid (ABA) and ABA-catabolizing bacteria effectively increase the metal bioavailability and uptake in hyperaccumulator

plants (Lu *et al.*, 2019). On the contrary to these results, Kuziemska *et al.* (2021) reported that application of organic amendments such as cattle and chicken manure and spent mushroom substrate reduced the toxic effects of Cu in *Dactylis glomerata* plants by reducing Cu uptake, which may be associated with the immobilization of the metals in the soil.

Abdel Latef and colleagues studied the potential of two PGPR (*Paenibacillus polymyxa* and *Bacillus circulans*) to mitigate Cu stress in maize seedlings. They pre-soaked maize seeds in the bacterial inoculum, and the seeds with uniformly surface coated with bacterial strains were grown in soils artificially contaminated by Cu. The result revealed that PGPR inoculation alleviated Cu-induced reduction of growth, photosynthesis and uptake of nutrients, along with the regulation of osmolytes and antioxidants (Abdel Latef *et al.*, 2020).

2.10.2. Seed priming for mitigation of metal toxicity

Numerous seed priming methods have been developed in recent years to counteract the toxic and detrimental effects of heavy metals in crop plants and agricultural systems (Prajapati *et al.*, 2020). Seed priming is a pre-sowing treatment that permits dormancy to be broken, resulting in increased germination rate and uniformity by regulating seed hydration and activating several metabolic pathways prior to the radical protrusion in order to initiate germination metabolism (van Hulten *et al.*, 2006; Jisha *et al.*, 2013). There are several seed priming methods based on the priming agents: hormonal, chemical, hydro-, bio-, and nano-primings. By enhancing the seedling vigor, seed priming ensure healthy and productive plants under adverse growth conditions (Rhaman *et al.*, 2021).

Priming of wheat seeds with indole-3-acetic acid and spermidine alleviated the adverse effects of Cu stress in wheat seedlings by enhancing the

growth, accumulation of osmoprotectants, the activity of the antioxidant system and by improving the stem tissue structure, including increased thickness of the epidermis, the diameter of parenchyma cells and xylem vessels (Agami, 2016). Similarly, the pre-treatment of *Cajanus cajan* seeds with methyl jasmonate mitigated Cu and Cd toxicity in the seedlings by increased synthesis of proline, AsA and GSH, thus improving the redox status (Kaushik *et al.*, 2021). Combined pre-treatment of Indian mustard seeds with 24-epibrassinolide and salicylic acid played an imperative role in alleviating Pb toxicity by reducing the oxidative stress *via* modulation of antioxidant systems (Kohli *et al.*, 2018).

2.10.3. Exogenous application of hormones for enhanced metal tolerance

Generally, endogenous phytohormones trigger various signal transduction pathways in plants under abiotic stress conditions (Ku *et al.*, 2018). Foliar application of hormones has been shown to boost plant tolerance to heavy metals (Bücker-Neto *et al.*, 2017; Sytar *et al.*, 2019; Saini *et al.*, 2021). They play a pivotal role in protecting plants from heavy metal toxicity by triggering diverse defence-related pathways. The hormones such as auxins, cytokinins, abscisic acid, ethylene, gibberellic acid, salicylic acid, brassinosteroids, methyl jasmonates *etc*., were shown to be involved in heavy metal tolerance in plants (Saini *et al.*, 2021).

Exogenous indole acetic acid and gibberellic acid alleviated Mn and Cr toxicity in pea seedlings by reducing oxidative stress (Gangwar *et al.*, 2011a,b). Similarly, kinetin-mediated Cd tolerance and enhanced PSII efficiency were observed in *Trigonella* seedlings, which have arisen from the up-regulation of the AsA-GSH cycle (Bashri *et al.*, 2021). Shi *et al.* (2019) reported that exogenous application of abscisic acid stimulated the metal uptake and vascular loading in the roots, reduced ROS production and

enhanced photosynthesis in poplar plants subjected to Pb stress by up-regulating the genes involved in metal tolerance.

Foliar application of salicylic acid reduced the metal translocation and enhanced the biomass accumulation in wheat plants exposed to Zn stress (Stanislawska-Glubiak and Korzeniowska, 2022). According to Bukhari *et al.* (2016), foliar application of 24-epibrassinolide enhanced the photosynthetic performance, reduced the oxidative stress and metal bioaccumulation and regulated ion homeostasis in tobacco seedlings exposed to Cr stress. Similarly, foliar application of 24-epibrassinolide and 28-homobrassinolide effectively alleviated Zn toxicity in radish plants by enhancing the photosynthetic pigment composition, accumulation of antioxidants and activation of nitrate reductase and antioxidant enzymes (Ramakrishna and Rao, 2015). Table 3 represents the list of phytohormones involved in heavy metal stress tolerance in various plants.

2.10.4. Exogenous application of compounds other than plant hormones in metal stress tolerance

Similar to phytohormones, exogenous application of various other compounds such as proline, melatonin, nitric oxides and nutrients elements such as boron, silicon, Zn, *etc*., was found to be involved in heavy metal stress tolerance in plants. For example, exogenous application of melatonin was found to be involved in Cu stress amelioration in cucumber plants through activation of ROS scavenging, enhanced production of GSH and PCs, and improved Cu sequestration and nutrient element distribution *via* changing the levels of gene expression involved in metal tolerance (Cao *et al.*, 2019).

Mineral nutrient availability influences metabolic, physiological, and developmental processes in plants. They influence the biosynthesis of plant hormones for the enhanced tolerance to abiotic stresses. For example, soil

supplementation of P in the form of diammonium phosphate mitigated As stress in *Brassica juncea* by enhanced nitric oxide (NO) generation, which in turn up-regulated AsA-GSH system, proline metabolism and glyoxylase system, and alleviated the effects of As on photosynthesis and reduced the As translocation (Khan *et al.*, 2021). Similarly, application of P in the form of grounded calcium dihydrogen phosphate [$Ca(H_2PO_4)2H_2O$] to Cu-stressed grapevine grown in rhizobox alleviated Cu toxicity by enhancing the lateral root proliferation, growth of root and shoot, biomass accumulation, and better acquisition of nutrients such as P, K, Zn and Fe (Baldi *et al.*, 2018).

Similarly, the application of metal nanoparticles has been proved to be involved in heavy metal stress tolerance in plants. According to Faizan *et al.* (2021), the foliar fertigation of zinc nanoparticles along with salicylic acid ameliorates the As-induced oxidative stress in rice plants by modulating the antioxidant system.

2.10.5. Transgenic approaches for enhanced heavy metal uptake

For the efficient phytoremediation of contaminated lands, it is important to enhance the phytostabilization and/or phytoextraction potential of the plants. Recently, the genetic transformation of plants has been used as an efficient strategy for the enhanced phytoremediation of metal contaminated lands (Koźmińska *et al.*, 2018). Transgenic approaches are the precise and advanced technology that introduces or over-expresses genes involved in heavy metal absorption, translocation, and sequestration processes in plants to improve phytoremediation potential (Mani and Kumar, 2014; Das *et al.*, 2016). Genetic manipulations in hyperaccumulator plants with a slow growth rate and less biomass can also be utilized to improve biomass accumulation and phytoextraction (Saxena *et al.*, 2020). The knock-down or over-expression of genes involved in the synthesis of phytochelatins and

metallothioneins can specifically contribute to the enhanced chelation and sequestration of toxic metal ions in plants.

Over-expression of a novel *Streptococcus thermophilus*-γ-glutamylcysteine synthetase-glutathione synthetase (StGCS-GS) synthesizes GSH with limited feedback inhibition in *Beta vulgaris* resulting in three transgenic lines with enhanced tolerance to different concentrations of Cd, Cu and Zn (Liu *et al.*, 2015). These transgenic sugar beet over-produces GSH and PCs, which in turn results in greater accumulation of the metals. Similar genome editing and transformation studies in various plants for enhanced phytoextraction were reviewed by Venegas-Rioseco *et al.* (2022).

Table 1. Non-edible plants showing phytoremediation potential under different heavy metal/metalloid stresses.

Plant species	Growth conditions	Heavy metals/metalloids in medium	Metal concentration in the plant parts (µg/g DW)		Promising benefits	References
			Root	Shoot		
Arundo donax (Giant reed)	As_2O_3 in Hoagland solution	As (1000g/L)	121	615.61	a) Bioethanol and biogas b) Eco-restoration c) Maximum CO_2 uptake of 37 µmol $m^{-2}s^{-1}$	Mirza *et al.*, 2011; Elhawat *et al.*, 2014; Barbosa *et al.*, 2015; D'Imporzano *et al.*, 2018
	Soil treatment with sludge contamination	Cr (600 ppm)	34±17	13±4		
		Pb (900 ppm)	34±7	6.6±1.1		
		Zn (900 ppm)	118±32	116±29		
	$CuSO_4.5H_2O$ in nutrient solution	Cu (26.8 mg/L)	76.57	47.72		
Cannabis sativa (Hemp)	$CdCl_2.2.5H_2O$ in acid-washed sand and perlite (5:4)	Cd (200 ppm)	4052.8±225.6	101.5±8	a) Biodiesel and bioethanol b) Soil regeneration, c) CO_2 uptake of 20 tons ha^{-1}	Shi and Cai, 2009a,2010; Jasinskas *et al.*, 2020
	$ZnSO_4.7H_2O$ in acid-washed sand and perlite (5:4)	Zn (800 ppm)	5029±138.3	657.5±35.5		
Cynara cardunculus (Cardoon)	Soil treatment with As and Cd	As (6.5 mM)	400	300	a) Carbon sequestration b) 30-40% hexose containing polysaccharides for bioethanol production	Leonardi *et al.*, 2016; Fernandes *et al.*, 2018
		Cd (13 mM)	150	25		
Festuca rubra (Red fescue)	Soil treatment with $CdCl_2$	Cd (120 ppm)	3277	266	a) Biofuel b) 3.35 Mg C ha^{-1} yr^{-1} of soil organic carbon	Qian *et al.*, 2010; Gołda and Korzeniowska, 2016

(*Continued*)

Table 1. (*Continued*)

Plant species	Growth conditions	Heavy metals/metalloids in medium	Metal concentration in the plant parts (µg/g DW)		Promising benefits	References
			Root	Shoot		
Hibiscus cannabinus (Kenaf)	Contaminated soil	Cd	-	2.49	a) Bioethanol b) biodiesel and biogas c) biochar yield of 30% wt	Arbaoui *et al.*, 2013; Khiari *et al.*, 2020
		Zn	-	82.5		
Jatropha curcas (Physic nut)	Contaminated soil	Cd	3.86±0.25	14.25±1.78	a) Biodiesel b) Eco-restoration c) Seed contains 30-50% of oil	Chang *et al.*, 2014
		Cr	29.08±8.67	33.4±7.54		
		Ni	16.45±2.47	45.05±10.46		
		Zn	57.6±4.1	195.33±14.04		
		Cu	37.51±2.31	53.58±4.8		
Miscanthus floridulus (Giant Chinese silver grass)	$CdCl_2$ in Hoagland solution	Cd (200µM)	6000	500	a) Biofuel b) Increase soil organic carbon	Barbosa *et al.*, 2015; Guo *et al.*, 2016
	Industrial sludge containing 3.5 % Zn	Zn	154±53	114±42		
Miscanthus giganteus (Silver grass)	Industrial sludge containing 3.5 % Zn	Zn	197±49	143±20	a) Biofuel, contributing 10% of bioenergy b) carbon sequestration of 2 Mg C ha^{-1}	Barbosa *et al.*, 2015; Nakajima *et al.*, 2018
Miscanthus sinensis (Elephant grass)	Industrial sludge containing 3.5 % Zn	Zn	181±32	172±66	a) Biofuel b) Carbon sequestration of 1 Mg C ha^{-1}	Barbosa *et al.*, 2015; Nakajima *et al.*, 2018

(*Continued*)

Table 1. (*Continued*)

Plant species	Growth conditions	Heavy metals/metalloids in medium	Metal concentration in the plant parts (µg/g DW)		Promising benefits	References
			Root	Shoot		
Miscanthus sacchariflorus (Amur silver-grass)	$CdCl_2$ in Hoagland solution	Cd (200µM)	4000	80	a) Biofuel b) Improve soil quality	Guo *et al.*, 2016
Populus deltoids (Poplar)	$Zn(NO_3)_2.6H_2O$ in Hoagland solution	Zn (1 mM)	3229±598	1007±209.6	a) Biofuel b) Carbon sequestration	Stoláriková *et al.*, 2015
Ricinus communis (Castor)	$Na_2HAsO_4.7H_2O$ in Hoagland solution	As (200 µM)	17.31±1.32	2.87±0.23	a) 149.6 g biodiesel kg^{-1} castor b) 30.1 g bioethanol kg^{-1} castor c) soil reclamation	Shi and Cai, 2009a,2010; Bateni and Karimi, 2016; Singh *et al.*, 2019
	$CdCl_2.2.5H_2O$ and $ZnSO_4.7H_2O$ in acid-washed sand and perlite (5:4)	Cd (200 ppm)	2517.9±178.7	59.8±7.5		
		Zn (800 ppm)	2779±27	915±26		
Salix alba (Willow)	$Na_2HAsO_4.7H_2O$ in Hoagland solution	As (250 µM)	5000	65	a) Biofuel b) Carbon sequestration of 1Mg ha^{-1} y^{-1} C	Purdy and Smart, 2008; Milan *et al.*, 2012; Niksa *et al.*, 2020
	Soil treatment with $CdCl_2.H_2O$	Cd (4.68 ppm)	104.4±11.4	24.1±4.8		
Thlaspi caerulescens (Alpine penny-cress)	Metalliferrous habitat	Cd	80	19.1	a) Biofuel b) Eco-restoration	Banásová *et al.*, 2008
		Cu	21	30		
		Pb	528	3		
		Zn	5869	19410		

Table 2. Earlier reports on the potential of *R. communis* for heavy metal phytoremediation.

Metals/ metalloids	Concentration of metal in the growing medium	Experiment type and exposure time	Major outcome	References
As	100 and 200 µM $Na_2HAsO_4.7H_2O$	Vermiculite irrigated with Hoagland nutrient solution with 28 days of As exposure	➢ Enhanced stomatal conductance, water use efficiency and photosynthesis. ➢ Enhanced activity of SOD, POD and GR, and regulation of GSH/GSSH ratio. ➢ Hence efficient ROS scavenging and thereby reduced MDA and As accumulation. ➢ Over-expression of nicotianamine synthase genes leading to enhanced chelation and transport of essential metals and enhanced As tolerance.	Singh *et al.*, 2019,2021a,b,c
Cu	100, 250, 500 and 750 µmol/L $CuSO_4.5H_2O$	Hydroponic experiment with 10 days of Cu exposure	➢ Enhanced organic and amino acids composition in the root exudates. ➢ High Cu phytoextraction capacity. ➢ Tolerance mechanisms were further enhanced by application of P fertilizers.	Huang *et al.*, 2016,2018
Cu	5, 10, 20, 40, 60, 80 and 100 mg/L $CuSO_4$	Hydroponic experiment with 20 days of Cu exposure	➢ Enhanced Cu bioaccumulation ➢ Thickened root cell walls, with large amount of high density electron bodies. ➢ Root cell walls acted as the major location for Cu detoxification.	Kang *et al.*, 2015

(*Continued*)

Table 2. (*Continued*)

Metals/ metalloids	Concentration of metal in the growing medium	Experiment type and exposure time	Major outcome	References
Cd	25, 50, 75, 100 and 150 mg Cd/kg soil	Pot experiments with 30, 60 and 90 days of Cd exposure	➢ Enhanced accumulation of proline, and enhanced antioxidant enzyme activities such as POD, CAT, APX, SOD and GR. ➢ Low shoot and high root metal concentrations, large amount of underground and aerial biomass, higher metal removal and tolerance efficiency, and low metal translocation factor. ➢ Accumulation of metal was further enhanced by application of organic and inorganic amendments.	Bauddh and Singh, 2012a,b, 2014; Bauddh *et al.*, 2015a,b,2016
Cd	50 ppm $(CH_3COO)_2Cd.2H_2O$	Pot experiments with 6 h of Cd exposure	➢ Enhanced expression of C-repeat binding factor/dehydration responsive element binding genes (DREB-1B, DREB-1F and CBF). ➢ Significant positive correlation of Cd accumulation, proline and phenolics content with the expression of these genes. ➢ Gene expression was further enhanced by foliar application of Mo.	Ali and Hadi, 2018
Ni	0.05, 0.1 and 0.2 mM $NiCl_2$	Hydroponic experiment with 14 days of Ni exposure	➢ Enhanced expression levels of stress responsive genes. ➢ Enhanced primary and secondary metabolism.	Çelik and Akdaş, 2019
Pb	100, 200 and 500 µM $Pb(NO_3)_2$	Hydroponic experiment with 12 days of Pb exposure	➢ Enhanced activity of CAT. ➢ Increased starch grains in the chloroplasts. ➢ About 5% of Pb accumulated in the roots, suggested the role of this plant in rhizofiltration of Pb contaminated water.	Khan *et al.*, 2018

(*Continued*)

Table 2. (*Continued*)

Metals/ metalloids	Concentration of metal in the growing medium	Experiment type and exposure time	Major outcome	References
Cd and Zn	25 mg $CdCl_2.2H_2O$/kg and 380 mg $ZnCl_2.2H_2O$/kg	Pot experiments with 19 days of metal exposure	➢ Cell wall played important role in Cd and Zn sequestration within the root itself. ➢ Cd (51-69%) and Zn (40-62%) mainly accumulated in the cell wall of the root.	He *et al.*, 2020a
Cd and Zn	1,5,10,20, and 40 mg $CdCl_2.2.5\ H_2O$/kg 100,200,400,600, and 800 mg $ZnCl_2$/kg	Pot experiment with 4 months of metal exposure	➢ Higher tolerance to the metal with enhanced translocation efficiency. ➢ Produced high biomass.	Wang *et al.*, 2016a
Cd, Fe, Mn, Pb and Zn	5.6-162 mg Cd/kg; 1672-2166 mg Fe/kg; 173-207 mg Mn/kg; 120-1152 mg Pb/kg; 158-325 mg Zn/kg	Plants grown in industrial waste contaminated sites in peri-urban Greater Hyderabad	➢ The trend of metal accumulation was Fe > Zn > Mn > Pb > Cd, with greater translocation of Cd and Pb. ➢ Reduced chlorophyll and protein contents, while increased proline and MDA contents due to its metal tolerance. ➢ Higher amount of ricinoleic acid in the seed. ➢ Fatty acid composition of seeds of plants grown in polluted areas was almost similar to that of the control. ➢ Therefore, efficiently employed for reclamation of heavy metal contaminated soils.	Boda *et al.*, 2017
Cu, Cr, Pb and Zn	309±12 mg Cu/kg; 1010±23 mg Cr/kg; 488±10 mg Pb/kg; 1023±36 mg Zn/kg	Pot experiment with dredged sediment from river near to industrialized area	➢ Increased rate of phytoextraction. ➢ Addition of chelators such as EDTA, NTA, and citric acid enhanced the phytostabilization	Fuentes *et al.*, 2018
Cd, Ni, Pb and Zn	0.36±0.08 mg Cd/kg; 5.00±0.95 mg Ni/kg; 3.45±0.85 mg Pb/kg; 117.6±12.7 mg Zn/kg	Plants grown under roadside air pollution	➢ Minimal reduction in transpiration rate and stomatal conductance. ➢ Elevated internal CO_2 concentration and water use efficiency. ➢ Increased total antioxidant activity and amino acids content.	Khalid *et al.*, 2019

Table 3. Phytohormone-mediated enhanced heavy metal tolerance in various plants.

Plants	Heavy metals	Phytohormones	Mode of hormone application	Remarks	References
Arabidopsis thaliana	As	Indole-3-acetic acid	Pre-treatment in the growing medium	➢ Improved As(III) tolerance in *aux1* (Auxin Transporter mutant) seedlings. ➢ Demonstrated the key role of transport and signaling of auxin in regulating root growth and metal tolerance.	Krishnamurthy and Rathinasabapathi, 2013
Brassica juncea	Pb	24-epibrassinolide and salicylic acid	Seed priming	➢ Enhanced dry matter content, osmolytes and heavy metal tolerance index. ➢ Mitigated the adverse effects of metal stress by up-regulation of antioxidant genes and modulation of antioxidative defense response.	Kohli *et al.*, 2018
Hordeum vulgare	Cd and Mo	Gibberellic acid	Applied in the germination medium	➢ Reduced the inhibitory effects on hydrolytic enzymes during seed germination, thereby enhanced the mobilization of starch and protein in the endosperm. ➢ Alleviated the negative effects of Cd and Mo stress	Amri *et al.*, 2016
Pisum sativum	Mn	Indole acetic acid	Applied in the growing nutrient medium	➢ Reduced H_2O_2 levels and MDA content ➢ Increased antioxidant enzymes activities, promoted growth and alleviated Mn toxicity.	Gangwar *et al.*, 2011a
Pisum sativum	Cr	Gibberellic acid	Applied in the growing nutrient medium	➢ Increased levels of antioxidants counteract adverse effects of Cr toxicity. ➢ Sustained activities of enzymes involved in nitrogen assimilation.	Gangwar *et al.*, 2011b

(*Continued*)

Table 3. (*Continued*)

Plants	Heavy metals	Phytohormones	Mode of hormone application	Remarks	References
Populus×canescens	Pb	Abscisic acid	Applied in the growing nutrient medium	➢ Stimulated expression levels of genes involved in metal uptake, transport and detoxification. ➢ Enhanced Pb uptake, reduced Pb deposition in the cortex and enhanced Pb vascular loading in the roots.	Shi *et al.*, 2019
Solanum lycopersicum	Co	6-benzylaminopurine and abscisic acid	Applied in the growing nutrient medium	➢ Activation of morpho-physiological and antioxidative defense responses. ➢ Increased plant biomass by alleviating Co-induced phytotoxicity. ➢ Minimizing Co uptake, translocation and consequently bioaccumulation.	Kamran *et al.*, 2021
Solanum lycopersicum	Cd	Kinetin	Foliar application	➢ Alleviated the negative effects of Cd on the fresh mass and lowered the ROS level by positively affecting PSII photochemistry and further rise in AsA-GSH cycle enzymes and their metabolites.	Singh *et al.*, 2018
Trigonella foenum-graecum	Cd	Kinetin	Foliar application	➢ Restoration of carbonic anhydrase activity. ➢ Enhanced the ratio of AsA/DHA and GSH/GSSG. ➢ Maintained the redox status of cells.	Bashri *et al.*, 2021
Triticum aestivum	Zn	Salicylic acid	Foliar application	➢ Higher biomass production and yield. ➢ Reduced Zn translocation and alleviation of Zn phytotoxicity	Stanislawska-Glubiak and Korzeniowska, 2022
Zea mays	Cd	Indole-3-butyric acid	Applied in the growing nutrient medium	➢ Decreased the concentration of H_2O_2 ➢ Improved the uptake of essential nutrients and growth, and alleviated Cd toxicity.	Šípošová *et al.*, 2021

MATERIALS AND METHODS

3.1. Materials

3.1.1. Collection of seeds

The seeds of castor (*Ricinus communis* L. var. TMV 5) were procured from Tapioca and Castor Research Station (TCRS), Tamil Nadu Agricultural University, Salem, India.

3.1.2. Chemicals

Analytical reagent (AR) or guaranteed reagent (GR) chemicals were purchased from Himedia, Merck, SRL, Qualigens and Spectrochem companies. Bovine serum albumin (BSA), riboflavin, glutaraldehyde, methyl viologen, 3-(3,4-dichlorophenyl)-1,1-dimethyl urea (DCMU), L-ascorbate, ascorbate oxidase, L-dehydroascorbic acid, kinetin and 6-benzylaminopurine were purchased from Sigma-Aldrich Co., USA.

3.2. Preliminary screening for heavy metal concentrations in the soil and plant samples collected from the polluted lands with luxuriant growth of *R. communis*

Soil and plant samples were collected from five different locations in Kozhikode city limits (1-10 m away from roadsides), with luxuriant growth of *R. communis*. For soil sampling, five sub-samples of the top soil in the rhizosphere (0-5 cm) were collected from each site and mixed thoroughly to get a representative sample. The root and leaf samples of *R. communis* were also collected from the same locations, in which five sub-samples were taken and mixed to get a representative sample. The leaf and root samples were washed thoroughly in running tap water to remove adherent soil particles and dust.

The soil, root and leaf samples were dried in an oven at 100°C for 1 h, followed by 60°C until a constant weight was achieved. From the samples, 1 g of each was transferred into Kjeldahl flasks, and then digested by refluxing in HNO_3 using a heating mantle at 60°C until the solution became colorless. Subsequently, the digest was filtered using Whatman's filter paper, transferred to a standard flask, and volume was made up to 50 ml with distilled water. The concentrations of various heavy metals in the samples were determined using inductively coupled plasma mass spectrometry (ICPMS, Agilent 7800, Santa Clara, United States).

3.3. Composition and preparation of Hoagland nutrient solution

Hoagland nutrient solution was used for the hydroponic culture studies (Hoagland and Arnon, 1950). For the efficient growth of *R. communis* seedlings in the nutrient medium, phosphate and sulphate in the standard Hoagland medium was replaced with chloride and nitrate respectively according to Kiran and Prasad (2017) (Table 4).

Table 4. Composition of modified Hoagland nutrient solution used in the study.

Compounds		Molecular weight	Concentration of stock solution		Volume of stock/L of final solution
		g/mol	mM	g/L	mL
Macronutrients	KNO_3	101.10	1000	101.0	6.0
	$Ca(NO_3)_2.4H_2O$	236.16	1000	236.16	4.0
	NH_4Cl	53.49	1000	53.49	2.0
	$Mg(NO_3)_2.6H_2O$	256.41	1000	256.41	1.0
Micronutrients	KCl	74.55	25	1.864	2.0
	H_3BO_3	61.83	12.5	0.773	
	$ZnSO_4.7H_2O$	287.54	1.0	0.288	
	$MnSO_4.H_2O$	169.01	1.0	0.169	
	$CuSO_4.5H_2O$	249.68	0.25	0.062	
	H_2MoO_4	161.97	0.25	0.04	
	NaFeEDTA	558.50	53.7	30.0	0.3

The stock solution of each nutrient was prepared separately just before use, from which an appropriate volume of each was mixed together to make up the final volume and concentration of the nutrient solution. The pH of the solution was adjusted to 6.8 using 0.1 N HCl or 0.1 N NaOH.

3.4. Experimental set-up

Seeds of castor were surface sterilized with 0.1% $HgCl_2$ solution for 10 min and further washed thoroughly with distilled water. The seeds were germinated in paper cups filled with sterilized sand (The sterilized sand was prepared by solarization, *i.e.*, mulching the sand with a transparent polyethylene cover to trap solar energy, which causes physical, chemical, and biological changes in the soil, thereby decontamination of the sand from soil-borne pathogens, insects and mites were achieved). Ten days old seedlings were transferred into glass bottles (9 × 5 cm, 120 mL) filled with quarter strength modified Hoagland media. The nutrient media was replaced every 3 d toensure a fresh supply of nutrient elements and also to avoidalgal growth. Plants were maintained in greenhouse under controlled conditions of temperature (25 ± 5°C), light intensity (12 h daylight in the range of 28-600 μmol/m^2/s), and relative humidity (60 ± 2%) (Fig. 1).

3.4.1. Determination of $CuSO_4$ concentration at which plants exhibit highest level of tolerance

Ricinus communis seedlings with 30 d of growth period were treated with varying concentrations of $CuSO_4$ (0, 40, 80, 120, 160, 200, 240 and 280 μM), prepared in quarter strength modified Hoagland nutrient medium. The phenotypic changes and toxicity symptoms observed in the seedlings due to excess Cu were analyzed.

3.4.2. Treatment with $CuSO_4$ solution

The *R. communis* seedlings with a growth period of 30 d (after complete emergence of the first pair of primary leaves) were treated with varying concentrations of $CuSO_4$ solution (40, 80, 120, 160 and 200 μM) prepared in quarter strength modified Hoagland nutrient medium for 10 d. The plants growing in quarter strength Hoagland solution were taken as the control plants. Various physiological, biochemical and anatomical parameters were analyzed in the roots, cotyledonary and primary leaves on alternate days of $CuSO_4$ exposure up to 10 d. In the case of cotyledonary leaves, the abscission occurs after 6 d at higher Cu concentrations (120, 160 and 200 μM $CuSO_4$) and therefore, Cu toxicity symptoms and tolerance mechanisms were analyzed up to 6 d of treatment in the case of cotyledonary leaves.

3.4.3. Determination of effective concentration of cytokinins to analyze the Cu stress ameliorative effects in the cotyledonary leaves of *R. communis* seedlings

From the different concentrations of $CuSO_4$ analyzed, one mild and one severe stress concentrations (80 and 160 μM $CuSO_4$ respectively) were selected to determine the stress ameliorative effects of two different cytokinins [kinetin (KIN) and 6-benzylaminopurine (BAP)]. 80 and 160 μM $CuSO_4$ treated *R. communis* seedlings were subjected to treatment with 5, 10, 15, 20 and 25 μM KIN and BAP as foliar spray. The photosynthetic pigment composition and accumulation of malondialdehyde (MDA) content in the cotyledonary leaves on 6 d of exposure to $CuSO_4$ and cytokinins were analyzed to select the effective concentrations of KIN and BAP.

3.4.4. Treatment with kinetin (KIN) and 6-benzylaminopurine (BAP)

Stock solutions of kinetin (KIN) and 6-benzylaminopurine (BAP) were prepared in double-distilled water. The $CuSO_4$ treated seedlings (80 and 160

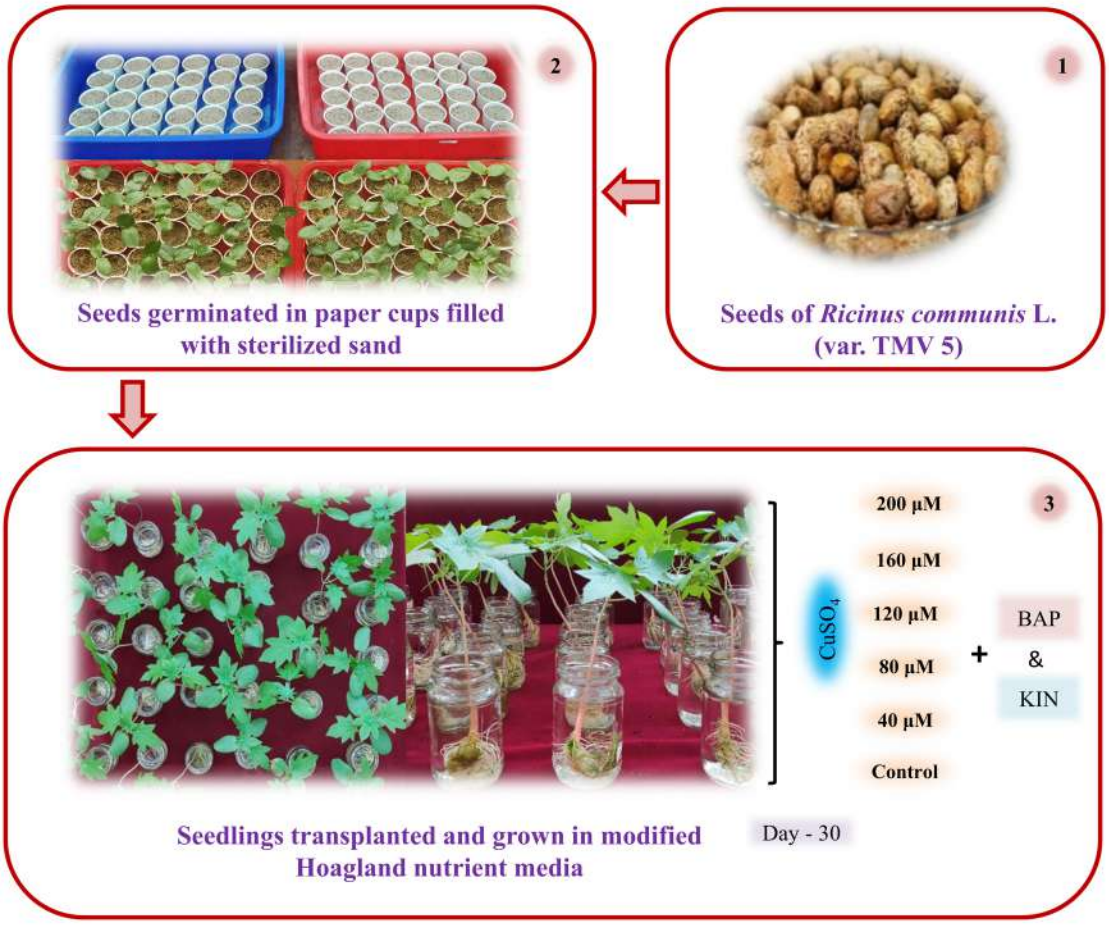

Figure 1. Experimental set-up

μM) were applied with 15 μM each of kinetin (KIN) and 6-benzylaminopurine (BAP), prepared in 0.1% teepol as the surfactant (5 mL per plant) (the selection of 15 μM as the most effective concentration for both KIN and BAP was based on a standardization study). The control plants were treated with 0.1% teepol prepared in water. The cotyledonary leaves were harvested on 6 d for further analysis.

3.5. Physiological parameters

3.5.1. Dry weight (DW) % and moisture content (MC) %

To determine the dry weight percentage (DW%) and moisture content percentage (MC%), the fresh weight of the samples were recorded and then oven-dried at 100°C for 1 h, followed by lowering the temperature of the oven to 60°C. The samples were re-weighed at regular intervals until the weights became constant. DW% and MC% were calculated by using the following equation,

$$\text{DW\%} = \frac{\text{Dry weight}}{\text{Fresh weight}} \times 100$$

$$\text{MC\%} = \frac{\text{Fresh weight} - \text{Dry weight}}{\text{Fresh weight}} \times 100$$

3.5.2. Relative water content (RWC)

The protocol proposed by Weatherley (1950) was used to determine relative water content (RWC). After determining the fresh weight, small pieces of the samples were immersed in distilled water and kept in the dark for 12 h. Consequently, leaves were blotted; turgid weight was measured, followed by the dry weight measurements, and RWC was calculated by the following equation,

$$\text{RWC} = \frac{\text{Fresh weight} - \text{Dry weight}}{\text{Turgid weight} - \text{Dry weight}} \times 100$$

3.5.3. Total chlorophyll and carotenoids contents

Leaf pigments such as total chlorophyll and carotenoid contents were estimated according to the methods of Arnon (1949) and Lichtenthaler and Wellburnn (1983) respectively. Fifty milligrams of fresh leaf sample was weighed using electronic balance and crushed in 80% acetone using pre-chilled mortar and pestle. The homogenate was centrifuged at 5000 rpm for 10 min at 4°C (Sorvall legend X1R, ThermoFisher Scientific, India) and the supernatant was collected. The residue was re-extracted with 80% acetone and centrifuged. The process was repeated until the pellet became colourless. The final volume of the pooled supernatant was noted, and the absorbance was recorded at 663, 646, 750 and 470 nm against the solvent blank (80% acetone) using UV-VIS spectrophotometer (Systronics 2201, Ahmedabad, India). Total chlorophyll (Chl *a*+*b*) and carotenoids present in the extract was calculated as micrograms chlorophyll and carotenoids per gram fresh weight using the following formula,

$$\text{Chlorophyll a + b} = \frac{20.12\,(A_{646} - A_{750}) + 8.02\,(A_{663} - A_{750})}{\text{Fresh weight of the sample}} \times \text{volume}$$

$$\text{Carotenoids} = \frac{1000\,(A_{470}) + 3.27\,(\text{Chl } a - \text{Chl } b)}{\text{Fresh weight of the sample} \times 229} \times \text{volume}$$

Where,

$$\text{Chlorophyll } a = \frac{12.69\,(A_{663} - A_{750}) - 2.69\,(A_{646} - A_{750})}{\text{Fresh weight of the sample}} \times \text{volume}$$

$$\text{Chlorophyll } b = \frac{22.9\,(A_{646} - A_{750}) - 4.68\,(A_{663} - A\,750)}{\text{Fresh weight of the sample}} \times \text{volume}$$

3.5.4. Photosystem (PS) I and II activities

Thylakoids from leaves were isolated according to Puthur (2000). The photochemical activities of the isolated thylakoids were assayed polarographically with a Clark-type oxygen electrode (DW1/AD, Hansatech, Norfolk, UK) which was connected to a digital control box (OXYG1, Hansatech) at 4°C. The light dependent O_2 uptake/evolution was measured by irradiating the sample with saturating intensity of white light (1800 µmol photons $m^{-2}s^{-1}$), provided by a 100W halogen lamp (LS2, Hansatech). The activities of PSI and PSII were expressed in terms of µmol of O_2 consumed (PSI)/evolved (PSII) min^{-1} mg^{-1} chlorophyll.

Isolation of thylakoids: 500 mg of fresh tissue was homogenized in 5 mL ice-cold isolation buffer (pH 7.8), containing 400 mM sucrose, 10 mM NaCl, and 20 mM tricine with pre-chilled mortar and pestle. The homogenate was filtered with 4 layered cheesecloth and then centrifuged at 4°C for 6 min at 5000 rpm. After centrifugation, the supernatant was discarded, and the pellet was suspended in 500 µM suspension buffer (pH 7.5), containing 100 mM sucrose, 10 mM NaCl, 20 mM HEPES [N(2-hydroxyethyl)piperazine-N-(2-ethanesulphonic acid)], and 2 mM $MgCl_2$. This thylakoid suspension was stored at 4°C and used to analyze thylakoid electron transport activities.

Estimation of chlorophyll content of thylakoid membranes: Chlorophyll content of the thylakoid samples was estimated according to the method of Arnon (1949). 40 µL of the thylakoid suspension was added to the test tube containing 3 mL of 80% acetone (v/v). The contents of the tubes were mixed thoroughly using a vortex mixer, and the homogenate was centrifuged at 5000 rpm for 5 min, and the supernatant was collected. The absorbance was measured at 645, 663 and 750 nm against the solvent blank (80% acetone). The total chlorophyll content of the thylakoids was calculated using the following equation,

$$Total\ chl = 20.12\ (A_{646}\text{-}A_{750}) + 8.02\ (A_{663}\text{-}A_{750}) \times Dilution\ factor$$

Analysis of thylakoid electron transport activities: For the measurement of PSI activity, stock solutions of 500 mM DCMU (3-(3,4-dichlorophenyl)-1,1-dimethylurea), 10 mM DCPIP (2,6-dichlorophenolindophenol), 500 mM ascorbate, 5 mM MV (methyl viologen) and 1 M NaN_3 were prepared. The 2 mL reaction mixture containing 20 µL each of DCMU, DCPIP, ascorbate and MV, 10 µL NaN_3, and 40 µL thylakoid extract was prepared in suspension buffer (pH 7.5). PSI activity was measured in terms of oxygen consumption by using DCPIP as an artificial electron donor and MV as an exogenous electron acceptor.

To measure PSII activity, a stock solution of 50 mM PBQ (p-benzoquinone) was prepared. The 2 mL reaction mixture containing 20 µL PBQ and 40 µL thylakoid extract was prepared in suspension buffer (pH 7.5). PSII activity was measured in terms of oxygen evolution using PBQ as an artificial electron acceptor.

The light dependent electron transport in the thylakoid membrane was blocked in certain steps by artificial electron acceptors and donors for estimating the PSI and PSII activities based on the O_2 uptake/evolution from/into the medium. For measuring PSI activity, PSII activity was blocked initially by adding DCMU to the medium. Electron transport to PSI was maintained by artificial electron donors, ascorbate and DCPIP in the medium, where ascorbate acted as reductant by donating electrons to DCPIP and further the electrons supplied by DCPIP to plastocyanin were transferred to PSI. Electrons from PSI were bypassed to an artificial electron acceptor, MV in the reaction mixture. MV reacts with O_2 molecules in the medium and produces H_2O_2. Further, the dissociation of H_2O_2 to form O_2 and H_2O by the action of catalase was arrested by NaN_3 added in the reaction mixture. Thus

the O_2 consumption by the activity of PSI alone was measured by the oxygen electrode system.

To measure the PSII activity, artificial electron acceptor PBQ was added to the medium, and it will scavenge the electrons from plastoquinone. The transfer of electrons from plastoquinone to cytochrome is terminated, so the activity of PSII alone was measured. Splitting of water for transferring of electrons to PSII results in evolution of oxygen molecules in the medium, and it was measured by oxygen electrode system.

3.5.5. Chlorophyll *a* fluorescence analysis

Chlorophyll *a* fluorescence measurements were carried out using Plant Efficiency Analyzer (Handy PEA, Hansatech Ltd., Norfolk, UK). The leaf samples were subjected to dark adaptation for 20 min using light exclusion clips attached to the leaf surface. Fluorescence measurements were recorded up to 1 s with a data acquisition rate of 10 µs for the first 2 ms and 1 ms thereafter, by illuminating with a continuous red light (3000 µmol photons m^{-2} s^{-1}, 650 nm) by an array of three light-emitting diodes, focused on a 5 mm diameter of the leaf surface. The data obtained from Handy PEA was analyzed with the help of Biolyzer software (Bioenergetics Laboratory, University of Geneva, Switzerland) (Strasser *et al.*, 2004). All the fluorescence parameters selected for the study are represented in Table 5.

Table 5. Explanations for various chlorophyll *a* fluorescence parameters used in the present study.

Parameters	Description
Phases in fluorescence induction curve	
O = Fo	Minimal fluorescence/first step of chl*a* fluorescence transient
J = Fj	Intermediate step in the chl*a* fluorescence transient at 30 ms
I = Fi	Intermediate step in the chl*a* fluorescence transient at 2 ms

P = Fm	Maximal fluorescence level/final step of chl *a* fluorescence transient
OJ-phase	Represents the reduction of the acceptor side of PSII
JI-phase	Represents the reduction of the PQ (plastoquinone) pool
IP-phase	Represents the reduction of the acceptor side PSI
Area	Area above the fluorescence induction curve
Tf(max)	Time taken to reach Fm
Other JIP parameters	
Fv = Fm - Fo	Maximal variable fluorescence
Fv/Fo	Maximum efficiency of water splitting complex
Fv/Fm	Capturing and conversion efficiency of harvested light energy or maximum quantum yield of PSII
Vj	Relative variable fluorescence at J phase of the fluorescence induction curve
N	Turn over number of Q_A indicates the number of times Q_A was reduced from 0 to Tf(max)
SFI(abs)	Structure-function-index or the vitality index of PSII
PI(abs)	Performance index of PSII on absorption basis
PI(total)	Performance index of electron flux to the final PSI electron acceptors
DF(total)	PSII-relative driving force
Fluorescence yield parameters	
PHI(Po)	Maximum quantum yield of primary PSII photochemistry (at t = 0)
PHI(Eo)	Quantum yield (at t = 0) for electron transport from Q_A^- to plastoquinone
PSIo	Probability (at t = 0) that a trapped exciton moves an electron into the electron transport chain beyond Q_A
Phenomenological energy flux parameters	
ABS/CSm	Absorption of energy per excited cross-section (CS) approximated by Fm
TRo/CSm	Excitation energy flux trapped by PSII of a photosynthesizing sample cross-section (CS) approximated by Fm
ETo/CSm	Electron transport flux transported by PSII of a photosynthesizing sample cross-section (CS) approximated by Fm

DIo/CSm	Heat dissipation of excitation energy by PSII of a photosynthesizing sample cross-section (CS) approximated by Fm
Specific energy flux parameters	
ABS/RC	Absorption flux per reaction center (RC) corresponding directly to its apparent antenna size
TRo/RC	Trapping flux leading to Q_A reduction per RC at t = 0
ETo/RC	Electron transport flux from Q_A to plastoquinone per RC at t = 0
DIo/RC	Dissipated energy flux per RC at the initial moment of the measurement, *i.e.*, at t = 0

3.5.6. Chlorophyll stability index (CSI)

Chlorophyll stability index (CSI) was measured as per Mishra *et al.* (2016). To analyze CSI, 50 mg of leaf tissue was cut into small pieces and placed in test tubes (in two sets) containing 10 mL of distilled water. One set was kept in the water bath for 1 h at 50°C, and another set was left as control under room temperature. After draining the water, 5 mL of dimethyl sulphoxide (DMSO) was added to both sets and kept in a hot air oven at 70°C till the leaves became pale. The absorbance of both the supernatants was measured at 646 and 663 nm using UV-VIS spectrophotometer, and chlorophyll content in the samples was calculated (Arnon, 1949). CSI was then calculated with the following equation:

$$CSI = (C1 / C2) \times 100$$

Where C1 and C2 are the chlorophyll contents in temperature treated and control sets, respectively.

3.5.7. Osmolality

Osmolality was measured according to Hura *et al.* (2007), using Vapor pressure osmometer (Wescor, 5520, USA). Calibration of the osmometer

chamber was done using 100, 290 and 1000 mmol/kg standard solutions (Wescor, 5520, USA). Cell sap from leaves and roots was collected by the freeze-thawing method. Ten leaf discs (diameter 10 mm) taken from the middle portions of leaves were pooled in an Eppendorf tube. Leaf discs were frozen by keeping in deep freezer (-80°C) for 30 min. For the estimation, samples were thawed to room temperature, and the sap extruding from the leaf discs was collected with a 10 µL pipette and quickly transferred to the disc chamber of the osmometer, and the readings were recorded. The osmolality of the cell sap was expressed in mmol/kg.

3.6. Analysis of reactive oxygen species

3.6.1. Superoxide ($^{\bullet}O_2^-$) content

Superoxide content was estimated as described by Doke (1983).

***Extraction*:** Pre-weighed plant samples were cut into 1×1 mm size and immersed in 5 mL of 0.01 M potassium phosphate buffer (pH 7.8) containing 0.05% NBT and 10 mM NaN_3. The mixture was initially kept at room temperature for 1 h, later transferred to water bath (85°C) and incubated for 15 min. After incubation, the mixture was quickly transferred to ice bath to reduce the temperature.

***Estimation*:** After cooling, the absorbance of the mixture was measured at 580 nm using UV-VIS spectrophotometer. The calculation and determination of $^{\bullet}O_2^-$ content in the plant samples were carried out using the extinction coefficient of 12.3 $mM^{-1}cm^{-1}$. The $^{\bullet}O_2^-$ content in the plant samples was expressed in millimoles per gram fresh weight.

3.6.2. Hydrogen peroxide (H_2O_2) content

Hydrogen peroxide content was estimated as described by Junglee *et al.* (2014).

***Extraction*:** Pre-weighed plant samples were homogenized in 5 mL of 0.1% ice-cold trichloroacetic acid (TCA) using mortar and pestle. The homogenate was centrifuged at 12,000 rpm for 15 min at 4°C. The supernatant was collected and used for the estimation of H_2O_2 content.

***Estimation*:** One millilitre of the supernatant was mixed with an equal volume of potassium phosphate buffer (pH 7), followed by 1 mL of 1 M potassium iodide. The absorbance of the mixture was measured at 390 nm using UV-VIS spectrophotometer. Hydrogen peroxide was used as the standard. The H_2O_2 content in the plant samples was expressed in micrograms per gram fresh weight.

3.7. ROS induced membrane damage

3.7.1. Lipid peroxidation

The rate of lipid peroxidation was assessed by estimating malondialdehyde (MDA) content. Estimation of MDA was done according to Heath and Packer (1968).

Extraction: Pre-weighed plant tissues were homogenized in 5 mL of 5% TCA using mortar and pestle. At room temperature, the homogenate was centrifuged at 12,000 rpm for 15 min. The supernatant was collected and used for the estimation of MDA.

Estimation: 2 mL of the supernatant was mixed with an equal volume of 0.5% of thiobarbituric acid (TBA) prepared in 20% TCA. The solution was heated in water bath (95°C) for 24 min, cooled and then centrifuged at 3000 rpm for 2 min. The absorbance of the supernatant was measured at 532 and 600 nm using UV-VIS spectrophotometer. By subtracting the absorbance value at 600 nm from the absorbance value of 532 nm, the non-specific turbidity was corrected, and the MDA content was calculated using its

extinction coefficient of 155 $mM^{-1}cm^{-1}$. The MDA content in the plant samples was expressed in micromoles per gram fresh weight.

3.7.2. Membrane stability index (MSI)

Membrane stability index (MSI) was determined as described by Sairam *et al.* (1997).Pre-weighed fresh tissue samples were cut into 10 mm^2 sized segments and placed in tubes containing 20 mL of distilled water in two sets. One set was kept at 40°C for 30 min (C_1), and another set was kept in boiling water bath (100°C) for 15 min (C_2). The electrical conductivities of both the solutions (EC_1 and EC_2, respectively) were measured using multi-parameter PCSTestor (Eutech Instruments, Vernon Hills, USA). The MSI was calculated as,

$$MSI = [1- (EC_1/EC_2)] \times 100$$

Where, EC_1 and EC_2 were the electrical conductivities of 40°C and 100°C treated sets, respectively.

3.7.3. Electrolyte leakage (EL%)

Electrolyte leakage (EL%) was estimated as described by Lutts *et al.* (1996) with some modifications. Pre-weighed fresh tissue samples were cut into 10 mm^2 sized segments and placed in tubes containing 20 mL of distilled water. The samples were kept at 4°C for 24 h, then brought to room temperature, and the solution was transferred to another tube (C_1). Further, the tissue was again immersed in 20 mL distilled water and then autoclaved for 15 min at 120°C (C_2). After reaching to room temeperature, the electrical conductivity of both the solutions (EC_1 and EC_2, respectively) was measured using Multi-parameter PCSTestor (Eutech Instruments, Vernon Hills, USA). The EL% was calculated as,

$$EL\% = (EC_1/EC_2) \times 100$$

3.8. Estimation of primary metabolites

3.8.1. Total soluble sugars content

Total soluble sugars content was estimated using phenol-sulphuric acid method (Dubois *et al.*, 1956).

***Extraction**:* Pre-weighed plant samples were homogenized in 5 mL of 80% ethanol using pre-chilled mortar and pestle. The homogenate was centrifuged at 10000 rpm for 10 min at 4°C, and the supernatant was collected. The pellet was re-extracted using 80% ethanol, the supernatant was pooled and was used for the estimation of total soluble sugars content.

***Estimation**:* From the supernatant, a known volume of aliquot was pipette out and made up to 2 mL using distilled water. To this, 1 mL of 5% (w/v) phenol was added and mixed well. Then, 5 mL of concentrated sulphuric acid was added to the tube and cooled. The optical density of the solution was read at 490 nm using a UV-VIS spectrophotometer. D-glucose was used as the standard. Total soluble sugars content was expressed as glucose equivalents in milligrams per gram fresh weight.

3.8.2. Total proteins content

Total proteins content was estimated according to Lowry *et al.* (1951).

***Extraction**:* Pre-weighed plant samples were homogenized in 5 mL of sodium phosphate buffer (pH 7) using pre-chilled mortar and pestle. A known volume of the homogenate was pipetted out into a centrifuge tube, and an equal volume of 10% (W/V) trichloroacetic acid (TCA) was added. This mixture was kept in a refrigerator (4°C) for 1 h for flocculation. The protein precipitate was collected by centrifugation at 5000 rpm for 10 min. The supernatant was decanted off, and the residue was washed twice with cold 2% TCA. The residue was then washed with 30% perchloric acid, diethyl ether

and 80% acetone to remove starch, lipids and chlorophyll pigments respectively.

Preparation of alkaline copper reagent: Mix 50 mLof reagent A with 1 mL of reagent B prior to use.

Reagent A: 2% Na_2CO_3 in 0.1 N NaOH

Reagent B: 0.5% $CuSO_4$ in 1% sodium potassium tartarate

Estimation*:* The pellet obtained after centrifugation was dried and then digested in 5 mL 0.1 N NaOH by heating in a boiling water bath for 10 min. After cooling, the suspension was cleared by centrifugation (5000 rpm for 10 min), and the supernatant was collected. Known volume of aliquot was pipetted and made up to 1 mL with distilled water. To the aliquots, 5 mL of alkaline copper reagent was added and shaken well. After 10 min, 0.5 mL of 1 N Folin-ciocalteu phenol reagent was added and shaken well immediately. The tubes were kept in the dark for 30 min for colour development. The optical density of the solution was read at 700 nm using a UV-VIS spectrophotometer. Bovine serum albumin (BSA) fraction V powder was used as the standard. Total proteins content was expressed as BSA equivalents in milligrams per gram fresh weight.

3.8.3. Total free amino acids content

Total free amino acids content in the plant tissues was estimated according to the method of Moore and Stein (1948) using ninhydrin-hydrindantin reagent.

Extraction*:* Pre-weighed plant samples were homogenized in 5 mL of 80% ethanol using pre-chilled mortar and pestle. The homogenate was centrifuged at 10000 rpm for 10 min at 4°C, and the supernatant was collected. The pellet

was re-extracted using 80% ethanol, the supernatant was pooled and used to estimate total free amino acids content.

***Preparation of reagent solution*:** Dissolved 2 g ninhydrin and 0.3 g hydrindantin in 75 mL 2-methoxy ethanol (methyl cellosolve) and stirred carefully to avoid air bubbles in the solution. To this solution, 25 mL of sodium acetate buffer (pH 5.5) was added (3:1 ratio). The resulting reagent solution was immediately transferred into dark bottle.

Estimation: From the supernatant, a known volume of aliquot was pipette out and made up to 1 mL using distilled water. To this, 1 mL of freshly prepared reagent solution was added and kept in boiling water bath for 15 min. After cooling, 5 mL of diluent (n-propanol and distilled water in 1:1 ratio) was added, mixed well and incubated at room temperature for 15 min. The absorbance was measured at 570 nm using UV-VIS spectrophotometer. L-leucine was used as the standard. The free amino acids content in the plant samples was expressed as leucine equivalents in milligrams per gram fresh weight.

3.8.4. Proline content

Proline content in the plant samples was estimated according to the method of Bates *et al.*(1973) using ninhydrin reagent.

***Extraction**:* Pre-weighed fresh samples were homogenized in 5 mL of 3% (w/v) aqueous sulfosalicylic acid using pre-chilled mortar and pestle. The homogenate was centrifuged at 10000 rpm for 10 min at 4°C. The supernatant was collected and used for the estimation of proline.

Preparation of ninhydrin reagent solution: Mixed 20 mL of 6 M orthophosphoric acid and 30 mL glacial acetic acid. 1.25 g of ninhydrin (2.5% w/v) was dissolved in the acid mixture.

Estimation: To a known volume of supernatant, an equal volume of glacial acetic acid and ninhydrin reagent was added and mixed well. The mixture was heated in boiling water bath for 1 h, and then the reaction was terminated by placing the tubes in ice bath. After cooling, 4 mL of toluene was added to the reaction mixture and stirred well for 30 s using vortex mixer. The upper chromophoric toluene layer was separated, and the optical density was measured at 520 nm using UV-VIS spectrophotometer. L-proline was used as the standard. The proline content in the plant samples was expressed in milligrams per gram fresh weight.

3.9. Free radical scavenging mechanisms

3.9.1. Enzymatic antioxidants

3.9.1.1. Glutathione reductase (GR, EC 1.6.4.2)

Glutathione reductase (GR) activity was assayed by following the method of Kalt-Torres *et al.* (1984) with some modifications.

Extraction: Pre-weighed fresh plant samples were homogenized in 5 mL of 50 mM sodium phosphate buffer (pH 7.0) containing 0.2 mM EDTA using pre-chilled glass mortar and pestle. The homogenate was filtered through four-layered muslin cloth, and the filtrate was centrifuged at 14000 rpm for 20 min at 4°C, and the supernatant was used for the enzyme assay.

Enzyme assay:The reaction mixture (3 mL) contained 1.8 mL of 50 mM sodium phosphate buffer (pH 7.6), 0.3 mL each of 3 mM EDTA, 0.1 mM NADPH, 0.1 mM oxidized glutathione (GSSG) and enzyme extract. The activity of GR was recorded by decrease in absorbance due to the oxidation of NADPH per minute at 340 nm for 3 min at 30 s interval using UV-VIS spectrophotometer. One unit of GR activity was defined as the amount of enzyme required to oxidize 1 μmol of NADPH per min.

3.9.1.2. Monodehydroascorbate reductase (MDHAR, EC 1.6.5.4)

Monodehydroascorbate reductase (MDHAR) activity was assayed according to Hossain *et al.* (1984) with some modifications.

***Extraction**:* Pre-weighed fresh plant samples were homogenized in 5 mL of 50 mM sodium phosphate buffer (pH 7.0) containing 0.2 mM EDTA using pre-chilled glass mortar and pestle. The homogenate was filtered through four-layered muslin cloth, and the filtrate was centrifuged at 14000 rpm for 20 min at 4°C, and the supernatant was used for the enzyme assay.

***Enzyme assay**:* The reaction mixture (3 mL) contained 1.5 mL of 150 mM sodium phosphate buffer (pH 7.0), 0.3 mL of 0.1 mM EDTA, 0.2 mL of 0.25% of triton X-100, 0.25 mL of 30 mM ascorbate, 0.2 mL of 3 mM NADH, 0.25 mL of 0.25 units ascorbate oxidase and 0.3 mL of enzyme extract. The activity of MDHAR was recorded by decrease in absorbance due to the oxidation of NADH per minute at 340 nm for 3 min at 30 s interval using UV-VIS spectrophotometer. One unit of MDHAR activity was defined as the amount of enzyme required to oxidize 1 μmol of NADH per min.

3.9.1.3. Dehydroascorbate reductase (DHAR, EC 1.8.5.1)

Dehydroascorbate reductase (DHAR) activity was assayed as per the protocol of Dalton *et al.* (1987) with some modifications.

***Extraction**:* Pre-weighed fresh plant samples were homogenized in 5 mL of 50 mM sodium phosphate buffer (pH 7.0) containing 0.2 mM EDTA using pre-chilled glass mortar and pestle. The homogenate was filtered through four-layered muslin cloth, and the filtrate was centrifuged at 14000 rpm for 20 min at 4°C, and the supernatant was used for the enzyme assay.

***Enzyme assay**:* The reaction mixture (3 mL) contained 1.5 mL of 100 mM sodium phosphate buffer (pH 7.0), 0.3 mL of 1 mM EDTA, 0.5 mL of 15 mM

reduced glutathione (GSH), 0.3 mL of 2 mM dehydroascorbate and 0.4 mL of enzyme extract. The activity of DHAR was recorded by observing the increase in absorbance at 265 nm for 3 min at 30 s interval using UV-VIS spectrophotometer. One unit of DHAR activity was defined as the amount of enzyme required to catalyze the formation of 1 μmol of ascorbate per min.

3.9.1.4. Catalase (CAT, EC 1.11.1.6)

Catalase (CAT) activity in the fresh plant samples was assayed by the method of Chance and Maehly (1955) with some modifications.

Extraction: The enzyme extraction was carried out according to Polle *et al.* (1994). Pre-weighed fresh plant samples were homogenized in 5 mL of 100 mM potassium phosphate buffer (pH 7.0) containing 1 mM EDTA, using pre-chilled mortar and pestle. The homogenate was filtered through four-layered muslin cloth, and the filtrate was centrifuged at 14000 rpm for 15 min at 4°C, and the supernatant was used for the enzyme assay.

Enzyme assay: The reaction mixture contained 1 mL of 100 mM potassium phosphate buffer (pH 7.0), 1 mL of 30% (w/v) H_2O_2 and 0.1 mL of enzyme extract. The activity of CAT was recorded by observing the decrease in absorbance at 240 nm for 90 s at 15 s interval using UV-VIS spectrophotometer. One unit of CAT activity was defined as the amount of enzyme required for the decomposition of 1 μmol of H_2O_2 per min.

3.9.1.5. Guaiacol peroxidase (POD, EC 1.11.1.7)

POD activity in the fresh plant samples was measured according to the method of Gasper *et al.* (1975) with some modifications.

Extraction: The enzyme extraction was carried out according to the method of Polle *et al.* (1994). Pre-weighed fresh plant samples were homogenized in 5 mL of 100 mM potassium phosphate buffer (pH 7.0) containing 1 mM

EDTA, using pre-chilled glass mortar and pestle. The homogenate was filtered through four-layered muslin cloth, and the filtrate was centrifuged at 14000 rpm for 15 min at 4°C, and the supernatant was used for the enzyme assay.

Enzyme assay: The reaction mixture contained 30 µL of 1% guaiacol, 12 µL of 30% (w/v) H_2O_2 and 100 µL of enzyme extract, and made up to 3 mL with 100 mM potassium phosphate buffer (pH 7.0). The activity of POD was recorded by observing the increase in absorbance at 420 nm for 3 min at 30 s interval using UV-VIS spectrophotometer. One unit of POD activity was defined as the amount of enzyme required to oxidize 1 µmol of guaiacol per min.

3.9.1.6. Ascorbate peroxidase (APX, EC 1.11.1.11)

APX activity in the fresh plant samples was assayed by following the method of Nakano and Asada (1981).

Extraction*:* The enzyme extraction was carried out according to the method of Polle *et al.* (1994). Pre-weighed fresh plant samples were homogenized in 5 mL of 100 mM potassium phosphate buffer (pH 7.0) containing 1 mM EDTA, using pre-chilled glass mortar and pestle. The homogenate was filtered through four-layered muslin cloth, and the filtrate was centrifuged at 14000 rpm for 15 min at 4°C, and the supernatant was used for the enzyme assay.

Enzyme assay: The reaction mixture contained 15 µL of 0.5 mM ascorbate, 296 µL of 30% (w/v) hydrogen peroxide and 100 µL of enzyme extract, and made up to 3 mL with 100 mM potassium phosphate buffer (pH 7.0). The activity of APX was recorded by observing the decrease in absorbance at 290 nm for 3 min at 30 s interval using UV-VIS spectrophotometer. One unit of APX activity was defined as the amount of enzyme required to oxidize 1

µmol of ascorbate per min.

3.9.1.7. Superoxide dismutase (SOD, EC 1.15.1.1)

Assay of SOD activity in the fresh plant samples was done as per the modified protocol of Giannopolitis and Ries (1977).

***Extraction**:* The enzyme extraction was carried out according to the method of Polle *et al.* (1994). Pre-weighed fresh plant samples were homogenized in 5 mL of 100 mM potassium phosphate buffer (pH 7.0) containing 1 mM EDTA, using pre-chilled glass mortar and pestle. The homogenate was filtered through four-layered muslin cloth, and the filtrate was centrifuged at 14000 rpm for 15 min at 4°C, and the supernatant was used for the enzyme assay.

***Enzyme Assay**:* The reaction mixture consisted of 0.1 mL of 1.5 M sodium carbonate, 0.3 mL of 130 mM methionine, 0.3 mL of 13 µM riboflavin, 0.3 mL of 10 µM EDTA, 0.3 mL of 0.63 mM nitrobluetetrazolium (NBT) and 0.1 mL enzyme extract, and the reaction mixture was made up to 3 mL using 100 mM potassium phosphate buffer (pH 7.0). Different assay systems were set, *viz.* test samples, dark-control and light-control. Test tubes containing all the assay mixtures including enzyme extract, illuminated under fluorescent lamp for 30 min served as the test sample and the set of tubes placed in dark served as the dark control. The assay mixture without enzyme extract illuminated under fluorescent lamp for 30 min served as light control. The mixture without NBT and enzyme extract served as the blank. The blue formazan accumulation in different tubes was quantified using spectrophotometer by recording the absorbance at 560 nm against the blank. One unit of SOD activity was defined as the amount of enzyme required to inhibit the photochemical reduction of NBT to blue formazan by 50%.

Specific activity of each enzyme was calculated after determining

soluble protein concentration in the enzyme extract according to Bradford (1976).

$$\text{Specific activity} = \frac{\text{Enzyme activity in Units}}{\text{mg protein/mL enzyme extract}}$$

3.9.2. Non-enzymatic antioxidants

3.9.2.1. Ascorbate (AsA) content

The estimation of AsA content was carried out according to the method of Chen and Wang (2002) with some modifications.

Extraction: Pre-weighed fresh plant samples were homogenized in 5 mL of 5% (w/v) trichloroacetic acid (TCA) using mortar and pestle. The homogenate was centrifuged at 12000 rpm for 15 min at 4°C. The supernatant was collected and used for the estimation of AsA content.

Estimation: An aliquot of 0.5 mL of the supernatant was mixed well with 0.25 mL of 0.2 M sodium phosphate buffer (pH 7.4). To this mixture, 0.5 mL of 10% (w/v) TCA, 0.5 mL of 42% (v/v) phosphoric acid, 0.5 mL of 4% (w/v) bipyridyl (dissolved in 70% alcohol) and 0.25 mL of 3% (w/v) ferric chloride were added. The mixture was incubated at 40°C for 30 min. The absorbance was measured at 525 nm using UV-VIS spectrophotometer. Pure form of AsA was used as the standard. The AsA contents in the plant samples were expressed in milligrams per gram fresh weight.

3.9.2.2. Glutathione (GSH) content

The estimation of GSH content was carried out according to the method of Chen and Wang (2002) with some modifications.

Extraction: Pre-weighed fresh plant samples were homogenized in 5 mL of 5% (w/v) trichloroacetic acid (TCA) using mortar and pestle. The

homogenate was centrifuged at 12000 rpm for 15 min at 4°C. The supernatant was collected and used for the estimation of GSH content.

Estimation: An aliquot of 0.5 mL of the supernatant was mixed with 2.3 mL of 0.2 M sodium phosphate buffer (pH 6.8). To this mixture, 0.2 mL of 6 mM 5,5'-dithiobis-2-nitrobenzoic acid (DNTB/Ellman's reagent; dissolved in 0.2 M sodium phosphate buffer, pH 6.8) was added. The mixture was incubated at 30°C for 5 min. The absorbance was measured at 412 nm using UV-VIS spectrophotometer. Oxidized glutathione was used as the standard. The GSH contents in the plant samples were expressed in milligrams per gram fresh weight.

3.9.2.3. Total phenolics content

The estimation of total phenolics content was carried out according to the method of Folin and Denis (1915) using Folin-ciocalteu phenol reagent.

Extraction: Pre-weighed plant samples were homogenized in 5 mL of 80% ethanol using pre-chilled mortar and pestle. The homogenate was centrifuged at 10000 rpm for 10 min, and the supernatant was collected. The pellet was re-extracted using 80% ethanol, the pooled supernatant was used to estimate total phenolics content.

Estimation: From the supernatant, a known volume of aliquot was pipetted out and made up to 3 mL using distilled water. To this, 0.5 mL of 1 N Folin-ciocalteu phenol reagent was added and mixed well. After 3 min, 2 mL of 20% sodium carbonate was added. The mixture was thoroughly mixed and kept for 1 min for colour development. The optical density of the solution was read at 650 nm using UV-VIS spectrophotometer. Catechol was used as the standard. Total phenolics content was expressed in milligrams per gram fresh weight.

3.9.2.4. Flavonoids content

The extraction and estimation of flavonoids content were carried out according to Mirecki and Teramura (1984) with some modifications.

Extraction: Pre-weighed fresh plant samples were cut into 1×1 mm size andimmersed in 5 ml of solvent containing methanol, hydrochloric acid and water in 79:1:20 ratio. The mixture was incubated at room temperature for 24 h. After centrifugation, the resulting supernatant was used to estimate flavonoids content.

Estimation: The optical density of the supernatant was read at 315 nm using UV-VIS spectrophotometer. The flavonoids content was calculated using its molar extinction coefficient of 33 $mM^{-1}cm^{-1}$ and expressed in millimoles per gram fresh weight.

3.9.2.5. Anthocyanins content

The extraction and estimation of anthocyanins content were carried out according to the method of Mancinelli *et al.* (1975) with some modifications.

Extraction: Pre-weighed fresh plant samples were cut into 1×1 mm size andimmersed in 5 ml of solvent containing methanol and hydrochloric acid in 99:1 ratio. The mixture was incubated at 4°C for 24 h. After centrifugation, the resulting supernatant was used to estimate anthocyanins content.

Estimation: The optical density of the supernatant was read at 530 nm using UV-VIS spectrophotometer. The anthocyanins content was calculated using its molar extinction coefficient of 34.3 $mM^{-1}cm^{-1}$ and expressed in millimoles per gram fresh weight.

3.10. Bioaccumulation and distributional patterns of elements

3.10.1. Bioaccumulation and translocation of Cu

The digestion of plant samples to analyze the Cu bioaccumulation was carried out according to the method of Allan (1969). The samples of root, stem, cotyledonary and primary leaves from the control and $CuSO_4$ treated plants on 6 and 10 d were harvested and dried in an oven at 100°C for 1 h, followed by 60°C until a constant weight was achieved. The dry weight of each sample was determined, transferred into Kjeldahl flasks, and then a mixture of nitric and perchloric acids prepared in 10:4 ratio was added. The samples were refluxed for digestion in the heating mantle at 60°C until the solution became colorless. Subsequently, the digest was filtered using Whatman's filter paper, transferred to a standard flask, and volume was made up to 50 ml with distilled water. Atomic absorption spectrophotometer (AA-7000, Shimadzu, Kyoto, Japan) was used to estimate Cu present in the digested samples. The bioaccumulation of Cu in the plant samples was expressed in micrograms per gram dry weight. The translocation factor (TF) of Cu in the leaves was calculated by using the following equation,

$$\text{Translocation factor(TF)} = \frac{\text{Concentration of Cu in the leaves}}{\text{Concentration of Cu in the roots}}$$

3.10.2. Subcellular distribution pattern of Cu

The subcellular distribution pattern of Cu was determined as per Weigel and Jäger (1980).

Fractionation of the samples: On 6 d of exposure to Cu stress, 5 g of fresh tissue was collected from both the control as well as 200 µM $CuSO_4$ treated seedlings. Generally, the cells are divided into three fractions such as cell wall, organellar and cytoplasmic or soluble fractions. The plant samples were homogenized in 50 mM cold Tris-HCl buffer (pH 7.5), containing 250 mM

sucrose and 1 mM dithiothreitol, using pre-chilled mortar and pestle. The homogenate was centrifuged at 3000 g for 30 seconds at 4°C. The precipitate was designated as fraction 1, containing cell wall and debris. The remaining supernatant was then centrifuged at 20,000 g for 45 min at 4°C (Ultracentrifuge Sorvall WX100 Plus, ThermoFisher Scientific, United States). The resultant pellet was designated as fraction 2, consisting of the cell organelles, and the supernatant was the soluble/cytoplasmic fraction (fraction 3).

Digestion of fractions and estimation of Cu: All the three fractions were oven-dried at 60°C, and then digested by refluxing in HNO_3 until the solution became colourless using Kjeldahl flasks heated in the heating mantle at 60°C. Subsequently, the digest was filtered using Whatman's filter paper, transferred to standard flask, and volume was made up to 50 ml with distilled water. The Cu concentrations in the samples were determined using ICPMS (Agilent 7800, Santa Clara, United States).

3.11. Leaf micromorphological characters

Micromorphology of cotyledonary and primary leaves of *R. communis* seedlings was evaluated using scanning electron microscope (SEM) on 6 and 10 d of exposure to $CuSO_4$ and cytokinins. The leaf cuttings of different treatments were fixed in 2.5% glutaraldehyde, prepared in 0.2 M sodium cacodylate buffer (pH 7.4). The specimens were dehydrated by passing through ascending acetone series. Then the samples were dehydrated using Critical Point Dryer (Quorum K850, Houston, Texas). Dried specimens were mounted on aluminium stubs using double side adhesive conducting carbon tapes and further subjected to gold-palladium coating for 60 sec using Sputter Coater (Quorum SC7626, Houston, Texas). Photomicrographs were taken using field emission scanning electron microscope (FESEM Carl-Zeiss Gemini 300, Jena, Germany).

3.12. Anatomical studies

3.12.1. Histochemistry

Root, stem, primary and cotyledonary leaves of control as well as 200 µM $CuSO_4$ treated seedlings were collected and fixed in FAA (100 mL FAA contains 10 mL formalin, 5 mL acetic acid, 50 mL alcohol and 35 mL distilled water). Free-hand sections were taken and stained with toluidine blue. Photomicrographs were taken using compound microscope (LEICA DM2000 LED microscope attached with LEICA DMC4500 camera).

3.12.2. Scanning Electron Microscopy (SEM) and Energy-Dispersive X-ray (EDX) Analysis

The anatomical studies of root, stem, cotyledonary and primary leaves of *R. communis* seedlings were evaluated using field emission scanning electron microscope (FESEM) on 6 d of exposure to $CuSO_4$ and cytokinins. Free-hand sections of plant samples were fixed in 2.5% glutaraldehyde, prepared in 0.2 M sodium cacodylate buffer (pH 7.4). The sections were dehydrated by passing through ascending acetone series. Then the samples were dehydrated using Critical Point Dryer (Quorum K850, Houston, Texas). Dried specimens were mounted on aluminium stubs using double side adhesive conducting carbon tapes and further subjected to gold-palladium coating for 60 sec using Sputter Coater. Photomicrographs were taken using field emission scanning electron microscope.

Quantitative compositional analysis of Cu and other essential elements in the xylem tissues of root, stem, cotyledonary and primary leaves of *R. communis* seedlings were evaluated using FESEM attached with Energy Dispersive X-ray spectroscope (Ametek EDAX Octane Plus, New Jersey, USA).

3.13. Analysis for bioactive compounds by Gas chromatography and mass spectrometry (GCMS)

The sample preparation and extraction were carried out according to Canini *et al.* (2007) with some modifications.

Sample preparation: The roots, cotyledonary and primary leaves of *R. communis* seedlings on 6 d of exposure to $CuSO_4$ and cytokinins were collected and washed with distilled water. The samples were cut into small pieces and shade dried at room temperature for 3-4 weeks. After drying, they were ground into fine powder with a mechanical grinder and stored in air-tight containers until use.

Preparation of extract: Two grams of powdered root and leaf samples were extracted in soxhlet apparatus with 20 ml of aqueous methanol (v/v) at 75°C for 24 h. After cooling, the extract was filtered to remove the plant residues and was concentrated in rotary evaporator at 40°C. The crude extract was stored in air-tight vials at -20°C until use.

GCMS analysis: The identification of bioactive compounds in the methanolic extracts was carried out using GCMS (Shimadzu QP2010S, Kyoto, Japan). An ELITE-5MS column (30 m length × 0.25 mm ID × 0.25 µm thickness) was used for GC separation. At start, the column oven temperature was maintained at 80°C for 4 min and then increased to 260°C for 6 min. The specifications of the instrument were, injection mode - split less; injection temperature - 260°C; sample injection volume - 1 µL; total flow - 54.01 mL/min; column flow - 1.00 mL/min; pressure - 65.2 kPa; solvent cut time - 6.50 min; purge flow - 3.0 mL/min; and detector gain mode - relative. The compounds in the samples were identified by comparing with the mass spectra on WILEY 8 and National Institute of Standard and Technology (NIST 11) libraries using GCMS Solutions software.

3.14. Fourier Transform Infrared (FTIR) spectroscopic analysis

The roots, cotyledonary and primary leaves of *R. communis* seedlings on 6 d of exposure to $CuSO_4$ and cytokinins were collected and washed with distilled water. The separation procedure of the cell wall was performed as stated in section 3.9.2. After separation, the cell wall fraction was dried at 30°C for 3-4 weeks. After drying, they were ground into fine powder with a mechanical grinder and stored in air-tight containers until use. The powdered samples were made into pellets by mixing with dried potassium bromide (KBr). The pellets were placed in the path of the beam, and evaluation of solid-state spectrum was done by using FTIR spectrometer (Jasco-4100, Shanghai, China) in 400–4000 cm^{-1} range with 2 cm^{-1} resolution. The data were analyzed using Origin Pro 8.

3.15. Statistical analysis

Analysis of variance (ANOVA) was performed using SPSS software 20.0. Duncan's test was used to compare the means at 5% probability level. The data is an average of recordings from three independent experiments, each with three replicates (*i.e.*, n=9). The data represent mean ± standard error (SE). Pearson's correlation analysis was performed to evaluate the relationships between the various photosynthetic variables and antioxidation mechanisms in the cotyledonary and primary leaves and roots of *R. communis* seedlings exposed to $CuSO_4$ and cytokinins.

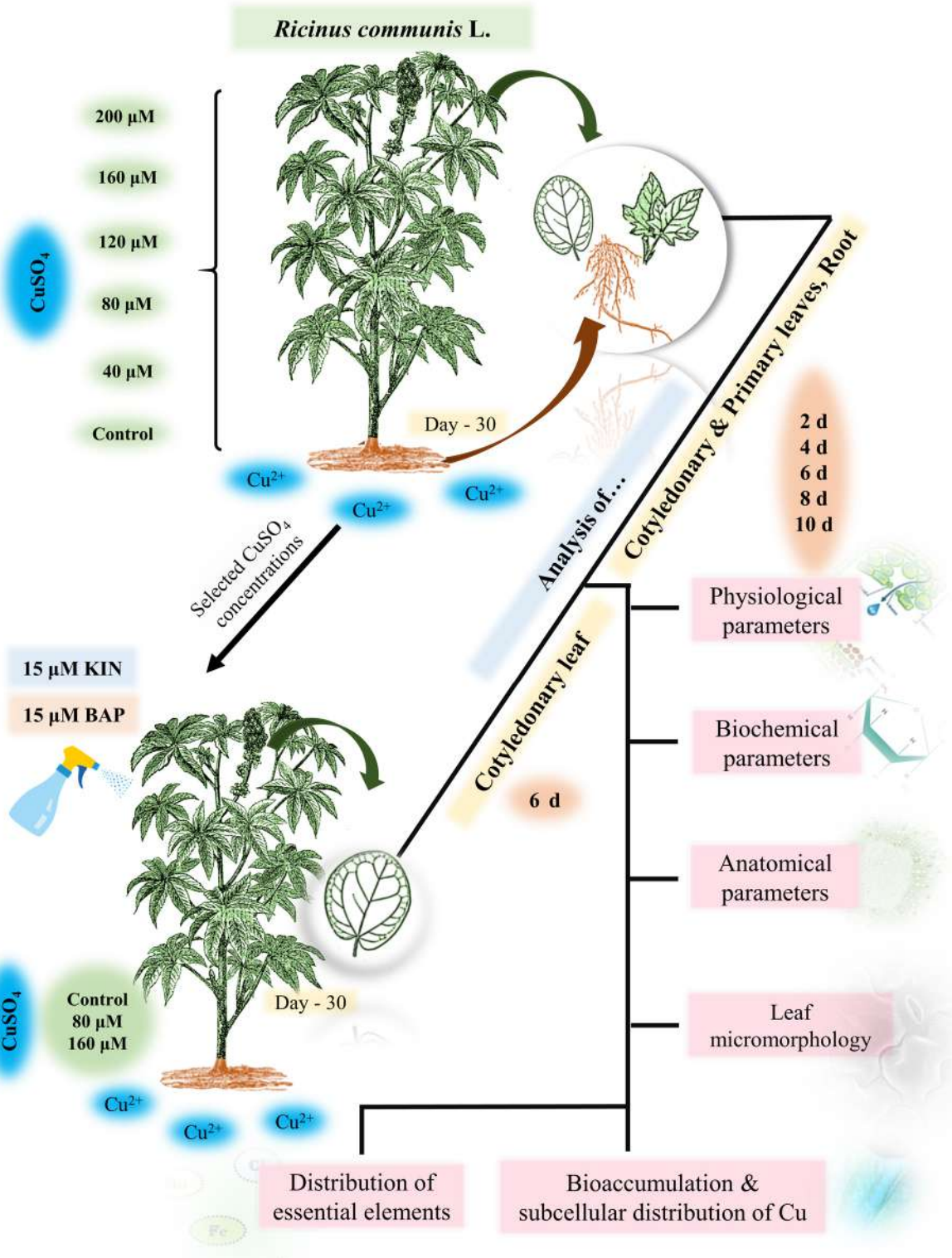

Figure 2. Schematic representation of the work

RESULTS

4.1. Preliminary screening

4.1.1. Analysis of soil and plant samples collected from the polluted lands with luxuriant growth of *Ricinus communis* for detecting heavy metals

The concentration of heavy metals such as As, Cd, Co, Cr, Cu, Ni, Pb and Zn in the soil and *R. communis* root and leaf samples collected from different locations of polluted lands are represented in Table 6. As per the results, the study locations are largely polluted with these heavy metals and the *R. communis* plants grown in these areas exhibited exceptionally higher tolerance towards these metals. The range of different metal concentrations were 0.39-0.69, 0.51-6.01, 2.33-3.68, 13.82-47.79, 23.57-169.29, 11.79-27.53, 18.75-91.52 and 9.94-46.79 μg/g DW for As, Cd, Co, Cr, Cu, Ni, Pb and Zn respectively in the soil samples collected from the five different locations. The order of heavy metal concentrations in the soil was Cu > Pb >Cr > Zn > Ni > Cd > Co > As. Among them, As and Cd seen were accumulated in the leaves of *R. communis* and this was higher than the concentrations in the soil, and it ranged between 1-3 and 6.6-47.2 folds increases respectively in the leaves as compared to the soil. Moreover, the concentrations of all the metals studied were higher in the leaves of *R. communis* plants than in the roots. The concentration of Cu in the leaves was higher than present in the soil in plants grown in site 3, 4 and 5, and the increases were 1.1, 1.2 and 1.4 folds respectively as compared to the respective concentrations of Cu in the soil. Furthermore, all the leaf samples had comparatively higher concentrations of Cu, and thus further study was carried out with Cu.

4.1.2. Selection of effective concentration of $CuSO_4$ at which the plants exhibited highest level of tolerance

The preliminary screening to identify the concentrations of $CuSO_4$ in which the *R. communis* seedlings exhibited the highest level of tolerance was carried out with one month old healthy seedlings. The seedlings were subjected to 40, 80, 120, 160, 200, 240 and 280 μM $CuSO_4$ prepared in quarter strength modified Hoagland nutrient medium for 10 d. The seedlings grown in Hoagland nutrient medium were designated as the control. In the experimental period, the $CuSO_4$ concentrations above 200 μM induced toxicity symptoms such as decaying of root and abscission of cotyledonary leaves from 2 d of exposure to $CuSO_4$ onwards. Therefore, the concentrations of $CuSO_4$ below 200 μM were selected for growing *R. communis* seedlings so as to analyze the physiochemical features and tolerance mechanisms adopted by the plant with increasing concentrations of $CuSO_4$ (Fig. 3).

4.1.3. Selection of effective concentration of kinetin (KIN) and 6-benzylaminopurine (BAP) to analyze the Cu stress ameliorative effects in the cotyledonary leaves of *R. communis*.

From the different concentrations of $CuSO_4$ analyzed, one mild and one severe stress concentrations (80 and 160 μM $CuSO_4$ respectively) were selected to analyze the stress ameliorative effects of two different cytokinins [kinetin (KIN) and 6-benzylaminopurine (BAP)]. 80 and 160 μM $CuSO_4$treated *R. communis* seedlings were subjected to 5, 10, 15, 20 and 25 μM KIN and BAP as foliar spray. The photosynthetic pigment composition and extent of membrane lipid peroxidation were analyzed to select the effective concentrations of KIN and BAP (Table 7).

During KIN application, the maximum restoration of total chlorophyll and carotenoid contents was observed in the cotyledonary leaves when the Cu-treated seedlings were subjected to 20 μM KIN. However, the accumulation of MDA content was least in the cotyledonary leaves of 160 μM

Table 6. Concentration of different heavy metals in the soil and *R. communis* root and leaf samples collected from the polluted lands of Kozhikode city limits with luxuriant growth of *R. communis*.

Location	Type of samples	Concentration of heavy metals (µg/g DW)							
		As	Cd	Co	Cr	Cu	Ni	Pb	Zn
Site 1	Soil	0.393 ± 0.020	3.844 ± 0.192	2.397 ± 0.120	13.818 ± 0.691	23.569 ± 1.178	15.031 ± 0.752	18.750 ± 0.938	17.429 ± 0.871
	Root	0.0932 ± 0.005	0.335 ± 0.167	0.084 ± 0.004	2.210 ± 0.111	10.683 ± 0.534	0.637 ± 0.032	2.824 ± 0.141	1.147 ± 0.057
	Leaf	1.104 ± 0.055	25.547 ± 1.278	0.317 ± 0.016	13.748 ± 0.687	17.543 ± 0.877	3.072 ± 0.154	9.599 ± 0.480	7.173 ± 0.359
Site 2	Soil	0.459 ± 0.023	2.374 ± 0.119	3.206 ± 0.160	30.129 ± 1.506	169.294 ± 8.465	19.654 ± 0.983	91.517 ± 4.576	32.714 ± 1.636
	Root	0.118 ± 0.006	0.188 ± 0.009	0.144 ± 0.007	2.682 ± 0.134	40.611 ± 2.031	0.834 ± 0.042	3.547 ± 0.177	2.091 ± 0.105
	Leaf	0.593 ± 0.030	112.120 ± 5.606	0.367 ± 0.018	10.319 ± 0.516	73.220 ± 3.661	2.569 ± 0.128	13.588 ± 0.679	8.221 ± 0.411
Site 3	Soil	0.691 ± 0.035	2.7807 ± 0.139	3.683 ± 0.184	18.019 ± 0.901	33.446 ± 1.672	27.530 ± 1.376	24.189 ± 1.209	46.788 ± 2.339
	Root	0.079 ± 0.004	0.121 ± 0.006	0.105 ± 0.005	2.395 ± 0.120	15.761 ± 0.788	1.088 ± 0.054	1.603 ± 0.080	3.777 ± 0.189
	Leaf	0.550 ± 0.028	27.757 ± 1.388	0.454 ± 0.023	11.374 ± 0.569	36.321 ± 1.816	3.055 ± 0.153	12.256 ± 0.613	9.175 ± 0.459
Site 4	Soil	0.511 ± 0.026	0.512 ± 0.026	3.598 ± 0.180	47.789 ± 2.389	35.995 ± 1.80	16.631 ± 0.832	54.340 ± 2.717	19.157 ± 0.958
	Root	0.107 ± 0.005	0.061 ± 0.003	0.107 ± 0.005	3.80 ± 0.189	19.272 ± 0.964	0.762 ± 0.038	3.713 ± 0.186	1.401 ± 0.701
	Leaf	0.584 ± 0.029	13.267 ± 0.663	0.355 ± 0.18	10.715 ± 0.536	44.889 ± 2.244	2.529 ± 0.126	14.316 ± 0.716	5.419 ± 0.271
Site 5	Soil	0.448 ± 0.022	6.008 ± 0.301	2.334 ± 0.117	25.010 ± 1.250	65.438 ± 3.272	11.795 ± 0.590	51.3653 ± 2.568	9.938 ± 0.497
	Root	0.106 ± 0.005	0.415 ± 0.021	0.074 ± 0.004	2.014 ± 0.101	25.612 ± 1.281	0.764 ± 0.038	4.007 ± 0.2003	1.593 ± 0.796
	Leaf	0.465 ± 0.023	145.889 ± 7.294	0.227 ± 0.011	10.184 ± 0.509	92.460 ± 4.623	2.205 ± 0.110	17.910 ± 0.895	6.465 ± 0.323

$CuSO_4$ treated seedlings along with 15 µM KIN. In the case of BAP application, the maximum restoration of total chlorophyll and carotenoid content was recorded in the cotyledonary leaves of 160 µM $CuSO_4$ treated seedlings along with 15 µM BAP. Similarly, lower accumulation of MDA was recorded when the seedlings were treated with 80 µM $CuSO_4$ + 15 µM BAP (Table 7).

Even though the chlorophyll and carotenoid contents were higher in the cotyledonary leaves of *R. communis* seedlings treated with 20 µM KIN along with $CuSO_4$, another important parameter, the rate of membrane lipid peroxidation was higher in 20 µM KIN as compared to 15 µM KIN. Therefore, for the easiness in comparison, an ideal concentration of 15 µM for both KIN and BAP was selected to analyze cytokinin-mediated Cu stress alleviation mechanisms in *R. communis* (Fig. 4).

4.2. Analysis of the Cu toxicity, tolerance mechanisms and Cu stress ameliorative effects of cytokinins in *R. communis* L. seedlings

4.2.1. Physiological studies

4.2.1.1. Dry weight (DW) %

Copper treatment resulted in the enhancement of DW% in both the leaves and roots of *R. communis* seedlings as compared to the respective controls (Table 8). In cotyledonary leaves, there was no significant variation observed in DW% on 2 d of $CuSO_4$ exposure. But, from 4 d onwards, a significant enhancement was observed at higher concentrations of $CuSO_4$ (120 to 200 µM). The enhancement in DW% was 2.8 folds higher upon exposure to 200 µM $CuSO_4$ on 4 d, which was further enhanced to 3.9 folds on 6 d.

In the case of primary leaves, the enhancement in DW% was insignificant during the experimental period. An increase of about 13-20% of

DW% only was observed upon exposure to 120-200 µM $CuSO_4$ on 4 d of treatment as compared to the control. In contrast, the abscission of cotyledonary leaves resulted in the enhancement of DW% in primary leaves. It was enhanced to 20-45% in all the treatments on 8-10 d of $CuSO_4$ exposure as compared to the primary leaves of the control, with the highest enhancement occurring in the case of 160 and 200 µM $CuSO_4$ treatments on 8 and 10 d of exposure (Table 8).

Exposure to Cu stress resulted in significant variations of DW% in the roots of *R. communis* seedlings. Exposure to 40 and 80 µM $CuSO_4$ resulted in the enhancement of DW% in the roots on initial days of treatment, and it was to the extent of 83 and 60% increase respectively on 4 d of exposure. In contrast, at higher concentrations of $CuSO_4$, the increase of DW% was minimum (10-17% on 4 d). Moreover, prolonged exposure to $CuSO_4$ resulted in the decrease of DW% in the roots of *R. communis* seedlings as compared to the roots of control seedlings. On exposure to 200 µM $CuSO_4$ for 10 d, 22% reduction in DW% was noticed in the roots (Table 8).

The increase of DW% of cotyledonary leaves was 2.5 and 3.4 folds on treatment with 80 and 160 µM $CuSO_4$ concentrations, respectively, compared to the control. Application of KIN and BAP reduced the DW% of cotyledonary leaves in *R. communis* subjected to both concentrations of $CuSO_4$ to a level as that of the control. The reduction of DW% was 52-66% and 65-73% on application of KIN and BAP respectively, along with $CuSO_4$ as compared to those exposed to $CuSO_4$ alone (Table 9).

4.2.1.2. Moisture content (MC) %

On initial days of $CuSO_4$ exposure, there was no significant variation observed in MC% of the cotyledonary leaves of *R. communis* seedlings as compared to the control (Table 10). But, Cu stress resulted in significant

Table 7. Total chlorophyll, carotenoids and MDA contents analyzed in the cotyledonary leaves of *R. communis* subjected to different concentrations of $CuSO_4$ (80 and 160 μM) and cytokinins (KIN and BAP in 5, 10, 15, 20 and 25 μM) on 6 d of treatment in Hoagland nutrient medium. Values are the mean ± SE of three independent experiments.

Treatments	Total chlorophyll content (mg/g FW)	Carotenoids content (mg/g FW)	MDA content (μmol/g FW)
Control	1.289 ± 0.03	0.423 ± 0.02	14.366 ± 0.17
80 μM $CuSO_4$	0.816 ± 0.02	0.252 ± 0.01	65.591 ± 11.87
160 μM $CuSO_4$	0.705 ± 0.01	0.215 ± 0.01	95.430 ± 11.56
80 μM Cu + 5 μM KIN	0.627 ± 0.02	0.281 ± 0.01	40.0 ± 0.64
80 μM Cu + 10 μM KIN	0.598 ± 0.06	0.259 ± 0.03	36.532 ± 0.89
80 μM Cu + 15 μM KIN	0.973 ± 0.22	0.285 ± 0.01	30.269 ± 0.16
80 μM Cu+ 20 μM KIN	1.443 ± 0.02	0.525 ± 0.01	28.145 ± 0.24
80 μM Cu + 25 μM KIN	1.919 ± 0.09	0.658 ± 0.02	31.532 ± 0.24
160 μM Cu + 5 μM KIN	0.929 ± 0.01	0.354 ± 0.01	38.105 ± 7.06
160 μM Cu + 10 μM KIN	0.972 ± 0.11	0.349 ± 0.04	31.854 ± 1.21
160 μM Cu + 15 μM KIN	1.055 ± 0.01	0.379 ± 0.01	26.427 ± 0.99
160 μM Cu + 20 μM KIN	1.407 ± 0.02	0.545 ± 0.01	41.835 ± 1.31
160 μM Cu + 25 μM KIN	0.711 ± 0.01	0.308 ± 0.01	35.806 ± 1.61
80 μM Cu+ 5 μM BAP	0.761 ± 0.01	0.320 ± 0.01	28.387 ± 0.32
80 μM Cu + 10 μM BAP	0.925 ± 0.01	0.337 ± 0.01	25.484 ± 0.32
80 μM Cu + 15 μM BAP	1.269 ± 0.01	0.422 ± 0.03	20.322 ± 1.29
80 μM Cu + 20 μM BAP	1.346 ± 0.01	0.491 ± 0.01	22.270 ± 0.19
80 μM Cu + 25 μM BAP	1.127 ± 0.01	0.402 ± 0.01	50.269 ± 1.08
160 μM Cu + 5 μM BAP	0.755 ± 0.01	0.321 ± 0.01	27.016 ± 0.40
160 μM Cu + 10 μM BAP	1.036 ± 0.01	0.368 ± 0.02	26.434 ± 0.45
160 μM Cu + 15 μM BAP	1.589 ± 0.01	0.621 ± 0.02	25.081 ± 0.08
160 μM Cu + 20 μM BAP	1.131 ± 0.01	0.322 ± 0.01	28.226 ± 0.32
160 μM Cu + 25 μM BAP	0.984 ± 0.01	0.398 ± 0.01	23.871 ± 0.86

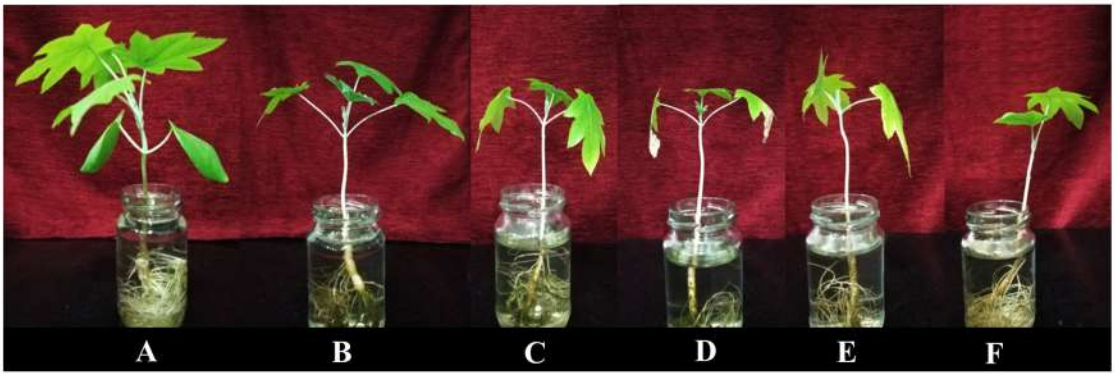

Figure 3. *Ricinus communis* after exposure to different concentrations of $CuSO_4$ for 10 d. A, B, C, D, E and F represents control, 40, 80, 120, 160 and 200 µM $CuSO_4$ treated seedlings.

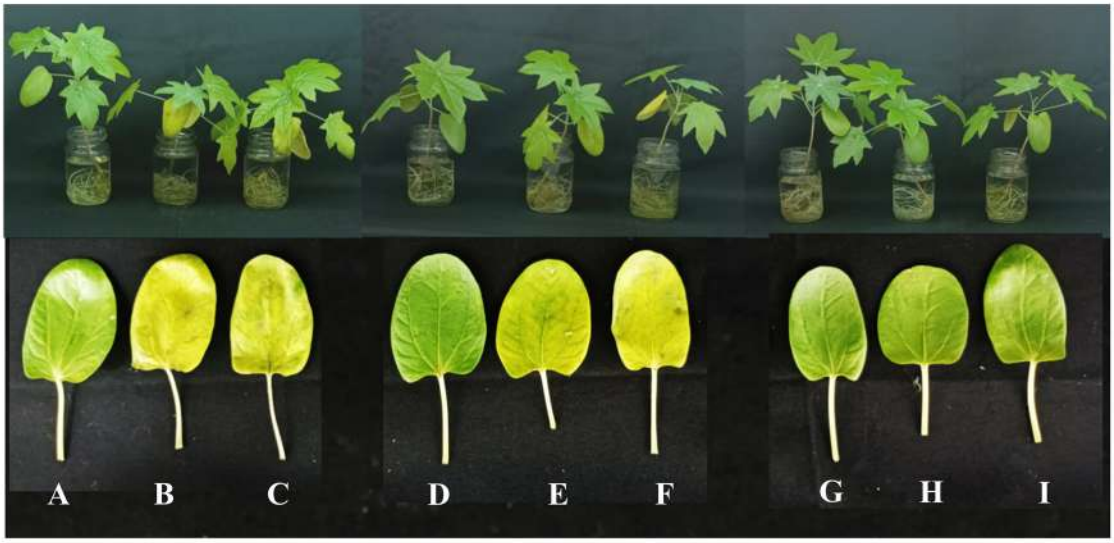

Figure 4. *Ricinus communis* seedlings and the phenotypic changes in the cotyledonary leaves after exposure to $CuSO_4$and cytokinins for 6 d. A: control; B: 80 µM $CuSO_4$; C: 160 µM $CuSO_4$; D: control + KIN; E: 80 µM $CuSO_4$+ KIN; F: 160 µM $CuSO_4$+ KIN; G: control + BAP; H: 80 µM $CuSO_4$+ BAP; and I: 160 µM $CuSO_4$+ BAP.

reductions of MC% in the cotyledonary leaves from 4 d of exposure. At concentrations above 120 μM $CuSO_4$, the reductions in MC% were to the extent of 14-20% on 4 d as compared to that of the control, which reduced further (27-33%) on 6 d of exposure.

An insignificant reduction in MC% was noticed in the primary leaves of *R. communis* seedlings subjected to Cu stress during the treatment period as compared to the respective controls. The reduction was only ≤ 2.5% in all the treatments up to 6 d of $CuSO_4$ exposure. On 10 d of treatment, the reduction of MC% in primary leaves was up to 5.4% at higher $CuSO_4$ concentrations as compared to the control (Table 10).

Similar to the primary leaves, the reduction of MC% was minimum and insignificant in the roots of *R. communis* seedlings, even at higher concentrations of the treatment period. A slight reduction of MC% (only 5%) was observed on exposure to 40 μM $CuSO_4$ on 4 d. But, on further days of exposure, the reduction of MC% became less and on 10 d, a minute enhancement (1.8%) in MC% was noticed in the roots at 200 μM $CuSO_4$ (Table 10).

The reductions in MC% were to the extent of 17 and 27% in cotyledonary leaves subjected to 80 and 160 μM $CuSO_4$ treatments respectively. On application of KIN and BAP along with $CuSO_4$, MC% of cotyledonary leaves was increased significantly. The enhancement was 23-28% and 23-39% respectively on application of KIN and BAP along with $CuSO_4$ as compared to those exposed to $CuSO_4$ alone (Table 9).

4.2.1.3. Relative water content (RWC)

Copper stress resulted in significant reductions of RWC in the cotyledonary leaves of *R. communis* seedlings (Table 11). On 2 d of Cu stress, the reduction was insignificant in the cotyledonary leaves even at higher

$CuSO_4$ concentrations, and the reduction was only 4-14% as compared to that of the control. In contrast, RWC was decreased to 58-72% in the cotyledonary leaves of *R. communis* seedlings exposed to 120-200 µM $CuSO_4$ on 4 and 6 d.

In the case of primary leaves, a gradual decline in RWC was observed upon increasing concentrations of $CuSO_4$ and days of exposure. The reductions in RWC were ≤ 14% in the primary leaves even on exposure to higher concentrations of $CuSO_4$ on 6 d. On exposure to 160 and 200 µM $CuSO_4$, the RWC of primary leaves were decreased significantly to the extent of 29-31% on 10 d as compared to that of the control (Table 11).

A comparatively insignificant reduction in RWC was observed in the roots of *R. communis* seedlings subjected to increasing concentrations of $CuSO_4$ up to 6 d. From 8 d onwards, the RWC of roots was enhanced and reached the level almost the same as that of the control (Table 11).

The reductions in RWC were to the extent of 60 and 68% in the cotyledonary leaves of *R. communis* on exposure to 80 and 160 µM $CuSO_4$ respectively. On application of KIN and BAP along with $CuSO_4$, RWC of cotyledonary leaves was increased significantly. The enhancement was recorded as 108 and 80% in 80 and 160 µM $CuSO_4$ treated cotyledonary leaves respectively during KIN application as compared to those exposed to $CuSO_4$ alone, whereas the increase was 138 and 131% on BAP application along with 80 and 160 µM $CuSO_4$ (Table 9).

4.2.1.4. Total chlorophyll content

Copper stress resulted in the decrease of total chlorophyll content in the cotyledonary leaves of *R. communis* seedlings. The reduction was found to be insignificant on 2 d of $CuSO_4$ exposure, but significant at later stages of the treatment period. On 6 d, the reduction of total chlorophyll content

Table 8. Dry weight percentage (DW%) in the cotyledonary leaves, primary leaves and roots of *R. communis* seedlings subjected to increasing concentrations of $CuSO_4$ (Control, 40, 80, 120, 160 and 200 µM) for 10 d. Values are the mean ± SE of three independent experiments. Different alphabetical letters indicate significant difference between treatments (Duncan's test $p \leq 0.05$).

Plant parts	$CuSO_4$ (µM)	Dry weight percentage (DW%)					
		0 d	2 d	4 d	6 d	8 d	10 d
Cotyledonary leaf	Control	10.24 ± 0.52^{a}	10.0 ± 0.61^{b}	9.91 ± 0.73^{c}	10.17 ± 0.65^{c}	-	-
	40	10.17 ± 0.68^{a}	10.34 ± 0.66^{ab}	8.65 ± 0.39^{c}	10.46 ± 0.66^{c}	-	-
	80	10.25 ± 0.61^{a}	9.56 ± 0.35^{b}	9.89 ± 0.53^{c}	25.81 ± 1.21^{b}	-	-
	120	10.18 ± 0.34^{a}	11.22 ± 0.72^{ab}	27.78 ± 0.85^{a}	40.0 ± 2.38^{a}	-	-
	160	10.31 ± 0.42^{a}	12.22 ± 0.68^{a}	22.86 ± 0.95^{b}	34.78 ± 3.65^{a}	-	-
	200	10.22 ± 0.55^{a}	11.34 ± 0.56^{ab}	28.0 ± 1.25^{a}	40.0 ± 5.29^{a}	-	-
Primary leaf	Control	11.90 ± 0.65^{a}	10.0 ± 0.34^{a}	9.47 ± 0.67^{ab}	9.48 ± 0.52^{a}	10.25 ± 0.68^{a}	10.56 ± 1.05^{a}
	40	9.52 ± 0.42^{a}	9.09 ± 0.57^{a}	9.41 ± 0.81^{b}	11.29 ± 1.19^{a}	13.04 ± 2.34^{a}	13.95 ± 1.59^{a}
	80	10.91 ± 0.58^{a}	9.76 ± 0.38^{a}	9.78 ± 0.61^{ab}	10.64 ± 1.24^{a}	12.33 ± 2.16^{a}	12.77 ± 2.19^{a}
	120	9.99 ± 0.64^{a}	11.11 ± 0.67^{a}	10.87 ± 0.37^{ab}	10.14 ± 1.35^{a}	12.50 ± 0.84^{a}	12.22 ± 3.04^{a}
	160	10.25 ± 0.24^{a}	10.714 ± 0.72^{a}	11.43 ± 0.51^{a}	11.76 ± 0.94^{a}	14.67 ± 1.29^{a}	15.38 ± 3.18^{a}
	200	11.13 ± 0.26^{a}	10.94 ± 0.84^{a}	11.39 ± 0.42^{a}	10.26 ± 0.86^{a}	14.75 ± 0.86^{a}	13.04 ± 3.64^{a}
Root	Control	5.60 ± 0.32^{a}	6.12 ± 0.43^{c}	5.88 ± 0.55^{c}	5.99 ± 0.55^{b}	8.11 ± 0.78^{ab}	7.43 ± 0.54^{ab}
	40	5.56 ± 0.34^{a}	7.76 ± 0.53^{abc}	10.78 ± 0.95^{a}	7.86 ± 0.24^{a}	8.55 ± 0.84^{ab}	7.40 ± 0.64^{ab}
	80	4.95 ± 0.24^{a}	6.60 ± 0.46^{c}	9.45 ± 1.62^{ab}	6.92 ± 0.34^{ab}	7.08 ± 0.67^{b}	8.45 ± 0.51^{a}
	120	5.12 ± 0.38^{a}	9.42 ± 0.58^{a}	6.49 ± 0.25^{c}	5.68 ± 0.37^{b}	9.92 ± 0.48^{a}	7.63 ± 0.72^{ab}
	160	4.96 ± 0.26^{a}	7.21 ± 0.64^{bc}	6.89 ± 0.42^{bc}	5.56 ± 0.72^{b}	9.30 ± 0.74^{ab}	7.40 ± 0.84^{ab}
	200	5.02 ± 0.37^{a}	8.54 ± 0.59^{ab}	6.67 ± 0.43^{c}	6.67 ± 0.34^{ab}	8.39 ± 0.68^{ab}	5.79 ± 0.39^{b}

Table 9. Dry weight percentage (DW%), moisture content percentage (MC%) and relative water content (RWC) in the cotyledonary leaves of *R. communis* on 6 d of exposure to $CuSO_4$ (80 and 160 µM) and cytokinins (KIN and BAP). Values are the mean ± SE of three independent experiments. Different alphabetical letters indicate significant difference between treatments (Duncan's test $p \leq 0.05$).

Treatments	DW%	MC%	RWC
Control	10.169 ± 0.51^{d}	89.831 ± 4.49^{a}	86.179 ± 4.31^{b}
80 µM $CuSO_4$	25.806 ± 1.29^{b}	74.194 ± 3.71^{b}	37.097 ± 1.85^{e}
160 µM $CuSO_4$	34.783 ± 1.74^{a}	65.217 ± 3.26^{c}	27.273 ± 1.36^{f}
Control + KIN	8.511 ± 0.426^{e}	91.489 ± 4.57^{a}	91.489 ± 4.57^{ab}
80 µM $CuSO_4$ + KIN	8.642 ± 0.43^{de}	91.358 ± 4.57^{a}	77.083 ± 3.85^{c}
160 µM $CuSO_4$ + KIN	16.667 ± 0.83^{c}	83.333 ± 4.17^{a}	49.180 ± 2.46^{d}
Control + BAP	8.421 ± 0.421^{e}	91.579 ± 4.58^{a}	93.548 ± 4.68^{a}
80 µM $CuSO_4$ + BAP	9.0 ± 0.45^{de}	91.0 ± 4.55^{a}	88.349 ± 4.42^{ab}
160 µM $CuSO_4$ + BAP	9.211 ± 0.46^{de}	90.789 ± 4.54^{a}	76.667 ± 3.83^{c}

Table 10. Moisture content percentage (MC%) in the cotyledonary leaves, primary leaves and roots of *R. communis* seedlings subjected to increasing concentrations of $CuSO_4$ (Control, 40, 80, 120, 160 and 200 µM) for 10 d. Values are the mean ± SE of three independent experiments. Different alphabetical letters indicate significant difference between treatments (Duncan's test $p \leq 0.05$).

Plant parts	$CuSO_4$ (µM)	Moisture content percentage (MC%)					
		0 d	2 d	4 d	6 d	8 d	10 d
Cotyledonary leaf	Control	89.76 ± 4.45^{a}	89.88 ± 5.24^{a}	90.09 ± 5.64^{ab}	89.83 ± 4.92^{a}	-	-
	40	89.83 ± 4.42^{a}	89.66 ± 3.95^{a}	91.35 ± 3.68^{a}	89.53 ± 4.19^{a}	-	-
	80	90.35 ± 4.58^{a}	90.43 ± 4.68^{a}	90.11 ± 3.53^{ab}	74.19 ± 4.32^{b}	-	-
	120	90.26 ± 4.28^{a}	88.78 ± 3.25^{a}	72.22 ± 5.21^{c}	60.0 ± 3.22^{c}	-	-
	160	91.67 ± 5.12^{a}	87.78 ± 2.25^{a}	77.14 ± 2.39^{bc}	65.22 ± 3.19^{bc}	-	-
	200	92.19 ± 5.3^{a}	88.66 ± 2.58^{a}	72.0 ± 3.24^{c}	60.0 ± 5.26^{c}	-	-
Primary leaf	Control	88.10 ± 5.6^{a}	90.0 ± 5.47^{a}	90.53 ± 4.59^{a}	90.52 ± 5.31^{a}	89.74 ± 3.45^{a}	89.44 ± 5.64^{a}
	40	90.48 ± 6.29^{a}	90.91 ± 4.16^{a}	90.59 ± 5.42^{a}	88.71 ± 3.25^{a}	86.95 ± 4.10^{a}	86.05 ± 4.08^{a}
	80	89.09 ± 6.16^{a}	90.24 ± 4.35^{a}	90.22 ± 5.21^{a}	89.36 ± 4.04^{a}	87.67 ± 3.16^{a}	87.23 ± 4.07^{a}
	120	91.25 ± 5.31^{a}	88.89 ± 5.73^{a}	89.13 ± 3.42^{a}	89.86 ± 3.86^{a}	87.5 ± 2.59^{a}	87.78 ± 3.94^{a}
	160	92.0 ± 7.28^{a}	89.28 ± 6.18^{a}	88.57 ± 3.75^{a}	88.23 ± 3.47^{a}	85.33 ± 3.58^{a}	84.62 ± 3.75^{a}
	200	90.25 ± 7.15^{a}	89.06 ± 3.48^{a}	88.61 ± 3.47^{a}	89.74 ± 3.09^{a}	85.24 ± 3.72^{a}	86.96 ± 2.95^{a}
Root	Control	94.40 ± 2.44^{a}	93.88 ± 3.31^{a}	94.11 ± 2.54^{a}	94.01 ± 3.21^{a}	91.89 ± 4.24^{a}	92.57 ± 3.31^{a}
	40	94.44 ± 3.48^{a}	92.24 ± 4.21^{a}	89.22 ± 4.21^{a}	92.14 ± 3.58^{a}	91.45 ± 3.25^{a}	92.59 ± 2.54^{a}
	80	95.25 ± 3.24^{a}	93.39 ± 3.51^{a}	90.55 ± 3.24^{a}	93.08 ± 2.57^{a}	92.92 ± 3.35^{a}	91.55 ± 3.33^{a}
	120	94.23 ± 3.31^{a}	90.58 ± 3.15^{a}	93.51 ± 3.58^{a}	94.32 ± 2.56^{a}	90.08 ± 2.38^{a}	92.37 ± 3.84^{a}
	160	96.20 ± 3.34^{a}	92.79 ± 3.21^{a}	93.10 ± 3.65^{a}	94.44 ± 2.85^{a}	90.69 ± 3.09^{a}	92.59 ± 3.20^{a}
	200	94.51 ± 4.32^{a}	91.46 ± 3.88^{a}	93.33 ± 3.53^{a}	93.33 ± 3.15^{a}	91.60 ± 3.75^{a}	94.20 ± 2.22^{a}

Table 11. Relative water content (RWC) in the cotyledonary leaves, primary leaves and roots of *R. communis* seedlings subjected to increasing concentrations of $CuSO_4$ (Control, 40, 80, 120, 160 and 200 µM) for 10 d. Values are the mean ± SE of three independent experiments. Different alphabetical letters indicate significant difference between treatments (Duncan's test $p \leq 0.05$).

Plant parts	$CuSO_4$ (µM)	Relative water content (RWC)					
		0 d	2 d	4 d	6 d	8 d	10 d
Cotyledonary leaf	Control	94.21 ± 5.56^{a}	95.58 ± 6.14^{a}	85.47 ± 5.16^{ab}	86.18 ± 4.25^{a}	-	-
	40	94.64 ± 6.25^{a}	91.23 ± 4.67^{a}	93.13 ± 4.57^{a}	78.57 ± 3.28^{a}	-	-
	80	94.25 ± 4.58^{a}	88.89 ± 4.28^{a}	78.09 ± 4.28^{b}	37.10 ± 3.64^{b}	-	-
	120	95.01 ± 3.25^{a}	85.29 ± 3.19^{a}	36.11 ± 2.58^{c}	21.95 ± 3.16^{c}	-	-
	160	93.86 ± 6.54^{a}	82.29 ± 5.18^{a}	32.93 ± 4.26^{c}	27.27 ± 2.17^{bc}	-	-
	200	95.20 ± 4.61^{a}	82.69 ± 6.25^{a}	32.73 ± 3.56^{c}	24.49 ± 2.19^{c}	-	-
Primary leaf	Control	97.37 ± 2.55^{a}	88.89 ± 5.54^{ab}	84.31 ± 5.64^{a}	86.06 ± 6.21^{a}	91.30 ± 4.21^{a}	90.07 ± 5.46^{a}
	40	98.70 ± 2.02^{a}	97.56 ± 1.36^{a}	79.38 ± 6.58^{a}	83.33 ± 5.48^{a}	83.33 ± 3.24^{ab}	81.32 ± 5.24^{a}
	80	97.66 ± 2.22^{a}	89.16 ± 4.35^{ab}	81.37 ± 4.28^{a}	84.85 ± 3.85^{a}	75.29 ± 4.25^{bc}	79.61 ± 4.21^{a}
	120	96.25 ± 3.05^{a}	84.70 ± 5.21^{ab}	75.92 ± 5.47^{a}	84.93 ± 6.21^{a}	76.83 ± 3.86^{bc}	79.0 ± 3.42^{a}
	160	92.50 ± 4.55^{a}	91.46 ± 4.35^{ab}	73.80 ± 6.24^{a}	82.19 ± 5.24^{a}	69.56 ± 3.15^{bc}	63.22 ± 4.88^{b}
	200	94.24 ± 5.26^{a}	74.02 ± 7.58^{b}	72.92 ± 8.21^{a}	73.68 ± 6.05^{a}	64.20 ± 3.85^{c}	62.50 ± 4.53^{b}
Root	Control	99.16 ± 0.22^{a}	97.87 ± 1.11^{a}	93.20 ± 2.54^{a}	98.37 ± 0.55^{a}	97.55 ± 0.92^{a}	93.10 ± 3.28^{ab}
	40	99.17 ± 0.55^{a}	95.53 ± 1.34^{ab}	81.98 ± 3.58^{b}	99.23 ± 0.25^{a}	98.07 ± 0.89^{a}	97.42 ± 1.05^{a}
	80	98.36 ± 1.02^{a}	90.0 ± 1.58^{b}	97.29 ± 1.01^{a}	90.98 ± 2.54^{a}	93.75 ± 1.29^{b}	98.24 ± 0.66^{a}
	120	94.25 ± 2.25^{a}	92.59 ± 2.10^{ab}	91.14 ± 2.31^{a}	97.65 ± 1.16^{a}	98.16 ± 0.55^{a}	85.21 ± 2.56^{b}
	160	97.35 ± 1.02^{a}	97.17 ± 1.22^{a}	93.91 ± 2.51^{a}	99.27 ± 1.08^{a}	99.15 ± 0.27^{a}	88.03 ± 3.43^{b}
	200	95.67 ± 3.04^{a}	77.32 ± 2.56^{c}	95.89 ± 2.56^{a}	92.72 ± 3.67^{a}	98.17 ± 0.65^{a}	98.48 ± 0.85^{a}

recorded in the cotyledonary leaves subjected to 160 and 200 μM $CuSO_4$ was 43 and 48% respectively, as compared to the control (Fig. 5A).

Similar to the cotyledonary leaves, total chlorophyll content in the primary leaves also decreased on exposure to Cu stress. On 6 d, the reduction in total chlorophyll content was ≤ 30% even at 200 μM $CuSO_4$ treatment. In contrast, on the following days of treatment (8 and 10 d), total chlorophyll content was decreased to 38-41% in the primary leaves of seedlings treated with 160 and 200 μM $CuSO_4$ with respect to that of the control (Fig. 5B).

Copper stress mediated reductions in total chlorophyll content in the cotyledonary leaves were 28 and 38% when exposed to 80 and 160 μM $CuSO_4$ respectively, as compared to the control. Exogenous application of KIN and BAP resulted in significant increase in total chlorophyll content as compared to $CuSO_4$ treatments alone. During KIN application, total chlorophyll contents were enhanced by 32 and 57% in 80 and 160 μM $CuSO_4$ treated cotyledonary leaves respectively as compared to those exposed to $CuSO_4$ alone. However, BAP application resulted in 77% enhancement in total chlorophyll content of cotyledonary leaves in seedlings exposed to both the $CuSO_4$ concentrations as compared to these exposed to $CuSO_4$ alone (Fig. 5C).

4.2.1.5. Carotenoids content

In contrast to the chlorophyll content, carotenoids content in the cotyledonary leaves was enhanced at mild doses of $CuSO_4$ on initial days, and the maximum enhancement (35%) was recorded on exposure to 40 μM $CuSO_4$ on 4 d. But, on 6 d of $CuSO_4$ exposure, carotenoids content was reduced significantly. At 200 μM $CuSO_4$ treatment, carotenoids content was decreased to 44% on 6 d with respect to that of the control (Fig. 6A).

In primary leaves, the carotenoids content was gradually and significantly decreased from 4 d onwards with increasing concentration of $CuSO_4$. Highly significant reduction in carotenoids content in the primary leaves of *R. communis* seedlings was observed on 8 and 10 d of $CuSO_4$ exposure, which was to the extent of 40-54% in all the treatments (Fig. 6B).

On exposure of *R. communis* seedlings to $CuSO_4$, there was a reduction in the carotenoids content (> 50%) in the cotyledonary leaves, and cytokinin application along with Cu stress lead to the enhancement in the carotenoids contents. On treatment of *R. communis* with 80 and 160 µM $CuSO_4$ along with KIN, carotenoids content in the cotyledonary leaves was enhanced by 14 and 81%, respectively, as compared to those exposed to $CuSO_4$ alone. During BAP application along with Cu stress, the enhancement was 150 and 96% in the cotyledonary leaves of 80 and 160 µM $CuSO_4$ treated seedlings as compared to that of Cu stress alone (Fig. 6C).

4.2.1.6. Photosystem (PS) I activities

A drastic reduction in the PSI activities was observed in the cotyledonary leaves of *R. communis* seedlings subjected to increasing concentrations of $CuSO_4$. The reduction was 5-34% on exposure to 40 to 200 µM $CuSO_4$ on 2 d of treatment with respect to the control, and the reductions became more severe on further days of $CuSO_4$ exposure. Treatment of *R. communis* seedlings with 160 and 200 µM $CuSO_4$ resulted in $\geq$ 80% reductions in the PSI activities of the cotyledonary leaves on 6 d (Fig. 7A).

Similar to the cotyledonary leaves, the PSI activities were reduced drastically and significantly in primary leaves also, on exposure to increasing concentrations of $CuSO_4$. The PSI activity was reduced by 8-58% in the primary leaves even at 2 d of $CuSO_4$ treatment. The reductions were 78 and

85% on 8 and 10 d respectively upon exposure to 200 µM $CuSO_4$ as compared to that of the controls (Fig. 7B).

The reductions in PSI activity were 66 and 82% in the cotyledonary leaves of 80 and 160 µM $CuSO_4$ treated *R. communis* seedlings as compared to that of the control. On application of KIN and BAP in Cu-stressed seedlings, the activities of PSI increased significantly. In the case of KIN application along with 80 and 160 µM $CuSO_4$, PSI activity was enhanced by 2 and 3 folds respectively, as compared to that of $CuSO_4$ alone. During BAP application, the enhancement in PSI activity was 3 and 4 folds in the cotyledonary leaves of seedlings exposed to 80 and 160 µM $CuSO_4$ respectively, as compared to that exposed to Cu stress alone (Fig. 7C).

4.2.1.7. Photosystem (PS) II activities

Similar to the reductions in the PSI activities, the activities of PSII were also significantly reduced in both the cotyledonary and primary leaves of *R. communis* seedlings with increase in the concentration of $CuSO_4$ and days of exposure (Fig. 8A and B). In the case of cotyledonary leaves, the PSII activity was reduced up to 60% with increase in $CuSO_4$ concentrations with respect to the control even on 2 d of exposure. On 6 d of exposure to $CuSO_4$, the reductions were 81-92% upon treatment with 120-200 µM $CuSO_4$ as compared to that of the control (Fig. 8A).

In primary leaves, the reduction in PSII activity was 22-56% on exposure to increasing concentrations of $CuSO_4$ up to 4 d of treatment, and the reductions were more severe on further days of $CuSO_4$ exposure. On 6 d of treatment, the reduction in PSII activity became 63%, which was further reduced to 66 and 88% on 8 and 10 d respectively in the primary leaves subjected to 200 µM $CuSO_4$ as compared to the respective controls (Fig. 8B).

Exposure to 80 and 160 µM $CuSO_4$ resulted in 70 and 86% reductions in PSII activities in the cotyledonary leaves of *R. communis* seedlings, which was more or less restored upon application of cytokinins, most significantly in seedlings exposed to BAP along with $CuSO_4$. During KIN and BAP application along with 80 and 160 µM $CuSO_4$, 2-6 folds increase in PSII activities were recorded in the cotyledonary leaves as compared to that exposed to Cu stress alone, with maximum enhancement of 6 folds in 160 µM $CuSO_4$ + BAP (Fig. 8C).

4.2.1.8. Chlorophyll *a* fluorescence induction curve and JIP parameters

4.2.1.8.1. Effects of Cu on chlorophyll *a* fluorescence induction curve and JIP parameters

The alterations in the light-dependent photosynthetic process in the cotyledonary and primary leaves of *R. communis* seedlings subjected to increasing concentrations of $CuSO_4$ were observed in the shape of induction curves of chlorophyll *a* fluorescence (Fig. 9). The fluorescence intensity represented on logarithmic time scale starts with initial fluorescence (Fo) at 'O' level, through transitional fluorescence Fj and Fi at 'J' and 'I' levels, respectively, to the point of maximum fluorescence (Fm) at 'P' level, reveals the proper functioning of PSII. Copper toxicity significantly modified the OJIP curve of the cotyledonary leaves as compared to the primary leaves of *R. communis* seedlings on 4 d of exposure (Fig. 9A and B). In the cotyledonary leaves, Cu stress resulted in the significant enhancement in Fo, which was increased by 16-67% in various concentrations of $CuSO_4$ as compared to the control. In the case of Fm, a severe reduction was observed in Cu-treated cotyledonary leaves, which was to the extent of 7-57% compared to the control. Cotyledonary leaves treated with 160 and 200 µM $CuSO_4$ resulted in the flattening of the OJIP curve, as the shape of the transient was significantly

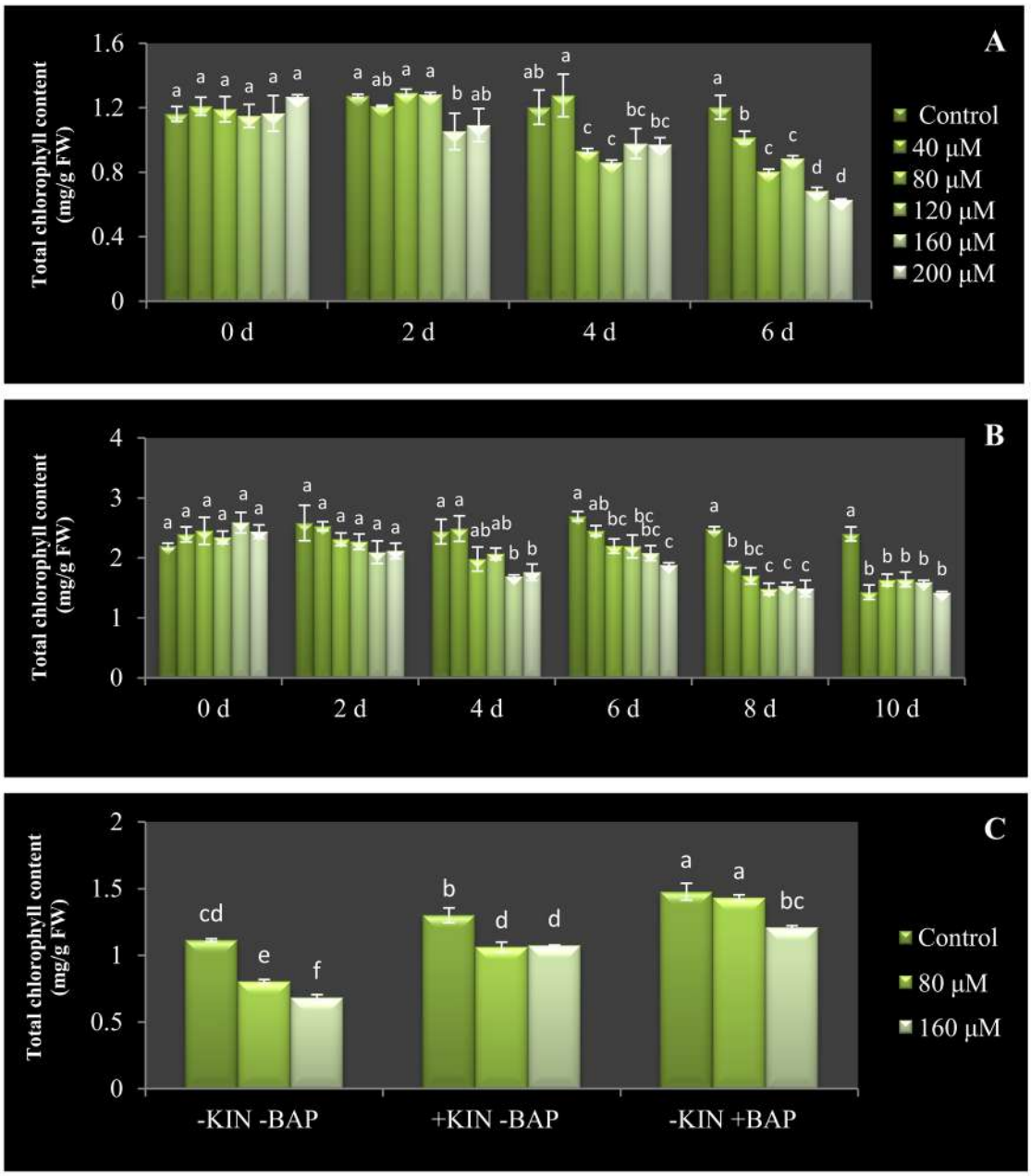

Figure 5. Total chlorophyll contents in the cotyledonary leaves (A), primary leaves (B), and cotyledonary leaves (exposed to cytokinins for 6 d) (C) of *R. communis* seedlings subjected to increasing concentrations of $CuSO_4$. Different alphabetical letters indicate significant difference between treatments (Duncan's test $p \leq 0.05$).

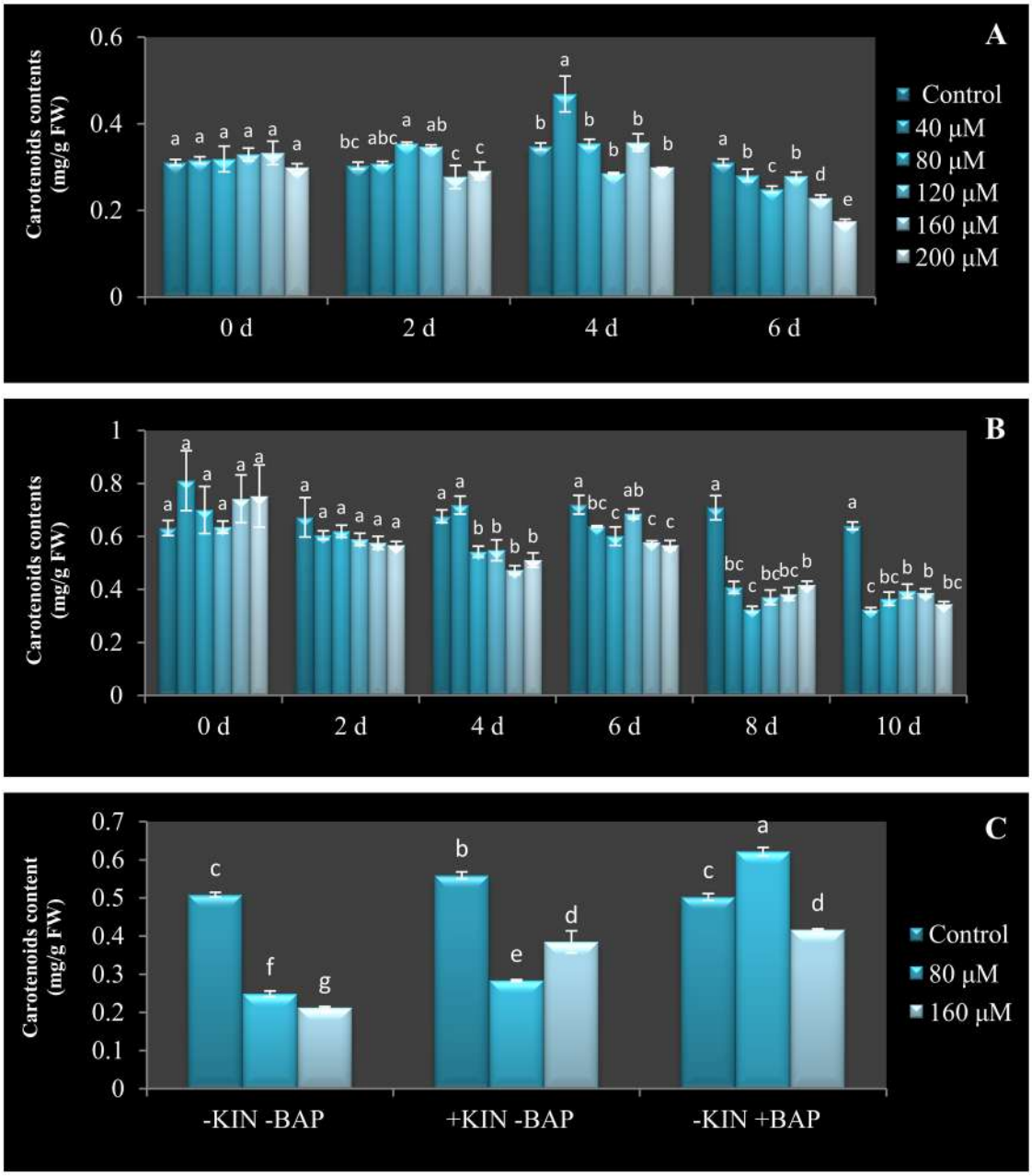

Figure 6. Carotenoids contents in the cotyledonary leaves (A), primary leaves (B), and cotyledonary leaves (exposed to cytokinins for 6 d) (C) of *R. communis* seedlings subjected to increasing concentrations of $CuSO_4$. Different alphabetical letters indicate significant difference between treatments (Duncan's test $p \leq 0.05$).

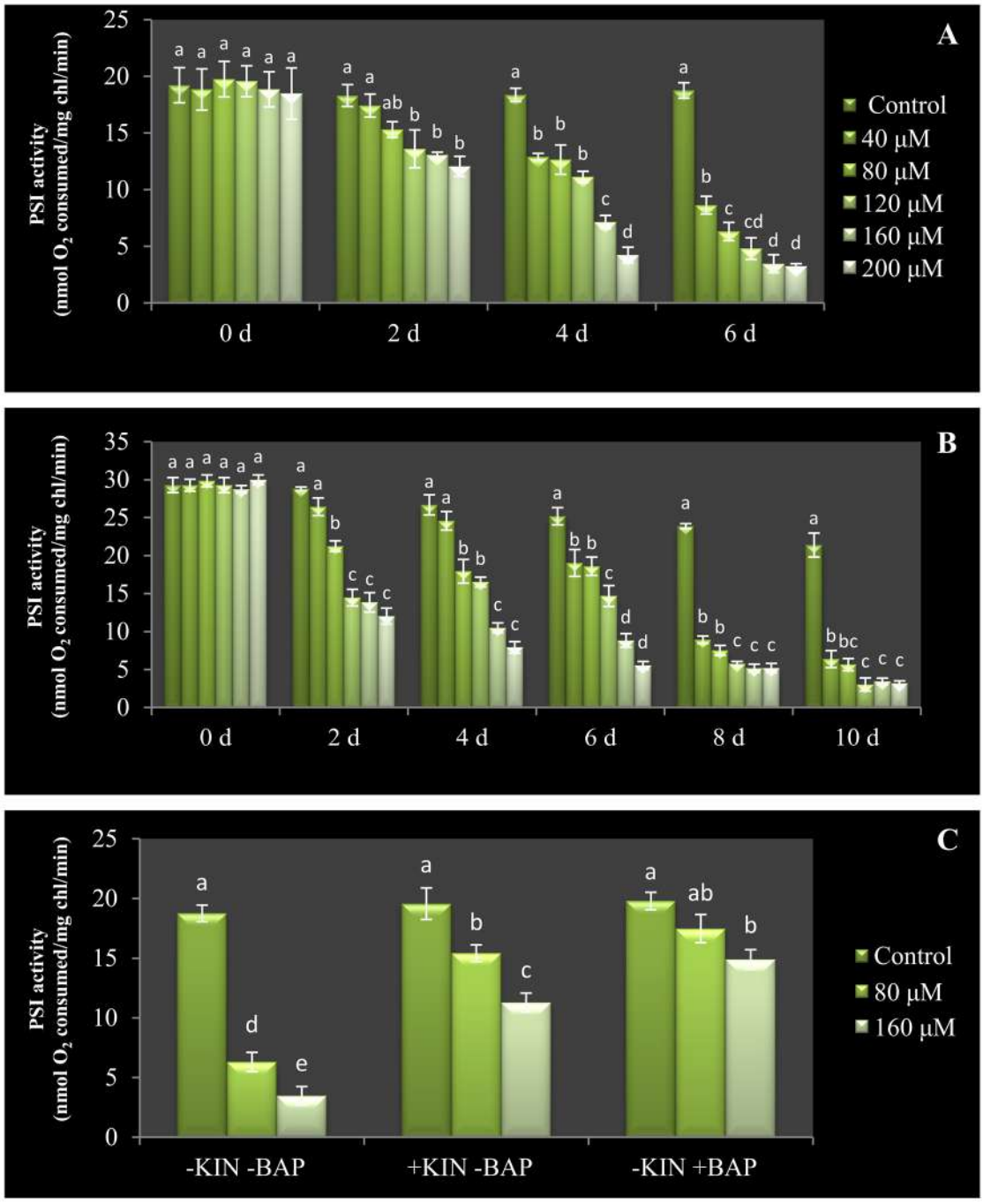

Figure 7. Photosystem (PS) I activities in the cotyledonary leaves (A), primary leaves (B), and cotyledonary leaves (exposed to cytokinins for 6 d) (C) of *R. communis* seedlings subjected to increasing concentrations of $CuSO_4$. Different alphabetical letters indicate significant difference between treatments (Duncan's test $p \leq 0.05$).

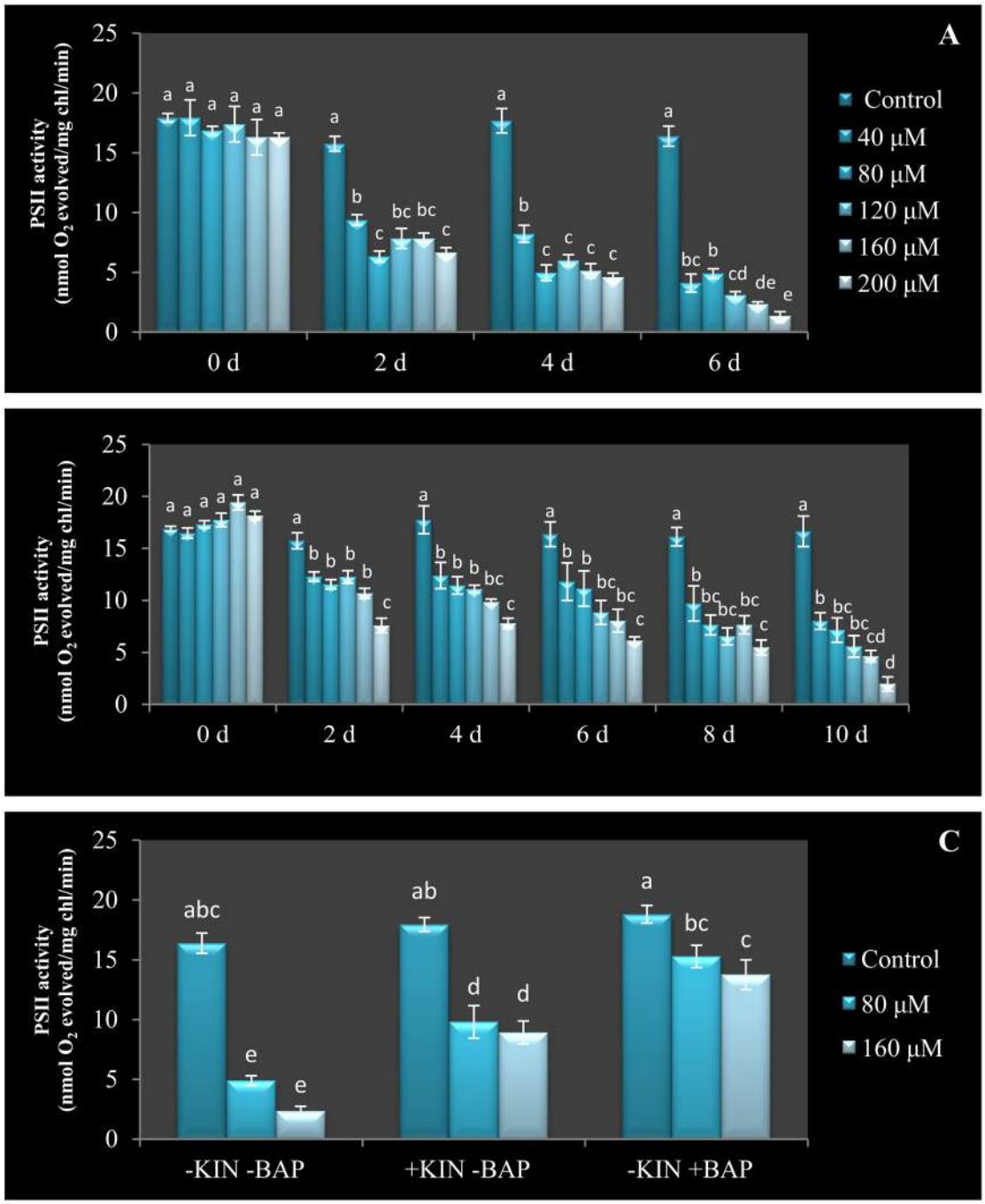

Figure 8. Photosystem (PS) II activities in the cotyledonary leaves (A), primary leaves (B), and cotyledonary leaves (exposed to cytokinins for 6 d) (C) of *R. communis* seedlings subjected to increasing concentrations of $CuSO_4$. Different alphabetical letters indicate significant difference between treatments (Duncan's test $p \leq 0.05$).

altered, especially at the J and I peak (chlorophyll fluorescence transient at 2 and 30 ms respectively).

In the case of primary leaves, Cu did not significantly affect the standard shape of the OJIP curves on 4 d of exposure to toxicity (Fig. 9B). Accordingly, the Fo and Fm values were maintained more or less similar to that of the control under Cu toxicity in the primary leaves. However, after the Cu-induced abscission of the cotyledonary leaves, a slight modification in the OJIP curve was observed in the primary leaves (Fig. 9C). On 10 d of $CuSO_4$ exposure, though no significant variation was observed in Fo, a 16% reduction in Fm was noticed at 200 μM $CuSO_4$.

In the radar plot representing various fluorescence parameters and performance indices, pronounced changes were observed in the cotyledonary leaves when subjected to Cu stress as compared to the control seedlings (Fig. 10A). A pronounced enhancement was observed in the Tf(max), time taken to reach Fm, in the cotyledonary leaves upon exposure to increasing levels of Cu. The increase in Tf(max) was 97% over the control in the cotyledonary leaves subjected to 200 μM $CuSO_4$. At the same time, the area above the chlorophyll *a* fluorescence curve between Fo and Fm was decreased drastically in the cotyledonary leaves as a result of Cu stress, and the reduction was about 34-82% with increase in concentration of $CuSO_4$. The maximum efficiency of water splitting complex represented as Fv/Fo, was also reduced due to $CuSO_4$ treatment in the cotyledonary leaves, and the prominent reduction was noticed on exposure to 120-200 μM $CuSO_4$ (Fig. 10A).

In the case of primary leaves, an insignificant variation was observed in the fluorescence parameters on 4 d of $CuSO_4$ treatment (Fig. 10B). A slight enhancement in Tf(max) was observed in primary leaves at low concentrations of $CuSO_4$ treatment (40 and 80 μM), whereas it was reduced at

higher concentrations (120-200 μM $CuSO_4$). On 10 d of $CuSO_4$ exposure, Tf(max) was reduced up to 34% in primary leaves. The reductions in area and Fv/Fo were ≤ 18 and 9% respectively for all the $CuSO_4$ treatments as compared to the respective controls. However, on 10 d of Cu stress, the reductions in area and Fv/Fo were more prominent in primary leaves, and reduced up to 57 and 35% respectively, as compared to the control (Fig. 10C).

Copper induced change in the turnover number of Q_A, as represented by N, was visualized in the radar plot. The reduction in N was up to 41% in cotyledonary leaves subjected to Cu stress on 4 d. However, the reductions in N were only 12 and 16% in primary leaves subjected 200 μM $CuSO_4$ on 4 and 10 d respectively (Fig). The structure-function-index or the vitality index of PSII as represented by SFI(abs) was declined significantly, and the reduction ranges from 44 to 89% in the cotyledonary leaves upon exposure to 40 to 200 μM $CuSO_4$ as compared to the control. However, the reduction in SFI(abs) was only 17-25% in primary leaves on exposure to 120-200 μM $CuSO_4$ as compared to the control on 4 d, though no variations were observed at 40 and 80 μM $CuSO_4$ treatments. On the other hand, the reduction in SFI(abs) was to the extent of 28-65% as compared to the control in the primary leaves on 10 d of exposure to 40-200 μM $CuSO_4$ (Fig. 10).

The fluorescence yield parameters, including photochemical and non-photochemical quantum yields, exhibited prominent variations during $CuSO_4$exposure. The values of PHI(Po), PHI(Eo) and PSIo were significantly reduced, and the reductions were 48, 77 and 65% respectively in cotyledonary leaves of *R. communis* seedlings subjected to 120-200 μM $CuSO_4$. On the other hand, the reductions in these yield parameters were ≤ 11% only as compared to the respective controls in the primary leaves even exposed to 200 μM$CuSO_4$ on 4 d. In contrast, on 10 d, the reductions in PHI(Po), PHI(Eo)

and PSIo exceeded 9, 42 and 36% respectively over the control in the primary leaves subjected to 200 μM $CuSO_4$ (Fig. 10).

The capturing and conversion efficiency of harvested light energy, represented as Fv/Fm, was decreased drastically in the cotyledonary leaves upon exposure to Cu stress. At normal conditions, the value of Fv/Fm was maintained in the range of 0.80 to 0.84. In the cotyledonary leaves of the control seedlings, the value was 0.834, which decreased to 0.795 on exposure to 40 μM $CuSO_4$ and further to 0.392 at 200 μM $CuSO_4$ treatments (53% reduction over the control) on 4 d. In contrast to this result, in primary leaves on 4 and 10 d of $CuSO_4$ exposure, the reduction in Fv/Fm was insignificant. The value of Fv/Fm noticed was 0.84 in control, which was reduced to 0.82 and 0.81 only in the primary leaves of seedlings exposed to 200 μM $CuSO_4$ on 4 and 10 d respectively (Table 12).

The relative variable fluorescence at J step represented as Vj measured in the cotyledonary leaves on exposure to 40-200 μM $CuSO_4$ on 4 d, increased to 22-58% as compared to the cotyledonary leaves of the control seedlings. In primary leaves on 4 d, the increase in Vj was only up to 14% upon exposure to increasing levels of $CuSO_4$. In contrast, on abscission of cotyledonary leaves, Vj was significantly enhanced in the primary leaves. The maximum increase in Vj was 58% in the primary leaves subjected to 200 μM $CuSO_4$ on 10 d as compared to the control (Table 12).

The performance indices such as PI(abs) and PI(total) were significantly reduced in both the leaves due to Cu toxicity. In cotyledonary leaves, the reduction in PI(abs) and PI(total) exceeded 90% on exposure to 200 μM $CuSO_4$ as compared to that of the control on 4 d. On the same day, the reduction in these parameters was ≤ 40% in primary leaves subjected to increasing concentrations of $CuSO_4$. However, on 10 d of $CuSO_4$ exposure, the reductions in PI(abs) and PI(total) were 76 and 82% respectively in

primary leaves subjected to 200 μM $CuSO_4$ compared to the control (Table 12).

The PSII-relative driving force, denoted as DF(total), was reduced drastically in both the leaves of *R. communis* seedlings during severe stress situations. In the cotyledonary leaves, DF(total) was found to be reduced by 3 to 4 folds on exposure to 120-200 μM $CuSO_4$ compared to the control on 4 d, whereas the reduction in DF(total) was less in primary leaves on the same day of $CuSO_4$ exposure. However, on 10 d of Cu stress, the DF(total) was significantly reduced in primary leaves, and the reduction recorded was up to 2 folds as compared to the control (Table 12).

The photosynthetic capabilities of the cotyledonary and primary leaves of *R. communis* under different concentrations of $CuSO_4$ is clearly visualized in the energy pipeline leaf models such as phenomenological energy fluxes per cross-section and phenomenological energy fluxes per single reaction center (Fig. 11, 12, 13, 14, 15 and 16). These models also describe the stepwise flow of energy through PSII at the level of cross-section (ABS/CSm, TRo/CSm, ETo/CSm and DIo/CSm) and in a single reaction center (ABS/RC, TRo/RC, ETo/RC and DIo/RC). Cross-section (CS) represents the surface of the excited region of the photosynthetic sample, including the response of both active and inactive reaction centers, whereas reaction center (RC) reflects the photosynthetically active reaction centers of PSII that can reduce Q_A.

A significant reduction was observed in the number of photons absorbed (ABS/CSm), trapped energy (TRo/CSm) and electron transport (ETo/CSm) per cross-sections in cotyledonary leaves on exposure to increasing concentrations of $CuSO_4$ on 4 d. The decreases in ABS/CSm, TRo/CSm and ETo/CSm were ranging between 8-57, 14-78 and 40-85% respectively in cotyledonary leaves of *R. communis* seedlings subjected to 40-

200 μM $CuSO_4$ on 4 d, whereas the reductions in these parameters were negligible in primary leaves on same day of the treatment (Fig. 11 and 12). However, significant reductions were observed in primary leaves on 10 d of $CuSO_4$ exposure. The decrease in ABS/CSm and TRo/CSm was least (≤ 11%) up to 160 μM $CuSO_4$ treatments on 10 d, whereas at 200 μM $CuSO_4$, the reduction was 16 and 24% respectively for ABS/CSm and TRo/CSm as compared to the control. In the case of ETo/CSm, ≤ 30% decrease was noticed in the primary leaves subjected to 40-160 μM $CuSO_4$ on 10 d, and it increased to 51% on exposure to 200 μM $CuSO_4$ as compared to the control (Fig. 13).

The value of DIo/CSm (dissipated energy per cross-section) was significantly elevated upon exposure to Cu stress, with maximum dissipation in cotyledonary leaves on 4 d. The value of DIo/CSm was enhanced up to 65% over the control in cotyledonary leaves on treatment with increasing concentrations of $CuSO_4$. In the case of primary leaves, the enhancement in DIo/CSm was 15 and 19% on 4 and 10 d respectively, over the control (Fig. 11, 12 and 13).

The phenomenological energy fluxes per reaction center were analyzed from the specific membrane model (Fig. 14, 15 and 16). It was found that TRo/RC (trapped energy per reaction center) and ETo/RC (electron transport per reaction center) were decreased drastically in cotyledonary leaves, but these parameters were slightly increased in primary leaves of *R. communis* seedlings subjected to various concentrations of $CuSO_4$ on 4 d. In the case of cotyledonary leaves, the reductions in TRo/RC and ETo/RC were 39 and 52 % respectively as compared to the control. A gradual increase in TRo/RC was observed in primary leaves on 10 d with increase in $CuSO_4$ concentrations, and the highest value was recorded in 200 μM $CuSO_4$ (49% enhancement over the control). Even though TRo/RC was high, the trapped energy was not

efficiently utilized for electron transport, as evidenced by the insignificant variations in ETo/RC in primary leaves on 10 d (Fig. 14, 15 and 16).

ABS/RC (absorption flux per reaction center) and DIo/RC (dissipation per reaction center) were found to be significantly increased in the cotyledonary leaves of *R. communis* subjected to increasing concentrations of $CuSO_4$ on 4 d. The enhancement in ABS/RC exceeds 100% in cotyledonary leaves, whereas the enhancement was insignificant in primary leaves on 4 d of Cu stress. In the case of primary leaves, on 10 d of treatment, the increase in ABS/RC was 65% over the control. Even though the absorption flux was high during $CuSO_4$ treatment, the absorbed energy was dissipated without being utilized for the photochemical processes. In the case of DIo/RC, 4-5 folds enhancement was observed in cotyledonary leaves treated with 120-200 μM $CuSO_4$ on 4 d, whereas the enhancement was negligible in primary leaves on the same days of $CuSO_4$ treatment. On 10 d of $CuSO_4$ exposure, DIo/RC was enhanced from 1.3 to 2.3 folds in primary leaves on exposure to 40-200 μM $CuSO_4$ (Fig. 14, 15 and 16).

4.2.1.8.2. Impact of cytokinins on chlorophyll *a* fluorescence induction curve and JIP parameters

In the cotyledonary leaves of *R. communis*, when subjected to Cu stress, the PSII efficiency was reduced drastically, and the reduction was severe upon exposure to 160 μM $CuSO_4$ as evidenced by the flattening of the fluorescence induction (OJIP) curve, especially at the J and I peak. However, on application of cytokinins to Cu stressed seedlings, the OJIP curve was restored to its standard shape similar to that of the control in all the cases except in the case of 160 μM $CuSO_4$ + KIN (Fig. 17A). The significant enhancement in Fo during Cu stress was reduced on application of cytokinins in Cu stressed seedlings, most prominently in the BAP treated seedlings. In the case of Fm, 26 and 70% reduction was recorded in the cotyledonary

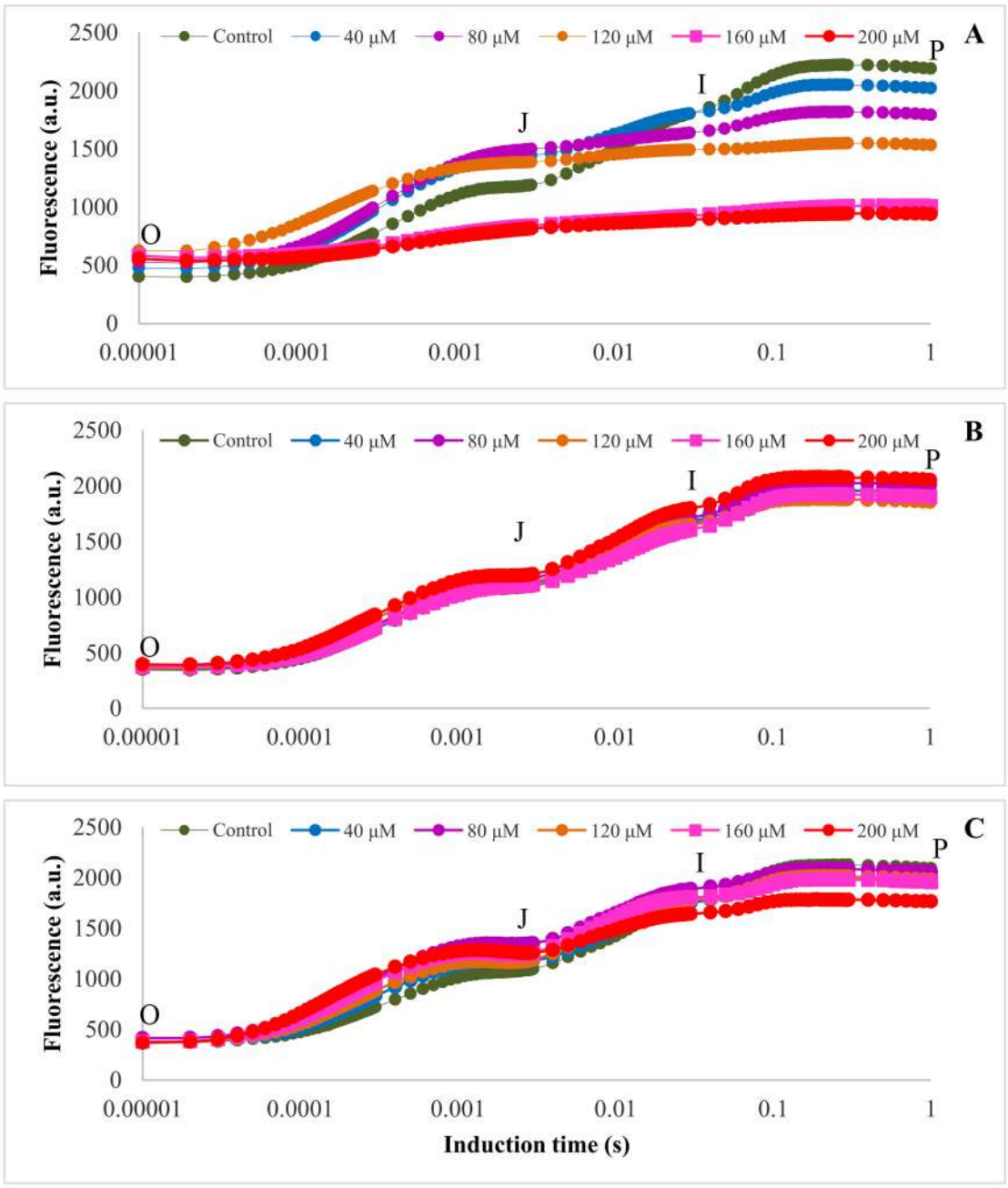

Figure 9. Chlorophyll *a* fluorescence induction curve in the cotyledonary leaves on 4 d (A) and primary leaves on 4 and 10 d (B and C respectively) in *R. communis* seedlings subjected to increasing concentrations of $CuSO_4$.

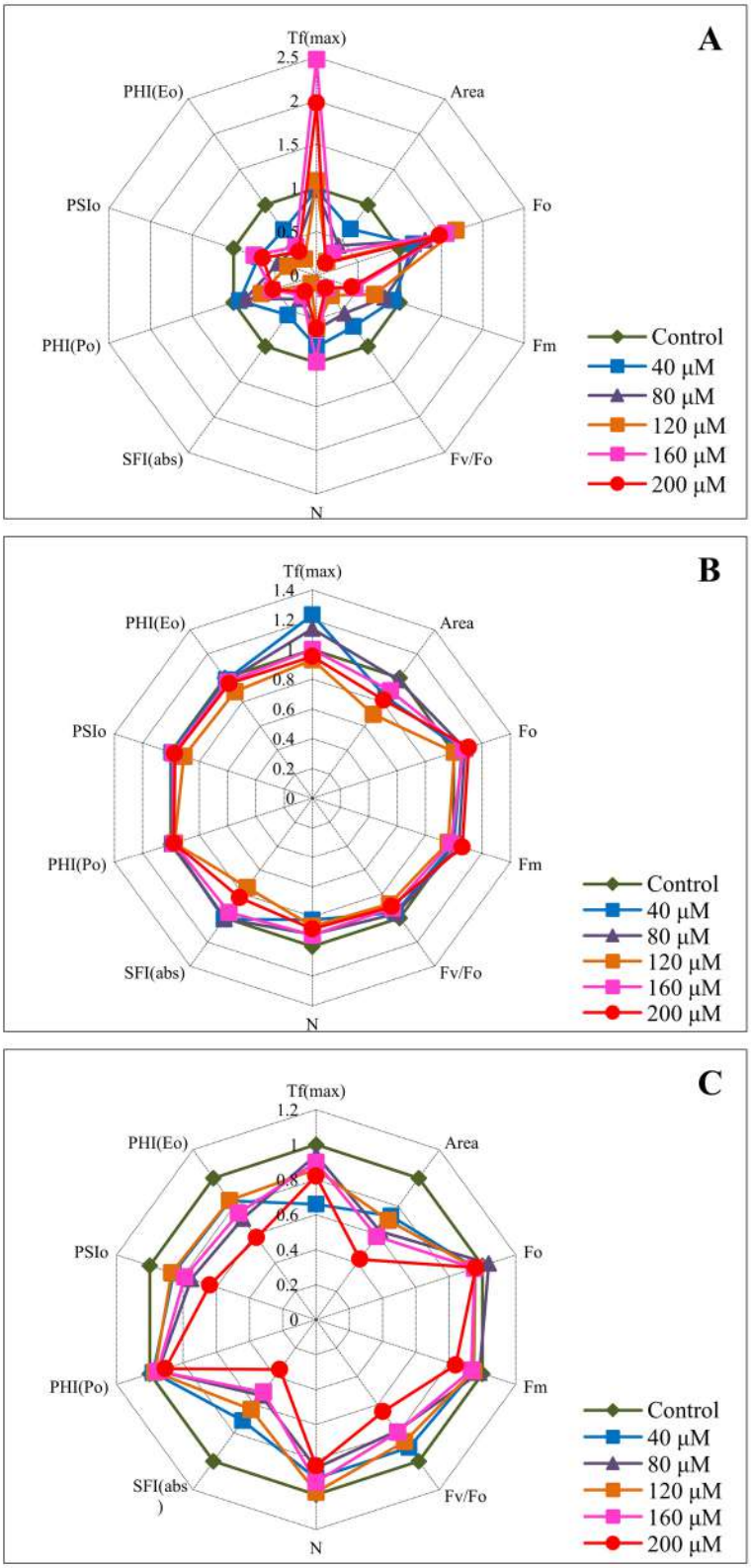

Figure 10. Radar plot representing various chlorophyll *a* fluorescence parameters and performance indices in the cotyledonary leaves on 4 d (A) and primary leaves on 4 and 10 d (B and C respectively) in *R. communis* seedlings subjected to increasing concentrations of $CuSO_4$.

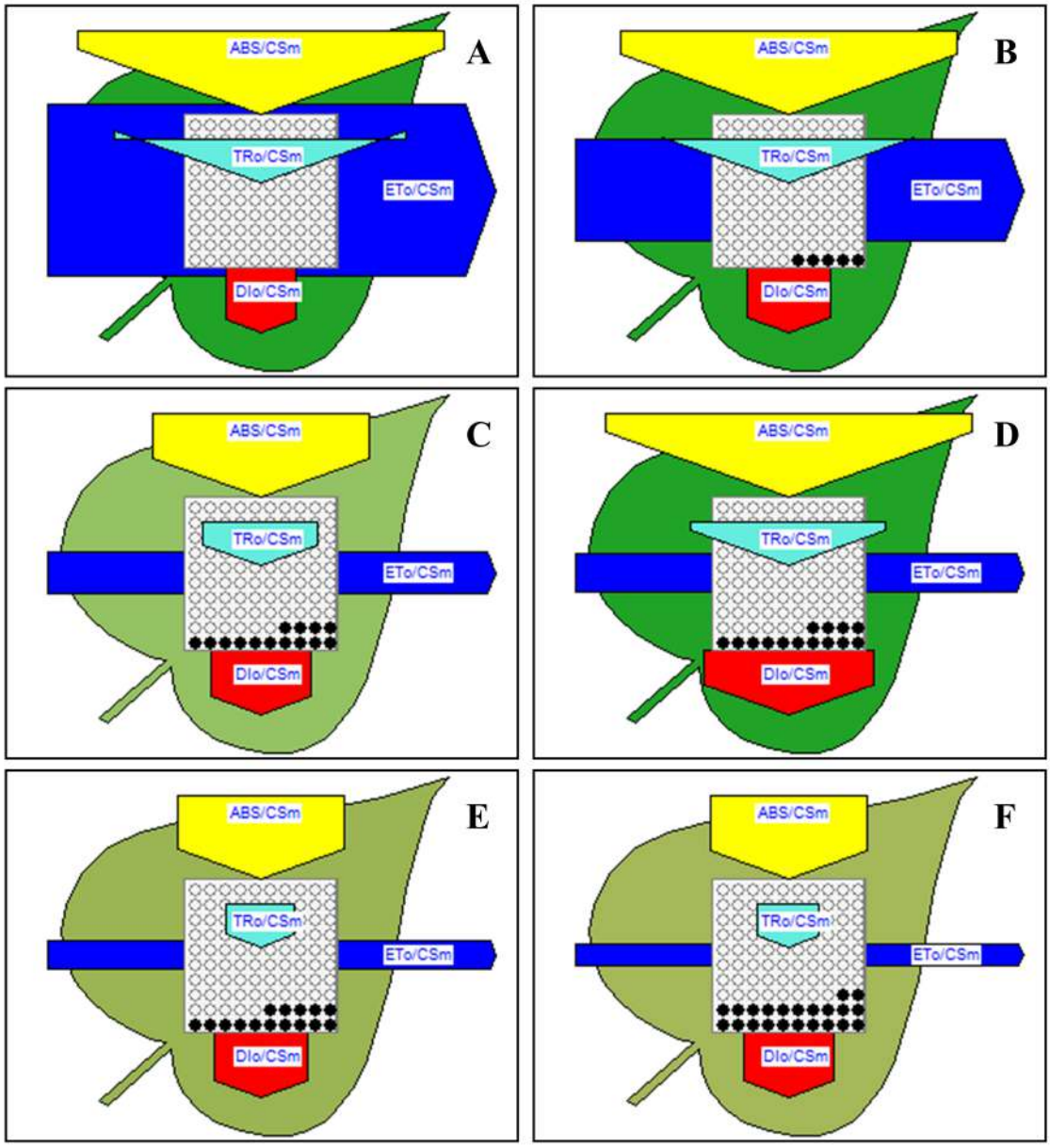

Figure 11. Phenomenological energy fluxes per cross-section in the cotyledonary leaves of *R. communis* seedlings subjected to increasing concentrations of $CuSO_4$ for 4 d. A, B, C, D, E and F representing the cotyledonary leaves of control, 40, 80, 120, 160 and 200 µM $CuSO_4$ treated seedlings respectively. The value of each parameter can be seen as relative changes in the width of each arrow.

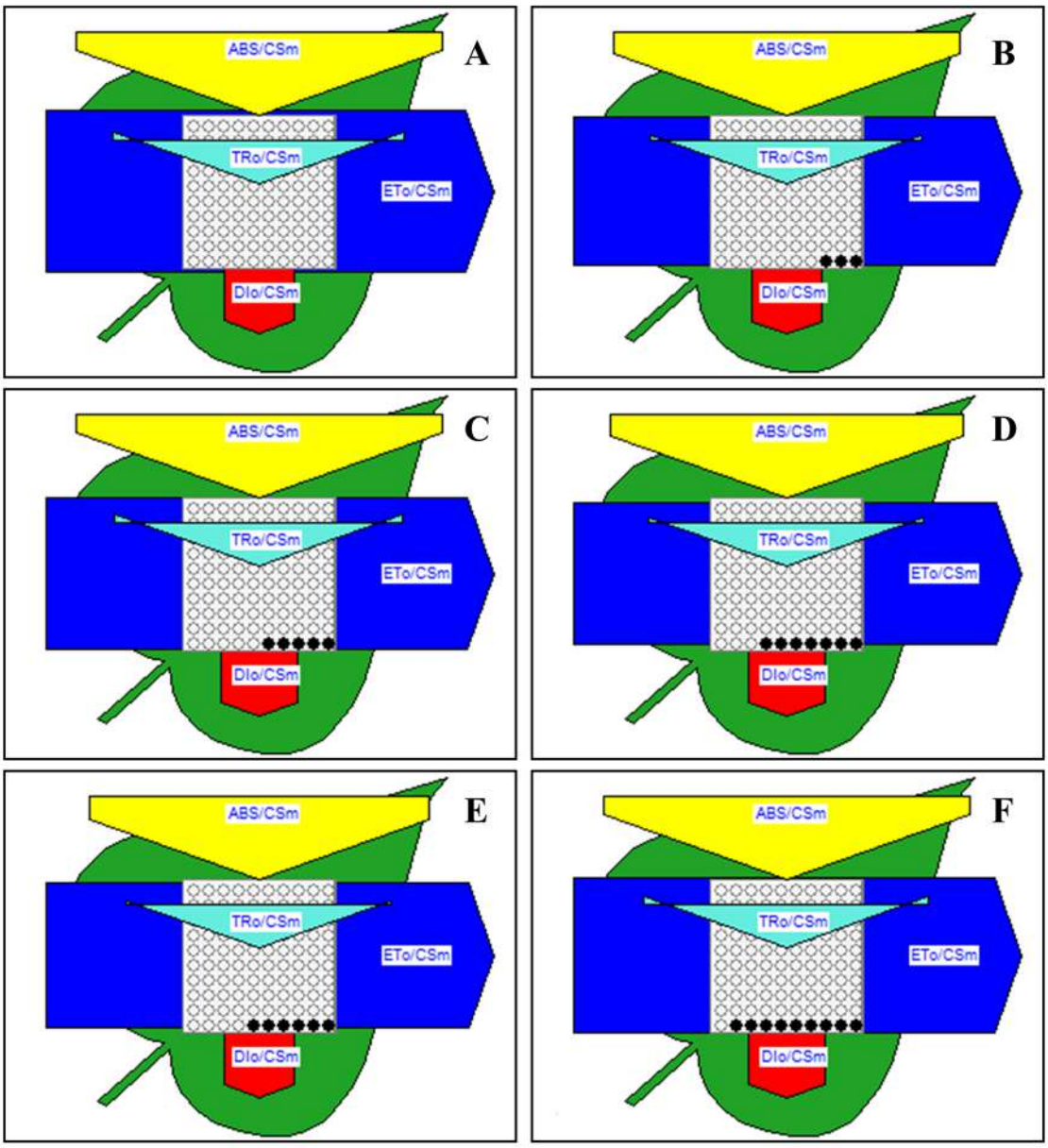

Figure 12. Phenomenological energy fluxes per cross-section in the primary leaves of *R. communis* seedlings subjected to increasing concentrations of $CuSO_4$ for 4 d. A, B, C, D, E and F representing the primary leaves of control, 40, 80, 120, 160 and 200 μM $CuSO_4$ treated seedlings respectively. The value of each parameter can be seen as relative changes in the width of each arrow.

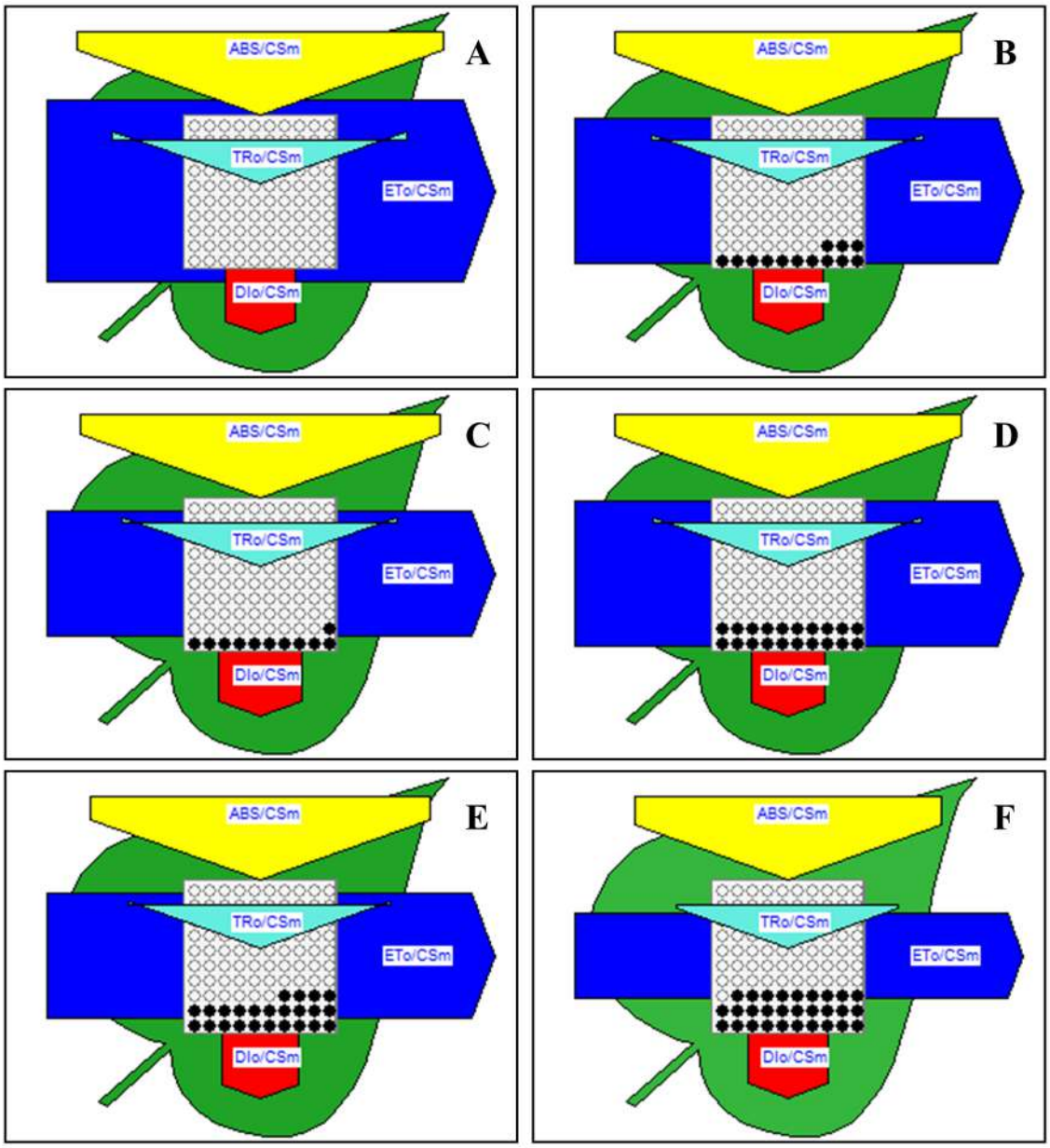

Figure 13. Phenomenological energy fluxes per cross-section in the primary leaves of *R. communis* seedlings subjected to increasing concentrations of $CuSO_4$ for 10 d. A, B, C, D, E and F representing the primary leaves of control, 40, 80, 120, 160 and 200 μM $CuSO_4$ treated seedlings respectively. The value of each parameter can be seen as relative changes in the width of each arrow.

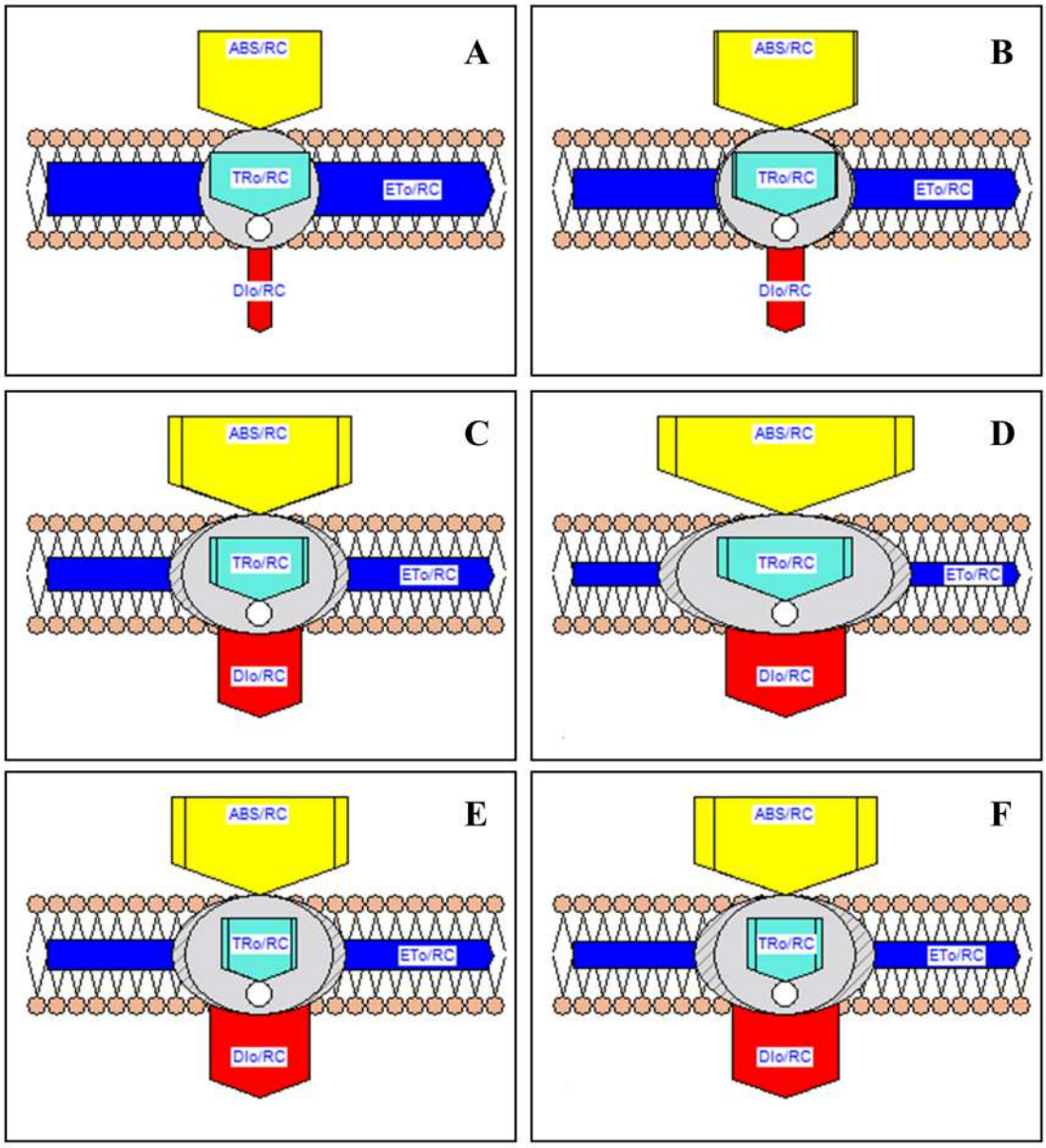

Figure 14. Phenomenological energy fluxes per single reaction center in the cotyledonary leaves of *R. communis* seedlings subjected to increasing concentrations of $CuSO_4$ for 4 d. A, B, C, D, E and F representing the cotyledonary leaves of control, 40, 80, 120, 160 and 200 μM $CuSO_4$ treated seedlings respectively. The value of each parameter can be seen as relative changes in the width of each arrow.

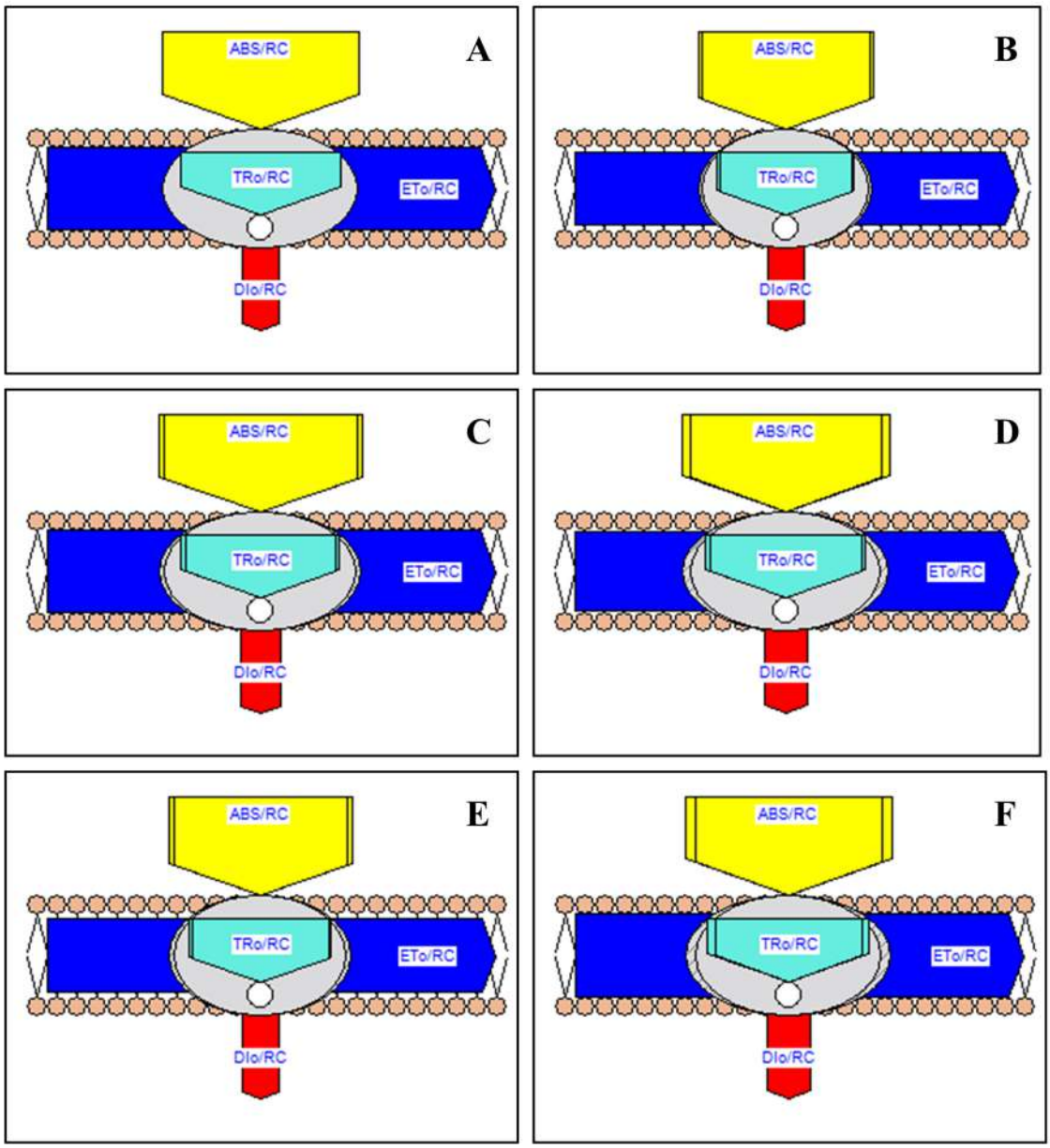

Figure 15. Phenomenological energy fluxes per single reaction center in the primary leaves of *R. communis* seedlings subjected to increasing concentrations of $CuSO_4$ for 4 d. A, B, C, D, E and F representing the primary leaves of control, 40, 80, 120, 160 and 200 μM $CuSO_4$ treated seedlings respectively. The value of each parameter can be seen as relative changes in the width of each arrow.

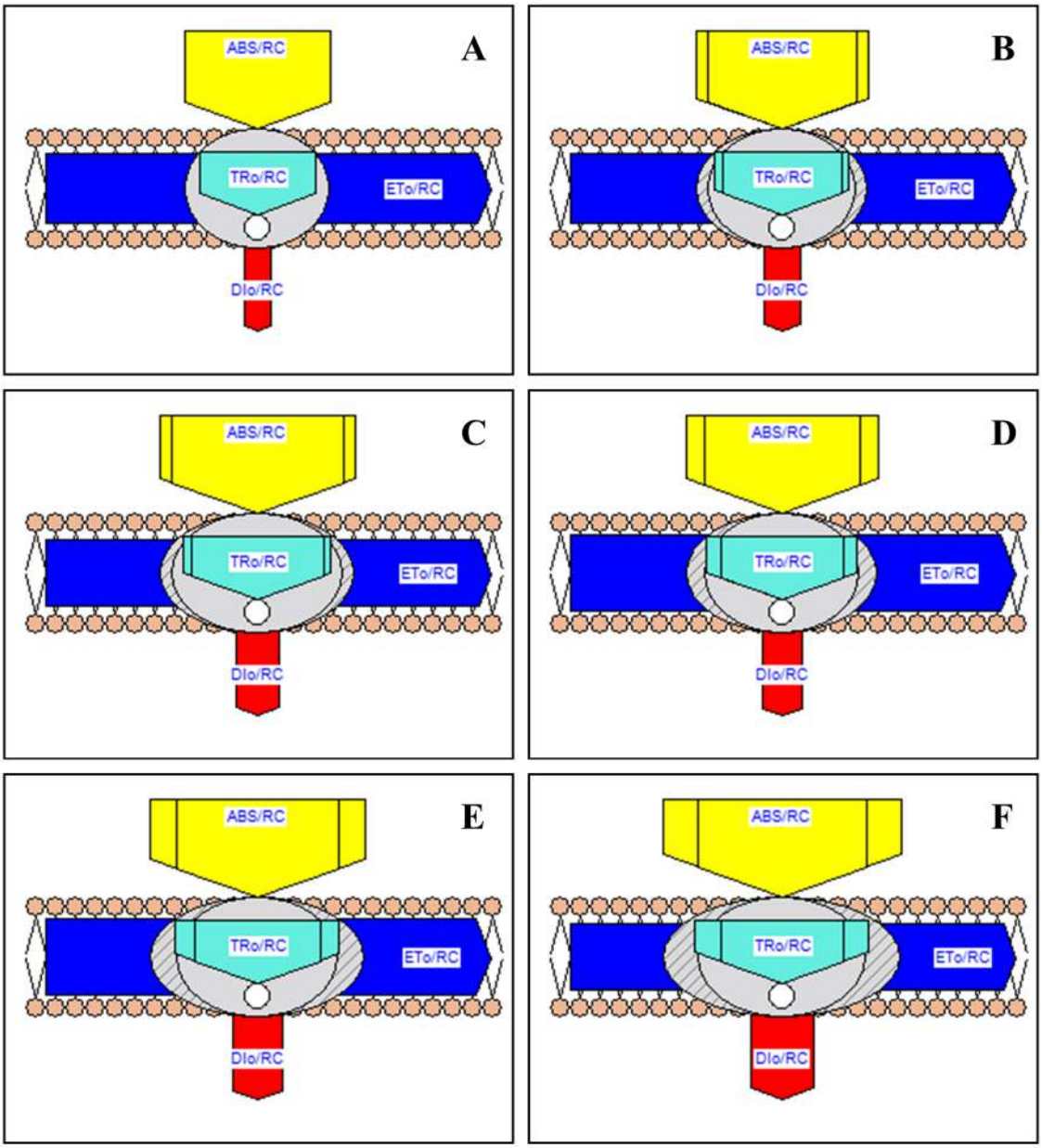

Figure 16. Phenomenological energy fluxes per single reaction center in the primary leaves of *R. communis* seedlings subjected to increasing concentrations of $CuSO_4$ for 10 d. A, B, C, D, E and F representing the primary leaves of control, 40, 80, 120, 160 and 200 μM $CuSO_4$ treated seedlings respectively. The value of each parameter can be seen as relative changes in the width of each arrow.

Table 12. Various chlorophyll *a* fluorescence parameters in the cotyledonary and primary leaves of *R. communis* seedlings subjected to increasing concentrations of $CuSO_4$ (Control, 40, 80, 120, 160 and 200 µM) for 10 d. Values are the mean ± SE of three independent experiments. Different alphabetical letters indicate significant difference between treatments (Duncan's test $p \leq 0.05$).

Leaf types	$CuSO_4$ (µM)	Fluorescence parameters (a.u.)				
		Fv/Fm	Vj	PI(abs)	PI(total)	DF(total)
Cotyledonary leaf (4 d)	Control	0.834 ± 0.008^{a}	0.429 ± 0.008^{c}	3.224 ± 0.106^{a}	2.149 ± 0.058^{a}	0.333 ± 0.011^{a}
	40	0.795 ± 0.007^{a}	0.620 ± 0.014^{bc}	1.035 ± 0.136^{b}	0.718 ± 0.071^{b}	-0.148 ± 0.043^{ab}
	80	0.737 ± 0.014^{a}	0.751 ± 0.015^{ab}	0.422 ± 0.071^{c}	0.476 ± 0.159^{bc}	-0.532 ± 0.218^{bc}
	120	0.613 ± 0.018^{ab}	0.822 ± 0.017^{ab}	0.093 ± 0.014^{c}	0.114 ± 0.028^{c}	-1.350 ± 0.100^{c}
	160	0.418 ± 0.122^{b}	0.493 ± 0.167^{c}	0.454 ± 0.259^{c}	0.447 ± 0.287^{bc}	-0.720 ± 0.494^{bc}
	200	0.392 ± 0.134^{b}	0.874 ± 0.012^{a}	0.209 ± 0.082^{c}	0.133 ± 0.096^{c}	-1.145 ± 0.346^{c}
Primary leaf (4 d)	Control	0.843 ± 0.013^{a}	0.454 ± 0.016^{b}	2.869 ± 0.055^{a}	1.485 ± 0.079^{a}	0.1707 ± 0.023^{a}
	40	0.836 ± 0.014^{a}	0.456 ± 0.016^{b}	2.705 ± 0.024^{ab}	1.249 ± 0.058^{ab}	0.111 ± 0.009^{a}
	80	0.836 ± 0.010^{a}	0.462 ± 0.019^{b}	2.584 ± 0.162^{ab}	1.431 ± 0.122^{a}	0.181 ± 0.025^{a}
	120	0.838 ± 0.014^{a}	0.515 ± 0.011^{a}	1.934 ± 0.047^{c}	0.885 ± 0.037^{b}	-0.069 ± 0.007^{b}
	160	0.834 ± 0.011^{a}	0.493 ± 0.015^{ab}	2.232 ± 0.246^{bc}	1.276 ± 0.241^{ab}	0.122 ± 0.058^{a}
	200	0.822 ± 0.013^{a}	0.502 ± 0.012^{ab}	2.052 ± 0.197^{c}	0.967 ± 0.072^{b}	0.012 ± 0.016^{b}
Primary leaf (10 d)	Control	0.841 ± 0.002^{a}	0.413 ± 0.006^{c}	3.436 ± 0.288^{a}	1.822 ± 0.140^{a}	0.266 ± 0.027^{a}
	40	0.839 ± 0.001^{a}	0.502 ± 0.014^{b}	2.189 ± 0.143^{b}	0.990 ± 0.117^{b}	-0.003 ± 0.052^{b}
	80	0.833 ± 0.006^{ab}	0.577 ± 0.038^{ab}	1.510 ± 0.323^{bc}	0.542 ± 0.104^{cd}	-0.293 ± 0.087^{cd}
	120	0.836 ± 0.006^{ab}	0.504 ± 0.032^{b}	2.058 ± 0.390^{b}	0.801 ± 0.199^{bc}	-0.134 ± 0.114^{bc}
	160	0.833 ± 0.006^{ab}	0.558 ± 0.006^{b}	1.479 ± 0.033^{bc}	0.484 ± 0.020^{cd}	-0.318 ± 0.015^{cd}
	200	0.819 ± 0.009^{b}	0.652 ± 0.029^{a}	0.841 ± 0.173^{c}	0.321 ± 0.067^{d}	-0.526 ± 0.096^{d}

leaves of *R. communis* seedlings exposed to 80 and 160 μM $CuSO_4$ as compared to the control. The reduced Fm was restored during application of BAP along with Cu stress, though no significant changes were recorded on KIN application (Fig. 17A).

In the radar plot representing various fluorescence parameters, pronounced variations were observed in the cotyledonary leaves when the seedlings were treated with $CuSO_4$, compared to the control. However, the restoration of the fluorescence parameters such as Tf(max), Area, Fv/Fo and N was noticed on application of BAP to the Cu-stressed seedlings. In contrast, no significant variation was recorded when KIN was applied to the Cu-stressed seedlings (Fig. 17B).

The fluorescence yield parameters, including photochemical and non-photochemical quantum yields, exhibited prominent reductions during $CuSO_4$ exposure. The reductions in PHI(Po), PHI(Eo), and PSIo were to the extent of 19-55 and 78-98% respectively for 80 and 160 μM $CuSO_4$ treated seedlings as compared to the control. On application of BAP along with $CuSO_4$, the photosynthetic efficiency was restored in the cotyledonary leaves, more or less similar to that of the control. In contrast, no significant variations were observed in cotyledonary leaves on KIN application along with $CuSO_4$ (Fig. 17B).

The value of Fv/Fm was reduced to 0.651 and 0.188 in 80 and 160 μM $CuSO_4$ treated cotyledonary leaves respectively. On application of KIN to 80 and 160 μM $CuSO_4$ stressed seedlings, Fv/Fm was enhanced to 0.77 and 0.348 respectively. But, BAP application resulted in the enhancement of Fv/Fm to 0.823 and 0.785 in 80 and 160 μM $CuSO_4$ treated cotyledonary leaves respectively (Table 13).

On the contrary, Vj (variable fluorescence) was found to be significantly enhanced upon exposure to 80 and 160 μM $CuSO_4$ (47 and 90% respectively). Cytokinin application resulted in the reduction of Vj in Cu stressed seedlings as compared to that exposed to Cu stress alone, and the reduction was lowered to 15 and 32% in KIN and BAP treated cotyledonary leaves respectively (Table 13).

The drastic reductions (> 90%) in the performance indices PI(abs) and PI(total) during Cu stress were recovered to some extent in the cotyledonary leaves upon exposure to cytokinins. On application of KIN to the seedlings treated with 80 μM $CuSO_4$, PI(abs) and PI(total) were enhanced to 3 and 4 folds respectively as compared to that exposed to $CuSO_4$ alone but no significant enhancement was recorded in 160 μM $CuSO_4$ + KIN treatments. Similarly, in the cotyledonary leaves of 80 μM $CuSO_4$ + BAP, PI(abs) and PI(total) were enhanced to 8 and 12 folds respectively as compared to that of 80 μM $CuSO_4$. However, in the case of 160 μM $CuSO_4$ + BAP, the performance indices were enhanced as compared to 160 μM $CuSO_4$, still a reduction of > 70 % was recorded as compared to the control (Table 13).

The PSII-relative driving force, DF(total) was reduced drastically in the cotyledonary leaves of *R. communis* seedlings exposed to Cu stress (12 and 22 folds reduction on 80 and 160 μM $CuSO_4$). Application of BAP to 80 μM $CuSO_4$ treated seedlings resulted in the enhancement in DF(total) and only 1.7 folds reduction was recorded as compared to the control, whereas, in the case of all other three stress situations (80 or 160 μM $CuSO_4$ + KIN and 160 μM $CuSO_4$ + BAP), the enhancement did not reach to a level as similar to that of the control (Table 13).

A significant reduction was observed in the number of photons absorbed (ABS/CSm, 26 and 70% reduction), trapped energy (TRo/CSm, 45 and 94% reduction), and electron transport (ETo/CSm, 67 and 99% reduction)

per cross-section in the cotyledonary leaves of *R. communis* subjected to 80 and 160μM $CuSO_4$ treatments. But the value of DIo/CSm (dissipated energy per cross-section) was significantly elevated to a maximum of 43% during $CuSO_4$ treatments. On application of cytokinins, the energy parameters ABS/CSm, TRo/CSm and ETo/CSm were considerably enhanced and DIo/CSm was reduced as compared to $CuSO_4$ treatments alone except in the case of 160 μM $CuSO_4$ + KIN. During the treatment with 80 μM $CuSO_4$ + KIN, ABS/CSm, TRo/CSm and ETo/CSm were enhanced to 12, 28 and 42% respectively as compared to those exposed to 80 μM $CuSO_4$. But these parameters were enhanced to 43, 90 and 206% respectively in 80 μM $CuSO_4$ + BAP as compared to 80 μM $CuSO_4$. The elevated DIo/CSm was reduced by 11 and 21% in KIN and BAP treated cotyledonary leaves of seedlings exposed to 80 μM $CuSO_4$ respectively. The closed RCs during Cu stress, represented as dark circles, were significantly reduced and the number of active RCs was increased in all the three cases except in the case of 160 μM $CuSO_4$ + KIN (Fig. 18).

The enhancement in the energy flux parameters such as ABS/RC, TRo/RC and DIo/RC and reduction in ETo/RC during Cu stress was effectively modulated on application of cytokinins, most significantly in BAP treated seedlings. KIN and BAP application to 80 μM $CuSO_4$ treated seedlings resulted in the reduction of ABS/RC, TRo/RC and DIo/RC by 30, 20 and 45%, and 44, 26 and 69% respectively as compared to those exposed to Cu stress alone. In the case of ETo/RC, 80 μM $CuSO_4$ + KIN treated seedlings showed 11% decrease as compared to 80 μM $CuSO_4$, whereas, in 80 μM $CuSO_4$ + BAP, ETo/RC was enhanced to 19% over 80 μM $CuSO_4$ (Fig. 19).

4.2.1.9. Chlorophyll stability index (CSI)

Copper stress significantly decreased chlorophyll stability index in both cotyledonary and primary leaves of *R. communis* seedlings (Fig. 20). In

cotyledonary leaves, the reduction in MSI was found to be significant even on 2 d of $CuSO_4$ exposure, and it was 22-50% on 2 d. On 6 d, the reduction in CSI recorded in the cotyledonary leaves subjected to 200 µM $CuSO_4$ was exceeding 80% as compared to the control (Fig. 20A).

Similar to the cotyledonary leaves, CSI in the primary leaves also decreased on exposure to Cu stress. On 2 d, the reduction in CSI was ≤ 22% only even at higher $CuSO_4$ treatments. In contrast, on the following days of treatment (4-10 d), CSI was decreased up to 38% in Cu-treated primary leaves with respect to that of the control (Fig. 20B).

The CSI was reduced by 51 and 65% in the cotyledonary leaves upon exposure to 80 and 160 µM $CuSO_4$, respectively. Cytokinin application in seedlings treated with 80 and 160 µM $CuSO_4$ resulted in the enhancement of CSI as compared to those exposed to Cu stress alone. The enhancement was to the extent of 47-58 and 65-92% on application of KIN and BAP respectively in seedlings treated with $CuSO_4$ as compared to the respective $CuSO_4$ treatments (Fig. 20C).

4.2.1.10. Osmolality

Copper treatment resulted in the enhancement of osmolality in both cotyledonary and primary leaves of *R. communis* seedlings as compared to the respective controls (Fig. 21). In cotyledonary leaves subjected to 40-160 µM $CuSO_4$, there was no significant variation observed in osmolality up to 4 d, whereas at 200 µM $CuSO_4$, a maximum of 53% enhancement over the control was observed on 4 d. But, on 6 d, a significant enhancement was observed at concentrations 80 to 200 µM $CuSO_4$, and the enhancement exceeds 2 folds as compared to the control (Fig. 21A).

In the case of primary leaves, the enhancement in osmolality was insignificant up to 6 d, and the increase was only 6-19% as compared to the

Table 13. Various chlorophyll *a* fluorescence parameters in the cotyledonary leaves of *R. communis* on 6 d of exposure to $CuSO_4$ (80 and 160 µM) and cytokinins (KIN and BAP). Values are the mean ± SE of three independent experiments. Different alphabetical letters indicate significant difference between treatments (Duncan's test $p \leq 0.05$).

Treatments	Fluorescence parameters (a.u.)				
	Fv/Fm	Vj	PI(abs)	PI(total)	DF(total)
Control	0.832 ± 0.005^{a}	0.514 ± 0.014^{d}	2.039 ± 0.237^{a}	0.787 ± 0.157^{a}	-0.121 ± 0.084^{a}
80 µM $CuSO_4$	0.651 ± 0.074^{b}	0.756 ± 0.053^{b}	0.212 ± 0.097^{d}	0.053 ± 0.022^{bc}	-1.432 ± 0.303^{c}
160 µM $CuSO_4$	0.188 ± 0.056^{d}	0.975 ± 0.011^{a}	0.007 ± 0.003^{d}	0.0035 ± 0.002^{c}	-3.042 ± 0.330^{d}
Control + KIN	0.816 ± 0.003^{a}	0.547 ± 0.004^{d}	1.421 ± 0.080^{b}	0.583 ± 0.029^{a}	-0.235 ± 0.021^{ab}
80 µM $CuSO_4$ + KIN	0.770 ± 0.005^{ab}	0.645 ± 0.004^{c}	0.642 ± 0.015^{c}	0.238 ± 0.014^{b}	-0.625 ± 0.026^{ab}
160 µM $CuSO_4$ + KIN	0.349 ± 0.077^{c}	0.931 ± 0.015^{a}	0.008 ± 0.006^{d}	0.0035 ± 0.001^{c}	-2.928 ± 0.330^{d}
Control + BAP	0.817 ± 0.003^{a}	0.545 ± 0.025^{d}	1.529 ± 0.192^{b}	0.621 ± 0.089^{a}	-0.217 ± 0.068^{ab}
80 µM $CuSO_4$ + BAP	0.826 ± 0.004^{a}	0.535 ± 0.011^{d}	1.648 ± 0.147^{b}	0.626 ± 0.067^{a}	-0.208 ± 0.046^{ab}
160 µM $CuSO_4$ + BAP	0.785 ± 0.011^{a}	0.665 ± 0.020^{c}	0.624 ± 0.112^{c}	0.202 ± 0.030^{bc}	-0.705 ± 0.072^{b}

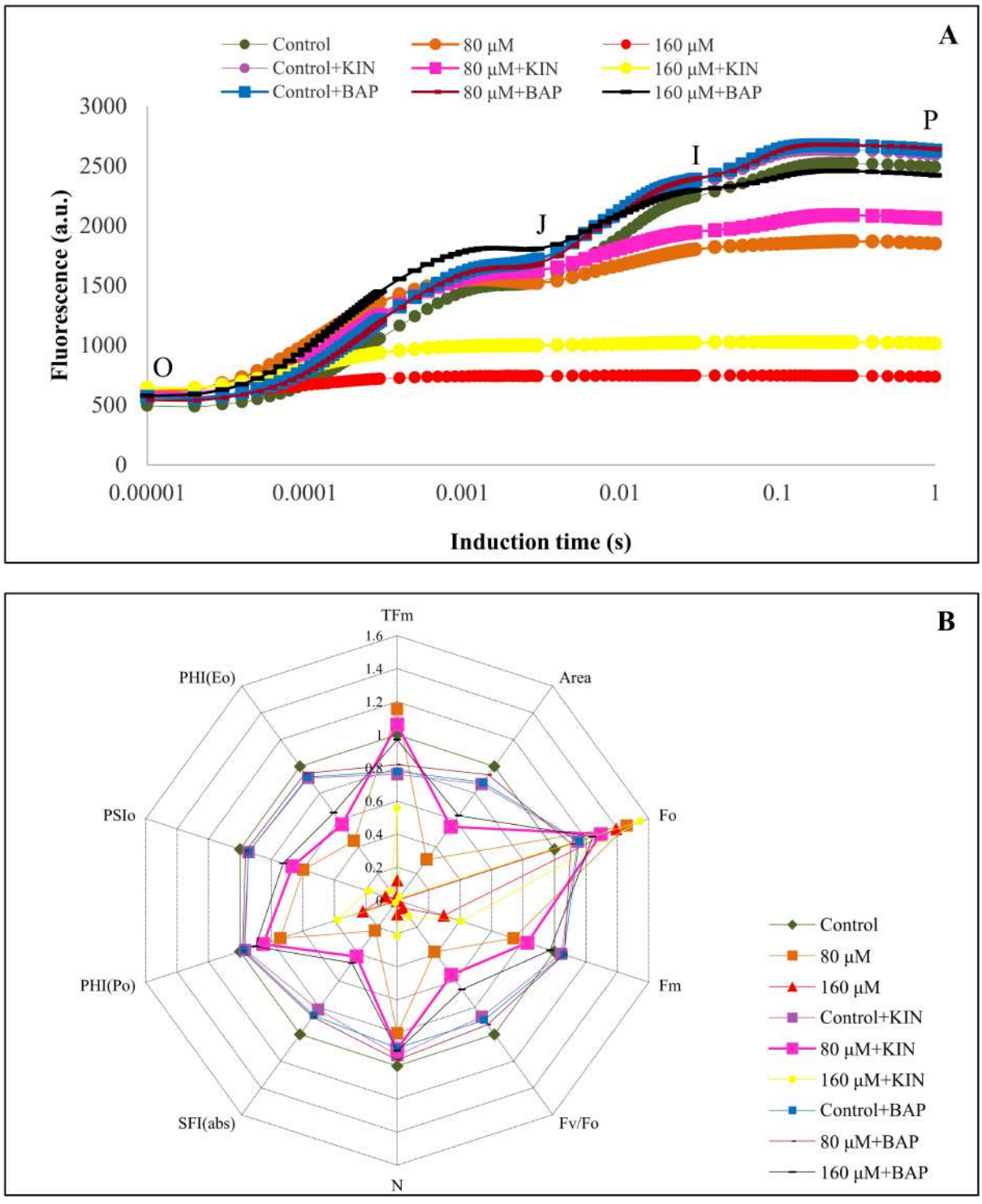

Figure 17. Chlorophyll *a* fluorescence induction curve (A) and radar plot representing various chlorophyll *a* fluorescence parameters (B) in the cotyledonary leaves of *R. communis* seedlings on 4 d of exposure to $CuSO_4$ (80 and 160 µM) and cytokinins (KIN and BAP).

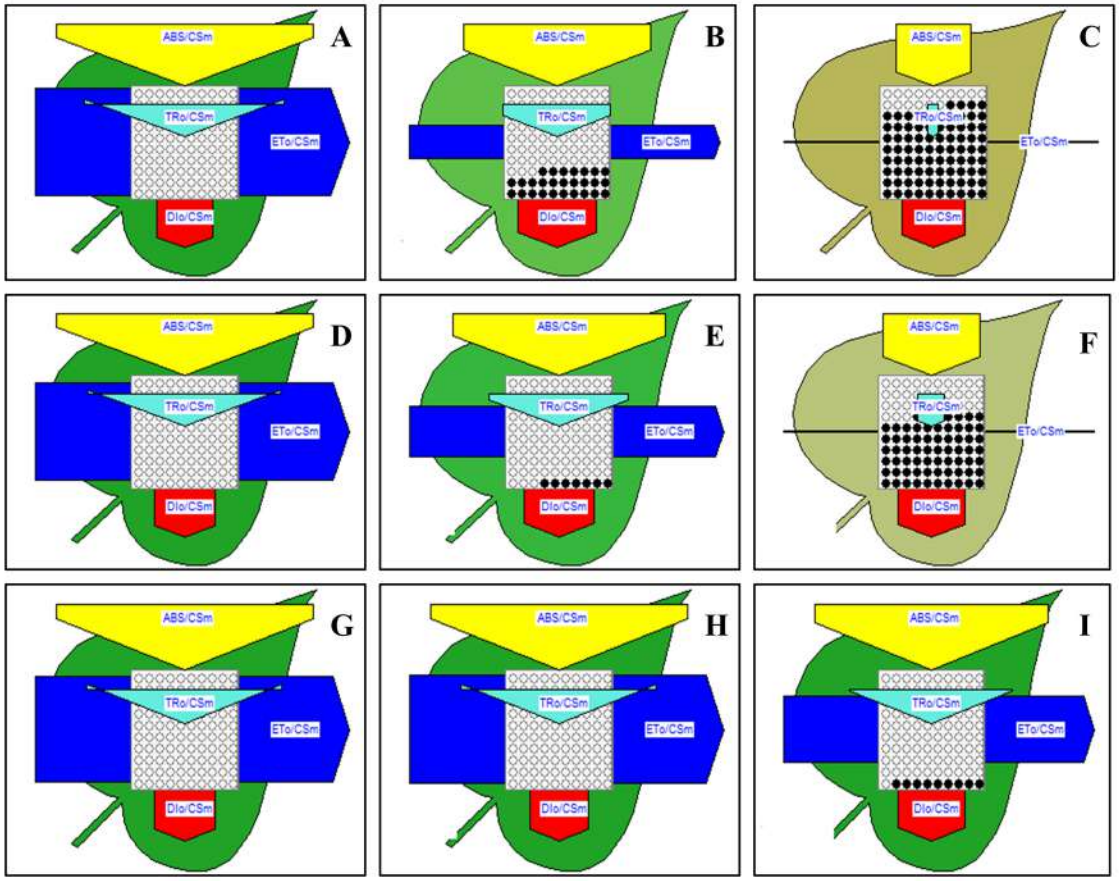

Figure 18. Phenomenological energy fluxes per cross-section in the cotyledonary leaves of *R. communis* seedlings on 4 d of exposure to $CuSO_4$ (80 and 160 µM) and cytokinins (KIN and BAP). A: control; B: 80 µM $CuSO_4$; C: 160 µM $CuSO_4$; D: control + KIN; E: 80 µM $CuSO_4$ + KIN; F: 160 µM $CuSO_4$ + KIN; G: control + BAP; H: 80 µM $CuSO_4$ + BAP; and I: 160 µM $CuSO_4$ + BAP treated seedlings. The value of each parameter can be seen as relative changes in the width of each arrow.

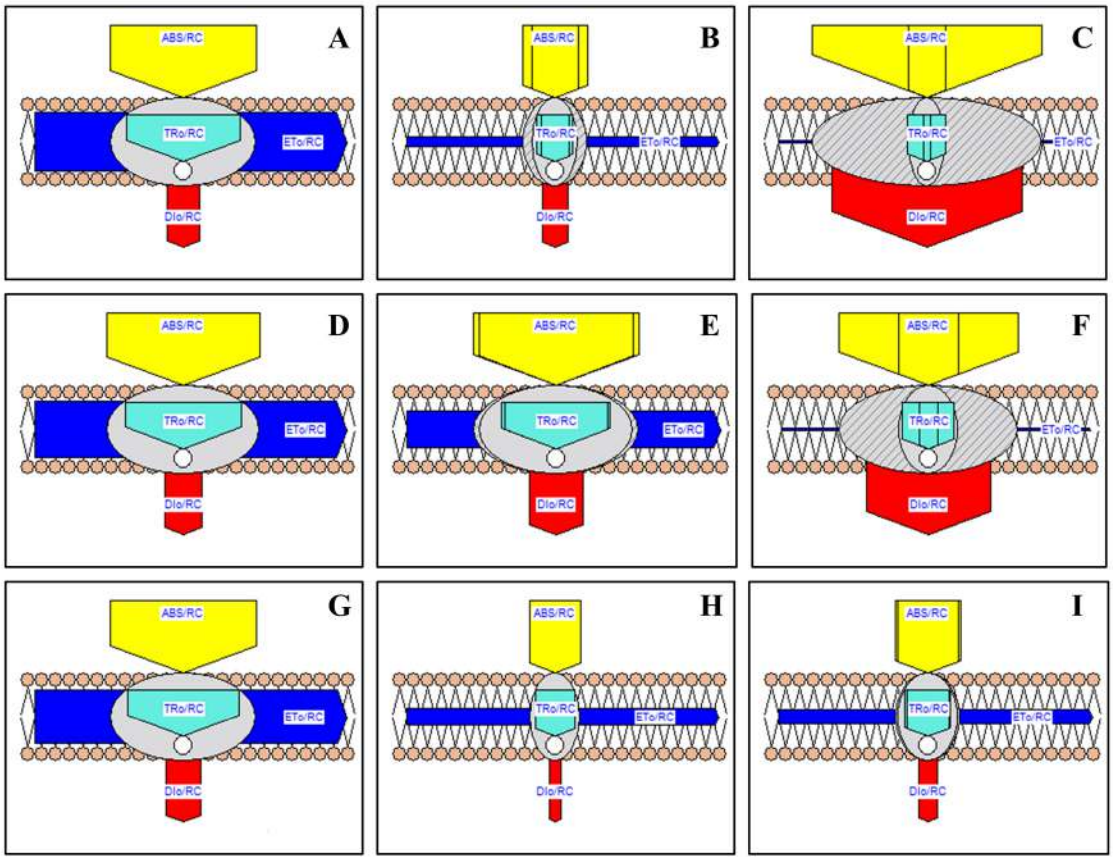

Figure 19. Phenomenological energy fluxes per single reaction center in the cotyledonary leaves of *R. communis* seedlings on 4 d of exposure to $CuSO_4$ (80 and 160 µM) and cytokinins (KIN and BAP). A: control; B: 80 µM $CuSO_4$; C: 160 µM $CuSO_4$; D: control + KIN; E: 80 µM $CuSO_4$ + KIN; F: 160 µM $CuSO_4$ + KIN; G: control + BAP; H: 80 µM $CuSO_4$+ BAP; and I: 160 µM $CuSO_4$ + BAP treated seedlings. The value of each parameter can be seen as relative changes in the width of each arrow.

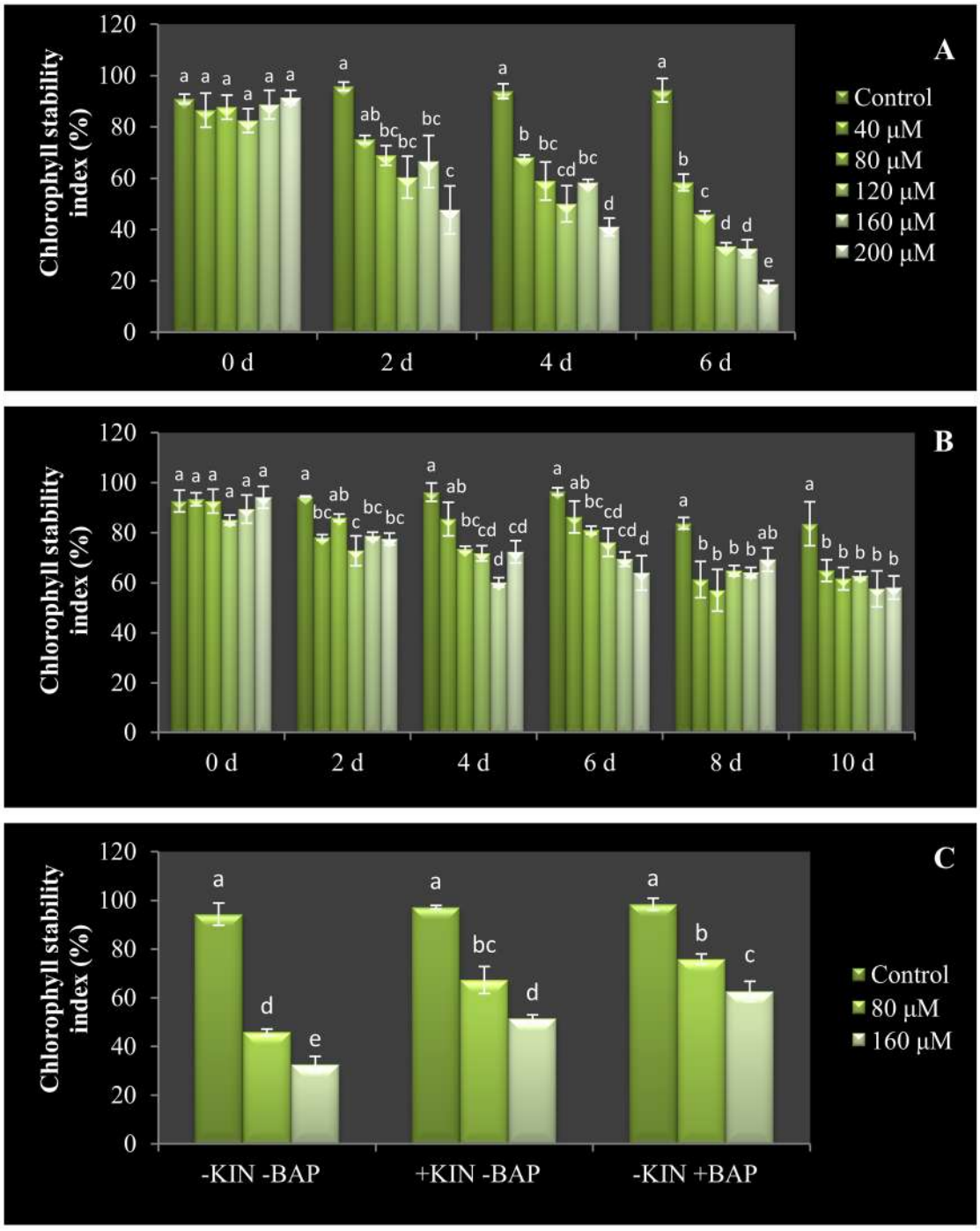

Figure 20. Chlorophyll stability index in the cotyledonary leaves (A), primary leaves (B), and cotyledonary leaves (exposed to cytokinins for 6 d) (C) of *R. communis* seedlings subjected to increasing concentrations of $CuSO_4$. Different alphabetical letters indicate significant difference between treatments (Duncan's test $p \leq 0.05$).

control. In contrast, the abscission of cotyledonary leaves resulted in significant enhancement of osmolality in primary leaves. It was enhanced up to 46% on 10 d of $CuSO_4$ exposure as compared to the primary leaves of the control (Fig. 21B).

Exposure to Cu stress resulted in variations in osmolality in the roots of *R. communis* seedlings.An insignificant enhancement in osmolality was observed on 2 d of $CuSO_4$ exposure.In contrast, on further days of treatment, the osmolality was decreased in roots as compared to the control roots. The reduction in osmolality was ≤ 17% even at higher $CuSO_4$ concentrations throughout the treatment period (Fig. 21C).

Ricinus communis seedlings subjected to Cu stress resulted in increased osmolality in the cotyledonary leaves, and it exceeds 100% when treated with 80 and 160 µM $CuSO_4$ as compared to the control seedlings. On application of KIN and BAP along with 80 and 160 µM $CuSO_4$,the osmolality decreased to the extent of 43-47% in the cotyledonary leaves of *R. communis* seedlings as compared to that exposed to Cu stress alone (Fig. 21D).

4.2.2. Reactive oxygen species production

4.2.2.1. Superoxide ($^{\bullet}O_2^-$) content

Superoxide anion ($^{\bullet}O_2^-$) accumulation was increased in both the leaves and roots during initial days of $CuSO_4$ exposure (Fig. 22). In the case of cotyledonary leaves, an insignificant increase in $^{\bullet}O_2^-$ content was observed on 2 d, which was then increased significantly on further days of Cu stress. The enhancement in $^{\bullet}O_2^-$ content exceeded 85% over the control on 4 d of 160 and 200 µM $CuSO_4$ treatments, which was then reduced to 55-59% on 6 d (Fig. 22A).

An insignificant increase in $^{\bullet}O_2^-$ content was noticed in the primary leaves of *R. communis* seedlings subjected to $CuSO_4$ treatments up to 6 d as compared to the respective controls. But, on 8 d onwards, a significant enhancement in accumulation of $^{\bullet}O_2^-$ content was observed in primary leaves.The enhancement in $^{\bullet}O_2^-$ content exceeded 80% over the control on 8 d in all the $CuSO_4$ treatments, which was then reduced to 31-52% on 10 d of Cu stress (Fig. 22B).

In the case of roots upon exposure to Cu stress, mild stress (40 and 80 μM $CuSO_4$) resulted in significant accumulation of $^{\bullet}O_2^-$ content on initial days of treatment. However, severe stress resulted in reduced accumulation of $^{\bullet}O_2^-$ content. On 2 d, 36-43% enhancement in the accumulation of $^{\bullet}O_2^-$ content was observed at 40 and 80 μM $CuSO_4$ treatments as compared to the control. In contrast, 36-75% reduction in the accumulation of $^{\bullet}O_2^-$ content was observed on 6-10 d in the roots subjected to 40-200 μM $CuSO_4$ (Fig. 22C).

The accumulation of superoxide ($^{\bullet}O_2^-$) molecules was increased by > 60% in the cotyledonary leaves of seedlings subjected to 80 and 160 μM $CuSO_4$ treatments as compared to those of the control seedlings. On application of KIN or BAP along with $CuSO_4$, $^{\bullet}O_2^-$ content was significantly reduced as compared to the $CuSO_4$ treatments alone. The reductions were 35-38% and 40-43% respectively in cotyledonary leaves of $CuSO_4$ treated seedlings along with KIN and BAP applications as compared to the respective $CuSO_4$ treatments (Fig. 22D).

4.2.2.2. Hydrogen peroxide (H_2O_2) content

A significant increase in the accumulation of H_2O_2 content was recorded in both the leaves and roots of *R. communis* on being subjected to increasing concentrations of $CuSO_4$ (Fig. 23). In cotyledonary leaves, the accumulation of H_2O_2 content was not significant on 2 d. However, on 4 d, a

drastic increase in H_2O_2 accumulation (7 folds) was recorded on treatment with 160 and 200 µM $CuSO_4$. In contrary, on 6 d of treatment, an enormous hike in H_2O_2 content was recorded even at lower concentrations of $CuSO_4$, and the increase was 7-12 folds as compared to the control (Fig. 23A).

In the case of primary leaves, H_2O_2 content increased gradually up to 6 d, and beyond which the increase was not significant as compared to that of the control. The maximum accumulation of H_2O_2 content was recorded on 6 d of $CuSO_4$ exposure in primary leaves, *i.e.*, 3.7 folds at 200 µM $CuSO_4$ over the control. On 8 and 10 d of Cu stress, a maximum of 70% enhancement in H_2O_2 accumulation was recorded over the control (Fig. 23B).

The accumulation of H_2O_2 content in the roots of *R. communis* seedlings was maximum on 2 d of treatment, which ranges from 80-110% of increase when treated with 120-200 µM $CuSO_4$. From 6 d onwards, the accumulation of H_2O_2 was insignificant, *i.e.*, a maximum of 48% increase was recorded over the control (Fig. 23C).

A drastic increase of 7 and 12 folds in H_2O_2 accumulation was recorded in the cotyledonary leaves treated with 80 and 160 µM $CuSO_4$, respectively, as compared to the control. When plants were exposed to foliar applied KIN or BAP along with $CuSO_4$, the content of H_2O_2 was found to be reduced significantly in cotyledonary leaves compared to the seedlings exposed to Cu stress alone, and the reductions were to the extent of 62-79% in both KIN and BAP applied cotyledonary leaves subjected to $CuSO_4$ (Fig. 23D).

4.2.3. ROS induced membrane damage

4.2.3.1. Lipid peroxidation

A significant increase in the rate of lipid peroxidation, as assessed by MDA content was recorded in both the leaves and roots upon treatment with

$CuSO_4$ (Fig. 24). The MDA content was found to be increased to the extent of 64% in the cotyledonary leaves on 2 d of exposure to 200 µM $CuSO_4$. But, a drastic and highly significant increase in MDA accumulation was observed on 4 d, *i.e.*, 3.5 to 7 folds increase, which further increased to 9 folds over the control on 6 d (Fig. 24A).

However, in primary leaves, a gradual increase in MDA accumulation was recorded upon treatment with increasing concentrations of $CuSO_4$ and days of exposure. About 20-75% increase in MDA accumulation was observed in the primary leaves on 2 d, which increased further to 47-100% over the control on 6 d of treatment. The maximum accumulation of MDA content was recorded in the primary leaves of *R. communis* seedlings subjected to 200 µM $CuSO_4$ on 10 d, and the increase was 113% over the control (Fig. 24B).

Similar to the primary leaves, a gradual increase in accumulation of MDA content was observed in roots of *R. communis* seedlings subjected to increasing concentrations of $CuSO_4$. An increase of ≤ 2 folds was observed on 2-4 d of treatment and was enhanced on further days of $CuSO_4$ treatment. The maximum accumulation of MDA content was recorded in the roots of *R. communis* seedlings subjected to 200 µM $CuSO_4$ on 10 d, *i.e.*, 2.7 folds increase over the control (Fig. 24C).

Compared to the control, the enhancement in MDA accumulation was ranging from 4 to 6 folds in cotyledonary leaves of seedlings exposed to 80 and 160 µM $CuSO_4$. However, on application of KIN or BAP in $CuSO_4$ treated seedlings, the MDA accumulation in the cotyledonary leaves was drastically reduced. KIN application resulted in the reduction of MDA content by 58 and 72% in the cotyledonary leaves of *R. communis* seedlings treated with 80 and 160 µM $CuSO_4$ respectively, as compared to those exposed to Cu stress alone. Similarly, 70 and 74% reduction of MDA content

was recorded in seedlings treated with 80 and 160 µM $CuSO_4$ respectively during BAP application (Fig. 24D).

4.2.3.2. Membrane stability index (MSI)

A significant gradual decrease in MSI was observed in both the leaves and roots upon exposure to $CuSO_4$, with the highest level of reduction recorded in the cotyledonary leaves (Fig. 25). A reduction of 65% on 2 d was further reduced to 86% on 6 d upon treatment with 200 µM $CuSO_4$ as compared to the control (Fig. 25A).

An insignificant reduction in MSI was observed in the primary leaves on treatment with increasing concentrations of $CuSO_4$ on 2 d. However, 4 d onwards, a significant reduction in MSI was recorded in the primary leaves. The reduction in MSI exceeded 60% compared to the control on 6 d of treatment, which was further reduced to 86% on 10 d of Cu stress (Fig. 25B).

In contrast to primary leaves, MSI was found to be reduced significantly in roots even from 2 d of treatment. On 6 d, a maximum of 50% reduction in MSI was recorded in the roots of Cu-treated seedlings, but the reduction reached to 80% with respect to control on 10 d of $CuSO_4$ treatments (Fig. 25C).

On exposure to 80 and 160 µM $CuSO_4$, the MSI was reduced to 57 and 67%, respectively, as compared to the control. However, upon application of KIN or BAP to 80 and 160 µM $CuSO_4$ treated seedlings, MSI of cotyledonary leaves was found to be restored in all four cases. The enhancement in MSI was 90-143 and 134-170% in KIN and BAP applied cotyledonary leaves respectively, subjected to Cu stress as compared to the respective cotyledonary leaves exposed to Cu stress alone (Fig. 25D).

4.2.3.3. Electrolyte leakage (EL%)

The leakage of electrolytes was increased significantly in *R. communis* by the toxic effects of Cu, which was further enhanced with the increase in metal exposure time (Fig. 26). Copper stress induced enhancement in EL% in the cotyledonary leaves was ≤ 50% in all the treatments except 200 μM $CuSO_4$ on 2 d, and an increase of 73% was recorded on exposure to 200 μM $CuSO_4$ over the control. The enhancement in EL% reached to 70-88% in the cotyledonary leaves over the control on 4-6 d of exposure to $CuSO_4$ treatments (Fig. 26A).

A significant and gradual increase in EL% was recorded in the primary leaves on treatment with $CuSO_4$, and a maximum increase was noticed in seedlings treated with 200 μM $CuSO_4$. Though the increase in EL% was 3-55% up to 6 d of $CuSO_4$ treatment in primary leaves, an enhancement of 35-56% was recorded on 10 d of the treatment (Fig. 26B).

In the roots of *R. communis* seedlings subjected to $CuSO_4$ treatments, the increase in EL% was to the extent of 14-40% and 26-63% when exposed to 40-200 μM $CuSO_4$ on 2 and 6 d respectively. However, 72-80% increase in EL% was recorded in the roots of *R. communis* seedlings treated with 120-200 μM $CuSO_4$ on 10 d (Fig. 26C).

Copper stress significantly enhanced (2-3 folds over the control) the electrolyte leakage in cells of the cotyledonary leaves of *R. communis* seedlings. On application of cytokinins in Cu stressed seedlings, the EL% was reduced significantly. KIN application resulted in the reduction of EL% (39-46%) in the cotyledonary leaves subjected to 80 and 160 μM $CuSO_4$ as compared to that exposed to $CuSO_4$alone, whereas the reduction was still higher (55-61%) on application of BAP (Fig. 26D).

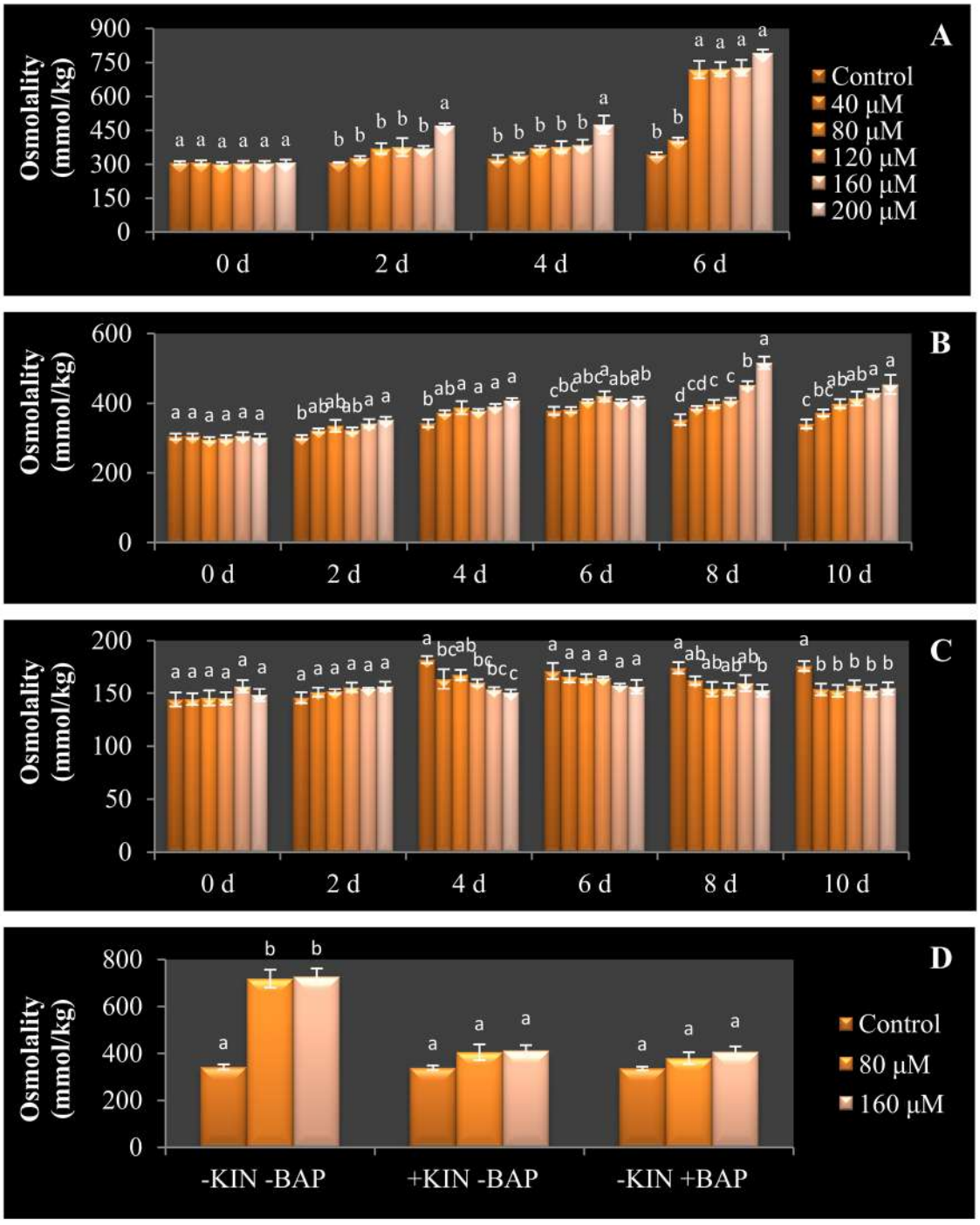

Figure 21. Osmolality in the cotyledonary leaves (A), primary leaves (B), roots (C), and cotyledonary leaves (exposed to cytokinins for 6 d) (D) of *R. communis* seedlings subjected to increasing concentrations of $CuSO_4$. Different alphabetical letters indicate significant difference between treatments (Duncan's test $p \leq 0.05$).

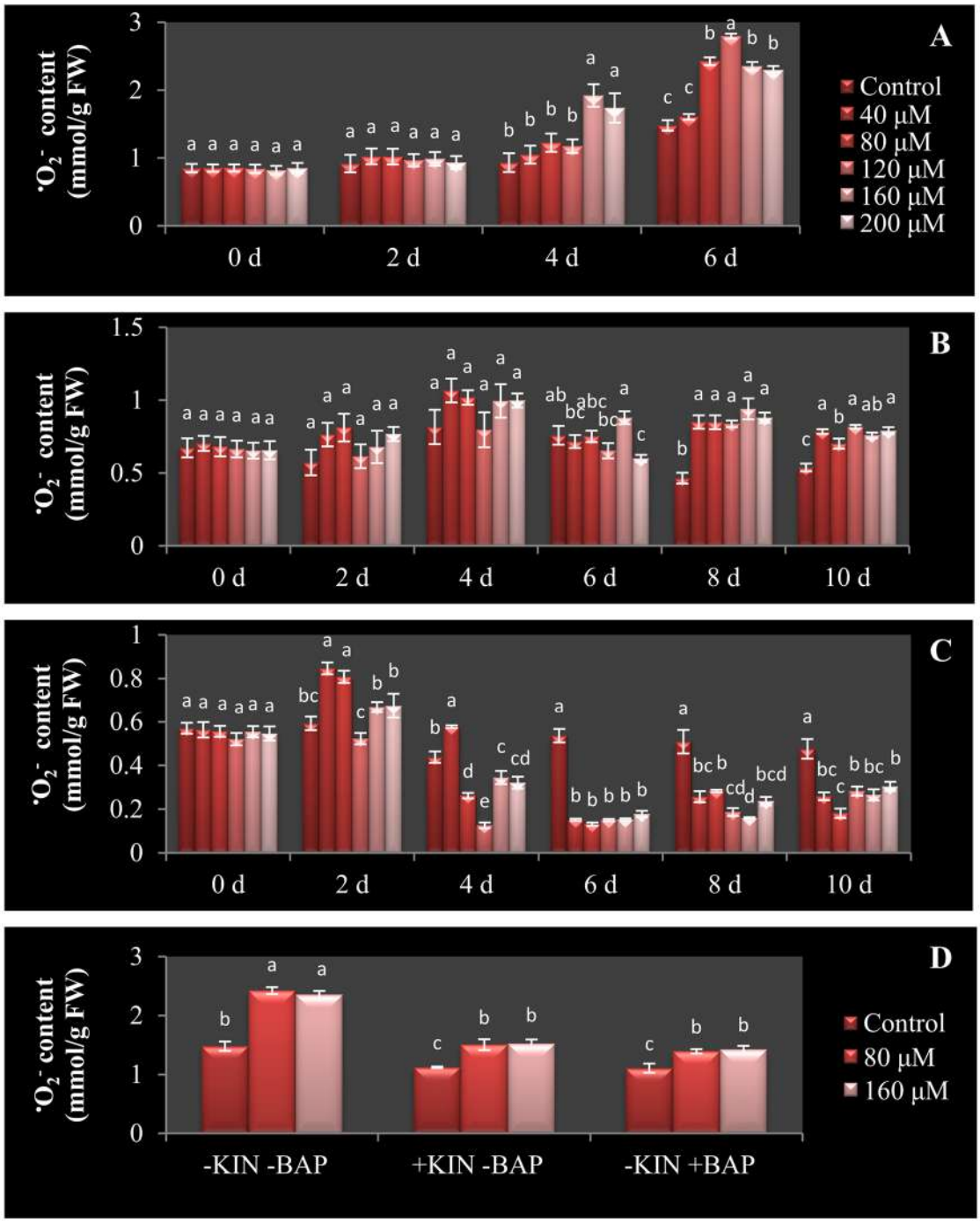

Figure 22. Superoxide ($^{\bullet}O_2^-$) content in the cotyledonary leaves (A), primary leaves (B), roots (C), and cotyledonary leaves (exposed to cytokinins for 6 d) (D) of *R. communis* seedlings subjected to increasing concentrations of $CuSO_4$. Different alphabetical letters indicate significant difference between treatments (Duncan's test $p \leq 0.05$).

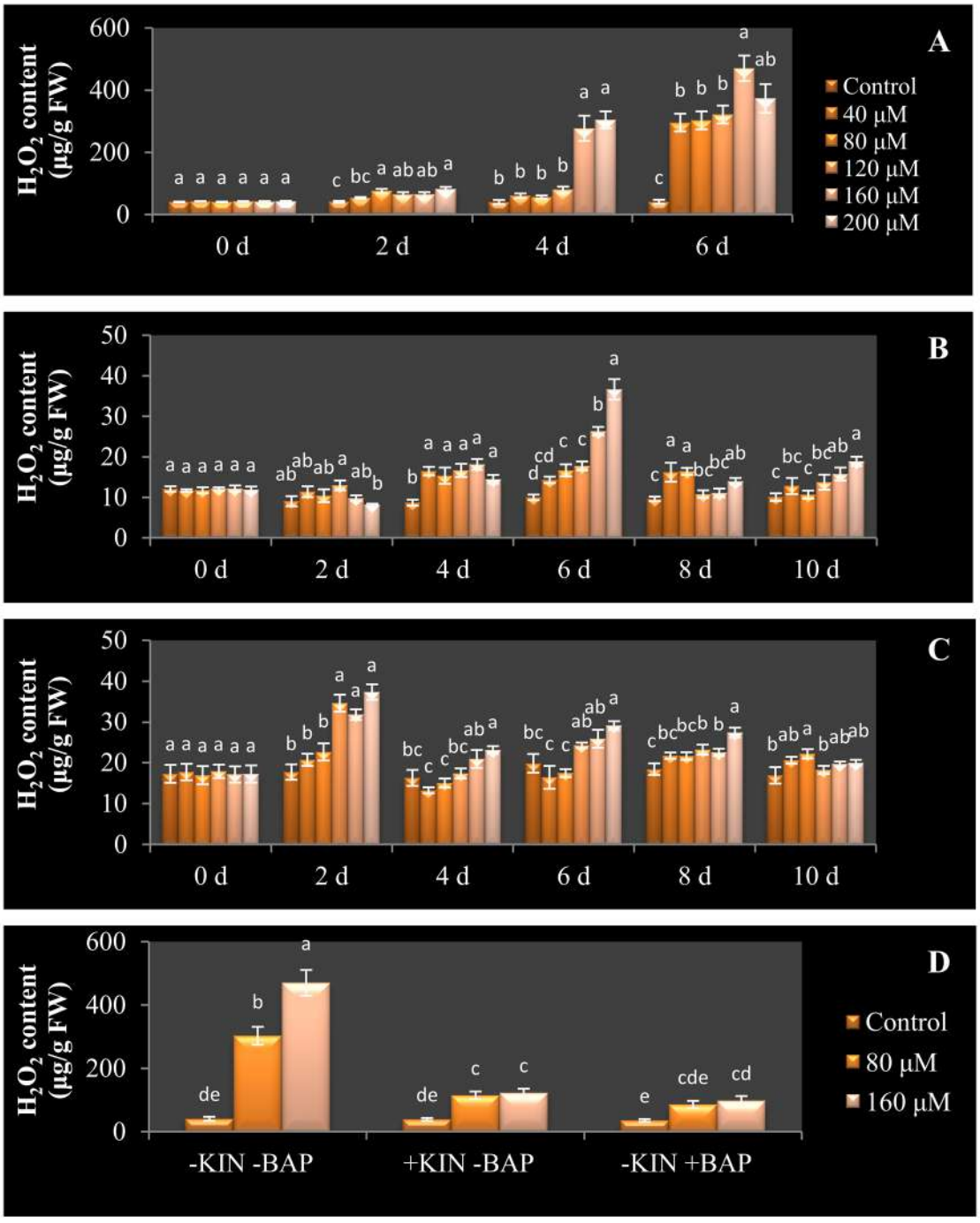

Figure 23. Hydrogen peroxide (H_2O_2) content in the cotyledonary leaves (A), primary leaves (B), roots (C), and cotyledonary leaves (exposed to cytokinins for 6 d) (D) of *R. communis* seedlings subjected to increasing concentrations of $CuSO_4$. Different alphabetical letters indicate significant difference between treatments (Duncan's test $p \leq 0.05$).

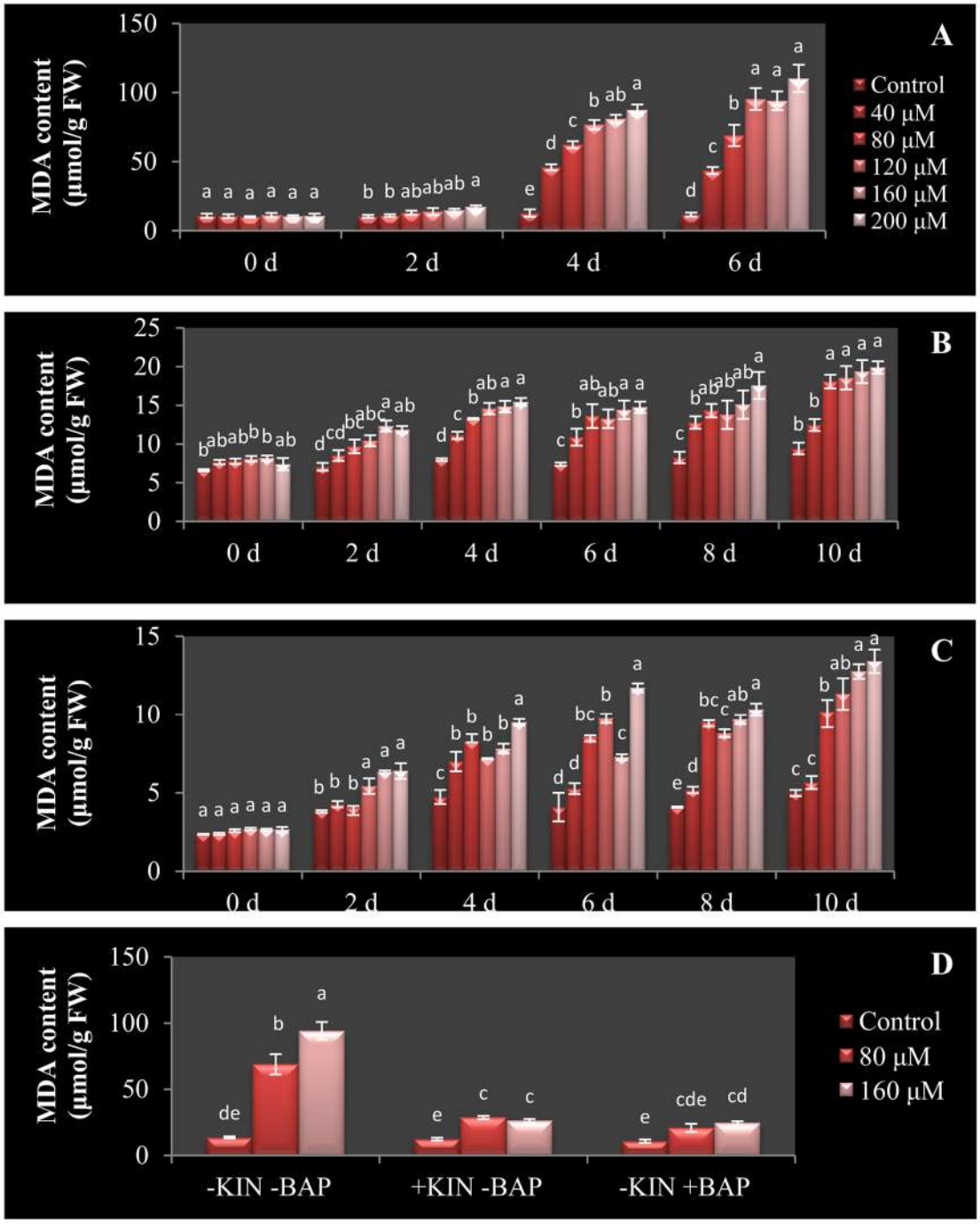

Figure 24. Malondialdehyde (MDA) content in the cotyledonary leaves (A), primary leaves (B), roots (C), and cotyledonary leaves (exposed to cytokinins for 6 d) (D) of *R. communis* seedlings subjected to increasing concentrations of $CuSO_4$. Different alphabetical letters indicate significant difference between treatments (Duncan's test $p \leq 0.05$).

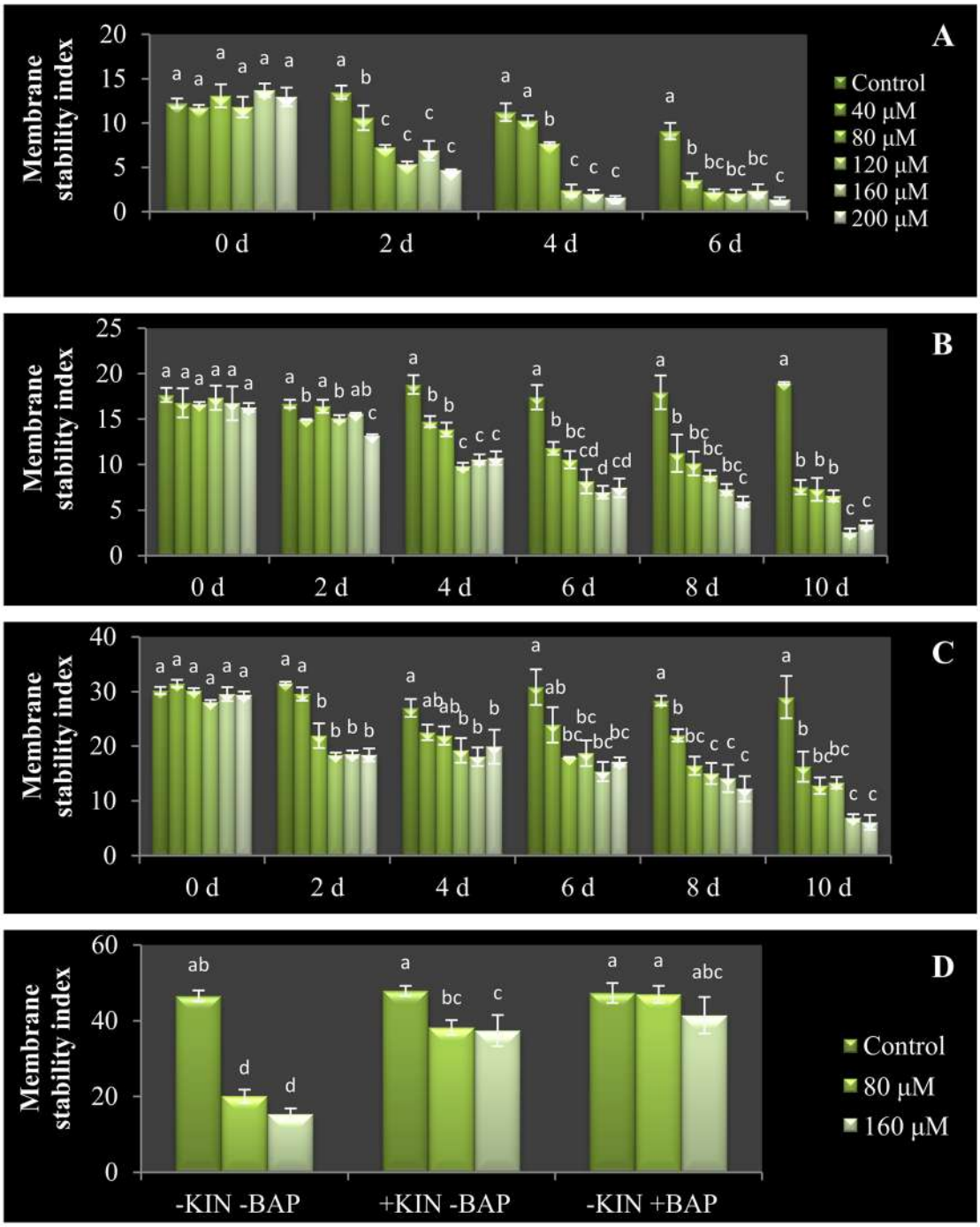

Figure 25. Membrane stability index (MSI) in the cotyledonary leaves (A), primary leaves (B), roots (C), and cotyledonary leaves (exposed to cytokinins for 6 d) (D) of *R. communis* seedlings subjected to increasing concentrations of $CuSO_4$. Different alphabetical letters indicate significant difference between treatments (Duncan's test $p \leq 0.05$).

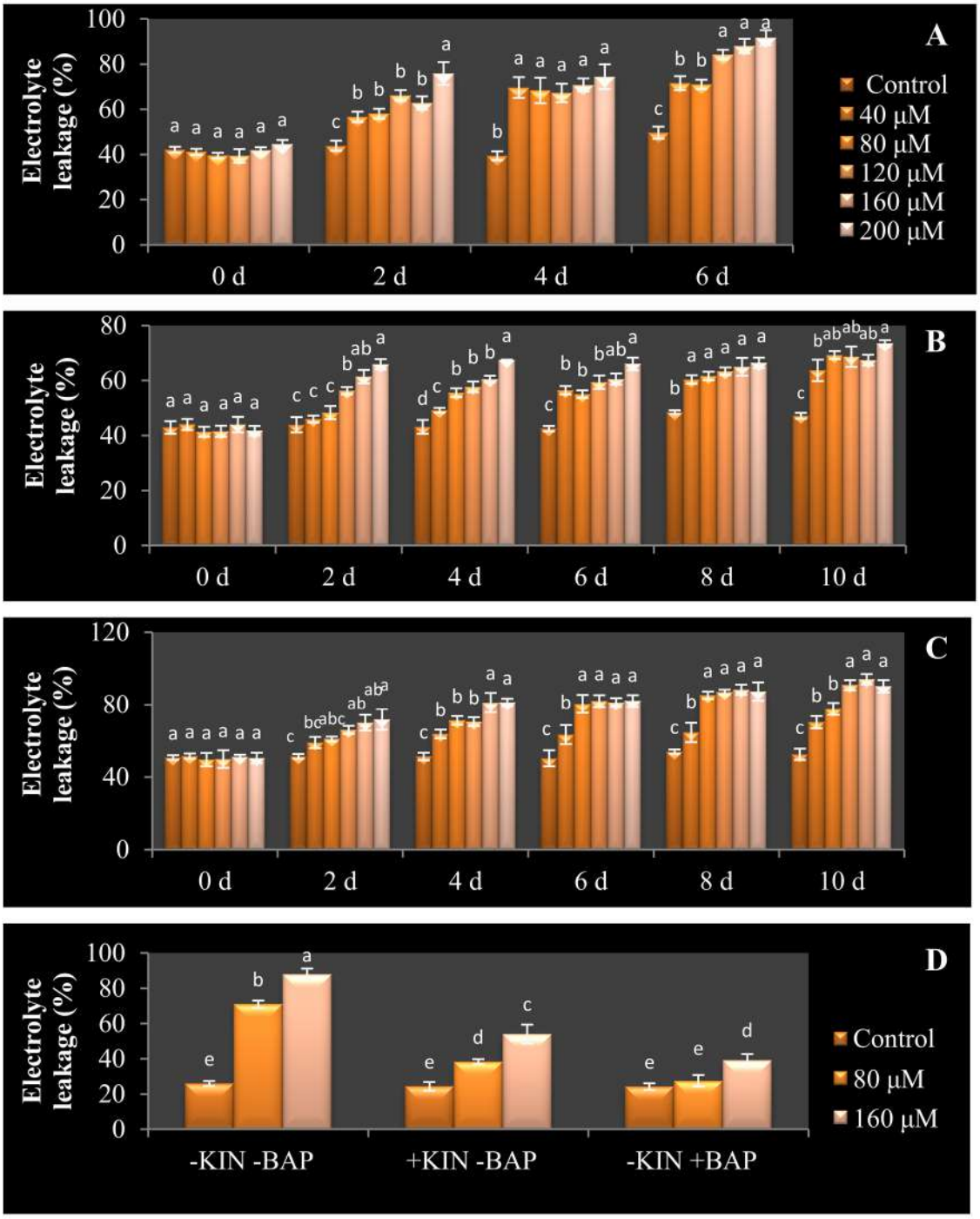

Figure 26. Electrolyte leakage (EL%) in the cotyledonary leaves (A), primary leaves (B), roots (C), and cotyledonary leaves (exposed to cytokinins for 6 d) (D) of *R. communis* seedlings subjected to increasing concentrations of $CuSO_4$. Different alphabetical letters indicate significant difference between treatments (Duncan's test $p \leq 0.05$).

4.2.4. Accumulation of primary metabolites

4.2.4.1. Total soluble sugar

Soluble sugar content was increased significantly in both cotyledonary and primary leaves of *R. communis* seedlings when exposed to increasing concentrations of $CuSO_4$. On the initial days of treatment (up to 4 d), the increase in total soluble sugar contents was insignificant in all the treatments except in 200 µM $CuSO_4$, which accumulated 2.6 folds higher soluble sugar content than that of the control. However, a drastic enhancement in the accumulation of soluble sugar content was observed on 6 d, which was to the extent of 2-8 folds over the control in treatments with 80-200 µM $CuSO_4$ (Fig. 27A).

A significant and gradual increase in total soluble sugar content was recorded in the primary leaves with increasing concentrations of $CuSO_4$ and days of exposure. On 2 d of treatment, the increase was 42% over the control in primary leaves of seedlings treated with 200 µM $CuSO_4$, which was enhanced to 67% on 6 d. Further from 8 d onwards, a steep increase in total soluble sugar content was recorded, and it was 2-3 folds higher over the control in all the treatments (Fig. 27B).

In contrast to the leaves, the total soluble sugar content in roots was significantly reduced in all the treatments. The reduction was 37-60% on 2 d of treatment, which was further reduced up to 68% on 4 d as compared to the respective controls. Prolonged exposure to Cu stress resulted in more severe reductions in the total soluble sugar content in the roots, which was to a maximum of 80% as compared to the control on 10 d (Fig. 27C).

Total soluble sugars content was significantly enhanced by 2 and 4 folds over the control in the cotyledonary leaves of *R. communis* seedlings subjected to 80 and 160 µM $CuSO_4$ respectively. On application of

cytokininsin $CuSO_4$ treated seedlings, accumulation of soluble sugars content was reduced to a significant level compared to that exposed to Cu stress alone. KIN application resulted in the reduction (33 and 62%) of soluble sugars content in cotyledonary leaves of 80 and 160 µM $CuSO_4$ treated seedlings as compared to those exposed to $CuSO_4$alone. Similarly, 25 and 61% reduction was recorded in 80 and 160 µM $CuSO_4$ treated seedlings respectively on application of BAP (Fig. 27D).

4.2.4.2. Total protein

Treatment with increasing concentrations of $CuSO_4$ resulted in the accumulation of total protein content in the cotyledonary leaves of *R. communis* seedlings. Though the accumulation was insignificant on 2 d, a significant and drastic increase in the accumulation of protein content was recorded in the cotyledonary leaves on 4 d of treatment with $CuSO_4$. The increase was to the extent of 1.9 to 4.9 folds at higher $CuSO_4$ concentrations (80-200 µM) on 4 d of treatment, and it was maximum at 120 µM $CuSO_4$. Beyond this, a reducing trend in protein content was observed in cotyledonary leaves, but still it was higher than that of the control (2-3 folds over the control) (Fig. 28A).

In contrary to soluble sugar content, total protein content was significantly reduced in the primary leaves on treatment with increasing concentrations of $CuSO_4$ and days of exposure. Even though the reduction was insignificant up to 6 d of treatment, 21-38% of reduction was recorded in the primary leaves of seedlings subjected to 120-200 µM $CuSO_4$ on 8-10 d (Fig. 28B).

Similar to the primary leaves, the total protein content was reduced significantly in the roots also. The reduction was 10-60% in the roots exposed to 40-200 µM $CuSO_4$ on 2-4 d as compared to the respective controls, beyond

which, the decline in total protein content extended up to 80% over the control (Fig. 28C).

Total protein content was enhanced to 2 and 3 folds in cotyledonary leaves exposed to 80 and 160 µM $CuSO_4$ respectively as compared to that of the control. However, cytokinin application resulted in the reduction of protein content in the cotyledonary leaves. On KIN application to Cu-treated seedlings, the protein content in cotyledonary leaves was reduced to 55 and 65% in seedlings subjected to 80 and 160 µM $CuSO_4$ respectively as compared to that of Cu stress alone. Similarly, 62 and 72% reduction was recorded in 80 and 160 µM $CuSO_4$ treated seedlings respectively on application of BAP (Fig. 28D).

4.2.4.3. Total free amino acids

A significant and gradual increase in total free amino acids content was observed in the cotyledonary leaves of *R. communis* with increase in concentration of $CuSO_4$ and days of exposure. The enhancement was 2-2.5 folds higher than that of the control on 2 d of $CuSO_4$ exposure, which further increased to 4-12 folds higher when exposed to 4-6 d of Cu stress (Fig. 29A).

The enhancement in total free amino acids content was insignificant in primary leaves up to 6 d of metal treatment. Thereafter, a significant enhancement was recorded. The increase in total free amino acids content was ranging between 2 to 2.9 folds over the control in primary leaves of *R. communis* exposed to 120-200 µM $CuSO_4$ (Fig. 29B).

Total free amino acids content was decreased significantly in the roots of *R. communis* on exposure to increasing concentrations of $CuSO_4$. On 2 d of exposure, the reduction was 25-47% in roots treated with 40-200 µM $CuSO_4$ as compared to the control. Thereafter, a gradual reduction in free amino acids

content was recorded, and a maximum reduction of 88% over the control was observed in roots treated with 200 µM $CuSO_4$ on 10 d (Fig. 29C).

Exposure to 80 and 160 µM $CuSO_4$ resulted in the accumulation (4 and 7 folds increase) of total free amino acids content in the cotyledonary leaves of *R. communis* seedlings. Foliar application of cytokinins resulted in the dramatic reduction of free amino acids content in the cotyledonary leaves of Cu-stressed *R. communis* seedlings. On application of KIN and BAP to 80 and 160 µM $CuSO_4$ treated seedlings, 84-90% reduction of free amino acids content was recorded in the cotyledonary leaves as compared to that exposed to $CuSO_4$alone (Fig. 29D).

4.2.4.4. Proline content

A significant and gradual increase in proline content was recorded in the cotyledonary as well as primary leaves of *R. communis* seedlings with increase in concentrations of $CuSO_4$ and days of treatments. In the case of cotyledonary leaves, a drastic hike in the proline content was recorded on 4 and 6 d of treatment, which was 14-19 folds higher than the control when treated with 160 and 200 µM $CuSO_4$ (Fig. 30A).

In the case of primary leaves, the increase in proline content was dependent on the concentration of $CuSO_4$ and the exposure time. On 6 d of treatment, the enhancement in proline content was ranging between 2-2.8 folds over the control. A maximum of 4 folds increase over the control was recorded in primary leaves when exposed to 200 µM $CuSO_4$ on 10 d (Fig. 30B).

Similar to other metabolites such as total sugar, total protein and total free amino acids, the proline content was also reduced significantly in the roots of *R. communis*. On 2 d, the reduction in proline content was only ≤

30% over the control. However, the level of reduction increased to 61% as compared to the control on 4-10 d of the treatment period (Fig. 30C).

In the case of proline content, a drastic accumulation (6 and 14 folds increase) was recorded in the cotyledonary leaves of *R. communis* seedlings subjected to 80 and 160 µM $CuSO_4$ respectively as compared to the control. However, application of KIN and BAP to the Cu-stressed seedlings leads to 75-90% reduction in proline content of the cotyledonary leaves as compared to those exposed to $CuSO_4$alone (Fig. 30D).

4.2.5. Free radical scavenging mechanisms

4.2.5.1. Enzymatic antioxidants

4.2.5.1.1. Glutathione reductase (GR)

A significant increase in GR activity was recorded in the cotyledonary leaves on exposure to increasing levels of $CuSO_4$. The activity of GR was gradually enhanced with increase in treatment period and exposure to 40-120 µM $CuSO_4$, and the increase was in the range of 1.3-2.6 folds with respect to the control on 2-6 d of exposure. In contrast, on exposure to 160 and 200 µM $CuSO_4$, 2.6 folds increase in GR activity was recorded over the control on 2 d, which was reduced to 2.4 and 2.0 folds on 4 and 6 d respectively as compared to the control (Fig. 31A).

In primary leaves, the increase in GR activity was ≤ 2 folds over the control up to 8 d of exposure to low concentrations of $CuSO_4$ (40-120 µM). When *R. communis* seedlings were exposed to higher concentrations of $CuSO_4$ (200 µM), GR activity was enhanced to a maximum of 2.8 folds up to 4 d, which was reduced and became insignificant on 6 d. Furthermore, upon exposure to 160 and 200 µM $CuSO_4$, the activity of GR was drastically

enhanced to a maximum of 5 and 15 folds on 8 and 10 d respectively over the control (Fig. 31B).

In the case of roots, a significant enhancement in GR activity was recorded and depended on the concentration of $CuSO_4$. Up to 4 d of $CuSO_4$ exposure, the activity was gradually increased and reached to a maximum of 12 folds over the control. On 10 d, further enhancement (up to 17 folds) was observed over the control on exposure to increasing levels of $CuSO_4$, with a maximum increase of 17 folds in the roots exposed to 160 and 200 µM $CuSO_4$ (Fig. 31C).

Exposure to $CuSO_4$ treatment resulted in 2 folds increase of GR activity in the cotyledonary leaves of *R. communis* seedlings. On application of cytokinins, the GR activity was further enhanced. The enhancement was least in Cu stressed cotyledonary leaves of seedlings upon exposure to KIN. In contrast, BAP application significantly enhanced GR activity in cotyledonary leaves, as compared to those subjected to $CuSO_4$ alone. The enhancement was 32 and 34% in BAP treated seedlings along with 80 and 160 µM $CuSO_4$, respectively (Fig. 31D).

4.2.5.1.2. Monodehydroascorbate reductase (MDHAR)

Copper stress resulted in highly significant enhancements in MDHAR activity in the leaves and roots of *R. communis* seedlings (Fig. 32). In cotyledonary leaves, the MDHAR activity was increased up to 2.5 folds over the control on 2 d of exposure to 200 µM $CuSO_4$. On further days of $CuSO_4$ exposure, the MDHAR activity increased to a maximum of 4 and 5 folds with respect to that of the control on 4 and 6 d respectively (Fig. 32A).

The MDHAR activity was gradually increased in the primary leaves of *R. communis* seedlings subjected to increasing concentrations of $CuSO_4$ throughout the treatment period. On 2 d of exposure to Cu stress, the

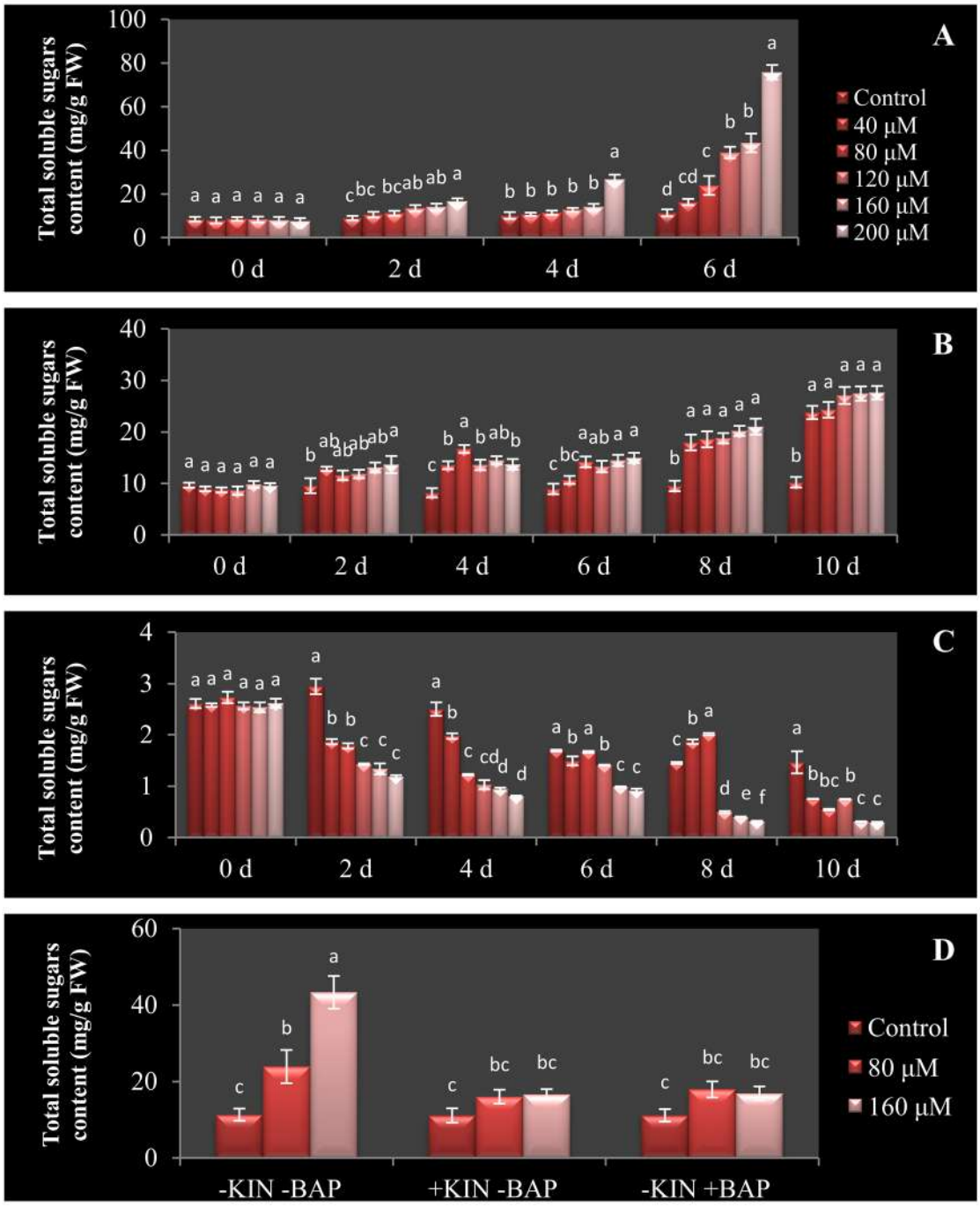

Figure 27. Total soluble sugars content in the cotyledonary leaves (A), primary leaves (B), roots (C), and cotyledonary leaves (exposed to cytokinins for 6 d) (D) of *R. communis* seedlings subjected to increasing concentrations of $CuSO_4$. Different alphabetical letters indicate significant difference between treatments (Duncan's test $p \leq 0.05$).

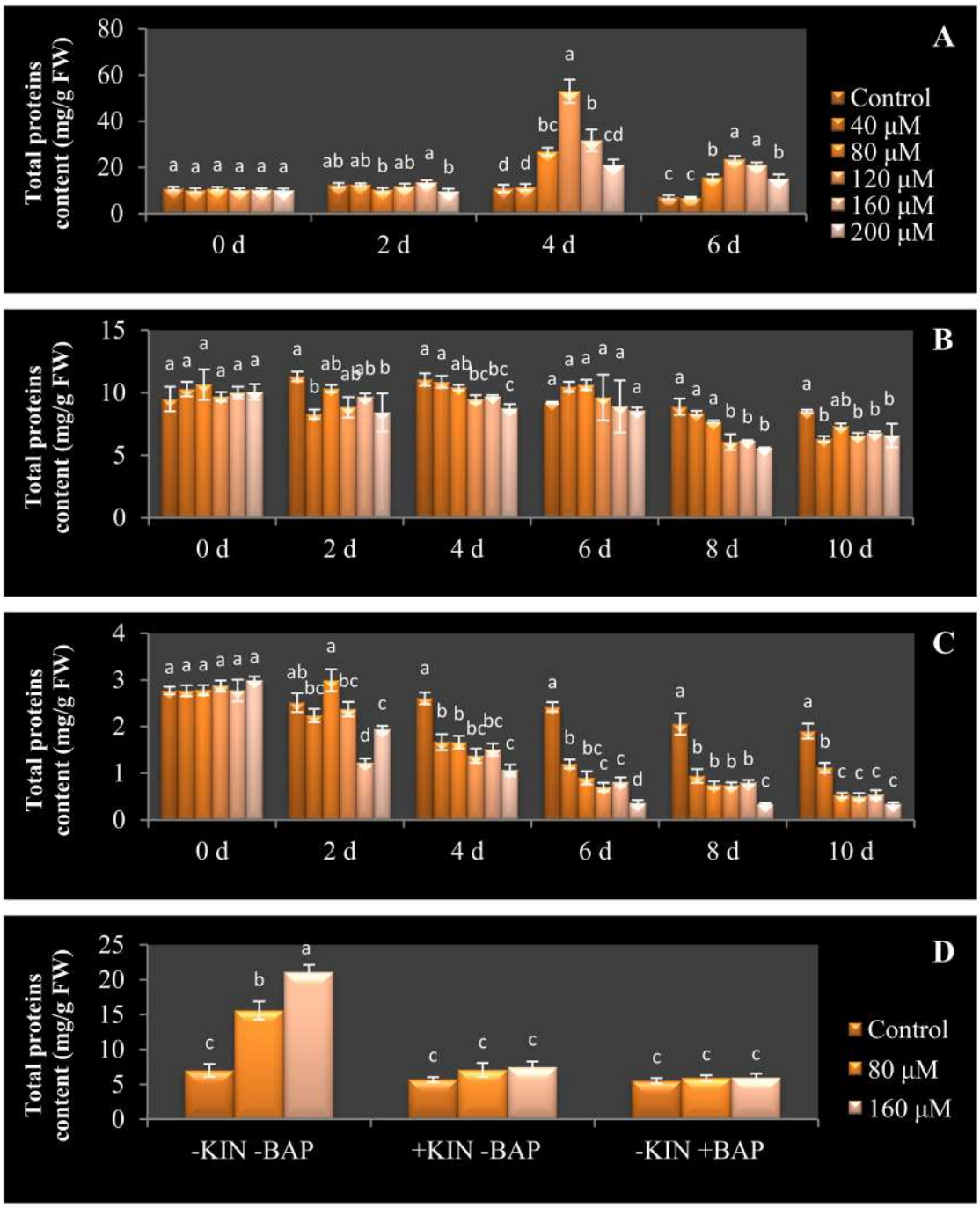

Figure 28. Total proteins content in the cotyledonary leaves (A), primary leaves (B), roots (C), and cotyledonary leaves (exposed to cytokinins for 6 d) (D) of *R. communis* seedlings subjected to increasing concentrations of $CuSO_4$. Different alphabetical letters indicate significant difference between treatments (Duncan's test $p \leq 0.05$).

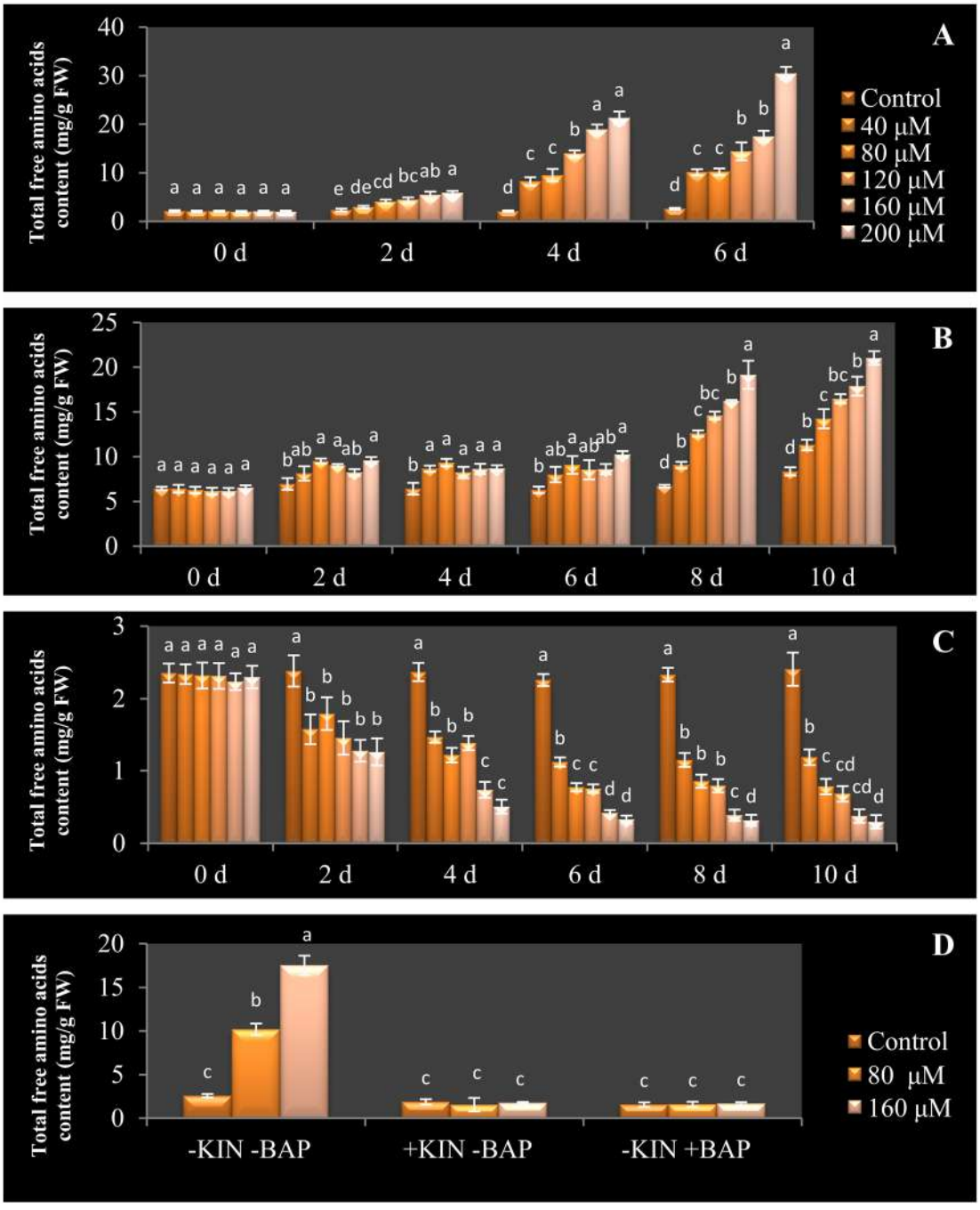

Figure 29. Total free amino acids content in the cotyledonary leaves (A), primary leaves (B), roots (C), and cotyledonary leaves (exposed to cytokinins for 6 d) (D) of *R. communis* seedlings subjected to increasing concentrations of $CuSO_4$. Different alphabetical letters indicate significant difference between treatments (Duncan's test $p \leq 0.05$).

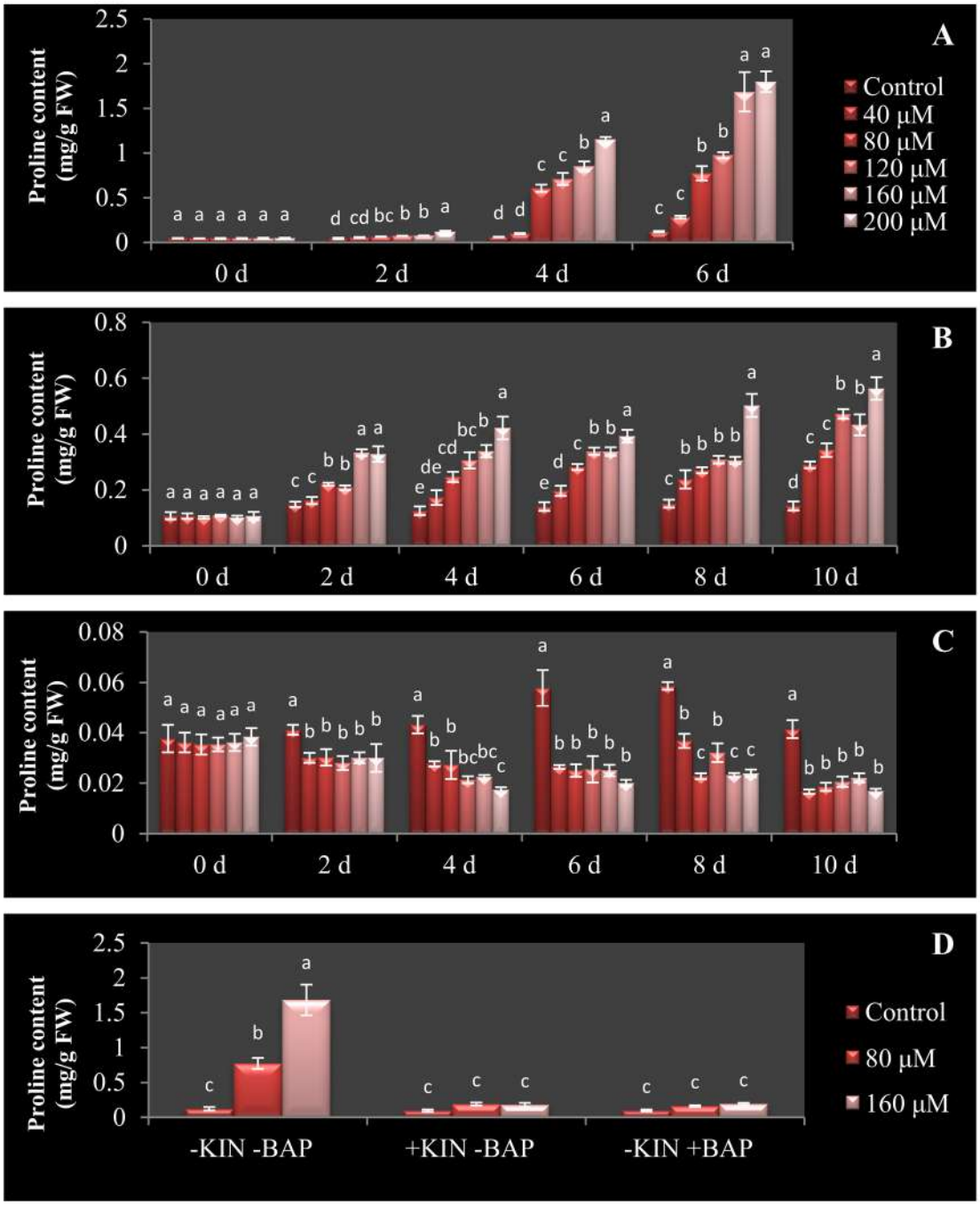

Figure 30. Proline content in the cotyledonary leaves (A), primary leaves (B), roots (C), and cotyledonary leaves (exposed to cytokinins for 6 d) (D) of *R. communis* seedlings subjected to increasing concentrations of $CuSO_4$. Different alphabetical letters indicate significant difference between treatments (Duncan's test $p \leq 0.05$).

enhancement in MDHAR activity was insignificant and was only 1.2 to 1.6 folds higher than the control. In contrast, a significant enhancement in activity was observed from 4 d onwards. About 2-3 folds increase in activity of MDHAR was recorded over the control on 6 d and further enhanced to a maximum of 3.7 folds as compared to the control on 10 d of $CuSO_4$ stress (Fig. 32B).

In the case of roots, no significant enhancement was noticed in MDHAR activity on 2 d of $CuSO_4$ treatment; but the activity was significantly enhanced from 4 d onwards. The increase in MDHAR activity in root was 1.5-4.0 folds over the control in treatments ranging from 40-200 µM $CuSO_4$ on 4 d, which was enhanced up to 5 folds on 6 and 8 d. On 10 d, a maximum of 6 and 7 folds increase in activity over the control was recorded in the roots of seedlings treated with 80 and 120 µM $CuSO_4$ respectively.In contrast, the enhancement in MDHAR activity was 3-4 folds only when treated with 160 and 200 µM $CuSO_4$ on 10 d (Fig. 32C).

The enhancement in MDHAR activity was 1.5 and 3.7 folds higher in 80 and 160 µM $CuSO_4$ treated cotyledonary leaves of *R. communis* than that of the control. Cytokinin application to Cu-stressed *R. communis* seedlings resulted in further enhancement of MDHAR activity in the cotyledonary leaves. On application of KIN to 80 and 160 µM $CuSO_4$ treated seedlings, MDHAR activity in cotyledonary leaves was enhanced to a maximum of 1.7 folds as compared to that exposed to $CuSO_4$alone. But, on exposure of 80 and 160 µM $CuSO_4$ treated seedlings to BAP, MDHAR activity was significantly enhanced by 4.5 and 1.5 folds, as compared to the seedlings exposed to $CuSO_4$alone (Fig. 32D).

4.2.5.1.3. Dehydroascorbate reductase (DHAR)

The activity of DHAR was gradually increased in the cotyledonary leaves of *R. communis* seedlings exposed to an increase in the concentration

of $CuSO_4$ in a time-dependent manner. On 2 d, the DHAR activity was enhanced up to 1.8-3.6 folds over the control on exposure to 40-200 μM $CuSO_4$, which was further enhanced to a maximum of 4 and 7.5 folds over the control on 4 and 6 d respectively (Fig. 33A).

Similar to cotyledonary leaves, a gradual increase in DHAR activity was observed in primary leaves also up to 4 d of $CuSO_4$ exposure, with a maximum increase of 1.5 and 2.3 folds over the control on 2 and 4 d respectively. On 6 d, the increase in DHAR activity was reduced, and only 1.5-1.8 folds increase over the control was recorded. But, the activity was again enhanced to a range of 2.5-3.0 and 2.7-3.6 folds with respect to that of the control on 8 and 10 d respectively upon exposure to 80-200 μM $CuSO_4$ (Fig. 33B).

A highly significant increase in DHAR activity was recorded in the roots of *R. communis* seedlings subjected to increasing levels of Cu. The activity was enhanced to 3-8 folds over the control in the seedlings subjected to 40-200 μM $CuSO_4$ on 2 d. When the $CuSO_4$ exposure was prolonged, the enzyme activity was again enhanced, and reached to a maximum of 12 and 14 folds over the control on 6 and 8 d. Furthermore, the increase in DHAR activity was only 7-10 folds with respect to the control when subjected to 40-160 μM $CuSO_4$, which was reduced to 5.6 folds increase over the control at 200 μM $CuSO_4$ on 10 d (Fig. 33C).

Exposure to $CuSO_4$ treatment resulted in 4 folds increase of DHAR activities in the cotyledonary leaves of *R. communis* seedlings. On application of cytokinins, the DHAR activity was further enhanced. KIN application resulted in 37 and 7% enhancement in DHAR activity in the cotyledonary leaves of 80 and 160 μM $CuSO_4$ treated seedlings respectively as compared to that exposed to $CuSO_4$alone. Similarly, 45 and 12% increase in activity was

recorded in the seedlings treated with BAP along with 80 and 160 µM $CuSO_4$ (Fig. 33D).

4.2.5.1.4. Catalase (CAT)

Exposure to Cu stress resulted in the enhanced activity of CAT in both the leaves and roots of *R. communis* (Fig. 34). Though the increase in CAT activity was insignificant at low concentrations of $CuSO_4$ (40-120 µM) on 2 and 4 d of treatment, a significant increase (2-6 folds) was observed at higher concentrations (160-200 µM). A drastic increase in CAT activity was recorded in the cotyledonary leaves on 6 d of $CuSO_4$ treatment, and the increase was 9-14 folds over the control on exposure to 80-200 µM $CuSO_4$ (Fig. 34A).

The increase in CAT activity was 2 folds over the control in the primary leaves of *R. communis* subjected to 120-200 µM $CuSO_4$ treatments even on 2 d of exposure, which was extended up to 5 folds on 6 d and reached to 7 folds over the control on 10 d of $CuSO_4$ exposure (Fig. 34B).

In the case of roots, a maximum of 2 folds increase in CAT activity was recorded upon exposure to increasing concentrations of $CuSO_4$ up to 6 d of treatment as compared to that of the control. However, the increase in CAT activity reached 9 folds over the control in the roots of *R. communis* subjected to 200 µM $CuSO_4$ on 10 d (Fig. 34C).

The enhancement in CAT activity was 9 and 14 folds higher in 80 and 160 µM $CuSO_4$ treated cotyledonary leaves of *R. communis* than that of the control, and cytokinin application resulted in further enhancement of CAT activity. On application of KIN to 80 and 160 µM $CuSO_4$ treated seedlings, CAT activity in cotyledonary leaves was enhanced to 45 and 27% as compared to that exposed to $CuSO_4$alone. Similarly, during exposure to 80 and 160 µM $CuSO_4$ treated seedlings to BAP, CAT activity was enhanced to

55 and 77% respectively, as compared to the seedlings exposed to $CuSO_4$alone (Fig. 34D).

4.2.5.1.5. Guaiacol peroxidase (POD)

A significant and gradual increase in POD activity was observed in the cotyledonary and primary leaves of *R. communis*. On 2 d, the increase in POD activity was ≤ 4 folds over the control, which enhanced to 8 and 14 folds in the cotyledonary leaves of seedlings subjected to 200 μM $CuSO_4$ on 4 and 6 d respectively (Fig. 35A).

The increase in POD activity was less in primary leaves as compared to that of cotyledonary leaves. On 2 d, the enhancement in POD activity was ranging between 1.6-1.8 folds in the primary leaves subjected to 120-200 μM $CuSO_4$. On the following day of treatment (4 d), the enhancement in POD activity ranged between 2-3 folds over the control in the primary leaves of seedlings exposed to 40-200 μM $CuSO_4$. But no further significant enhancement in POD activity was recorded on 6 and 8 d of $CuSO_4$ exposure. In contrast, the enhancement in POD activity reached to a maximum of 3.5 folds on exposure to 200 μM $CuSO_4$ for 10 d as compared to that of the control (Fig. 35B).

A drastic increase in POD activity was recorded in the roots on 2 d of exposure to $CuSO_4$. On 2 d, the enhancement was 5 folds over the control upon exposure to 40 μM $CuSO_4$, which was increased to 17-19 folds over the control in the roots of *R. communis* seedlings exposed to 120-200 μM $CuSO_4$. From 4 d onwards, the enhancement in POD activity was reduced (only ≤ 3 folds increase over the control) at higher $CuSO_4$ concentrations (120-200 μM). In contrast, at mild stresses (40 and 80 μM $CuSO_4$), the POD activity increased (3 to 6 folds over the control) on further days of exposure (Fig. 35C).

Exposure to $CuSO_4$ treatment resulted in 12 folds increase of POD activity in the cotyledonary leaves of *R. communis* seedlings. On application of cytokinins, the POD activity was further enhanced. KIN application resulted in negligible enhancement in POD activity in the cotyledonary leaves of 80 and 160 µM $CuSO_4$ treated seedlings respectively as compared to that exposed to $CuSO_4$alone. In contrast, significant increase in activity was recorded in the seedlings treated with BAP along with $CuSO_4$. Of which, 80 µM $CuSO_4$ + BAP treated cotyledonary leaves recorded 40% increase in POD activity as compared to that treated with 80 µM $CuSO_4$ (Fig. 35D).

4.2.5.1.6. Ascorbate peroxidase (APX)

A significant and gradual increase in APX activity was observed in the leaves and roots of *R. communis* exposed to $CuSO_4$ in a time-dependent manner (Fig. 36). The increase in APX activity was 2-8 folds over the control in the cotyledonary leaves subjected to 40-200 µM $CuSO_4$ for 2-4 d. However, the activity was drastically increased on 6 d, to the extent of 20-23 folds in the cotyledonary leaves exposed to 80-200 µM $CuSO_4$ as compared to the control (Fig. 36A).

In the case of primary leaves, a gradual increase in APX activity was observed up to 10 d, and a maximum of 2 folds increase was recorded with increase in concentrations of $CuSO_4$ and days of exposure as compared to the control (Fig. 36B).

The activity of APX was gradually increased in the roots of *R. communis* subjected to $CuSO_4$ treatments. Up to 6 d of $CuSO_4$ exposure, the enhancement in APX activity was $\leq$ 8 folds over the control in all the $CuSO_4$ treatments. Thereafter, the activity was increased to $\geq$ 10 folds over the control. Maximum APX activity of 18 and 16 folds was recorded in the roots treated with 200 µM $CuSO_4$ on 8 and 10 d respectively (Fig. 36C).

The enhancement in APX activity was 20 and 23 folds, respectively, for 80 and 160 µM $CuSO_4$ treated cotyledonary leaves of seedlings than that of the control. The activity of APX was found to be significantly enhanced further with the application of KIN and BAP along with $CuSO_4$ than that of the cotyledonary leaves of *R. communis* exposed to $CuSO_4$alone. On application of KIN to 80 and 160 µM $CuSO_4$ treated seedlings, 53 and 67% increase in APX activity was recorded as compared to that of Cu stress alone. In contrast, a maximum of only 12% increase in APX activity was recorded upon application of BAP to Cu stressed seedlings (Fig. 36D).

4.2.5.1.7. Superoxide dismutase (SOD)

A significant enhancement in SOD activity was observed in the cotyledonary leaves of *R. communis* subjected to $CuSO_4$ treatment from 4 d onwards. The increase was 2 to 3.3 folds over the control with increase in concentrations of $CuSO_4$ (80-200 µM) on 4 d, which reached up to 4.5 to 6.8 folds over the control on 6 d of exposure (Fig. 37A).

A significant increase in SOD activity in the primary leaves was observed from 4 d onwards and extended up to 8 d. On 6 and 8 d, the maximum increase in SOD activity was observed on exposure to 120 µM $CuSO_4$, and it was 61 and 46% respectively as compared to the control. In contrast, on 10 d of exposure, a gradual reduction in SOD activity was recorded, and it reached up to 26% as compared to the control (Fig. 37B).

A significant and gradual increase of SOD activity was recorded in the roots on exposure to $CuSO_4$. An increase of 3.7-4.5 folds over the control was recorded up to 6 d of treatment at 200 µM $CuSO_4$, which extended to 10 and 13 folds as compared to the respective controls on 8 and 10 d respectively in the roots of *R. communis* (Fig. 37C).

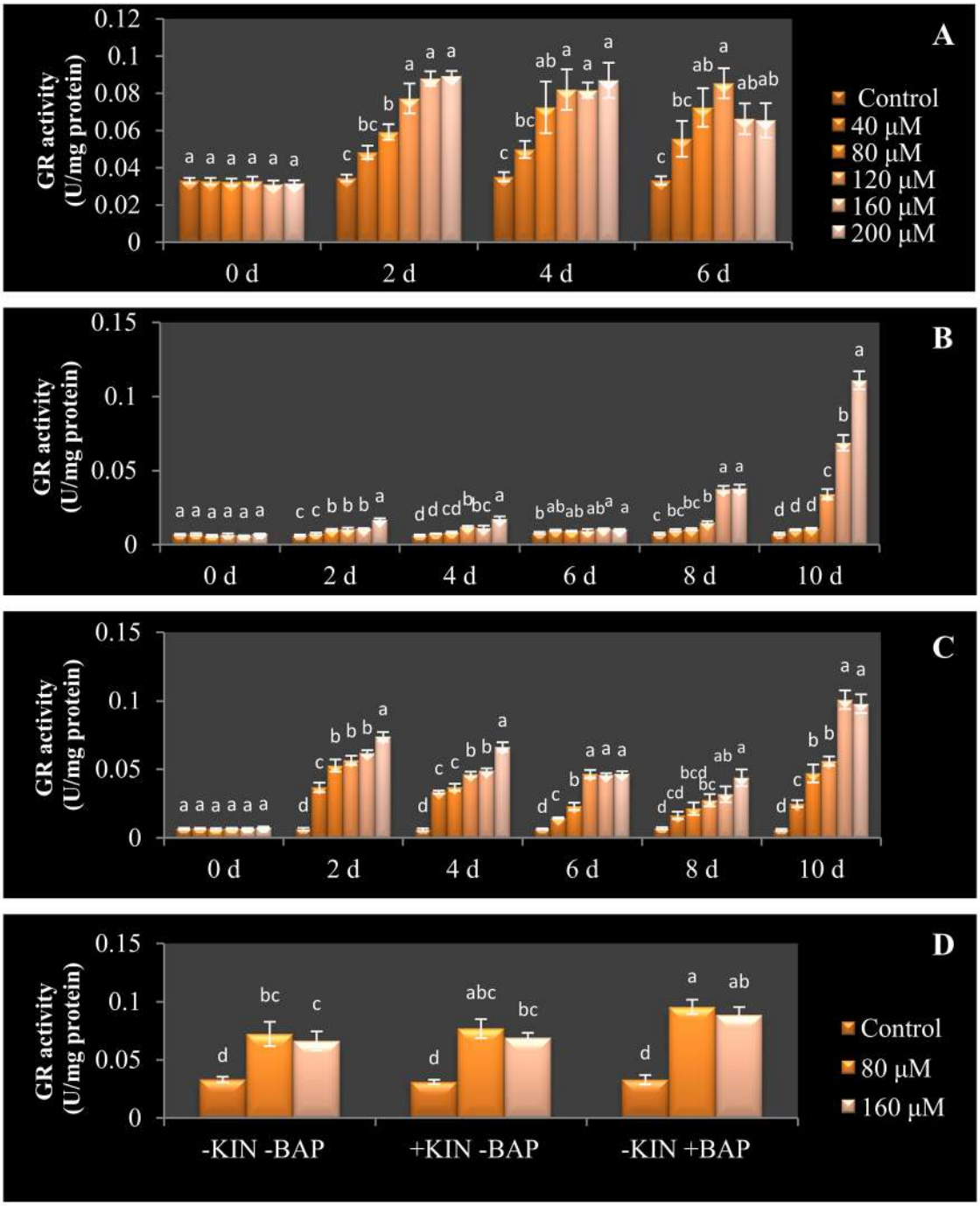

Figure 31. Glutathione reductase (GR) activity in the cotyledonary leaves (A), primary leaves (B), roots (C), and cotyledonary leaves (exposed to cytokinins for 6 d) (D) of *R. communis* seedlings subjected to increasing concentrations of $CuSO_4$. Different alphabetical letters indicate significant difference between treatments (Duncan's test $p \leq 0.05$).

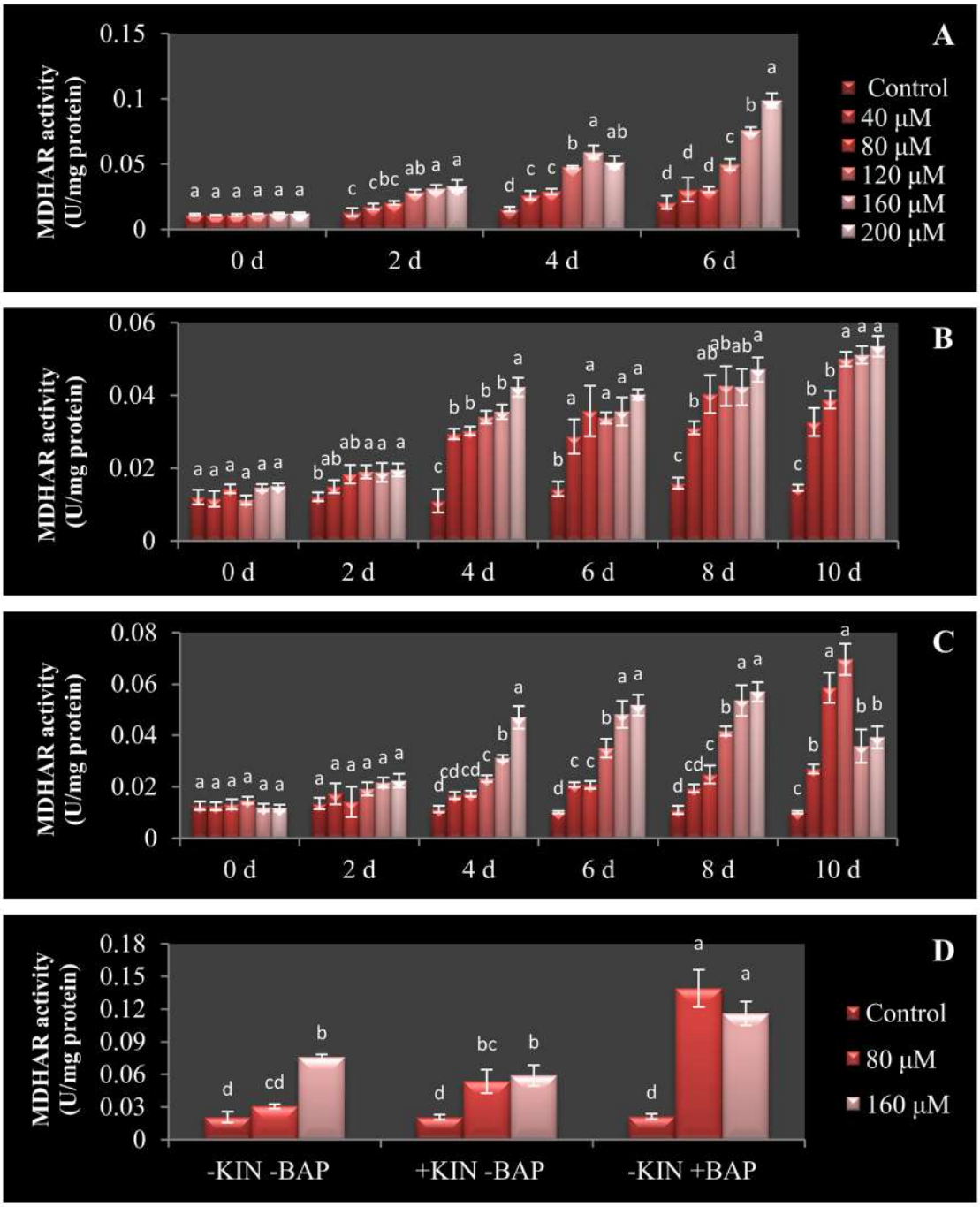

Figure 32. Monodehydroascorbate reductase (MDHAR) activity in the cotyledonary leaves (A), primary leaves (B), roots (C), and cotyledonary leaves (exposed to cytokinins for 6 d) (D) of *R. communis* seedlings subjected to increasing concentrations of $CuSO_4$. Different alphabetical letters indicate significant difference between treatments (Duncan's test $p \leq 0.05$).

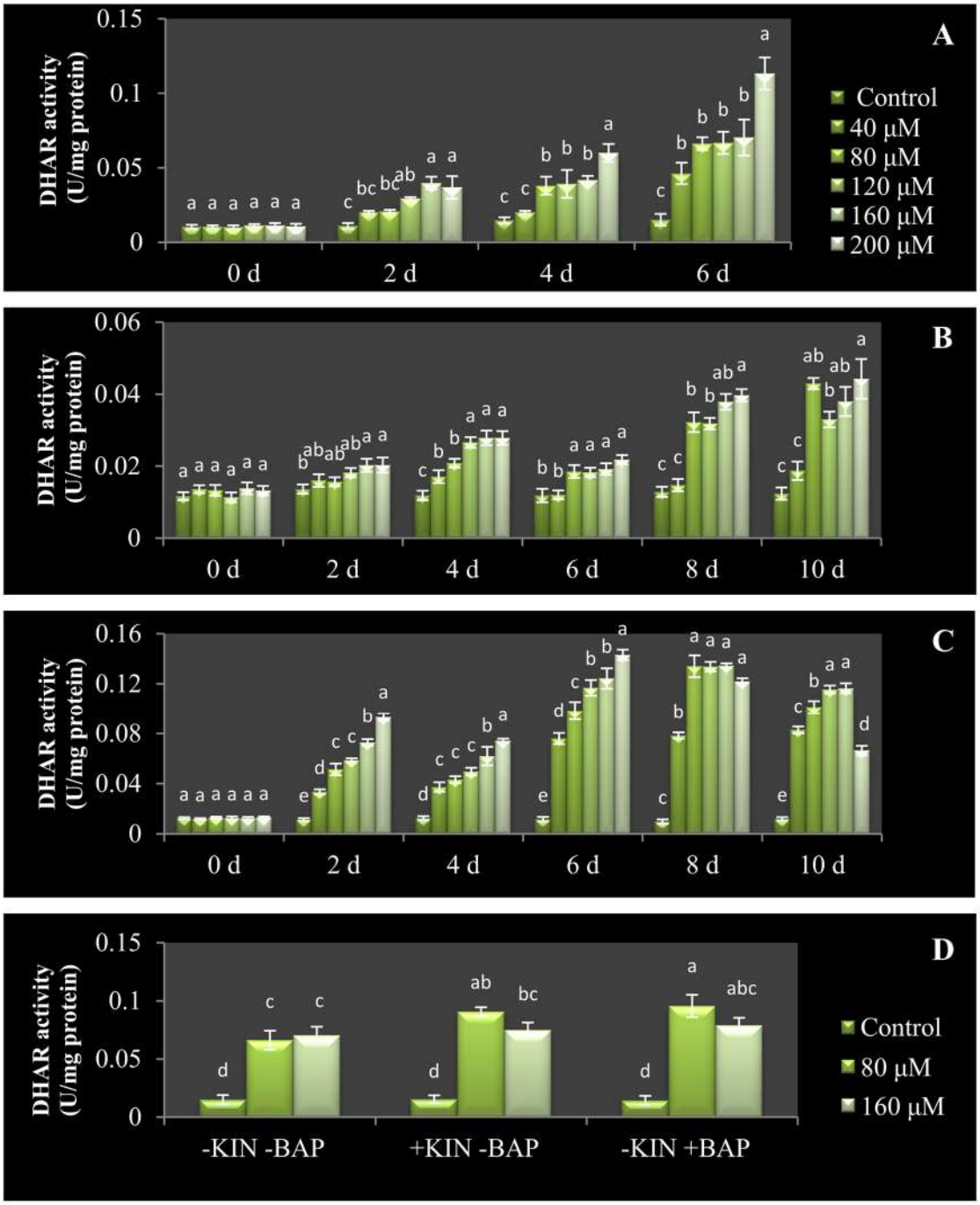

Figure 33. Dehydroascorbate reductase (DHAR) activity in the cotyledonary leaves (A), primary leaves (B), roots (C), and cotyledonary leaves (exposed to cytokinins for 6 d) (D) of *R. communis* seedlings subjected to increasing concentrations of $CuSO_4$. Different alphabetical letters indicate significant difference between treatments (Duncan's test $p \leq 0.05$).

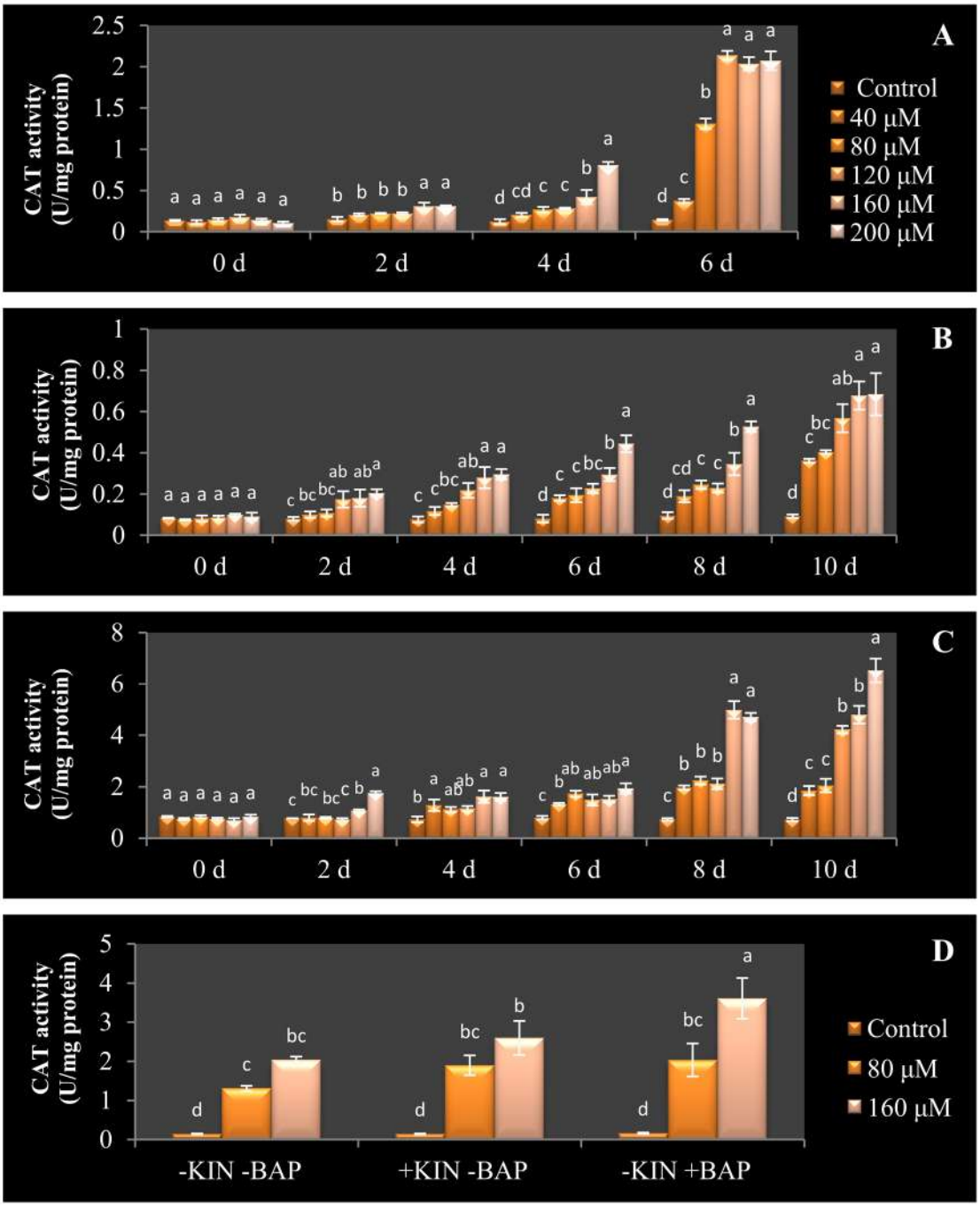

Figure 34. Catalase (CAT) activity in the cotyledonary leaves (A), primary leaves (B), roots (C), and cotyledonary leaves (exposed to cytokinins for 6 d) (D) of *R. communis* seedlings subjected to increasing concentrations of $CuSO_4$. Different alphabetical letters indicate significant difference between treatments (Duncan's test $p \leq 0.05$).

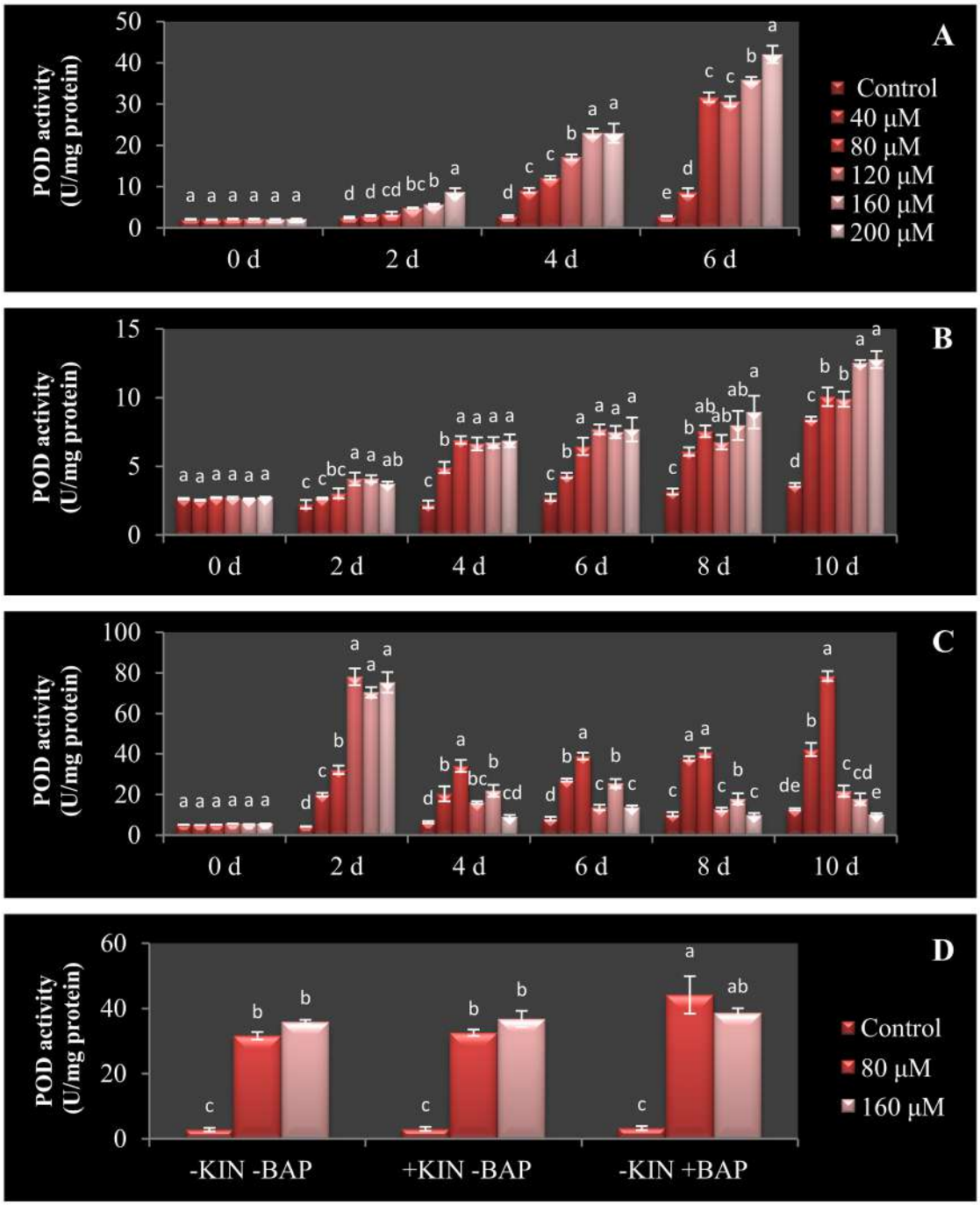

Figure 35. Guaiacol peroxidase (POD) activity in the cotyledonary leaves (A), primary leaves (B), roots (C), and cotyledonary leaves (exposed to cytokinins for 6 d) (D) of *R. communis* seedlings subjected to increasing concentrations of $CuSO_4$. Different alphabetical letters indicate significant difference between treatments (Duncan's test $p \leq 0.05$).

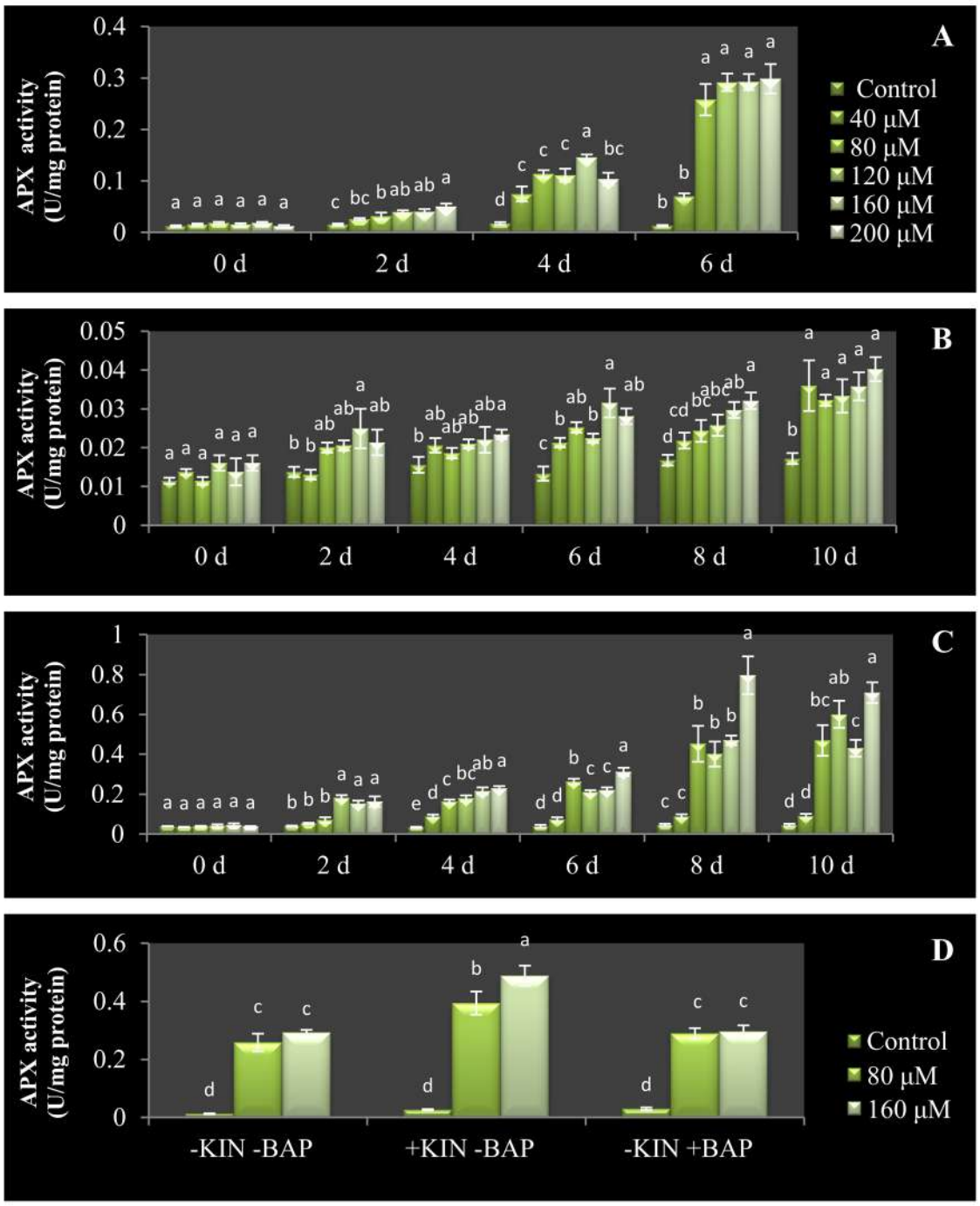

Figure 36. Ascorbate peroxidase (APX) activity in the cotyledonary leaves (A), primary leaves (B), roots (C), and cotyledonary leaves (exposed to cytokinins for 6 d) (D) of *R. communis* seedlings subjected to increasing concentrations of $CuSO_4$. Different alphabetical letters indicate significant difference between treatments (Duncan's test $p \leq 0.05$).

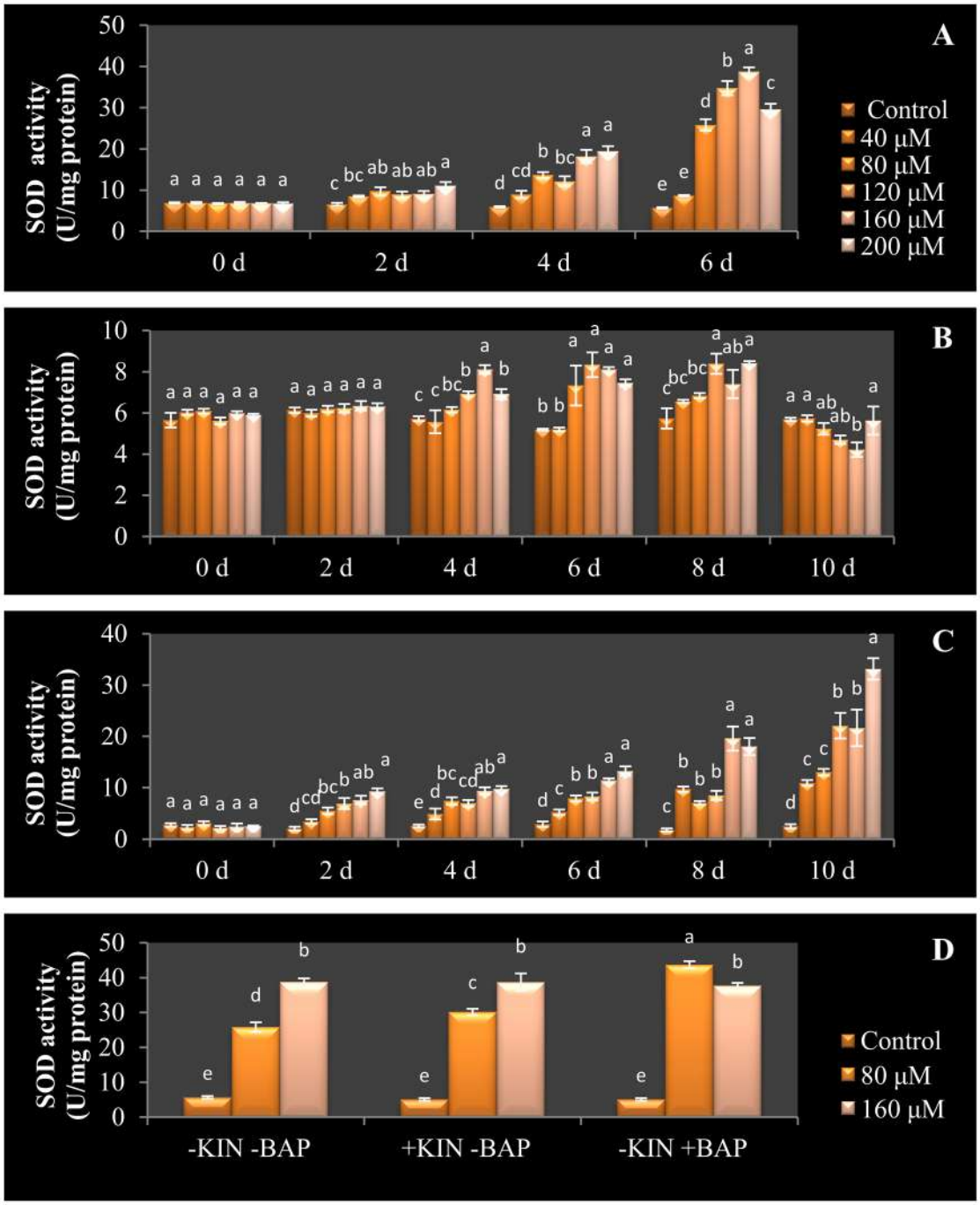

Figure 37. Superoxide dismutase (SOD) activity in the cotyledonary leaves (A), primary leaves (B), roots (C), and cotyledonary leaves (exposed to cytokinins for 6 d) (D) of *R. communis* seedlings subjected to increasing concentrations of $CuSO_4$. Different alphabetical letters indicate significant difference between treatments (Duncan's test $p \leq 0.05$).

Exposure to 80 and 160 µM $CuSO_4$ treatment resulted in 5 and 7 folds increase of SOD activity in the cotyledonary leaves of *R. communis* seedlings. On application of cytokinins to 80 µM $CuSO_4$ treated seedlings, SOD activity was further enhanced, and the increase was to the extent of 17 and 69% on application of KIN and BAP respectively as compared to that treated with 80 µM $CuSO_4$. But no significant changes were recorded on application of KIN and BAP to 160 µM $CuSO_4$ treated seedlings (Fig. 37D)

4.2.5.2. Non-enzymatic antioxidants

4.2.5.2.1. Ascorbate (AsA) content

An insignificant increase in AsA content was observed in the cotyledonary leaves on 2 d of exposure to increasing concentrations of $CuSO_4$. However, on 4 d, AsA content increased to an extent of 1.5-3.5 folds with respect to the control. In contrast, a maximum of 4 folds increase over the control was recorded in the cotyledonary leaves subjected to 120 µM $CuSO_4$ on 6 d, and beyond this concentration, AsA accumulation was reduced to $\leq$ 3 folds as compared to the control (Fig. 38A).

The accumulation of AsA was gradually increased in primary leaves depending on the concentration and time of exposure to $CuSO_4$. Up to 6 d, AsA accumulation was $\leq$ 2 folds with respect to the control in the primary leaves, which enhanced to a maximum of 3.5 and 3.8 folds over the control on 8 and 10 d respectively subjected to 200 µM $CuSO_4$ (Fig. 38B).

In contrast to the cotyledonary and primary leaves, the accumulation of AsA was significantly reduced in the roots depending on the exposure time and concentration of $CuSO_4$. The insignificant reduction recorded in the roots of *R. communis* seedlings on 2 and 4 d of Cu stress was significantly reduced to 26-56% as compared to the control on 6 d. Prolonged exposure to Cu stress

resulted in further reductions in AsA content in roots, with a maximum reduction of 84% in the roots exposed to 200 µM $CuSO_4$ for 10 d (Fig. 38C).

The increase in AsA accumulation was 135 and 172% in the cotyledonary leaves of 80 and 160 µM $CuSO_4$ treated *R. communis* seedlings as compared to the control. On application of KIN or BAP, AsA accumulation was further increased. KIN application resulted in 11 and 29% enhancement in AsA content in the cotyledonary leaves of 80 and 160 µM $CuSO_4$ treated seedlings respectively as compared to that exposed to Cu stress alone. Similarly, 7 and 22% increase was recorded in the seedlings treated with 80 and 160 µM $CuSO_4$ respectively along with BAP (Fig. 38D).

4.2.5.2.2. Glutathione (GSH) content

Glutathione accumulation was significantly enhanced in the cotyledonary leaves upon exposure to increasing concentrations of $CuSO_4$. An increase of 1.6-4.3 folds on 2 d was further enhanced to 3-14 and 5-26 folds over the control on 4 and 6 d respectively (Fig. 39A).

In the case of primary leaves, exposure to low concentration of $CuSO_4$ (40-120 µM) resulted in an insignificant enhancement in the accumulation of GSH up to 6 d. In contrast, at higher Cu stress (160-200 µM $CuSO_4$), GSH was accumulated to the extent of 1.5-3.8 folds over the control upon exposure for 2 to 6 d. From 8 d onwards, a gradual and significant increase in accumulation of GSH was recorded upon exposure to increasing concentrations of $CuSO_4$, with a maximum accumulation (4.3 folds over the control) in the primary leaves subjected to 200 µM $CuSO_4$ for 10 d (Fig. 39B).

Similar to cotyledonary and primary leaves, a gradual increase in the accumulation of GSH was recorded in the roots also. On exposure to low concentration of $CuSO_4$ (40-120 µM), GSH accumulation was ≤ 70% over the

control throughout the treatment period (2-10 d). In contrast, at higher $CuSO_4$ concentrations (160-200 μM), a maximum of 77-100% and 98-138% increases were recorded in the roots of *R. communis* seedlings on 8 and 10 d respectively as compared to the control (Fig. 39C).

A drastic enhancement in GSH accumulation was recorded in the cotyledonary leaves of 80 and 160 μM $CuSO_4$ (20 and 25 folds respectively) treated *R. communis* seedlings as compared to the control. However, application of cytokinins resulted in significant reduction (≥ 80% as compared to the respective $CuSO_4$ treatments) in GSH content in the cotyledonary leaves and reached a level approximately equal to that of the control (Fig. 39D).

4.2.5.2.3. Total phenolics content

Total phenolics content was gradually increased in both the cotyledonary and primary leaves upon exposure to increasing concentrations of $CuSO_4$. In the case of cotyledonary leaves, the enhancement in phenolics content accumulation was insignificant on 2 d, but was significantly enhanced on 4 and 6 d of Cu stress. A maximum of 4 and 5 folds increase in phenolics content accumulation was recorded in the cotyledonary leaves on exposure to 200 μM $CuSO_4$ on 4 and 6 d respectively (Fig. 40A).

The increase in phenolics content was insignificant (≤ 30% as compared to the control) in the primary leaves up to 4 d of $CuSO_4$ exposure. From 6 d onwards, the accumulation was gradually increased depending on the concentration and days of exposure. The accumulation of phenolics recorded a maximum of 94 and 111% over the control in primary leaves on 8 and 10 d respectively of exposure to 200 μM $CuSO_4$ (Fig. 40B).

In contrast to the cotyledonary and primary leaves, the accumulation of phenolics significantly reduced in the roots, depending on the concentration

and days of exposure to $CuSO_4$. About 31-72% reduction of phenolics content was recorded on 2 d of $CuSO_4$ exposure, and further recorded a maximum of 85 and 91% reductions as compared to the control on 6 and 10 d respectively (Fig. 40C).

Similar to the GSH content, Cu stress mediated enhancement in total phenolics content in the cotyledonary leaves of *R. communis* seedlings was effectively modulated by the exogenous application of cytokinins. Phenolics accumulation was 1.7 and 3 folds higher in the cotyledonary leaves of 80 and 160 µM $CuSO_4$ treated *R. communis* seedlings as compared to the control. On application of KIN and BAP, 44-73% reduction in phenolics accumulation was recorded in the cotyledonary leaves as compared to the respective $CuSO_4$ treatments (Fig. 40D).

4.2.5.2.4. Flavonoids content

A gradual increase in the accumulation of flavonoids was recorded in the cotyledonary leaves subjected to increasing concentrations of $CuSO_4$. About 34-38% increase over the control was recorded on 2 d of $CuSO_4$ exposure irrespective of the concentrations, which reached to a maximum of 98 and 120% increase over the control on 4 and 6 d respectively (Fig. 41A).

Similar to the cotyledonary leaves, the accumulation of flavonoids was enhanced in the primary leaves also, and the enhancement was $\leq$ 20% over the control up to 6 d of $CuSO_4$ exposure. On further days of treatment, the accumulation of flavonoids in the primary leaves reached to a maximum of 32% as compared to the control, and the enhancement was insignificant on 10 d (Fig. 41B).

Contrary to that of cotyledonary and primary leaves, the flavonoids content was reduced depending on $CuSO_4$ concentration and time of exposure, and the reduction was insignificant up to 4 d. A reduction of 10-

43% was recorded in the roots of *R. communis* seedlings on 6 d of $CuSO_4$ exposure and further reduced to a maximum of 49% over the control on 10 d (Fig. 41C).

Similar to the GSH and phenolics content, Cu stress mediated enhancement in flavonoids content in the cotyledonary leaves of *R. communis* seedlings was reduced significantly on application of cytokinins and reached to a level similar to that of the control. The enhancement in flavonoids content exceeds 100% in both 80 and 160 µM $CuSO_4$ treated cotyledonary leaves of *R. communis*. Application of KIN and BAP reduced the accumulation of flavonoids content, and the reduction was to the extent of 33-43% as compared to the $CuSO_4$ treatments alone (Fig. 41D).

4.2.5.2.5. Anthocyanin content

The enhanced accumulation of anthocyanin content was recorded in the cotyledonary leaves when exposed to low concentrations of $CuSO_4$ (40-120 µM) on 2 d, and the increase was 23% over the control. Beyond this concentration, the anthocyanin accumulation was reduced insignificantly (7-11% reduction over the control) in the cotyledonary leaves on 2 d of exposure. On increasing the exposure time, the accumulation was significantly reduced. The maximum reduction recorded was 21 and 35% as compared to the control on 4 and 6 d respectively on exposure to 200 µM $CuSO_4$ (Fig. 42A).

In the case of primary leaves, the accumulation of anthocyanin was significantly enhanced up to 6 d of $CuSO_4$ exposure irrespective of the concentrations, and the enhancement ranged between 31-54% with respect to the control. On 8 d, a significant enhancement of 63-71% over the control was recorded when exposed to 40-80 µM $CuSO_4$. Beyond this concentration and

exposure time, the accumulation of anthocyanin was insignificant with respect to the control (Fig. 42B).

A gradual increase in the accumulation of anthocyanin was recorded in the roots of *R. communis* seedlings subjected to increasing concentrations of $CuSO_4$ up to 6 d of treatment. The maximum accumulation of 39% was recorded in the roots of seedlings exposed to 200 µM $CuSO_4$ with respect to the control on 2 d. Later an enhancement of 61 and 96% was recorded on 4 and 6 d respectively as compared to that of the control. But the accumulation was reduced to 13 and 29% over the control on 8 and 10 d respectively upon exposure to 160-200 µM $CuSO_4$. In contrast, during exposure to low concentration of $CuSO_4$ (40-120 µM), the accumulation of anthocyanin was further enhanced to a maximum of 63 and 91% on 8 and 10 d respectively (Fig. 42C).

In contrast to all other non-enzymatic antioxidants, the reduction in the accumulation of anthocyanin on exposure to $CuSO_4$ (28 and 31% reduction in 80 and 160 µM $CuSO_4$, respectively) was seen to increase on application of KIN and BAP as compared to the Cu stressalone. The enhancement in the accumulation of anthocyanin content ranged between 14-36% compared to the respective $CuSO_4$ treatments, with the highest enhancement recorded in the BAP treated ones (Fig. 42D).

4.2.6. Bioaccumulation and translocation of Cu

In general, Cu uptake by *R. communis* seedlings gradually increased with the increase in concentrations of $CuSO_4$ (Table 14). But most of the accumulated Cu was retained in the root itself, and only a small portion was found to be transported into the aerial parts of the plant. Since Cu is an essential element and a minimum amount is present in the Hoagland nutrient solution, a basal level of Cu was detected even in the control seedlings. The

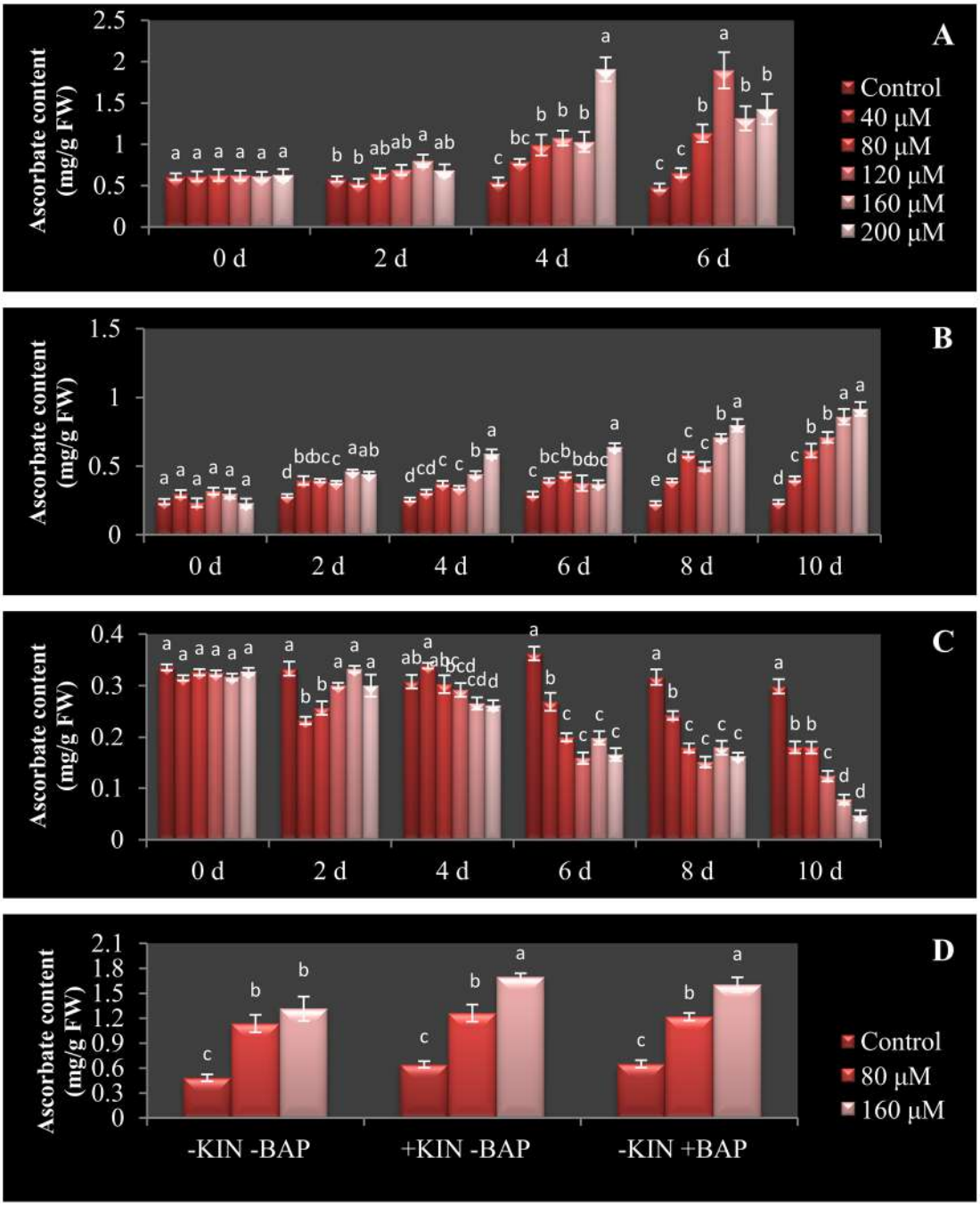

Figure 38. Ascorbate (AsA) content in the cotyledonary leaves (A), primary leaves (B), roots (C), and cotyledonary leaves (exposed to cytokinins for 6 d) (D) of *R. communis* seedlings subjected to increasing concentrations of $CuSO_4$. Different alphabetical letters indicate significant difference between treatments (Duncan's test $p \leq 0.05$).

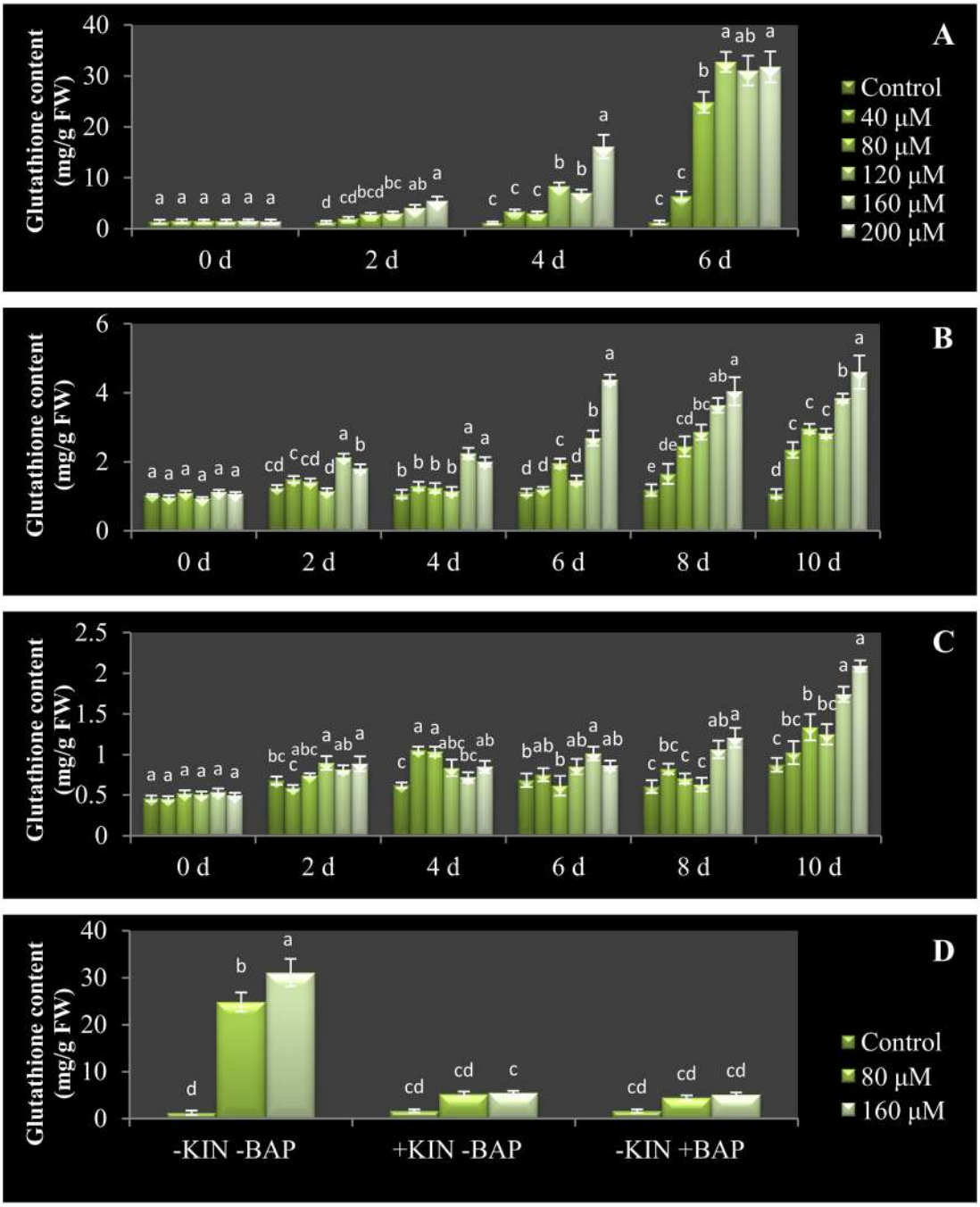

Figure 39. Glutathione (GSH) content in the cotyledonary leaves (A), primary leaves (B), roots (C), and cotyledonary leaves (exposed to cytokinins for 6 d) (D) of *R. communis* seedlings subjected to increasing concentrations of $CuSO_4$. Different alphabetical letters indicate significant difference between treatments (Duncan's test $p \leq 0.05$).

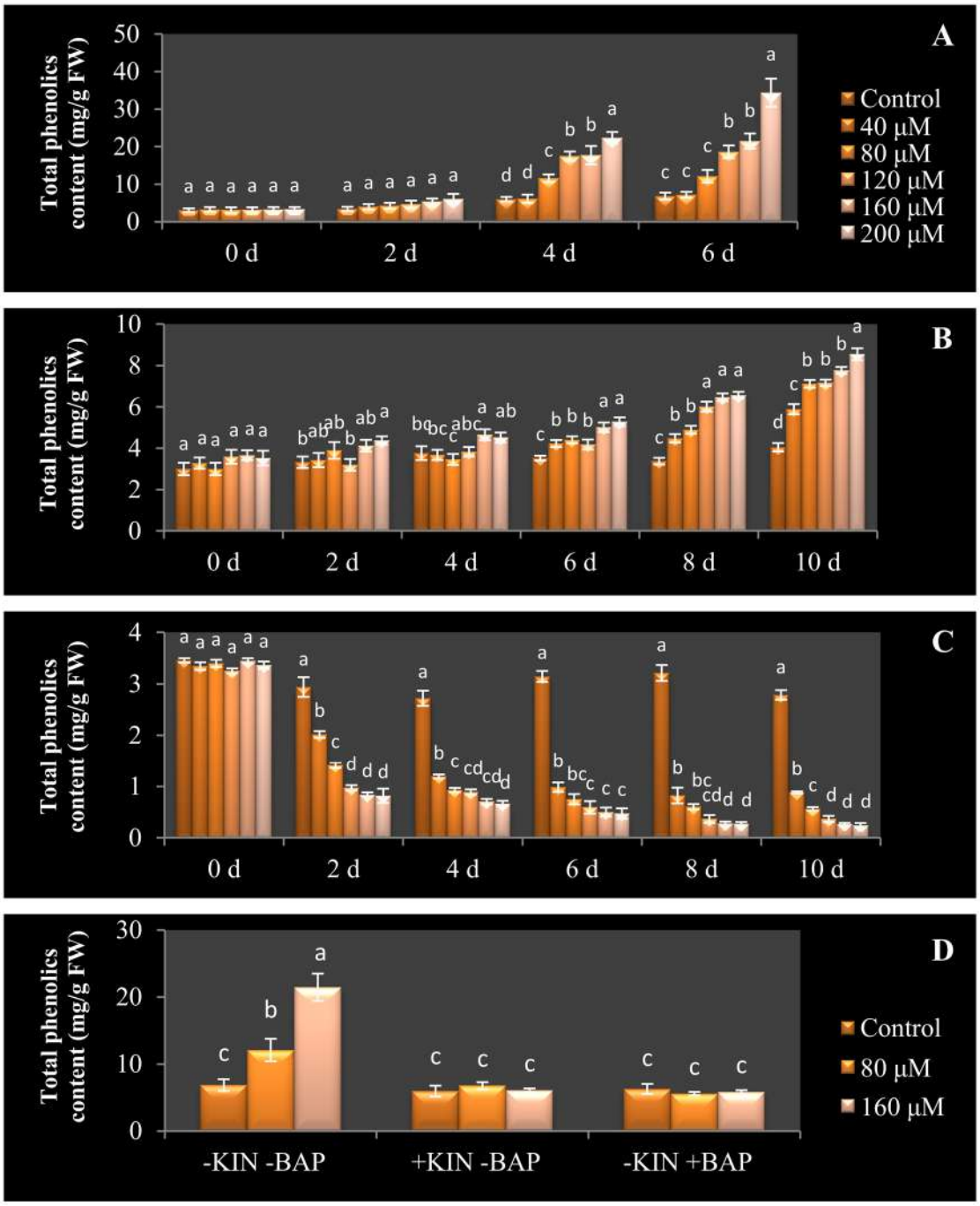

Figure 40. Total phenolics content in the cotyledonary leaves (A), primary leaves (B), roots (C), and cotyledonary leaves (exposed to cytokinins for 6 d) (D) of *R. communis* seedlings subjected to increasing concentrations of $CuSO_4$. Different alphabetical letters indicate significant difference between treatments (Duncan's test $p \leq 0.05$).

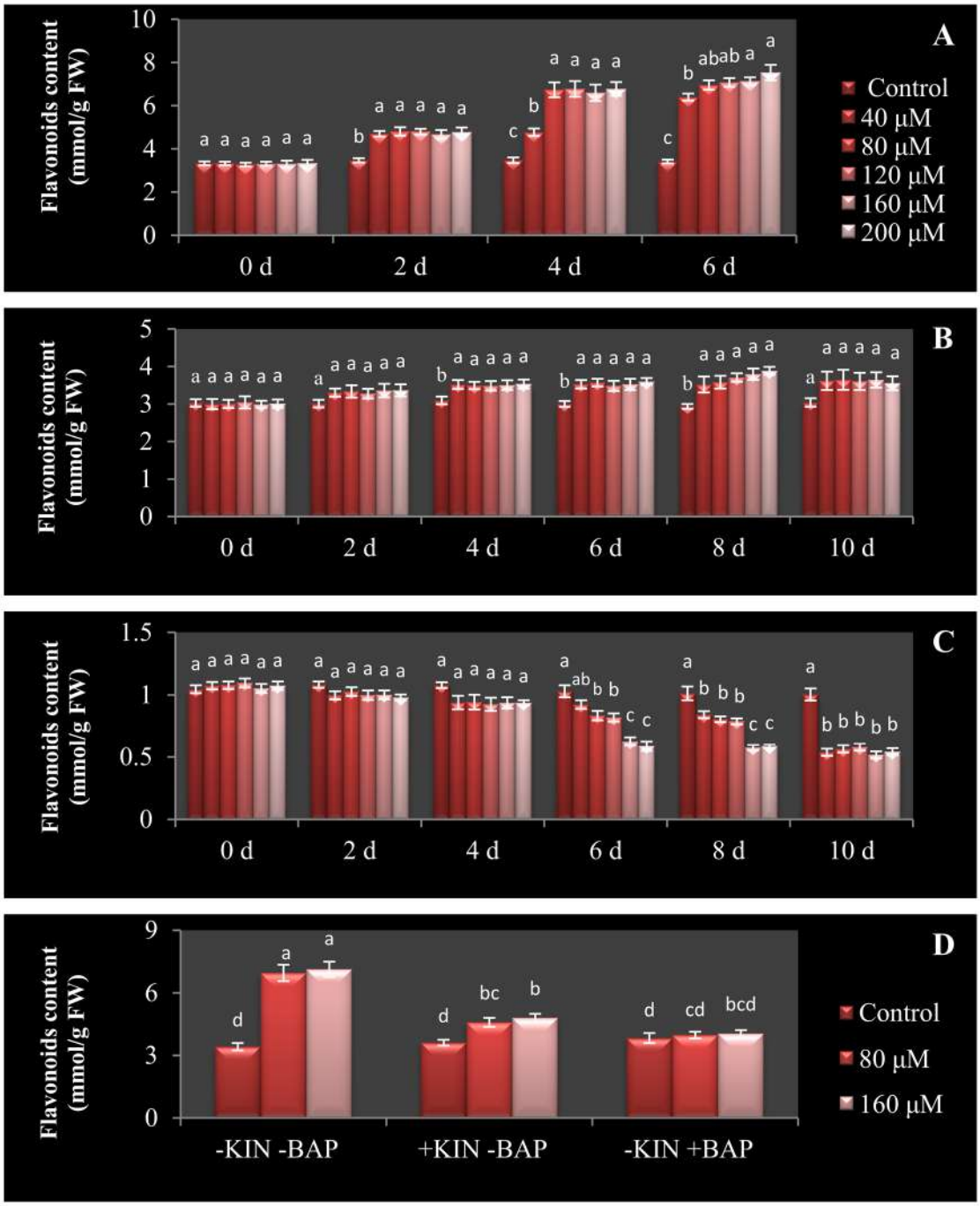

Figure 41. Flavonoids content in the cotyledonary leaves (A), primary leaves (B), roots (C), and cotyledonary leaves (exposed to cytokinins for 6 d) (D) of *R. communis* seedlings subjected to increasing concentrations of $CuSO_4$. Different alphabetical letters indicate significant difference between treatments (Duncan's test $p \leq 0.05$).

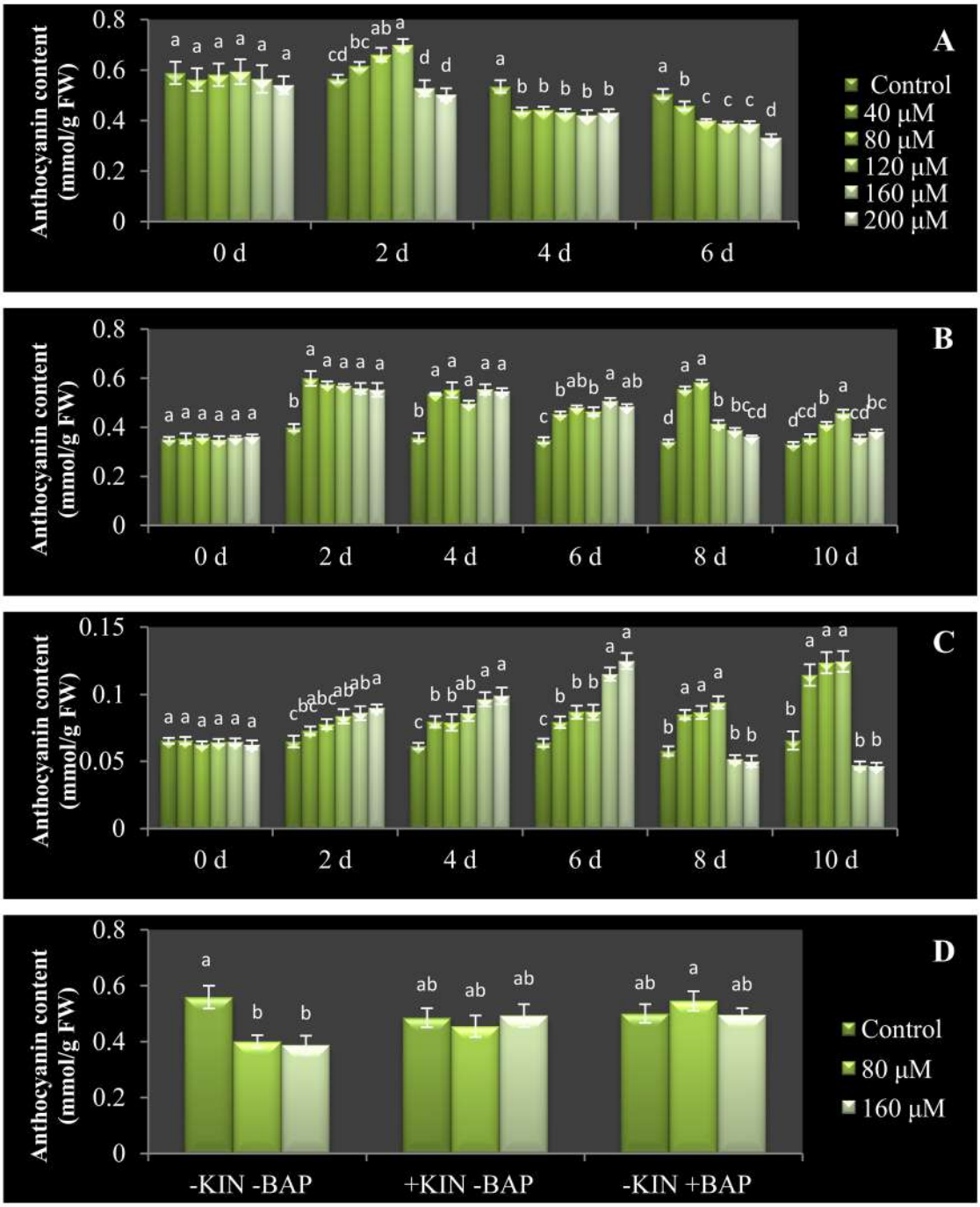

Figure 42. Anthocyanin content in the cotyledonary leaves (A), primary leaves (B), roots (C), and cotyledonary leaves (exposed to cytokinins for 6 d) (D) of *R. communis* seedlings subjected to increasing concentrations of $CuSO_4$. Different alphabetical letters indicate significant difference between treatments (Duncan's test $p \leq 0.05$).

concentration of Cu in the roots of 40 μM $CuSO_4$ treated seedlings was 1198 ± 83 μg/g DW, whereas it was increased up to 1598 ± 38 μg/g DW in 200 μM $CuSO_4$ (44 folds increase over the control) on 6 d of treatment period. Similarly, in the case of stem, the bioaccumulation was 157 ± 6.91 μg/g DW in 40 μM treated seedlings, which further enhanced to 1205 ± 46.27 μg/g DW in 200 μM $CuSO_4$ treated seedlings (20 folds increase over the control) (Table 14).

Comparatively an increased accumulation level of Cu was recorded in the cotyledonary leaves than in the primary leaves. The accumulation was 2.6 folds higher in cotyledonary leaves at 200 μM $CuSO_4$, at the same time it was only 1.4 folds in the case of primary leaves as compared to the respective controls on 6 d of treatment. The Cu bioaccumulation was 40.50 ± 1.88 and 19.15 ± 1.08 μg/g DW in cotyledonary and primary leaves respectively upon exposure to 200 μM $CuSO_4$. In contrast to these results, on 10 d of $CuSO_4$ exposure, a significant increase in the bioaccumulation of Cu was recorded in the primary leaves. The accumulation was ranging between 34.75 ± 3.61 to 36.34 ±3.64 μg/g DW (1.7 folds higher over the control) in the primary leaves subjected to 120-200 μM $CuSO_4$ on 10 d (Table 14).

Translocation factor (TF) indicates the proportion of Cu translocated into specific plant parts from the root system. Comparatively low level of Cu was accumulated in the roots, and almost similar content got accumulated in cotyledonary and primary leaves, which was uptaken from the Hoagland nutrient medium in the control seedlings, giving rise to higher TF values for the cotyledonary and primary leaves of the control seedlings on 6 and 10 d of analysis. On the other hand, the TFvalues of cotyledonary and primary leaves on 6 d were approximately 0.02 and 0.01 respectively when subjected to different concentrations of $CuSO_4$. Further, on 10 d, the TF value was

increased to 0.02 in the primary leaves on exposure to 120-200 µM $CuSO_4$ (Table 14).

Exogenous application of KIN and BAP along with $CuSO_4$ significantly reduced the Cu concentrations in the aerial parts of the seedlings as compared to the seedlings treated with $CuSO_4$ alone. In the case of cotyledonary leaves subjected to 160 µM $CuSO_4$, the Cu bioaccumulation of 37.80 ± 1.9 µg/g DW was reduced to 28.33 ± 0.47 and 18.22 ± 0.59 µg/g DW upon exposure to KIN and BAP respectively. Therefore, the TF values were also reduced in the cotyledonary leaves when subjected to KIN and BAP treatments along with Cu stress as compared to the TF of cotyledonary leaves exposed to Cu stress alone. The TF value was 0.022 for the cotyledonary leaves of *R. communis* seedlings exposed to 160 µM $CuSO_4$, which was reduced to 0.018 and 0.013 in cotyledonary leaves subjected to KIN and BAP respectively along with 160 µM $CuSO_4$ (Table 15).

4.2.7. Distribution of Cu in the xylem tissues

The distribution of the accumulated Cu in the xylem tissues of root, stem, cotyledonary and primary leaves of *R. communis* seedlings was analyzed by SEM-EDX microanalysis (Fig. 43 and 44). Significant difference in the distribution of Cu was observed in the xylem tissues upon treatment with $CuSO_4$ as compared to that of the control seedlings. Since Cu is an essential element and is a constituent of the Hoagland nutrient solution, a basal level of Cu was detected even in the xylem tissues of the control seedlings. In the case of xylem tissues of roots, 8 folds increase in the distribution of Cu was recorded upon treatment with 200 µM $CuSO_4$ over that of the control. In contrast, the xylem tissues of stem were found to have a more or less similar distribution pattern of Cu in both the control and Cu-treated seedlings. The xylem tissues of cotyledonary leaves recorded the highest proportion of Cu content upon $CuSO_4$ treatment, and it was extended

Table 14. Bioaccumulation of copper (Cu) in the root, stem, cotyledonary and primary leaves, and translocation factor (TF) in the cotyledonary and primary leaves of *R. communis* seedlings subjected to increasing concentrations of $CuSO_4$ (Control, 40, 80, 120, 160 and 200 μM) on 6 and 10 d. Values are the mean ± SE of three independent experiments. Different alphabetical letters indicate significant difference between treatments (Duncan's test $p \leq 0.05$).

Days	$CuSO_4$ (μM)	Cu bioaccumulation (μg/g DW)				Translocation factor (TF)	
		Root	Stem	Cotyledonary leaf	Primary leaf	Cotyledonary leaf	Primary leaf
6 d	Control	36.3 ± 5^{c}	58.6 ± 4.3^{f}	15.36 ± 1.79^{c}	13.65 ± 1.96^{b}	0.423	0.376
	40	1198 ± 83^{b}	157 ± 6.91^{e}	25.93 ± 2.65^{b}	13.97 ± 0.87^{ab}	0.021	0.012
	80	1562 ± 54^{a}	430 ± 8.82^{d}	33.32 ± 2.94^{ab}	14.69 ± 0.69^{ab}	0.021	0.009
	120	1573 ± 30^{a}	741 ± 9.13^{c}	39.12 ± 2.23^{a}	15.05 ± 0.11^{ab}	0.025	0.010
	160	1592 ± 16^{a}	814 ± 11.28^{b}	38.91 ± 3.68^{a}	15.06 ± 0.54^{ab}	0.024	0.009
	200	1598 ± 38^{a}	1205 ± 46.27^{a}	40.50 ± 1.88^{a}	19.15 ± 1.08^{a}	0.025	0.012
10 d	Control	34.0 ± 4.56^{b}	50.41 ± 7.16^{d}	NA	20.58 ± 2.69^{b}	NA	0.605
	40	1506 ± 234.36^{a}	230.45 ± 20.33^{d}	NA	22.89 ± 2.50^{b}	NA	0.015
	80	1634 ± 185.95^{a}	1008.62 ± 32.37^{bc}	NA	21.11 ± 3.33^{b}	NA	0.013
	120	1663 ± 198.11^{a}	888.38 ± 21.26^{c}	NA	34.75 ± 3.61^{a}	NA	0.021
	160	1674 ± 159.87^{a}	1203.0 ± 114.32^{ab}	NA	36.44 ± 1.69^{a}	NA	0.022
	200	1794 ± 241.81^{a}	1369.50 ± 132.80^{a}	NA	36.34 ± 3.64^{a}	NA	0.020

*NA: not applicable

Table 15. Bioaccumulation of Cu (µg/g DW) in the root, stem, cotyledonary leaves and primary leaves and translocation factor (TF) in *R. communis* seedlings on 6 d of exposure to $CuSO_4$ (80 and 160 µM) and cytokinins (KIN and BAP). Values are the mean ± SE of three independent experiments. Different alphabetical letters indicate significant differences between treatments (Duncan's test $p \leq 0.05$).

Treatments	Cu bioaccumulation (µg/g DW)				Translocation factor (TF)	
	Root	Stem	Cotyledonary leaf	Primary leaf	Cotyledonary leaf	Primary leaf
Control	35.80 ± 1.79^{f}	51.54 ± 2.58^{g}	15.0 ± 0.75^{f}	13.54 ± 0.68^{cde}	0.419	0.378
80 µM $CuSO_4$	1513.70 ± 84.1^{bc}	499.33 ± 23.05^{d}	31.80 ± 1.6^{b}	14.55 ± 0.73^{bc}	0.021	0.010
160 µM $CuSO_4$	1715.33 ± 85.77^{a}	905.22 ± 40.74^{a}	37.80 ± 1.9^{a}	16.78 ± 0.84^{a}	0.022	0.010
80 µM $CuSO_4$+KIN	1388.64 ± 76.38^{d}	377.70 ± 12.59^{e}	24.0 ± 0.86^{d}	14.40 ± 0.45^{bcd}	0.017	0.010
160 µM $CuSO_4$+KIN	1544.20 ± 77.21^{b}	728.11 ± 29.79^{b}	28.33 ± 0.47^{c}	15.11 ± 0.38^{b}	0.018	0.010
80 µM $CuSO_4$+BAP	1080.21 ± 54.0^{e}	232.25 ± 11.61^{f}	16.36 ± 0.6^{ef}	13.09 ± 0.3^{de}	0.015	0.012
160 µM $CuSO_4$+BAP	1402.91 ± 70.15^{cd}	677.36 ± 27.89^{c}	18.22 ± 0.59^{e}	12.36 ± 0.34^{e}	0.013	0.009

to 17 folds increase over the control. In the case of primary leaves, Cu was distributed in the xylem tissues, and it was higher by 71% upon exposure to $CuSO_4$ treatment as compared to that of the control (Fig. 43 and 44, Table 16).

Significant differences in the distribution of Cu were observed in the xylem tissues upon treatment with 160 μM $CuSO_4$ in the presence and absence of KIN and BAP application as compared to that of the control seedlings. The xylem tissues of cotyledonary leaves subjected to 160 μM $CuSO_4$had the highest proportion of Cu content, and it was 8 folds higher than the control. On application of cytokinins to 160 μM $CuSO_4$ treated seedlings, the proportion of Cu content was significantly reduced, and the reduction was 85 and 62% in KIN and BAP treated cotyledonary leaves as compared to Cu stress alone (Fig. 45, Table 17).

4.2.8. Subcellular distribution pattern of Cu

The subcellular distribution of Cu in various plant parts of *R. communis* seedlings on 6 d of exposure to 200 μM $CuSO_4$ revealed that most of the accumulated Cu was localized in the cell wall regions (Table 18). Of the total concentrations of Cu accumulated in the roots of 200 μM $CuSO_4$ treated seedlings, 77% was localized in the cell wall, and only 16 and 7% were distributed in the organellar and cytoplasmic fractions respectively. In the case of stem, 60% of Cu was localized in the cell wall fraction, and 26% and 14% of Cu in the cytoplasmic and organellar fractions respectively. In cotyledonary leaves, 79% of the bioaccumulated Cu was localized to the cell wall, 18% in the cytoplasmic fraction and only 3% of the Cu was localized in the organelles. Similarly, in the case of primary leaves, 55 and 35% of the Cu was localized in the cell wall and cytoplasmic fractions respectively, and the remaining 10% was distributed in the organellar fractions (Table 18).

4.2.9. Distribution pattern of essential elements in the xylem tissues

4.2.9.1. Influence of Cu on essential elemental distribution

The influence of Cu stress on the distribution of various essential elements in the xylem elements was analyzed by SEM-EDX analysis. *R. communis* seedlings treated with $CuSO_4$ recorded significant variations in SEM-EDX peaks denoting various macro and micro-elemental distribution patterns in the xylem tissues. The variations in the peaks were more significant in the roots and cotyledonary leaves of 200 µM $CuSO_4$ treated seedlings as compared to the controls (Fig. 43 and 44, Table 16).

4.2.9.1.1. Macro-elements

Among the essential elements identified, the major portion constitutes C and O in all the plant tissues. The distribution of C was significantly reduced in the xylem tissues of cotyledonary leaves (30%) and roots (45%) exposed to Cu stress as compared to the control. Whereas the distribution of C was negligibly reduced in primary leaves, and no variation was recorded in the stem tissues. In the distribution of O, a 33% reduction was observed in the xylem tissues of cotyledonary leaves upon exposure to Cu stress. But no significant variations were recorded in other plant parts subjected to Cu stress (Table 16).

The distributional pattern of Ca was significantly enhanced in the cotyledonary leaves and roots during $CuSO_4$ treatments, and the increase was 11 and 17 folds over the control in cotyledonary leaves and roots respectively. In contrast, a negligible increase and reduction of Ca were recorded in stem and primary leaves respectively on exposure to $CuSO_4$. Cu stress resulted in the enhancement of P distribution in the xylem tissues of all the plant parts except in cotyledonary leaves. Primary leaves recorded the highest distribution of P and 5 folds increase was recorded as compared to the control.

Similar to the distribution of P, the distribution of Mg was also enhanced in the xylem tissues of primary leaves, stem and root of *R. communis* seedlings, and the increase ranged between 2-4 folds over the control. In contrast, in the case of cotyledonary leaves, Mg was below the detectable level (BDL) on treatment with $CuSO_4$ (Table 16).

In the case of the distribution pattern of K, the xylem tissues of cotyledonary leaves recorded 17 folds increase when exposed to Cu stress as compared to the control, whereas no significant variations were recorded in the xylem tissues of primary leaves, stem and roots of *R. communis* seedlings during Cu stress. The distribution of S was enhanced by 50 and 35% in the xylem tissues of cotyledonary leaves and roots respectively over the control during $CuSO_4$ treatment, whereas, it was reduced by 40 and 14% in primary leaves and stem respectively over the control. The proportion of Si distribution was very less in the xylem tissues of all the plant parts and was below detectable level in the xylem of cotyledonary leaves exposed to $CuSO_4$ (Table 16).

4.2.9.1.2. Micro-elements

The distribution of Zn was enhanced in the xylem tissues of all the plant parts on exposure to $CuSO_4$, except in the case of stem, with a maximum increase of 23 folds over the control in the cotyledonary leaves. In the case of Fe and Cl, the distribution was enhanced in the cotyledonary leaves and roots upon exposure to $CuSO_4$, whereas it was decreased in the primary leaves and stem. The enhancement was to the extent of 3-8 folds for Fe and Cl in the xylem tissues of cotyledonary leaves and roots. The proportion of B distribution was reduced in the xylem tissues of cotyledonary leaves, stem and roots, whereas it was enhanced in the primary leaves upon exposure to $CuSO_4$, with the highest reduction of 98% in cotyledonary leaves (Table 16).

4.2.9.2. Impact of cytokinins on essential elemental distribution in the cotyledonary leaves

The EDX results indicate that Cu stress in the presence and absence of cytokinins resulted in the induction of significant changes in the cellular distribution of various macro and microelements in the xylem tissues of cotyledonary leaves as compared to that of the control seedlings (Fig. 45, Table 17).

4.2.9.2.1. Macro-elements

Among the essential elements, the major portion constitutes C and O. The distribution of C was significantly reduced by 33% in the xylem tissues of cotyledonary leaves upon exposure to 160 μM $CuSO_4$ as compared to the control. However, C distribution in the xylem tissues of cotyledonary leaves was considerably restored upon application of KIN and BAP in 160 μM $CuSO_4$ treated seedlings. In contrast, no significant variations were observed in the distribution of O in the xylem tissues of cotyledonary leaves of 160 μM $CuSO_4$ treated seedlings in the presence and absence of cytokinins as compared to that of the control (Table 17).

The seedlings treated with $CuSO_4$ recorded a sharp enhancement in Ca distribution, i.e., about 8 folds increase of Ca content in the cotyledonary leaves of 160 μM $CuSO_4$ treated seedlings as compared to that of the control. In contrast, P and Mg distributions were found to be decreased significantly in cotyledonary leaves of seedlings treated with 160 μM $CuSO_4$. P content was reduced to 60% as compared to that of the control, while Mg was below the detectable level when exposed to $CuSO_4$. On application of KIN or BAP along with 160 μM $CuSO_4$, Ca content was reduced, and P and Mg contents were enhanced significantly as compared to seedlings subjected to Cu stress alone. In the case of Ca content, the reductions were 86 and 69% respectively

for KIN and BAP-treated cotyledonary leaves along with 160 μM $CuSO_4$ as compared to the cotyledonary leaves treated with 160 μM $CuSO_4$ alone. The content of Mg was increased to 4 and 8 folds respectively in KIN and BAP treated cotyledonary leaves over the control. But Mg content was below the detectable level on exposure to $CuSO_4$ alone. On application of KIN and BAP, P distribution was enhanced to 3 and 10 folds respectively as compared to the cotyledonary leaves treated with 160 μM $CuSO_4$ alone (Table 17).

K distribution was increased significantly in the cotyledonary leaves of seedlings subjected to Cu stress in the presence and absence of cytokinins. An enhancement of 16% in the distribution of S was recorded in the cotyledonary leaves of *R. communis* seedlings exposed to $CuSO_4$ as compared to that of the control. However, on application of KIN and BAP, the distribution of S was reduced as compared to that of Cu stress alone, with a significant reduction of 36% in the case of BAP treated leaves. In the case of Si, which was below the detectable level on exposure to 160 μM $CuSO_4$, got enhanced to 7.5 and 6 folds higher on application of KIN and BAP respectively to 160 μM $CuSO_4$ treated seedlings as compared to the control (Table 17).

4.2.9.2.2. Micro-elements

The essential micro-elements such as Zn and Fe contents were increased to the extent of 6 and 7 folds in the cotyledonary leaves of 160 μM $CuSO_4$ treated seedlings over the control seedlings. On application of KIN or BAP along with 160 μM $CuSO_4$, the accumulation of Zn and Fe was reduced drastically as compared to Cu stress alone. Exposure to KIN and BAP resulted in the reduction of Zn and Fe distribution to the extent of 83 and 89% respectively as compared to 160 μM $CuSO_4$. Similar to Zn and Fe, Cl distribution was also enhanced to 2.8 folds in the Cu-treated cotyledonary leaves as compared to the control, which was reduced to 48 and 74% on application of KIN and BAP respectively as compared to that of Cu stress

alone. The significant reduction (96%) in the distribution of B on exposure to $CuSO_4$ was restored on application of KIN and BAP (Table 17).

4.2.10. Leaf micromorphological characters

4.2.10.1. Effect of Cu on leaf micromorphological characters

The leaf micromorphological characters of *R. communis* were significantly modified upon exposure to $CuSO_4$ (Fig. 46). In the case of cotyledonary leaves, the number of stomata per unit area was significantly reduced in both adaxial and abaxial surfaces on exposure to 200 µM $CuSO_4$ treatment as compared to the control on 6 d. During Cu stress, the adaxial stomata were completely closed, whereas the abaxial stomata were partially closed as compared to the respective controls. Copper stress also resulted in slight changes in the shape and size of guard cells, resulting in the structural loss of the stomata (Fig. 46).

In the case of primary leaves, the stomatal variations were analyzed on 6 and 10 d of exposure to 200 µM $CuSO_4$. The distribution of stomata was uninterrupted in the primary leaves upon exposure to $CuSO_4$ as compared to the control. On 6 d of exposure to $CuSO_4$, the adaxial stoma was completely closed in the primary leaves, but no significant variations were recorded in the abaxial stomata during Cu stress as compared to the control. In contrast, on 10 d of exposure to $CuSO_4$, both the adaxial and abaxial stomata were completely closed in the primary leaves. (Fig. 47 and 48).

4.2.10.2. Impact of cytokinins on micromorphology of cotyledonary leaves

The responses of stomatal opening on exposure to $CuSO_4$and cytokinin application in adaxial and abaxial leaf surfaces are shown in Fig. 49 and 50. The reduced number of stomata per unit area in both adaxial and abaxial

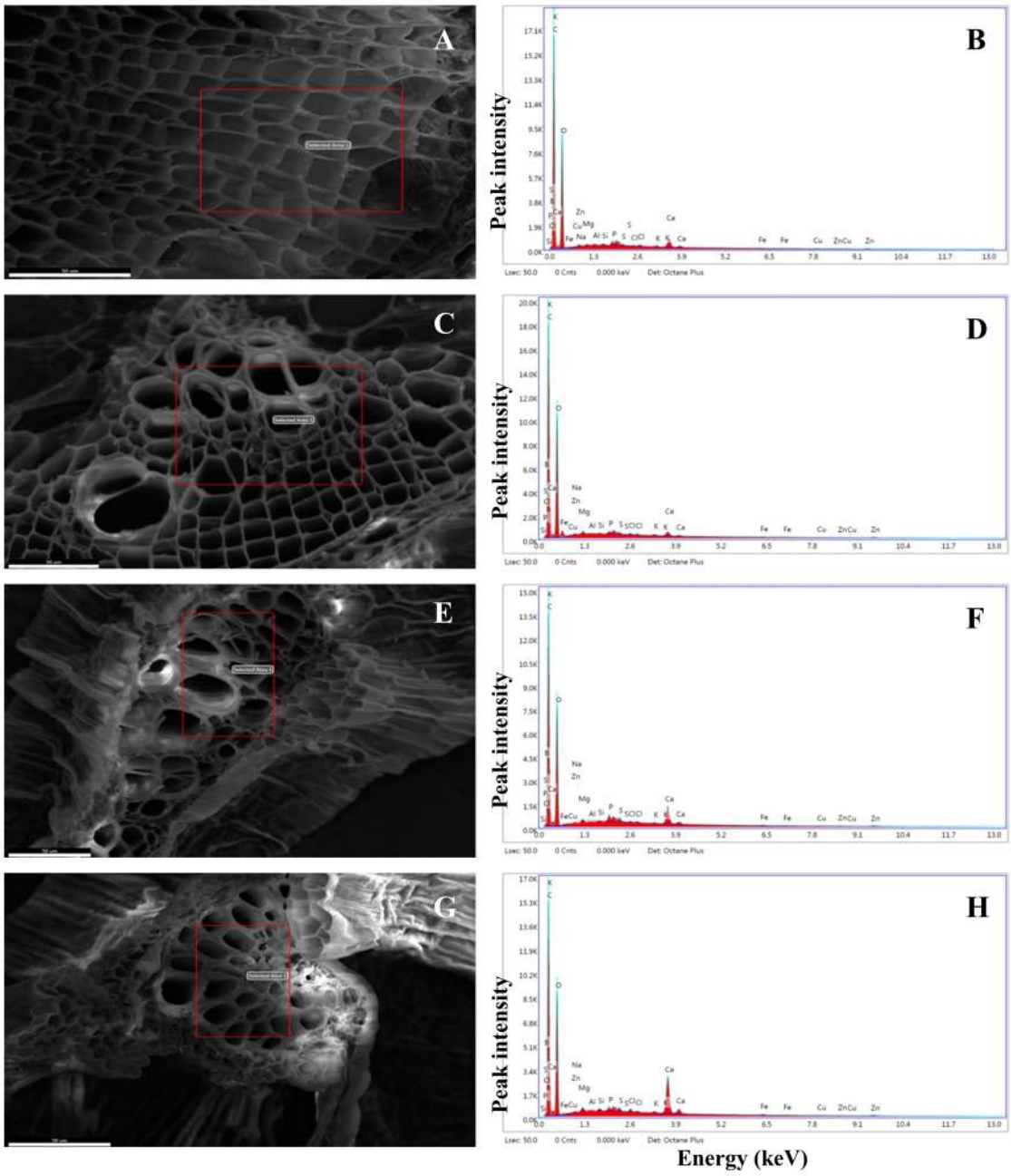

Figure 43. SEM-EDX spectra of xylem tissues of root (A&B), stem (C&D), cotyledonary leaf (E&F) and primary leaf (G&H) of control seedlings of *R. communis*.

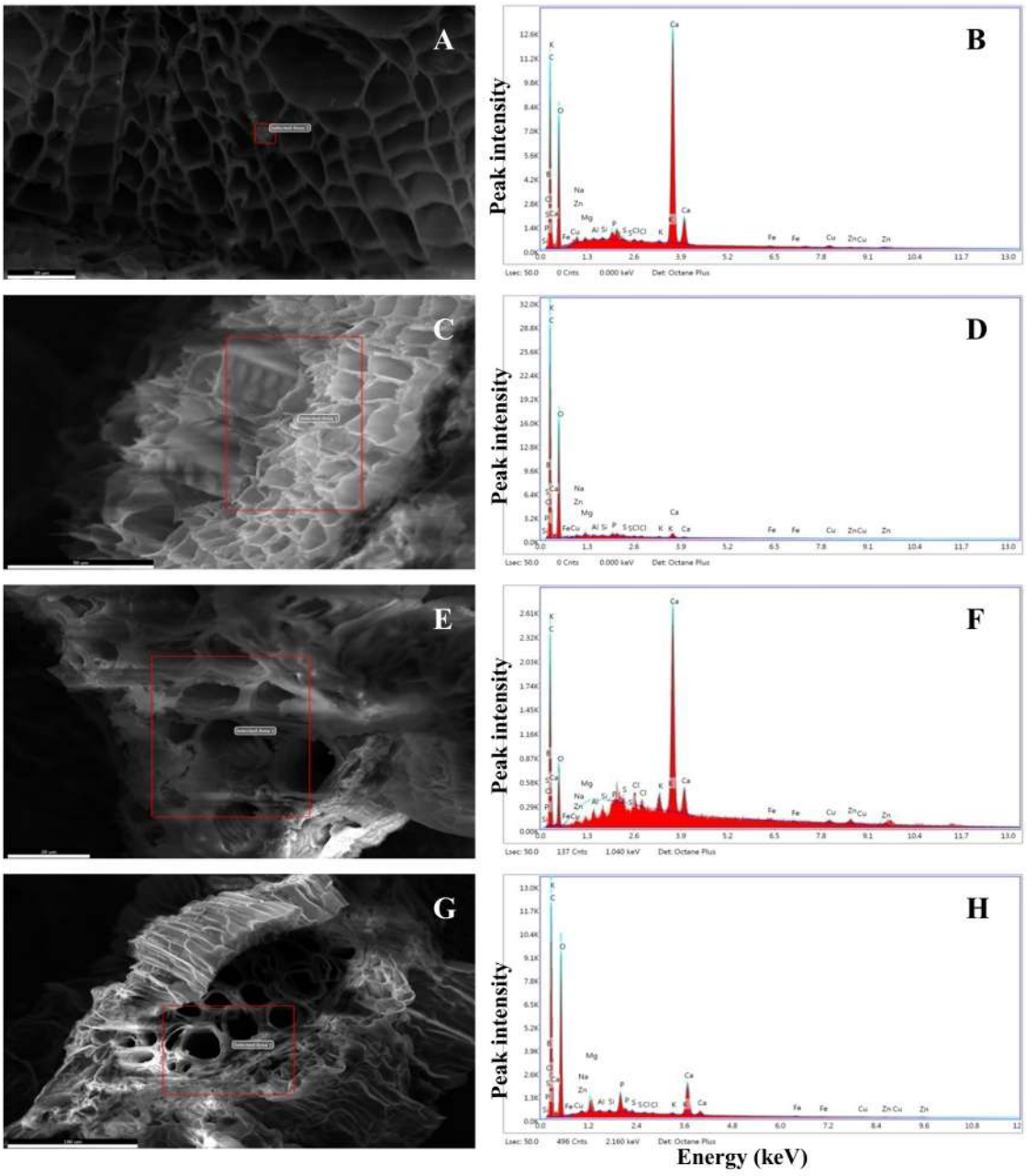

Figure 44. SEM-EDX spectra of xylem tissues of root (A&B), stem (C&D), cotyledonary leaf (E&F) and primary leaf (G&H) of *R. communis* seedlings on exposure to 200 µM $CuSO_4$ on 6 d.

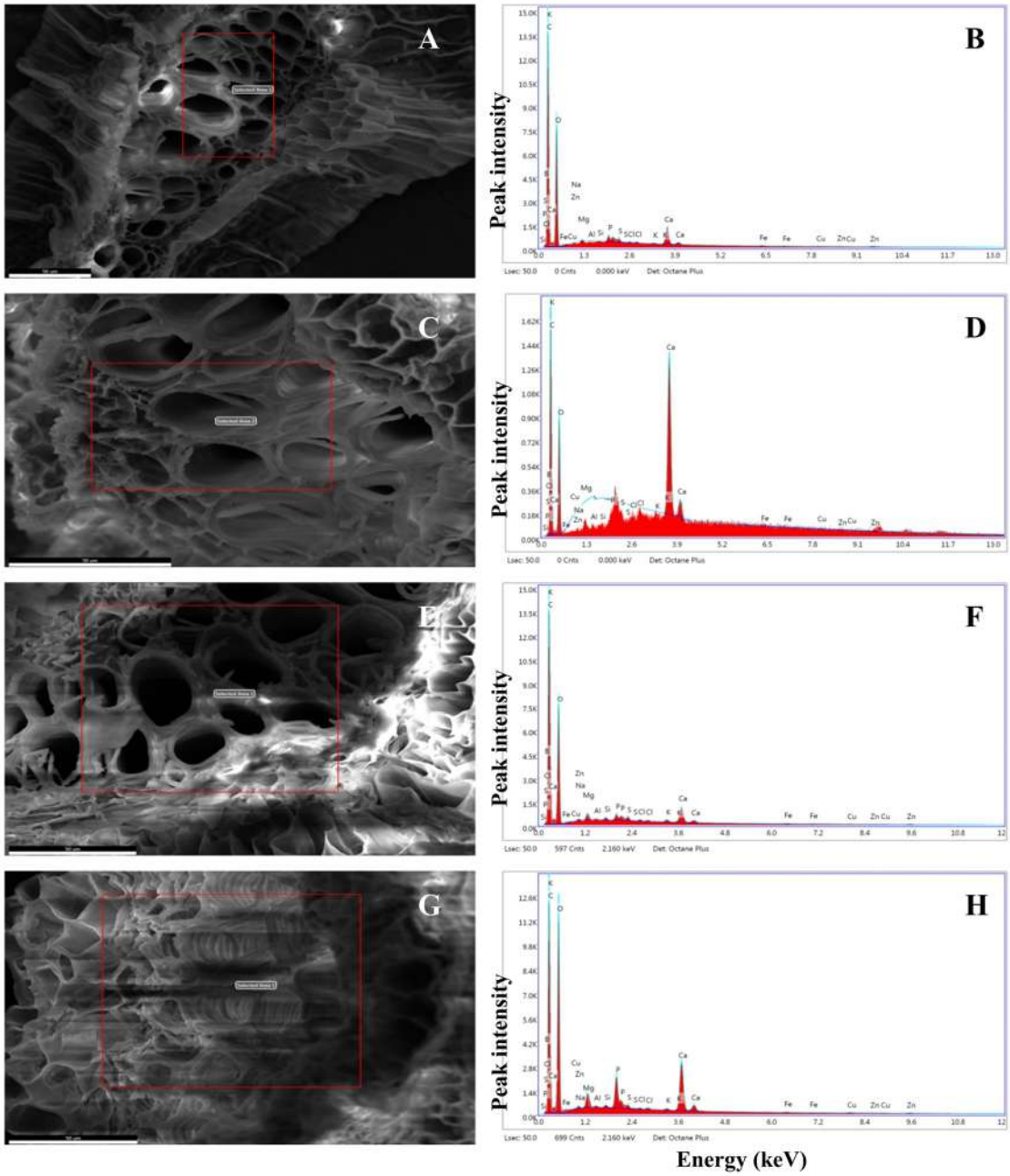

Figure 45. SEM-EDX spectra of xylem tissues in cotyledonary leaves of *R. communis* seedlings on 6 d of exposure to 160 µM $CuSO_4$ and cytokinins (KIN and BAP). A&B: control; C&D: 160 µM $CuSO_4$; E&F: 160 µM $CuSO_4$+ KIN; and G&H: 160 µM $CuSO_4$+ BAP.

Table 16. SEM-EDX data showing the distribution of various macro and micro-elements (weight %) in the xylem tissues of root, stem, cotyledonary and primary leaves of *R. communis* seedlings on 6 d of $CuSO_4$ (control and 200 µM) treatments.

Essential elements		Distribution of elements (weight %)							
		Root		Stem		Cotyledonary leaf		Primary leaf	
		Control	200 µM $CuSO_4$	Control	200 µM $CuSO_4$	Control	200 µM $CuSO_4$	Control	200 µM $CuSO_4$
Macro-elements	C	54.1	29.41	53.15	53.5	52.19	36.58	49.29	45.65
	O	42.22	43.1	43.77	43.44	42.72	28.64	43.21	44.66
	Ca	1.33	23.27	0.6	0.68	2.38	26.65	4.86	4.5
	P	0.39	0.66	0.25	0.3	0.5	0.25	0.31	1.43
	Mg	0.09	0.28	0.21	0.43	0.14	BDL	0.29	1.1
	K	0.14	0.2	0.13	0.09	0.09	1.53	0.16	0.18
	S	0.23	0.31	0.21	0.18	0.36	0.54	0.32	0.19
	Si	0.1	0.16	0.04	0.1	0.02	BDL	0.14	0.11
Micro-elements	Cu	0.11	0.86	0.06	0.07	0.09	1.49	0.07	0.12
	Zn	0.08	0.24	0.05	0.01	0.12	2.8	0.09	0.18
	Fe	0.06	0.19	0.07	0.05	0.15	0.63	0.18	0.16
	Cl	0.07	0.18	0.13	0.08	0.11	0.87	0.25	0.08
	B	1.03	0.83	1.34	0.97	1.13	0.02	0.82	1.34

*BDL: below detectable level

Table 17. SEM-EDX data showing the macro and micro-elements (weight %) in the cotyledonary leaves of *R. communis* seedlings on 6 d of $CuSO_4$ (160 µM) and cytokinins (KIN and BAP) treatments.

Essential elements		Distribution of elements (weight %)			
		Control	160 µM $CuSO_4$	160 µM $CuSO_4$ + KIN	160 µM $CuSO_4$ + BAP
Macro-elements	C	52.19	35.02	52.21	41.93
	O	42.72	41.89	40.92	45.56
	Ca	2.38	19.48	2.66	6.1
	P	0.5	0.2	0.55	2.17
	Mg	0.14	BDL	0.55	1.18
	K	0.09	0.15	0.32	0.16
	S	0.36	0.42	0.39	0.27
	Si	0.02	BDL	0.15	0.12
Micro-elements	Cu	0.09	0.76	0.11	0.29
	Zn	0.12	0.66	0.11	0.07
	Fe	0.15	1.07	0.18	0.14
	Cl	0.11	0.31	0.16	0.08
	B	1.13	0.04	1.43	1.67

*BDL: below detectable level

Table 18. Subcellular distribution of copper (Cu) in the root, stem, cotyledonary and primary leaves of *R. communis* seedlings subjected to $CuSO_4$ treatment (control and 200 µM) on 6 d. Values are the mean ± SE of three independent experiments.

Treatments	Plant parts	Subcellular distribution of Cu (µg/g DW)		
		Fraction 1 (Cell wall fraction)	Fraction 2 (Organellar fraction)	Fraction 3 (Cytoplasmic fraction)
Control	Root	26.716 ± 1.34	4.694 ± 0.23	9.952 ± 0.50
	Stem	40.671 ± 2.03	8.370 ± 0.42	12.926 ± 0.65
	Cotyledonary leaf	9.216 ± 0.46	1.446 ± 0.07	4.344 ± 0.22
	Primary leaf	7.606 ± 0.38	2.173 ± 0.11	5.406 ± 0.27
200 µM $CuSO_4$	Root	1247.121 ± 62.36	260.476 ± 13.02	119.450 ± 5.97
	Stem	708.858 ± 35.44	165.634 ± 8.28	314.556 ± 15.73
	Cotyledonary leaf	34.169 ± 1.71	1.288 ± 0.06	7.704 ± 0.38
	Primary leaf	11.079 ± 0.55	1.939 ± 0.10	7.065 ± 0.35

surfaces of cotyledonary leavesof *R. communis* when treated with 160 μM$CuSO_4$was enhanced on exogenous application of KIN and BAP.The adaxial stomata were completely closed, whereas the abaxial stomata were partially closed during Cu stress (160 μM$CuSO_4$), as compared to the control. However, on application of cytokinins, the stomata opened on both adaxial and abaxial surfaces. In contrast to the KIN application, the stomatal opening was more prominent with the application of BAP (Fig. 49 and 50).

4.2.11. Anatomical modifications

4.2.11.1. Effect of Cu on anatomical modifications

The root cross-sections of *R. communis* seedlings exhibited single-layered epidermis, followed by a few-layered cortex and vascular cylinder. Some of the epidermal cells gave rise to unicellular root hairs. Cortex was composed of thin-walled, loosely arranged, parenchymatous cells with intercellular spaces. The stele is tetrarch and exarch, with a central pith region (Fig. 51 and 52). The anatomy reveals that, due to the Cu stress mediated decaying of the roots, the anatomical variation in the epidermis and cortex was not clearly observed in the roots of *R. communis* seedlings subjected to 200 μM $CuSO_4$. The number and size of xylem vessels were significantly reduced in the roots exposed to $CuSO_4$ as compared to the control. The scanning electron micrographs of the root cross-sections of *R. communis* seedlings after exposure to 200 μM $CuSO_4$ on 6 d of treatment were carried out. In the case of the stelar region, the thickness of the xylem wall was enhanced from 1.494 ± 0.135 μm in control to 2.947 ± 0.290 μm in 200 μM $CuSO_4$ treated roots (97% increase as compared to the control). The SEM images also revealed some clotted depositions in the xylem walls on exposure to $CuSO_4$ (Fig. 53 and 54, Table 19).

The cross-section of the stem of *R. communis* seedlings consists of single-layered epidermis, followed by ground tissue and stele. The outer wall of the epidermis is cuticularized. The ground tissue is differentiated into hypodermis and cortex. The hypodermis is 2-3 layered, collenchymatous and with angular thickening. Cortex consisted of loosely packed thin-walled parenchymatous cells. The cortex and stele were separated by single-layered, compactly arranged endodermis. The vascular bundles are wedge-shaped, conjoint, collateral and open, 7-9 in number and arranged in a ring in the primary structure of the stem. The vascular bundles are endarch, consisting of phloem and xylem, followed by a large pith region. The thickening of the hypodermis was increased on imparting Cu stress as compared to the control. No other significant variations were observed in the stem anatomy of *R. communis* seedlings upon exposure to $CuSO_4$ (Fig. 51 and 52). The scanning electron microscopic images of the secondary thickening of the vascular region revealed that the degradation of xylem tissues was initiated in the stem of *R. communis* seedlings subjected to 200 μM $CuSO_4$ as compared to the control. Moreover, the thickness of the xylem walls of the stem was enhanced from 0.931 ± 0.171 μm in control to 3.109 ± 0.438 μm in 200 μM $CuSO_4$ treated seedlings. Similar to the roots, some clotted depositions in the xylem walls were observed in the stem also on exposure to $CuSO_4$ (Fig. 53 and 54, Table 19).

The cotyledonary and primary leaves are covered on both surfaces by single-layered epidermis (adaxial and abaxial epidermis) along with cuticle as observed in the cross-section of both the cotyledonary and primary leaves through the midrib. The epidermis is uniseriate, compactly arranged parenchymatous cells. The tissue between the adaxial and abaxial epidermis consists of thin-walled parenchymatous mesophylls. The cells of mesophyll constitute upper palisade tissue and lower spongy tissue. A 2-3 layered compactly arranged collenchyma tissue lies just near to both the adaxial and

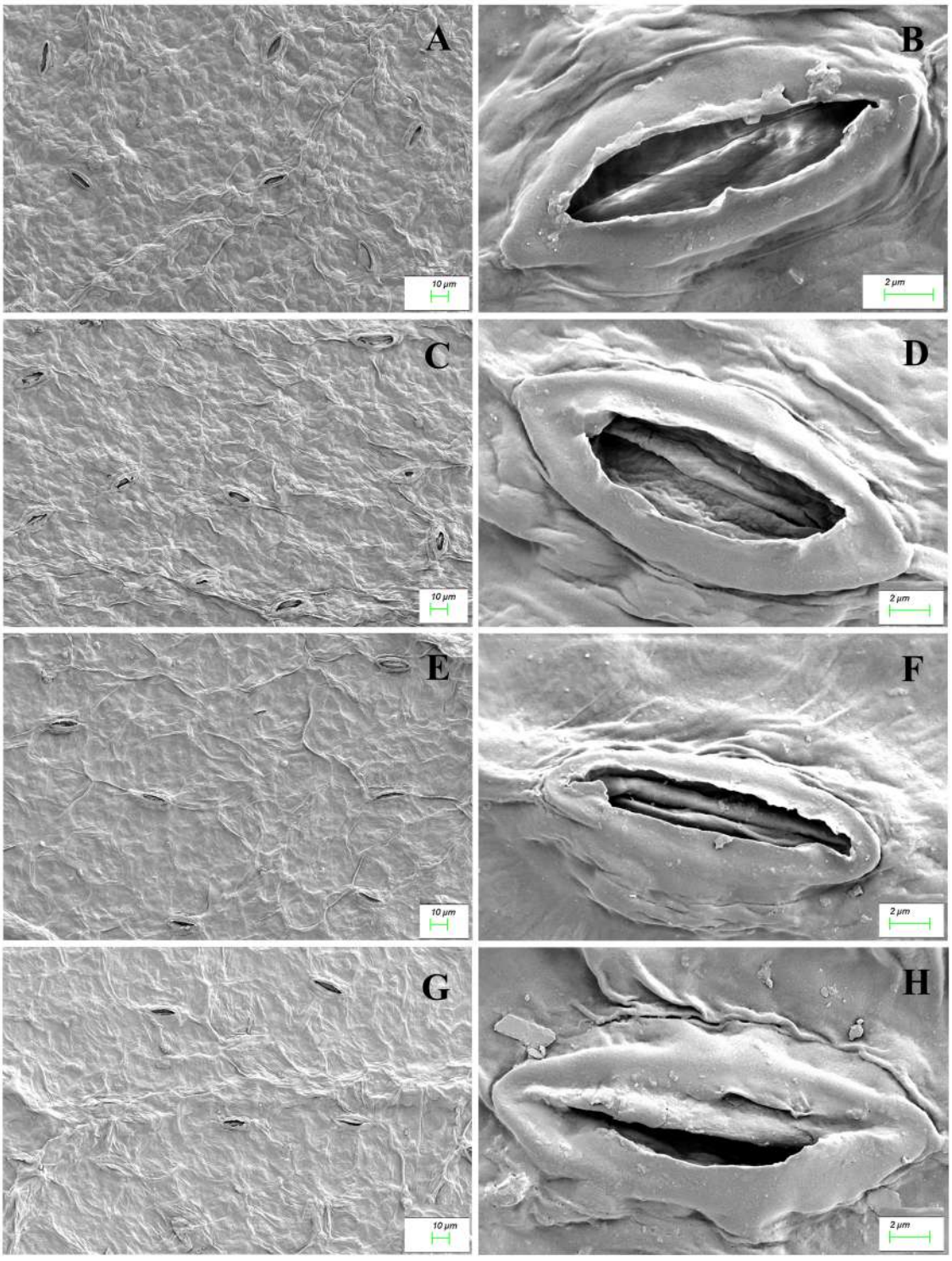

Figure 46. Scanning electron micrographs of adaxial and abaxial stomata in the cotyledonary leaves of *R. communis* seedlings on exposure to $CuSO_4$ for 6 d. A&B: control - adaxial stomata; C&D: control - abaxial stomata; E&F: 200 µM $CuSO_4$ - adaxial stomata; and G&H: 200 µM $CuSO_4$ - abaxial stomata.

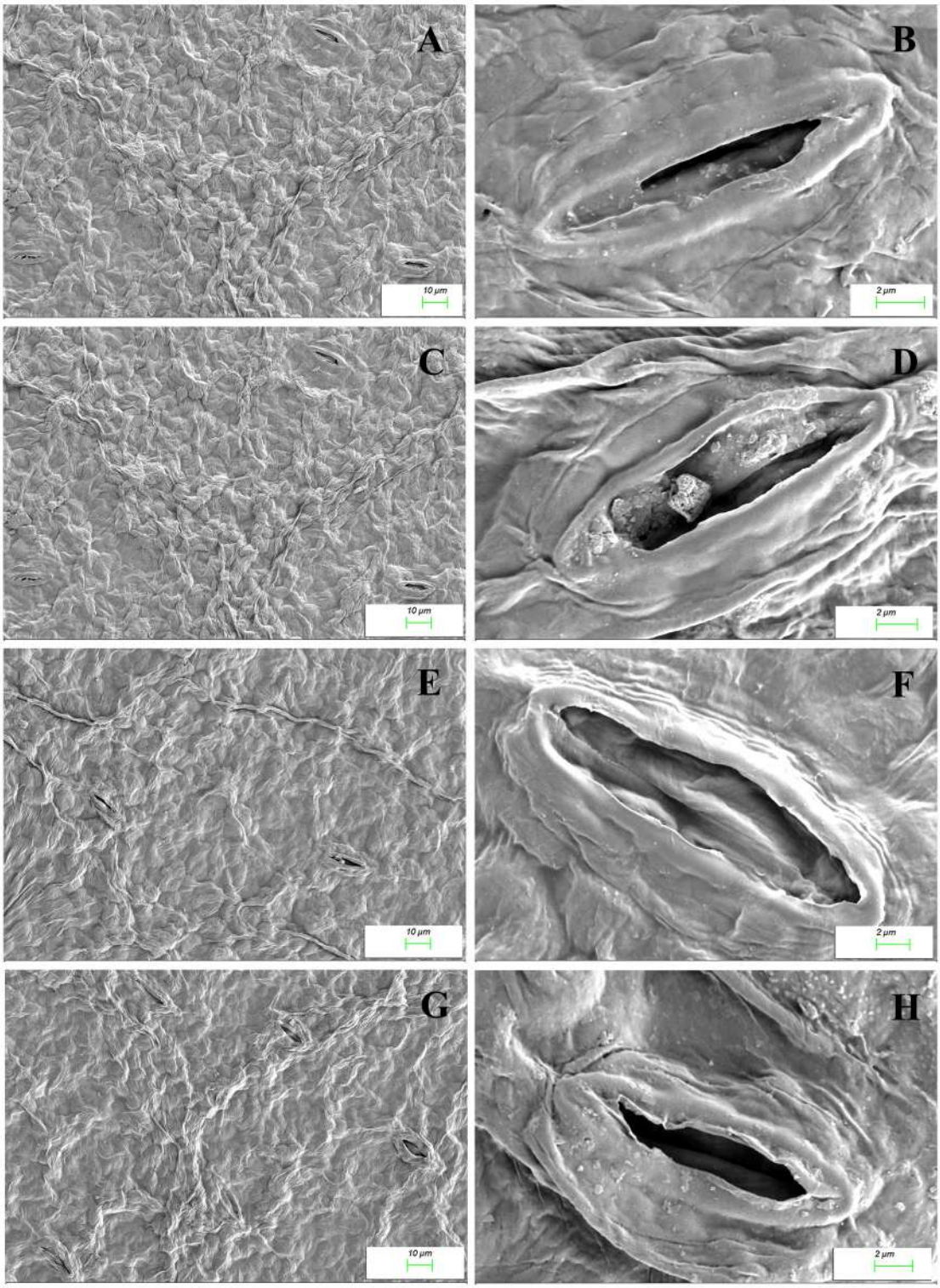

Figure 47. Scanning electron micrographs of adaxial and abaxial stomata in the primary leaves of *R. communis* seedlings on exposure to $CuSO_4$ for 6 d. A&B: control - adaxial stomata; C&D: control - abaxial stomata; E&F: 200 µM $CuSO_4$ - adaxial stomata; and G&H: 200 µM $CuSO_4$ - abaxial stomata.

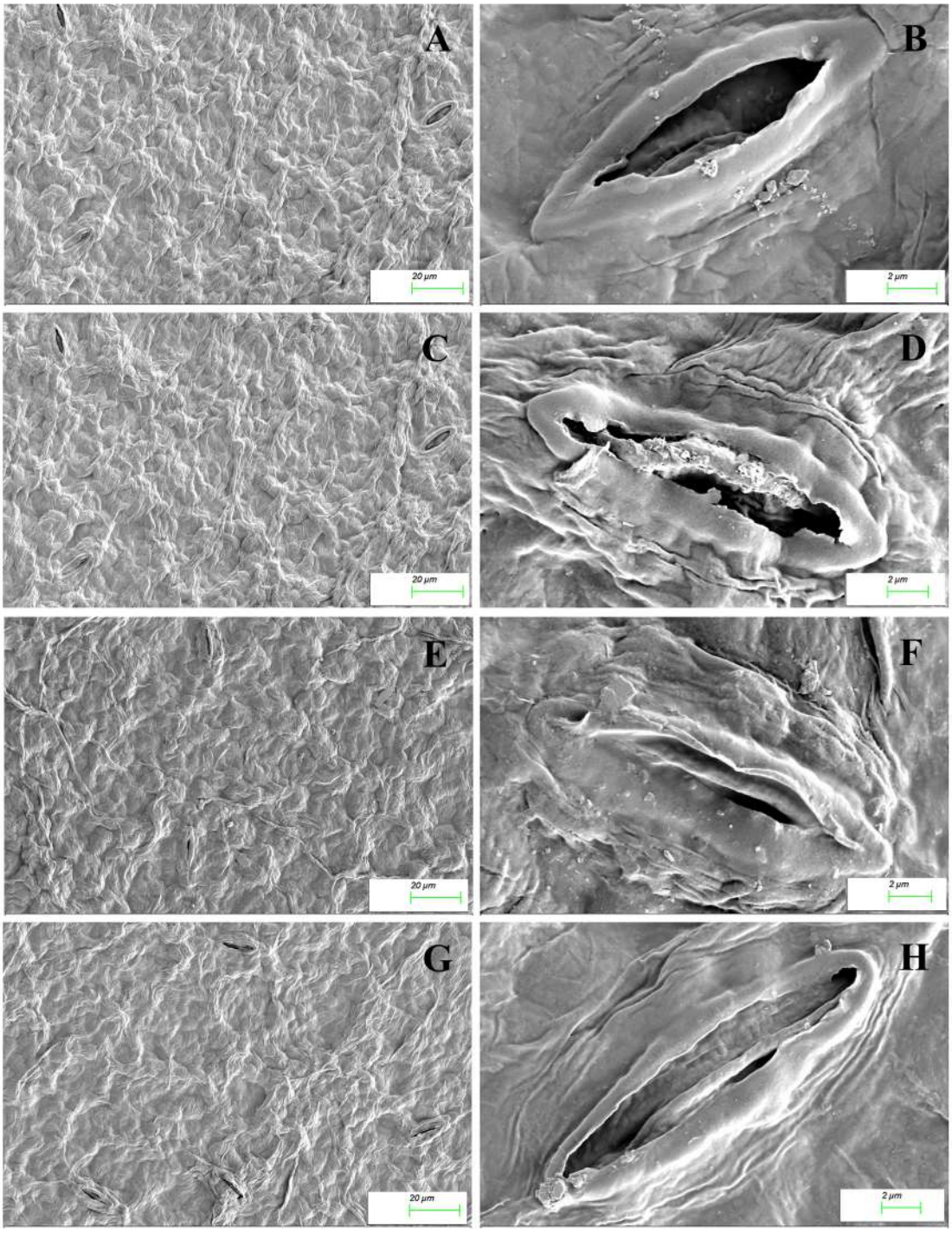

Figure 48. Scanning electron micrographs of adaxial and abaxial stomata in the primary leaves of *R. communis* seedlings on exposure to $CuSO_4$ for 10 d. A&B: control - adaxial stomata; C&D: control - abaxial stomata; E&F: 200 µM $CuSO_4$ - adaxial stomata; and G&H: 200 µM $CuSO_4$ - abaxial stomata.

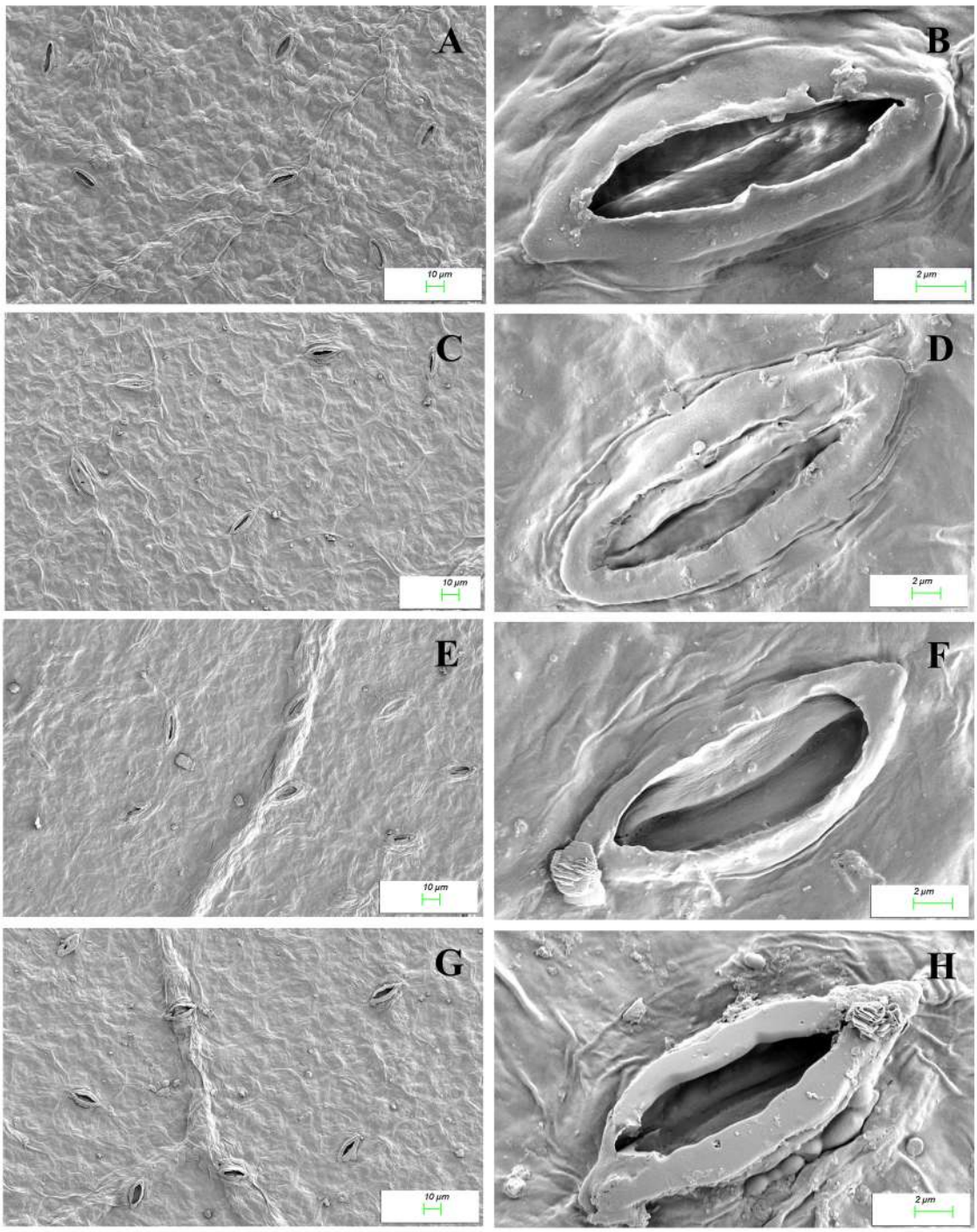

Figure 49. Scanning electron micrographs of adaxial stomata in the cotyledonary leaves of *R. communis* seedlings on 6 d of exposure to 160 µM $CuSO_4$ and cytokinins (KIN and BAP). A&B: control; C&D: 160 µM $CuSO_4$; E&F: 160 µM $CuSO_4$ + KIN; G&H: 160 µM $CuSO_4$ + BAP.

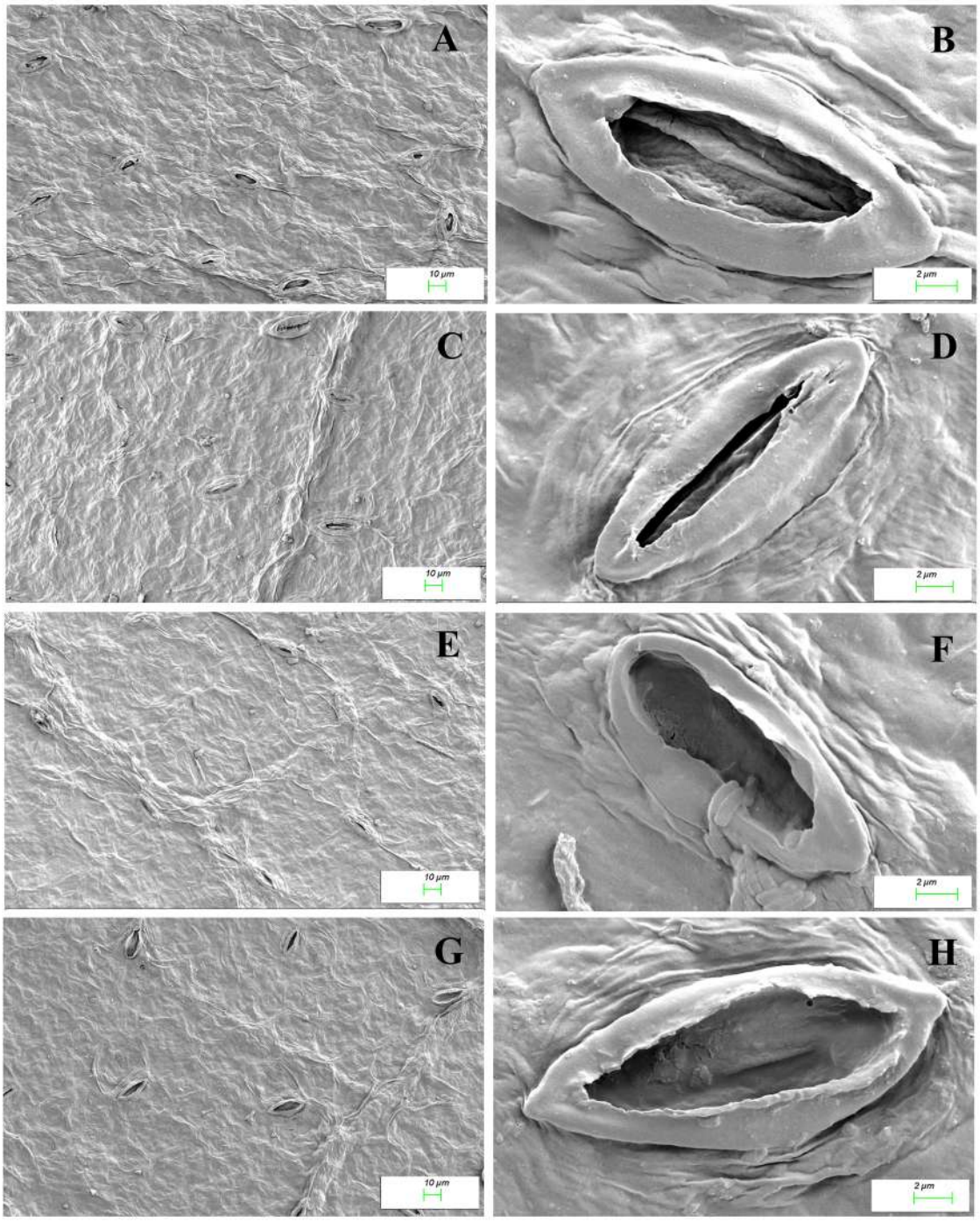

Figure 50. Scanning electron micrographs of abaxial stomata in the cotyledonary leaves of *R. communis* seedlings on 6 d of exposure to 160 µM $CuSO_4$ and cytokinins (KIN and BAP). A&B: control; C&D: 160 µM $CuSO_4$; E&F: 160 µM $CuSO_4$ + KIN; G&H: 160 µM $CuSO_4$ + BAP.

abaxial epidermis at the region of mid-vein, most prominently in the cotyledonary leaves. The vascular bundles are conjoint, collateral and closed, with a larger mid-vein bundle. Xylem lies towards the adaxial surface, and phloem lies towards the abaxial surface. In the xylem tissues of the mid-vein vascular bundle, protoxylem is situated towards adaxial surface and metaxylem towards the abaxial surface. No significant variations were recorded in the anatomy of both the leaves when treated with $CuSO_4$ as compared to the control (Fig. 51 and 52). The scanning electron microscopic analysis of the xylem tissues revealed that the thickness of the xylem wall was increased in both the leaves upon exposure to $CuSO_4$. In cotyledonary leaves, the xylem wall thickness was 3.407 ± 0.137 µm in control, which enhanced to 4.448 ± 0.205 µm when treated with 200 µM $CuSO_4$ (31% increase as compared to the control). In the case of primary leaves, the xylem wall thickness were 3.637 ± 0.147 and 3.9872 ± 0.161 µm in control and 200 µM $CuSO_4$ treated seedlings respectively (10% increase over the control). The clotted depositions were observed in the xylem walls of cotyledonary leaves on Cu stress but not observed in the primary leaves (Fig. 53 and 54, and Table 19).

Table 19. Xylem wall thickening in the root, stem, cotyledonary and primary leaves of *R. communis* seedlings subjected to $CuSO_4$ treatments (control and 200 µM) on 6 d. Values are the mean ± SE of three independent experiments.

Plant samples	Xylem wall thickening (µm)	
	Control	200 µM $CuSO_4$
Root	1.494 ± 0.135	2.947 ± 0.290
Stem	0.931 ± 0.171	3.109 ± 0.438
Cotyledonary leaf	3.407 ± 0.137	4.448 ± 0.205
Primary leaf	3.637 ± 0.147	3.9872 ± 0.161

4.2.11.2. Impact of cytokinins on anatomical modifications in the cotyledonary leaves

Scanning electron microscopic analysis was performed in the cross-sections of cotyledonary leaves of *R. communis* seedlings to determine the anatomical changes during exposure to 160 μM $CuSO_4$ in the presence and absence of applied cytokinins. It was observed that marked changes occur in the thickening of the xylem wall as compared to that of the control. Similarly, the presence of clotted depositions observed in between the walls of the xylem and bundle cap cells in the cotyledonary leaves of 160 μM $CuSO_4$ treated seedlings was comparatively reduced on application of cytokinins (Fig. 55).

4.2.12. GCMS analysis of bioactive compounds

4.2.12.1. Effect of Cu on GCMS analysis of bioactive compounds

The phytochemical composition of cotyledonary and primary leaves and roots of *R. communis* seedlings on 6 d of exposure to 200 μM $CuSO_4$ in comparison with the control was analyzed by comparing the retention times (rt), molecular weight (m/z), peak area, peak area %, height and height %. The phytocompound neophytadiene was detected in all the parts of both the control and Cu-treated seedlings, but the peak area % varied among them (Fig. 56, 57 and 58, Table 20).

In the case of cotyledonary leaves, 8 compounds such as (E)-phytol; delta-tetradecalactone; androst-5-en-7-one, 3-(acetyloxy)-, (3-beta.)-; androsta-4,16-dien-3-one; cis,cis,cis-7,10,13-hexadecatrienal; hexadecanoic acid; lupeol; and neophytadiene were detected commonly in both the control as well as Cu-treated seedlings, but in different proportion. 3,7,11,15-tetramethyl-2-hexadecen-1-ol; 3-cyclopentylpropionic acid, 2-isopropoxyphenyl ester; beyerene; isophytol acetate; methyl palmitate;

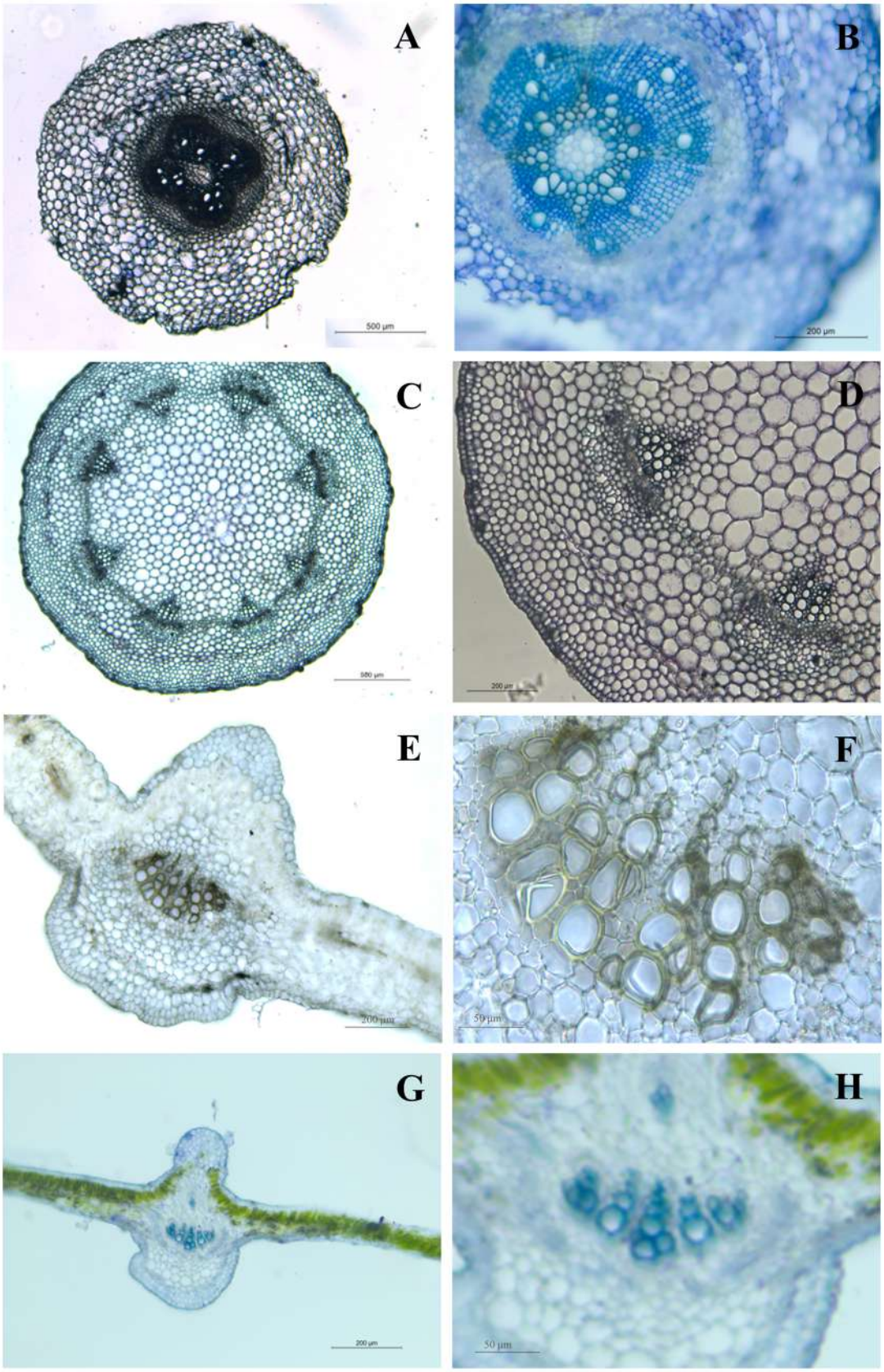

Figure 51. Histochemically stained of cross sections of root (A&B), stem (C&D), cotyledonary leaf (E&F) and primary leaf (G&H) of control seedlings of *R. communis*.

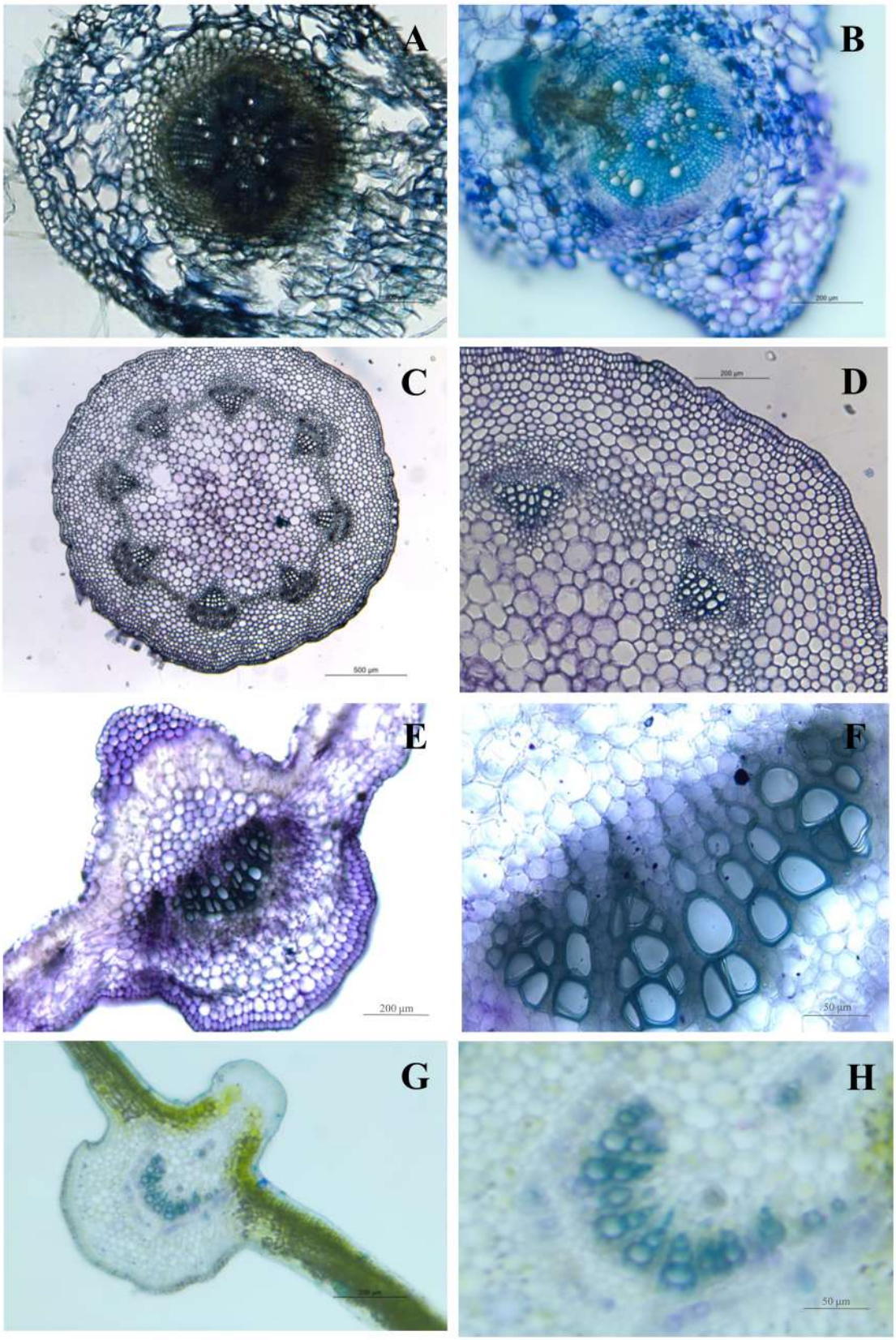

Figure 52. Histochemically stained cross sections of root (A&B), stem (C&D), cotyledonary leaf (E&F) and primary leaf (G&H) of *R. communis* seedlings on exposure to 200 µM $CuSO_4$ fore 6 d.

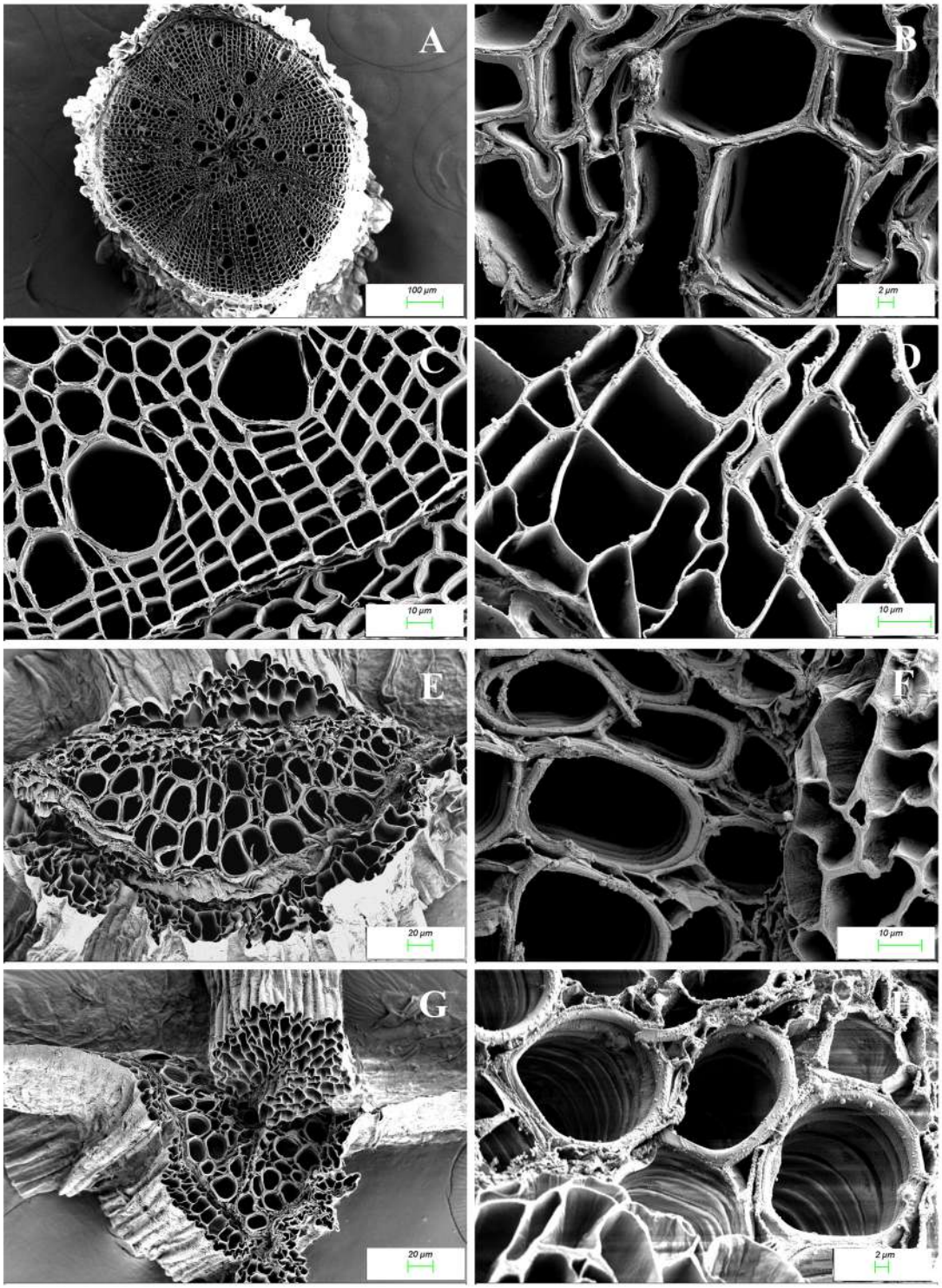

Figure 53. Scanning electron micrographs of cross sections of root (A&B), stem (C&D), cotyledonary leaf (E&F) and primary leaf (G&H) of control seedlings of *R. communis*.

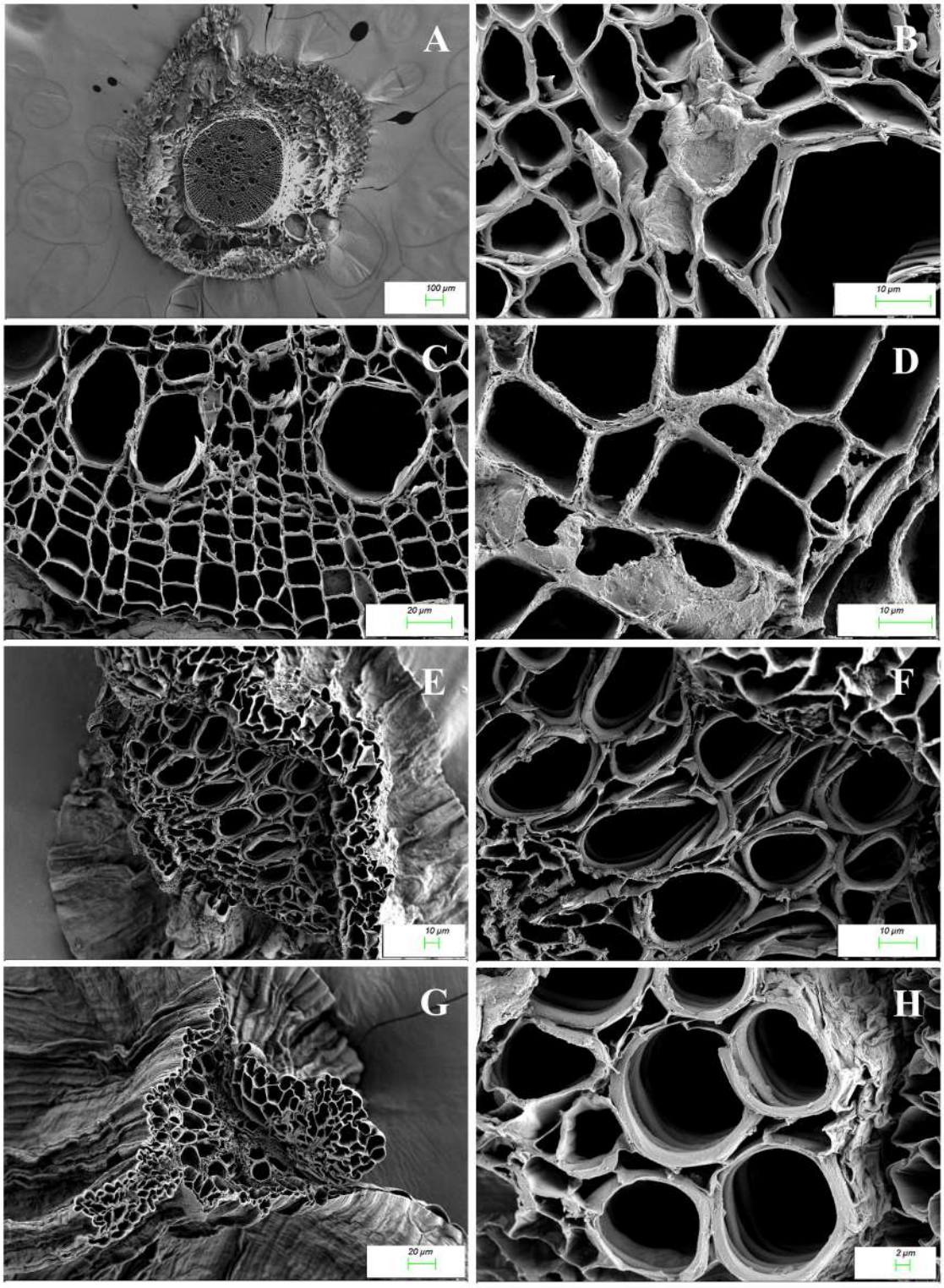

Figure 54. Scanning electron micrographs of cross sections of root (A&B), stem (C&D), cotyledonary leaf (E&F) and primary leaf (G&H) of *R. communis* seedlings on exposure to 200 µM $CuSO_4$ for 6 d.

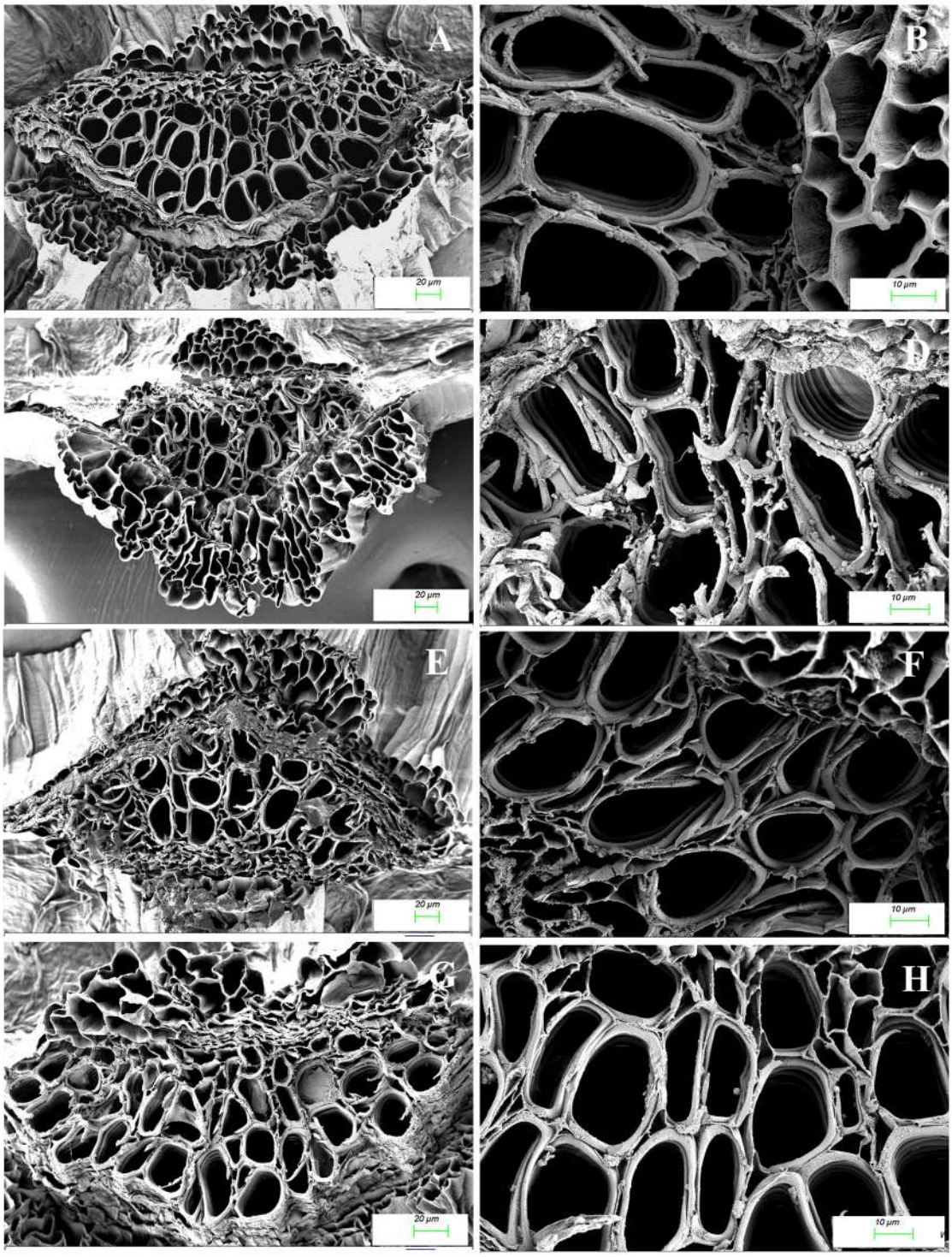

Figure 55. Scanning electron micrographs of cross-sections of cotyledonary leaves of *R. communis* seedlings on 6 d of exposure to 160 µM $CuSO_4$ and cytokinins (KIN and BAP). A&B: control; C&D: 160 µM $CuSO_4$; E&F: 160 µM $CuSO_4$ + KIN; G&H: 160 µM $CuSO_4$ + BAP.

oxacycloheptadec-8-en-2-one; and stigmasterol present in the cotyledonary leaves of the control seedlings disappeared on exposure to $CuSO_4$. Copper induced accumulation of 1,7-dioxaspiro[5.5]undec-2-ene; 17-norkaur-15-ene, 13-methyl-, (8-beta,13-beta.)-; 18-norisopimara-4(19),7,15-triene; 2-chloroethyl linoleate; 2-hexadecen-1-ol, 3,7,11,15-tetramethyl-, [R-[R*,R*-(E)]]-; 3-(3-methyl-5-oxo-4,5-dihydro-1h-pyrazol-4-yl)propanoic acid; calendin; phytol acetate; and tricyclo[20.8.0.0(7,16)]triaconta-1(22),7(16),9,13,24,28-hexaene were unique to the cotyledonary leaves subjected to Cu stress. Of which, 16.65% of peak area constitute the phytol acetate (Fig. 56, Table 20).

In the case of primary leaves, due to the accumulation of 93.72% proportion of lupeol in the control seedlings, only four phytocompounds, alpha-linolenic acid; hexadecanoic acid; neophytadiene; and phytol, were detected in the control seedlings. The phytocompounds such as alpha-linolenic acid; gamma-tocopherol; 8-dodecen-1-ol, acetate, (Z)-; octadecanoic acid; palmitoyl chloride; and vitamin E were unique to the $CuSO_4$ treated primary leaves. On $CuSO_4$ exposure, the proportion of the phytocompounds hexadecanoic acid, neophytadiene and phytol were enhanced in the primary leaves, whereas the proportion of lupeol was drastically reduced (72% reduction in peak area % as compared to the control) (Fig. 57, Table 20).

The phytocompounds (22E)-stigmasta-4,6,22-trien-3-yl acetate; 9,12-octadecadienoic acid, methyl ester; 9-octadecenoic acid (Z)-, methyl ester; cholestane-3,5-diol, 5-acetate, (3-beta,5-alpha.)-; cis-vaccenic acid; methyl 11,14-eicosadienoate; methyl isopimarate; and methyl stearate were reported only in the roots of *R. communis* seedlings. Of which, 9-octadecenoic acid (Z)-, methyl ester; and methyl isopimarate were common for both the control and $CuSO_4$ treated roots, however, the peak area % was reduced by 70 and 43% respectively during Cu stress as compared to the control. Four

phytocompounds, 9,12-octadecadienoic acid, methyl ester; cholestane-3,5-diol, 5-acetate, (3-beta,5-alpha.)-; isophytol acetate; and methyl stearate observed in the roots of the control seedlings were not present in seedlings exposed to Cu stress. Moreover, the compounds such as (E)-phytol; beyerene; cis-vaccenic acid; hexadecanoic acid; lupeol; methyl 11,14-eicosadienoate; and phytol acetate absent in the roots of the control seedlings were appearing in seedlings upon exposure to 200 μM $CuSO_4$, in which hexadecanoic acid alone constitute 45.87% of the peak area (Fig. 58, Table 20).

4.2.12.2. Impact of cytokinins on accumulation of bioactive compounds in the cotyledonary leaves

Variations in the bioactive compounds in cotyledonary leaves of *R. communis* seedlings subjected to Cu stress along with the application of cytokinins were evaluated by GCMS analysis (Fig. 56A, 59, 60 and 61, Table 21). The compounds such as 3-cyclopentylpropionic acid, 2-isopropoxyphenyl ester; cis,cis,cis-7,10,13-hexadecatrienal; and stigmasterol were not detected in seedlings subjected to Cu stress conditions with and without KIN and BAP (80 $CuSO_4$, 160 $CuSO_4$, 80 $CuSO_4$ + KIN, 160 $CuSO_4$ + KIN, 80 $CuSO_4$ + BAP, and 160 $CuSO_4$ + BAP). In contrast, the appearance of new compounds was observed in cotyledonary leaves of seedlings subjected to Cu stress, which were 1,7-dioxaspiro[5.5]undec-2-ene; 9,12,15-octadecatrienoic acid, (Z,Z,Z)-; delta-4,16-androstadien-3-one; hexahydrofarnesyl acetone; lup-20(29)-en-3-yl acetate; and phytol acetate. The compounds such as 1,7-dioxaspiro[5.5]undec-2-ene; 9,12,15-octadecatrienoic acid, (Z,Z,Z)-; delta-4,16-androstadien-3-one; and lup-20(29)-en-3-yl acetate were unique to the cytokinin treated seedlings subjected to Cu stress. Of these, 9,12,15-octadecatrienoic acid, (Z,Z,Z)- and lup-20(29)-en-3-yl acetate were present only in seedlings subjected to Cu stress along with BAP application (Table 21).

More than the production of new bioactive compounds, quantitative variations were observed between the control and seedlings subjected to Cu stress in the presence and absence of cytokinins. Upon exposure to Cu stress, a significant increase in peak area % of isophytol acetate was noticed, i.e., 41 and 32% in seedlings exposed to 80 and 160 µM $CuSO_4$, respectively. A prominent enhancement in the peak area % of lup-20(29)-en-3-yl acetate (43.24%) and lupeol (41%) was detected in 160 µM $CuSO_4$+BAP treated seedlings (Table 21).

4.2.13. Fourier Transform Infrared (FTIR) spectroscopic analysis

4.2.13.1. Effect of Cu on FTIR spectra

In order to differentiate the functional groups related to different carbohydrate structures, aldehydes, or phenols in the cell wall material of $CuSO_4$ treated *R. communis* seedlings, the infrared spectra of the root, cotyledonary and primary leaves were analyzed (Fig. 62). The peaks at 3397 cm^{-1} (peak No. 1) and 2923 cm^{-1} (peak No. 2) indicate the –OH stretching vibration corresponding with polysaccharides, celluloses and hemicelluloses, and –COOH and –CH3 stretching vibration associated with cellulose and proteins, respectively. Peak No. 3 (transmittance at 1635 cm^{-1}) is precise for amide bands representing the N–H bending vibration and C=O stretching vibration of peptide bonds. Peak No. 4 (transmittance at 1385 cm^{-1}) was a characteristic peak associated with the C–H symmetric bending vibration in terminal methyls. It was difficult to recognize the individual peaks in the low-frequency region due to the presence of complex polysaccharides (Fig. 62).

Compared with the control, the shape of FTIR spectral peaks of cotyledonary leaves, primary leaves and roots of 200 µM $CuSO_4$ treated seedlings remained structurally the same. However, characteristic peaks occurred at different degrees. When the seedlings were subjected to $CuSO_4$

treatment, the peak No. 1 and 2 of both the leaves and roots became weak and shifted to a low-frequency region, and peak No. 3 became shallow as compared to that of the control. In contrast, peak No. 4 became much stronger and deep with $CuSO_4$ treatment than the control (Fig. 62).

4.2.13.2. Impact of cytokinins on FTIR spectra of cotyledonary leaves

As compared to the control, peak no. 1 was shifted to a higher frequency region and became weaker in both the $CuSO_4$ treatments (80 and 160 µM). On application of cytokinins along with $CuSO_4$, peak no. 1 shifted to the low-frequency region and at the same time increased in height as compared to that of the control. A stronger peak was observed in the case of cotyledonary leaves of seedlings with BAP application than that of KIN (Fig. 63).

Peak No. 2 (transmittance at 2923 cm^{-1}) was weak during Cu stress, became as strong as the control when treated with BAP, but no significant variation was observed in KIN treated cotyledonary leaves. In the case of peak No. 3 (transmittance at 1635 cm^{-1}), which was shallow during Cu stress, became much deeper on application of cytokinins, most significantly in BAP treated ones. The peak No. 4 (transmittance at 1385 cm^{-1}) was associated with the C–H bending vibration with terminal methyls, which became sharper when subjected to both $CuSO_4$ treatments. On application of KIN and BAP along with $CuSO_4$, the strength of the peak was reduced and maintained as that of the control (Fig. 63).

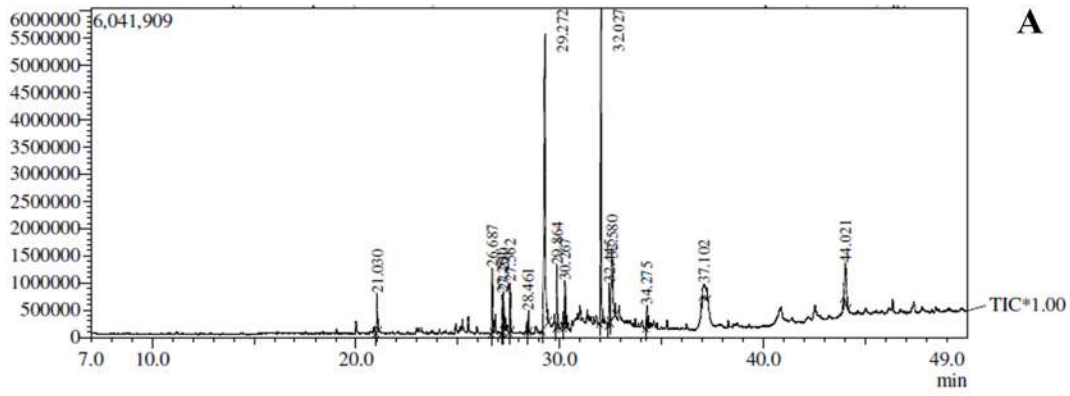

Peak Report TIC

Peak#	R.Time	Area	Area%	Height	Height%	Name	Base m/z
1	21.030	2181994	2.89	714464	3.41	.DELTA.-TETRADECALACTONE	100.05
2	26.687	3048994	4.04	1199797	5.73	NEOPHYTADIENE	68.05
3	27.201	1908244	2.53	689760	3.30	3,7,11,15-Tetramethyl-2-hexadecen-1-ol	82.10
4	27.250	2270728	3.01	726116	3.47	3-Cyclopentylpropionic acid, 2-isopropoxyphenyl ester	110.00
5	27.562	2248724	2.98	893327	4.27	(E)-PHYTOL	82.05
6	28.461	905224	1.20	375074	1.79	METHYL PALMITATE	74.00
7	29.272	24002471	31.82	5373512	25.67	HEXADECANOIC ACID	73.00
8	29.864	3090352	4.10	1148225	5.49	Androsta-4,16-dien-3-one	91.05
9	30.267	2687352	3.56	856118	4.09	ANDROST-5-EN-7-ONE, 3-(ACETYLOXY)-, (3.BETA.)-	91.00
10	32.027	15003894	19.89	5765437	27.54	Isophytol, acetate	71.05
11	32.445	2522400	3.34	730731	3.49	OXACYCLOHEPTADEC-8-EN-2-ONE	67.05
12	32.580	7677547	10.18	1096072	5.24	cis,cis,cis-7,10,13-Hexadecatrienal	79.05
13	34.275	1137034	1.51	409354	1.96	BEYERENE	135.10
14	37.102	2652331	3.52	245389	1.17	Stigmasterol	55.05
15	44.021	4094176	5.43	710068	3.39	Lupeol	55.05
		75431465	100.00	20933444	100.00		

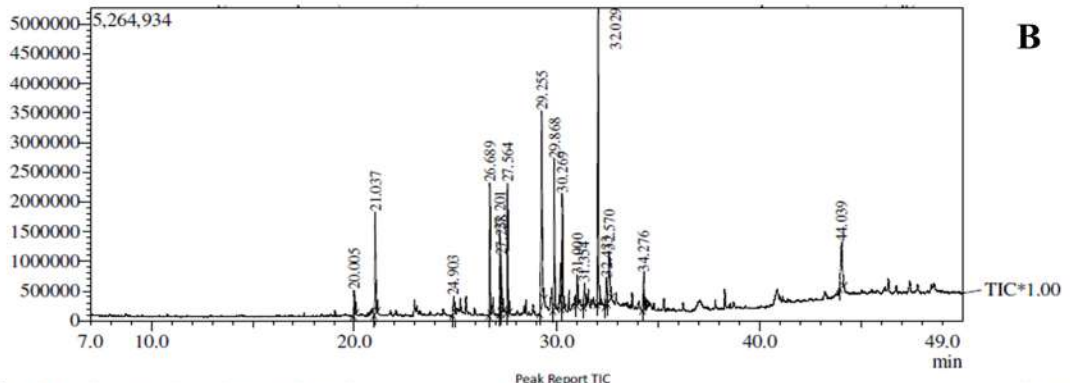

Peak Report TIC

Peak#	R.Time	Area	Area%	Height	Height%	Name	Base m/z
1	20.005	1182300	1.48	410626	1.61	1,7-Dioxaspiro[5.5]undec-2-ene	98.10
2	21.037	5139566	6.45	1714865	6.74	.DELTA.-TETRADECALACTONE	100.05
3	24.903	1254980	1.57	300148	1.18	CALENDIN	111.10
4	26.689	5554370	6.97	2213479	8.70	NEOPHYTADIENE	68.05
5	27.201	3845155	4.82	1367414	5.38	(E)-PHYTOL	82.10
6	27.258	2761890	3.46	942918	3.71	3-(3-METHYL-5-OXO-4,5-DIHYDRO-1H-PYRAZOL-4-YL)PROPANOIC ACID	110.05
7	27.564	5237200	6.57	2175771	8.56	2-HEXADECEN-1-OL, 3,7,11,15-TETRAMETHYL-, [R-[R*,R*-(E)]]-	82.05
8	29.255	12839281	16.11	3279069	12.90	HEXADECANOIC ACID	73.05
9	29.868	6930785	8.69	2526743	9.94	Androsta-4,16-dien-3-one	91.05
10	30.269	6308651	7.91	1937783	7.62	ANDROST-5-EN-7-ONE, 3-(ACETYLOXY)-, (3.BETA.)-	91.05
11	31.000	1358803	1.70	491637	1.93	18-NORISOPIMARA-4(19),7,15-TRIENE	91.05
12	31.354	1572605	1.97	391131	1.54	Tricyclo[20.8.0.0(7,16)]triaconta-1(22),7(16),9,13,24,28-hexaene	270.30
13	32.029	13275317	16.65	4983183	19.60	Phytol, acetate	71.05
14	32.433	1638519	2.06	464524	1.83	2-CHLOROETHYL LINOLEATE	67.05
15	32.570	4616045	5.79	840267	3.30	cis,cis,cis-7,10,13-Hexadecatrienal	79.05
16	34.276	1843499	2.31	630498	2.48	17-Norkaur-15-ene, 13-methyl-, (8.beta.,13.beta.)-	135.15
17	44.039	4363152	5.47	757996	2.98	Lupeol	95.05
		79722118	100.00	25428052	100.00		

Figure 56. GCMS chromatograms and peak reports of bioactive compounds from the methanolic extracts of the cotyledonary leaves of *R. communis* seedlings on exposure to $CuSO_4$. A: control; and B: 200 µM $CuSO_4$.

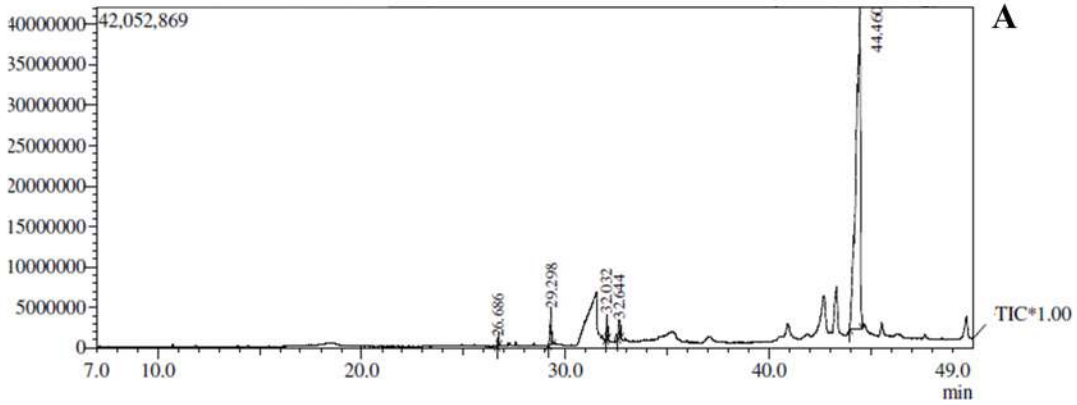

Peak Report TIC

Peak#	R.Time	Area	Area%	Height	Height%	Name	Base m/z
1	26.686	2218308	0.35	916945	1.81	NEOPHYTADIENE	68.05
2	29.298	20182244	3.21	4565981	9.04	HEXADECANOIC ACID	73.00
3	32.032	7375362	1.17	3061101	6.06	Phytol	71.05
4	32.644	9777776	1.55	2277223	4.51	alpha.-Linolenic acid	79.05
5	44.460	590056868	93.72	39709408	78.58	Lupeol	95.10
		629610558	100.00	50530658	100.00		

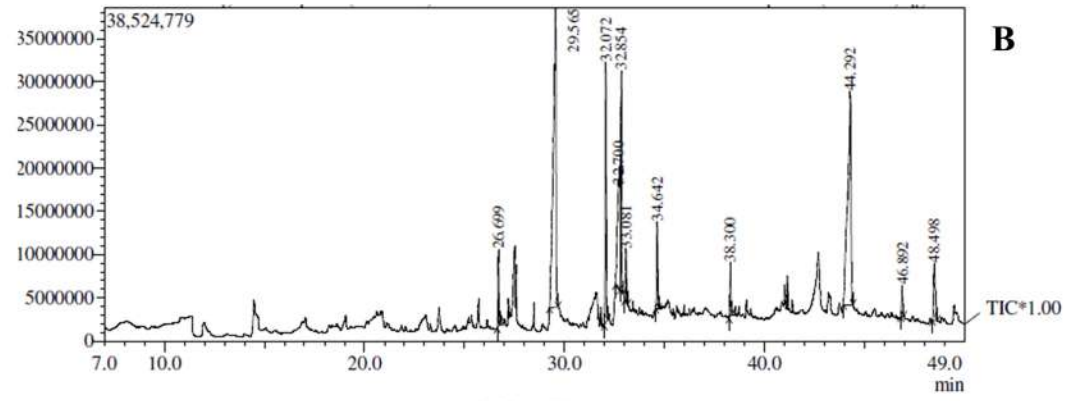

Peak Report TIC

Peak#	R.Time	Area	Area%	Height	Height%	Name	Base m/z
1	26.699	22897090	2.15	8762030	5.23	NEOPHYTADIENE	68.05
2	29.565	317225395	29.78	34574870	20.62	HEXADECANOIC ACID	73.00
3	32.072	92887501	8.72	30076965	17.94	Phytol	71.05
4	32.700	104201595	9.78	11822318	7.05	8-Dodecen-1-ol, acetate, (Z)-	81.05
5	32.854	129579464	12.16	25426002	15.16	.alpha.-Linolenic acid	79.05
6	33.081	18691748	1.75	6118235	3.65	Octadecanoic acid	73.00
7	34.642	32728772	3.07	10004669	5.97	(+)-Beyerene	105.10
8	38.300	18138349	1.70	6125384	3.65	Palmitoyl chloride	98.10
9	44.292	275144674	25.83	24584693	14.66	Lupeol	95.10
10	46.892	13254763	1.24	3570506	2.13	.gamma.-Tocopherol	151.05
11	48.498	40447782	3.80	6618747	3.95	Vitamin E	165.05
		1065197133	100.00	167684419	100.00		

Figure 57. GCMS chromatograms and peak reports of bioactive compounds from the methanolic extracts of the primary leaves of *R. communis* seedlings on exposure to $CuSO_4$. A: control; and B: 200 µM $CuSO_4$.

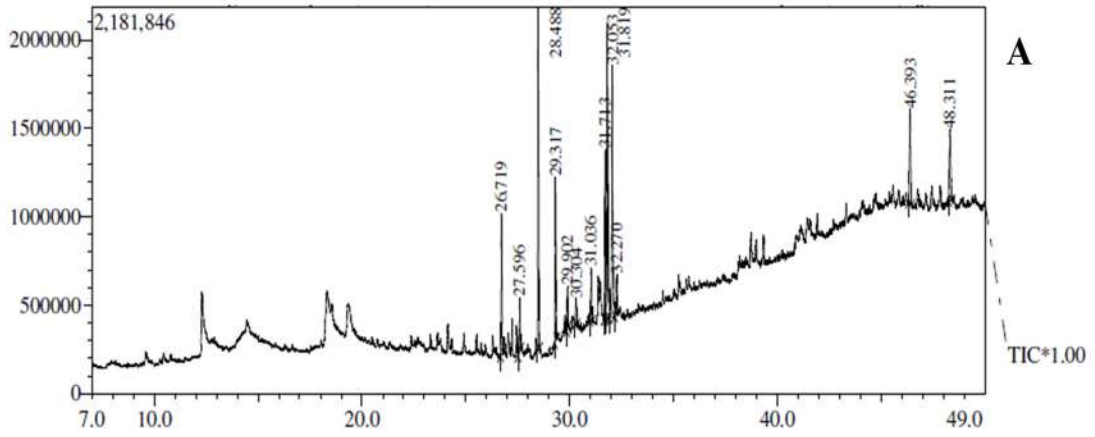

Peak Report TIC

Peak#	R.Time	Area	Area%	Height	Height%	Name	Base m/z
1	26.719	2024142	6.77	800329	8.11	NEOPHYTADIENE	68.10
2	27.596	798278	2.67	304809	3.09	3,7,11,15-Tetramethyl-2-hexadecen-1-ol	82.10
3	28.488	4962227	16.59	1923869	19.49	METHYL PALMITATE	74.05
4	29.317	2404494	8.04	922660	9.35	Dibutyl phthalate	149.05
5	29.902	669786	2.24	234903	2.38	ANDROSTA-4,16-DIEN-3-ONE	93.05
6	30.304	465266	1.56	146661	1.49	Androst-5-en-7-one, 3-(acetyloxy)-, (3.beta.)-	270.25
7	31.036	854652	2.86	301573	3.06	Methyl isopimarate	105.05
8	31.713	2412219	8.07	962021	9.75	9,12-Octadecadienoic acid, methyl ester	67.05
9	31.819	5630766	18.83	1675692	16.98	9-OCTADECENOIC ACID (Z)-, METHYL ESTER	55.05
10	32.053	5087371	17.01	1425350	14.44	Isophytol, acetate	71.05
11	32.270	811530	2.71	233589	2.37	Methyl stearate	74.05
12	46.393	2013571	6.73	536016	5.43	(22E)-STIGMASTA-4,6,22-TRIEN-3-YL ACETATE #	83.05
13	48.311	1773257	5.93	401278	4.07	Cholestane-3,5-diol, 5-acetate, (3.beta.,5.alpha.)-	55.05
		29907559	100.00	9868750	100.00		

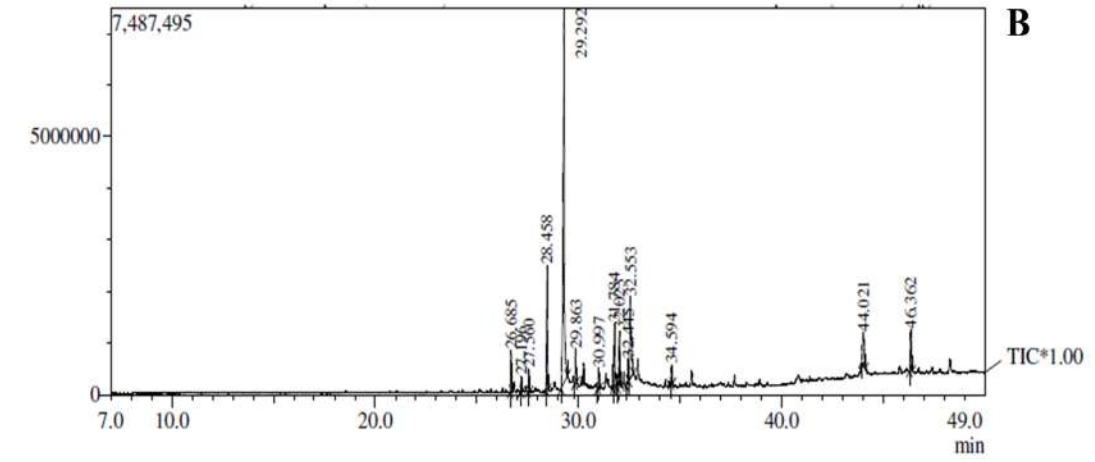

Peak Report TIC

Peak#	R.Time	Area	Area%	Height	Height%	Name	Base m/z
1	26.685	1995491	2.85	796157	4.33	NEOPHYTADIENE	68.05
2	27.196	803625	1.15	293647	1.60	(E)-PHYTOL	82.05
3	27.560	1120897	1.60	428537	2.33	3,7,11,15-Tetramethyl-2-hexadecen-1-ol	82.05
4	28.458	6065249	8.67	2400655	13.05	METHYLPALMITATE	74.00
5	29.292	32070506	45.87	7248676	39.39	HEXADECANOIC ACID	73.05
6	29.863	1843384	2.64	660218	3.59	Androsta-4,16-dien-3-one	91.05
7	30.997	1138992	1.63	398504	2.17	Methyl isopimarate	91.05
8	31.784	3969333	5.68	1232032	6.70	9-OCTADECENOIC ACID (Z)-, METHYL ESTER	55.05
9	32.023	3351394	4.79	1088483	5.92	Phytol, acetate	71.05
10	32.445	1652195	2.36	447802	2.43	METHYL 11,14-EICOSADIENOATE	67.05
11	32.553	8629314	12.34	1587870	8.63	cis-Vaccenic acid	55.05
12	34.594	976589	1.40	365565	1.99	(+)-Beyerene	105.05
13	44.021	3348436	4.79	642725	3.49	Lupeol	95.15
14	46.362	2956233	4.23	811000	4.41	3.beta.-Acetoxystigmasta-4,6,22-triene	83.10
		69921638	100.00	18401871	100.00		

Figure 58. GCMS chromatograms and peak reports of bioactive compounds from the methanolic extracts of the roots of *R. communis* seedlings on exposure to $CuSO_4$. A: control; and B: 200 µM $CuSO_4$.

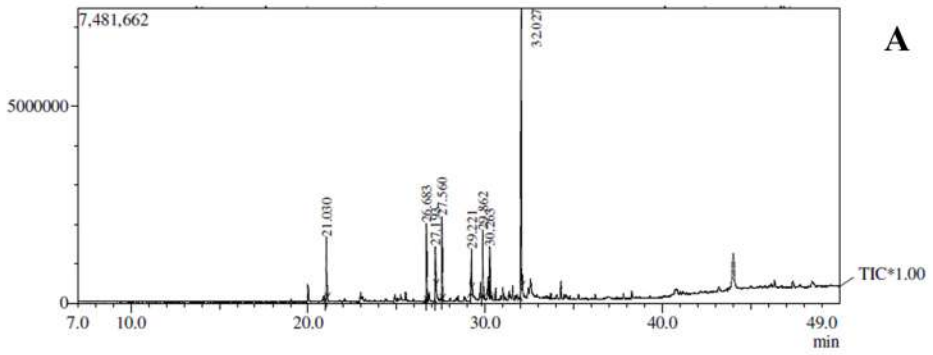

Peak Report TIC

Peak#	R.Time	Area	Area%	Height	Height%	Name	Base m/z
1	21.030	4374709	9.63	1564789	8.81	.DELTA.-TETRADECALACTONE	100.05
2	26.683	4667792	10.28	1922331	10.82	NEOPHYTADIENE	68.05
3	27.193	2486408	5.47	1146503	6.45	3,7,11,15-Tetramethyl-2-hexadecen-1-ol	82.05
4	27.560	4770633	10.50	2071529	11.66	Phytol, acetate	82.05
5	29.221	2558068	5.63	1037570	5.84	HEXADECANOIC ACID	73.00
6	29.862	4469505	9.84	1676938	9.44	Androsta-4,16-dien-3-one	91.05
7	30.263	3410602	7.51	1168074	6.58	Androst-5-en-7-one, 3-(acetyloxy)-, (3.beta.)-	91.05
8	32.027	18685342	41.14	7177580	40.40	Isophytol, acetate	71.05
		45423059	100.00	17765314	100.00		

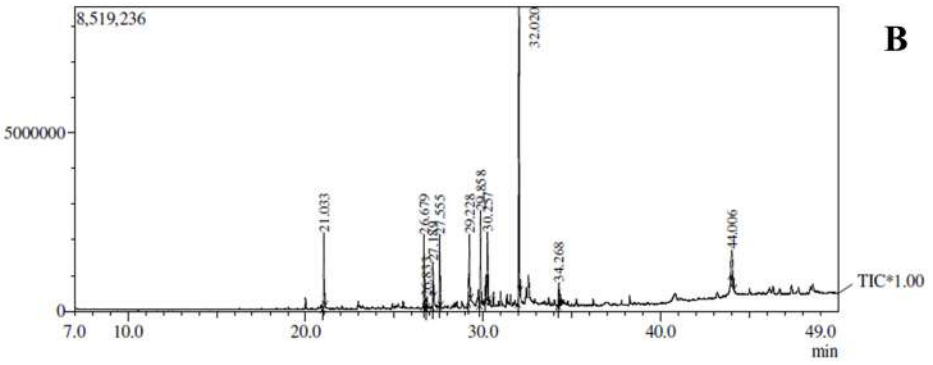

Peak Report TIC

Peak#	R.Time	Area	Area%	Height	Height%	Name	Base m/z
1	21.033	5540923	8.43	2079648	8.86	.DELTA.-TETRADECALACTONE	100.10
2	26.679	4826448	7.34	2026546	8.64	NEOPHYTADIENE	68.05
3	26.833	713486	1.09	282352	1.20	HEXAHYDROFARNESYLACETONE	58.05
4	27.189	2630536	4.00	1096423	4.67	(E)-PHYTOL	82.05
5	27.555	4845418	7.37	1998547	8.52	3,7,11,15-Tetramethyl-2-hexadecen-1-ol	82.10
6	29.228	6066911	9.23	1862342	7.94	HEXADECANOIC ACID	73.05
7	29.858	7149377	10.88	2614916	11.14	ANDROSTA-4,16-DIEN-3-ONE	91.05
8	30.257	7237501	11.01	1914680	8.16	ANDROST-5-EN-7-ONE, 3-(ACETYLOXY)-, (3.BETA.)-	91.05
9	32.020	20920636	31.83	8121625	34.61	Isophytol, acetate	71.05
10	34.268	1811138	2.76	646212	2.75	BEYERENE	135.15
11	44.006	3988855	6.07	823960	3.51	Lupeol	95.10
		65731229	100.00	23467251	100.00		

Figure 59. GCMS chromatograms and peak reports of bioactive compounds from the methanolic extracts of the cotyledonary leaves of *R. communis* seedlings on exposure to $CuSO_4$. A: 80 µM $CuSO_4$; and B: 160 µM $CuSO_4$.

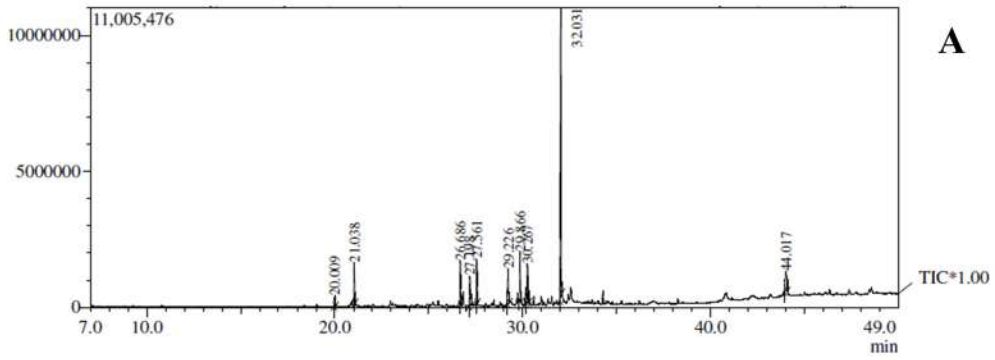

Peak Report TIC

Peak#	R.Time	Area	Area%	Height	Height%	Name	Base m/z
1	20.009	1008999	1.70	362604	1.66	1,7-DIOXASPIRO[5.5]UNDEC-2-ENE	98.10
2	21.038	3563897	6.00	1432949	6.56	.DELTA.-TETRADECALACTONE	100.05
3	26.686	3555301	5.99	1554278	7.11	NEOPHYTADIENE	68.05
4	27.198	3858465	6.50	1095143	5.01	3,7,11,15-Tetramethyl-2-hexadecen-1-ol	82.05
5	27.561	3601744	6.07	1564610	7.16	Phytol, acetate	82.05
6	29.226	4404899	7.42	1267272	5.80	HEXADECANOIC ACID	73.00
7	29.866	4704090	7.92	1836361	8.40	Androsta-4,16-dien-3-one	91.05
8	30.267	4471365	7.53	1407330	6.44	DELTA4,16-ANDROSTADIEN-3-ONE	91.05
9	32.031	26360634	44.40	10612863	48.55	Phytol	71.05
10	44.017	3841743	6.47	726861	3.33	Lupeol	95.10
		59371137	100.00	21860271	100.00		

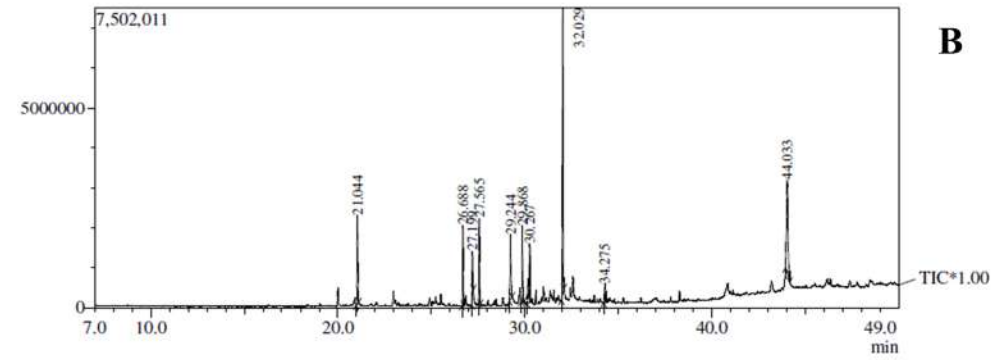

Peak Report TIC

Peak#	R.Time	Area	Area%	Height	Height%	Name	Base m/z
1	21.044	6283383	9.13	2213613	9.87	.DELTA.-TETRADECALACTONE	100.05
2	26.688	4881105	7.09	2000506	8.92	NEOPHYTADIENE	68.05
3	27.199	2617784	3.80	1136651	5.07	Phytol, acetate	82.05
4	27.565	5020879	7.29	2129787	9.49	3,7,11,15-Tetramethyl-2-hexadecen-1-ol	82.05
5	29.244	5405668	7.85	1616570	7.21	HEXADECANOIC ACID	73.00
6	29.868	5135456	7.46	1891443	8.43	ANDROSTA-4,16-DIEN-3-ONE	91.05
7	30.267	6775314	9.84	1472090	6.56	ANDROST-5-EN-7-ONE, 3-(ACETYLOXY)-, (3.BETA.)-	91.05
8	32.029	18865780	27.41	7164584	31.93	Phytol	71.05
9	34.275	1364532	1.98	470258	2.10	(+)-Beyerene	135.15
10	44.033	12489175	18.14	2340726	10.43	Lupeol	95.10
		68839076	100.00	22436228	100.00		

Figure 60. GCMS chromatograms and peak reports of bioactive compounds from the methanolic extracts of the cotyledonary leaves of *R. communis* seedlings on exposure to $CuSO_4$ and KIN. A: 80 µM $CuSO_4$ + KIN; and B: 160 µM $CuSO_4$ + KIN.

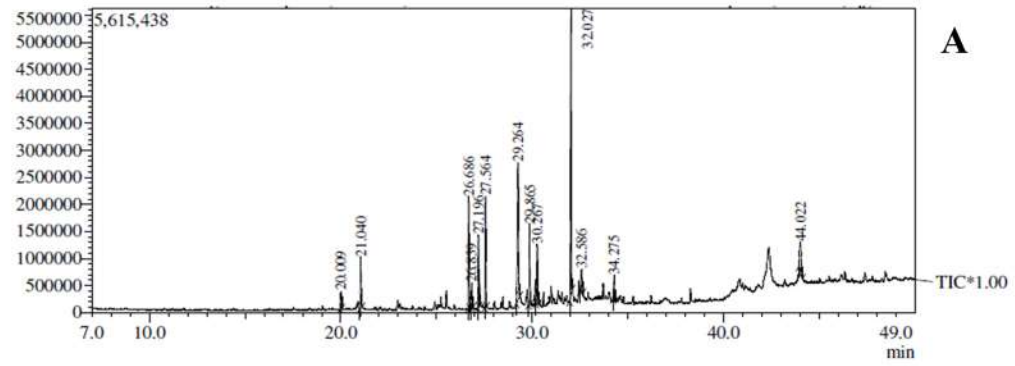

Peak Report TIC

Peak#	R.Time	Area	Area%	Height	Height%	Name	Base m/z
1	20.009	841151	1.54	317012	1.67	1,7-DIOXASPIRO[5.5]UNDEC-2-ENE	98.05
2	21.040	2799800	5.13	943715	4.96	.DELTA.-TETRADECALACTONE	100.05
3	26.686	5047888	9.26	2074418	10.91	NEOPHYTADIENE	68.05
4	26.839	1030500	1.89	454420	2.39	Hexahydrofarnesyl acetone	58.05
5	27.196	3525058	6.46	1326902	6.98	Phytol, acetate	82.05
6	27.564	4995054	9.16	2053248	10.79	3,7,11,15-Tetramethyl-2-hexadecen-1-ol	82.05
7	29.264	9571720	17.55	2534263	13.32	HEXADECANOIC ACID	73.00
8	29.865	3990646	7.32	1486938	7.82	ANDROSTA-4,16-DIEN-3-ONE	91.05
9	30.267	3722861	6.83	1111869	5.85	ANDROST-5-EN-7-ONE, 3-(ACETYLOXY)-, (3.BETA.)-	91.05
10	32.027	13120202	24.06	5302710	27.88	Phytol	71.05
11	32.586	1860630	3.41	420067	2.21	9,12,15-Octadecatrienoic acid, (Z,Z,Z)-	79.05
12	34.275	1181084	2.17	454605	2.39	(+)-Beyerene	135.10
13	44.022	2839762	5.21	540355	2.84	Lupeol	95.10
		54526356	100.00	19020522	100.00		

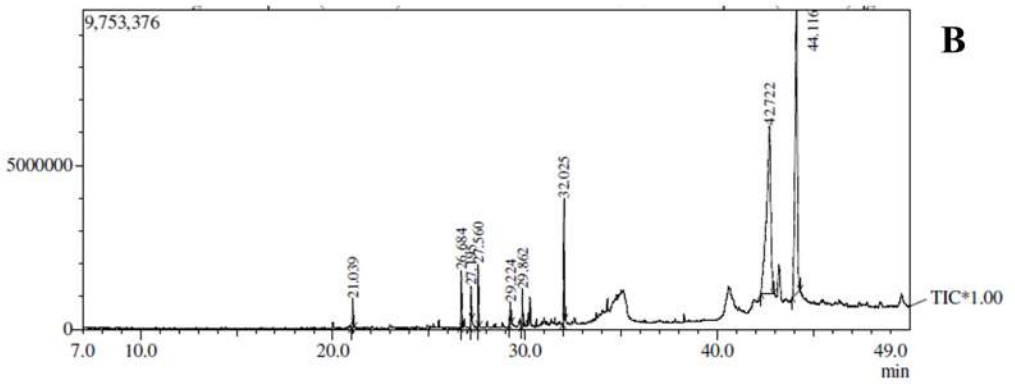

Peak Report TIC

Peak#	R.Time	Area	Area%	Height	Height%	Name	Base m/z
1	21.039	2520073	1.39	870655	3.50	.DELTA.-TETRADECALACTONE	100.05
2	26.684	4247130	2.34	1728302	6.94	NEOPHYTADIENE	68.05
3	27.195	2568562	1.42	1083398	4.35	3,7,11,15-Tetramethyl-2-hexadecen-1-ol	82.05
4	27.560	4727196	2.61	1899053	7.63	Phytol, acetate	82.05
5	29.224	2017626	1.11	679244	2.73	HEXADECANOIC ACID	73.00
6	29.862	3089538	1.70	1122277	4.51	Androsta-4,16-dien-3-one	91.05
7	32.025	9473580	5.22	3732003	14.99	Phytol	71.05
8	42.722	78421857	43.24	5120361	20.57	LUP-20(29)-EN-3-YL ACETATE	95.10
9	44.116	74291115	40.96	8656146	34.78	Lupeol	95.10
		181356677	100.00	24891439	100.00		

Figure 61. GCMS chromatograms and peak reports of bioactive compounds from the methanolic extracts of the cotyledonary leaves of *R. communis* seedlings on exposure to $CuSO_4$ and BAP. A: 80 µM $CuSO_4$ + BAP; and B: 160 µM $CuSO_4$ + BAP.

Table 20. Bioactive compounds detected in the methanolic extracts of cotyledonary leaf, primary leaf and roots of *R. communis* seedlings on 6 d of $CuSO_4$ (control and 200 µM) treatments.

Sl. No.	Name of the compound	Peak area percentage (%)					
		Cotyledonary leaf		Primary leaf		Root	
		Control	200 µM $CuSO_4$	Control	200 µM $CuSO_4$	Control	200 µM $CuSO_4$
1	(22E)-Stigmasta-4,6,22-trien-3-yl acetate	-	-	-	-	6.73	4.23
2	(E)-Phytol	2.98	4.82	-	-	-	1.15
3	1,7-Dioxaspiro[5.5]undec-2-ene	-	1.48	-	-	-	-
4	17-Norkaur-15-ene, 13-methyl-, (8-beta,13-beta)-	-	2.31	-	-	-	-
5	18-Norisopimara-4(19),7,15-triene	-	1.70	-	-	-	-
6	2-Chloroethyl linoleate	-	2.06	-	-	-	-
7	2-Hexadecen-1-ol, 3,7,11,15-tetramethyl-, [R-[R*,R*-(E)]]-	-	6.57	-	-	-	-
8	3-(3-Methyl-5-oxo-4,5-dihydro-1h-pyrazol-4-yl)propanoic acid	-	3.46	-	-	-	-
9	3,7,11,15-Tetramethyl-2-hexadecen-1-ol	2.53	-	-	-	2.67	1.60
10	3-Cyclopentylpropionic acid, 2-isopropoxyphenyl ester	3.01	-	-	-	-	-
11	8-Dodecen-1-ol, acetate, (Z)-	-	-	-	9.78	-	-
12	9,12-Octadecadienoic acid, methyl ester	-	-	-	-	8.07	-
13	9-octadecenoic acid (Z)-, methyl ester	-	-	-	-	18.83	5.68
14	Alpha-linolenic acid	-	-	-	12.16	-	-
15	Alpha-Linolenic acid	-	-	1.55	-	-	-
16	Androst-5-en-7-one, 3-(acetyloxy)-, (3-beta)-	3.56	7.91	-	-	1.56	-
17	Androsta-4,16-dien-3-one	4.10	8.69	-	-	2.24	2.64
18	Beyerene	1.51	-	-	3.07	-	1.40
19	Calendin	-	1.57	-	-	-	-

(*Continued*)

Table 20. (*Continued*)

Sl. No.	Name of the compound	Peak area percentage (%)					
		Cotyledonary leaf		Primary leaf		Root	
		Control	200 µM $CuSO_4$	Control	200 µM $CuSO_4$	Control	200 µM $CuSO_4$
20	Cholestane-3,5-diol, 5-acetate, (3-beta,5-alpha)-	-	-	-	-	5.93	-
21	Cis,cis,cis-7,10,13-Hexadecatrienal	10.18	5.79	-	-	-	-
22	Cis-Vaccenic acid	-	-	-	-	-	12.34
23	Delta-tetradecalactone	2.89	6.45		-	-	-
24	Gamma-tocopherol	-	-	-	1.24	-	-
25	Hexadecanoic acid	31.82	16.11	3.21	29.78	-	45.87
26	Isophytol acetate	19.89	-	-	-	17.01	-
27	Lupeol	5.43	5.47	93.72	25.83	-	4.79
28	Methyl 11,14-eicosadienoate	-	-	-	-	-	2.36
29	Methyl isopimarate	-	-	-	-	2.86	1.63
30	Methyl palmitate	1.20	-	-	-	16.59	8.67
31	Methyl stearate	-	-	-	-	2.71	-
32	Neophytadiene	4.04	6.97	0.35	2.15	6.77	2.85
33	Octadecanoic acid	-	-	-	1.75	-	-
34	Oxacycloheptadec-8-en-2-one	3.34	-	-	-	-	-
35	Palmitoyl chloride	-	-	-	1.70	-	-
36	Phytol	-	-	1.17	8.72	-	-
37	Phytol acetate	-	16.65	-	-	-	4.79
38	Stigmasterol	3.52	-	-	-	-	-
39	Tricyclo[20.8.0.0(7,16)]triaconta-1(22),7(16),9,13,24,28-hexaene	-	1.97	-	-	-	-
40	Vitamin E	-	-	-	3.80	-	-

Table 21. Bioactive compounds detected in the methanolic extracts of cotyledonary leaves of *R. communis* seedlings on 6 d of $CuSO_4$ (80 and 160 µM) and cytokinins (KIN and BAP) treatments.

Sl. No.	Name of the compound	Peak area percentage (%)						
		Control	80 $CuSO_4$	160 $CuSO_4$	80 $CuSO_4$ + KIN	160 $CuSO_4$ + KIN	80 $CuSO_4$ + BAP	160 $CuSO_4$ + BAP
1	1,7-Dioxaspiro[5.5]undec-2-ene	-	-	-	1.70	-	1.54	-
2	3,7,11,15-Tetramethyl-2-hexadecen-1-ol	2.53	5.47	7.37	6.50	7.29	9.16	1.42
3	3-Cyclopentylpropionic acid, 2-isopropoxyphenyl ester	3.01	-	-	-	-	-	-
4	9,12,15-Octadecatrienoic acid, (Z,Z,Z)-	-	-	-	-	-	3.41	-
5	(E)-phytol	2.98	-	4.00	-	-	-	-
6	Androst-5-en-7-one, 3-(acetyloxy)-, (3-beta)-	3.56	7.51	11.01	-	9.84	6.83	-
7	Androsta-4,16-dien-3-one	4.10	9.84	10.88	7.92	7.46	7.32	1.70
8	Beyerene	1.51	-	2.76	-	1.98	2.17	-
9	cis,cis,cis-7,10,13-Hexadecatrienal	10.18	-	-	-	-	-	-
10	Delta-4,16-androstadien-3-one	-	-	-	7.53	-	-	-
11	Delta-tetradecalactone	2.89	9.63	8.43	6.00	9.13	5.13	1.39
12	Hexadecanoic acid	33.02	5.63	9.23	7.42	7.85	17.55	1.11
13	Hexahydrofarnesyl acetone	-	-	1.09	-	-	1.89	-
14	Isophytol, acetate	19.89	41.14	31.83	-	-	-	-
15	Lup-20(29)-en-3-yl acetate	-	-	-	-	-	-	43.24
16	Lupeol	5.43	-	6.07	6.47	18.14	5.21	40.96
17	Neophytadiene	4.04	10.28	7.34	5.99	7.09	9.26	2.34
18	Oxacycloheptadec-8-en-2-one	3.34	-	-	-	-	-	-
19	Phytol	-	-	-	44.40	27.41	24.06	5.22
20	Phytol, acetate	-	10.50	-	6.07	3.80	6.46	2.61
21	Stigmasterol	3.52	-	-	-	-	-	-

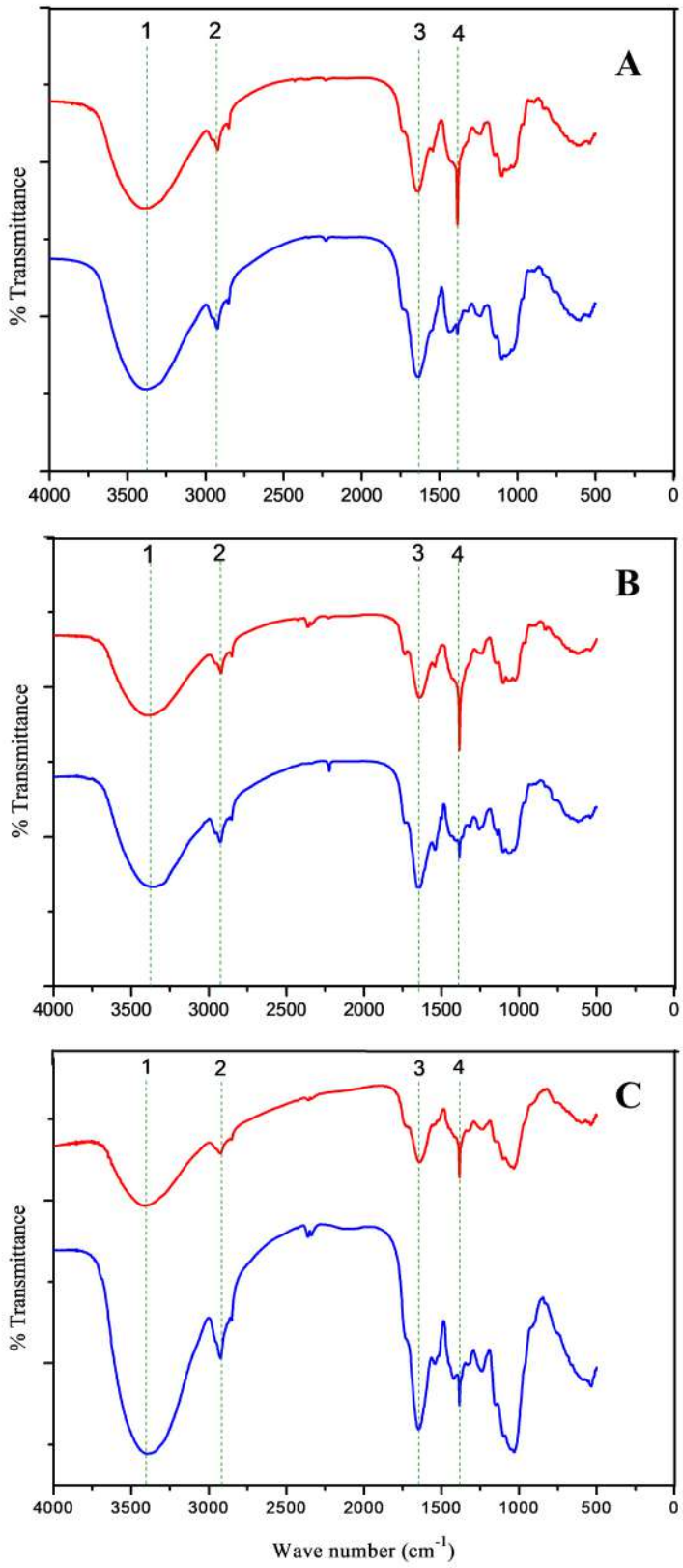

Figure 62. FTIR spectra of the cell wall fractions of cotyledonary leaf (A), primary leaf (B) and roots (C) of *R. communis* seedlings on exposure to $CuSO_4$. Blue and red lines represent control and 200 µM $CuSO_4$ treated seedlings.

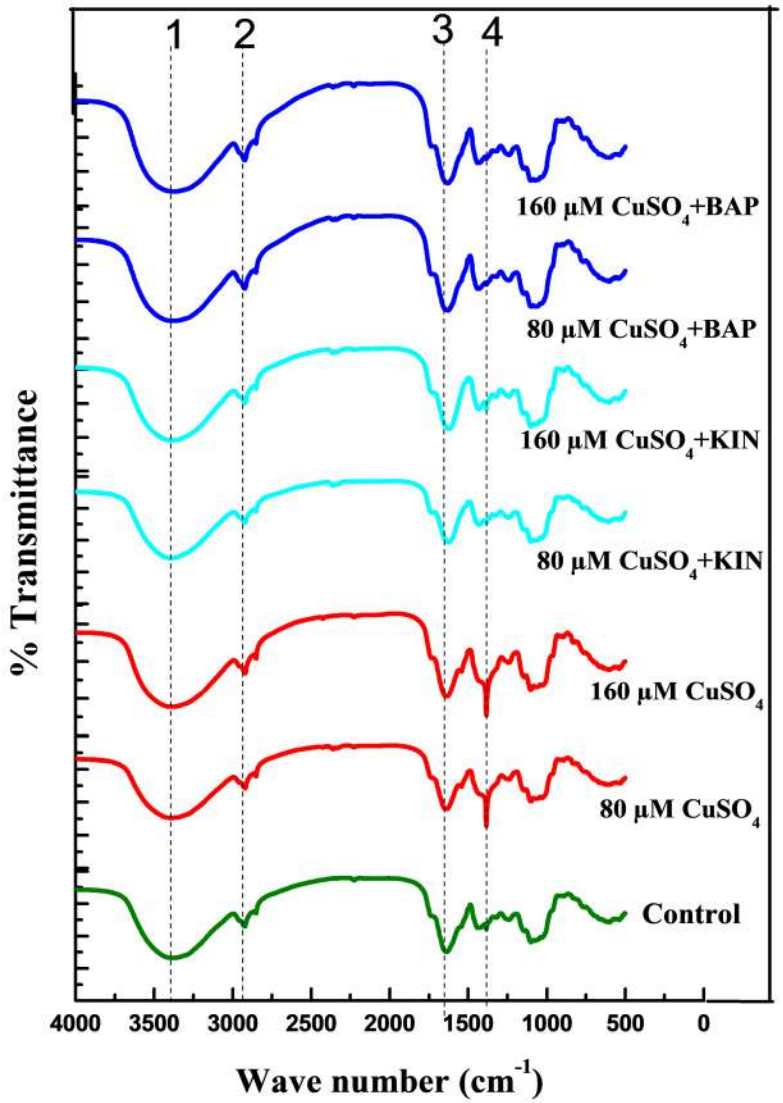

Figure 63. FTIR spectra of the cell wall fractions of cotyledonary leaves of *R. communis* seedlings on 6 d of exposure to $CuSO_4$ (80 and 160 µM) and cytokinins (KIN and BAP).

Table 22. Pearson's correlation coefficients between various parameters related to photosynthesis in the cotyledonary leaves of *R. communis* seedlings exposed to $CuSO_4$.

	RWC	Total Chlorophyll	Carotenoids	PSI activity	PSII activity	Area	Fv/Fm	Vj	PI(abs)	PI(total)	DF(total)	MDA	$\bullet O_2^-$	H_2O_2	CSI
RWC	1														
Total Chlorophyll	.822*	1													
Carotenoids	.974**	.876*	1												
PSI activity	.958**	.673	.914*	1											
PSII activity	.981**	.744	.968**	.974**	1										
Area	.290	.237	.185	.383	.198	1									
Fv/Fm	.830*	.522	.798	.800	.837*	.151	1								
Vj	-.960**	-.673	-.935**	-.989**	-.986**	-.298	-.863*	1							
PI(abs)	.978**	.738	.965**	.978**	.992**	.272	.873*	-.994**	1						
PI(total)	.970**	.721	.954**	.972**	.981**	.300	.898*	-.992**	.997**	1					
DF(total)	.864*	.557	.860*	.856*	.900*	.090	.977**	-.919**	.925**	.940**	1				
MDA	-.954**	-.689	-.939**	-.971**	-.973**	-.314	-.900*	.993**	-.993**	-.998**	-.944**	1			
$\bullet O_2^-$	-.821*	-.538	-.716	-.902*	-.812*	-.552	-.530	.831*	-.799	-.783	-.572	.778	1		
H_2O_2	-.931**	-.666	-.916*	-.987**	-.970**	-.311	-.748	.980**	-.967**	-.955**	-.836*	.956**	.874*	1	
CSI	.942**	.637	.903*	.970**	.955**	.369	.912*	-.987**	.981**	.990**	.940**	-.994**	-.800	-.942**	1

**. Correlation is significant at the 0.01 level (2-tailed).

*. Correlation is significant at the 0.05 level (2-tailed).

Table 23. Pearson's correlation coefficients between various parameters related to photosynthesis in the primary leaves of *R. communis* seedlings exposed to $CuSO_4$.

	RWC	Total Chlorophyll	Carotenoids	PSI activity	PSII activity	Area	Fv/Fm	Vj	PI(abs)	PI(total)	DF(total)	MDA	$\bullet O_2^-$	H_2O_2	CSI
RWC	1														
Total Chlorophyll	.117	1													
Carotenoids	.336	.950**	1												
PSI activity	.480	.750	.889*	1											
PSII activity	.360	.921**	.961**	.926**	1										
Area	.295	.403	.387	.282	.483	1									
Fv/Fm	.341	.306	.293	.435	.531	.731	1								
Vj	-.323	-.439	-.501	-.752	-.711	-.426	-.847*	1							
PI(abs)	.678	.538	.664	.865*	.789	.272	.648	-.842*	1						
PI(total)	.637	.547	.708	.924**	.790	.125	.479	-.786	.969**	1					
DF(total)	.477	.641	.780	.954**	.827*	.032	.352	-.735	.901*	.972**	1				
MDA	-.529	-.819*	-.941**	-.983**	-.961**	-.382	-.447	.696	-.851*	-.888*	-.909*	1			
$\bullet O_2^-$	-.488	-.495	-.645	-.591	-.479	.273	.347	-.028	-.436	-.576	-.643	.619	1		
H_2O_2	-.133	-.768	-.822*	-.921**	-.880*	-.129	-.390	.766	-.753	-.823*	-.912*	.871*	.446	1	
CSI	.788	.535	.711	.887*	.777	.240	.497	-.715	.967**	.971**	.907*	-.887*	-.607	-.705	1

**. Correlation is significant at the 0.01 level (2-tailed).

*. Correlation is significant at the 0.05 level (2-tailed).

Table 24. Pearson's correlation coefficients between various parameters related to photosynthesis in the cotyledonary leaves of *R. communis* seedlings exposed to $CuSO_4$ along with kinetin (KIN).

	RWC	Total Chlorophyll	Carotenoids	PSI activity	PSII activity	Area	Fv/Fm	Vj	PI(abs)	PI(total)	DF(total)	MDA	$\bullet O_2^-$	H_2O_2	CSI
RWC	1														
Total Chlorophyll	.376	1													
Carotenoids	.257	.556	1												
PSI activity	.895**	.398	.453	1											
PSII activity	.651	.227	.768*	.764*	1										
Area	.504	.258	.427	.456	.532	1									
Fv/Fm	.921**	.261	.228	.877**	.625	.256	1								
Vj	-.977**	-.345	-.362	-.943**	-.741*	-.449	-.957**	1							
PI(abs)	.870**	.552	.669*	.906**	.847**	.604	.767*	-.898**	1						
PI(total)	.845**	.581	.646	.868**	.786*	.583	.726*	-.862**	.988**	1					
DF(total)	.950**	.297	.263	.900**	.656	.311	.996**	-.979**	.815**	.779*	1				
MDA	-.556	-.509	-.856**	-.631	-.847**	-.772*	-.390	.592	-.829**	-.787*	-.447	1			
$\bullet O_2^-$	-.118	.229	-.124	-.351	-.244	-.008	-.220	.218	-.265	-.321	-.222	.006	1		
H_2O_2	-.707*	-.495	-.698*	-.718*	-.805**	-.857**	-.528	.710*	-.854**	-.803**	-.580	.956**	-.058	1	
CSI	.901**	.607	.588	.859**	.767*	.692*	.761*	-.886**	.968**	.957**	.808**	-.810**	-.108	-.884**	1

**. Correlation is significant at the 0.01 level (2-tailed).

*. Correlation is significant at the 0.05 level (2-tailed).

Table 25. Pearson's correlation coefficients between various parameters related to photosynthesis in the cotyledonary leaves of *R. communis* seedlings exposed to $CuSO_4$ along with 6-benzylaminopurine (BAP).

	RWC	Total Chlorophyll	Carotenoids	PSI activity	PSII activity	Area	Fv/Fm	Vj	PI(abs)	PI(total)	DF(total)	MDA	$\bullet O_2^-$	H_2O_2	CSI
RWC	1														
Total Chlorophyll	.367	1													
Carotenoids	.732*	.708*	1												
PSI activity	.536	-.130	.449	1											
PSII activity	.480	-.043	.284	.457	1										
Area	.506	-.432	-.071	.252	.339	1									
Fv/Fm	.621	.107	.661	.792*	.644	.065	1								
Vj	-.744*	-.106	-.713*	-.841**	-.591	-.220	-.965**	1							
PI(abs)	.699*	-.031	.600	.845**	.493	.247	.939**	-.974**	1						
PI(total)	.728*	-.022	.568	.812**	.398	.262	.872**	-.933**	.981**	1					
DF(total)	.770*	.096	.694*	.849**	.559	.241	.947**	-.994**	.982**	.961**	1				
MDA	-.284	.409	-.282	-.695*	-.504	-.209	-.734*	.750*	-.773*	-.719*	-.738*	1			
$\bullet O_2^-$	-.373	-.370	-.179	-.017	.244	.028	.145	-.018	-.017	-.183	-.072	-.225	1		
H_2O_2	-.502	.491	-.104	-.499	-.420	-.904**	-.347	.476	-.497	-.461	-.472	.531	-.260	1	
CSI	.604	-.310	.317	.612	.506	.499	.777*	-.790*	.865**	.838**	.794*	-.701*	.192	-.686*	1

**. Correlation is significant at the 0.01 level (2-tailed).

*. Correlation is significant at the 0.05 level (2-tailed).

Table 26. Pearson's correlation coefficients between various parameters related to antioxidation mechanisms in the cotyledonary leaves of *R. communis* seedlings exposed to $CuSO_4$.

	Osmolality	$\bullet O_2^-$	H_2O_2	MSI	EL	GR	MDHAR	DHAR	CAT	POD	APX	SOD	AsA	GSH	Phenolics	Favonoids	Anthocyanins	Cu content
Osmolality	1																	
$\bullet O_2^-$	.971**	1																
H_2O_2	.952**	.905*	1															
MSI	-.978**	-.902*	-.956**	1														
EL	.965**	.963**	.924**	-.914*	1													
GR	.830*	.791	.943**	-.836*	.855*	1												
MDHAR	.980**	.933**	.931**	-.971**	.969**	.844*	1											
DHAR	.971**	.973**	.879*	-.914*	.983**	.760	.967**	1										
CAT	.994**	.970**	.972**	-.971**	.956**	.856*	.959**	.950**	1									
POD	.988**	.964**	.940**	-.958**	.991**	.848*	.991**	.986**	.975**	1								
APX	.964**	.929**	.966**	-.948**	.981**	.924**	.979**	.945**	.961**	.984**	1							
SOD	.997**	.978**	.956**	-.970**	.958**	.831*	.964**	.962**	.998**	.979**	.955**	1						
AsA	.941**	.962**	.800	-.871*	.924**	.634	.916*	.976**	.915*	.937**	.863*	.937**	1					
GSH	.968**	.928**	.995**	-.961**	.957**	.936**	.956**	.917*	.980**	.967**	.986**	.968**	.840*	1				
Phenolics	.951**	.937**	.880*	-.906*	.989**	.799	.974**	.987**	.927**	.985**	.964**	.935**	.934**	.922**	1			
Favonoids	.989**	.958**	.970**	-.975**	.935**	.844*	.947**	.932**	.998**	.961**	.945**	.995**	.902*	.973**	.903*	1		
Anthocyanins	-.961**	-.997**	-.879*	.885*	-.966**	-.771	-.933**	-.980**	-.953**	-.963**	-.923**	-.965**	-.972**	-.910*	-.948**	-.937**	1	
Cu content	.964**	.962**	.976**	-.925**	.971**	.925**	.943**	.934**	.977**	.967**	.979**	.970**	.870*	.987**	.929**	.965**	-.950**	1

**. Correlation is significant at the 0.01 level (2-tailed).

*. Correlation is significant at the 0.05 level (2-tailed).

Table 27. Pearson's correlation coefficients between various parameters related to antioxidation mechanisms in the primary leaves of *R. communis* seedlings exposed to $CuSO_4$.

	Osmolality	$\bullet O_2^-$	H_2O_2	MSI	EL	GR	MDHAR	DHAR	CAT	POD	APX	SOD	AsA	GSH	Phenolics	Favonoids	Anthocyanins	Cu content
Osmolality	1																	
$\bullet O_2^-$	-.471	1																
H_2O_2	.728	-.755	1															
MSI	-.921**	.726	-.910*	1														
EL	.854*	-.737	.955**	-.976**	1													
GR	.666	-.234	.740	-.735	.774	1												
MDHAR	.805	-.684	.945**	-.953**	.954**	.845*	1											
DHAR	.556	-.851*	.868*	-.819*	.888*	.642	.853*	1										
CAT	.849*	-.744	.917**	-.979**	.986**	.785	.965**	.905*	1									
POD	.843*	-.720	.962**	-.940**	.967**	.681	.896*	.799	.914*	1								
APX	.789	-.545	.872*	-.906*	.936**	.931**	.951**	.848*	.953**	.839*	1							
SOD	.719	-.718	.993**	-.906*	.948**	.796	.967**	.868*	.923**	.935**	.902*	1						
AsA	.792	-.685	.991**	-.934**	.966**	.799	.963**	.830*	.931**	.967**	.905*	.991**	1					
GSH	.708	-.738	.985**	-.910*	.954**	.806	.974**	.905*	.941**	.918**	.923**	.995**	.980**	1				
Phenolics	.860*	-.694	.920**	-.971**	.992**	.812*	.951**	.888*	.993**	.932**	.963**	.922**	.939**	.936**	1			
Favonoids	.815*	-.875*	.890*	-.961**	.954**	.594	.900*	.904*	.964**	.907*	.840*	.872*	.880*	.889*	.943**	1		
Anthocyanins	.767	-.794	.927**	-.951**	.949**	.757	.981**	.913*	.975**	.873*	.921**	.942**	.927**	.961**	.947**	.948**	1	
Cu content	.477	-.961**	.776	-.701	.737	.188	.630	.795	.698	.780	.492	.716	.704	.717	.674	.838*	.717	1

**. Correlation is significant at the 0.01 level (2-tailed).

*. Correlation is significant at the 0.05 level (2-tailed).

Table 28. Pearson's correlation coefficients between various parameters related to antioxidation mechanisms in the roots of *R. communis* seedlings exposed to $CuSO_4$.

	Osmolality	$\bullet O_2^-$	H_2O_2	MSI	EL	GR	MDHAR	DHAR	CAT	POD	APX	SOD	AsA	GSH	Phenolics	Favonoids	Anthocyanins	Cu content
Osmolality	1																	
$\bullet O_2^-$	.448	1																
H_2O_2	-.709	-.832*	1															
MSI	.806	.812*	-.847*	1														
EL	-.496	-.966**	.830*	-.760	1													
GR	-.552	-.984**	.873*	-.889*	.927**	1												
MDHAR	-.576	-.972**	.905*	-.896*	.946**	.979**	1											
DHAR	-.642	-.972**	.882*	-.915*	.947**	.988**	.981**	1										
CAT	-.696	-.881*	.772	-.878*	.842*	.923**	.860*	.942**	1									
POD	-.538	-.896*	.675	-.737	.942**	.861*	.852*	.907*	.889*	1								
APX	-.592	-.960**	.844*	-.893*	.895*	.989**	.944**	.981**	.965**	.866*	1							
SOD	-.569	-.953**	.790	-.889*	.883*	.980**	.929**	.973**	.967**	.880*	.994**	1						
AsA	.604	.970**	-.877*	.843*	-.958**	-.974**	-.950**	-.983**	-.947**	-.919**	-.975**	-.959**	1					
GSH	-.778	-.546	.732	-.731	.479	.662	.576	.668	.797	.476	.735	.698	-.697	1				
Phenolics	.537	.983**	-.822*	.887*	-.926**	-.994**	-.969**	-.987**	-.933**	-.891*	-.987**	-.989**	.966**	-.624	1			
Favonoids	.524	.963**	-.759	.795	-.964**	-.944**	-.918**	-.962**	-.934**	-.977**	-.946**	-.952**	.973**	-.568	.960**	1		
Anthocyanins	-.454	-.991**	.858*	-.839*	.946**	.983**	.988**	.966**	.846*	.848*	.947**	.937**	-.946**	.529	-.976**	-.926**	1	
Cu content	-.611	-.978**	.866*	-.896*	.947**	.991**	.973**	.998**	.950**	.913*	.988**	.982**	-.988**	.672	-.991**	-.971**	.967**	1

**. Correlation is significant at the 0.01 level (2-tailed).

*. Correlation is significant at the 0.05 level (2-tailed).

Table 29. Pearson's correlation coefficients between various parameters related to antioxidation mechanisms in the cotyledonary leaves of *R. communis* seedlings exposed to $CuSO_4$ along with kinetin (KIN).

	Osmolality	$\bullet O_2^-$	H_2O_2	MSI	EL	GR	MDHAR	DHAR	CAT	POD	APX	SOD	AsA	GSH	Phenolics	Favonoids	Anthocyanins	Cu content
Osmolality	1																	
$\bullet O_2^-$	.221	1																
H_2O_2	.538	-.058	1															
MSI	-.717*	-.082	-.584	1														
EL	.711*	.260	.783*	-.595	1													
GR	.767*	.250	.787*	-.540	.674*	1												
MDHAR	.523	-.121	.932**	-.621	.766*	.621	1											
DHAR	.697*	.167	.875**	-.724*	.703*	.904**	.794*	1										
CAT	.632	.322	.857**	-.785*	.866**	.717*	.816**	.837**	1									
POD	.648	.128	.887**	-.709*	.768*	.883**	.726*	.899**	.878**	1								
APX	.710*	.094	.854**	-.793*	.810**	.841**	.744*	.888**	.882**	.979**	1							
SOD	.639	.118	.869**	-.742*	.817**	.818**	.742*	.858**	.898**	.985**	.991**	1						
AsA	.720*	.245	.848**	-.632	.916**	.855**	.715*	.819**	.885**	.943**	.943**	.955**	1					
GSH	.803**	.172	.797*	-.824**	.748*	.874**	.657	.891**	.861**	.946**	.946**	.922**	.895**	1				
Phenolics	-.448	.319	-.188	.244	-.246	-.259	-.214	-.063	-.105	-.260	-.328	-.307	-.318	-.245	1			
Favonoids	.582	-.054	.984**	-.668*	.807**	.734*	.957**	.856**	.892**	.857**	.843**	.851**	.828**	.805**	-.197	1		
Anthocyanins	-.759*	-.235	-.435	.596	-.525	-.628	-.394	-.702*	-.503	-.499	-.533	-.451	-.503	-.688*	-.184	-.467	1	
Cu content	.720*	.222	.853**	-.763*	.876**	.814**	.736*	.830**	.941**	.960**	.964**	.974**	.972**	.941**	-.309	.860**	-.502	1

**. Correlation is significant at the 0.01 level (2-tailed).

*. Correlation is significant at the 0.05 level (2-tailed).

Table 30. Pearson's correlation coefficients between various parameters related to antioxidation mechanisms in the cotyledonary leaves of *R. communis* seedlings exposed to $CuSO_4$ along with 6-benzylaminopurine (BAP).

	Osmolality	$\bullet O_2^-$	H_2O_2	MSI	EL	GR	MDHAR	DHAR	CAT	POD	APX	SOD	AsA	GSH	Phenolics	Favonoids	Anthocyanins	Cu content
Osmolality	1																	
$\bullet O_2^-$	-.021	1																
H_2O_2	.587	-.260	1															
MSI	-.145	.404	.120	1														
EL	.771*	.132	.491	-.315	1													
GR	.564	-.335	.862**	.034	.407	1												
MDHAR	.496	-.360	.891**	.055	.326	.961**	1											
DHAR	.528	-.209	.812**	-.005	.387	.924**	.963**	1										
CAT	.824**	-.021	.820**	-.231	.802**	.752*	.721*	.763*	1									
POD	.469	-.433	.760*	-.131	.279	.953**	.899**	.878**	.693*	1								
APX	.616	-.271	.873**	-.143	.503	.947**	.954**	.966**	.867**	.920**	1							
SOD	.549	-.346	.811**	-.102	.377	.970**	.965**	.971**	.765*	.961**	.979**	1						
AsA	.674*	-.189	.887**	-.186	.702*	.894**	.845**	.838**	.937**	.841**	.937**	.873**	1					
GSH	.615	-.446	.673*	-.474	.485	.805**	.749*	.778*	.804**	.897**	.876**	.867**	.845**	1				
Phenolics	-.275	.615	-.472	.273	-.053	-.554	-.608	-.469	-.316	-.540	-.534	-.562	-.438	-.450	1			
Favonoids	.708*	-.589	.578	-.496	.580	.661	.673*	.671*	.677*	.640	.728*	.720*	.675*	.783*	-.593	1		
Anthocyanins	-.284	-.170	-.319	.343	-.503	-.146	-.225	-.391	-.564	-.174	-.401	-.280	-.416	-.436	-.305	-.312	1	
Cu content	.643	-.490	.554	-.648	.663	.609	.502	.476	.750*	.673*	.664	.615	.778*	.870**	-.457	.770*	-.308	1

**. Correlation is significant at the 0.01 level (2-tailed).

*. Correlation is significant at the 0.05 level (2-tailed).

DISCUSSION

For the past few years, anthropogenic activities have resulted in environmental pollution with heavy metals. Along with industrial effluents, injudicious agricultural activities, including the long-term use of excessive chemical fertilizers, fungicides and pesticides, have led to the dramatic accumulation of toxic metal ions in the soil, water and air. Soil pollution with heavy metals produces many environmental concerns and imparts damaging impact on plants as well as animals. In response to these harsh environmental conditions, plants develop intricate physiological and molecular processes for improved tolerance, adaptation and survival. Hence this situation warrants the need to study the physiochemical responses of *R. communis* upon exposure to copper (Cu) stress, as this plant can grow luxuriantly with high tolerance under harsh environmental conditions, including heavy metal toxicity. Understanding the basic mechanisms involved in the removal of contaminants can lead us to design strategies to achieve a more efficient removal of environmental pollutants.

Heavy metals are a key abiotic stress factor that can interact with nutrient elements and thereby negatively affect nutrient absorption by the plants. Heavy metals cause damage to the plants by interfering with important physiological and metabolic processes, resulting in growth retardation. Heavy metal poisoning in plants is usually associated with leaf chlorosis, necrosis, turgor loss, hampered photosynthetic system and progressively senescence and death. Copper is an essential redox-active transition metal with significant roles in plant growth and developmental processes, but it becomes a potential stress factor at concentrations above the threshold level.

Since plants are immobile, the only way to avoid the toxicity exerted by the hazardous metals is to adjust their physiological systems to adapt to the environment in which they thrive. Copper phytotoxicity can negatively affect

seed germination, growth and development in plants (Rehman *et al.*, 2019). Many of the plant species have been successfully absorbed and accumulated the toxic ions, including essential and non-essential elements, to the above-ground tissues without showing any toxicity symptoms. There are several investigations already done on heavy metal hyperaccumulators and the tolerance mechanisms operational in these plants.

According to the observations of Trigueros and Rossini-Oliva (2021), *Erica australis* can withstand up to 200 μM $CuSO_4$ in the nutrient medium, but the leaves lost the turgor due to the reduced water uptake at this concentration of $CuSO_4$. The authors also observed that at concentrations above 200 μM $CuSO_4$, death of the plant was noticed within 20 days of treatment. Similar results were observed in the present research also, in which concentrations above 200 μM $CuSO_4$ led to symptoms of plant death. Therefore, the concentrations of $CuSO_4$ from 0 to 200 μM (0, 40, 80, 120, 160 and 200 μM $CuSO_4$) were selected to analyze the Cu stress effects and tolerance mechanisms operational in *R. communis* seedlings when exposed to increasing concentrations of $CuSO_4$.

Plant growth and development have been observed to be improved by priming the seeds or seedlings with phytohormones under adverse environmental conditions, including heavy metal stress (Mir *et al.*, 2018; Bali *et al.*, 2018; Alam *et al.*, 2019; Kaya *et al.*, 2019; Sytar *et al.*, 2019). The plant growth regulators modulate the principal metabolic processes in plants under stress by interacting with the other biomolecules to develop defence strategies (Ahmad *et al.*, 2016a, b).Cytokinins are an essential group of phytohormones that promote cell division and differentiation. There is additional evidence that cytokinins play an important function in the stress response of plants (Werner *et al.*, 2001; Jiang *et al.*, 2019a). Exogenous application of growth hormone has recently been investigated as a potential strategy for alleviating and establishing tolerance in plants under abiotic stress conditions (Wang and Zhang, 2017; Acidri *et al.*, 2020). It was reported that

heavy metal stress resulted in the N- and O-glycosylation mediated deactivation of cytokinins and thereby reduced the pool size of active cytokinins (Piotrowska-Niczyporuk *et al.*, 2020). However, exogenous cytokinins can restore the endogenous cytokinin homeostasis by the synergistic action of auxins which will reduce the metal toxicity (Saini *et al.*, 2021). Despite the fact thatearlier research has revealed endogenous cytokinin-mediated stress tolerance pathways, a thorough understanding of the exogenous cytokinin mediated plant tolerance to metal stress is unclear.

The cytokinin mediated Cu stress alleviation in the cotyledonary leaves of *R. communis* seedlings was evaluated by the exogenous application of cytokinins to the Cu stressed seedlings. From the different concentrations of $CuSO_4$, 80 and 160 μM were selected to analyze the stress alleviating effects of two cytokinins, kinetin (KIN) and 6-benzylaminopurine (BAP). When comparing the effects of various concentrations of KIN and BAP on photosynthetic pigment composition and extent of membrane lipid peroxidation, 15 μM was taken as an effective concentration for further analysis. Therefore, a comparative analysis of the effects of exogenous application of KIN and BAP on the metal bioaccumulation and tolerance mechanisms in the cotyledonary leaves of *R.communis* seedlings subjected to Cu stress on 6 d was performed.

5.1. Analysis of soil and plant samples for trace and heavy metal concentrations collected from the polluted lands with luxuriant growth of *R. communis*

Roadsides are surrounded by intense vehicular traffics, and therefore they are the highest source of various heavy metals, which negatively affect the growth and development of roadside plants. The impact of vehicular pollution on roadside plants due to the elevated heavy metal concentrations were reviewed in detail by Muthu *et al.* (2021), and the authors revealed that vehicular emissions of heavy metals and other pollutants resulted in the foliar injury and necrosis, clogging of stomata, chlorosis and reduced photosynthesis, decreased species diversity, carbon

nanotoxicity, alterations in the leaf anatomy, reduced flowering and seed development and biochemical aberrations in these plants. Due to the sensitive nature of majority of the plants towards these traffic emissions, highly tolerant hyperaccumulator plants could be the dominant species in these areas, which will lead to reduced species diversity. The capability of *R. communis* to become the dominant species along the roadsides is an indication of the potential of this plant towards harsh environmental conditions and heavy metal tolerance (Altaf *et al*., 2021).

The bioaccumulation studies of heavy metals such as As, Cd, Co, Cr, Cu, Ni, Pb and Zn in the soil and plant samples collected from the polluted roadside soils with luxuriant growth of *R. communis* revealed that, these experimental sites were heavily polluted with various heavy metals, and *R. communis* plants showed exceptionally higher accumulation and tolerance potential towards these heavy metals. The highly significant enhanced accumulation of the analyzed heavy metals in the root and leaves is a clear indication of the phytoextraction potential of *R. communis*. Of the various heavy metals analyzed, As, Cd and Cu content in the leaves were higher than that present in the soil and roots, indicating the hyperaccumulation potential of this plant. Furthermore, Cu was found in relatively higher concentrations in all the study locations. Therefore, in order to analyze the heavy metal toxicity and tolerance mechanisms adopted by *R. communis*, the heavy metal Cu was selected for further studies, and the Cu-induced functional and structural modulations in *R. communis* were investigated in detail.

5.2. Analysis of tissue water status

5.2.1. Cu induced reduction in tissue water status

Abiotic stresses, including the toxicity of metals, restrict the growth and development of plants (Giannakoula *et al.*, 2021). Copper stress resulted in the reduction in the tissue RWC and MC% but enhanced DW% in the root, cotyledonary and primary leaves of *R. communis* seedlings, and the variations were severe in the cotyledonary leaves. This reduction of tissue water status

was associated with reduced water use efficiency and photosynthesis under abiotic stress conditions, including heavy metal stress (Sharma *et al.*, 2020a). These results are in agreement with the significant positive correlation observed in RWC with PSI ($r = 0.958$, $p \leq 0.01$) and PSII ($r = 0.981$, $p \leq 0.01$) activities, Fv/Fm ($r = 0.830$, $p \leq 0.05$), PI(abs) ($r = 0.978$, $p \leq 0.01$), and CSI ($r = 0.942$, $p \leq 0.01$) in the cotyledonary leaves upon exposure to Cu stress. Due to the stress shielding effect of cotyledonary leaves towards the primary leaves, the RWC and photosynthetic machinery are least affected in the primary leaves (Table 18 and 19).

The RWC provides an estimate of the mass of water in the tissues in relation to their maximum water holding capacity and highlights the abilities of plants to retain water under stress conditions (Chaparzadeh etal., 2003). The significant reduction in RWC and MC% in the cotyledonary leaves of *R. communis* seedlings exposed to increasing levels of Cu stress is an indication of the negative effects of absorbed metal on the water intake processes and thereby reduced tissue water status (Kaya *et al.*, 2007). It has been reported that a higher concentration of trace metals resulted in plant growth inhibition due to water deficiency, nutrient imbalances and thereby photosynthesis (Bankaji *et al.*, 2014). The reason for the reduced entry of water to the plant system and the method adopted by the plant to reduce the transpirational loss of water is detailed in later sections (5.9.1. and 5.10.1).

5.2.2. Effect of cytokinins on maintaining tissue water status

Upon application of cytokinins, the tissue water status was regained to normal conditions in the cotyledonary leaves of *R. communis* seedlings under Cu stress. Joshi *et al.* (2018) studied cytokinin oxidase (*OsCKX2*) mutant rice plants under stress, and they revealed that endogenous cytokinins are directly involved in maintaining the tissue water status during abiotic stress. According to Wu *et al.* (2012), exogenous cytokinins can enhance water use

efficiency under stress situations, and thereby effectively alleviate the photosynthetic damages in the plants caused due to various abiotic stresses. Likewise, cytokinins prevent the chloroplast disassembly and degradation of pigments, proteins, and nucleic acids during senescence, resulting in delayed senescence and prolonged photosynthesis in leaves (Wu *et al.*, 2021). The phenotype of *R. communis* especially that of the cotyledonary leaves, indicated that the application of cytokinins effectively alleviated Cu-induced alterations in the tissue water status and enhanced the tolerance potential, and this would ensure prolonged photosynthetic functions in cotyledonary leaves even under Cu stress and would immensely help in the seedling establishment. The enhanced root water uptake during cytokinin application was mediated by the transpirational pull and is detailed in section 5.9.2. The significant positive correlation recorded in RWC with the photosynthetic performance index PI(abs) in KIN ($r = 0.870$, $p \leq 0.01$) and BAP ($r = 0.699$, $p \leq 0.05$) treated cotyledonary leaves substantiate cytokinin mediated maintenance of tissue water status and photosynthetic performance under Cu stress (Table 20 and 21).

5.3. Photosynthesis and JIP parameters

5.3.1. Effects of Cu on photosynthesis and JIP parameters

Copper stress induces various toxicity symptoms in the metabolism of plants, of which photosynthesis is the most sensitive process (Giannakoula *et al.*, 2021). Photosynthesis is an inevitable process in plants, through which the light energy absorbed by the leaf is converted to high energy molecules, and the trapping of the sunlight is carried out by the photosynthetic pigments chlorophylls and carotenoids. Exposure to Cu stress reduced photosynthetic pigment composition and photosynthetic efficiency in both the cotyledonary and primary leaves of *R. communis* plants.According to Vijayarengan and Jose (2014), toxic levels of Cu substitute for Mg in the chlorophyll and also

induce deficiencies in iron and magnesium ions in the plant, leading to the inhibition of protochlorophyllide and phytoene synthesis, which are the intermediary products of chlorophyll and carotenoid biosynthesis respectively, and thereby causing reduction in the chlorophylls and carotenoid levels. Binding of Cu to the -SH group of ALA (aminolevulinic acid) dehydratase (converts aminolevulinic acid to porphobilinogen) and protochlorophyllide reductase (participates in the porphyrin and chlorophyll metabolism) also destroys the structure and function of chloroplast (Myśliwa-Kurdziel *et al.*, 2004).

Dall'Osto *et al.* (2012) reported that carotenoids protect the chlorophylls from peroxidation, so that elevated levels of chlorophyll destruction was observed due to reduction in carotenoids during Cu stress, which is in accordance with the significant positive correlation recorded between total chlorophyll and carotenoids contents ($r = 0.876$, $p \leq 0.05$ and $r = 0.950$, $p \leq 0.01$ in cotyledonary and primary leaves respectively) in the present study (Table 18 and 19).

Besides photoprotection, carotenoids especially xanthophylls have roles in LHC assembly and PSI core translation and stability (Dall'Osto *et al.*, 2013). Xue *et al.* (2013) noticed that the prime reason for leaf chlorosis during metal stress is the destruction of pigments in the older leaves and inhibition of its biosynthesis in younger leaves. In *R. communis*, the reduction in the photosynthetic pigments of the cotyledonary leaves is higher, and that of primary leaves was comparatively less on 6 d of Cu exposure, indicating that cotyledonary leaves receive the initial brunt of Cu stress and the impact of which was higher as compared to primary leaves. Therefore, the primary leaves of *R. communis* showed better photosynthetic performance in the seedling stage when exposed to Cu stress.

Photosynthesis is a key phenomenon that contributes significantly to plant growth and development (Kalaji *et al.*, 2017). Heavy metal stress resulted in the degradation of the thylakoid membrane protein complex, which resulted in the blockage of electron transfer and thereby diminished the photosystem activities (Wang *et al.*, 2014; Shackira and Puthur, 2019). Photosystem activities (PSI and PSII) were extremely sensitive to heavy metal stress and were significantly reduced in the cotyledonary leaves under Cu stress. During environmental stresses, PSI and PSII activities maintain ATP/NADPH levels *via* cyclic and non-cyclic electron transport; however, they were inactivated during extreme stress situations (Huan *et al.*, 2014). Therefore, in the present study, due to extreme stress effects in the cotyledonary leaves, both PSI and II activities were drastically reduced even at low concentrations of $CuSO_4$. At the same time, the reductions in photosystem activities were least in primary leaves upon exposure to low concentrations of $CuSO_4$ during the initial days. However, due to the highly sensitive nature of photosystems to heavy metals, drastic reductions were observed in the primary leaves during later stages of the stress exposure.

Chlorophyll *a* fluorescence kinetics can provide details regarding the structure and function of the photosynthetic apparatus, especially that of PSII under different environmental stresses (Stirbet and Govindjee, 2011). Copper-induced chlorophyll degradation and reduced photosystem (PS) II efficiency in the cotyledonary leaves of *R. communis* were already reported in our previous studies (Sameena and Puthur, 2021a,c). During Cu stress, Fo was increased and Fm was reduced significantly, resulting in the flattening of the OJIP transient curve in the cotyledonary leaves of *R. communis* seedlings. The increase in Fo and decrease in Fm during Cu toxicity indicates the lowering of energy trapping by PSII reaction centers, resulting from the physical dissociation of PSII core LHC (Ouzounidou *et al.*, 2003). Similar to

this result, Janeeshma *et al.* (2021a) observed Cd induced reduction in Fm and associated flattening of the OJIP transient curve in maize seedlings.

The area above the chlorophyll fluorescence curve between Fo and Fm, which is proportional to the pool size of the electron acceptor Q_A on the reducing side of PSII (Strasser *et al.*, 2004), was decreased in both types of leaves as a result of $CuSO_4$ treatment. The noticeable reduction in the area with the increasing metal stress in the cotyledonary leaves is a clear indication of reduced pool size of oxidized Q_A and blockage of electron transfer from RC to the quinone pool (Mathur *et al.*, 2016).

A highly significant reduction in Fv/Fo in cotyledonary leaves of Cu-treated plants corresponds to the destabilization of photosynthetic apparatus and water-splitting complex on the donor side of PSII.The Fv/Fm ratio represents the capturing and conversion efficiency of primary light energy and is used to assess the quantum yield of primary photochemistry of PSII (Strasser *et al.*, 2004). A significant reduction in Fm and Fv/Fm was observed in the cotyledonary leaves of seedlings treated with $CuSO_4$. These reductions indicate the inactivation of PSII reaction centers because of the oxidation or degradation of the D1 proteins (Marwood *et al.*, 2001). The decline in the Fv/Fm ratio in the cotyledonary leaves of *R. communis* seedlings suggests that Cu inhibited the quantum efficiency of PSII photochemistry by reducing the rate of primary charge separation and also by the release of some minor antenna complex from PSII (Mathur *et al.*, 2016). In the cotyledonary leaves of *R. communis* seedlings subjected to increasing concentrations of $CuSO_4$, Tf(max) was drastically enhanced. According to Kalaji *et al.* (2017), the physiological characterization of Tf(max) is missing, but still, it has a strong sensitivity to the size of the PSI acceptor side as well as the PSII/PSI ratio. The enhancement in the Tf(max) was associated with the cumulative effects

of D1 protein degradation, enhanced number of inactive reaction centers and reduced Fm values during Cu stress (Sruthi and Puthur, 2020).

The turnover number of Q_A (N) indicates the number of times Q_A reduced from 0 to Tf(max), and a higher turnover number enhances the efficiency of the acceptor side of PSII (Sayyad-Amin *et al.*, 2014). During Cu stress, N was significantly reduced in the cotyledonary leaves of *R. communis* seedlings, and this reduction in N indicates the lesser number of excited electrons, leading to the lowering of the PSII efficiency in cotyledonary leaves of plants subjected to Cu stress. At the same time, the reduction in N was least in the primary leaves on 4 d of Cu exposure, which was enhanced after the early abscission of cotyledonary leaves due to Cu stress. The results indicated that primary leaves keep up the efficiency of electron migration as indicated from the value of N, similar to that of control on 4 d of Cu stress, but the inefficiency in maintaining the N value with an increase in period of treatment (10 d) indicates that it is more sensitive to Cu at later stages of Cu stress.

The performance index, an indicator of plant vitality [PI(total), PI(abs) and SFI(abs)] was decreased drastically in cotyledonary leaves but was less affected in primary leaves of *R. communis* on 4 d of Cu exposure, and gradually reduced in primary leaves on 10 d of Cu exposure. Performance indices give an outline on the functioning of RC, the proportion of energy flux reaching to the RC and its utilization for electron transport (Mehta *et al.*, 2010). The drastic reduction in performance indices in the cotyledonary leaves during Cu stress indicates the negative effect of metal ions on the efficiency and charge separation capability of PSII in these leaves.The results are in agreement with the observations of Tomar *et al.* (2015), in which they found that the performance of PSII was negatively affected by an organic

pollutant in soybean with increasing concentration of the pollutant and the time of exposure.

Variable fluorescence (Vj) gives information regarding the photosynthetic electron transport beyond Q_A, and the physiological characterization of Vj reveals that it depends on the redox state of the PQ pool in darkness (Tóth *et al.*, 2007). The increased value of Vj correlates with the negative effect of the electron transport at the acceptor side of PSII and disruption of the electron transport from RCs to the plastoquinone pool (Sruthi and Puthur, 2018). These are in accordance with the significant negative correlation observed in Vj with PSI ($r = -0.989$, $p \leq 0.01$) and PSII ($r = -0.986$, $p \leq 0.01$) activities, PI(abs) ($r = -0.994$, $p \leq 0.01$) and PI(total) ($r = -0.992$, $p \leq 0.01$) in the cotyledonary leaves exposed to Cu stress (Table 18). The significant increase in the value of Vj in cotyledonary leaves of *R. communis* seedlings when subjected to higher concentrations of $CuSO_4$ and the maintenance of the same without a minor increase in the primary leaves as compared to that control on 4 d of Cu stress points out that an early breakdown of photosynthetic machinery occurs in the cotyledonary leaves. This strategy could shield the immature/younger plant parts (developing primary leaves) with lesser impacts of Cu stress on the normal growth and development. However, the increase of Vj was observed in the primary leaves on 10 d of Cu exposure, *i.e.*, after the Cu-induced abscission of cotyledonary leaves.

The driving force of photosynthesis calculated on cross-section basis, as represented by DF(total), indicates the importance of individual components in driving the processes in PSII. The significant reduction in DF(total) of cotyledonary leaves of *R. communis* seedlings subjected to Cu stress was mainly due to the reduction in the partial driving force for the conversion of excitation energy required for the electron transport beyond Q_A

(Krüger *et al.*, 2014). The photosynthetic yield parameters such as PHI(Po), PHI(Eo), and PSIo, denoting the proportion of energy absorbed by chlorophyll molecules associated with PSII, were susceptible to Cu stress, as evidenced by the decrease in the values of PHI(Po), PHI(Eo) and PSIo in the cotyledonary leaves of *R. communis* seedlings as compared to that of control. The reduction in these parameters indicates the Cu induced impairment of the electron transfer from Q_A to plastoquinone most significantly in the cotyledonary leaves of *R. communis* seedlings as compared to the least reduction of these parameters in the primary leaves.

The diminished photochemical activities in the cotyledonary leaves cannot be solely attributed to the reduced activities of the photosystems, but partly also due to the decreased photosynthetic pigment composition. The metal which gets accumulated in cotyledonary leaves would be hindering the photosynthesis function, and at the same time, the primary leaves were less affected. But on Cu induced abscission of cotyledonary leaves, the sink for metal accumulation turns out to be the primary leaves and hence the reduction of photosynthesis was noted in these leaves.

The visualization of the energy pipeline leaf model represent the various activities of photosynthetic apparatus such as absorption, maximum trapping flux beyond Q_A, electron transport and dissipation of absorbed energy, expressed per excited cross-section (ABS/CSm, TRo/CSm, ETo/CSm and DIo/CSm) and the membrane model represents the specific activity in a single reaction center of PSII (ABS/RC, TRo/RC, ETo/RC and DIo/RC). In these dynamic models, the width of each arrow represents the energy fluxes of the corresponding energy parameter. It was very clear in the model that ABS/CSm, TRo/CSm and ETo/CSm were declining with increase in $CuSO_4$ concentrations, and the decrease was very sharp in the cotyledonary leaves but not significant in the primary leaves on 4 d. However, the reductions in

these parameters were significant in primary leaves on 10 d, i.e., after Cu-induced abscission of cotyledonary leaves.The reduction in the number of active RCs in plants subjected to metal toxicity leads to the transformation of electron excitation energy to heat energy, ultimately culminating in photo-inhibition (Paunov *et al.*, 2018). Therefore, it could be deduced that Cu stress results in the inactivation of the donor side of PSII due to the disorganization of the antenna molecules and reaction centers, attributed to the increased Cu stress effects in the cotyledonary leaves.

ABS/CSm indicates the absorption of photon flux by antenna chlorophyll molecules of active and inactive reaction centers of PSII per excited active cross-section of leaf area. The decrease in ABS/CSm highlights the decrease in energy absorptive potential of the reaction center in response to higher $CuSO_4$ concentrations, and it may be either due to the reduction in the antenna size of PSII or due to the structural alteration in minor antenna LHC components of PSII, leading to the decline in energy absorption by chlorophyll molecules (Tongra *et al.*, 2011). The reduction in TRo/CSm could be related to the decreased density of the active reaction centers, suggesting that the down regulation of PSII was possible through the inactivation of the reaction centers that eventually reduce the efficiency of trapping (Tomar *et al*., 2015). The pronounced reduction in ETo/CSm in cotyledonary leaves subjected to higher concentrations of $CuSO_4$ could be due to the additive effects of lower energy absorption by antenna molecules (ABS/CSm) and lower energy trapping by the reaction centers (TRo/CSm).

ABS/RC, indicating the absorption per active reaction center, was increased with increase in $CuSO_4$ concentrations in both cotyledonary and primary leaves due to the reduction in the number of active reaction centers. Although ABS/RC was increased on exposure to Cu stress, the same was not reflected in ABS/CSm as the distribution frequency of active reaction centers

in a cross-sectional area was less. The fewer RC in a unit area would have forced the existing RC to harvest the light energy to the maximum capacity.Interestingly, it was noticed that TRo/RC was decreased in the cotyledonary leaves with respect to the control when the stress condition was prolonged.In the case of ETo/RC (maximum electron transport flux per reaction center), mild increase in primary leaves and severe decrease in cotyledonary leaves were observed upon exposure to Cu stress.Habibi and Vaziri (2017) also observed such similar results of TRo/RC and ETo/RC in maize seedlings exposed to low and high concentrations of salicylic acid (SA), in which the author observed that low concentration of SA caused mild increases and high doses caused significant reduction of both TRo/RC and ETo/RC.Even though ABS/RC was higher in stressed leaves, the absorbed light energy was found to be dissipated without being utilized for photochemistry, as represented by higher values of DIo/RC in the cotyledonary leaves.These results are in agreement with the observations of Faseela (2018), in which the author analyzed two rice cultivars subjected to high light and UV-B stresses; and found that DIo/RC was significantly increased in stress-sensitive cultivar whereas least increase was observed in the stress-tolerant cultivar. These results indicate that higher levels of $CuSO_4$ cause inactivation of the donor side of PSII due to the disorganization of the antenna molecules and reaction centers in the cotyledonary leaves, which was attributed to the increased stress effects on the cotyledonary leaves as compared to the primary leaves.

Surprisingly, it was noticed that in the cotyledonary leaves at higher $CuSO_4$ concentrations, the data for the energy pipeline leaf model per cross-section and specific membrane model per reaction center were too small for calculation on 6 d, which is an indication of complete damage of the PSII at higher concentrations on 6 d; at the same time, the same concentrations of $CuSO_4$was posing least damage to the primary leaves. Therefore, for better

comparison, the fluorescence analysis was carried out in both the cotyledonary and primary leaves on 4 d of Cu treatment.

Chlorophyll stability index (CSI) is an indicator of the stress tolerance potential of the plants. Exposure of *R. communis* seedlings to Cu stress resulted in the reduction of chlorophyll stability compared to the control most significantly in the cotyledonary leaves, probably due to the enhanced chlorophyll degradation in these leaves. Similar to these results, several authors observed decreased CSI in plants exposed to heavy metal stress. According to Siddhu *et al.* (2008), the destruction of chlorophyll stability was observed in *Solanum melongena* subjected to Cd stress. In the present study, the chlorophyll stability was least affected in primary leaves, which helps the plant to withstand the metal stress and ensure higher productivity.

5.3.2. Modulation of photosynthesis by application of cytokinins

The results indicated that exogenous application of cytokinins ameliorated the negative effect of Cu on the photosynthetic pigment composition, which was evidenced by the increased level of chlorophyll and carotenoid contents in the cotyledonary leaves subjected to Cu stress along with cytokinins as compared to those subjected to Cu stress alone. Talla *et al.* (2016) observed the cytokinin-induced up-regulation of genes involved in the chlorophyll cycle and enhanced accumulation of the chlorophyll cycle intermediate, 7-hydroxymethyl chlorophyll, in rice seedlings. Therefore, it can be stated that exogenous cytokinins play significant roles in maintaining the photosynthetic pigments in plants subjected to diverse stress situations *via* the up-regulation of genes involved in the synthesis of various intermediates coming up in the chlorophyll cycle. Similarly, Gangwar *et al.* (2014) observed cytokinin mediated enhancement in the expression of genes that encoded the proteins involved in the biosynthesis of photosynthetic pigments and resulted

in the enhancement in the biosynthesis of pigments, thereby efficiently modulated photosynthetic processes.

The significant reduction in the PSI and PSII activities in the cotyledonary leaves of *R. communis* plants subjected to Cu stress was significantly nullified by the exogenous application of cytokinins, as evidenced by the enhancement in the photosystem activities in cytokinin treated plants along with $CuSO_4$. This enhancement in photosystem activities during cytokinin application was due to the enhanced expression of the genes encoding the chlorophyll binding proteins *Lhcb4* and *Lhcb6* in light-harvesting complex (LHC) (Talla *et al.*, 2016). This integrated networking of LHC genes resulted in the maintenance of the antenna size of PSII, underlining the efficient role of cytokinin in maintaining the photosynthetic functions even under severe stress conditions. According to the observations of Gujjar *et al.* (2020), exogenous application of a synthetic cytokinin, N-2-(chloro-4-pyridyl)-N-phenyl urea), improved the chlorophyll contents and photosynthesis in rice plants under drought stress.

In order to elucidate the enhanced tolerance of PSII towards Cu stress in the cotyledonary leaves of *R. communis* upon exposure to cytokinins, the primary photochemistry of cotyledonary leaves was explored *via* chlorophyll *a* fluorescence. The application of BAP efficiently modulated the changes in the OJIP transient curve and other fluorescence parameters caused by Cu stress. In contrast, KIN application along with $CuSO_4$ did not impart any significant variations in PSII photochemistry as evidenced by the variations in the OJIP kinetics and energy pipeline models as compared to those exposed to Cu stress alone.

A significant restoration of Fo and Fm observed in the cotyledonary leaves of *R. communis* subjected to Cu toxicity along with BAP reflects the stress ameliorative function of BAP, and it was much better than that

observed with KIN. The restoration of flattened OJIP curve due to Cu stress by the application of BAP is yet another proof for the stress-relieving function of BAP, and again this feature was also much better than KIN. According to Gururani *et al.* (2015), the increase in Fo due to heat stress can be mitigated by the exogenous application of ABA, indicating the capability of this phytohormone in regulating the stability of the PSII complex.

Highly significant restoration of reduced Fv/Fo in cotyledonary leaves of Cu-treated plants on application of cytokinins, especially with BAP, corresponds to the BAP mediated stabilization of photosynthetic apparatus and water-splitting complex on the donor side of PSII. Similarly, the enhanced turnover number (N) during cytokinin application corresponds to the enhanced number of excited electrons, leading to the improved PSII efficiency in cotyledonary leaves of plants subjected to Cu stress.There was an enhancement in Area on BAP application, denoting the enhanced pool size of oxidized Q_A and thereby activation of electron transport from RC to quinone pool. Likewise, all the fluorescence parameters were restored similar to that of control in the cotyledonary leaves of *R. communis* seedlings on exogenous application of cytokinins, most significantly during BAP application. Cytokinin-induced improvements in these fluorescence parameters could be correlated with the enhanced number of active reaction centers and restoration of the degraded D1 protein due to the effective antioxidation mechanisms, supported by the antisenescing function of cytokinins (Bashri *et al.*, 2021). Moreover, BAP application along with $CuSO_4$ enhanced the photosynthetic yield parameters (PHI(Po), PHI(Eo), and PSIo), indicating the enhanced photosynthetic functions in the cotyledonary leaves of *R. communis* under Cu toxicity.

Exogenous application of BAP along with $CuSO_4$ efficiently modulated the variations in photosynthetic functions and energy fluxes as

evidenced by the variations in the energy pipeline and membrane models as compared to those exposed to Cu stress alone. In contrast, KIN application failed to impart significant variations in energy flux parameters caused by Cu stress. Similarly, on exposure to BAP, the number of active RCs was increased, contributing to the enhanced photosynthetic efficiency in the cotyledonary leaves exposed to Cu stress. Similar to our results, cytokinin-mediated enhancement in energy flux parameters in *Trigonella* seedlings subjected to Cd stress was observed by Bashri and co-workers (Bashri *et al.*, 2021). This mitigation of photosystem damages in the cotyledonary leaves of *R. communis* during Cu stress was due to the efficient action of the antioxidation system, influenced by cytokinins, which will be discussed later in the section 5.4.2.

It has been reported that the gibberellic acid enhanced the stability of LHC complex and photosynthetic efficiency in sunflower subjected to Cu stress, reflecting the role of this phytohormone in photoprotection (Ouzounidou and Ilias, 2005). Similar to this result, in the present investigation, there was reduced chlorophyll destruction, which was indicated by the higher values of CSI in the cotyledonary leaves of *R. communis* seedlings exposed to Cu stress along with KIN or BAP, and it was clear that BAP was more effective than KIN in maintaining the chlorophyll stability. Compared with our results, BAP mediated the protection of photosynthetic apparatus in *Zea mays* subjected to drought stress, as demonstrated by Shao *et al.* (2010). The authors also stated that this cytokinin mediated photo-protective acclimation during drought stress in maize was achieved by stabilizing the PSII complex and enhancing the electron donation capacity of PSII. The higher value of CSI calculated in the case of cotyledonary leaves of *R. communis* seedlings exposed to Cu stress along with KIN or BAP indicates the ability of plants to tolerate the Cu stress situation through improved stability of chlorophyll molecules, which resulted in efficient photosynthesis.

The significant positive correlation recorded in CSI with the photosynthetic performance index PI(abs) in KIN and BAP (r = 0.968 and 0.865, $p \leq 0.01$) treated cotyledonary leaves substantiate cytokinin mediated maintenance of chlorophyll stability and associated photosynthetic performance under Cu stress (Table 20 and 21). The restoration of photosynthesis and fluorescence parameters on the application of BAP along with $CuSO_4$was in agreement with Wu *et al.* (2021), wherein they observed that exogenous application of BAP effectively modulated the photosynthetic efficiency in *Solanum melongena* plants under salinity stress. The role of cytokinins to overcome the high light stress-induced photo-damage in *Arabidopsis thaliana* plants was demonstrated by Cortleven *et al.* (2014), wherein the authors proposed that cytokinin deficient transgenic *A. thaliana* and cytokinin receptor mutants exposed to high light stress exhibited stronger photoinhibition and drastic decline in the quantum efficiency of PSII. These observations underline the significant role played by cytokinins in effectively modulating the photosynthetic functions of plants under different abiotic stresses.

The above discussed features revealed that $CuSO_4$ negatively affects the photosynthetic efficiency in cotyledonary leaves of *R. communis* seedlings, which was overcome to some extent by the exogenous application of cytokinins. It was clear from the results that, of the two cytokinins used, BAP was most effective in maintaining photosynthesis in the cotyledonary leaves of *R. communis* seedlings subjected to Cu stress. Even though the direct influence of BAP in the regulation of photosynthesis is unknown, the activation of genes involved in photosynthesis by the action of cytokinins was frequently discussed (Takei *et al.*, 2002).

5.4. ROS accumulation and oxidative stress

5.4.1. Cu-induced ROS accumulation and oxidative stress

Heavy metal toxicity resulted in oxidative stress in plant cells due to the disturbances in the homeostatic events, thereby accumulating ROS molecules (AbdElgawad *et al.*, 2020). Generally, a low level of ROS production is a normal phenomenon in the chloroplast membrane due to the reduction of $NADP^+$ to NADPH (Marshall *et al.*, 2002). However, the overproduction of ROS due to heavy metal stress activates the programmes associated with the over-excitation of PSII, ultimately resulting in photosystem damages (Foyer, 2018). The declined photosynthetic efficiency and enhanced ROS accumulation in the cotyledonary leaves of *R. communis* seedlings during Cu stress in the present study is in agreement with the studies of Acidri *et al.* (2020), wherein the authors found that stress-mediated decline of CO_2 fixation along with reduced PSII efficiency leads to photoinhibition and associated overproduction of ROS molecules in *Coffea arabica* plants.

The enhanced accumulation of MDA content in the cotyledonary leaves of *R. communis* seedlings subjected to Cu stress indicated Cu-induced oxidative stress and associated reactive oxygen species (ROS) generation, resulting in membrane lipid peroxidation (Shabbir *et al.*, 2020). Copper stress resulted in the drastic photoinhibition and accumulation of ROS molecules in the chloroplast, leading to significant levels of membrane lipid peroxidation. According to Malnoë (2018), excess excitation energy due to photoinhibition causes electron leakage, irreversible reduction of electron acceptors, and over-accumulation of ROS. The increased accumulation of ROS molecules in the present study indicates the inefficiency in transferring absorbed energy to PSII reaction centers and the insufficiency of an antioxidative system necessary to scavenge the overproduced ROS.

In the present study, toxic levels of Cu in the growing medium resulted in the generation of free Cu^{2+} in the cells, which induced the generation of hydrogen peroxides (H_2O_2) and superoxide anions ($^{\bullet}O_2^-$) in the cotyledonary leaves of *R. communis* seedlings. Hydrogen peroxide is a chief signaling molecule for several physiological processes in plants during a wide variety of environmental stresses, which can induce tolerance towards various stresses (Hieno *et al.*, 2019). The major sites of ROS production in plants are chloroplasts (via photochemistry and electron transport), peroxisomes (via photorespiration), mitochondria (via respiratory electron transport), cell membrane and cytosol (by the activity of peroxidase enzymes) (Apel and Hirt, 2004). Therefore, the over-accumulation of ROS molecules results in irreparable oxidative damage to cellular components like proteins and DNA, and subsequently leads to cell death (de Souza *et al.*, 2017).The significant negative correlation recorded in ROS molecules with the photosynthetic parameters is the clear indication of ROS mediated photodamage occurred in the cotyledonary leaves of *R. communis* as a result of Cu toxicity. For example, the negative correlation observed in H_2O_2 molecules with PSI and PSII activities (r = -0.987 and -0.970 respectively at $p \leq 0.01$), PI(abs) (r = -0.967, $p \leq 0.01$), PI(total) (r = -0.955, $p \leq 0.01$), and DF(total) (r = -0.836, $p \leq 0.05$) in the cotyledonary leaves. Likewise, negative correlations were also recorded in the $^{\bullet}O_2^-$ content with PSI and PSII activities (r = -0.902 and -0.812 respectively at $p \leq 0.05$) (Table 18).

Overproduced ROS within the cells converts the membrane fatty acids into toxic lipid peroxides, leading to the destruction of the biological membranes, ion leakage by the plasma membrane, and ultimately causing cell death (Rangani *et al.*, 2018; Kamran *et al.*, 2020). The overaccumulation of MDA content is also an indication of the disturbances in the chlorophyll stability and associated photodamage in the leaves, which is in agreement with the significant negative correlation observed between MDA content and

CSI in the cotyledonary and primary leaves (r = -0.994 at $p \leq 0.01$ and -0.887 at $p \leq 0.05$ respectively) (Table 18 and 19).

MDA, the product of membrane lipid peroxidation, is considered as an index of plant oxidative stress, and the elevated level of MDA indicates the extent of membrane damage caused by ROS generated as a result of environmental stresses (Meng *et al.*, 2007). There are several reports regarding the increased lipid peroxidation and concomitant accumulation of MDA with increase in Cu stress in various plants (Jiang *et al.*, 2013; Ayala *et al.*, 2014). The increased MDA content in *R. communis* plant parts most prominently in the cotyledonary leaves indicates the occurrence of oxidative stress in the seedlings subjected to varying concentrations of $CuSO_4$. Comparatively lesser accumulation of MDA in the primary leaves than the cotyledonary leaves was due to the activation of various antioxidant mechanisms so as to control and detoxify ROS, and thereby reducing the rate of lipid peroxidation in primary leaves. According to AbdElgawad *et al.* (2020), the oxidative stress induced by the heavy metals was less affected in the younger leaves as compared to the older leaves due to higher growth rate and enhanced ROS signaling in the younger leaves.

The elevated ROS levels, electrolyte leakage, and reduced membrane and chlorophyll stability indices arise from Cu-induced oxidative stress, which triggers various stress responses (Rehman *et al.*, 2019). The significant positive correlation observed between H_2O_2 accumulation and MDA content in the cotyledonary and primary leaves (r = 0.956 at $p \leq 0.01$ and 0.871 at $p \leq 0.05$, respectively) indicated the ROS mediated membrane damage and concomitant MDA accumulation in these leaves (Table 18 and 19).

The increased membrane peroxidation by oxidative stress negatively affects membrane stability and integrity, ultimately resulting in the leakage of essential elements, and electrolyte leakage is considered as the stress intensity

marker in intact plant cells, which is commonly used to assess the stress-induced injury of plant cells as well as plant stress tolerance (Djebali *et al.*, 2005; Demidchik *et al.*, 2014). The results indicate that enhanced production of ROS under Cu stress disrupts membrane integrity and lowers the MSI. The significant negative correlation recorded in MSI with the $^{\bullet}O_2^-$ ($r = -0.902$ at $p \leq 0.05$) and H_2O_2 ($r = -0.956$ at $p \leq 0.01$) contents and positive correlation of EL% with $^{\bullet}O_2^-$ and H_2O_2 ($r = 0.963$ and $r = 0.924$ respectively at $p \leq 0.01$) in the cotyledonary leaves highlights the ROS mediated membrane damage and EL% in the cells (Table 22). Similarly, the ROS mediated destruction of MSI was also experienced in the primary leaves and roots, which was evident from the significant negative correlation between H_2O_2 and MSI in the primary leaves and roots ($r = -0.910$ and $r = -0.847$ respectively at $p \leq 0.05$) of Cu-treated *R. communis* seedlings (Table 23 and 24). These results are supported by the observations of Malik *et al.* (2019), wherein the authors pointed out that mercury stress leads to over-accumulation of ROS and thereby reduce MSI and increases EL% in chicory plants. Giannakoula *et al.* (2021) demonstrated the Cu stress mediated oxidative stress, ROS accumulation, membrane lipid peroxidation and disruption of membrane integrity in *Citrus aurantium*, which finally resulted in the decline of the photosynthetic activity.

5.4.2. Cytokinin mediated alleviation of ROS accumulation and oxidative stress

Exogenous application of cytokinins efficiently reduced the accumulation of ROS molecules in the cotyledonary leaves of *R. communis* seedlings, thereby alleviating oxidative stress. It has been reported that exogenously applied cytokinins act as cellular membrane stabilizer in plants under heavy metal stress (Wang *et al.*, 2015b). Cytokinins can reduce the metal induced photodamage and elevate the antioxidation mechanisms in the cotyledonary leaves of *R. communis* seedlings, which in turn reduce the

oxidative stress. Liu *et al.* (2014b) stated that reduced accumulation of H_2O_2 is correlated with the enhanced tolerance potential of the maize plants, and similar result was achieved in cotyledonary leaves of *R. communis* seedlings as a result of exogenous application of cytokinins.

On application of KIN and BAP, the content of MDA was reduced to a level that of control. Similarly, the $^{\bullet}O_2^-$ and H_2O_2 accumulations were drastically reduced on exposure to cytokinin in Cu-stressed seedlings, in which enhanced membrane stability and reduced electrolyte leakage occurs simultaneously in these leaves. The results indicated that ROS scavenging was efficiently carried out in *R. communis* seedlings when exogenous cytokinin was applied. Previous studies indicated that applying a low concentration of phytohormones such as ABA and BAP confers metal stress tolerance *via* enhanced ROS scavenging by activating the antioxidation potential (Shi *et al.*, 2019; Kamran *et al.*, 2021). It was also reported that BAP significantly enhances antioxidant activities in perennial ryegrass under salinity stress and reduces oxidative stress (Ma *et al.*, 2016). Therefore, BAP can be considered as membrane stabilizer and oxidative stress alleviator.

5.5. Metabolic dynamisms and osmotic adjustment

5.5.1. Cu-induced alterations in primary metabolites and osmolality

Accumulation of low molecular weight, non-toxic organic compounds in the cell is an important stress tolerance mechanism operating in plants under heavy metal toxicity (Garg *et al.*, 2002; Sruthi *et al.*, 2017). The increase in total sugars, total proteins, total free amino acids and proline contents in the present study can be correlated with the adaptive mechanism of *R. communis* towards Cu stress under hydroponic culture conditions. According to Xiong *et al.* (2006), the elevated levels of various metabolites in Cu stressed *Brassica pekinensis* contribute towards the detoxification of Cu.

The enhanced accumulation and distribution of metabolites in *R. communis* is found to be most prominent mechanisms in the cotyledonary leaves as compared to the primary leaves. The higher metabolite reserves in the cotyledonary leaves would be a conducive environment for the interconversion of metabolites suitable for the situation. The higher enhancement of metabolite accumulation in the cotyledonary leaves and lesser extent of enhancement in the primary leaves in *R. communis* seedlings exposed to Cu toxicity highlights the extreme stress effects in the cotyledonary leaves and minor stress effects in the primary leaves. Therefore, the cotyledonary leaves are more prone to oxidative stress in *R. communis* seedlings.

The increase in sugar content in both the cotyledonary and primary leaves of *R. communis* seedlings subjected to Cu stress is an indication of metal induced up-regulation of sugar metabolism in order to meet the increased energy demands to cope up with the stress situations (Rosa *et al.*, 2009; Mishra *et al.*, 2014). Moreover, the accumulation of sugars during ROS outbreak is involved in the regulation of the osmotic stress *via* the preservation of the biological membranes and molecules, which facilitate in maintaining the membrane integrity (Shackira *et al.*, 2017). According to the observations of Carrino *et al.* (2020), the sugars accumulated during abiotic stress conditions are the major contributors of osmotic adjustment in the leaves of *R. communis*. Though the Cu stress resulted in the reduced photosynthetic activity, the enhanced sugar accumulation in the leaves could be largely contributed by the excessive degradation of the starch (Dong and Beckles, 2019).

The enhancement in sugar accumulation in both the cotyledonary and primary leaves of *R. communis* seedlings depended on the concentration of $CuSO_4$ and days of Cu exposure. This finding is in consistent with the

observations of Contreras *et al.* (2018), wherein the authors revealed that the accumulation of various sugars such as galactose and raffinose, and sugar alcohols such as alditols, play osmoprotective and antioxidant roles in Antarctic *Colobanthus quitensis* plants during Cu stress, and their level of accumulation were strictly dependent on the concentrations of $CuSO_4$.

The increased protein content in the cotyledonary and primary leaves on initial days of Cu exposure would be largely contributed from the enhanced synthesis of stress proteins such as phytochelatins, metallothioneins and heat shock proteins which protect the plant from metal induced damages. According to Hall (2002), induction of protein biosynthesis is an immediate effect of heavy metal toxicity in plants. This might be the prime reason for enhanced synthesis and accumulation of protein in *R. communis* leaves on initial days of Cu toxicity. Therefore, the quick accumulation of proteins on initial days of Cu stress might have largely contributed by the synthesis of phytochelatins, which helps to sequester toxic metal ions into the vacuoles.

Furthermore, the enhanced synthesis of proteins during metal stress also contributes towards the specific protective functions and synthesis of enzymes involved in antioxidative defence mechanisms as well as in maintaining cellular membrane integrity (Omidifar *et al.*, 2021). Similar to the behavior of *R. communis*, Olkhovych *et al.* (2016) reported the enhanced synthesis of stress proteins in *Pistia stratiotes* exposed to Cu nanoparticles. Hence, the accumulation of proteins in *R. communis* seedlings during Cu exposure implies enhanced metal tolerance mechanisms in the plant.

Though the accumulation of protein was drastic in the cotyleonary leaves on initial days of Cu exposure, the accumulation was reduced with the increase in the treatment period and concentration of $CuSO_4$. This result denoted the interferences that occurred in the biosynthetic processes of protein due to extreme stress effects. Furthermore, the onset of senescence in

the cotyledonary leaves owing to toxic metal ions might be a contributing factor to the reduced protein levels. But, after the Cu stress induced abscission of cotyledonary leaves, the primary leaves became the principal site for metal toxicity, and therefore, the protein accumulation was reduced in these leaves also. Similar to our results, Hasan *et al.* (2017) observed the metal induced disturbances in the cellular protein homeostasis by interfering with the protein folding and stimulating the aggregation of nascent proteins, resulting in reduced cell viability.

Amino acids, the precursors of proteins, play significant roles in plant stress metabolism. The enhanced accumulation of free amino acids content in both the cotyledonary and primary leaves of *R. communis* seedlings will contribute towards the increased production of stress proteins such as phytochelatins and metallothioneins during Cu stress. This enhanced free amino acids content points towards the significant role played by amino acids in stress related metabolism of plants. Moreover, the increase in amino acids creates a nitrogen reserve, resulting in the dynamic adjustment of nitrogen metabolism, thereby enhancing antioxidation mechanisms and osmotic adjustment under stress conditions (Zhong *et al.*, 2017). Cu also forms stable complexes with amino acids in the xylem sap, which facilitate the translocation of this metal from root to shoot in hyperaccumulator plants (Shabbir *et al.*, 2020).

Proline executes various significant beneficial functions under heavy metal toxicity, such as role in cellular osmotic adjustment, ROS scavenging, protection of cell organelles from dehydration injury, maintenance of membrane integrity *etc.* (Trovato *et al.* 2008; Sharma *et al.* 2020b). The drastic increase in proline concentration in the cotyledonary leaves on 4 and 6 d of $CuSO_4$ exposure reveals the severity of the stress in the plant organ than that of the primary leaves. The amplified accumulation of proline with respect

to the increasing stress effects in the present study is consistent with many of the previous reports (Shackira and Puthur, 2017; Sruthi and Puthur, 2019; Janeeshma *et al.*, 2021b), which indicates the role of antioxidative activity of proline towards Cu induced injury in *R. communis* seedlings.

The enhanced accumulation of metabolites in the cotyledonaryleaves is an adaptive mechanism of the *R. communis* plants toward Cu toxicity, which can be actively involved in the Cu detoxification mechanisms in plants (Wang *et al.*, 2020). The existing metabolite reserves in the cotyledonary leaves would also create a favorable situation to overcome the stress environment by converting one form to another (Dubey *et al.*, 2018). These metabolites have a protective role against heavy metal stress by restricting the metal bioaccumulation in the photosynthetically active leaves, thereby allowing them to maintain cellular metal homeostasis (Piotrowska- Niczyporuk *et al.*, 2012; Anjitha *et al.*, 2021). These metabolites play an active role in the amelioration of ROS and thus provide stability to the structures of macromolecules (Llanes *et al.*, 2013).

In contrast to the cotyledonary and primary leaves, the accumulation of metabolites was significantly reduced in the roots of *R. communis* seedlings. According to Wang *et al.* (2021a), Cd stress resulted in a significant reduction in the accumulation of amino acids and other related metabolites in the roots of maize seedlings. Because of the reduced root growth, decreased uptake of essential elements, and root dieback due to metal stress, the metabolic activities in the roots become highly disturbed, which may be the prime reason for the reduced accumulation of metabolites in the roots (Sanaei *et al.*, 2021).

Due to the accumulation/deposition of metals inside the xylem vessels and other spaces, the water transport from the external environment to the shoot system was decreased, which leads to the decreased availability of

water to the plant, and therefore plants experience high osmotic stress (Haider *et al.*, 2021). During osmotic stress, lowering of the solute potential occurs, and the process is termed as osmotic adjustment. By the accumulation of suitable metabolites as well as by the production of stress proteins, plants have evolved ways to cope up with the cell osmoticum (Yadav *et al.*, 2021). These metabolites assist in lowering of osmotic potential to maintain the osmotic balance of the cell and keep the cell active under various stress conditions, including heavy metal stress (Mirshad and Puthur, 2017). These metabolites also protect the cellular structures and scavenge reactive oxygen species (Slama *et al.*, 2015).

The increase in osmolality in the cotyledonary and primary leaves of *R. communis* seedlings subjected to Cu stress was mainly due to the accumulation of various metabolites such as sugars, proteins, free amino acids and proline contents. The significant positive correlation recorded between the osmolality and Cu bioaccumulation in the cotyledonary leaves ($r = 0.964$ at $p \leq 0.01$) points out the Cu stress mediated accumulation of metabolites and enhanced osmolality in these leaves (Table 22). This indicates that enhanced accumulation of various osmolytes in both types of leaves helps to maintain a better osmotic adjustment to escape from the osmotic stress (Lintunen *et al.*, 2016). Thus, *R. communis* seedlings cope up with the Cu stress effects by the enhanced synthesis of organic solutes and metabolites, which help the plant to tolerate harsh environmental conditions.

5.5.2. Modulation of primary metabolites and osmolality by cytokinin application

The enhanced accumulation of metabolites in the cotyledonary leaves of *R. communis* seedlings subjected to Cu stress was reverted to a level similar to that of control seedlings upon exposure to cytokinins. As cytokinins can link external signals and internal metabolic processes, this group of

phytohormones can be considered the master regulators of plant growth and development (Emamverdian *et al.*, 2021). They are actively involved in the physiological and metabolic processes of plants, including nitrogen and phosphorous metabolism, and maintaining water status under stress situations (Hönig *et al.*, 2018). Gupta *et al.* (2012) studied the role of BAP in abiotic stress tolerance, and the authors revealed that BAP could effectively regulate the metabolite concentration in the plants under stress, thereby maintaining the membrane integrity and keeping the cells intact. Thus, it is quite apparent that cytokinin application plays a crucial role in protecting the plants from Cu toxicity by triggering various defence related metabolic pathways.

The Cu-induced osmotic stress was effectively alleviated in the cotyledonary leaves by the application of KIN and BAP, which regulate the accumulation of metabolites. Therefore, the osmolality was reduced to the level as that of control leaves. It has been reported that cytokinins regulate ethylene signaling, which plays a significant role in the biosynthesis and accumulation of osmolytes in plants under stress (Shen *et al.*, 2014). According to Ha *et al.* (2012), the cytokinin receptor histidine kinase, *AHK1*, is an osmotic sensor that positively regulates the stress responses in plants. Therefore, the osmotic stress perception and the related stress response would be comparatively quick and effective when cytokinin is involved along with Cu-induced osmotic stress.

5.6. Antioxidant defence mechanisms

5.6.1. Cu stress mediated elicitation of antioxidant defence mechanisms

Under normal environmental conditions, the antioxidant system actively participates in the detoxification of ROS molecules and maintains a balance between the activities of antioxidant enzymes and the production of ROS. Any changes in the environment disrupt this balance, resulting in an

increase in ROS.The tolerance potential of *R. communis* towards Cu phytotoxicity was apparent from the higher activities of various antioxidation enzymes and the accumulation of non-enzymatic antioxidants. These antioxidants were actively involved in the detoxification of ROS molecules (Singh *et al.*, 2017b; Hasanuzzaman *et al.*, 2019; Janeeshma *et al.*, 2021a). The significant enhancement in these antioxidant enzyme activities and the accumulation of non-enzymatic antioxidants in the root, cotyledonary and primary leaves of *R. communis* seedlings exposed to Cu stress help the plant to counter the over-accumulation of ROS in the chloroplasts, mitochondria, peroxisomes and cytosol.

Antioxidant defence system constitutes several antioxidant enzymes like CAT, POD and SOD, and the enzymes of AsA-GSH cycle such as GR, MDHAR, DHAR and APX, and non-enzymatic antioxidants such as AsA, GSH, phenolics, flavonoids and anthocyanins, mediate scavenging of toxic ROS from the cells of *R. communis* seedlings. Enhanced accumulation of various antioxidants and increased activities of antioxidant enzymes result in quick scavenging of ROS, thereby reducing oxidative stress (Alqarawi*et al.*, 2014; Hashem *et al.*, 2016). These results suggested that the induction of antioxidant defence system upon exposure to Cu stress may be an adaptive strategy developed by the plants to curtail oxidative stress. Similar to our results, induction of antioxidant enzyme activities was observed in mung bean seedlings during Cu stress, which helps to tolerate the Cu-induced oxidative stress (Gaur *et al.*, 2021). According to Yap *et al.* (2021), the antioxidant enzymes such as APX, CAT, POD and SOD activities were enhanced considerably to reduce the oxidative stress caused by ROS molecules during Cu stress in *Centella asiatica*.

SOD is the major antioxidant enzyme involved in primary resistance against ROS, catalyzing the dismutation of $^{\bullet}O_2^-$ and consequently producing

H_2O_2 and O_2 (Gill *et al.*, 2015). The enhanced level of $^{\bullet}O_2^-$ accumulations stimulates SOD enzyme activity; thereby $^{\bullet}O_2^-$ produced in cells are quickly transformed to H_2O_2 by the activity of SOD (Dixit *et al.*, 2001). The significant positive correlation recorded between SOD activity with $^{\bullet}O_2^-$ content (r = 0.978 at $p \leq 0.01$) and H_2O_2 content (r = 0.956 at $p \leq 0.01$) in the cotyledonary leaves of *R. communis* seedlings is a clear indication of $^{\bullet}O_2^-$ mediated enhancement in SOD activity and the associated accumulation of H_2O_2 in these leaves (Table 22). Apart from the ROS scavenging, SOD has recently been discovered to have key roles in diverse metabolic processes. It acts as a nuclear transcription factor, RNA binding protein, and signal modulator of glucose metabolisms (Chung, 2017). The majority of them are independent of their usual antioxidant properties, which indirectly help to regulate oxidative stress (Wang *et al.*, 2018).

As the rate of H_2O_2 radicals gets enhanced by SOD activity, the enzymes such as CAT, POD and APX activities were induced, aiding in the removal of H_2O_2 radicals from the cells (Zhang *et al.*, 2017b). These results are supported by the significant positive correlation recorded in SOD activity with CAT, POD and APX activities (r = 0.998, 0.979 and 0.955 respectively at $p \leq 0.01$) in the cotyledonary leaves of *R. communis* seedlings (Table 22), indicating the effective alleviation of destructive oxygen species by the integrated network of the enzymatic antioxidants, which probably acted as the protective system in the plant cells.

Catalases are predominantly peroxisomal enzymes, which can degrade the H_2O_2 without using any reducing power and is mainly active at comparatively higher H_2O_2 concentrations (Anjum *et al.*, 2016b). CAT is involved in the direct conversion of H_2O_2 into H_2O and O_2 or in the indirect conversion through the oxidation of substrates such as formaldehyde, formate, methanol, ethanol and nitrite with H_2O_2 and release of H_2O and O_2 (Sharma

and Ahamed, 2014; Su *et al.*, 2018). In *R. communis*, the activity of CAT was gradually enhanced in the root, primary and cotyledonary leaves upon exposure to Cu stress. The significant positive correlation recorded between CAT activity and H_2O_2 content in the cotyledonary and primary leaves (r = 0.972 and 0.917 respectively at $p \leq 0.01$) confirms the elevation of CAT activity due to the higher accumulation of H_2O_2 in *R. communis* seedlings (Table 22 and 23). Similar to our results, Cu-stress mediated elevation of CAT activity was observed in many plants such as *Abutilon indicum*, *Withania somnifera*, bamboo, maize *etc*., which help the plant for the effective alleviation of H_2O_2 and to tolerate Cu-stress mediated oxidative stress (Rout and Sahoo, 2013; Emamverdian and Ding, 2017; Rout *et al.*, 2017; Liu *et al.*, 2018c; Yap *et al.*, 2021). According to Su *et al.* (2018), the deletion mutation of CAT genes resulted in defective plant growth, disturbed redox state and enhanced sensitivity to environmental stresses, indicating the major role played by the CAT enzyme in the growth and development of plants under stress.

Guaiacol peroxidases (POD) are heme-containing enzymatic ROS scavengers, which participate in the biosynthetic mechanisms involved in the plant defence against environmental stresses (Gill and Tuteja, 2010). It can oxidize aromatic electron donors like guaiacol and pyrogallol in the presence of H_2O_2 to form H_2O (Sharma *et al.*, 2012). The gradual enhancement of POD activity in the cotyledonary and primary leaves is a clear indication of Cu-stress mediated H_2O_2 production and oxidative stress in these leaves. This can be supported by the significant positive correlation recorded between POD activity and H_2O_2 content in the cotyledonary and primary leaves (r = 0.940 and 0.962 respectively at $p \leq 0.01$) (Table 22 and 23). In the case of roots, drastic enhancement in POD activity was recorded on 2 d of Cu exposure. In contrast, due to the extreme stress effects, POD activity was gradually reduced in the roots from 4 d onwards. According to Yap *et al.* (2021),

Centella asiatica plants exposed to Cu stress had enhanced POD activity in the roots and leaves, followed by other antioxidant enzymes, which indicates the higher affinity of POD towards H_2O_2 than CAT and APX enzymes. Similarly, POD played a major role at the initial stages of Cu stress in the roots of *R. communis* seedlings as evidenced by drastic enhancement in activity on 2 d, and further, other enzymes such as CAT and APX majority took over the role of H_2O_2 detoxification.

Enzymes such as APX, MDHAR, DHAR and GR are the components of the AsA-GSH cycle in plants, and they work together to detoxify H_2O_2 into water and molecular oxygen (Shan *et al.*, 2015). APX, having a higher affinity towards H_2O_2, catalyzes the reduction of H_2O_2 into H_2O using AsA as a specific electron donor in the organelles such as chloroplasts, cytosol, mitochondria, and peroxisomes (Anjum *et al.*, 2016b; Chalanika De silva and Asaeda, 2017). Though CAT and APX both have heme, they have different affinities for H_2O_2 and different requirements for reducing power during H_2O_2 metabolism (Anjum *et al.*, 2014). Because of the higher affinity of APX towards H_2O_2, it can efficiently eliminate even low levels of H_2O_2. A significant positive correlation was recorded between H_2O_2 levels and APX activity in cotyledonary leaves ($r = 0.966$ at $p \leq 0.01$), primary leaves ($r = 0.872$ at $p \leq 0.05$) and roots ($r = 0.844$ at $p \leq 0.05$) of *R. communis* seedlings upon exposure to Cu stress indicates the effective enhancement of APX activity with increasing accumulation of H_2O_2, mostly in the cotyledonary leaves as evidenced from the higher r values as compared to primary leaves and roots (Table 22, 23 and 24). This would ensure the effective alleviation of H_2O_2 and enhanced tolerance of *R. communis* towards the Cu induced oxidative stress. According to Caverzan*et al.* (2012), transgenic tall fescue plants with higher APX gene expression showed significant enhancement in the APX activity when exposed to Cu stress. The diverse effects of knockout and knockdown of different APX genes on plant growth and antioxidant

metabolisms highlight the role played by APX in maintaining the redox signaling, which emphasizes the complexity of interactions of APX with other antioxidants in fine-tuning the antioxidant metabolism in plants (Caverzan*et al.*, 2012). The variable responses of antioxidant enzymes in *Hibiscus cannabinus* upon exposure to increasing concentrations of $CuSO_4$ were observed by Saleem *et al.* (2020).

Increased APX activity under Cu stress resulted in the increased activity of all other enzymes of the AsA-GSH cycle, i.e., MDHAR, DHAR and GR, which was evidenced by the significant positive correlations recorded in APX activity with MDHAR, DHAR and GR activities in the root, cotyledonary and primary leaves of *R. communis* seedlings subjected to Cu stress (Table 22, 23 and 24). This APX mediated enhancement in MDHAR, DHAR and GR activities helps the plant for recycling the DHA to AsA and thus re-equips the APX for further reduction of H_2O_2. Similar results of enhanced activities of AsA-GSH cycle enzymes were observed in various plants treated with $CuSO_4$, which promotes the neutralization of ROS for the improved protection of cellular functioning (Zaheer *et al.*, 2015; Abdulmajeed *et al.*, 2021). The increased activities of antioxidant enzymes in *R. communis* seedlings, most significantly in roots and cotyledonary leaves under Cu stress, indicate that these plant parts of *R. communis* encounter with the highest level of Cu stress. Therefore, a balance between various enzymatic antioxidants is indispensable to maintain the steady-state level of ROS in cells during abiotic stress (Sachdev *et al.*, 2021).

The ROS scavenging potential in plants is also associated with the level of various non-enzymatic antioxidants, which are low molecular weight compounds and can neutralize or transform ROS to maintain the cellular redox status (Mittler, 2017; Carvalho *et al.*, 2018). Ascorbate is a hydrophilic redox buffer that protects plants from ROS-induced oxidative damages. In

addition, the proteinaceous thiol compounds, including GSH, also participate in the metabolism of ROS to maintain redox homeostasis (Kapoor *et al.*, 2015). Ascorbate and GSH directly interact and neutralize superoxide and hydroxyl radicals, and AsA became electron donors for APX catalyzed H_2O_2 reduction (Soares *et al.*, 2019). According to Xiao *et al.* (2021), AsA has at least triple roles in plant stress responses: act as antioxidant for ROS scavenging, function as cofactor in plant metabolic processes, and take part to regulate various signal pathways under stress. Therefore, the enhanced accumulation of AsA content in the cotyledonary and primary leaves of *R. communis* seedlings helps the plant to tolerate Cu induced oxidative stress. As AsA is mainly located in the photosynthetic tissues in its reduced form, it can act as an alternative electron donor of PSII when the oxygen evolving complex is inactivated due to stress. Thus, AsA protects the entire photosynthetic machinery during stress (Nagy *et al.*, 2016). The reduction in the accumulation of AsA in the roots of Cu-stressed *R. communis* seedlings might be due to the enhanced activity of APX, and the enhanced MDHAR and DHAR activities may not be sufficient to restore the AsA in the roots.

Glutathione is considered as one of the most important antioxidants, which scavenge the ROS such as H_2O_2, singlet molecular oxygen ($^1O_2$) and hydroxyl radicals ($OH^{\bullet}$) (Gill and Tuteja, 2010). It is involved in the regeneration of AsA through the AsA-GSH cycle and acts as a redox buffer to keep the reduced state of the intracellular environment. The significant enhancement in the accumulation of GSH in *R. communis* seedlings helps the plant to tackle the stress situation, thereby reducing the Cu induced oxidative stress. Heavy metal chelation by phytochelatins (PCs) is one of the ubiquitous detoxification mechanisms in metal accumulator plants, synthesized enzymatically from GSH (Yadav, 2010). Therefore, enhanced accumulation of GSH in plants subjected to heavy metal stress is a necessity for metal accumulator plants. The significant positive correlation recorded in AsA and

GSH contents with $^{\bullet}O_2^-$ and H_2O_2 accumulation in the roots, cotyledonary and primary leaves manifests the role of these antioxidant molecules in supporting the detoxification of ROS in *R. communis* seedlings. Of these, the higher r values observed during correlation of GSH content with H_2O_2 accumulation in the cotyledonary and primary leaves (r = 0.995 and 0.985 respectively at $p \leq 0.01$) is a clear indication of the role of GSH in H_2O_2 detoxification in the leaves (Table 22, 23 and 24).

Phenolics are a wide group of compounds with principal role in antioxidant defence mechanisms in plants. Phenolics, having antioxidant action and metal chelation properties, produced as a stress response in plants, can help the plant to adapt to the metal stress environment (Kısa *et al.*, 2016). In the present study, treatment of *R. communis* seedlings with $CuSO_4$ resulted in the enhanced accumulation of phenolics contents in the leaves, which helped the plants to scavenge the excess ROS molecules. The antioxidant capacity of phenolics is related to their aromatic ring structure with –OH or –OCH_3 substituents, which is suitable for trapping free radicals (Dumanović *et al.*, 2021). Phenolic compounds with *o*-dihydroxy groups in their structure can be complex with toxic metal ions and thus prevent the formation of ROS through Fenton reactions. Thus, the phenolic compounds accumulated in the cotyledonary and primary leaves of *R. communis* seedlings during Cu stress help the plant to sequester the toxic levels of Cu^{2+} and thereby reduce ROS accumulation.

Flavonoids are phenolic compounds with dihydroxy B-ring in the structure that can scavenge ROS produced by heavy metal stress (Davies *et al.*, 2018). The gradual increase in flavonoids content in the cotyledonary and primary leaves of *R. communis* seedlings subjected to Cu stress is a strategy adopted by the plant to scavenge enhanced ROS accumulation in these leaves. But in the case of roots, which experiences extreme stress effects, gradual

reduction in total phenolics and flavonoids contents were observed. These results are in agreement with the observations of Chrysargyris *et al.* (2021). They reported that minor stress resulted in the accumulation of phenolics and flavonoids contents in *Pelargonium graveolens* plants subjected to $CuSO_4$ in nutrient medium, whereas severe stress resulted in lesser accumulation of these metabolites. The authors also stated that the strong correlation recorded between flavonoids accumulation and antioxidant enzyme assays during Cu stress suggests the role of this class of compounds in the pool of antioxidant molecules, which helps the plant to tolerate mild effects of Cu stress (Chrysargyris *et al.*, 2021). Similarly, the enhanced flavonoids content in the leaves of *R. communis* seedlings can also help to reduce the oxidative stress induced by Cu stress.

Anthocyanins are water-soluble pigments that are accumulated during metal stress in plants. They act as antioxidants and metal chelators to protect the plant cells from metal induced oxidative damages and thereby assist in stress tolerance (Janeeshma *et al.*, 2021c). According to Naing and Kim (2021), among other heavy metals, Cu was found to be the most potent inducer of anthocyanin synthesis, and the produced anthocyanins help to protect the cells against Cu toxicity by scavenging the toxic ROS molecules. In the present study, the accumulation of anthocyanins was gradually enhanced in all the plant parts of *R. communis* seedlings during exposure to low concentrations of $CuSO_4$, indicating the role of anthocyanin in regulating oxidative stress during mild/moderate stresses. However, metal induced anthocyanins may be effective in mild/moderate stresses but may not be sufficiently effective at severe metal stresses (Naing and Kim, 2021).

The significant enhancement in the activities of antioxidant enzymes and anthocyanin accumulation in *Brassica juncea* subjected to Cd exposure was observed by Kapoor *et al.* (2019), wherein the authors suggested the

enhanced photosynthesis and tolerance of this plant was possible through triggering of efficient ROS scavenging by various antioxidants. In contrast, according to Giannakoula *et al.* (2021), Cu toxicity resulted in enhanced ROS production and membrane damage, reduced photosynthetic pigment synthesis and declined photosynthetic activity in citrus plants and the elevated antioxidation mechanisms could not successfully counteract the ROS induced photosynthetic damage.

5.6.2. Cytokinin mediated modulation of antioxidant defence mechanisms

Exogenous application of cytokininsefficiently enhanced the antioxidative defence mechanisms in the cotyledonary leaves of *R. communis* seedlings exposed to Cu stress, which effectively alleviated oxidative stress. The enhanced photosynthetic efficiency and associated enhancement in stability indices and reductions in the MDA accumulation and EL% in the cotyledonary leaves of *R. communis* seedlings subjected to KIN or BAP along with Cu stress were ascribed to the integrated network of antioxidation mechanisms.The significant positive correlations recorded between various enzymatic and non-enzymatic antioxidants in the cotyledonary leaves of *R. communis* seedlings along with cytokinin application indicate that all the antioxidation mechanisms are interconnected to one another (Table 25 and 26). Previously, many studies have reported that the application of a lower concentration of phytohormones enhanced the ROS scavenging ability by boosting the antioxidant enzyme activities in plants under heavy metal stress (Jiang *et al.*, 2019b; Bashri *et al.*, 2021; Kamran *et al.*, 2021). According to Kumari *et al.* (2018), the maintenance of stability indices and efficient photosynthesis resulting from BAP application is largely due to enhanced ROS scavenging mechanisms in wheat under drought and high temperature stress situations. Therefore, these phytohormones primarily assist in strengthening the antioxidant machinery in plants exposed to heavy metals.

It was shown that the cytokinins act as oxidative stress alleviators and membrane stabilizers by enhancing the enzymatic antioxidant system (Jia *et*

al., 2017). According to Bashri *et al.* (2021), exogenous cytokinins mitigate the photosystem damages in *Trigonella* seedlings subjected to Cd stress by restoring D1 proteins and reaction centers *via* modulation of enhanced antioxidant enzyme activities. The cytokinin-mediated enhanced antioxidation in the cotyledonary leaves of *R. communis*, along with the antisenescing function of cytokinins, resulted in the prolonged photosynthetic functions and thereby seedling establishment in *R. communis* under adverse environmental conditions.

The enhanced activities of antioxidant enzymes accompanied by an enhanced level of AsA in the cotyledonary leaves exposed to Cu stress along with the exogenous application of cytokinins indicates the prominent role played by KIN and BAP under Cu stress in regulating ROS-induced oxidative stress, and thereby effectively modulating photosynthetic efficiency in *R. communis* seedlings. This amending effect of exogenous cytokinin could be correlated with the reduced accumulation of ROS in Cu stressed leaves through modulation of antioxidative functions, thereby improving the resistance of plants towards the oxidative stress caused by $CuSO_4$ (Hasanuzzaman *et al.*, 2017; Jung *et al.*, 2020). It was also reported that BAP significantly enhances antioxidant activities in perennial ryegrass under salinity stress. Therefore, this phytohormone can be considered as a membrane stabilizer and oxidative stress alleviator.

Previously, studies have proved that applying a low concentration of phytohormones such as ABA and BAP confers metal stress tolerance *via* enhanced ROS scavenging by activating antioxidant activities (Shi *et al.*, 2019; Kamran *et al.*, 2021). Upon application of cytokinins, the anthocyanin contents were also increased, indicating the enhanced potential of the plant to negotiate the ROS-induced oxidative and photosystem damages. This resulted in the reduction of ROS accumulation in thylakoid membranes and improved photosynthesis in *R. communis* seedlings exposed to Cu stress along with applied cytokinins. The accumulation of endogenous anthocyanin contents on

the application of cytokinins can contribute towards the enhanced antioxidation potential and strongly supplements with the ROS scavenging potential to the plant (Thind *et al.*, 2021).

On application of KIN and BAP along with Cu stress, accumulation of antioxidants such as GSH, total phenolics and flavonoids decreased drastically and reached a level similar to that of the control. These reductions could be justified with the enhanced stress alleviation of cytokinins by increased antioxidant enzyme activities and less demand for non-enzymatic antioxidants to be in action. In contrast, Zhou *et al.* (2019) observed that the application of *trans*-zeatin along with Cd and Zn toxicity resulted in the accumulation of non-protein thiols, including GSH, and enhanced stress tolerance in a halophytic plant *Kosteletzkya pentacarpos*. In contrast, Piotrowska-Niczyporuk *et al.* (2020) observed that exogenous cytokinins confer Pb tolerance in a green alga *Acutodesmus obliquus*, by effective modulation of endogenous cytokinin levels, which act as an inhibitory factor for the production of thiol mediated compounds. This action of cytokinins as a negative regulator of the synthesis of thiol-rich compounds and phytochelatins in plants under stress situations will not promote the sequestration of the metal into the algal cells but stimulate the metal exclusion.

5.7. Bioaccumulation of Cu and distributional patterns

5.7.1. Enhanced Cu bioaccumulation and cellular as well as subcellular distribution patterns

Copper is an essential plant micronutrient that tends to accumulate in different parts of the plant. The trend of bioaccumulation in *R. communis* after $CuSO_4$ treatment was root > stem > stem > cotyledonary leaf > primary leaf. The bioaccumulation of Cu by *R. communis* increased gradually with increase

in Cu concentration in the medium as well as with increase in the treatment period, and the major part of the uptaken Cu was retained in the root itself, and only a small portion was found to be transported to the aerial parts. This is in accordance with the studies of Fulekar (2016), where the author established that the metal content concentrates more in the roots than the shoots because the roots receive the metal entering the plants as a result of nutrient uptake. According to Peng *et al.* (2015), the immobilization of higher amount of metal in the root system is a chief tolerance mechanism against heavy metal toxicity in plants. In plants, the absorption of metal depends on the metal availability in the soil and the physiological requirement of the metal to the plant (DalCorso *et al.*, 2013). Since Cu concentration was higher in the roots, it can strongly bind to the root cell wall, resulting in the restricted mobility of the metal and reduced translocation to the aerial parts (Marques *et al.*, 2018). When the bioaccumulation of Cu in cotyledonary and primary leaves was compared, it was found that the higher content of Cu was translocated into the cotyledonary leaves than the primary leaves. Similar results were also observed by Yan and co-workers (2010) in *Avicennia marina*, in which they reported that the accumulation of Pb occurred mainly in the roots, with some accumulation in cotyledonary leaves but very little in primary leaves.

With the increase in the concentration of Cu in the growing medium, there was a greater uptake of this metal and an accumulation of the same in various plant parts.On abscission of cotyledonary leaves, the principal site for Cu sequestration became the primary leaves, and therefore the Cu bioaccumulation was significantly enhanced in the primary leaves on 10 d of treatment. The study revealed that, when *R. communis* seedlings subjected to increasing concentrations of $CuSO_4$, toxic levels of Cu pose least damages to the photosynthetic machinery of first pair of primary leaves in the presence of cotyledonary leaves, whereas, excision of cotyledonary leaves resulted in

severe oxidative stress and photosynthetic damages in the primary leaves of *R. communis* seedlings (Sameena and Puthur, 2021b).

The TF value of cotyledonary leaves was twice higher than the primary leaves. This result indicates the translocation of toxic levels of Cu to the cotyledonary leaves and is a shielding mechanism of cotyledonary leaves by which the normal physiological and biochemical activities of primary leaves were more or less maintained normal even under Cu phytotoxicity. The TF values were < 1 in both the cotyledonary and primary leaves, which indicates the strong capability to hold Cu^{2+} in the root cells avoiding the transport into the aboveground tissues in *R. communis* plants. It was also noticed that at higher $CuSO_4$ concentrations (120-200 μM $CuSO_4$), the abscission of cotyledonary leaves occurs within 6 d of the treatment period indicating the high toxicity encountered by cotyledonary leaves by which it perishes until then it protects the primary leaves from phytotoxicity induced by Cu. But on abscission of cotyledonary leaves, the translocation of Cu to the primary leaves was enhanced, and therefore higher TF values were recorded in the primary leaves on 10 d of $CuSO_4$ treatment.

As the absorbed metal is highly concentrated in the roots, the detoxification of the metal at the subcellular level is also crucial to reduce the bioavailability and toxicity in plants. The major detoxification mechanisms operational in plants are the binding of the metal ions to the cell wall as well as the sequestration into the vacuole (Zhou *et al.*, 2017; Cao *et al.*, 2018). The first barrier for metal uptake is the cell wall, which comprises cellulose, hemicelluloses, pectin and protein, which can bind with metal ions and thereby restrict the entry into the cytoplasm. In the present study, the major portion of the uptaken Cu was sequestered in the cell wall, as evidenced by the higher Cu concentrations in the cell wall fractions. According to Zhang *et al.* (2021b), the maize plants exposed to Pb stress showed 50% or above

proportion of the absorbed Pb in the cell wall fractions, and only the remaining portion was localized in the organellar and soluble fractions.

In mature plant cells, vacuole comprises as much as 90% of the total cell volume. They consist of S-rich peptides and organic acids, which helps in the chelation and compartmentalization of toxic metal ions in plants (Shen *et al.*, 2021). According to Wang *et al.* (2016b), the soluble (cytoplasmic) fraction consisted of mostly vacuoles, which act as a preferential site for Cu sequestration after the cell wall. In accordance with these observations, in the case of stem, the absorbed Cu was localized in the cytoplasmic fraction after the cell wall fraction, indicating the vacuolar sequestration of Cu in the stem of *R. communis* seedlings. But in the case of root, the second largest site of Cu localization was in the organellar fraction, which may negatively affect the root cell metabolism and may be the reason for the reduced metabolites reserves in the roots of Cu treated seedlings. In the case of both cotyledonary and primary leaves, most of the accumulated Cu was localized in the cell wall fraction, which might be one of the tolerance strategies adopted by the plant in order to keep the photosynthetic machinery undisturbed. After the cell wall, vacuoles act as the preferential site for the sequestration of Cu, as evidenced by the comparatively higher values of Cu content in the cytoplasmic fractions in the cotyledonary and primary leaves upon exposure to 200 μM $CuSO_4$ as compared to that of the control. The Cu content in the organellar fractions of cotyledonary and primary leaves of *R. communis* seedlings subjected to 200 μM $CuSO_4$ was approximately near the Cu content recorded in the organellar fractions of both the leaves of control seedlings. This indicates the efficient cell wall sequestration of toxic levels of Cu in these leaves, and thereby preventing the organelles from the toxic concentrations of Cu. Similar to our results, Pan *et al.* (2019) reported that 83% of the absorbed metal was localized in the cell wall and vacuolar fractions in *Xanthium strumarium* plants subjected to Mn stress.

5.7.2. Influence of cytokinins on Cu bioaccumulation and distribution

Exogenous application of cytokinins serves as a potential candidate for the effective amelioration of the heavy metal toxicity in plants by influencing the metal biosorption and stress adaptation (Saini *et al.*, 2021). They act as chemical messengers to improve stress tolerance, thereby allowing normal growth and development even under metal toxicity. On exogenous application of cytokinins, the heavy metal entry was strongly restricted to the shoot, as evidenced by the lower Cu bioaccumulation and TF values in the cotyledonary and primary leaves of *R. communis* seedlings subjected to KIN or BAP along with 80 and 160 µM $CuSO_4$. These results are in agreement with the observations of Piotrowska-Niczyporuk *et al.* (2020), in which the authors reported that exogenous application of three cytokinins such as *trans*-zeatin, kinetin, and N,N'-diphenylurea played as a negative regulator of metal detoxification machinery and also stimulated the metal exclusion and antioxidative defence mechanisms in green alga *Acutodesmus obliquus* exposed to Pb stress. Similarly, Massoud *et al.* (2018) reported that exogenous auxin (IAA) and gibberellic acid (GA_3) have protective effects in pea seedlings subjected to Cu stress by lowering the Cu bioaccumulation to the plant system.

On comparing the Cu bioaccumulation and EDX results in the cytokinin treated cotyledonary leaves of *R. communis* seedlings subjected to Cu stress, it was noticed that cytokinins effectively regulated the Cu translocation to the cotyledonary leaves, which help the plant in efficient photosynthesis. Similar to our results, Kamran *et al.* (2021) reported that application of BAP alone or in combination with ABA reduced the metal uptake in tomato seedlings exposed to Co stress, reduced the chlorophyll destruction and up-regulated antioxidative mechanisms and thereby enhanced the photosynthesis and growth of the plant.

5.8. Distribution of essential elements in the xylem tissues

5.8.1. Influence of Cu on distribution of essential elements

Being the divalent cation, Cu may compete with the uptake of other micro and macro-elements such as Zn, Ca, Mg, Fe, *etc*., bytransceptors or sensorsacross the membranes (Fan *et al.*, 2021). This competition between the nutrient and toxic elements for binding sites resulted in disturbances in the distribution of nutrient elements in plants (Shackira and Puthur, 2019). According to the observations of Fan *et al.* (2021), there is a strong cross-talk existing between the uptake of nutrient elements, their homeostasis and signaling in plants. From the chemical point of view, the chemical interactions and nutrient dynamics can result from the chemical similarities or analogy between elements, which share the same transporter to take up the elements (Courbet *et al.*, 2019).

Ricinus communis seedlings treated with $CuSO_4$ lead to the reduction in C content in the roots and cotyledonary leaves, which might be due to the limited fixation of CO_2 by the leaves and consequently reduced C export in the form of photoassimilates to the roots. This limited CO_2 fixation was also reflected in O content in the cotyledonary leaves. Calcium acts as a universal second messenger in plants under normal functioning as well as during environmental stresses. Plants have myriads of Ca sensing proteins such as calmodulins (CaMs), Ca^{2+}-dependent protein kinases (CDPKs), calcineurin B-like proteins (CBLs) *etc*., which binds to Ca^{2+} ions in the cells and trigger the downstream regulation of signaling pathways such as ABA-dependent stomatal closure (Jalmi *et al.*, 2018; Schulze *et al.*, 2021). The enhanced Ca distribution in the cotyledonary leaves and roots of Cu-treated seedlings indicates the activation of the Ca-mediated signaling processes and confirms its role in stomatal closure and thereby preventing excess water loss during stress. It was reported that there was a cross-talk between the Cu-induced

intracellular signals like calcium and H_2O_2 levels, leading to the activation of Ca-dependent gene expression of antioxidant proteins *via* CaMs and CDPKs in *Ulva compressa* exposed to Cu stress (González *et al.*, 2012). The role of Ca^{2+} in heavy metal sequestration to the cell wall has been discussed in section 5.10.1.

The accumulation of P content in the xylem tissues of *R. communis* seedlings was significantly enhanced during Cu stress, most probably in the xylem of root and primary leaf, whereas the accumulation was reduced in the xylem of cotyledonary leaves. Phosphorous is involved in various metabolic and regulatory processes in plants and constitutes the structural skeleton of biomolecules such as ATP, NADPH, nucleic acids *etc*. (Razaq *et al.*, 2017; Bechtaoui *et al.*, 2021). Therefore, the enhanced accumulation of P content helps the plant to counteract the Cu induced growth and photosynthetic damages *via* enhanced production of ATP and NADPH. This would also ensure the enhanced mitochondrial activity and activation of antioxidant enzymes. According to the report of Hayes *et al.* (2019), enhanced Ca levels in the plant also modulate the leaf cell-specific allocation of P to the palisade mesophyll cells during high P conditions that also contribute to the efficient photosynthesis in these leaves even under Cu toxicity.

Similar to the P content, the Mg content was also significantly enhanced in the xylem tissues of root, stem and primary leaves of *R. communis* seedlings upon exposure to Cu stress, whereas in the case of xylem of cotyledonary leaves, the Mg content was significantly reduced and recorded below detectable limit during Cu stress. Magnesium is an essential mineral nutrient involved in the photosynthetic metabolism and phloem loading, and its deficiency resulted in the decline in net carbon assimilation rate (Tränkner *et al.*, 2018). The enhanced Mg content would be aiding in the

maintenance of the photosynthetic processes and allocation of photoassimilates in *R. communis* seedlings even under Cu stress.

In contrast, the reduced P and Mg content in the cotyledonary leaves may be due to mineral element remobilization in these leaves prior to abscission. According to the observations of Maillard *et al.* (2015), the remobilization of P and Mg from older leaves to younger leaves occurred in most of the plant species in order to modulate the nutrient deficiency and also the remobilization efficiency is largely dependent on the extent of mineral deficiency in essential parts such as primary leaves. Since majority of the assimilated P and Mg were stored in the chloroplasts as photosynthetic proteins, the remobilization of the components of chloroplasts is characteristics of senescence (Zentgraf *et al.*, 2022). Therefore, the up-regulation of the chloroplast dismantling and protein degradation in the cotyledonary leaves might be the prime reason for the reduced distribution of P and Mg in these leaves. The decreased chlorophyll molecules and associated reduction in photosynthetic efficiency in the cotyledonary leaves of *R. communis* seedlings under Cu stress were already discussed in section 5.3.1.

In the case of K distribution, it was drastically enhanced in the xylem tissues of cotyledonary leaves on exposure to Cu stress, whereas no significant changes were recorded in all other plant parts. Similar to Mg, K also significantly contributes towards the proper functioning of photosynthesis (Tränkner *et al.*, 2018). Because of the role of K as a coenzyme or activator of many enzyme systems, the increased K content in the cotyledonary leaves of *R. communis* seedlings subjected to Cu stress might account for the enhanced antioxidant enzyme activities. Moreover, adequate K status induces the solute accumulation, lowers the osmotic potential and helps to maintain plant cell turgor (Wang *et al.*, 2013). This

would help to equalize the heavy metal toxicity in plants by forming the solutes such as metabolites and nitrogen compounds in the cell sap, thereby maintaining the osmoticum and improving the stress tolerance (Kumar *et al.*, 2020). Similar to our results, significant enhancement in the K content in the leaves of *Erica australis* subjected to Cu stress was observed by Trigueros and Rossini-Oliva (2021). Therefore, K can efficiently minimize the metal toxicity in plants by the cumulative effect of enhanced accumulation of mineral elements, metabolites, and activity of antioxidant enzymes (Ahmad *et al.*, 2016a).

Exposure of *R. communis* to Cu stress enhanced the distribution of S in the root and cotyledonary leaves. Sulphur has several functions in plant growth and development, ranging from being a structural element of macro-biomolecules to influencing multiple physiological processes including abiotic stress tolerance (Zenda *et al.*, 2021). Being an essential component of amino acid cysteine, and thereby GSH and phytochelatins, S offers the plants protection against oxidative stress induced by heavy metals. Therefore, the enhanced S in cotyledonary leaves and roots of *R. communis* seedlings can be correlated to enhanced synthesis of S containing amino acids and thereby GSH and phytochelatins. The toxicity imparted by Cu^{2+} in *R. communis* might be partially alleviated by the enhanced accumulation of these metal chelators.

Silicon improves the vigor and resistance of plants when exposed to environmental stresses as well as gives mechanical strength to the stem (Luyckx *et al.*, 2017). The significant enhancement in the distribution of Si was observed in the xylem tissues of stem, and in all other plant parts, the variations in the distribution were insignificant. It has been reported that Si forms complexes with heavy metals, and their deposition and redistribution are responsible for better resistance of the plants against toxic metal ions (Lux *et al.*, 2020; Janeeshma *et al.*, 2021d).

The drastic increase in Zn distribution was recorded in the xylem tissues of all the plant parts of *R. communis* seedlings except in the case of stem when treated with $CuSO_4$. Zinc is an indispensable micronutrient, which activates the enzymes involved in protein synthesis and metabolism of carbohydrates, lipids and nucleic acids (Hassan *et al.*, 2020). According to the observations of Thounaojam *et al.* (2014), Zn improves the resistance of the plants and alleviates the oxidative stress under Cu toxicity by stimulating the antioxidation mechanisms and also by restricting the accumulation of toxic levels of Cu in the plant system. Therefore, the enhanced accumulation of Zn in the roots and leaves of *R. communis* seedlings exposed to Cu stress could help the plant to tide over the toxicity imposed by Cu.

The distribution of Fe was found to be significantly enhanced in the xylem tissues of roots and cotyledonary leaves of *R. communis* seedlings, whereas no significant variations were recorded in the stem and primary leaves. Iron is essential in many of the vital processes of plants, including DNA synthesis, photosynthesis, respiration and nitrogen reduction (Rai *et al.*, 2021b). In photosynthesis and respiration, Fe serves as a critical cofactor for electron transport components in the chloroplast and mitochondrion (Rout and Sahoo, 2015). The crosstalk between Cu and Fe has been documented in many previous studies (Waters and Armbrust, 2013; Waters *et al.*, 2014; Rai *et al.*, 2021b). In order to prevent Cu mediated inhibition of photosynthesis and respiration, the entry and accumulation of Fe were promoted, which helps to alleviate Cu toxicity to some extent.

Similar to the distribution of Fe, Cl distribution was also significantly enhanced in the xylem tissues of roots and cotyledonary leaves of *R. communis* seedlings exposed to Cu stress. It can act as a cofactor for PSII and regulate the enzymes activities (Franco-Navarro *et al.*, 2021). Chlorine is a major osmotically active solute in the vacuole and activates tonoplast-V-type

H^+-ATPases, which helps to establish the proton gradient and thereby facilitates the turgor regulation and nutrient homeostasis (Raven, 2017). Due to the osmotic property of Cl^- ions, Cl accumulation resulted in the lowering of osmotic potential and increase in water contents of plants under stress (Koch *et al.*, 2021). The enhanced Cl distribution in *R. communis* seedlings will reduce the Cu induced osmotic and nutrient imbalances in the plant.

As B is an essential micronutrient and boric acid is a major component of the Hoagland nutrient medium, a basal level of B was observed in the xylem tissues throughout the plant. Though B is required for the normal growth and development of plants, its specific role in plant metabolism is still being debated (Lewis, 2019; Brdar-Jokanović, 2020). On exposure to Cu stress, B distribution was significantly reduced in the xylem tissues in all the parts of *R. communis* seedlings, except in the case of primary leaves, which might be due to the reduced root uptake of B due to Cu stress. Usually, the root uptake and transport of B were mediated by the regulation of the Major Intrinsic Protein (MIP) family (Matthes *et al.*, 2020; Pereira *et al.*, 2021). According to the observations of Ligaba *et al.* (2011), 0.2 mM $CuCl_2$down-regulated the transcript level of root MIP genes. This can be correlated with the reduced distribution of B in the root and cotyledonary leaves of *R. communis* seedlings. However, according to the observations of Chen *et al.* (2019), exogenous B has a stress alleviating role in rice plants exposed to Cd stress by improving the antioxidative potential and suppressing the metal uptake and transport. Since primary leaves experienced only mild stress effects, B distribution was significantly enhanced, which might help the primary leaves to tackle the stress situation.

5.8.2. Cytokinin mediated modulation of essential elemental distribution

The significant reductions observed in the distribution of C content in the xylem tissues of cotyledonary leaves of *R. communis* seedlings on

exposure to $CuSO_4$ were effectively recovered on exogenous application of cytokinins. This indicates the efficient CO_2 fixation and photosynthesis in the cotyledonary leaves, mediated by the cytokinins. According to the observations of Di Benedetto *et al.* (2015), exogenous application of BAP alone or in combination with IAA resulted in the enhanced carbon fixation and net photosynthetic rate in *Epipremnum aureum*.

Due to severe stress effects in the cotyledonary leaves, P content was drastically reduced in the xylem tissues of cotyledonary leaves upon exposure to $CuSO_4$. In contrast, the distribution was enhanced on application of cytokinins, most significantly in BAP treated cotyledonary leaves. Cytokinin mediated enhancement in P content helps the plant to counteract Cu stress effects *via* enhanced photosynthesis, respiration and activity of antioxidant enzymes. Wang *et al.* (2006) reported that exogenous cytokinins reversed the expression changes responsive to phosphate starvation along with the increases in the intracellular phosphate level, indicating the subtle interaction between cytokinin and phosphate signaling pathway.

On exposure to $CuSO_4$, Mg distribution became below detectable level in the xylem tissues of cotyledonary leaves, which was significantly enhanced on cytokinin treatments, with the highest enhancement in BAP treated cotyledonary leaves. The crosstalk between phytohormones and cell Mg levels was studied by Guo *et al.* (2015), and the authors recognized that some uncharted signal pathways from phytohormones are interconnected with Mg transporters in plants. This linkage may help the plant to recover the reduced Mg levels in the cotyledonary leaves of *R. communis* seedlings subjected to Cu stress and thereby help in enhancing the photosynthesis rate.

Due to the reduced Cu stress effects by the application of cytokinins, the enhanced Ca level was significantly reduced in both KIN and BAP applied cotyledonary leaves. On cytokinins application, the Cu-treated plants

experienced reduced oxidative stress. Therefore, the role of Ca signaling for stress tolerance was limited, resulting in reduced Ca distribution in the xylem tissues of cotyledonary leaves subjected to cytokinin application along with $CuSO_4$ treatment. Calcium-phytohormone crosstalk in plants under abiotic stress was very well reviewed by Aslam *et al.* (2021), but there is no clear evidence in the Ca-cytokinin crosstalk under heavy metal stress.

As an essential component of GSH and phytochelatins, the enhancement in the distribution of S was important for the efficient sequestration of heavy metals. Since phytohormone application reduced the metal uptake and translocation to the shoot, these metal sequestering proteins are less in use, which may be the reason for the reduced distribution of S in the xylem tissues of cotyledonary leaves applied with cytokinins. The interrelationship between S and phytohormones in *Arabidopsis* was studied by Maruyama-Nakashita *et al.* (2004), and they observed that cytokinins are believed to be involved in the negative regulation of S metabolism through the inhibition of sulphate transporter (*SULTR*) by cytokinin response 1/wooden leg/Arabidopsis histidine kinase 4 cytokinin receptor (*CRE1/WOL/AHK4*). Similar results were also observed by Werner *et al.* (2010). Because of these reasons, the distribution of S was significantly reduced in the cotyledonary leaves of *R. communis* seedlings during cytokinin application.

Due to the reduced Cu stress effects in the cotyledonary leaves on application of cytokinins, the distribution of Zn was decreased in the xylem tissues. On the other hand, Zn is an activator of several metabolic processes in plants, thereby offering resistance to the plant during Cu stress. Since the plant experienced least oxidative stress during cytokinin application, the accumulation of metabolites was drastically reduced; this in turn leads to less Zn in action. According to Krishna *et al.* (2020), the transporters included in

Zn-regulated Fe-regulated transporter-like proteins (*ZIP*) family are involved in the cellular uptake and transport of Zn in plants. Gao *et al.* (2019) reported that these ZIP family transporter genes are strictly controlled by cytokinins. The authors observed that the *ZIP* family transporter genes were down-regulated in cytokinin-depleted dominant mutant root enhancer1 (*ren1-D*) during Zn sufficient conditions, and therefore Zn uptake was regulated in a highly dynamic way in response to cytokinins and vice versa. Therefore, on exogenous application of cytokinins, the Zn uptake and transport were reduced significantly in the cotyledonary leaves of *R. communis* seedlings.

Similar to the distribution of Zn, the drastic increase in the distribution of Fe in the xylem tissues of cotyledonary leaves treated with $CuSO_4$ was reduced significantly upon exposure to cytokinins and reached to a level similar to that of control. Hindt and Guerinot (2012) reviewed the regulation of Fe homeostasis by cytokinin levels, and they observed that exogenous application of cytokinins resulted in the repression of the plasma-membrane divalent cation transporter *IRT1* (responsible for root Fe transport) and membrane-bound ferric chelate reductase *FRO2* (responsible for the reduction of Fe^{3+} to Fe^{2+}), both depend on cytokinin receptors. This might be the reason for reduced Fe distribution in the xylem tissues of cotyledonary leaves when exposed to cytokinins.

Similarly, the enhanced distribution of Cl was also reduced to a level as that of control when seedlings were exposed to exogenous application of cytokinins. According to Gurmani *et al.* (2011), the pre-treatment of rice seeds with BAP and ABA effectively regulated the Cl^- ions in the plants under salinity stress by efficient osmoregulation. The crosstalk of the Cl^- ions with leaf physiology, plant hormone signal transduction and photosynthesis in tobacco plants was studied by Wang *et al.* (2020), and the authors revealed that this crosstalk helps the plant in contributing towards abiotic stress

tolerance of plants. According to the observations of Li *et al.* (2016), the stelar localized transporter (Nitrate Transporter 1/Peptide Transporter family, NPF) proteins (an anion/H^+ co-transporter) mediates loading of Cl^- to the root xylem tissues. Wen *et al.* (2020) reported that exogenous application of BAP regulated the expression of this gene family. Therefore, the activity of cytokinins leads to a decrease in the transport of Cl^- to the stelar region and accordingly, a decrease in the distribution of Cl^- in cotyledonary leaves exposed to cytokinins was observed.

The considerable increase in the distribution of K content in the cotyledonary leaves upon exposure to $CuSO_4$ in the presence of cytokinins indicates the role of K in enhanced antioxidation mechanisms under Cu stress. Similarly, the enhanced K content also speeds up the cytokinin mediated stomatal responses, thereby accelerating CO_2 fixation and photosynthesis during Cu stress (Hu *et al.*, 2013). Further, the interaction between endogenous hormone biosynthesis and K^+ ions during environmental stresses was reviewed by Sardans and Peñuelas (2021). The authors concluded that wide arrays of K^+ functions are important for the stress responses in plants, which are performed by membrane K^+ transporters that act within a cascade of processes involving the control of gene transcription associated with the up and down-regulation of plant hormones.

The enhanced distribution of Si during exogenous application of cytokinins improves the resistance of the plant and gives mechanical strength to the plant. According to Hosseini *et al.* (2017, 2019), the crosstalk between Si and endogenous phytohormones, including iso-pentenyladenine (a cytokinin), enhanced the tolerance towards osmotic stress in *Hordeum vulgare* and *Zea mays* plants. According to the observations of Markovich *et al.* (2017), a strong positive correlation was observed between cytokinin and Si uptake in *Arabidopsis* and sorghum plants. Therefore, this interconnection

between Si and cytokinin may be the reason for the enhanced distribution of Si in the xylem tissues of cotyledonary leaves exposed to Cu stress and applied with cytokinins.

Copper stress mediated reduced uptake and distribution of B was effectively restored on exogenous application of cytokinins in the xylem tissues of cotyledonary leaves. According to the observations of Eggert and von Wirén (2017), the concentration of B in the shoot is strongly associated with cytokinins, and the B-dependent growth responses appeared to be initiated mainly by cytokinins, suggesting the nutritional status of B was strongly interconnected with cytokinins such as *cis*-zeatin and isopentenyladenine.

5.9. Leaf micromorphological characters

5.9.1. Effect of Cu on leaf micromorphological characters

Heavy metal stress frequently favours stomatal closure, which is one of the major limitations tophotosynthesis under heavy metal stress in plants (Sagardoy *et al.*, 2010). The disturbances in the stomatal opening and closing trigger enhanced production of ROS and inhibit the electron transport chain, and thereby reducing the plant metabolism (Hoque *et al.*, 2021). In the present study, the closure of stomata in the cotyledonary leaves on 6 d of exposure and primary leaves on 10 d of exposure to 200 µM $CuSO_4$ in *R. communis* seedlings would largely contribute to the reduced photosynthetic functions in these leaves. This metal-induced stomatal closure can be correlated with the reduced tissue water status during Cu stress. It may be induced by the direct interaction of metal ions with the guard cells or as an early impact of metal toxicity in the roots (Rucińska-Sobkowiak, 2016).

The complete closure of stomata in the adaxial surfaces of both cotyledonary and primary leaves is one of the primary responses of the plant

to the reduced water use efficiency, thereby preventing the transpirational loss of water. According to Gálusová *et al.* (2020), the reduction in the size of the stomata during heavy metal stress is to avoid further loss of water from the leaves. Moreover, heavy metals stimulate the accumulation of stress hormone ABA in the cells, and ABA mediates a series of signal cascades to regulate the stomatal aperture by guard cells and thereby reducing the transpirational loss of water (Bharath *et al.*, 2021). It was reported that *R. communis* plants have higher stomatal resistance during water-scarce situations, which is one of the drought tolerance mechanisms along with the early physiological reactions (Papazoglou *et al.*, 2020). This would ensure the increased resistance of the plant towards reduced tissue water status and help the plant to acclimatize the stress situations. Furthermore, the closing of the stomata during heavy metal stress resulted in reduced transpiration and hence reduced the translocation of toxic metal ions from roots to shoots (Shi *et al.*, 2019).

5.9.2. Impact of cytokinin on leaf micromorphological characters

Exogenous application of cytokinins resulted in the increase of the stomatal aperture in the cotyledonary leaves of *R. communis* seedlings exposed to $CuSO_4$ treatments. This may be one of the reasons for enhanced water use efficiency and photosynthesis in the cotyledonary leaves of *R. communis* during Cu stress, most significantly in BAP treated seedlings. In plants, endogenous cytokinins act as antagonists of ABA, leading to the increased stomatal conductance and modulation of leaf gas exchange (Hönig *et al.*, 2018). These results are also in agreement with the observations of Nguyen *et al.* (2021), wherein the authors proposed that the reduced level of cytokinins in plants due to the detrimental effect of metal stress can be recovered by external supplementation of cytokinins to the natural levels, which in turn help the plant to overcome the stress situation and recovery of photosynthesis. According to the observations of Ahanger *et al.* (2018),

application of KIN resulted in the enhanced uptake of K^+ and Ca^{2+} ions and increased K^+/Na^+ and Ca^{2+}/Na^+ ratios, thereby enhancing stomatal performance and maintenance of relative water content in *Solanum lycopersicum* exposed to NaCl stress. Similarly, Kamran *et al.* (2021) observed the enhancement of tissue water status by improved water and mineral uptake by roots and stomatal conductance on exogenous application of BAP in tomato plants exposed to Co stress. These findings were consistent with the present observation, in which exogenous application of KIN and BAP to the Cu-stressed *R. communis* seedlings resulted in the increase of stomatal aperture and thereby enhancing the tissue water status and photosynthesis.

5.10. Anatomical modifications

5.10.1. Impact of Cu on anatomical characters

Copper stress resulted in the severe damage of epidermal and cortical cells of roots in *R. communis* seedlings. This cellular degradation during heavy metal stress is associated with the prevention of the metal entry into shoots which is one of the tolerance mechanisms adopted by the plants during exposure to extreme stresses (Ren *et al.*, 2016). Similar to our results, Al faifi and El-Shabasy (2021) observed the degradation of cell wall materials of epidermis and cortex in the roots of *Cenchrus ciliaris* grown near a cement dust factory polluted with diverse heavy metals including Cu. Copper stress mediated changes in the number and size of the xylem vessels in the roots might be due to the Cu-mediated interferences in plant water relations, thereby reducing the tissue water status and moisture content in the shoots.

The significant enhancement in the thickness of xylem walls and the presence of clotted depositions in the xylem are indications for the sequestration of Cu^{2+} in the xylem walls of roots, which in turn prevent the

translocation of the toxic ions to the shoots. It was reported that cell walls are the major site of metal immobilization, in which the cell wall polysaccharides exhibit highest metal binding capacity (Chmielowska-Bąk and Deckert, 2021). During metal stress, as an adaptation, plants modulate the cell wall composition by increasing the polysaccharides pectins and callose levels, which consequently enhances the cell wall thickening, metal binding capacity and metal immobilization (Sarath *et al.*, 2022). Similar to the present study, Rucińska-Sobkowiak *et al.* (2013) observed the cell wall thickening and callose depositions in the vascular cylinder in lupin roots exposed to Pb stress. Similarly, Ca^{2+} modifies the physical properties of the cell wall by ionically interacting with pectin, most specifically in the unmethylated homogalacturonans (most abundant polymer of pectin, having –ve charge when unmethylated), resulting in the enhanced rigidity of the cell wall (Ochoa-Villarreal *et al.*, 2012; Thor, 2019). Therefore, the enhanced Ca distribution upon treatment with $CuSO_4$ is a clear evidence for the stress mediated enhancement in cell wall composition to enable the metal sequestration processes (Olmedo *et al.*, 2021; Wang *et al.*, 2021b). These results also indicate that the metal induced wall thickening and depositions may be responsible for the prevention of water diffusion from the apoplast that surrounds the xylem tissues. Also, the Cu accumulation in the xylem walls may also account for the reduced water flow to the shoot (discussed in section 5.2).

The highest enhancement in the xylem wall thickening was observed in the roots of *R. communis* subjected to Cu stress, along with higher distribution of Ca, as evidenced from the EDX results. The highest proportion of absorbed Cu in the cell wall fraction as observed in the subcellular distribution studies indicates the efficient sequestration of Cu ions in the root cell wall. The regulation of metal transport from root to shoot was reviewed in detail by Angulo-Bejarano *et al.* (2021), and they observed that, as the roots are the

first contact zone of heavy metals, significant anatomical changes can occur in the roots along with the efficient cell wall sequestration of the metal. Likewise, majority of the transported metal was sequestered in the cell walls of stem and a comparatively to a lesser extent in the leaves, which was evident from the analysis of the subcellular distribution of Cu. The enhanced synthesis of cell wall materials and associated thickening and metal sequestration to the cell wall was reviewed by Chmielowska-Bąk and Deckert (2021), and the authors observed that about 50-70% of the uptaken metal could sequester into the cell wall.

The variations in cell wall thickening are not limited to the root system but proceed up to the cell walls of stem in *R. communis* seedlings exposed to $CuSO_4$, as observed in the hypodermis as well as in the xylem tissues. The binding of the metal ions in the cell walls of stem prevents the further movement of ions to the leaf, thereby protecting the leaves from metal induced photosynthetic damages. The minor degradation of xylem tissues as observed in the SEM images of stem indicates metal induced autophagy, which is a biological self-destruction process to maintain the cellular homeostasis by engulfing of the damaged organelles into the vacuole during stress situations (Hasan *et al.*, 2017). The variations observed in the anatomy of cotyledonary and primary leaves of *R. communis* seedlings upon exposure to 200 μM $CuSO_4$ were the thickening of the xylem walls as well as the presence of clotted depositions, most evidently in the cotyledonary leaves.

5.10.2. Cytokinin mediated anatomical characters

Application of cytokinins reduced the Cu translocation from root to shoot, and therefore, the content of Cu was found in low concentrations in the cotyledonary leaves of seedlings subjected to both the cytokinin treatments, *i.e.*, 160 μM $CuSO_4$ + KIN and 160 μM $CuSO_4$ + BAP. Due to the reduced Cu translocation to the cotyledonary leaves upon cytokinins application, the need

for cell wall sequestration also gets reduced, which can be cited as the reason for decreased xylem wall thickness and reduced Ca distribution in cotyledonary leaves exposed to cytokinins. Since cytokinins have the capacity to bring about cell wall modifications, it would be an added advantage for metal binding. Kinetin mediated cell wall modification and changes in cell ultrastructure in wheat plants under salt stress were observed by Aldesuquy *et al.* (2014), this largely contributes towards the salt stress mitigation in wheat plants. Similarly, the phytohormone brassinosteroid mediated cell wall remodeling by the reorientation of cellulose microfibrils in plants under heavy metal stress was reported by Rao and Dixon (2017). Therefore, even the low level of metal taken up would be effectively sequestered and taken care.

5.11. GCMS analysis of bioactive compounds

5.11.1. Effect of Cu stress on the distribution of bioactive compounds

The GCMS analysis of the bioactive compounds revealed that both qualitative and quantitative variations were recorded in the root, cotyledonary and primary leaves of *R. communis* seedlings exposed to $CuSO_4$ as compared to that of the control. According to Janeeshma *et al.* (2021b), heavy metals elicit alterations in the composition of various bioactive compounds in plants. The enhanced biosynthesis and accumulation of various bioactive secondary metabolites in plants is a tolerance mechanism adopted by the plants during heavy metal stress (Anjitha *et al.*, 2021). Most of these secondary metabolites are phenolic or flavonoid compounds, having antioxidant properties (Karimi *et al.*, 2012; Anjitha *et al.*, 2021).

In the present study, the enhanced accumulation of a diterpene, neophytadiene, was observed in both cotyledonary and primary leaves upon exposure to $CuSO_4$ as compared to the control. According to the observations of Rani *et al.* (2021), the increased levels of terpenes, including

neophytadiene are the products of heavy metal stress related metabolism in plants, which help the plant to tolerate the higher concentrations of the metal. It was reported that the terpene synthase enzyme requires a divalent cation (Mg^{2+} or Mn^{2+} under normal conditions) as a co-factor for their optimal activity (Ashaari *et al.*, 2021). During low concentrations of Cu^{2+} ions, it becomes the co-factor for terpene synthase and enhances the biosynthesis of terpenes. In contrast, at higher concentrations of Cu^{2+}, the enzyme activity was interrupted (Hojati *et al.*, 2017). This may be the reason for the enhanced neophytadiene accumulation in both the cotyledonary and primary leaves where the Cu^{2+} level was less, and the reduced accumulation in the roots of *R. communis* where the Cu^{2+} level was high.

On exposure to $CuSO_4$, the composition of (E)-phytol was significantly enhanced in the cotyledonary leaves as compared to the control, along with the accumulation of a phytol, 2-hexadecen-1-ol, 3,7,11,15-tetramethyl-, [R-[R*,R*-(E)]]- and phytol acetate. Since phytol is an isoprenoid alcohol bound with chlorophyll molecule *via* ester linkage, the degradation of chlorophyll results in the accumulation of phytol and its derivatives in the cells (Gutbrod *et al.*, 2021). In the present study, Cu resulted in the early senescence of the cotyledonary leaves, which in turn induces the degradation of chlorophyll molecules and the concomitant accumulation of various phytol derivatives in these leaves. But in the case of primary leaves, less accumulation of phytol derivatives was observed during Cu stress, as compared to that of the cotyledonary leaves. The results indicate that Cu mediated chlorophyll destruction was most prominent in the cotyledonary leaves, and they act as a shield to protect the primary leaves from Cu induced chlorophyll degradation.

Ricinus communis leaves are rich source of lupeol (a pentacyclic triterpenoid) accumulating as a predominant constituent having anti-inflammatory properties (Li *et al.*, 2021c; Liu *et al.*, 2021). But, the large

proportion of lupeol present in the primary leaves of control was drastically reduced on exposure to $CuSO_4$. According to the observations of Rogowska and Szakiel (2021), during stress situations, the biosynthetic pathways of triterpenoids and sterols get changed significantly. This might be the reason for reduced lupeol in primary leaves of *R. communis* seedlings treated with $CuSO_4$.

Fatty acids have multiple roles in plant heavy metal stress tolerance (He and Ding 2020). Significant enhancement in the distribution of fatty acids such as cis-vaccenic and hexadecanoic acids and reductions in the distribution of fatty acid methyl esters such as methyl palmitate and methyl stearate were observed in the roots of *R. communis* seedlings upon exposure to $CuSO_4$. According to the studies conducted by Elloumi *et al.* (2014), a significant alteration in the fatty acid composition was observed in *Prunus dulcis* exposed to Cd, and the authors concluded that these variations were related to the extent of membrane lipid peroxidation in the plant. Similar variations in the relative abundance of fatty acids and their derivatives were observed in the roots of *Zea mays* under Cu stress (Chaffai *et al.*, 2009). Cadmium induced suppression of fatty acid metabolism in the roots of *Sedum plumbizincicola* was reported by Sun *et al.* (2020). Therefore, the significant enhancement in the distribution of fatty acids most severely in the roots of *R. communis* seedlings indicates the extent of lipid peroxidation due to Cu stress in the roots.

5.11.2. Impact of cytokinins on Cu stress induced alterations in bioactive compounds

Significant changes in the distribution of the bioactive compounds were observed in the cotyledonary leaves of *R. communis* seedlings subjected to Cu stress on application of KIN and BAP. The enhanced accumulation of phytol acetate and isophytol acetate during Cu stress was effectively reduced

on exogenous application of BAP, indicating the BAP-mediated regulation of chlorophyll destruction in these leaves. But, the higher proportion of phytol and its derivatives in the cotyledonary leaves, even in the presence of KIN, indicates application of KIN was not capable of preventing Cu-induced chlorophyll degradation.

3,7,11,15-tetramethyl-2-hexadecen-1-ol is a tocopherol biosynthesis intermediate, and the proportion of the same was increased in cotyledonary leaves on cytokinin application, indicating cytokinin mediated tocopherol biosynthesis during Cu stress. According to the observations of Ali *et al.* (2020), tocopherols can improve the heavy metal stress tolerance in *Brassica napus*. Due to the presence of an increased proportion of lupeol and lup-20(29)-en-3-yl acetate in seedlings subjected to 160 µM $CuSO_4$ along with BAP, other compounds were detected in the least proportion. These compounds exhibit a broad spectrum of biological properties, and the antioxidant activity of the same was described in several plants (Gallo and Sarachine 2009; Lalthanpuii and Lalchhandama 2020). Other plant growth regulators like auxin could also mediate the enhancement in lupeol synthesis in *R. communis* seedlings (Li *et al.*, 2021c).

5.12. Fourier Transform Infrared (FTIR) spectroscopic analysis

5.12.1. Variation in functional groups of cell wall materials during Cu stress

As mentioned in the subcellular distribution studies (section 5.7.1.), Cu was mainly accumulated in the cell wall of different organs in the *R. communis* seedlings. The functional groups associated with polysaccharides (including cellulose, hemicelluloses, and pectin) and proteins in the cell wall serve as binding and adsorption sites for heavy metals before they are crossing the cell membrane (He *et al.*, 2020a). The characteristic functional

groups associated with cell wall materials were identified by FTIR analysis. Though the shape of the FTIR spectral peaks of the various plant parts of Cu treated and control was structurally the same, characteristic peaks were observed at different wavenumbers. Peak No. 1 (at 3397 cm^{-1}) and 2 (at 2923 cm^{-1}) represent the stretching vibration associated with the celluloses, hemicelluloses, polysaccharides and proteins corresponding to the –OH and –COOH groups (Thakur *et al.*, 2018). It was reported that major Cu binding sites in the cell wall are functional groups (hydroxyl and carboxyl) associated with polysaccharides, cellulose, and hemicellulose in *Bruguiera cylindrica* (Sruthi and Puthur, 2019). These hydroxyl and carboxyl groups act as chemisorbing complexes, which binds to the metal ion, forming stable complexes (Kang *et al.*, 2015). Therefore, the results indicate that these hydroxyl and carboxyl groups of the cell wall compounds can act as principal Cu binding sites and have significant roles in Cu sequestration in *R. communis* seedlings subjected to $CuSO_4$ treatments.

Peak No. 3 (at 1635 cm^{-1}) represents the N–H bending vibration and C=O stretching vibration of peptides present in the cell wall materials (Chutia *et al.*, 2013). The spectral shifting and reduced intensity of the peak during Cu stress were due to the interaction of metal ions with the O and N atoms of the cell wall protein. Similar results were observed by Alhazmi (2019), wherein the author allowed the heavy metal to interact with bovine serum albumin at physiological pH, and the FTIR spectroscopic screening indicates that metal binding resulted in the spectral shifting of the peak between 1700-1600 cm^{-1}. Similar to our results, He *et al.* (2020a) observed that the functional groups –OH, –NH, –CN and –COOH associated with the cell wall materials provide the major binding sites for Cd and Zn stress in *R. communis* seedlings.

Peak No. 4 (at 1385 cm^{-1}) represents the C-H symmetric bending vibration in terminal methyls. The significant vibration enhancement at peak

No. 4 was due to the increase in the methylation and accumulation of peroxidation products of aliphatic ketones formed due to Cu stress (Xue *et al.*, 2011), which was similar in the roots, cotyledonary and primary leaves. Even though Cu accumulation in primary leaves was comparatively lesser than in cotyledonary leaves, the sequestration or detoxification of Cu in cell walls was as efficient and followed the same mechanism as in cotyledonary leaves.

5.12.2. Cytokinin mediated variation in functional groups of cell wall materials

The occurrence of a strong peak at 3397 (peak No. 1) and 2923 cm^{-1} (peak No. 2) in cytokinin treated cotyledonary leaves of seedlings as compared to that of the seedlings exposed to Cu stress alone denotes the cytokinin mediated synthesis of cell wall polysaccharides during Cu stress. This resulted in higher sequestration of Cu^{2+} ions to the cell walls in the cotyledonary leaves of cytokinin treated seedlings.

The deep peak observed in peak No. 3 (at 1635 cm^{-1}) of the cytokinin treated cotyledonary leaves and its spectral shift indicates the enhanced cell wall peptide synthesis during Cu stress. The significant sharpness at peak No. 4 (at 1385 cm^{-1}) in Cu stressed seedlings was due to the methylation and accumulation of peroxidation products during stress (Xue *et al.*, 2011). Due to the effective ROS scavenging by exogenous cytokinins *via* modulation of the antioxidation machinery, the accumulation of peroxidation products reduced significantly in the cotyledonary leaves of *R. communis* seedling, which was reflected in the reduced peak intensity.

SUMMARY AND CONCLUSIONS

Heavy metal tolerance potential of a non-edible bioenergy plant – *R. communis* L. (castor oil plant) was evaluated under hydroponic culture conditions with special reference to $CuSO_4$. The seedlings raised from the castor seeds in sterilized sand were grown in modified Hoagland nutrient medium. The seedlings with a growth period of 30 d (after complete emergence of the first pair of primary leaves) were treated with varying concentrations of $CuSO_4$ solution (40, 80, 120, 160 and 200 μM) prepared in quarter strength modified Hoagland nutrient medium for 10 d. The plants growing in quarter strength Hoagland medium without any metal treatment served as the control. Analyses of various functional and structural aspects in the roots, cotyledonary and primary leaves were carried out on alternate days of $CuSO_4$ exposure up to 10 d. In the case of cotyledonary leaves, the abscission occurs after 6 d at higher concentrations of Cu stress (120, 160 and 200 μM $CuSO_4$), and therefore, Cu toxicity symptoms and tolerance mechanisms were analyzed up to 6 d of treatment in the case of cotyledonary leaves.

From the different concentrations of $CuSO_4$ analyzed, one mild and one severe stress concentrations (80 and 160 μM $CuSO_4$ respectively) were selected to determine the stress ameliorative effects of two different cytokinins [kinetin (KIN) and 6-benzylaminopurine (BAP)]. 80 and 160 μM $CuSO_4$ treated *R. communis* seedlings were applied with standardized concentration (15 μM) of KIN and BAP (prepared in 0.1% teepol as the surfactant) as foliar spray. The control plants were treated with 0.1% teepol prepared in water. Analyses of various functional and structural aspects in the cotyledonary leaves were performed on 6 d of $CuSO_4$ and cytokinin

treatments to analyze the Cu-stress ameliorative effects of KIN and BAP in *R. communis* seedlings.

Major conclusions derived from the present study are summarized below:

- Due to the stress shielding effects of cotyledonary leaves towards primary leaves, the toxicity symptoms induced by Cu, such as oxidative stress and photosynthetic damages were least in primary leaves in the presence of cotyledonary leaves (up to 6 d of Cu stress), and accordingly, cotyledonary leaves receive the initial brunt of Cu stress. However, toxicity symptoms were developed in the primary leaves after the Cu-induced abscission of cotyledonary leaves.

- Copper stress significantly reduced the tissue water status, thereby enhancing DW% in the leaves and roots of *R. communis* seedlings. This is a common feature in plants exposed to heavy metal stress as the metal interferes with the xylem transport and eventually on other metabolic processes. Upon application of cytokinins, the tissue water status was regained to normal conditions in cotyledonary leaves, and this would ensure prolonged photosynthetic functions in cotyledonary leaves even under Cu stress and would immensely help in the seedling establishment.

- Photosystem activities were extremely sensitive to Cu even at concentrations of mild stress, which was resulted from the inhibition of photosynthetic machinery most significantly in the cotyledonary leaves, due to the extensive degradation of photosynthetic pigments, restricted stomatal opening and the functional impairment of PSII activity, including the reduced energy flux parameters, inefficiency in the electron transport and water-splitting complex. The increased

chlorophyll degradation in cotyledonary leaves during Cu stress contributes significantly towards the decrease of CSI in these leaves.

- Application of cytokinin maintained the photosynthetic efficiency of cotyledonary leaves of *R. communis* more necessarily during BAP application by improving the pigment content, preventing stomatal closure, maintaining the efficiency of photosystems and electron transport activities. This was confirmed by analyzing the OJIP transient curve and other fluorescence parameters, which are used to assess the stress intensity and the tolerance potential of *R. communis* in the presence and absence of exogenous phytohormones.

- The cellular ROS homeostasis was profoundly unbalanced due to higher Cu^{2+} in the cytoplasm, which resulted in severe oxidative burst and membrane damage. This cellular membrane damage was reflected in the accumulation of MDA content, reduced MSI and enhanced EL% in the leaves and roots of *R. communis* seedlings.

- Cytokinin application mitigated the Cu-induced oxidative stress by regulating the over-accumulation of ROS molecules and preventing membrane degradation and electrolyte leakage, which was ascribed to the recoupment of the integrated network of antioxidation mechanisms.

- Exposure to $CuSO_4$ caused prominent alterations in the metabolic dynamism and osmotic adjustment in *R. communis* seedlings. The enhanced accumulation of primary metabolites in the leaves would be a conducive environment for converting one form of metabolite to the other to suit the stress situation and help to counter oxidative stress. In contrast, the reduced accumulation of metabolites in the roots indicates the extreme stress effects encountered by the roots, which resulted in the inhibition of metabolic processes.

- The enhanced accumulation of protein content in both the cotyledonary and primary leaves on initial days of $CuSO_4$ exposure would be largely contributed from the enhanced synthesis of stress proteins such as phytochelatins and metallothioneins, heat shock proteins and enzymes involved in the antioxidant defence mechanisms; all of which contributes towards the protection of the plant from the metal induced damages as an immediate effect of heavy metal toxicity in plants. But, the significant reduction in protein content in the leaves during the later stages of Cu stress denoted the interferences that occurred in the biosynthetic processes of protein due to severe stress effects.

- As cytokinins are the master regulators of plant growth and development and can link external signals and internal metabolic processes, the enhanced accumulation of metabolites in the cotyledonary leaves of *R. communis* seedlings subjected to Cu stress was reverted to a level similar to that of control upon exposure to cytokinins.

- Due to the reduced tissue water status, the cotyledonary leaves experience higher osmotic stress and lowering of solute potential. But, the accumulation of the metabolite aids to cope up with the cell osmoticum and assist in lowering of osmotic potential to maintain the osmotic balance of the cell and keep up the cell water status under stress.

- Copper-induced ROS accumulation and oxidative stress elicited the activation of antioxidant enzymes and accumulation of non-enzymatic antioxidants in the leaves and roots of *R. communis* seedlings indicating that well-organized antioxidant machinery is operational in this plant during heavy metal stress, and the integrated network of these antioxidants contribute towards the detoxification of ROS

molecules. But these elevated antioxidation mechanisms could not successfully counteract the ROS-induced photosynthetic damage in cotyledonary leaves. The reduced accumulation of these antioxidants in the roots indicated the extreme stress experienced in the roots.

- The enhanced AsA in the leaves acted as an alternative electron donor of PSII and also helped to regulate the signal transduction pathways and protect the photosynthetic machinery during Cu stress in *R. communis*. The reduced accumulation of AsA in the roots could be correlated to the enhanced activity of APX, and the enhanced MDHAR and DHAR activities may not be sufficient to restore the AsA in the roots.

- Exogenous application of cytokininsefficiently enhanced the antioxidative defence mechanisms in the cotyledonary leaves of *R. communis* exposed to Cu stress, which resulted in the effective alleviation of oxidative stress. Reduced accumulation of antioxidants such as GSH and phenolic compounds to a level similar to that of the control in the cotyledonary leaves during cytokinin application could be justified with the enhanced stress alleviation of cytokinins by increased antioxidant enzyme activities and less demand for non-enzymatic antioxidants to be in action. Therefore, cytokinins acted as oxidative stress alleviators and membrane stabilizers.

- The bioaccumulation pattern of Cu revealed that major part of the uptaken Cu was retained in the root itself, and only a small portion was found to be transported to the aerial parts. This reflects the phytostabilization property with low TF and the effective tolerance mechanism of the plant. The TF value for cotyledonary leaves was twice higher than the primary leaves, indicating the effective translocation of toxic levels of Cu into the former, and therefore the

latter was kept unhampered and thereby maintained the normal photosynthetic and metabolic processes in the presence of cotyledonary leaves.

- On exogenous application of cytokinins, entry of Cu was strongly restricted to the shoot, as evidenced by the lower Cu bioaccumulation and TF values in the cotyledonary and primary leaves subjected to KIN or BAP along with 80 and 160 µM $CuSO_4$, which was more apparent on BAP application.

- The subcellular distribution studies of Cu indicated that the major detoxification mechanism operational in *R. communis* is the cell wall sequestration, thereby restricting the entry of toxic levels of Cu^{2+} into the cytoplasm. This might be one of the tolerance strategies adopted by the plant in order to keep the photosynthetic machinery undisturbed. After the cell wall, the vacuoles acted as the preferential site for Cu sequestration, which was evident from the ICPMS analysis of the subcellular fractions of the plant.

- The disturbances in the distribution of nutrient elements found in the xylem tissues of *R. communis* were largely due to the competition of Cu^{2+} with the nutrient elements for binding sites of the transporter proteins. The increased Ca distribution observed during Cu stress in the xylem tissues confirms its role in stomatal closure, thereby preventing excess water loss. Moreover, the significant enhancement in Ca distribution in the cotyledonary leaves may be correlated with enhanced antioxidation mechanisms in these leaves, which may be developed from the activation of Ca-dependent gene expression of antioxidant proteins.

- The drastic increase in K distribution during Cu stress is correlated with significant enhancement in metabolite accumulation and antioxidant activities in the cotyledonary leaves, indicating the role played by K in maintaining the osmotic potential and oxidative stress respectively, and thereby improved the stress tolerance potential of the plant. Similarly, enhanced S distribution in the roots and cotyledonary leaves can be correlated with enhanced GSH levels in these organs, indicating the chelation of Cu^{2+}.

- Maintenance of the distribution of essential elements in the cotyledonary leaves on cytokinin application indicated the cytokinin mediated enhanced nutrient uptake as well as reduced oxidative stress during Cu stress.

- Closure of stomata during Cu stress increases the tolerance of the plant towards reduced tissue water status and helps the plant to acclimatize the stress situations. Furthermore, stomatal closure resulted in reduced transpiration and hence reduced the translocation of Cu^{2+} from roots to shoots. During exogenous application of cytokinins, the stomatal aperture was increased and thereby enhanced the tissue water status and photosynthesis.

- Degradation of epidermal and cortical cells in the roots of *R. communis* during exposure to $CuSO_4$ is associated with the prevention of Cu^{2+} entry into shoots which is one of the tolerance mechanisms adopted by the plant during exposure to extreme stress.

- The enhanced cell wall thickness, increased distribution of Ca in the xylem walls and higher proportion of accumulated Cu in the cell wall fraction, indicates the crucial role of cell wall in Cu sequestration.

- Due to the reduced Cu translocation to the cotyledonary leaves upon cytokinins application, the need for cell wall sequestration also gets reduced, which can be cited as the reason for decreased xylem wall thickness and reduced Ca distribution in cotyledonary leaves exposed to cytokinins.

- The reduced accumulation of neophytadiene in the roots resulted from terpene synthase inactivation due to higher concentration of Cu^{2+} in the roots. Meanwhile, the proportion of this terpene was enhanced in the cotyledonary and primary leaves at low Cu^{2+} levels, which may be due to the role played by Cu^{2+} for the activation of terpene synthase as the co-factor.

- The enhanced accumulation of phytol derivatives and Cu-induced early senescence of cotyledonary leaves was due to the degradation of chlorophyll molecules in these leaves, which in turn protect the primary leaves from the stress effects of Cu as indicated in the comparatively reduced distribution of phytol derivatives in the primary leaves.

- The reduced accumulation of phytol and its derivatives in the cotyledonary leaves during BAP application and the insignificant changes on KIN application along with Cu-stress indicated that application of KIN was not capable of protecting Cu-induced chlorophyll destruction.

- The FTIR spectral analysis of the cell wall fraction revealed that the hydroxyl and carboxyl groups associated with polysaccharides and proteins of the cell wall materials acted as the chemisorbing complexes, which confirmed the role of the cell wall in Cu sequestration. Similarly, the C-H bending vibration (at 1385 cm^{-1})

represents the accumulation of peroxidation products of aliphatic ketones formed due to Cu stress. Even though Cu bioaccumulation in primary leaves was comparatively lesser than in cotyledonary leaves, the sequestration or detoxification of Cu in cell walls was as efficient and followed the same mechanism as in cotyledonary leaves.

- The occurrence of a strong peak at 3397 and 2923 cm^{-1} during cytokinin application denoted the cytokinin mediated enhancement in the synthesis of cell wall polysaccharides in the cotyledonary leaves, which can ensure enhanced sequestration of Cu^{2+} to the cell walls. Cytokinin application also resulted in reduced peak intensity at 1385 cm^{-1} indicating the reduced accumulation of peroxidation products, which can be attributed to the effective ROS scavenging by exogenous cytokinins *via* modulation of the antioxidation machinery.

As per the findings, *R. communis* could withstand higher levels of Cu by modulating the antioxidation machinery and osmotic adjustment, and allocating the translocated Cu^{2+} more into the cotyledonary leaves, thereby favorably modulating the photosynthetic efficiency in primary leaves. This result suggested that cotyledonary leaves have got the potential to evade Cu toxicity and have an efficient buffering action towards the primary leaves during stress. The enhanced enzymatic and non-enzymatic antioxidant system could successfully scavenge the ROS molecules, leading to reduced oxidative damage in primary leaves. The enhanced synthesis of cell wall polysaccharides and pectic compounds helps in efficient sequestration of metal ions in the cell wall, thereby preventing the presence of free toxic ions in the cytoplasm. This integrated networking of multiple stress response processes could ensure enhanced Cu stress tolerance in *R. communis*.

Ricinus communis plants could tolerate Cu-induced oxidative stress on application of exogenous cytokinins, which assisted in restoring cellular redox

status in the cotyledonary leaves. Furthermore, the photosynthetic efficiency was improved by efficient antioxidation systems, decreased ROS generation, and effective stomatal responses, ensuring the amelioration of Cu toxicity in these leaves. This antisenescing function of cytokinins helps the plant in the establishment of seedlings exhibiting profused growth under adverse environmental conditions. It was also observed that BAP was found to be more efficient than KIN in preventing Cu-induced early abscission and keeping the cotyledonary leaves photosynthetically active. As a result, exogenous application of BAP can be utilized as an effective strategy to increase the tolerance potential with fewer toxicity symptoms in hyperaccumulator plants. Furthermore, the exploitation of the molecular means associated with Cu-stress amelioration by BAP will be helpful to develop transgenic plants with the potential to overproduce cytokinins, which might be a more effective technique in ameliorating Cu stress.

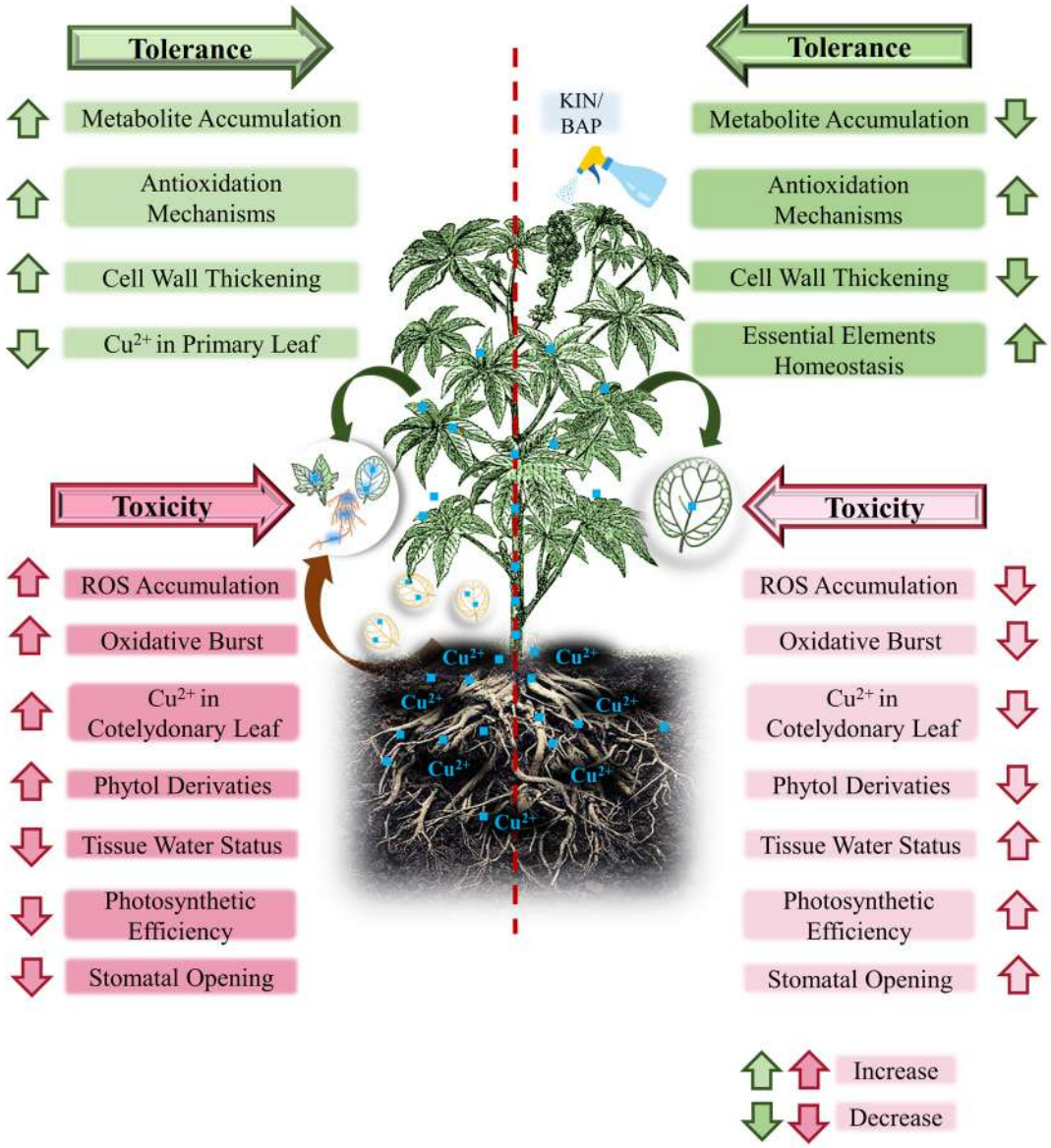

SUMMARY OF THE WORK

REFERENCES

Abdel Latef, A. A. H., Zaid, A., Abo-Baker, A. B. A. E., Salem, W. and Abu Alhmad, M. F. (2020). Mitigation of copper stress in maize by inoculation with *Paenibacillus polymyxa* and *Bacillus circulans*. *Plants*, 9(11), 1513.

AbdElgawad, H., Zinta, G., Hamed, B. A., Selim, S., Beemster, G., Hozzein, W. N., Wadaan, M. A. M., Asard, H. and Abuelsoud, W. (2020). Maize roots and shoots show distinct profiles of oxidative stress and antioxidant defense under heavy metal toxicity. *Environmental Pollution*, 258, 113705.

Abdelsalam, I. M., Elshobary, M., Eladawy, M. M. and Nagah, M. (2019). Utilization of multi-tasking non-edible plants for phytoremediation and bioenergy source - A review. *Phyton*, 88(2), 69.

Abdulmajeed, A. M., Alnusairi, G. S., Alharbi, M. H., Almushhin, A., Hasan, M. M. and Soliman, M. H. (2021). Alleviation of copper phytotoxicity by acetylsalicylic acid and nitric oxide application in mung bean involves the up-regulation of antioxidants, osmolytes and glyoxalase system. *Journal of Plant Interactions*, 16(1), 201-212.

Abhilash, P. C., Powell, J. R., Singh, H. B. and Singh, B. K. (2012). Plant microbe interactions: Novel applications for exploitation in multipurpose remediation technologies. *Trends in Biotechnology*, 30, 416-420.

Abioye, O. P., Ijah, U. J. J. and Aransiola, S. A. (2017). Phytoremediation of soil contaminants by the biodiesel plant *Jatropha curcas*. In: *Phytoremediation Potential of Bioenergy Plants*, Bauddh, K., Singh, B. and Korstad, J. (Eds.), Springer, Singapore, pp. 97-137.

Acidri, R., Sawai, Y., Sugimoto, Y., Handa, T., Sasagawa, D., Masunaga, T., Yamamoto, S. and Nishihara, E. (2020). Exogenous kinetin promotes the nonenzymatic antioxidant system and photosynthetic activity of coffee (*Coffea arabica* L.) plants under cold stress conditions. *Plants*, 9, 281.

Adejumo, S. A., Oniosun, B., Akpoilih, O. A., Adeseko, A. and Arowo, D. O. (2021). Anatomical changes, osmolytes accumulation and distribution in the native plants growing on Pb-contaminated sites. *Environmental Geochemistry and Health*, 43(4), 1537-1549.

Agami, R. A. (2016). Pre-soaking in indole-3-acetic acid or spermidine enhances copper tolerance in wheat seedlings. *South African Journal of Botany*, 104, 167-174.

Agency for Toxic Substances and Disease Registry (ATSDR) (2020). *Toxicological Profile for Lead (Draft for Public Comment)*. Department of Health and Human Services Atlanta, GA, USA, p. 582.

Ager, F. J., Ynsa, M. D., Dominguez-Solis, J. R., Gotor, C., Respaldiza, M. A. and Romero, L. C. (2002). Cadmium localization and quantification in the plant *Arabidopsis thaliana* using micro-PIXE. *Nuclear Instruments and Methods in Physics Research Section B*, 189, 494-98.

Ahammed, G. J., Choudhary, S. P., Chen, S., Xia, X. J., Shi, K., Zhou, Y. H. and Yu, J. Q. (2013). Role of brassinosteroids in alleviation of phenanthrene - methylation and chromatin patterning cadmium co-contamination-induced photosynthetic inhibition and oxidative stress in tomato. *Journal of Experimental Botany*, 64, 199-213.

Ahanger, M. A., Alyemeni, M. N., Wijaya, L., Alamri, S. A., Alam, P., Ashraf, M. and Ahmad, P. (2018). Potential of exogenously sourced kinetin in protecting *Solanum lycopersicum* from NaCl-induced oxidative stress through up-regulation of the antioxidant system, ascorbate-glutathione cycle and glyoxalase system. *PLoS One*, 13(9), e0202175.

Ahmad, P., Abdel Latef, A. A., Abd_Allah, E. F., Hashem, A., Sarwat, M., Anjum, N. A. and Gucel, S. (2016a). Calcium and potassium supplementation enhanced growth, osmolyte secondary metabolite production, and enzymatic antioxidant machinery in cadmium-exposed chickpea (*Cicer arietinum* L.). *Frontiers in Plant Science*, 7, 513.

Ahmad, P., Abdel Latef, A. A., Hashem, A., AbdAllah, E. F., Gucel, S. and Tran, L. S. P. (2016b). Nitric oxide mitigates salt stress by regulating levels of osmolytes and antioxidant enzymes in chickpea. *Frontiers in Plant Science*, 7, 347.

Ahmad, S. and Guo, Y. (2019). Signal transduction in leaf senescence: Progress and perspective. *Plants*, 8(10), 405.

Akhtar, F. Z., Archana, K. M., Krishnaswamy, V. G. and Rajagopal, R. (2020). Remediation of heavy metals (Cr, Zn) using physical, chemical and biological methods: A novel approach. *SN Applied Sciences*, 2, 267.

Al faifi, T. and El-Shabasy, A. (2021). Effect of heavy metals in the cement dust pollution on morphological and anatomical characteristics of *Cenchrus ciliaris* L. *Saudi Journal of Biological Sciences*, 28(1), 1069-1079.

Alam, P., Albalawi, T. H., Altalayan, F. H., Bakht, M. A., Ahanger, M. A., Raja, V., Ashraf, M. and Ahmad, P. (2019). 24-Epibrassinolide (EBR) confers tolerance against NaCl stress in soybean plants by up-regulating antioxidant system, ascorbate-glutathione cycle, and glyoxalase system. *Biomolecules*, 9, 640.

Aldesuquy, H., Baka, Z. and Mickky, B. (2014). Kinetin and spermine mediated induction of salt tolerance in wheat plants: Leaf area, photosynthesis and chloroplast ultrastructure of flag leaf at ear emergence. *Egyptian Journal of Basic and Applied Sciences*, 1(2), 77-87.

Ale, S., Femeena, P. V., Mehan, S. and Cibin, R. (2019). Environmental impacts of bioenergy crop production and benefits of multifunctional bioenergy systems. In: *Bioenergy with Carbon Capture and Storage: Using Natural Resources for Sustainable Development*, Pires, J. C. M. and Gonçalves, A. L. C. (Eds.), Academic Press, Elsevier, Cambridge, United States, pp. 195-217.

Alhazmi, H. A. (2019). FTIR spectroscopy for the identification of binding sites and measurements of the binding interactions of important metal ions with bovine serum albumin. *Scientia Pharmaceutica*, 87(1), 5.

Ali, B., Hasan, S. A., Hayat, S., Hayat, Q., Yadav, S., Fariduddin, Q. and Ahmad, A. (2008). A role for brassinosteroids in the amelioration of aluminium stress through antioxidant system in mung bean (*Vigna radiata* L. Wilczek). *Environmental and Experimental Botany*, 62, 153-159.

Ali, E., Hassan, Z., Irfan, M., Hussain, S., Rehman, H. U., Shah, J. M. and Ali, S. (2020). Indigenous tocopherol improves tolerance of oilseed rape to cadmium stress. *Frontiers in Plant Science*, 1536.

Ali, H. and Khan, E. (2018). What are heavy metals? Long-standing controversy over the scientific use of the term 'heavy metals' - proposal of a comprehensive definition. *Toxicological and Environmental Chemistry*, 100(1), 6-19.

Ali, H., Khan, E. and Ilahi, I. (2019). Environmental chemistry and ecotoxicology of hazardous heavy metals: Environmental persistence, toxicity and bioaccumulation. *Journal of Chemistry*, 2019, 6730305.

Ali, H., Khan, E. and Sajad, M. A. (2013). Phytoremediation of heavy metals - concepts and applications. *Chemosphere*, 91(7), 869-881.

Ali, N. and Hadi, F. (2018). CBF/DREB transcription factor genes play role in cadmium tolerance and phytoaccumulation in *Ricinus communis* under molybdenum treatments. *Chemosphere*, 208, 425-432.

Allamin, I. A., Halmi, M. I. E., Yasid, N. A., Ahmad, S. A., Abdullah, S. R. S. and Shukor, Y. (2020). Rhizodegradation of petroleum oily sludge-contaminated soil using *Cajanus cajan* increases the diversity of soil microbial community. *Scientific Reports*, 10(1), 1-11.

Allan, J. E. (1969). The preparation of agricultural samples for analysis by atomic absorption spectrometry, *Varian Techtron Bulletin*, 12-69.

Almehdi, A., El-Keblawy, A., Shehadi, I., El-Naggar, M., Saadoun, I., Mosa, K. A. and Abhilash, P. C. (2019). Old leaves accumulate more heavy metals than other parts of the desert shrub *Calotropis procera* at a traffic-polluted site as assessed by two analytical techniques. *International Journal of Phytoremediation*, 21(12), 1254-1262.

Alqarawi, A. A., Abd Allah, E. F. and Hashem, A. (2014). Alleviation of salt-induced adverse impact *via* mycorrhizal fungi in *Ephedra aphylla* Forssk. *Journal of Plant Interactions*, 9(1), 802-810.

Altaf, R., Altaf, S., Hussain, M., Shah, R. U., Ullah, R., Ullah, M. I., Rauf, A., Ansari, M. V., Alharbi, S. A., Alfarraj, S. and Datta, R. (2021). Heavy metal accumulation by roadside vegetation and implications for pollution control. *PLoS One*, 16(5), e0249147.

Altangerel, N., Ariunbold, G. and Gorman, C. (2017). In vivo diagnostics of early abiotic plant stress response *via* Raman spectroscopy. *Proceedings of the National Academy of Sciences of the United States of America*, 114, 3393-3396.

Amri, B., Khamassi, K., Ali, M. B., da Silva, J. A. T. and Kaab, L. B. B. (2016). Effects of gibberellic acid on the process of organic reserve mobilization in barley grains germinated in the presence of cadmium and molybdenum. *South African Journal of Botany*, 106, 35-40.

Angulo-Bejarano, P. I., Puente-Rivera, J. and Cruz-Ortega, R. (2021). Metal and metalloid toxicity in plants: An overview on molecular aspects. *Plants*, 10(4), 635.

Anjitha, K. S., Sameena, P. P. and Puthur, J. T. (2021). Functional aspects of plant secondary metabolites in metal stress tolerance and their importance in pharmacology. *Plant Stress*, 2, 100038.

Anjum, N. A., Gill, S. S., Gill, R., Hasanuzzaman, M., Duarte, A. C., Pereira, E., Ahmad, I., Tuteja, R. and Tuteja, N. (2014). Metal/metalloid stress tolerance in plants: Role of ascorbate, its redox couple, and associated enzymes. *Protoplasma*, 251(6), 1265-1283.

Anjum, N. A., Hasanuzzaman, M., Hossain, M. A., Thangavel, P., Roychoudhury, A., Gill, S. S., Rodrigo, M. A. M., Adam, V., Fujita, M., Kizek, R., Duarte, A. C., Pereira, E. and Ahmad, I. (2015). Jacks of metal/metalloid chelation trade in plants - An overview. *Frontiers in Plant Science*, 6, 192.

Anjum, N. A., Sharma, P., Gill, S. S., Hasanuzzaman, M., Khan, E. A., Kachhap, K., Mohamed, A. A., Thangavel, P., Devi, G. D., Vasudhevan, P., Sofo, A., Khan, N. A., Misra, A. N., Lukatkin, A. S., Singh, H. P., Pereira, E. and Tuteja, N. (2016b). Catalase and ascorbate peroxidase - representative H_2O_2-detoxifying heme enzymes in plants. *Environmental Science and Pollution Research*, 23(19), 19002-19029.

Anjum, S. A., Tanveer, M., Hussain, S., Shahzad, B., Ashraf, U., Fahad, S., Hassan, W., Jan, S., Khan, I., Saleem, M. F., Bajwa, A. A., Wang, L., Mahmood, A., Samad, R. A. and Tung, S. A. (2016a). Osmoregulation and antioxidant production in maize under combined cadmium and arsenic stress. *Environmental Science and Pollution Research*, 23, 11864-11875.

Apel, K. and Hirt, H. (2004). Reactive oxygen species: Metabolism, oxidative stress, and signal transduction. *Annual Review of Plant Biology*, 55, 373-399.

Arbaoui, S., Evlard, A., Mhamdi, M. W., Campanella, B., Paul, R. and Bettaieb, T. (2013). Potential of kenaf (*Hibiscus cannabinus* L.) and corn (*Zea mays* L.) for phytoremediation of dredging sludge contaminated by trace metals. *Biodegradation*, 24, 563-567.

Arif, N., Yadav, V., Singh, S., Singh, S., Ahmad, P., Mishra, R.K., Sharma, S., Tripathi, D. K., Dubey, N. K. and Chauhan, D. K. (2016). Influence of high and low levels of plant beneficial heavy metal ions on plant growth and development. *Frontiers in Environmental Science*, 4, 69.

Arnold, C. W., Parfitt, D. G. and Kaltreider, M. (2007). Phytovolatilization of oxygenated gasoline-impacted groundwater at an underground storage tank site *via* conifers. *International Journal of Phytoremediation*, 9, 53-69.

Arnon, D. I. (1949). Copper enzymes in isolated chloroplasts: Polyphenoloxidase in *Beta vulgaris*. *Plant Physiology*, 24(1), 1.

Arsenov, D., Župunski, M., Borišev, M., Nikolić, N., Pilipovic, A., Orlovic, S., Kebert, M. and Pajevic, S. (2020). Citric acid as soil amendment in cadmium removal by *Salix viminalis* L., alterations on biometric attributes and photosynthesis. *International Journal of Phytoremediation*, 22, 1-11.

Asad, S. A., Farooq, M., Afzal, A. and West H. (2019). Integrated phytobial heavy metals remediation strategies for sustainable clean environment - A review. *Chemosphere*, 217, 925-941.

Asada, K. (2006). Production and scavenging of reactive oxygen species in chloroplasts and their functions. *Plant Physiology*, 141(2), 391-396.

Asaf, S., Khan, M. A., Khan, A. L., Waqas, M., Shahzad, R., Kim, A. Y., Kang, S. M. and Lee, I. J. (2017). Bacterial endophytes from arid land plants regulate endogenous hormone content and promote growth in crop plants: An example of *Sphingomonas* sp. and *Serratia marcescens*. *Journal of Plant Interactions*, 12(1), 31-38.

Asemaneh, T., Ghaderian, S. M., Crawford, S. A., Marshall, A. T. and Baker, A. J. M. (2006). Cellular and subcellular compartmentation of Ni in the Eurasian serpentine plants *Alyssum bracteatum*, *Alyssum murale* (Brassicaceae) and *Cleome heratensis* (Capparaceae). *Planta*, 225, 193-202.

Ashaari, N. S., Sabri, S., Lai, K. S., Song, A. A. L., Rahim, R. A. and Abdullah, J. O. (2021). Kinetic studies and homology modeling of a dual-substrate linalool/nerolidol synthase from *Plectranthus amboinicus*. *Scientific Reports*, 11(1), 1-16.

Ashraf, M. and Foolad, M. R. (2007). Roles of glycine betaine and proline in improving plant abiotic stress tolerance. *Environmental and Experimental Botany*, 59, 206-216.

Aslam, M. M., Waseem, M., Jakada, B. H., Okal, E. J., Lei, Z., Saqib, H. S. A., Yuan, W., Xu, W. and Zhang, Q. (2022). Mechanisms of abscisic acid-mediated drought stress responses in plants. *International Journal of Molecular Sciences*, 23(3), 1084.

Aslam, S., Gul, N., Mir, M. A., Asgher, M., Al-Sulami, N., Abulfaraj, A. A. and Qari, S. (2021). Role of jasmonates, calcium, and glutathione in plants to combat abiotic stresses through precise signaling cascade. *Frontiers in Plant Science*, 1172, 668029.

Atici, Ö., Ağar, G. and Battal, P. (2005). Changes in phytohormone contents in chickpea seeds germinating under lead or zinc stress. *Biologia Plantarum*, 49(2), 215-222.

Ayala, A., Muñoz, M. F. and Argüelles, S. (2014). Lipid peroxidation: Production, metabolism, and signaling mechanisms of malondialdehyde and 4-hydroxy-2-nonenal. *Oxidative Medicine and Cellular Longevity*, 2014, 360438.

Azzarello, E., Pandolfi, C., Giordano, C., Rossi, M., Mugnai, V. and Mancuso S. (2012). Ultramorphological and physiological modifications induced by high zinc levels in *Paulownia tomentosa*. *Environmental and Experimental Botany*, 81, 11-17.

Babu, S. M. O. F., Hossain, M. B., Rahman, M. S., Rahman, M., Ahmed, A. S. S., Hasan, M. M., Rakib, A., Emran, T. B., Xiao, J. and Simal-Gandara, J. (2021). Phytoremediation of toxic metals: A sustainable green solution for clean environment. *Applied Sciences*, 11(21), 10348.

Bai, Z. G., Dent, D. L., Olsson, L. and Schaepman, M. E. (2008). Global assessment of land degradation and improvement 1. Identification by remote sensing, Wageningen Report 5, ISRIC - World Soil Information, International Soil Reference and Information Centre, p.70.

Baldi, E., Miotto, A., Ceretta, C. A., Quartieri, M., Sorrenti, G., Brunetto, G. and Toselli, M. (2018). Soil-applied phosphorous is an effective tool to mitigate the toxicity of copper excess on grapevine grown in rhizobox. *Scientia Horticulturae*, 227, 102-111.

Bali, S., Kaur, P., Kohli, S. K., Ohri, P., Thukral, A. K., Bhardwaj, R., Wijaya, L., Alyemeni, M. N. and Ahmad, P. (2018). Jasmonic acid induced changes in physio-biochemical attributes and ascorbate-glutathione pathway in *Lycopersicon esculentum* under lead stress at different growth stages. *Science of the Total Environment*, 645, 1344-1360.

Balkhair, K. S. and Ashraf, M. A. (2016). Field accumulation risks of heavy metals in soil and vegetable crop irrigated with sewage water in western region of Saudi Arabia. *Saudi Journal of Biological Sciences*, 23, 32-44.

Banásová, V., Horak, O., Nadubinská, M., Čiamporová, M. and Lichtscheidl, I. (2008). Heavy metal content in *Thlaspi caerulescens* J. et C. Presl growing on metalliferous and non-metalliferous soils in Central Slovakia. *International Journal of Environment and Pollution*, 33, 133-145.

Bankaji, I., Sleimi, N., López-Climent, M. F., Perez-Clemente, R. M. and Gomez-Cadenas, A. (2014). Effects of combined abiotic stresses on growth, trace element accumulation, and phytohormone regulation in two halophytic species. *Journal of Plant Growth Regulation*, 33(3), 632-643.

Barbosa, B., Boléo, S., Sidella, S., Costa, J., Duarte, M. P., Mendes, B., Cosentino, S. L. and Fernando, A. L. (2015). Phytoremediation of heavy metal-contaminated soils using the perennial energy crops *Miscanthus spp*. and *Arundo donax* L. *BioEnergy Research*, 8, 1500-1511.

Bashri, G., Singh, S., Prasad, S. M., Ansari, M. J., Usmani, S., Alfarraj, S., Alharbi, S. A. and Brestic, M. (2021). Kinetin mitigates Cd-induced damages to growth, photosynthesis and PSII photochemistry of *Trigonella* seedlings by up-regulating ascorbate-glutathione cycle. *PLoS One*, 16(6), e0249230.

Bateni, H. and Karimi, K. (2016). Biodiesel production from castor plant integrating ethanol production *via* a biorefinery approach. *Chemical Engineering Research and Design*, 107, 4-12.

Bates, L. S., Waldren, R. P. and Teare, I. D. (1973). Rapid determination of free proline for water-stress studies. *Plant and Soil*, 39(1), 205-207.

Bauddh, K. and Singh, R. P. (2012a). Cadmium tolerance and its phytoremediation by two oil yielding plants *Ricinus communis* (L.) and *Brassica juncea* (L.) from the contaminated soil. *International Journal of Phytoremediation*, 14, 772-785.

Bauddh, K. and Singh, R. P. (2012b). Growth, tolerance efficiency and phytoremediation potential of *Ricinus communis* (L.) and *Brassica juncea* (L.) in salinity and drought affected cadmium contaminated soil. *Ecotoxicology and Environmental Safety*, 85, 13-22.

Bauddh, K. and Singh, R. P. (2014). Effects of organic and inorganic amendments on bio-accumulation and partitioning of Cd in *Brassica juncea* and *Ricinus communis*. *Ecological Engineering*, 74, 93-100.

Bauddh, K., Bhaskar, S. B. and Korstad, J. (2017). *Phytoremediation Potential of Bioenergy Plants*, Springer, Singapore.

Bauddh, K., Kumar, A., Srivastava, S., Singh, R. P. and Tripathi, R. (2016). A study on the effect of cadmium on the antioxidative defense system and alteration in different functional groups in castor bean and Indian mustard. *Archives of Agronomy and Soil Science*, 62(6), 877-891.

Bauddh, K., Singh, K. and Singh, R. P. (2015a). *Ricinus communis* L.: A value added crop for remediation of cadmium contaminated soil. *Bulletin of Environmental Contamination and Toxicology*, 96, 265-269.

Bauddh, K., Singh, K., Singh, B. and Singh R. P. (2015b). *Ricinus communis*: A robust plant for bioenergy and phytoremediation of toxic metals from contaminated soil. *Ecological Engineering*, 84, 640-652.

Bechtaoui, N., Rabiu, M. K., Raklami, A., Oufdou, K., Hafidi, M. and Jemo, M. (2021). Phosphate-dependent regulation of growth and stresses management in plants. *Frontiers in Plant Science*, 12, 679916.

Bharath, P., Gahir, S. and Raghavendra, A. S. (2021). Abscisic acid-induced stomatal closure: An important component of plant defense against abiotic and biotic stress. *Frontiers in Plant Science*, 12, 615114.

Bhattacharyya, R., Ghosh, B. N., Mishra, P. K., Mandal, B., Rao, C. S., Sarkar, D., Das, K., Anil, K. S., Lalitha, M., Hati, K. M. and Franzluebbers, A. J. (2015). Soil degradation in India: Challenges and potential solutions. *Sustainability*, 7, 3528-3570.

Blum, A. (2011). Plant water relations, plant stress and plant production. In: *Plant Breeding for Water Limited Environments*, Blum, A. (Ed.), Springer, New York, pp. 11-52.

Boda, R. K., Majeti, N. V. P. and Suthari, S. (2017). *Ricinus communis* L. (castor bean) as a potential candidate for revegetating industrial waste contaminated sites in peri-urban Greater Hyderabad: Remarks on seed oil. *Environmental Science and Pollution Research*, 24(24), 19955-19964.

Bolan, N. S., Park, J. H., Robinson, B., Naidu, R. and Huh, K. Y. (2011). Phytostabilization: A green approach to contaminant. *Advances in Agronomy*, 112, 145-204.

Boller, M. A. and Steiner, M. (2002). Diffuse emission and control of copper in urban surface runoff. *Water Science and Technology*, 46, 173-181.

Bradford, M. M. (1976). A rapid and sensitive method for the quantitation of microgram quantities of protein utilizing the principle of protein-dye binding. *Analytical Biochemistry*, 72(1-2), 248-254.

Brdar-Jokanović, M. (2020). Boron toxicity and deficiency in agricultural plants. *International Journal of Molecular Sciences*, 21(4), 1424.

Briassoulis, H. (2019). Combating land degradation and desertification: The land-use planning quandary. *Land*, 8(2), 27.

Briffa, J., Sinagra, E. and Blundell, R. (2020). Heavy metal pollution in the environment and their toxicological effects on humans. *Heliyon*, 6(9), e04691.

Broadhurst, C. L., Chaney, R. L., Angle, J. S., Maucel, T. K., Erbe, E. F. and Murphy, C. A. (2004). Simultaneous hyperaccumulation of nickel, manganese and calcium in *Alyssum* leaf trichomes. *Environmental Science and Technology*, 38, 5797-802.

Bücker-Neto, L., Paiva, A. L. S., Machado, R. D., Arenhart, R. A. and Margis-Pinheiro, M. (2017). Interactions between plant hormones and heavy metals responses. *Genetics and Molecular Biology*, 40, 373-386.

Bukhari, S. A. H., Wang, R., Wang, W., Ahmed, I. M., Zheng, W. and Cao, F. (2016). Genotype-dependent effect of exogenous 24-epibrassinolide on chromium-induced changes in ultrastructure and physicochemical traits in

tobacco seedlings. *Environmental Science and Pollution Research*, 23 (18), 18229-18238.

Burkhead, J. L., Gogolin Reynolds, K. A., Abdel-Ghany, S. E., Cohu, C. M. and Pilon, M. (2009). Copper homeostasis. *New Phytologist*, 182(4), 799-816.

Cai, T., Meng, X., Liu, X., Liu, T., Wang, H., Jia, Z., Yang, D. and Ren, X. (2018). Exogenous hormonal application regulates the occurrence of wheat tillers by changing endogenous hormones. *Frontiers in Plant Science*, 9, 1886.

Canini, A., Alesiani, D., D'Arcangelo, G. and Tagliatesta, P. (2007). Gas chromatography-mass spectrometry analysis of phenolic compounds from *Carica papaya* L. leaf. *Journal of Food Composition and Analysis*, 20(7), 584-590.

Cao, Y. Y., Qi, C. D., Li, S., Wang, Z., Wang, X., Wang, J., Ren, S., Li, X., Zhang, N. and Guo, Y. D. (2019). Melatonin alleviates copper toxicity *via* improving copper sequestration and ROS scavenging in cucumber. *Plant and Cell Physiology*, 60(3), 562-574.

Cao, Z. Z., Qin, M. L., Lin, X. Y., Zhu, Z. W. and Chen, M. X. (2018). Sulfur supply reduces cadmium uptake and translocation in rice grains (*Oryza sativa* L.) by enhancing iron plaque formation, cadmium chelation and vacuolar sequestration. *Environmental Pollution*, 238, 76-84.

Carrino, L., Visconti, D., Fiorentino, N. and Fagnano, M. (2020). Biofuel production with castor bean: A win-win strategy for marginal land. *Agronomy*, 10(11), 1690.

Carvalho, M. E. A., de Camargo, P. R., Gaziola, S. A. and Azevedo, R. A. (2018). Is seaweed extract an elicitor compound? Changing proline content in drought-stressed bean plants. *Comunicata Scientiae*, 9(2), 292-297.

Caverzan, A., Passaia, G., Rosa, S. B., Ribeiro, C. W., Lazzarotto, F. and Margis-Pinheiro, M. (2012). Plant responses to stresses: Role of ascorbate peroxidase in the antioxidant protection. *Genetics and Molecular Biology*, 35(4), 1011-1019.

Çelik, Ö. and Akdaş, E. Y. (2019). Tissue-specific transcriptional regulation of seven heavy metal stress-responsive miRNAs and their putative targets in nickel indicator castor bean (*R. communis* L.) plants. *Ecotoxicology and Environmental Safety*, 170, 682-690.

Chaffai, R., Seybou, T., Marzouk, B. and Ferjani, E. (2009). A comparative analysis of fatty acid composition of root and shoot lipids in *Zea mays* under copper and cadmium stress. *Acta Biologica Hungarica*, 60(1), 109-125.

Chalanika De Silva, H. C. and Asaeda, T. (2017). Effects of heat stress on growth, photosynthetic pigments, oxidative damage and competitive capacity of three submerged macrophytes. *Journal of Plant Interactions*, 12(1), 228-236.

Chance, B. and Maehly, A. C. (1955). Assay of catalases and peroxidases. *Methods in Enzymology*, 764-775.

Chandra, R. and Kang, H. (2016). Mixed heavy metal stress on photosynthesis, transpiration rate, and chlorophyll content in poplar hybrids. *Forest Science and Technology*, 12(2), 55-61.

Chandra, R., Cho, W. and Kang, H. (2016). Phytoextraction potential of four poplar hybrids under greenhouse conditions. *Forest Science and Technology*, 12, 199-206.

Chang, F. C., Ko, C. H., Tsai, M. J., Wang, Y. N. and Chung, C. Y. (2014). Phytoremediation of heavy metal contaminated soil by *Jatropha curcas*. *Ecotoxicology*, 23, 1969-1978.

Chaparzadeh, N., Khavari-Nejad, R. A., Navari-Izzo, F. and Izzo, R. (2003). Water relations and ionic balance in *Calendula officinalis* L. under salinity conditions. *Agrochimica*, 47, 69-79.

Chattopadhyay, M. K., Kern, R., Mistou, M. Y., Dandekar, A. M., Uratsu, S. L. and Richarme, G. (2004). The chemical chaperone proline relieves the thermosensitivity of a dnaK deletion mutant at 42°C. *Journal of Bacteriology*, 186(23), 8149-8152.

Chauhan, P. and Mathur, J. (2020). Phytoremediation efficiency of *Helianthus annuus* L. for reclamation of heavy metals-contaminated industrial soil. *Environmental Science and Pollution Research*, 27, 29954-29966.

Chen, D., Chen, D., Xue, R., Long, J., Lin, X., Lin, Y., Jia, L., Zheng, R. and Song, Y. (2019). Effects of boron, silicon and their interactions on cadmium accumulation and toxicity in rice plants. *Journal of Hazardous Materials*, 367, 447-455.

Chen, J. X. and Wang, X. F. (2002). *Guide to Plant Physiological Experiments*. South China University of Technology Press, Guangzhou, pp. 123-127.

Chen, J., Shafi, M., Li, S., Wang, Y.,Wu, J., Ye, Z., Peng, D., Yan,W. and Liu, D. (2015). Copper induced oxidative stresses, antioxidant responses and phytoremediation potential of Moso bamboo (*Phyllostachys pubescens*). *Scientific Reports*, 5, 13554.

Chen, L., Long, C., Wang, D. and Yang, J. (2020a). Phytoremediation of cadmium (Cd) and uranium (U) contaminated soils by *Brassica juncea* L. enhanced with exogenous application of plant growth regulators. *Chemosphere*, 242, 125112.

Chen, L., Yang, J. and Wang, D. (2020b). Phytoremediation of uranium and cadmium contaminated soils by sunflower (*Helianthus annuus* L.) enhanced with biodegradable chelating agents. *Journal of Cleaner Production*, 263, 121491.

Chen, T., Cai, X., Wu, X., Karahara, I., Schreiber, L. and Lin, J. (2011). Casparian strip development and its potential function in salt tolerance. *Plant Signaling and Behavior*, 6(10), 1499-1502.

Chen, Z., Kuschk, P., Reiche, N., Borsdorf, H., Kästner, M. and Köser, H. (2012). Comparative evaluation of pilot scale horizontal subsurface-flow constructed wetlands and plant root mats for treating groundwater contaminated with benzene and MTBE. *Journal of Hazardous Materials*, 209, 510-515.

Chibuike, G. U. and Obiora, S. C. (2014). Heavy metal polluted soils: Effect on plants and bioremediation methods. *Applied and Environmetal Soil Science*, 2014, 752708.

Chmielowska-Bąk, J. and Deckert, J. (2021). Plant recovery after metal stress - A review. *Plants*, 10(3), 450.

Choi, Y. E., Harada, E., Wada, M., Tsuboi, H., Morita, Y., Kusanom, T. and Sano, H. (2001). Detoxification of cadmium in tobacco plants: Formation and active excretion of crystals containing cadmium and calcium through trichomes. *Planta*, 213, 45-50.

Chrysargyris, A., Maggini, R., Incrocci, L., Pardossi, A. and Tzortzakis, N. (2021). Copper tolerance and accumulation on *Pelargonium graveolens* L'Hér. grown in hydroponic culture. *Plants*, 10(8), 1663.

Chung, W. H. (2017). Unraveling new functions of superoxide dismutase using yeast model system: Beyond its conventional role in superoxide radical scavenging. *Journal of Microbiology*, 55(6), 409-416.

Chutia, R. S., Kataki, R. and Bhaskar, T. (2013). Thermogravimetric and decomposition kinetic studies of *Mesua ferrea* L. deoiled cake. *Bioresource Technology*, 139, 66-72.

Clemens, S., Palmgren, M. G. and Krämer, U. (2002). A long way ahead: Understanding and engineering plant metal accumulation. *Trends in Plant Science*, 7, 309-315.

Clemente, R., Pardo, T., Madejón, P., Madejón, E. and Bernal, M. P. (2015). Food byproducts as amendments in trace elements contaminated soils. *Food Research International*, 73, 176-189.

Cobbett, C. and Goldsbrough, P. (2002). Phytochelatins and metallothioneins: Roles in heavy metal detoxification and homeostasis. *Annual Review of Plant Biology*, 53(1), 159-182.

Cobbett, C. S. (2000). Phytochelatins and their roles in heavy metal detoxification. *Plant Physiology*, 123, 825-832.

Colebrook, E. H., Thomas, S. G., Phillips, A. L. and Hedden, P. (2014). The role of gibberellin signalling in plant responses to abiotic stress. *Journal of Experimental Biology*, 217(1), 67-75.

Contreras, R. A., Pizarro, M., Köhler, H., Sáez, C. A. and Zúñiga, G. E. (2018). Copper stress induces antioxidant responses and accumulation of sugars and phytochelatins in Antarctic *Colobanthus quitensis* (Kunth) Bartl. *Biological Research*, 51, 48.

Cortleven, A., Nitschke, S., Klaumunzer, M., AbdElgawad, H., Asard, H., Grimm, B., Riefler, M. and Schmulling, T. (2014). A novel protective function for cytokinin in the light stress response is mediated by the *Arabidopsis* Histidine Kinase2 and *Arabidopsis* Histidine Kinase3 receptors. *Plant Physiology*, 164, 1470-1483.

Cosio, C., DeSantis, L., Frey, B., Diallo, S. and Keller, C. (2005). Distribution of cadmium in leaves of *Thlaspi caerulescens*. *Journal of Experimental Botany*, 56, 765-75.

Cosio, C., Vollenweider, P. and Keller, C. (2006). Localization and effects of cadmium in leaves of a cadmium-tolerant willow (*Salix viminalis* L.) I. Macrolocalization and phytotoxic effects of cadmium. *Environmental and Experimental Botany*, 58, 64-74.

Courbet, G., Gallardo, K., Vigani, G., Brunel-Muguet, S., Trouverie, J., Salon, C. and Ourry, A. (2019). Disentangling the complexity and diversity of crosstalk between sulfur and other mineral nutrients in cultivated plants. *Journal of Experimental Botany*, 70, 4183-4196.

Cui, J. L., Luo, C. L., Tang, C. W. Y., Chan, T. S. and Li, X. D. (2017). Speciation and leaching of trace metal contaminants from e-waste contaminated soils. *Journal of Hazardous Materials*, 329, 150-158.

Cuypers, A., Remans, T., Weyens, N., Colpaert, J., Vassilev, A. and Vangronsveld, J. (2013). Soil-plant relationships of heavy metals and metalloids. In: *Heavy Metals in Soils*, Alloway, B. J. (Ed.), Springer, Dordrecht, Netherlands, pp. 161-193.

D'Imporzano, G., Pilu, R., Corno, L. and Adani, F. (2018). *Arundo donax* L. can substitute traditional energy crops for more efficient, environmentally-friendly production of biogas: A life cycle assessment approach. *Bioresource Technology*, 267, 249-256.

DalCorso, G., Fasani, E., Manara, A., Visioli, G. and Furini, A. (2019). Heavy metal pollutions: State of the art and innovation in phytoremediation. *International Journal of Molecular Sciences*, 20, 3412.

DalCorso, G., Manara, A. and Furini, A. (2013). An overview of heavy metal challenge in plants: From roots to shoots. *Metallomics*, 5(9), 1117-1132.

Dall'Osto, L., Holt, N. E., Kaligotla, S., Fuciman, M., Cazzaniga, S., Carbonera, D., Frank, H. A., Alric, J. and Bassi, R. (2012). Zeaxanthin protects plant photosynthesis by modulating chlorophyll triplet yield in specific light-harvesting antenna subunits. *Journal of Biological Chemistry*, 287(50), 41820-41834.

Dall'Osto, L., Piques, M., Ronzani, M., Molesini, B., Alboresi, A., Cazzaniga, S. and Bassi, R. (2013). The *Arabidopsis* nox mutant lacking carotene hydroxylase activity reveals a critical role for xanthophylls in photosystem I biogenesis. *The Plant Cell*, 25(2), 591-608.

Dalton, D. A., Hanus, F. J., Russell, S. A. and Evans, H. J. (1987). Purification, properties and distribution of ascorbate peroxidase in legume root nodules. *Plant Physiology*, 83, 789-794.

Das, N., Bhattacharya, S. and Maiti, M. K. (2016). Enhanced cadmium accumulation and tolerance in transgenic tobacco over-expressing rice metal tolerance protein gene *OsMTP1* is promising for phytoremediation. *Plant Physiology and Biochemistry*, 105, 297-309.

Das, P., Datta, R., Makris, K. C. and Sarkar, D. (2010). Vetiver grass is capable of removing TNT from soil in the presence of urea. *Environmental Pollution*, 158, 1980-1983.

Davies, K. M., Albert, N. W., Zhou, Y. and Schwinn, K. E. (2018). Functions of flavonoid and betalain pigments in abiotic stress tolerance in plants. *Annual Plant Reviews Online*, 21-62.

de Souza, A., Wang, J. Z. and Dehesh, K. (2017). Retrograde signals: Integrators of interorganellar communication and orchestrators of plant development. *Annual Review of Plant Biology*, 68, 85-108.

Demidchik, V., Straltsova, D., Medvedev, S. S., Pozhvanov, G. A., Sokolik, A. and Yurin, V. (2014). Stress-induced electrolyte leakage: The role of K^+-permeable channels and involvement in programmed cell death and metabolic adjustment. *Journal of Experimental Botany*, 65(5), 1259-1270.

Demirevska-Kepova, K., Simova-Stoilova, L., Stoyanova, Z., Hölzer, R. and Feller, U. (2004). Biochemical changes in barley plants after excessive supply of copper and manganese. *Environmental and Experimental Botany*, 52(3), 253-266.

Dennis, K. K., Liu, K. H., Uppal, K., Go, Y. M. and Jones, D. P. (2021). Distribution of phytochelatins, metal-binding compounds, in plant foods: A survey of commonly consumed fruits, vegetables, grains and legumes. *Food Chemistry*, 339, 128051.

Di Benedetto, A., Galmarini, C. and Tognetti, J. (2015). Effects of combined or single exogenous auxin and/or cytokinin applications on growth and leaf area development in *Epipremnum aureum*. *The Journal of Horticultural Science and Biotechnology*, 90(6), 643-654.

Dixit, V., Pandey, V. and Shyam, R. (2001). Differential antioxidative responses to cadmium in roots and leaves of pea (*Pisum sativum* L. cv. Azad). *Journal of Experimental Botany*, 52(358), 1101-1109.

Djebali, W., Zarrouk, M., Brouquisse, R., El Kahoui, S., Limam, F., Ghorbel, M. H. and Chaïbi, W. (2005). Ultrastructure and lipid alterations induced by cadmium in tomato (*Lycopersicon esculentum*) chloroplast membranes. *Plant Biology*, 7(04), 358-368.

Doke, N. (1983). Involvement of superoxide anion generation in the hypersensitive response of potato tuber tissues to infection with an incompatible race of *Phytophthora infestans* and to the hyphal wall components. *Physiological Plant Pathology*, 23(3), 345-357.

Dominguez-Solis, J. R., Lopez-Martin, M. C., Ager, F. J., Ynsa, M. D., Romero, L. C. and Gotor, C. (2004). Increased cysteine availability is essential for cadmium tolerance and accumulation in *Arabidopsis thalian*a. *Plant Biotechnology Journal*, 2, 469-476.

Dong, S. and Beckles, D. M. (2019). Dynamic changes in the starch-sugar interconversion within plant source and sink tissues promote a better abiotic stress response. *Journal of Plant Physiology*, 234, 80-93.

Du, Y., Gao, B., Zhou, H., Ju, X., Hao, H. and Yin, S. (2013). Health risk assessment of heavy metals in road dusts in urban parks of Beijing, China. *Procedia Environmental Sciences*, 18, 299-309.

Dubey, A. K., Kumar, A., Kumar, N., Kumar, S., Meenakshi, Gautam, A., Ansari, M. A., Manika, N., Lal, S., Behera, S. K., Mallick, S. and Sanyal, I. (2021). Over-expression of chickpea metallothionein 1 gene confers tolerance against major toxic heavy metal stress in *Arabidopsis*. *Physiology and Molecular Biology of Plants*, 27(12), 2665-2678.

Dubey, S., Shri, M., Gupta, A., Rani, V. and Chakrabarty, D. (2018). Toxicity and detoxification of heavy metals during plant growth and metabolism. *Environmental Chemistry Letters*, 16, 1169-1192.

Dubois, M., Gilles, K. A., Hamilton, J. K., Rebers, P. T. and Smith, F. (1956). Colorimetric method for determination of sugars and related substances. *Analytical Chemistry*, 28(3), 350-356.

Dumanović, J., Nepovimova, E., Natić, M., Kuča, K. and Jaćević, V. (2021). The significance of reactive oxygen species and antioxidant defense system in plants: A concise overview. *Frontiers Plant Science*, 11, 552969.

Durand, M., Porcheron, B., Hennion, N., Maurousset, L., Lemoine, R. and Pourtau, N. (2016). Water deficit enhances C export to the roots in *Arabidopsis*

thaliana plants with contribution of sucrose transporters in both shoot and roots. *Plant Physiology*, 170, 1460-1479.

Eggert, K. and von Wirén, N. (2017). Response of the plant hormone network to boron deficiency. *New Phytologist*, 216(3), 868-881.

El-Beltagi, H. S., Mohamed, H. I. and Sofy, M. R. (2020). Role of ascorbic acid, glutathione and proline applied as singly or in sequence combination in improving chickpea plant through physiological change and antioxidant defense under different levels of irrigation intervals. *Molecules*, 25(7), 1702.

Elhawat, N., Alshaal, T., Domokos-Szabolcsy, E., El-Ramady, H., Márton, L., Czakó, M., Kátai, J., Balogh, P., Sztrik, A., Molnár, M., Popp, J. and Fári, M. G. (2014). Phytoaccumulation potentials of two biotechnologically propagated ecotypes of *Arundo donax* in copper-contaminated synthetic wastewater. *Environmental Science and Pollution Research*, 21, 7773-7780.

Elkelish, A. A., Alnusaire, T. S., Soliman, M. H., Gowayed, S., Senousy, H. H. and Fahad, S. (2019). Calcium availability regulates antioxidant system, physio-biochemical activities and alleviates salinity stress mediated oxidative damage in soybean seedlings. *Journal of Applied Botany and Food Quality*, 92, 258-266.

Elloumi, N., Zouari, M., Chaari, L., Jomni, C., Marzouk, B. and Ben Abdallah, F. (2014). Effects of cadmium on lipids of almond seedlings (*Prunus dulcis*). *Botanical Studies*, 55(1), 1-9.

Emamverdian, A. and Ding, Y. (2017). HMs induced changes on growth, antioxidant enzyme's activity, gas exchange parameters and protein structures in *Sasa kongosanensis f. aureo–striatus*. *Polish Journal of Environmental Studies*, 26(2), 585-592.

Emamverdian, A., Ding, Y., Mokhberdoran, F. and Ahmad, Z. (2021). Mechanisms of selected plant hormones under heavy metal stress. *Polish Journal of Environmental Studies*, 30(1), 497-508.

Emamverdian, A., Ding, Y., Mokhberdoran, F. and Xie, Y. (2015). Heavy metal stress and some mechanisms of plant defense response. *Scientific World Journal*, 2015, 756120.

Fagnano, M., Visconti, D. and Fiorentino, N. (2020). Agronomic approaches for characterization, remediation, and monitoring of contaminated sites. *Agronomy*, 10(9), 1335.

Fahad, S., Hussain, S., Matloob, A., Khan, F. A., Khaliq, A., Saud, S., Hassan, S., Shan, D., Khan, F., Ullah, N., Faiq, M., Khan, M. R., Tareen, A. K., Khan, A., Ullah, A., Ullah, N. and Huang, J. L. (2015). Phytohormones and plant responses to salinity stress: A review. *Plant Growth Regulation*, 75, 391.

Fahr, M., Laplaze, L., Bendaou, N., Hocher, V., Mzibri, M., Bogusz, D. and Smouni, A. (2013). Effect of lead on root growth. *Frontiers in Plant Science*, 4, 175.

Fairless, D. (2007). The little shrub that could-maybe: India, like many countries, has high hopes for *Jatropha* as a biofuel source, but little is known about how to make it a successful crop. Daemon Fairless digs for the roots of a new enthusiasm. *Nature*, 449(7163), 652-656.

Faizan, M., Sehar, S., Rajput, V. D., Faraz, A., Afzal, S., Minkina, T., Sushkova, S., Adil, M. F., Yu, F., Alatar, A. A., Akhter, F. and Faisal, M. (2021). Modulation of cellular redox status and antioxidant defense system after synergistic application of zinc oxide nanoparticles and salicylic acid in rice (*Oryza sativa*) plant under arsenic stress. *Plants*, 10(11), 2254.

Fan, S. K., Fang, X. Z., Guan, M. Y., Ye, Y. Q., Lin, X. Y., Du, S. T. and Jin, C. W. (2014). Exogenous abscisic acid application decreases cadmium accumulation in *Arabidopsis* plants, which is associated with the inhibition of IRT1-mediated cadmium uptake. *Frontiers in Plant Science*, 5, 721.

Fan, X., Zhou, X., Chen, H., Tang, M. and Xie, X. (2021). Cross-talks between macro- and micronutrient uptake and signaling in plants. *Frontiers in Plant Science*, 12, 663477.

Faseela, P. (2018). Functional imprints of high intensity light and UV-B radiation in selected rice (*Oryza sativa* L.) varieties. Ph.D. Thesis. University of Calicut, Kerala.

Fazekašová, D. and Fazekaš, J. (2020). Soil quality and heavy metal pollution assessment of iron ore mines in NiznaSlana (Slovakia). *Sustainability*, 12(6), 2549.

Fernandes, M. C., Ferro, M. D., Paulino, A. F. C., Chaves, H. T., Evtuguin, D. V. and Xavier, A. M. R. B. (2018). Comparative study on hydrolysis and bioethanol production from cardoon and rockrose pretreated by dilute acid hydrolysis. *Industrial Crops and Products*, 111, 633-641.

Ferreira, P. A. A., Ceretta, C. A., Soriani, H. H., Tiecher, T. L., Soares, C. R. F. S., Rossato, L. V., Nicoloso, F. T., Brunetto, G., Paranhos, J. T. and Cornejo, P. (2015). *Rhizophagus clarus* and phosphate alter the physiological responses of *Crotalaria juncea* cultivated in soil with a high Cu level. *Applied Soil Ecology*, 91, 37-47.

Ferro, A. M., Kennedy, J. and LaRue, J. C. (2013). Phytoremediation of 1,4-dioxane-containing recovered groundwater. *International Journal of Phytoremediation*, 15, 911-923.

Fjällborg, B. and Dave, G. (2003). Toxicity of copper in sewage sludge. *Environment International*, 28, 761-769.

Folin, O. and Denis, W. (1915). A colorimetric method for the determination of phenols (and phenol derivatives) in urine. *Journal of Biological Chemistry*, 22(2), 305-308.

Food and Agricultural organization of United States (FAO), 2018. The state of the food security and nutrition in the world, Building climate resilience for food security and nutrition.

Foyer, C. H. (2018). Reactive oxygen species, oxidative signaling and the regulation of photosynthesis. *Environmental and Experimental Botany*, 154, 134-142.

Franco-Navarro, J. D., Díaz-Rueda, P., Rivero-Núñez, C. M., Brumós, J., Rubio-Casal, A. E., de Cires, A., Colmenero-Flores, J. M. and Rosales, M. A. (2021). Chloride nutrition improves drought resistance by enhancing water deficit avoidance and tolerance mechanisms. *Journal of Experimental Botany*, 72(14), 5246-5261.

Freeman, J. L., Zhang, L. H., Marcus, M. A., Fakra, S., McGrath, S. P. and Pilon-Smits, E. A. (2006). Spatial imaging, speciation, and quantification of selenium in the hyperaccumulator plants *Astragalus bisulcatus* and *Stanleya pinnata*. *Plant Physiology*, 142, 124-134.

Fu, L., Chen, C., Wang, B., Zhou, X., Li, S., Guo, P., Shen, Z., Wang, G. and Chen, Y. (2015). Differences in copper absorption and accumulation between copper-exclusion and copper-enrichment plants: A comparison of structure and physiological responses. *PLoS One*, 10(7), e0133424.

Fuentes, A. L. B, José, C., de Los Ríos, A., do Carmo, L. I., de Iorio, A. F. and Rendina, A. E. (2018). Phytoextraction of heavy metals from a multiply contaminated dredged sediment by chicory (*Cichorium intybus* L.) and castor bean (*Ricinus communis* L.) enhanced with EDTA, NTA, and citric acid application. *International Journal of Phytoremediation*, 20(13), 1354-1361.

Fulekar, M. H. (2016). Phytoremediation of heavy metals by *Helianthus annuus* in aquatic and soil environment. *International Journal of Current Microbiology and Applied Sciences*, 5(7), 392-404.

Gajić, G., Djurdjević, L., Kostić, O., Jarić, S., Mitrović, M. and Pavlović, P. (2018). Ecological potential of plants for phytoremediation and ecorestoration of fly ash deposits and mine wastes. *Frontiers in Environmental Science*, 6, 124.

Gallo, M. B. and Sarachine, M. J. (2009). Biological activities of lupeol. *International Journal of Biomedical and Pharmaceutical Sciences*, 3(1), 46-66.

Gálusová, T., Piršelová, B., Rybanský, Ľ., Krasylenko, Y., Mészáros, P., Blehová, A., Bardáčová, M., Moravčíková, J. and Matušíková, I. (2020). Plasticity of

soybean stomatal responses to arsenic and cadmium at the whole plant level. *Polish Journal of Environmental Studies*, 29(5), 3569-3580.

Gangola, M. R., Bharathi, R. and Ramadoss, B. R. (2018). Sugars play a critical role in abiotic stress tolerance in plants. In: *Biochemical, Physiological and Molecular Avenues for Combating Abiotic Stress Tolerance in Plants*, Wani, S. H. (Ed.), Academic Press, London, UK, pp. 17-38.

Gangwar, S., Singh, V. P., Prasad, S. M. and Maurya, J. N. (2011a). Differential responses of pea seedlings to indole acetic acid under manganese toxicity. *Acta Physiologiae Plantarum*, 33(2), 451-462.

Gangwar, S., Singh, V. P., Srivastava, P. K. and Maurya, J. N. (2011b). Modification of chromium (VI) phytotoxicity by exogenous gibberellic acid application in *Pisum sativum* (L.) seedlings. *Acta Physiologiae Plantarum*, 33(4), 1385-1397.

Gangwar, S., Singh, V. P., Tripathi, D. K., Chauhan, D. K., Prasad, S. M. and Maurya, J. N. (2014). Plant responses to metal stress. *Emerging Technologies and Management of Crop Stress Tolerance*, 2, 215-248.

Gao, S., Xiao, Y., Xu, F., Gao, X., Cao, S., Zhang, F., Wang, G., Sanders, D. and Chu, C. (2019). Cytokinin-dependent regulatory module underlies the maintenance of zinc nutrition in rice. *New Phytologist*, 224(1), 202-215.

García-Plazaola, J. I., Esteban, R., Fernández-Marín, B., Kranner, I. and Porcar-Castell, A. (2012). Thermal energy dissipation and xanthophyll cycles beyond the *Arabidopsis* model. *Photosynthesis Research*, 113(1), 89-103.

Garg, A. K., Kim, J. K., Owens, T. G., Ranwala, A. P., Do Choi, Y., Kochian, L. V. and Wu, R. J. (2002). Trehalose accumulation in rice plants confers high tolerance levels to different abiotic stresses. *Proceedings of the National Academy of Sciences of the United States of America*, 99(25), 15898-15903.

Gaspar, T., Penel, C. and Greppin, H. (1975). Peroxidase and isoperoxidase in relation to root and flower formation. *The Plant Biochemistry Journal*, 2, 33-47.

Gaur, S., Kumar, J., Prasad, S. M., Sharma, S., Bhat, J. A., Sahi, S., Singh, V. P., Tripathi, D. K. and Chauhan, D. K. (2021). Silicon and nitric oxide interplay alleviates copper induced toxicity in mung bean seedlings. *Plant Physiology and Biochemistry*, 167, 713-722.

Giannakoula, A., Therios, I. and Chatzissavvidis, C. (2021). Effect of lead and copper on photosynthetic apparatus in citrus (*Citrus aurantium* L.) plants. The role of antioxidants in oxidative damage as a response to heavy metal stress. *Plants*, 10(1), 155.

Giannopolitis, C. N. and Ries, S. K. (1977). Superoxide dismutases: I. Occurrence in higher plants. *Plant Physiology*, 59(2), 309-314.

Gibbs, H. K. and Salmon, J. M. (2015). Mapping the world's degraded lands. *Applied Geography*, 57, 12-21.

Gill, S. S. and Tuteja, N. (2010). Reactive oxygen species and antioxidant machinery in abiotic stress tolerance in crop plants. *Plant Physiology and Biochemistry*, 48, 909-930.

Gill, S. S., Anjum, N. A., Gill, R., Yadav, S., Hasanuzzaman, M., Fujita, M., Mishra, P., Sabat, S. C. and Tuteja, N. (2015). Superoxide dismutase - mentor of abiotic stress tolerance in crop plants. *Environmental Science and Pollution Research*, 22(14), 10375-10394.

Gołda, S. and Korzeniowska, J. (2016). Comparison of phytoremediation potential of three grass species in soil contaminated with cadmium. *Environmental Protection and Natural Resources*, 27, 8-14.

González, A., Cabrera, M. D. L. Á., Henríquez, M. J., Contreras, R. A., Morales, B. and Moenne, A. (2012). Cross talk among calcium, hydrogen peroxide, and nitric oxide and activation of gene expression involving calmodulins and calcium-dependent protein kinases in *Ulva compressa* exposed to copper excess. *Plant Physiology*, 158(3), 1451-1462.

Gonzalez-Mendoza, D., Espadas y Gil, F., Escoboza-Garcia, F., Santamaria, J. M. and Zapata-Perez, O. (2013). Copper stress on photosynthesis of black

mangle (*Avicennia germinans*). *Anais da Academia Brasileira de Ciências*, 85(2), 665-670.

Grennan, A. K. (2011). Metallothioneins, a diverse protein family. *Plant Physiology*, 155(4), 1750-1751.

Grill, E., Löffler, S., Winnacker, E. L. and Zenk, M. H. (1989). Phytochelatins, the heavy-metal-binding peptides of plants, are synthesized from glutathione by a specific γ-glutamylcysteine dipeptidyl transpeptidase (phytochelatin synthase). *Proceedings of the National Academy of Sciences of the United States of America*, 86(18), 6838-6842.

Grzegórska, A., Rybarczyk, P., Rogala, A. and Zabrocki, D. (2020). Phytoremediation - from environment cleaning to energy generation - current status and future perspectives. *Energies*, 13(11), 2905.

Gujjar, R. S., Banyen, P., Chuekong, W., Worakan, P., Roytrakul, S. and Supaibulwatana, K. (2020). A synthetic cytokinin improves photosynthesis in rice under drought stress by modulating the abundance of proteins related to stomatal conductance, chlorophyll contents, and rubisco activity. *Plants*, 9(9), 1106.

Guo, H., Hong, C., Chen, X., Xu, Y., Liu, Y., Jiang, D. and Zheng, B. (2016). Different growth and physiological responses to cadmium of the three *Miscanthus species*. *PLoS One*, 11(4), e0153475.

Guo, W., Chen, S., Hussain, N., Cong, Y., Liang, Z. and Chen, K. (2015). Magnesium stress signaling in plant: Just a beginning. *Plant Signaling and Behavior*, 10(3), e992287.

Gupta, D. K. and Sandiolo, L. M. (2012). Metal toxicity in plants: Perception, signaling and remediation, Springer, Singapore.

Gupta, S., Agarwal, V. P. and Gupta, N. K. (2012). Efficacy of putrescine and benzyladenine on photosynthesis and productivity in relation to drought tolerance in wheat (*Triticum aestivum* L.). *Physiology and Molecular Biology of Plants*, 18(4), 331-336.

Gurmani, A. R., Bano, A., Khan, S. U., Din, J. and Zhang, J. L. (2011). Alleviation of salt stress by seed treatment with abscisic acid (ABA), 6-benzylaminopurine (BA) and chlormequat chloride (CCC) optimizes ion and organic matter accumulation and increases yield of rice (‘*Oryza sativa*’ L.). *Australian Journal of Crop Science*, 5(10), 1278-1285.

Gurrieri, L., Merico, M., Trost, P., Forlani, G. and Sparla, F. (2020). Impact of drought on soluble sugars and free proline content in selected *Arabidopsis* mutants. *Biology*, 9(11), 367.

Gururani, M. A., Mohanta, T. K. and Bae, H. (2015). Current understanding of the interplay between phytohormones and photosynthesis under environmental stress. *International Journal of Molecular Sciences*, 16, 19055-19085.

Gustin, J. L., Zanis, M. J. and Salt, D. E. (2011). Structure and evolution of the plant cation diffusion facilitator family of ion transporters. *BMC Evolutionary Biology*, 11(1), 1-13.

Gutbrod, P., Yang, W., Grujicic, G. V., Peisker, H., Gutbrod, K., Du, L. F. and Dörmann, P. (2021). Phytol derived from chlorophyll hydrolysis in plants is metabolized *via*phytenal. *Journal of Biological Chemistry*, 296, 100530.

Ha, S., Vankova, R., Yamaguchi-Shinozaki, K., Shinozaki, K. and Tran, L. S. P. (2012). Cytokinins: Metabolism and function in plant adaptation to environmental stresses. *Trends in Plant Science*, 17(3), 172-179.

Habibi, G. and Vaziri, A. (2017). High salicylic acid concentration alters the electron flow associated with photosystem II in barley. *Acta Agriculturae Slovenica*, 109(2), 393-402.

Haider, F. U., Liqun, C., Coulter, J. A., Cheema, S. A., Wu, J., Zhang, R., Wenjun, M. and Farooq, M. (2021). Cadmium toxicity in plants: Impacts and remediation strategies. *Ecotoxicology and Environmental Safety*, 211, 111887.

Halbac-Cotoara-Zamfir, R., Smiraglia, D., Quaranta, G., Salvia, R., Salvati, L. and Giménez-Morera, A. (2020). Land degradation and mitigation policies in the mediterranean region: A brief commentary. *Sustainability*, 12(20), 8313.

Hall, J. Á. (2002). Cellular mechanisms for heavy metal detoxification and tolerance. *Journal of Experimental Botany*, 53(366), 1-11.

Hannink, N., Subramanian, N., Rosser, S. J., Basran, A., Murray, J. A. H. and Shanks, J. V. (2007). Enhanced transformation of TNT by tobacco plants expressing a bacterial nitroreductase. *International Journal of Phytoremediation*, 9, 385-401.

Hasan, M., Cheng, Y., Kanwar, M. K., Chu, X. Y., Ahammed, G. J. and Qi, Z. Y. (2017). Responses of plant proteins to heavy metal stress - a review. *Frontiers in Plant Science*, 8, 1492.

Hasanuzzaman, M., Bhuyan, M. H. M., Anee, T. I., Parvin, K., Nahar, K., Mahmud, J. A. and Fujita, M. (2019). Regulation of ascorbate-glutathione pathway in mitigating oxidative damage in plants under abiotic stress. *Antioxidants*, 8(9), 384.

Hasanuzzaman, M., Bhuyan, M. H. M., Parvin, K., Bhuiyan, T. F., Anee, T. I., Nahar, K., Hossen, M. S., Zulfiqar, F., Alam, M. M. and Fujita, M. (2020b). Regulation of ROS metabolism in plants under environmental stress: A review of recent experimental evidence. *International Journal of Molecular Sciences*, 21(22), 8695.

Hasanuzzaman, M., Bhuyan, M. H. M., Raza, A., Hawrylak-Nowak, B., Matraszek-Gawron, R., Nahar, K. and Fujita, M. (2020a). Selenium toxicity in plants and environment: Biogeochemistry and remediation possibilities. *Plants*, 9(12), 1711.

Hasanuzzaman, M., Bhuyan, M. H. M., Zulfiqar, F., Raza, A., Mohsin, S. M., Mahmud, J. A., Fujita, M. and Fotopoulos, V. (2020c). Reactive oxygen species and antioxidant defense in plants under abiotic stress: Revisiting the crucial role of a universal defense regulator. *Antioxidants*, 9(8), 681.

Hasanuzzaman, M., Nahar, K., Anee, T. I. and Fujita, M. (2017). Glutathione in plants: Biosynthesis and physiological role in environmental stress tolerance. *Physiology and Molecular Biology of Plants*, 23(2), 249-268.

Hashem, A., Abd_Allah, E. F., Alqarawi, A. A. and Egamberdieva, D. (2016). Bioremediation of adverse impact of cadmium toxicity on *Cassia italica* Mill by arbuscular mycorrhizal fungi. *Saudi Journal of Biological Sciences*, 23(1), 39-47.

Hassan, M. U., Aamer, M., Chattha, M. U., Haiying, T., Shahzad, B., Barbanti, L., Nawaz, M., Rasheed, A., Afzal, A., Liu, Y. and Guoqin, H. (2020). The critical role of zinc in plants facing the drought stress. *Agriculture*, 10(9), 396.

Hassinen, V. H., Tervahauta, A. I., Schat, H. and Kärenlampi, S. O. (2011). Plant metallothioneins - metal chelators with ROS scavenging activity? *Plant Biology*, 13(2), 225-232.

Hayat, S., Ali, B., Aiman Hasan, S. and Ahmad, A. (2007). Brassinosteroid enhanced the level of antioxidants under cadmium stress in *Brassica juncea*. *Environmental and Experimental Botany*, 60, 33-41.

Hayes, P. E., Clode, P. L., Guilherme-Pereira, C. and Lambers, H. (2019). Calcium modulates leaf cell-specific phosphorus allocation in Proteaceae from southwestern Australia. *Journal of Experimental Botany*, 70, 3995-4009.

He, C., Zhao, Y., Wang, F., Oh, K., Zhao, Z., Wu, C., Zhang, X., Chen, X. and Liu, X. (2020a). Phytoremediation of soil heavy metals (Cd and Zn) by castor seedlings: Tolerance, accumulation and subcellular distribution. *Chemosphere*, 252, 126471.

He, H., Ye, Z., Yang, D., Yan, J., Xiao, L., Zhong, T., Yuan, M., Cai, X., Fang, Z. and Jing, Y. (2013). Characterization of endophytic *Rahnella sp*. JN6 from *Polygonum pubescens* and its potential in promoting growth and Cd, Pb, Zn uptake by *Brassica napus*. *Chemosphere*, 90(6), 1960-1965.

He, M. and Ding, N. Z. (2020). Plant unsaturated fatty acids: Multiple roles in stress response. *Frontiers in Plant Science*, 11, 562785.

He, X., Xu, M., Wei, Q., Tang, M., Guan, L., Lou, L., Xu, X., Hu, Z., Chen, Y., Shen, Z. and Xia, Y. (2020b). Promotion of growth and phytoextraction of cadmium and lead in *Solanum nigrum* L. mediated by plant-growth-

promoting rhizobacteria. *Ecotoxicology and Environmental Safety*, 205, 111333.

He, Z., Shentu, J., Yang, X., Baligar, V. C., Zhang, T. and Stoffella, P. J. (2015). Heavy metal contamination of soils: Sources, indicators and assessment. *Journal of Environmental Indicators,* 9, 17-18.

Heath, R. L. and Packer, L. (1968). Photoperoxidation in isolated chloroplasts: I. Kinetics and stoichiometry of fatty acid peroxidation. *Archives of Biochemistry and Biophysics*, 125(1), 189-198.

Henao, S. G. and Ghneim-Herrera, T. (2021). Heavy metals in soils and the remediation potential of bacteria associated with the plant microbiome. *Frontiers in Environmental Science*, 15.

Hernández, L. E., Ortega-Villasante, C., Montero-Palmero, M. B., Escobar, C. and Carpena, R. O. (2012). Heavy metal perception in a microscale environment: A model system using high doses of pollutants. In: *Metal Toxicity in Plants: Perception, Signaling and Remediation*, Gupta, D. K. and Sandalio, L. M. (Eds.), Springer, Heidelberg, Germany, pp. 23-39.

Hieno, A., Ara, N. H. and Yamamoto, Y. Y. (2019). H_2O_2-mediated biotic and abiotic stress responses in plants. In: *Redox Homeostasis in Plants: From Signaling to Stress Tolerance*, Panda, S. and Yamamoto Y. (Eds.), Springer, Cham, pp. 19-42.

Hindt, M. N. and Guerinot, M. L. (2012). Getting a sense for signals: Regulation of the plant iron deficiency response. *Biochimica et Biophysica Acta (BBA)-Molecular Cell Research*, 1823(9), 1521-1530.

Hir, R. L., Spinner, L., Klemens, P. A. W., Chakraborti, D., Marco, F., Vilaine, F., Wolff, N., Lemoine, R., Porcheron, B., Géry, C., Téoulé, E., Chabout, S., Mouille, G., Neuhaus, H. E., Dinant, S. and Bellini, C. (2015). Disruption of the sugar transporters *AtSWEET11* and *AtSWEET12* affects vascular development and freezing tolerance in *Arabidopsis*. *Molecular Plant*, 8, 1687-1690.

Hoagland, D. R. and Arnon, D. I. (1950). The water-culture method for growing plants without soil. *Circular Califonia Agricultural Experiment Station*, 347, 1-32.

Hodson, M. J. (2012). Metal toxicity and tolerance in plants. *Biochemical Society*, 34, 28-32.

Hojati, M., Modarres-Sanavy, S., Enferadi, S., Majdi, M., Ghanati, F., Farzadfar, S. and Pazoki, A. (2017). Cadmium and copper induced changes in growth, oxidative metabolism and terpenoids of *Tanacetum parthenium*. *Environmental Science and Pollution Research*, 24(13), 12261-12272.

Hönig, M., Plíhalová, L., Husičková, A., Nisler, J. and Doležal, K. (2018). Role of cytokinins in senescence, antioxidant defence and photosynthesis. *International Journal of Molecular Sciences*, 19(12), 4045.

Hoque, M. N., Tahjib-Ul-Arif, M., Hannan, A., Sultana, N., Akhter, S., Hasanuzzaman, M., Akter, F., Hossain, M. S., Sayed, M. A., Hasan, M. T., Skalicky, M., Li X. and Brestič, M. (2021). Melatonin modulates plant tolerance to heavy metal stress: Morphological responses to molecular mechanisms. *International Journal of Molecular Sciences*, 22(21), 11445.

Hossain, M. A., Nakano, Y. and Asada, K. (1984). Monodehydroascorbatereductase in spinach chloroplasts and its participation in regeneration of ascorbate for scavenging hydrogen peroxide. *Plant Cell Physiology*, 25, 385-95.

Hosseini, S. A., Maillard, A., Hajirezaei, M. R., Ali, N., Schwarzenberg, A., Jamois, F. and Yvin, J. C. (2017). Induction of barley silicon transporter HvLsi1 and HvLsi2, increased silicon concentration in the shoot and regulated starch and ABA homeostasis under osmotic stress and concomitant potassium deficiency. *Frontiers in Plant Science*, 8, 1359.

Hosseini, S. A., Naseri Rad, S., Ali, N. and Yvin, J. C. (2019). The ameliorative effect of silicon on maize plants grown in Mg-deficient conditions. *International Journal of Molecular Sciences*, 20(4), 969.

Hou, D., O'Connor, D., Igalavithana, A. D., Alessi, D. S., Luo, J., Tsang, D. C. W., Sparks, D. L., Yamauchi, Y., Rinklebe, J. and Ok, Y. S. (2020). Metal

contamination and bioremediation of agricultural soils for food safety and sustainability. *Nature Reviews Earth and Environment*, 1, 366-381.

Hu, L., Wang, Z. and Huang, B. (2013). Effects of cytokinin and potassium on stomatal and photosynthetic recovery of Kentucky bluegrass from drought stress. *Crop Science*, 53(1), 221-231.

Huan, L., Xie, X., Zheng, Z., Sun, F., Wu, S., Li, M., Gao, S., Gu, W. and Wang, G. (2014). Positive correlation between PSI response and oxidative pentose phosphate pathway activity during salt stress in an intertidal macroalga. *Plant and Cell Physiology*, 55(8), 1395-1403.

Huang, C. X. and Van Steveninck, R. F. M. (1989). The role of particular pericycle cells in the apoplastic transport in root meristems of barley. *Journal of Plant Physiology*, 135, 554-558.

Huang, G., Guo, G., Yao, S., Zhang, N. and Hu, H. (2016). Organic acids, amino acids compositions in the root exudates and Cu-accumulation in castor (*Ricinus communis* L.) under Cu stress. *International Journal of Phytoremediation*, 18(1), 33-40.

Huang, G., Rizwan, M. S., Ren, C., Guo, G., Fu, Q., Zhu, J. and Hu, H. (2018). Influence of phosphorous fertilization on copper phytoextraction and antioxidant defenses in castor bean (*Ricinus communis* L.). *Environmental Science and Pollution Research*, 25(1), 115-123.

Huang, W., Yang, Y. J. and Zhang, S. B. (2019). The role of water-water cycle in regulating the redox state of photosystem I under fluctuating light. *Biochimica et Biophysica Acta (BBA)-Bioenergetics*, 1860(5), 383-390.

Hunce, S. Y., Clemente, R. and Bernal M. P. (2019). Energy production potential of phytoremediation plant biomass: *Helianthus annuus* and *Silybum marianum*. *Industrial Crops and Products*, 135, 206-216.

Hura, T., Grzesiak, S., Hura, K., Thiemt, E., Tokarz, K. and Wędzony, M. (2007). Physiological and biochemical tools useful in drought-tolerance detection in genotypes of winter triticale: Accumulation of ferulic acid correlates with drought tolerance. *Annals of Botany*, 100(4), 767-775.

Ibañez, S., Talano, M., Ontañon, O., Suman, J., Medina, M. I., Macek, T. and Agostini, E. (2016). Transgenic plants and hairy roots: Exploiting the potential of plant species to remediate contaminants. *New Biotechnology*, 33, 625-635.

Jabeen, R., Ahmad, A. and Iqbal, M. (2009). Phytoremediation of heavy metals: Physiological and molecular mechanisms. *The Botanical Review*, 75, 339-364.

Jain, M., Tiwary, S. and Gadre, R. (2018). Modulation of δ-aminolevulinic acid dehydratase activity by the sorbitolinduced osmotic stress in maize leaf segments. *Biochemistry (Moscow)*, 83(1), 32-36.

Jalmi, S. K., Bhagat, P. K., Verma, D., Noryang, S., Tayyeba, S., Singh, K., Sharma, D. and Sinha, A. K. (2018). Traversing the links between heavy metal stress and plant signaling. *Frontiers in Plant Science*, 9, 12.

Janeczko, A., Koscielniak, J., Pilipowicz, M., Szarek-Lukaszewska, G. and Skoczowski, A. (2005). Protection of winter rape photosystem 2 by 24-epibrassinolide under cadmium stress. *Photosynthetica*, 43, 293-298.

Janeeshma, E. and Puthur, J. T. (2020). Direct and indirect influence of arbuscular mycorrhizae on enhancing metal tolerance of plants. *Archives of Microbiology*, 202(1), 1-16.

Janeeshma, E., Kalaji, H. M. and Puthur, J. T. (2021a). Differential responses in the photosynthetic efficiency of *Oryza sativa* and *Zea mays* on exposure to Cd and Zn toxicity. *Acta Physiologia Plantarum*, 43(1), 1-12.

Janeeshma, E., Puthur, J. T. and Ahmad, P. (2021d). Silicon distribution in leaves and roots of rice and maize in response to cadmium and zinc toxicity and the associated histological variations. *Physiologia Plantarum*. 173(1), 460-471.

Janeeshma, E., Puthur, J. T., Wróbel, J. and Kalaji, H. M. (2021b). Metabolic alterations elicited by Cd and Zn toxicity in *Zea mays* with the association of *Claroideoglomus claroideum*. *Ecotoxicology*, 31(1), 92-113.

Janeeshma, E., Rajan, V. K. and Puthur, J. T. (2021c). Spectral variations associated with anthocyanin accumulation; an apt tool to evaluate zinc stress in *Zea mays* L. *Chemistry and Ecology*, 37(1), 32-49.

Jasinskas, A., Streikus, D. and Vonžodas, T. (2020). Fibrous hemp (Felina 32, USO 31, Finola) and fibrous nettle processing and usage of pressed biofuel for energy purposes. *Renewable Energy*, 149, 11-21.

Jáuregui-Zùñiga, D., Ferrer, M. A., Calderón, A. A., Muñoz, R. and Moreno, A. (2005). Heavy metal stress reduces the deposition of calcium oxalate crystals in leaves of *Phaseolus vulgaris*. *Journal of Plant Physiology*, 162, 1183-1187.

Javaid, S., uz Zaman, Q., Sultan, K., Riaz, U., Aslam, A., Sharif, S., Ehsan, N., Aslam, S., Jamil, A. and Ibraheem, S. (2020). Heavy metals stress, mechanism and remediation techniques in rice (*Oryza sativa* L.): A review. *Pure and Applied Biology*, 9(1), 403-426.

Jha, A. B., Misra, A. N. and Sharma, P. (2017). Phytoremediation of heavy metal-contaminated soil using bioenergy crops. In: *Phytoremediation Potential of Bioenergy Plants*, Bauddh, K., Singh, B. and Korstad, J. (Eds.), Springer, Singapore, pp. 63-96.

Jia, L. E., Liu, S., Duan, X. M., Zhang, C., Wu, Z. H., Liu, M. C., Guo, S. G., Zuo, J. H. and Wang, L. B. (2017). 6-benzylaminopurine treatment maintains the quality of Chinese chive (*Allium tuberosum* Rottler ex Spreng.) by enhancing antioxidant enzyme activity. *Journal of Integrative Agriculture*, 16(9), 1968-1977.

Jiang, A., Zuo, J., Zheng, Q., Guo, L., Gao, L., Zhao, S., Wang, Q. and Hu, W. (2019b). Red LED irradiation maintains the post-harvest quality of broccoli by elevating antioxidant enzyme activity and reducing the expression of senescence-related genes. *Scientia Horticulturae*, 251, 73-79.

Jiang, K. and Asami, T. (2018). Chemical regulators of plant hormones and their applications in basic research and agriculture. *Bioscience, Biotechnology and Biochemistry*, 82(8), 1265-1300.

Jiang, L., Liu, C., Cao, H., Chen, Z., Yang, J., Cao, S. and Wei, Z. (2019a). The role of cytokinin in selenium stress response in *Arabidopsis*. *Plant Science*, 281, 122-132.

Jiang, L., Shi, G., Ding, Y., Lou, L. and Cai, Q. (2013). Differential responses of two bamboo species (*Phyllostachys auresulcata* 'Spectabilis' and *Pleioblastus chino* 'Hisauchii') to excess copper. *BioEnergy Research*, 6, 1223-1229.

Jiang, Y., Lei, M., Duan, L. and Longhurst, P. (2015). Integrating phytoremediation with biomass valorisation and critical element recovery: A UK contaminated land perspective. *Biomass and Bioenergy*, 83, 328-339.

Jibran, R., A Hunter, D. and P Dijkwel, P. (2013). Hormonal regulation of leaf senescence through integration of developmental and stress signals. *Plant Molecular Biology*, 82(6), 547-561.

Jisha, K. C., Vijayakumari, K. and Puthur, J. T. (2013). Seed priming for abiotic stress tolerance: An overview. *Acta Physiologiae Plantarum*, 35(5), 1381-1396.

Jogawat, A., Yadav, B. and Narayan, O. P. (2021). Metal transporters in organelles and their roles in heavy metal transportation and sequestration mechanisms in plants. *Physiologia Plantarum*, 173(1), 259-275.

Joshi, R., Sahoo, K. K., Tripathi, A. K., Kumar, R., Gupta, B. K., Pareek, A. and Singla-Pareek, S. L. (2018). Knockdown of an inflorescence meristem-specific cytokinin oxidase-*OsCKX2* in rice reduces yield penalty under salinity stress condition. *Plant, Cell and Environment*, 41(5), 936-946.

Joshi, V., Joung, J. G., Fei, Z. and Jander, G. (2010). Interdependence of threonine, methionine and isoleucine metabolismin plants: Accumulation and transcriptional regulation under abiotic stress. *Amino Acids*, 39, 933-947.

Jung, H. I., Lee, B. R., Chae, M. J., Lee, E. J., Lee, T. G., Jung, G. B., Kim, M. S. and Lee, J. (2020). Ascorbate-mediated modulation of cadmium stress

responses: Reactive oxygen species and redox status in *Brassica napus*. *Frontiers in Plant Science*, 11, 1823.

Jung, Y., Ha, M., Lee, J., Ahn, Y. G., Kwak, J. H., Ryu, D. H. and Hwang, G. S. (2015). Metabolite profiling of the response of burdock roots to copper stress. *Journal of Agricultural and Food Chemistry*, 63(4), 1309-1317.

Junglee, S., Urban, L., Sallanon, H. and Lopez-Lauri, F. (2014). Optimized assay for hydrogen peroxide determination in plant tissue using potassium iodide. *American Journal of Analytical Chemistry*, 5(11), 730.

Kaddour, K., Smail, M., Hocine, B., Bouzaza, A. and Hacen, B. (2017). Assessment of heavy metal pollution due to the lead-zinc mine at the Ain Azel area (northeast of Algeria). *E3 Journal of Environmental Research and Management*, 8, 1-11.

Kalaji, H. M., Schansker, G., Brestic, M., Bussotti, F., Calatayud, A., Ferroni, L., Goltsev, V., Guidi, L., Jajoo, A., Li, P., Losciale, P., Mishra, V. K., Misra, A. N., Nebauer, S. G., Pancaldi, S., Penella, C., Pollastrini, M., Suresh, K., Tambussi, E., Yanniccari, M., Zivcak, M., Cetner, M. D., Samborska, I. A., Stirbet, A., Olsovska, K., Kunderlikova, K., Shelonzek, H., Rusinowski, S. and Bąba, W. (2017). Frequently asked questions about chlorophyll fluorescence, the sequel. *Photosynthesis Research*, 132(1), 13-66.

Kalt-Torres, W., Burke, J. J. and Anderson, J. M. (1984). Chloroplast glutathione reductase: Purification and properties. *Physiologia Plantarum*, 61(2), 271-278.

Kamal, K. J. and Joshi, S. D. (2006). *Medicinal and aromatic plants used in Nepal, Tibet and Trans- Himalayan region*. Author House, Indiana, USA, pp. 166-167.

Kamran, M., Danish, M., Saleem, M. H., Malik, Z., Parveen, A., Abbasi, G. H., Jamil, M., Ali, S., Afzal S., Riaz, M., Rizwan, M., Ali, M. and Zhou, Y. (2021). Application of abscisic acid and 6-benzylaminopurine modulated morpho-physiological and antioxidative defense responses of tomato

(*Solanum lycopersicum* L.) by minimizing cobalt uptake. *Chemosphere*, 263, 128169.

Kamran, M., Malik, Z., Parveen, A., Huang, L., Riaz, M., Bashir, S., Mustafa, A., Abbasi, G. H., Xue, B. and Ali, U. (2020). Ameliorative effects of biochar on rapeseed (*Brassica napus* L.) growth and heavy metal immobilization in soil irrigated with untreated wastewater. *Journal of Plant Growth Regulation*, 39(1), 266-281.

Kang, W., Bao, J., Zheng, J., Hu, H. and Du, J. (2015). Distribution and chemical forms of copper in the root cells of castor seedlings and their tolerance to copper phytotoxicity in hydroponic culture. *Environmental Science and Pollution Research*, 22(10), 7726-7734.

Kapoor, D., Sharma, R., Handa, N., Kaur, H., Rattan, A., Yadav, P., Gautam, V., Kaur, R. and Bhardwaj, R. (2015). Redox homeostasis in plants under abiotic stress: Role of electron carriers, energy metabolism mediators and proteinaceous thiols. *Frontiers in Environmental Science*, 3, 13.

Kapoor, D., Singh, M. P., Kaur, S., Bhardwaj, R., Zheng, B. and Sharma, A. (2019). Modulation of the functional components of growth, photosynthesis, and anti-oxidant stress markers in cadmium exposed *Brassica juncea* L. *Plants*, 8(8), 260.

Karabourniotis, G., Liakopoulos, G., Nikolopoulos, D. and Bresta, P. (2020). Protective and defensive roles of non-glandular trichomes against multiple stresses: Structure-function coordination. *Journal of Forestry Research*, 31(1), 1-12.

Karimi, P., Khavari-Nejad, R. A., Niknam, V., Ghahremaninejad, F. and Najafi, F. (2012). The effects of excess copper on antioxidative enzymes, lipid peroxidation, proline, chlorophyll, and concentration of Mn, Fe, and Cu in *Astragalus neo-mobayenii*. *The Scientific World Journal*, 2012, 615670.

Karlen, D. and Rice, C. (2015). Soil degradation: Will humankind ever learn?. *Sustainability*, 7, 12490-12501.

Katyal, J. C. and Vlek, P. L. G. (2000). Desertification: Concept, causes and amelioration. ZEF Discussion Papers on Development. *Policy*, 33.

Kaur, R. and Bhaskar, T. (2020). Potential of castor plant (*Ricinus communis*) for production of biofuels, chemicals, and value-added products. In: *Waste Biorefinery*, Bhaskar, T., Pandey, A., Mohan, S. V., Lee, D. J. and Khanal, S. K. (Eds.), Elsevier, Amsterdam, Netherlands, pp. 269-310.

Kaushik, S., Sharma, P., Kaur, G., Singh, A. K., Al-Misned, F. A., Shafik, H. M. and Sirhindi, G. (2021). Seed priming with methyl jasmonate mitigates copper and cadmium toxicity by modifying biochemical attributes and antioxidants in *Cajanus cajan*. *Saudi Journal of Biological Sciences*, 9(2), 721-729.

Kawachi, M., Kobae, Y., Mori, H., Tomioka, R., Lee, Y. and Maeshima, M. (2009). A mutant strain *Arabidopsis thaliana* that lacks vacuolar membrane zinc transporter *MTP1* revealed the latent tolerance to excessive zinc. *Plant and Cell Physiology*, 50(6), 1156-1170.

Kaya, C., Ashraf, M., Wijaya, L. and Ahmad, P. (2019). The putative role of endogenous nitric oxide in brassinosteroid-induced antioxidant defence system in pepper (*Capsicum annuum* L.) plants under water stress. *Plant Physiology and Biochemistry*, 143, 119-128.

Kaya, C., Tuna, A. L., Ashraf, M. and Altunlu, H. (2007). Improved salt tolerance of melon (*Cucumis melo* L.) by the addition of proline and potassium nitrate. *Environmental and Experimental Botany*, 60(3), 397-403.

Kazan, K. (2015). Diverse roles of jasmonates and ethylene in abiotic stress tolerance. *Trends in Plant Science*, 20(4), 219-229.

Keltjens, W. G. and Van Beusichem, M. L. (1998). Phytochelatins as biomarkers for heavy metal toxicity in maize: Single metal effects of copper and cadmium. *Journal of Plant Nutrition*, 21(4), 635-648.

Keunen, E., Schellingen, K., Vangronsveld, J. and Cuypers, A. (2016). Ethylene and metal stress: Small molecule, big impact. *Frontiers in Plant Science*, 7, 23.

Khalid, N., Masood, A., Noman, A., Aqeel, M. and Qasim, M. (2019). Study of the responses of two biomonitor plant species (*Datura alba* & *Ricinus communis*) to roadside air pollution. *Chemosphere*, 235, 832-841.

Khalid, S., Shahid, M., Niazi, N. K., Murtaza, B., Bibi, I. and Dumat, C. (2017). A comparison of technologies for remediation of heavy metal contaminated soils. *Journal of Geochemical Exploration*, 182, 247-268.

Khan, A. L., Hamayun, M., Kim, Y. H., Kang, S. M., Lee, J. H. and Lee, I. J. (2011). Gibberellins producing endophytic *Aspergillus fumigatus* sp. LH02 influenced endogenous phytohormonal levels, isoflavonoids production and plant growth in salinity stress. *Process Biochemistry*, 46(2), 440-447.

Khan, M. I. R. and Khan, N. A. (2014). Ethylene reverses photosynthetic inhibition by nickel and zinc in mustard through changes in PS II activity, photosynthetic nitrogen use efficiency, and antioxidant metabolism. *Protoplasma*, 251, 1007-1019.

Khan, M. I. R., Jahan, B., Alajmi, M. F., Rehman, M. T. and Khan, N. A. (2019). Exogenously-sourced ethylene modulates defense mechanisms and promotes tolerance to zinc stress in mustard (*Brassica juncea* L.). *Plants*, 8(12), 540.

Khan, M. I. R., Khan, N. A., Jahan, B., Goyal, V., Hamid, J., Khan, S., Iqbal, N., Alamri, S. and Siddiqui, M. H. (2021). Phosphorus supplementation modulates nitric oxide biosynthesis and stabilizes the defence system to improve arsenic stress tolerance in mustard. *Plant Biology*, 23, 152-161.

Khan, M. M., Islam, E., Irem, S., Akhtar, K., Ashraf, M. Y., Iqbal, J. and Liu, D. (2018). Pb-induced phytotoxicity in para grass (*Brachiaria mutica*) and Castorbean (*Ricinus communis* L.): Antioxidant and ultrastructural studies. *Chemosphere*, 200, 257-265.

Khan, N. A., Asgher, M., Per, T. S., Masood, A., Fatma, M. and Khan, M. I. R. (2016). Ethylene potentiates sulfur-mediated reversal of cadmium inhibited photosynthetic responses in mustard. *Frontiers in Plant Science*, 7, 1628.

Khiari, B., Ghouma, I., Ferjani, A. I., Azzaz, A. A., Jellali, S., Limousy, L. and Jeguirim, M. (2020). Kenaf stems: Thermal characterization and conversion for biofuel and biochar production. *Fuel*, 262, 116654.

Kidd, P. S., Bani, A., Benizri, E., Gonnelli, C., Hazotte, C., Kisser, J., Konstantinou, M., Kuppens, T., Kyrkas, D., Laubie, B., Malina, R., Morel, J. L., Olcay, H., Pardo, T., Pons, M. N., Prieto-Fernández, A., Puschenreiter,M., Quintela-Sabarís, C., Ridard, C., Rodríguez-Garrido, B., Rosenkranz, T., Rozpądek, P., Saad, R., Selvi, F., Simonnot, M. O., Tognacchini, A., Turnau, K., Ważny, R., Witters, N. and Echevarria, G. (2018). Developing sustainable agromining systems in agricultural ultramafic soils for nickel recovery. *Frontiers in Environmental Science*, 6, 44.

Kim, Y. and Kang, H. (2018). Comparative expression analysis of genes encoding metallothioneins in response to heavy metals and abiotic stresses in rice (*Oryza sativa*) and *Arabidopsis thaliana*. *Bioscience, Biotechnology and Biochemistry*, 82, 1656-1665.

Kiran, B. R. and Prasad, M. N. V. (2017). Responses of *Ricinus communis* L. (castor bean, phytoremediation crop) seedlings to lead (Pb) toxicity in hydroponics. *Selcuk Journal of Agriculture and Food Sciences*, 31, 73-80.

Kısa, D., Elmastaş, M., Öztürk, L. and Kayır, Ö. (2016). Responses of the phenolic compounds of *Zea mays* under heavy metal stress. *Applied Biological Chemistry*, 59(6), 813-820.

Koç, E., Üstün, A. S. and Celik, N. (2013). Effect of exogenously applied salicylic acid on cadmium chloride-induced oxidative stress and nitrogen metabolism in tomato (*Lycopersicon esculentum* L.). *Turkish Journal of Biology*, 37(3), 361-369.

Koch, M. T., Pawelzik, E. and Kautz, T. (2021). Chloride changes soil - plant water relations in potato (*Solanum tuberosum* L.). *Agronomy*, 11, 736.

Kohli, S. K., Handa, N., Bali, S., Arora, S., Sharma, A., Kaur, R. and Bhardwaj, R. (2018). Modulation of antioxidative defense expression and osmolyte content by co-application of 24-epibrassinolide and salicylic acid in Pb exposed

Indian mustard plants. *Ecotoxicology and Environmental Safety*, 147, 382-393.

Kohli, S. K., Handa, N., Gautam, V., Bali, S., Sharma, A., Khanna, K., Arora, S., Thukral, A. K., Ohri, P., Karpets, Y., Kolupaev, Y. E. and Bhardwaj, R. (2017). ROS signaling in plants under heavy metal stress. In: *Reactive Oxygen Species and Antioxidant Systems in Plants: Role and Regulation under Abiotic Stress*, Khan, M. I. R. and Khanm N. A. (Eds.), Springer, Singapore, pp. 185-214.

Koźmińska, A., Wiszniewska, A., Hanus-Fajerska, E. and Muszyńska, E. (2018). Recent strategies of increasing metal tolerance and phytoremediation potential using genetic transformation of plants. *Plant Biotechnology Reports*, 12(1), 1-14.

Krämer, U., Grime, G. W., Smith, J. A. C., Hawes, C. R. and Baker, A. J. M. (1997). Micro-PIXE as a technique for studying nickel localization in leaves of the hyperaccumulator plant *Alyssum lesbiacum*. *Nuclear Instruments and Methods in Physics Research Section B: Beam Interactions with Materials and Atoms*, 130, 346-350.

Krishna, T. P. A., Maharajan, T., Victor Roch, G., Ignacimuthu, S. and Antony Ceasar, S. (2020). Structure, function, regulation and phylogenetic relationship of ZIP family transporters of plants. *Frontiers in Plant Science*, 11, 662.

Krishnamurthy, A. and Rathinasabapathi, B. (2013). Auxin and its transport play a role in plant tolerance to arsenite-induced oxidative stress in *Arabidopsis thaliana*. *Plant, Cell and Environment*, 36(10), 1838-1849.

Krüger, G. H. J., De Villiers, M. F., Strauss, A. J., De Beer, M., Van Heerden, P. D. R., Maldonado, R. and Strasser, R. J. (2014). Inhibition of photosystem II activities in soybean (*Glycine max*) genotypes differing in chilling sensitivity. *South African Journal of Botany*, 95, 85-96.

Krzesłowska, M. (2011). The cell wall in plant cell response to trace metals: Polysaccharide remodeling and its role in defense strategy. *Acta Physiologia Plantarum*, 33, 35-51.

Ku, Y. S., Sintaha, M., Cheung, M. Y. and Lam, H. M. (2018). Plant hormone signaling crosstalks between biotic and abiotic stress responses. *International Journal of Molecular Sciences*, 19(10), 3206.

Kumar, P. and Sharma, P. K. (2020). Soil salinity and food security in India. *Frontiers in Sustainable Food Systems*, 4, 174.

Kumar, P., Kumar, T., Singh, S., Tuteja, N., Prasad, R. and Singh, J. (2020). Potassium: A key modulator for cell homeostasis. *Journal of Biotechnology*, 324, 198-210.

Kumar, V., Pandita, S., Sidhu, G. P. S., Sharma, A., Khanna, K., Kaur, P., Bali, A. S. and Setia, R. (2021). Copper bioavailability, uptake, toxicity and tolerance in plants: A comprehensive review. *Chemosphere*, 262, 127810.

Kumar, V., Thakur, R. K. and Kumar, P. (2019). Assessment of heavy metals uptake by cauliflower (*Brassica oleracea* var. botrytis) grown in integrated industrial effluent irrigated soils: A prediction modeling study. *Scientia Horticulturae*, 257, 108682.

Kumari, S., Kumar, S. and Prakash, P. (2018). Exogenous application of cytokinin (6-BAP) ameliorates the adverse effect of combined drought and high temperature stress in wheat seedling. *Journal of Pharmacognosy and Phytochemistry*, 7(1), 1176-1180.

Kupiec, M., Pienkowski, P., Bosiacka, B., Gutowska, I., Kupnicka, P., Prokopowicz, A., Chlubek, D. and Baranowska-Bosiacka, I. (2019). Old and new threats - trace metals and fluoride contamination in soils at defunct smithy sites. *International Journal of Environmental Research and Public Health*, 16 (5), 819.

Küpper, H., G€otz, B., Mijovilovich, A., Küpper, F. C. and Meyer-Klaucke, W. (2009). Complexation and toxicity of copper in higher plants. I.

characterization of copper accumulation, speciation, and toxicity in *Crassula helmsii* as a new copper accumulator. *Plant Physiology*, 151(2), 702-714.

Küpper, H., Šetlík, I., Setlikova, E., Ferimazova, N., Spiller, M. and Küpper, F. C. (2003). Copper-induced inhibition of photosynthesis: Limiting steps of in vivo copper chlorophyll formation in *Scmedesmus quadricanda*. *Functional Plant Biology*, 30, 1187-1190.

Küpper, H., Šetlík, I., Spiller, M., Küpper, F. C. and Prášil, O. (2002). Heavy metal-induced inhibition of photosynthesis: Targets of in vivo heavy metal chlorophyll formation1. *Journal of Phycology*, 38(3), 429-441.

Kuziemska, B., Trębicka, J., Wysokinski, A. and Jaremko, D. (2021). Supplementation of organic amendments improve yield and adaptability by reducing the toxic effect of copper in cocksfoot grass (*Dactylis glomerata* L. Cv Amera). *Agronomy*, 11(4), 791.

Lalthanpuii, P. B. and Lalchhandama, K. (2020). Chemical composition and broad-spectrum anthelmintic activity of a cultivar of toothache plant, *Acmella oleracea*, from Mizoram, India. *Pharmaceutical Biology*, 58(1), 393-399.

Lan, M. M., Liu, C., Liu, S. J., Qiu, R. L. and Tang, Y. T. (2020). Phytostabilization of Cd and Pb in highly polluted farmland soils using ramie and amendments. *International Journal of Environmental Research and Public Health*, 17(5), 1661.

Laporte, D., Rodríguez, F., González, A., Zúñiga, A., Castro-Nallar, E., Sáez, C. A. and Moenne, A. (2020). Copper-induced concomitant increases in photosynthesis, respiration, and C, N and S assimilation revealed by transcriptomic analyses in *Ulva compressa* (Chlorophyta). *BMC Plant Biology*, 20, 25.

Lebreton, S., Cabassa-Hourton, C., Savouré, A., Funck, D. and Forlani, G. (2020). Appropriate activity assays are crucial for the specific determination of proline dehydrogenase and pyrroline-5-carboxylate reductase activities. *Frontiers in Plant Science*, 11, 2113.

Leitenmaier, B. and Küpper, H. (2011). Cadmium uptake and sequestration kinetics in individual leaf cell protoplasts of the Cd/Zn hyperaccumulator *Thlaspi caerulescens*. *Plant, Cell and Environment*, 34(2), 208-219.

Leonardi, C., Pappalardo, H., Genovese, C., Puglia, G., Bua, G. D., Dugo, G. and Raccuia, S. A. (2016). Mechanisms of phytoextraction in *Cynara cardunculus* L. growing under cadmium and arsenic stress. *Acta Horticulturae*, 1147, 139-144.

Leszczyszyn, O. I., Imam, H. T. and Blindauer, C. A. (2013). Diversity and distribution of plant metallothioneins: A review of structure, properties and functions. *Metallomics*, 5(9), 1146-1169.

Lewis, D. H. (2019). Boron: The essential element for vascular plants that never was. *New Phytologist*, 221, 1685-1690.

Li, B., Byrt, C., Qiu, J., Baumann, U., Hrmova, M., Evrard, A., Johnson, A. A. T., Birnbaum, K. D., Mayo, G. M., Jha, D., Henderson, S. W., Tester, M., Gilliham, M. and Roy, S. J. (2016). Identification of a stelar-localized transport protein that facilitates root-to-shoot transfer of chloride in *Arabidopsis*. *Plant Physiology*, 170(2), 1014-1029.

Li, D., Pan, C., Lu, J., Zaman, W., Zhao, H., Zhang, J. and Lü, S. (2021c). Lupeol accumulation correlates with auxin in the epidermis of castor. *Molecules*, 26(10), 2978.

Li, J., Chang, Y., Al-Huqail, A. A., Ding, Z., Al-Harbi, M. S., Ali, E. F., Abeed, A. H. A., Rekaby, S. A., Eissa, M. A., Ghoneim, A. M. and Tammam, S. A. (2021b). Effect of manure and compost on the phytostabilization potential of heavy metals by the halophytic plant wavy-leaved saltbush. *Plants*, 10(10), 2176.

Li, J., Zhang, M., Sun, J., Mao, X., Wang, J., Liu, H., Zheng, H., Li, X., Zhao, H. and Zou, D. (2020b). Heavy metal stress-associated proteins in rice and *Arabidopsis*: Genome-wide identification, phylogenetics, duplication, and expression profiles analysis. *Frontiers in Genetics*, 11, 477.

Li, N., Euring, D., Cha, J. Y., Lin, Z., Lu, M., Huang, L. J. and Kim, W. Y. (2021a). Plant hormone-mediated regulation of heat tolerance in response to global climate change. *Frontiers in Plant Science*, 11, 2318.

Li, X. F., Su, M., Yang, M. F., Shen, S. H., Jiang, G. M., Qi, D. M., Chen, S. Y. and Liu, G. S. (2010). Major energy plants and their potential for bioenergy development in China. *Environmental Management*, 46(4), 579-589.

Li, X., Song, Y., Bian, Y., Gu, C., Yang, X., Wang, F. and Jiang, X. (2020a). Insights into the mechanisms underlying efficient Rhizodegradation of PAHs in biochar-amended soil: From microbial communities to soil metabolomics. *Environment International*, 144, 105995.

Liao, W., Yang, Y., Li, Y., Wang, G. and Peng, M. (2016). Genome-wide identification of cassava *R2R3MYB* family genes related to abscission zone separation after environmental-stress-induced abscission. *Scientific Reports*, 6(1), 1-12.

Lichtenthaler, H. K. and Wellburn, A. R. (1983). Determinations of total carotenoids and chlorophylls a and b of leaf extracts in different solvents. *Biochemical Society Transactions*, 11, 591-592.

Ligaba, A., Katsuhara, M., Shibasaka, M. and Djira, G. (2011). Abiotic stresses modulate expression of major intrinsic proteins in barley (*Hordeum vulgare*). *Comptes Rendus Biologies*, 334(2), 127-139.

Lima, L. R., Silva, H. F., Brignoni, A. S., Silva, F. G., Camargos, L. S. and Souza, L. A. (2019). Characterization of biomass sorghum for copper phytoremediation: Photosynthetic response and possibility as a bioenergy feedstock from contaminated land. *Physiology and Molecular Biology of Plants*, 25(2), 433-441.

Limmer, M. and Burken, J. (2016). Phytovolatilization of organic contaminants. *Environmental Science and Technology*, 50(13), 6632-6643.

Lin, L., Wu, J., Jiang, M. and Wang, Y. (2021). Plant mitogen-activated protein kinase cascades in environmental stresses. *International Journal of Molecular Sciences*, 22(4), 1543.

Lintunen, A., Paljakka, T., Jyske, T., Peltoniemi, M., Sterck, F., von Arx, G., Cochard, H., Copini, P., Caldeira, M. C., Delzon, S., Gebauer, R., Grönlund, L., Kiorapostolou, N., Lechthaler, S., Lobo-do-Vale, R., Peters, R. L., Petit, G., Prendin, A. L., Salmon, Y., Steppe, K., Urban, J., Juan, S. R. and Hölttä, T. (2016). Osmolality and non-structural carbohydrate composition in the secondary phloem of trees across a latitudinal gradient in Europe. *Frontiers in Plant Science*, 7, 726.

Liu, D. and Kottke, I. (2004). Subcellular localization of copper in the root cells of *Allium sativum* by electron energy loss spectroscopy (EELS). *Bioresource Technology*, 94, 153-158.

Liu, D., An, Z., Mao, Z., Ma, L. and Lu, Z. (2015). Enhanced heavy metal tolerance and accumulation by transgenic sugar beets expressing *Streptococcus thermophilus StGCS-GS* in the presence of Cd, Zn and Cu alone or in combination. *PLoS One*, 10(6), e0128824.

Liu, H., Hussain, S., Peng, S., Huang, J., Cui, K. and Nie, L. (2014a). Potentially toxic elements concentration in milled rice differ among various planting patterns. *Field Crops Research*, 168, 19-26.

Liu, J. J., Wei, Z. and Li, J. H. (2014b). Effects of copper on leaf membrane structure and root activity of maize seedling. *Botanical Studies*, 55(1), 1-6.

Liu, J., Wang, J., Lee, S. and Wen, R. (2018c). Copper-caused oxidative stress triggers the activation of antioxidant enzymes *via ZmMPK3* in maize leaves. *PLoS One*, 13(9), e0203612.

Liu, L., Li, W., Song, W. and Guo, M. (2018a). Remediation techniques for heavy metal-contaminated soils: Principles and applicability. *Science of the Total Environment*, 633, 206-219.

Liu, X., Li, R., Lu, W., Zhou, Z., Jiang, X., Zhao, H., Yang, B. and Lü, S. (2021). Transcriptome analysis identifies key genes involved in the regulation of epidermal lupeol biosynthesis in *Ricinus communis*. *Industrial Crops and Products*, 160, 113100.

Liu, Y., Liu, G., Yuan, Z., Liu, H. and Lam, P.K.S. (2018b). Heavy metals (As, Hg and V) and stable isotope ratios (d13C and d15N) in fish from Yellow River Estuary, China. *Science of the Total Environment*, 613-614, 462-471.

Llanes, A., Bertazza, G., Palacio, G. and Luna, V. (2013). Different sodium salts cause different solute accumulation in the halophyte *Prosopis strombulifera*. *Plant Biology*, 15, 118-125.

Llerena, J. P. P., Coasaca, R. L., Rodriguez, H. O. L., Llerena, S. Á. P., Valencia, Y. D. and Mazzafera, P. (2021). Metallothionein production is a common tolerance mechanism in four species growing in polluted Cu mining areas in Peru. *Ecotoxicology and Environmental Safety*, 212, 112009.

Lowry, O. H., Rosebrough, N. J., Farr, A. L. and Randall, R. J. (1951). Protein measurement with the Folin phenol reagent. *Journal of Biological Chemistry*, 193, 265-275.

Lu, Q., Weng, Y., You, Y., Xu, Q., Li, H., Li, Y., Liu, H. and Du, S. (2019). Inoculation with abscisic acid (ABA)-catabolizing bacteria can improve phytoextraction of heavy metal in contaminated soil. *Environmental Pollutio*n, 113497.

Lutts, S., Kinet, J. M. and Bouharmont, J. (1996). NaCl-induced senescence in leaves of rice (*Oryza sativa* L.) cultivars differing in salinity resistance. *Annals of Botany*, 78(3), 389-398.

Lux, A., Lukačová, Z., Vaculík, M., Švubová, R., Kohanová, J., Soukup, M., Martinka, M. and Bokor, B. (2020). Silicification of root tissues. *Plants*, 9(1), 111.

Lux, A., Martinka, M., Vaculik, M. and White P. J. (2011). Root responses to cadmium in the rhizosphere: A review. *Journal of Experimental Botany*, 62, 21-37.

Luyckx, M., Hausman, J. F., Lutts, S. and Guerriero, G. (2017). Impact of silicon in plant biomass production: Focus on bast fibres, hypotheses and perspectives. *Plants*, 6(3), 37.

Lwalaba, J. L. W., Louis, L. T., Zvobgo, G., Richmond, M. E. A., Fu, L., Naz, S., Mwamba, M., Mundende, R. P. M. and Zhang, G. (2020). Physiological and molecular mechanisms of cobalt and copper interaction in causing phyto-toxicity to two barley genotypes differing in Co tolerance. *Ecotoxicology and Environmental Safety*, 187, 109866.

Ma, J. F., Ueno, D., Zhao, F. and McGrath, S. P. (2005). Subcellular localisation of Cd and Zn in the leaves of a Cd-hyperaccumulating ecotype of *Thlaspi caerulescens*. *Planta*, 220, 731-736.

Ma, X., Zhang, J. and Huang, B. (2016). Cytokinin-mitigation of salt-induced leaf senescence in perennial ryegrass involving the activation of antioxidant systems and ionic balance. *Environmental and Experimental Botany*, 125, 1-11.

Mahar, A., Wang, P., Ali, A., Awasthi, M. K., Lahori, A. H., Wang, Q., Li, R. and Zhang, Z. (2016). Challenges and opportunities in the phytoremediation of heavy metals contaminated soils: A review. *Ecotoxicology and Environmental Safety*, 126, 111-121.

Maillard, A., Diquélou, S., Billard, V., Laîné, P., Garnica, M., Prudent, M., Garcia-Mina, J. M., Yvin, J. C. and Ourry, A. (2015). Leaf mineral nutrient remobilization during leaf senescence and modulation by nutrient deficiency. *Frontiers in Plant Science*, 6, 317.

Maksymiec, W. and Krupa, Z. (2002). Jasmonic acid and heavy metals in *Arabidopsis* plants - A similar physiological response to both stressors? *Journal of Plant Physiology*, 159, 509-515.

Malik, B., Pirzadah, T. B., Tahir, I. and Rehman, R. U. (2019). Growth and physiological responses in chicory towards mercury induced in vitro oxidative stress. *Plant Physiology Reports*, 24(2), 236-248.

Mallick, N. and Mohn, F. H. (2003). Use of chlorophyll fluorescence in metal-stress research: A case study with the green microalga *Scenedesmus*. *Ecotoxicology and Environmental Safety*, 55(1), 64-69.

Malnoë, M. (2018). Photoinhibition or photoprotection of photosynthesis? Update on the (newly termed) sustained quenching component qH. *Environmental and Experimental Botany*, 154, 123-133.

Mancinelli, A. L., Yang, C. P. H., Lindquist, P., Anderson, O. R. and Rabino, I. (1975). Photocontrol of anthocyanin synthesis: III. The action of streptomycin on the synthesis of chlorophyll and anthocyanin. *Plant Physiology*, 55, 251-257.

Mani, D. and Kumar, C. (2014). Biotechnological advances in bioremediation of heavy metals contaminated ecosystems: An overview with special reference to phytoremediation. *International Journal of Environmental Science and Technology*, 11, 843-872.

Markovich, O., Steiner, E., Kouřil, Š., Tarkowski, P., Aharoni, A. and Elbaum, R. (2017). Silicon promotes cytokinin biosynthesis and delays senescence in *Arabidopsis* and *Sorghum*. *Plant, Cell and Environment*, 40(7), 1189-1196.

Marques, D. M., Júnior, V. V., da Silva, A. B., Mantovani, J. R., Magalhães, P. C. and de Souza, T. C. (2018). Copper toxicity on photosynthetic responses and root morphology of *Hymenaea courbaril* L. (Caesalpinioideae). *Water, Air, and Soil Pollution*, 229(5), 1-14.

Marschner, H. (1995). Mineral nutrition of higher plants. 3rd edition, Academic Press, London, UK.

Marshall, J. A., Hovenden, M., Oda, T. and Hallegraeff, G. M. (2002). Photosynthesis does influence superoxide production in the ichthyotoxic alga *Chattonella marina* (Raphidophyceae). *Journal of Plankton Research*, 24 (11), 1231-1236.

Martins, J. P. R., de Vasconcelos, L. L., de Souza Braga, P. C., Rossini, F. P., Conde, L. T., Rodrigues, L. C. A., Falqueto, A. R. and Gontijo, A. B. P. L. (2020). Morphophysiological responses, bioaccumulation and tolerance of *Alternanthera tenella* Colla (Amaranthaceae) to excess copper under in vitro conditions. *Plant Cell Tissue and Organ Culture*, 143, 303-318.

Martins, J. P. R., Martins, A. D., Pires, M. F., Braga Junior, R. A., Reis, R. O., Dias, G. D. M. G. and Pasqual, M. (2016). Anatomical and physiological responses of *Billbergia zebrina* (Bromeliaceae) to copper excess in a controlled microenvironment. *Plant Cell, Tissue and Organ Culture*, 126(1), 43-57.

Maruyama-Nakashita, A., Nakamura, Y., Yamaya, T. and Takahashi, H. (2004). A novel regulatory pathway of sulfate uptake in *Arabidopsis* roots: Implication of CRE1/WOL/AHK4-mediated cytokinin-dependent regulation. *The Plant Journal*, 38(5), 779-789.

Marwood, C. A., Solomon, K. R. and Greenberg, B. M. (2001). Chlorophyll fluorescence as a bioindicator of effects on growth in aquatic macrophytes from mixtures of polycyclic aromatic hydrocarbons. *Environmental Toxicology and Chemistry*, 20(4), 890-898.

Masood, A., Iqbal, N. and Khan, N. A. (2012). Role of ethylene in alleviation of cadmium-induced photosynthetic capacity inhibition by sulphur in mustard. *Plant, Cell and Environment*, 35(3), 524-533.

Massoud, M. B., Sakouhi, L., Karmous, I., Zhu, Y., El Ferjani, E., Sheehan, D. and Chaoui, A. (2018). Protective role of exogenous phytohormones on redox status in pea seedlings under copper stress. *Journal of Plant Physiology*, 221, 51-61.

Mathur, S., Kalaji, H. M. and Jajoo, A. (2016). Investigation of deleterious effects of chromium phytotoxicity and photosynthesis in wheat plant. *Photosynthetica*, 54(2), 185-192.

Matthes, M. S., Robil, J. M. and McSteen, P. (2020). From element to development: The power of the essential micronutrient boron to shape morphological processes in plants. *Journal of Experimental Botany*, 71, 1681-1693.

Mazen, A. M. A. (2004). Calcium oxalate deposits in leaves of *Corchorus olitorius* as related to accumulation of toxic metals. *Russian Journal of Plant Physiology*, 51, 281-285.

McBride, M. B., Kelch, S., Schmidt, M., Zhou, Y., Aristilde, L. and Martinez, C. E. (2019). Lead solubility and mineral structures of coprecipitated lead/calcium oxalates. *Environmental Science and Technology*, 53, 13794-13801.

Mehmood, F., Khan, A. U. H. and Khan, Z. U. D. (2011). Appraisal of ecological significance of *Ricinus communis* Linn. in the wasteland of Lahore, Pakistan. *Biologia*, 57(1&2), 97-103.

Mehta, P., Jajoo, A., Mathur, S. and Bharti, S. (2010). Chlorophyll *a* fluorescence study revealing effects of high salt stress on photosystem II in wheat leaves. *Plant Physiology and Biochemistry*, 48(1), 16-20.

Mendes M. G., Santos Junior C. D., Dias A. C. C. and Bonetti A. M. (2015). Castor bean (*Ricinus communis* L.) as a potential environmental bioindicator. *Genetics and Molecular Research*, 14, 12880-12887.

Meng, Q., Zou, J., Zou, J. H., Jiang, W. S. and Liu, D. H. (2007). Effect of Cu^{2+} concentration on growth, antioxidant enzyme activity and malondialdehyde content in garlic (*Allium sativum* L.). *Acta Biologica Cracoviensia Botanica*, 49(1), 95-101.

Merewitz, E. B., Du, H., Yu, W., Liu, Y., Gianfagna, T. and Huang, B. (2012). Elevated cytokinin content in ipt transgenic creeping bentgrass promotes drought tolerance through regulating metabolite accumulation. *Journal of Experimental Botany*, 63(3), 1315-1328.

Milan, B., Slobodanka, P., Nataša, N., Borivoj, K., Milan, Ž., Marko, K., Andrej, P. and Saša, O. (2012). Response of *Salix alba* L. to heavy metals and diesel fuel contamination. *African Journal of Biotechnology*, 11, 14313-14319.

Milieu. (2008). *Environmental, Economic and Social Impacts of the use of Sewage Sludge on Land*. Available online: http://ec.europa.eu/environment/archives/waste/sludge/pdf/part_ii_report.pdf

Milman, O. (2015). Earth has lost a third of arable land in past 40 years, scientists say. *The Guardian*, 2, 12.

Mir, M. A., Sirhindi, G., Alyemeni, M. N., Alam, P. and Ahmad, P. (2018), Jasmonic acid improves growth performance of soybean under nickel toxicity by regulating nickel uptake, redox balance, and oxidative stress metabolism. *Journal of Plant Growth Regulation*, 37, 1195-1209.

Mirecki, R. M. and Teramura, A. H. (1984). Effects of ultraviolet-B irradiance on soybean: V. The dependence of plant sensitivity on the photosynthetic photon flux density during and after leaf expansion. *Plant Physiology*, 74, 475-480.

Mirshad, P. P. and Puthur, J. T. (2017). Drought tolerance of bioenergy grass *Saccharum spontaneum* L. enhanced by arbuscular mycorrhizae. *Rhizosphere*, 3, 1-8.

Mirza, N., Pervez, A., Mahmood, Q., Shah, M. M. and Shafqat, M. N. (2011). Ecological restoration of arsenic contaminated soil by *Arundo donax* L. *Ecological Engineering*, 37, 1949-1956.

Mishra, B. K., Srivastava, J. P., Lal, J. P. and Sheshshayee, M. S. (2016). Physiological and biochemical adaptations in lentil genotypes under drought stress. *Russian Journal of Plant Physiology*, 63(5), 695-708.

Mishra, B., Sangwan, R. S., Mishra, S., Jadaun, J. S., Sabir, F. and Sangwan, N. S. (2014). Effect of cadmium stress on inductive enzymatic and nonenzymatic responses of ROS and sugar metabolism in multiple shoot cultures of Ashwagandha (*Withania somnifera* Dunal). *Protoplasma*, 251 (5), 1031-1045.

Mittler, R. (2017). ROS are good. *Trends in Plant Science*, 22(1), 11-19.

Mohanty, M. (2016). Post-harvest management of phytoremediation technology. *Journal of Environmental and Analytical Toxicology*, 6, 398.

Montenegro, A. C., Ferreyroa, G. V., Parolo, M. E., Tudino, M. B., Lavado, R. S. and Molina, F. V. (2015). Copper speciation in soil: Time evolution and effect of clay amendment. *Water Air and Soil Pollution*, 226(9), 293.

Montero-Palmero, M. B., Martín-Barranco, A., Escobar, C. and Hernández, L. E. (2014a). Early transcriptional responses to mercury: A role for ethylene in mercury-induced stress. *New Phytologist*, 201(1), 116-130.

Montero-Palmero, M. B., Ortega-Villasante, C., Escobar, C. and Hernández, L. E. (2014b). Are plant endogenous factors like ethylene modulators of the early oxidative stress induced by mercury?. *Frontiers in Environmental Science*, 2, 34.

Moore, S. and Stein, W. H. (1948). Photometric ninhydrin method for use in the chromatography of amino acids. *Journal of Biological Chemistry*, 176, 367-388.

Mou, R. X., Cao, Z. Y., Lin, X. Y., Wu, L., Cao, Z. Z., Zhu, Z. W. and Chen, M. X. (2016). Characterization of the phytochelatins and their derivatives in rice exposed to cadmium based on high-performance liquid chromatography coupled with data-dependent hybrid linear ion trap orbitrap mass spectrometry. *Rapid Communications in Mass Spectrometry*, 30(16), 1891-1900.

Mourato, M. P., Moreira, I. N., Leitao, I., Pinto, F. R., Sales, J. R. and Martins, L. L. (2015). Effect of heavy metals in plants of the genus *Brassica*. *International Journal of Molecular Science*s, 16, 17975-17998.

Mukhtar, S., Bhatti, H. N., Khalid, M., Haq, M. A. and Shahzad, S. M. (2010). Potential of sunflower (*Helianthus annuus* L.) for phytoremediation of nickel (Ni) and lead (Pb) contaminated water. *Pakistan Journal of Botany*, 42, 4017-4026.

Müller, M. and Munné-Bosch, S. (2021). Hormonal impact on photosynthesis and photoprotection in plants. *Plant physiology*, 185(4), 1500-1522.

Muthu, M., Gopal, J., Kim, D. H. and Sivanesan, I. (2021). Reviewing the impact of vehicular pollution on road-side plants - future perspectives. *Sustainability*, 13(9), 5114.

Muthusaravanan, S., Sivarajasekar, N., Vivek, J. S., Paramasivan, T., Naushad, M., Prakashmaran, J., Gayathri, V. and Al-Duaij, O. K. (2018). Phytoremediation of heavy metals: Mechanisms, methods and enhancements. *Environmental Chemistry Letters*, 16, 1339-1359.

Myśliwa-Kurdziel, B., Prasad, M. N. V. and Strzałtka, K. (2004). Photosynthesis in heavy metal stressed plants. In: *Heavy Metal Stress in Plants*, Prasad, M. N. V. (Ed.), Springer, Berlin, Heidelberg, pp. 146-181.

Mythili, G. and Goedecke, J. (2016). Economics of land degradation in India. In: *Economics of Land Degradation and Improvement- A Global Assessment for Sustainable Development*, Nkonya, E., Mirzabaev, A. and von Braun, J. (Eds.), Cham, Springer, pp. 431-469.

Nagy, V., Vidal-Meireles, A., Tengölics, R., Rákhely, G., Garab, G., Kovács, L. and Tóth, S. Z. (2016). Ascorbate accumulation during sulphur deprivation and its effects on photosystem II activity and H_2 production of the green alga *Chlamydomonas reinhardtii*. *Plant, Cell and Environment*, 39, 1460-1472.

Naing, A. H. and Kim, C. K. (2018). Roles of *R2R3-MYB* transcription factors in transcriptional regulation of anthocyanin biosynthesis in horticultural plants. *Plant Molecular Biology*, 98, 1-18.

Naing, A. H. and Kim, C. K. (2021). Abiotic stress-induced anthocyanins in plants: Their role in tolerance to abiotic stresses. *Physiologia Plantarum*, 172(3), 1711-1723.

Nair, P. M. G. and Chung, I. M. (2015). Study on the correlation between copper oxide nanoparticles induced growth suppression and enhanced lignification in Indian mustard (*Brassica juncea* L.). *Ecotoxicology and Environmental Safety*, 113, 302-313.

Nakajima, T., Yamada, T., Anzoua, K. G., Kokubo, R. and Noborio, K. (2018). Carbon sequestration and yield performances of *Miscanthus* × *giganteus* and *Miscanthus sinensis*. *Carbon Management*, 9, 415-423.

Nakano, Y. and Asada, K. (1981). Hydrogen peroxide is scavenged by ascorbate-specific peroxidase in spinach chloroplasts. *Plant and Cell Physiology*, 22(5), 867-880.

Nawaz, H., Yasmeen, A., Anjum, M. A. and Hussain, N. (2016). Exogenous application of growth enhancers mitigate water stress in wheat by antioxidant elevation. *Frontiers in Plant Science*, 7, 597.

Nedjimi, B. (2021). Phytoremediation: A sustainable environmental technology for heavy metals decontamination. *SN Applied Sciences*, 3(3), 1-19.

Neto, A. D. A., Prisco, J. T. and Gomes-Filho, E. (2009). Changes in soluble amino-N, soluble proteins and free amino acids in leaves and roots of salt-stressed maize genotypes. *Journal of Plant Interactions*, 4(2), 137-144.

Neumann, D., ZurNieden, U., Lichtenberger, O. and Leopold, I. (1995). How does *Armeria maritime* tolerate high heavy metal concentrations?.*Journal of Plant Physiology*, 146, 704-717.

Nevo, Y. and Nelson, N. (2006). The NRAMP family of metal-ion transporters. *Biochimica et Biophysica Acta (BBA)-Molecular Cell Research*, 1763(7), 609-620.

Nguyen, T. Q., Sesin, V., Kisiala, A. and Emery, R. N. (2021). Phytohormonal roles in plant responses to heavy metal stress: Implications for using macrophytes in phytoremediation of aquatic ecosystems. *Environmental Toxicology and Chemistry*, 40(1), 7-22.

Niksa, D., Krzyżaniak, M. and Stolarski, M. J. (2020). The estimation of above- and below-ground biomass residues and carbon sequestration potential in soil on commercial willow plantation. In: *Renewable Energy Sources: Engineering, Technology, Innovation*, Wróbel, M., Jewiarz, M. and Szlęk, A. (Eds.), Springer International Publishing, Switzerland, pp. 257-266.

Noojipady, P., Prince, S. D. and Rishmawi, K. (2015). Reductions in productivity due to land degradation in the drylands of the southwestern United States. *Ecosystem Health and Sustainablity*, 1, 1-15.

Obenland, D. (1993). Purification and characterization of three soluble invertases from barley (*Hordeum vulgare* L.) leaves. *Plant Physiology*, 101(4), 1331-1339.

O'Brien, J. A. and Benková, E. (2013). Cytokinin cross-talking during biotic and abiotic stress responses. *Frontiers in Plant Science*, 4, 451.

Ochoa-Villarreal, M., Aispuro-Hernández, E., Vargas-Arispuro, I. and Martínez-Téllez, M. Á. (2012). Plant cell wall polymers: Function, structure and biological activity of their derivatives. In: *Polymerization*, Gomes, A. D. S. (Ed.) IntechOpen, London, pp. 63-86.

Oh, K., Li, T., Cheng, H., Hu, X., Lin, Q. and Xie, Y. (2013). A primary study on assessment of phytoremediation potential of biofuel crops in heavy metal contaminated soil. *Appied Mechanics and Materials*, 295, 1135-1138.

Ojuederie, O. B. and Babalola, O. O. (2017). Microbial and plant-assisted bioremediation of heavy metal polluted environments: A review. *International Journal of Environmental Research and Public Health*, 14(12), 1504.

Olivares, A. R., Carrillo-González, R., González-Chávez, M. D. C. A. and Hernández, R. M. S. (2013). Potential of castor bean (*Ricinus communis* L.) for phytoremediation of mine tailings and oil production. *Journal of Environmental Management*, 114, 316-323.

Olkhovych, O., Volkogon, M., Taran, N., Batsmanova, L. and Kravchenko, I. (2016). The effect of copper and zinc nanoparticles on the growth parameters, contents of ascorbic acid, and qualitative composition of amino acids and acylcarnitines in *Pistia stratiotes* L. (Araceae). *Nanoscale Research Letters*, 11(1), 1-9.

Olmedo, P., Zepeda, B., Rojas, B., Silva-Sanzana, C., Delgado-Rioseco, J., Fernández, K., Balic, I., Arriagada, C., Moreno, A. A., Defilippi, B. G. and Campos-Vargas, R. (2021). Cell wall calcium and hemicellulose have a role in the fruit firmness during storage of blueberry (*Vaccinium spp*.). *Plants*, 10(3), 553.

Omidifar, N., Nili-Ahmadabadi, A., Nakhostin-Ansari, A., Lankarani, K. B., Moghadami, M., Mousavi, S. M., Hashemi, S. A., Gholami, A., Shokripour, M. and Ebrahimi, Z. (2021). The modulatory potential of herbal antioxidants against oxidative stress and heavy metal pollution: Plants against environmental oxidative stress. *Environmental Science and Pollution Research*, 28(44), 61908-61918.

Osman, K. T. (2013a). Chemical soil degradation. In: *Soil Degradation, Conservation and Remediation*, Osman, K. T. (Ed.), Springer, Netherlands, pp. 125-148.

Osman, K. T. (2013b). Soil pollution. In: *Soil Degradation, Conservation and Remediation*, Osman, K. T. (Ed.), Springer, Netherlands, pp. 149-226.

Ouzounidou, G. and Ilias, I. (2005). Hormone-induced protection of sunflower photosynthetic apparatus against copper toxicity. *Biologia Plantarum*, 49(2), 223.

Ouzounidou, G., Ilias, I., Kabataidis, M. and Chatzimichail, A. (2003). Comparative study of nutrient deficiencies on growth and photochemistry of tobacco. *Journal of Plant Nutrition*, 26, 1605-1616.

Ouzounidou, G., Moustakas, M. and Strasser, R. J. (1997). Sites of action of copper in the photosynthetic apparatus of maize leaves: Kinetic analysis of chlorophyll fluorescence, oxygen evolution, absorption changes and thermal dissipation as monitored by photoacoustic signals. *Functional Plant Biology*, 24, 81-90.

Palanivel, T. M, Pracejus, B. and Victor, R. (2020). Phytoremediation potential of castor (*Ricinus communis* L.) in the soils of the abandoned copper mine in Northern Oman: Implications for arid regions. *Environmental Science and Pollution Research*, 27, 17359-17369.

Pan, G., Yan, W., Zhang, H., Xiao, Z., Li, X., Liu, W. and Zheng, L. (2019). Subcellular distribution and chemical forms involved in manganese accumulation and detoxification for *Xanthium strumarium* L. *Chemosphere*, 237, 124531.

Panagos, P., Ballabio, C., Lugato, E., Jones, A., Borrelli, P., Scarpa, S., Orgiazzi, A. and Montanarella, L. (2018). Potential sources of anthropogenic copper inputs to European agricultural soils. *Sustainability*, 10(7), 2380.

Pandey, P., Singh, J., Achary, V. and Reddy, M. K. (2015). Redox homeostasis *via* gene families of ascorbate-glutathione pathway. *Frontiers in Environmental Science*, 3, 25.

Papazoglou, E. G., Alexopoulou, E., Papadopoulos, G. K. and Economou-Antonaka, G. (2020). Tolerance to drought and water stress resistance mechanism of castor bean. *Agronomy*, 10(10), 1580.

Patel, V. R., Dumancas, G. G., Viswanath, L. C. K., Maples, R. and Subong, B. J. J. (2016). Castor oil: Properties, uses, and optimization of processing parameters in commercial production. *Lipid insights*, 9, 1-12.

Patniak, P. (2010). *Handbook of Environmental Analysis: Chemical Pollutants in Air, Water, Soil and Solid Wastes*. 2nd Edition, CRC Press, Taylor and Francis Group, Boca Raton, p. 770.

Patrick, J. W., Botha, F. C. and Birch, R. G. (2013). Metabolic engineering of sugars and simple sugar derivatives in plants. *Plant Biotechnology Journal*, 11, 142-156.

Paunov, M., Koleva, L., Vassilev, A., Vangronsveld, J. and Goltsev, V. (2018). Effects of different metals on photosynthesis: Cadmium and zinc affect chlorophyll fluorescence in durum wheat. *International Journal of Molecular Sciences*, 19(3), 787.

Pavlíková, D., Pavlík, M., Staszková, L., Motyka, V., Száková, J., Tlustoš, P. and Balík, J. (2008). Glutamate kinase as a potential biomarker of heavy metal stress in plants. *Ecotoxicology and Environmental Safety*, 70(2), 223-230.

Paz-Ferreiro, J. and Fu, S. (2016). Biological indices for soil quality evaluation: Perspectives and limitations. *Land Degradation and Development*, 27, 14-25.

Peleg, Z. and Blumwald, E. (2011). Hormone balance and abiotic stress tolerance in crop plants. *Current Opinion in Plant Biology*, 14(3), 290-295.

Peng, D., Shafi, M., Wang, Y., Li, S., Yan, W., Chen, J., Ye, Z. and Liu, D. (2015). Effect of Zn stresses on physiology, growth, Zn accumulation, and chlorophyll of *Phyllostachys pubescens*. *Environmental Science and Pollution Research*, 22(19), 14983-14992.

Peng, J. and Gong, J. (2014). Vacuolar sequestration capacity and long-distance metal transport in plants. *Frontiers in Plant Science*, 5, 19.

Pereira, G. L., Siqueira, J. A., Batista-Silva, W., Cardoso, F. B., Nunes-Nesi, A. and Araújo, W. L. (2021). Boron: More than an essential element for land plants?. *Frontiers in Plant Science*, 11, 610307.

Peter, L., Clausen, W., Broholm, M. M., Gosewinkel, U. and Trapp, S. (2017). Test of aerobic TCE degradation by willows (*Salix viminalis*) and willows inoculated with TCE-cometabolizing strains of *Burkholderia cepacia*. *Environmental Science and Pollution Research*, 24, 18320-18331.

Pilon-Smits, E. (2005). Phytoremediation. *Annual Review of Plant Biology*, 56, 15-39.

Piotrowska-Niczyporuk, A., Bajguz, A., Kotowska, U., Zambrzycka-Szelewa, E. and Sienkiewicz, A. (2020). Auxins and cytokinins regulate phytohormone homeostasis and thiol-mediated detoxification in the green alga *Acutodesmus obliquus* exposed to lead stress. *Scientific Reports*, 10(1), 1-14.

Piotrowska-Niczyporuk, A., Bajguz, A., Zambrzycka, E. and Godlewska-Żyłkiewicz, B. (2012). Phytohormones as regulators of heavy metal biosorption and toxicity in green alga *Chlorella vulgaris* (Chlorophyceae). *Plant Physiology and Biochemistry*, 52, 52-65.

Piotrowska-Niczyporuk, A., Bajguz, A., Zambrzycka-Szelewa, E. and Bralska, M. (2018). Exogenously applied auxins and cytokinins ameliorate lead toxicity by inducing antioxidant defense system in green alga *Acutodesmus obliquus*. *Plant Physiology and Biochemistry*, 132, 535-546.

Polle, A., Otter, T. and Seifert, F. (1994). Apoplastic peroxidases and lignification in needles of Norway spruce (*Piceaabies* L.). *Plant Physiology*, 106(1), 53-60.

Prajapati, R., Kataria, S. and Jain, M. (2020). Seed priming for alleviation of heavy metal toxicity in plants: An overview. *Plant Science Today*, 7(3), 308-313.

Printz, B., Lutts, S., Hausman, J. F. and Sergeant, K. (2016). Copper trafficking in plants and its implication on cell wall dynamics. *Frontiers in Plant Science*, 7, 601.

Purdy, J. J. and Smart, L. B. (2008). Hydroponic screening of shrub willow (*Salix spp*.) for arsenic tolerance and uptake. *International Journal of Phytoremediation*, 10, 515-28.

Puthur, J. T. (2000). *Photosynthetic events in Sesbania sesban (L.) Merrill in relation to osmotic stress during different developmental stages*. Ph.D. Thesis, Jamia Millia Islamia Central University, New Delhi, India.

Qian, Y., Follett, R. F. and Kimble, J. M. (2010). Soil organic carbon input from urban turfgrasses. *Soil Science Society of America Journal*, 74, 366-371.

Radziemska, M., Vaverková, M. D. and Baryła, A. (2017). Phytostabilization - management strategy for stabilizing trace elements in contaminated soils. *International Journal of Environmental Research and Public Health*, 14(9), 958.

Rai, K. K., Pandey, N., Meena, R. P. and Rai, S. P. (2021a). Biotechnological strategies for enhancing heavy metal tolerance in neglected and underutilized legume crops: A comprehensive review. *Ecotoxicology and Environmental Safety*, 208, 111750.

Rai, P. K., Lee, S. S., Zhang, M. M., Tsang, Y. F. and Kim, K. H. (2019). Heavy metals in food crops: Health risks, fate, mechanisms, and management. *Environment International*, 125, 365-385.

Rai, S., Singh, P. K., Mankotia, S., Swain, J. and Satbhai, S. B. (2021b). Iron homeostasis in plants and its crosstalk with copper, zinc, and manganese. *Plant Stress*, 1, 100008.

Rai, V. K. (2002). Role of amino acids in plant responses to stresses. *Biologia Plantarum*, 45, 481-487.

Ramakrishna, B. and Rao, S. S. R. (2015). Foliar application of brassinosteroids alleviates adverse effects of zinc toxicity in radish (*Raphanus sativus* L.) plants. *Protoplasma*, 252, 665-667.

Rangani, J., Panda, A., Patel, M. and Parida, A. K. (2018). Regulation of ROS through proficient modulations of antioxidative defense system maintains the structural and functional integrity of photosynthetic apparatus and confers drought tolerance in the facultative halophyte *Salvadora persica* L. *Journal of Photochemistry and Photobiology B: Biology*, 189, 214-233.

Rani, S., Singh, V., Sharma, M. K. and Sisodia, R. (2021). GC-MS based metabolite profiling of medicinal plant - *Catharanthus roseus* under cadmium stress. *Plant Physiology Reports*, 1-12.

Rao, X. and Dixon, R. A. (2017). Brassinosteroid mediated cell wall remodeling in grasses under abiotic stress. *Frontiers in Plant Science*, 8, 806.

Rascio, N. and Navari-Izzo, F. (2011). Heavy metal hyperaccumulating plants: How and why do they do it? And what makes them so interesting? *Plant Science*, 180, 169-181.

Rathika, R., Srinivasan, P., Alkahtani, J., Al-Humaid, L. A., Alwahibi, M. S., Mythili, R. and Selvankumar, T. (2021). Influence of biochar and EDTA on enhanced phytoremediation of lead contaminated soil by *Brassica juncea*. *Chemosphere*, 271, 129513.

Raven, J. A. (2017). Chloride: Essential micronutrient and multifunctional beneficial ion. *Journal of Experimental Botany*, 68(3), 359-367.

Razaq, M., Zhang, P., Shen, H. and Salahuddin, S. (2017). Influence of nitrogen and phosphorous on the growth and root morphology of *Acer mono*. *PLoS One*, 12, e0171321.

Reeves, R. D., Baker, A. J., Jaffre, T., Erskine, P. D., Echevarria, G. and van der Ent, A. (2018). A global database for plants that hyperaccumulate metal and metalloid trace elements. *New Phytologists*, 218, 407-411.

Rehman, M., Liu, L., Wang, Q., Saleem, M. H., Bashir, S., Ullah, S. and Peng, D. (2019). Copper environmental toxicology, recent advances, and future outlook: A review. *Environmental Science and Pollution Research*, 26(18), 18003-18016.

Ren, H., Li, Y. N., Zhao, F. F., Pu, X. J., Wei, L. J., Lv, X., Zhu, F. and Lin, H. H. (2016). The role of autophagy in alleviating damage of aluminum stress in *Arabidopsis thaliana*. *Plant Growth Regulation*, 79, 167-175.

Rhaman, M. S., Imran, S., Rauf, F., Khatun, M., Baskin, C. C., Murata, Y. and Hasanuzzaman, M. (2021). Seed priming with phytohormones: An effective approach for the mitigation of abiotic stress. *Plants*, 10(1), 37.

Rhodes, D., Nadolska-Orczyk, A. and Rich, P. J. (2002). Salinity, osmolytes and compatible solutes. In: *Salinity: Environment-Plants-Molecules*. Lauchli, A. and Luttge, U. (Eds.), Kluwer, Dordrecht, pp. 181-204.

Ritter, A., Dittami, S. M., Goulitquer, S., Correa, J. A., Boyen, C., Potin, P. and Tonon, T. (2014). Transcriptomic and metabolomic analysis of copper stress acclimation in *Ectocarpus siliculosus* highlights signaling and tolerance mechanisms in brown algae. *BMC Plant Biology*, 14(1), 1-17.

Riyazuddin, R., Nisha, N., Ejaz, B., Khan, M. I. R., Kumar, M., Ramteke, P. W. and Gupta, R. (2022). A Comprehensive review on the heavy metal toxicity and sequestration in plants. *Biomolecules*, 12(1), 43.

Rizwan, M., Ali, S., Adrees, M., Ibrahim, M., Tsang, D. C. W., Zia-ur-Rehman, M., Zahir, Z. A., Rinklebe, J., Tack F. M. G. and Ok, Y. S. (2017). A critical review on effects, tolerance mechanisms and management of cadmium in vegetables. *Chemosphere*, 182, 90-105.

Rogowska, A. and Szakiel, A. (2021). Enhancement of phytosterol and triterpenoid production in plant hairy root cultures - simultaneous stimulation or competition?. *Plants*, 10(10), 2028.

Roig, N., Sierra, J., Martí, E., Nadal, M., Schuhmacher, M. and Domingo, J. L. (2012). Long-term amendment of Spanish soils with sewage sludge: Effects on soil functioning. *Agriculture Ecosystem and Environment*, 158, 41-48.

Roitsch, T. and González, M. C. (2004). Function and regulation of plant invertases: Sweet sensations. *Trends in Plant Science*, 9(12), 606-613.

Romdhane, L., Panozzo, A., Radhouane, L., Dal Cortivo, C., Barion, G. and Vamerali, T. (2021). Root characteristics and metal uptake of maize (*Zea mays* L.) under extreme soil contamination. *Agronomy*, 11(1), 178.

Romic, M. and Romic, D. (2003). Heavy metals distribution in agricultural topsoils in urban area. *Environmental Geology*, 43, 795-805.

Roncarati, F., Sáez, C. A., Greco, M., Gledhill, M., Bitonti, M. B. and Brown, M. T. (2015). Response differences between *Ectocarpussiliculosus* populations to copper stress involve cellular exclusion and induction of the phytochelatin biosynthetic pathway. *Aquatic Toxicology*, 159, 167-175.

Rosa, M., Prado, C., Podazza, G., Interdonato, R., González, J. A., Hilal, M. and Prado, F. E. (2009). Soluble sugars: Metabolism, sensing and abiotic stress: A complex network in the life of plants. *Plant Signaling and Behavior*, 4 (5), 388-393.

Rosier, A., Medeiros, F. H. and Bais, H. P. (2018). Defining plant growth promoting rhizobacteria molecular and biochemical networks in beneficial plant-microbe interactions. *Plant and Soil*, 428(1), 35-55.

Rout, G. R. and Sahoo, S. (2015). Role of iron in plant growth and metabolism. *Reviews in Agricultural Sciences*, 3, 1-24.

Rout, J. R. and Sahoo, S. L. (2013). Antioxidant enzyme gene expression in response to copper stress in *Withania somnifera* L. *Plant Growth Regulation*, 71(1), 95-99.

Rout, J. R., Sahoo, S. L., Das, R., Ram, S. S., Chakraborty, A. and Sudarshan, M. (2017). Changes in antioxidant enzyme activities and elemental profiling of *Abutilon indicum* L. subjected to copper stress. *Proceedings of the National Academy of Sciences, India Section B: Biological Sciences*, 87(4), 1469-1478.

Ruan, Y. L. (2014). Sucrose metabolism: Gateway to diverse carbon use and sugar signaling. *Annual Review of Plant Biology*, 65(1), 33-67.

Rucińska-Sobkowiak, R. (2016). Water relations in plants subjected to heavy metal stresses. *Acta Physiologiae Plantarum*, 38(11), 1-13.

Rucińska-Sobkowiak, R., Nowaczyk, G., Krzesłowska, M., Rabęda, I. and Jurga, S. (2013). Water status and water diffusion transport in lupine roots exposed to lead. *Environmental and Experimental Botany*, 87, 100-109.

Saba, H., Jyoti, P. and Neha, S. (2013). Mycorrhizae and phytochelators as remedy in heavy metal contaminated land remediation. *International Research Journal of Environmental Sciences*, 2(1), 74-78.

Sachdev, S., Ansari, S. A., Ansari, M. I., Fujita, M. and Hasanuzzaman, M. (2021). Abiotic stress and reactive oxygen species: Generation, signaling, and defense mechanisms. *Antioxidants*, 10(2), 277.

Sagardoy, R., Vázquez, S., Florez-Sarasa, I. D., Albacete, A., Ribas-Carbó, M., Flexas, J., Abadía, J. and Morales, F. (2010). Stomatal and mesophyll conductances to CO_2 are the main limitations to photosynthesis in sugar beet (*Beta vulgaris*) plants grown with excess zinc. *New Phytologist*, 187 (1), 145-158.

Sağlam, A., Yetişsin, F., Demiralay, M. and Terzi, R. (2016). Copper stress and responses in plants. In: *Plant Metal Interaction: Emerging Remediation Techniques*, Ahmad, P. (Ed.), 1st edition, Elsevier, USA, pp. 21-40.

Saini, S., Kaur, N. and Pati, P. K. (2021). Phytohormones: Key players in the modulation of heavy metal stress tolerance in plants. *Ecotoxicology and Environmental Safety*, 223, 112578.

Sairam, R. K., Deshmukh, P. S. and Shukla, D. S. (1997). Tolerance of drought and temperature stress in relation to increased antioxidant enzyme activity in wheat. *Journal of Agronomy and Crop Science*, 178(3), 171-178.

Sakakibara, H., Honda, Y., Nakagawa, S., Ashida, H. and Kanazawa, K. (2003). Simultaneous determination of all polyphenols in vegetables, fruits, and teas. *Journal of Agricultural and Food Chemistry*, 51, 571-581.

Sakakibara, M., Watanabe, A., Inoue, M., Sano, S. and Kaise, T. (2010). Phytoextraction and phytovolatilization of arsenic from as-contaminated soils by *Pteris vittata*. *Proceedings of the Annual International Conference on Soils, Sediments, Water and Energy*, 12, 26.

Saleem, M. H., Fahad, S., Rehman, M., Saud, S., Jamal, Y., Khan, S. and Liu, L. (2020). Morpho-physiological traits, biochemical response and phytoextraction potential of short-term copper stress on kenaf (*Hibiscus cannabinus* L.) seedlings. *PeerJ*, 8, e8321.

Saleem, S., Mushtaq, N. U., Shah, W. H., Rasool, A. and Rehman, R. U. (2021). Microbial and plant-assisted bioremediation of heavy metal polluted environments. In: *Heavy Metal Toxicity in Plants: Physiological and Molecular Adaptations*, Aftab, T. and Hakeem, K. M. (Eds.), CRC Press, Taylor and Francis Group, New York, pp. 139-156.

Sall, M. L., Diaw, A. K. D., Gningue-Sall, D., Aaron, S. E. and Aaron, J. J. (2020). Toxic heavy metals: Impact on the environment and human health, and treatment with conducting organic polymers, a review. *Environmental Science and Pollution Research*, 27, 29927-29942.

Salt, D. E., Prince, R. C., Baker, A. J. M., Raskin, I. and Pickering, I. J. (1999). Zinc ligands in the metal hyperaccumulator *Thlaspi caerulescens* as determined using X-ray absorption spectroscopy. *Environmental Science and Technology*, 33, 713-717.

Salt, D. E., Prince, R. C., Pickering, I. J. and Raskin, I. (1995). Mechanisms of cadmium mobility and accumulation in Indian mustard. *Plant Physiology*, 109, 1427-1433.

Sameena P. P. and Puthur J. T. (2021c). Differential modulation of photosynthesis and defense strategies towards copper toxicity in primary and cotyledonary

leaves of *Ricinus communis* L. *Journal of Photochemistry and Photobiology*, 8, 100059.

Sameena, P. P. and Puthur, J. T. (2021a). Heavy metal phytoremediation by bioenergy plants and associated tolerance mechanisms. *Soil and Sediment Contamination: An International Journal*, 30(3), 253-274.

Sameena, P. P. and Puthur, J. T. (2021b). Cotyledonary leaves effectively shield the true leaves in *Ricinus communis* L. from copper toxicity. *International Journal of Phytoremediation*, 23(5), 492-504.

Sanaei, S., Sadeghinia, M., Meftahizade, H., Ardakani, A. F. and Ghorbanpour, M. (2021). Cadmium and lead differentially affect growth, physiology, and metal accumulation in guar (*Cyamopsis tetragonoloba* L.) genotypes. *Environmental Science and Pollution Research*, 1-13.

Santino, A., Taurino, M., De Domenico, S., Bonsegna, S., Poltronieri, P., Pastor, V. and Flors, V. (2013). Jasmonate signaling in plant development and defense response to multiple (a)biotic stresses. *Plant Cell Reports*, 32(7), 1085-1098.

Sarath, N. G., Shackira, A. M., El-Serehy, H. A., Hefft, D. I. and Puthur, J. T. (2022). Phytostabilization of arsenic and associated physio-anatomical changes in *Acanthus ilicifolius* L. *Environmental Pollution*, 118828.

Sardans, J. and Peñuelas, J. (2021). Potassium control of plant functions: Ecological and agricultural implications. *Plants*, 10(2), 419.

Sarret, G., Harada, E., Choi, Y. E., Isaure, M. P., Geoffroy, N., Fakra, S., Marcus, M. A., Birschwilks, M., Clemens, S. and Manceau, A. (2006). Trichomes of tobacco excrete zinc as zinc-substituted calcium carbonate and other zinc-containing compounds. *Plant Physiology*, 141, 1021-1034.

Saxena, G., Purchase, D., Mulla, S. I., Saratale, G. D. and Bharagava, R. N. (2020). Phytoremediation of heavy metal-contaminated sites: Eco-environmental concerns, field studies, sustainability issues, and future prospects. *Reviews of Environmental Contamination and Toxicology*, de Voogt, P. (Ed.), Springer Nature, Switzerland, pp. 71-131.

Sayyad-Amin, P., Borzouei, A. and Jahansouz, M. R. (2014). Assaying the photosynthetic performance of salt-affected soybean using chlorophyll *a* fluorescence transients. *International Journal of Plant, Animal and Environmental Sciences*, 4 (2), 677-689.

Scarlat, N., Dallemand, J.-F., Monforti-Ferrario, F., Banja, M. and Motola, V. (2015). Renewable energy policy framework and bioenergy contribution in the European Union – An overview from national renewable energy action plans and progress reports. *Renewable and Sustainable Energy Reviews*, 51, 969-985.

Schulze, S., Dubeaux, G., Ceciliato, P. H., Munemasa, S., Nuhkat, M., Yarmolinsky, D., Aguilar, J., Diaz, R., Azoulay-Shemer, T., Steinhorst, L., Offenborn, J. K., Kudla, J., Kollist, H. and Schroeder, J. I. (2021). A role for calcium-dependent protein kinases in differential CO_2-and ABA-controlled stomatal closing and low CO_2-induced stomatal opening in *Arabidopsis*. *New Phytologist*, 229(5), 2765-2779.

Sgherri, C., Quartacci, M. F. and Navari-Izzo, F. (2007). Early production of activated oxygen species in root apoplast of wheat following copper excess. *Journal of Plant Physiology*, 164, 1152-1160.

Shabbir, Z., Sardar, A., Shabbir, A., Abbas, G., Shamshad, S., Khalid, S., Natasha, N., Murtaza, G., Dumat, C. and Shahid, M. (2020). Copper uptake, essentiality, toxicity, detoxification and risk assessment in soil-plant environment. *Chemosphere*, 259, 127436.

Shackira, A. M. and Puthur J. T. (2019). Cd^{2+} influences metabolism and elemental distribution in roots of *Acanthus ilicifolius* L. *International Journal of Phytoremediation*, 21, 1-12.

Shackira, A. M. and Puthur, J. T. (2017). Enhanced phytostabilization of cadmium by a halophyte - *Acanthus ilicifolius* L. *International Journal of Phytoremediation*, 19(4), 319-326.

Shackira, A. M., Puthur, J. T. and Nabeesa-Salim, E. (2017). *Acanthus ilicifolius* L. a promising candidate for phytostabilization of zinc. *Environmental Monitoring and Assessment*, 189(6), 282.

Shahid, M., Dumat, C., Pourrut, B., Sabir, M. and Pinelli, E. (2014). Assessing the effect of metal speciation on lead toxicity to *Vicia faba* pigment contents. *Journal of Geochemical Exploration*, 144, 290-297.

Shan, C., Zhou, Y. and Liu, M. (2015). Nitric oxide participates in the regulation of the ascorbate-glutathione cycle by exogenous jasmonic acid in the leaves of wheat seedlings under drought stress. *Protoplasma*, 252, 1397-1405.

Shao, R., Wang, K. and Shangguan, Z. (2010). Cytokinin-induced photosynthetic adaptability of *Zea mays* L. to drought stress associated with nitric oxide signal: Probed by ESR spectroscopy and fast OJIP fluorescence rise. *Journal of Plant Physiology*, 167(6), 472-479.

Sharma, A., Kumar, V., Shahzad, B., Ramakrishnan, M., Singh Sidhu, G. P., Bali, A. S., Handa, N., Kapoor, D., Yadav, P., Khanna, K., Bakshi, P., Rehman, A., Kohli, S. K., Khan, E. A., Parihar, R. D., Yuan, H., Thukral, A. K., Bharadwaj, R. and Zheng, B. (2020a). Photosynthetic response of plants under different abiotic stresses: A review. *Journal of Plant Growth Regulation*, 39(2), 509-531.

Sharma, A., Wang, J., Xu, D., Tao, S., Chong, S., Yan, D., Li, Z., Yuan, H. and Zheng, B. (2020b). Melatonin regulates the functional components of photosynthesis, antioxidant system, gene expression, and metabolic pathways to induce drought resistance in grafted *Carya cathayensis* plants. *Science of the Total Environment*, 713, 136675.

Sharma, I. and Ahmad, P. (2014). Catalase: A versatile antioxidant in plants. In: *Oxidative Damage to Plants: Antioxidant Networks and Signaling*, Ahmad, P. (Ed.), Academic Press, Elsevier, United States, pp. 131-148.

Sharma, P., Jha, A. B., Dubey, R. S. and Pessarakli, M. (2012). Reactive oxygen species, oxidative damage, and antioxidative defense mechanism in plants under stressful conditions. *Journal of Botany*, 2012, 217037.

Sharma, R. K. and Archana, G. (2016). Cadmium minimization in food crops by cadmium resistant plant growth promoting rhizobacteria. *Applied Soil Ecology*, 107, 66-78.

Sharma, R., Bhardwaj, R., Handa, N., Gautam, V., Kohli, S.K., Bali, S., Kaur, P., Thukral, A. K., Arora, S., Ohri, P. and Vig, A. P. (2016b). Responses of phytochelatins and metallothioneins in alleviation of heavy metal stress in plants: An overview. In: *Plant Metal Interaction: Emerging Remediation Techniques*, Ahmad, P. (Ed.), Elsevier, Amsterdam, Netherlands, pp. 263-283.

Sharma, S. S., Dietz, K. J. and Mimura, T. (2016a). Vacuolar compartmentalization as indispensable component of heavy metal detoxification in plants. *Plant Cell and Environment*, 39, 1112-1126.

Sheldon, A. R. and Menzies, N. W. (2005). The effect of copper toxicity on the growth and root morphology of Rhodes grass (*Chloris gayana* Knuth.) in resin buffered solution culture. *Plant and Soil*, 278 (1-2), 341-349.

Shen, G., Niu, J. and Deng, Z. (2017). Abscisic acid treatment alleviates cadmium toxicity in purple flowering stalk (*Brassica campestris* L. ssp. chinensis var. purpurea Hort.) seedlings. *Plant Physiology and Biochemistry*, 118, 471-478.

Shen, X., Li, R., Chai, M., Cheng, S., Tam, N. F. Y. and Han, J. (2021). Does combined heavy metal stress enhance iron plaque formation and heavy metal bioaccumulation in *Kandelia obovata*?. *Environmental and Experimental Botany*, 186, 104463.

Shen, X., Wang, Z., Song, X., Xu, J., Jiang, C., Zhao, Y., Ma, C. and Zhang, H. (2014). Transcriptomic profiling revealed an important role of cell wall remodeling and ethylene signaling pathway during salt acclimation in *Arabidopsis*. *Plant Molecular Biology*, 86(3), 303-317.

Shi, G. and Cai, Q. (2009a). Cadmium tolerance and accumulation in eight potential energy crops. *Biotechnology Advances*, 27, 555-561.

Shi, G. and Cai, Q. (2009b). Leaf plasticity in peanut (*Arachis hypogaea* L.) in response to heavy metal stress. *Environmental and Experimental Botany*, 67, 112-117.

Shi, G. and Cai, Q. (2010). Zinc tolerance and accumulation in eight oil crops. *Journal of Plant Nutrition*, 33, 982-997.

Shi, Q., Sun, H., Timm, S., Zhang, S. and Huang, W. (2022). Photorespiration alleviates photoinhibition of photosystem I under fluctuating light in tomato. *Plants*, 11(2), 195.

Shi, W. G., Liu, W., Yu, W., Zhang, Y., Ding, S., Li, H., Mrak, T., Kraigher, H. and Luo, Z. B. (2019). Abscisic acid enhances lead translocation from the roots to the leaves and alleviates its toxicity in *Populus* × *canescens*. *Journal of Hazardous Materials*, 362, 275-285.

Shin, S. Y., Kim, M. H., Kim, Y. H., Park, H. M. and Yoon, H. S. (2013). Co-expression of monodehydroascorbate reductase and dehydroascorbate reductase from *Brassica rapa* effectively confers tolerance to freezing-induced oxidative stress. *Molecules and Cells*, 36(4), 304-315.

Siddhu, G., Sirohi, D. S., Kashyap, K., Khan, I. A. and Khan, M. A. (2008). Toxicity of cadmium on the growth and yield of *Solanum melongena* L. *Journal of Environmental Biology*, 29(6), 853-857.

Sidhu, G. P. S., Singh, H. P., Batish, D. R. and Kohli, R. K. (2016). Effect of lead on oxidative status, antioxidative response and metal accumulation in *Coronopus didymus*. *Plant Physiology and Biochemistry*, 105, 290-296.

Singh, G., Singh, P., Guldhe, A., Stenström, T. A., Bux, F. and Kumari, S. (2017a). Biotechnological intervention to enhance the potential ability of bioenergy plants for phytoremediation. In: *Phytoremediation Potential of Bioenergy Plants*, Bauddh, K., Singh, B. and Korstad, J. (Eds.), Springer, Singapore, pp. 387-408.

Singh, N. B., Kumar, A. and Rai, S. (2014). Potential production of bioenergy from biomass in an Indian perspective. *Renewable and Sustainable Energy Reviews*, 39, 65-78.

Singh, R., Jha, A. B., Misra, A. N., and Sharma, P. (2019). Differential responses of growth, photosynthesis, oxidative stress, metals accumulation and NRAMP genes in contrasting *Ricinus communis* genotypes under arsenic stress. *Environmental Science and Pollution Research*, 26, 31166-31177.

Singh, R., Misra, A. N. and Sharma, P. (2021a). Effect of arsenate toxicity on antioxidant enzymes and expression of nicotianamine synthase in contrasting genotypes of bioenergy crop *Ricinus communis*. *Environmental Science and Pollution Research*, 28(24), 31421-31430.

Singh, R., Misra, A. N. and Sharma, P. (2021b). Genome-wide transcriptional response of contrasting genotypes of industrial crop castor to As (V) stress: Identification of genes and mechanisms associated with As (V) tolerance. *Industrial Crops and Products*, 179, 114678.

Singh, R., Misra, A. N. and Sharma, P. (2021c). Differential responses of thiol metabolism and genes involved in arsenic detoxification in tolerant and sensitive genotypes of bioenergy crop *Ricinus communis*. *Protoplasma*, 258(2), 391-401.

Singh, R., Parihar, P., Singh, S., Mishra, R. K., Singh, V. P. and Prasad, S. M. (2017b). Reactive oxygen species signaling and stomatal movement: Current updates and future perspectives. *Redox Biology*, 11, 213-218.

Singh, S., Parihar, P., Singh, R., Singh, V. P. and Prasad, S. M. (2016). Heavy metal tolerance in plants: Role of transcriptomics, proteomics, metabolomics, and ionomics. *Frontiers in Plant Science*, 6, 1143.

Singh, S., Singh, A., Srivastava, P. K. and Prasad, S. M. (2018). Cadmium toxicity and its amelioration by kinetin in tomato seedlings vis-à-vis ascorbate-glutathione cycle. *Journal of Photochemistry and Photobiology B: Biology*, 178, 76-84.

Šípošová, K., Labancová, E., Kučerová, D., Kollárová, K. and Vivodová, Z. (2021). Effects of exogenous application of indole-3-butyric acid on maize plants cultivated in the presence or absence of cadmium. *Plants*, 10(11), 2503.

Skorbiłowicz, M., Skorbiłowicz, E. and Rogowska, W. (2021). Heavy metal concentrations in roadside soils on the Białystok-Budzisko Route in Northeastern Poland. *Minerals*, 11(11), 1290.

Slama, I., Abdelly, C., Bouchereau, A., Flowers, T. and Savoure, A. (2015). Diversity, distribution and roles of osmoprotective compounds accumulated in halophytes under abiotic stress. *Annals of Botany*, 115, 433-447.

Smith, A. T., Smith, K. P. and Rosenzweig, A. C. (2014). Diversity of the metal-transporting P1B-type ATPases. *Journal of Biological Inorganic Chemistry*, 19(6), 947-960.

Soares, C., Carvalho, M. E., Azevedo, R. A. and Fidalgo, F. (2019). Plants facing oxidative challenges - a little help from the antioxidant networks. *Environmental and Experimental Botany*, 161, 4-25.

Soliman, M. H., Alayafi, A. A. M., El Kelish, A. A. and Abu-Elsaoud, A. M. (2018). Acetylsalicylic acid enhance tolerance of *Phaseolus vulgaris* L. to chilling stress, improving photosynthesis, antioxidants and expression of cold stress responsive genes. *Botanical Studies*, 59(6), 1-17.

Song, W. Y., Mendoza-Cózatl, D. G., Lee, Y., Schroeder, J. I., Ahn, S. N., Lee, H. S., Wicker, T. and Martinoia, E. (2014). Phytochelatin-metal(loid) transport into vacuoles shows different substrate preferences in barley and *Arabidopsis*. *Plant, Cell and Environment*, 37(5), 1192-1201.

Souri, Z., Cardoso, A. A., da-Silva, C. J., de Oliveira, L. M., Dari, B., Sihi, D. and Karimi, N. (2019). Heavy metals and photosynthesis: Recent developments. In: *Photosynthesis, Productivity and Environmental Stress*, Ahmad, P., Ahanger, M. A., Alyemeni, M. N. and Alam, P. (Eds.), John Wiley & Sons, New Jersy, United States, pp. 107-134.

Srivastava, R. K. (2019). Bio-energy production by contribution of effective and suitable microbial system. *Material Science for Energy Technologies*, 2, 308-318.

Srivastava, S., Srivastava, A. K., Suprasanna, P. and D'souza, S. F. (2013). Identification and profiling of arsenic stress-induced microRNAs in *Brassica juncea*. *Journal of Experimental Botany*, 64(1), 303-315.

Sruthi, P. and Puthur, J. T. (2018). The modulation of various physiochemical changes in *Bruguiera cylindrica* (L.) Blume affected by high concentrations of NaCl. *Acta Physiologiae Plantarum*, 40, 160.

Sruthi, P. and Puthur, J. T. (2019). Characterization of physiochemical and anatomical features associated with enhanced phytostabilization of copper in *Bruguiera cylindrica* (L.) Blume. *International Journal of Phytoremediation*, 21(14), 1423-1441.

Sruthi, P. and Puthur, J. T. (2020). High NaCl tolerance potential of *Bruguiera cylindrica* (L.) Blume compromised by mild $CuSO_4$ concentration as evidenced by unique physiochemical features. *Marine Pollution Bulletin*, 156, 111260.

Sruthi, P., Shackira, A. M. and Puthur, J. T. (2017). Heavy metal detoxification mechanisms in halophytes: An overview. *Wetlands Ecology and Management*, 25(2), 129-148.

Stanislawska-Glubiak, E. and Korzeniowska, J. (2022). Effect of salicylic acid foliar application on two wheat cultivars grown under zinc stress. *Agronomy*, 12(1), 60.

Stein, O. and Granot, D. (2019). An overview of sucrose synthases in plants. *Frontiers in Plant Science*, 10, 95.

Stirbet, A. and Govindjee (2011). On the relation between the Kautsky effect (chlorophyll *a* fluorescence induction) and photosystem II: Basics and applications of the OJIP fluorescence transient. *Journal of Photochemistry and Photobioloby B: Biology*, 104, 236-257.

Stolárikova, V. M., Romeo, S., Minnocci, A., Luxová, M., Vaculík, M., Lux, A. and Sebastiani, L. (2015). Anatomical, biochemical and morphological responses of poplar *Populus deltoides* clone Lux to Zn excess. *Environmental and Experimental Botany*, 109, 235-243.

Stolt, J. P., Sneller, F. E. C., Bryngelsson, T., Lundborg, T. and Schat, H. (2003). Phytochelatin and cadmium accumulation in wheat. *Environmental and Experimental Botany*, 49, 21-28.

Strasser, R. J., Tsimilli-Michael, M. and Srivastava, A. (2004). Analysis of the chlorophyll a fluorescence transient. In: *Chlorophyll a Fluorescence: A Signature of Photosynthesis, Advances in Photosynthesis and Respiration*, Papageorgiou, G. C. and Govindjee (Eds.). Springer, Dordrecht, Netherlands, pp. 321-362.

Su, T., Wang, P., Li, H., Zhao, Y., Lu, Y., Dai, P., Ren, T., Wang, X., Li, X., Shao, Q., Zhao, D., Zhao, Y. and Ma, C. (2018). The *Arabidopsis* catalase triple mutant reveals important roles of catalases and peroxisome-derived signaling in plant development. *Journal of Integrative Plant Biology*, 60(7), 591-607.

Sun, L., Cao, X., Tan, C., Deng, Y., Cai, R., Peng, X. and Bai, J. (2020). Analysis of the effect of cadmium stress on root exudates of *Sedum plumbizincicola* based on metabolomics. *Ecotoxicology and Environmental Safety*, 205, 111152.

Sun, Y., Wen, C., Liang, X. and He, C. (2018). Determination of the phytoremediation efficiency of *Ricinus communis* L. and methane uptake from cadmium and nickel-contaminated soil using spent mushroom substrate. *Environmental Science and Pollution Research*, 25(32), 32603-32616.

Sun, Y., Zhou, Q., Xu, Y., Wang, L. and Liang, X. (2011). Phytoremediation for co-contaminated soils of benzo[a]pyrene (B[a]P) and heavy metals using ornamental plant *Tagetes patula*. *Journal of Hazardous Materials*, 186(2-3), 2075-2082.

Suprasanna, P., Nikalje, G. and Rai, A. N. (2015). Osmolyte accumulation and implications in plant abiotic stress tolerance. In: *Osmolytes and Plants Acclimation to Changing Environment: Emerging Omics Technologies*, Iqbal, N., Nazar, R. and Khan, N. A. (Eds.), Springer Nature, Switzerland, pp. 1-12.

Surriya, O., Saleem, S., Waqar, K. and Gul, A. (2015). Phytoremediation of soils: Prospects and challenges. In: *Soil Remediation and Plants*, Hakeem, K. R., Sabir, M., Öztürk, and Mermut, A. R. (Eds.), Academic Press, Elsevier, Cambridge, United States, pp. 1-36.

Susarla, S., Medina, V. and McCutcheon, S. C. (2002). Phytoremediation: An ecological solution to organic chemical contamination. *Ecological Engineering*, 18, 647-658.

Sytar, O., Kumari, P., Yadav, S., Brestic, M. and Rastogi, A. (2019). Phytohormone priming: Regulator for heavy metal stress in plants. *Journal of Plant Growth Regulation*, 38(2), 739-752.

Szabados, L. and Savoure, A. (2010). Proline: A multifunctional amino acid. *Trends in Plant Science*, 15, 89-97.

Tagmount, A., Berken, A. and Terry, N. (2002). An essential role of S-adenosyl-L-methionine: L-methionine S-methyltransferase in selenium volatilization by plants: Methylation of selenomethionine to seleniummethyl-L-selenium-methionine, the precursor of volatile selenium. *Journal of Plant Physiology*, 130, 847-856.

Takei, K., Takahashi, T., Sugiyama, T., Yamaya, T. and Sakakibara, H. (2002). Multiple routes communicating nitrogen availability from roots to shoots: A signal transduction pathway mediated by cytokinin. *Journal of Experimental Botany*, 53(370), 971-977.

Talla, S. K., Panigrahy, M., Kappara, S., Nirosha, P., Neelamraju, S. and Ramanan, R. (2016). Cytokinin delays dark-induced senescence in rice by maintaining the chlorophyll cycle and photosynthetic complexes. *Journal of Experimental Botany*, 67, 1839-1851.

Tarekegn, M. M., Salilih, F. Z. and Ishetu, A. I. (2020). Microbes used as a tool for bioremediation of heavy metal from the environment, *Cogent Food and Agriculture*, 6(1), 1783174.

Tennstedt, P., Peisker, D., Bottcher, C., Trampczynska, A. and Clemens, S. (2009). Phytochelatin synthesis is essential for the detoxification of excess zinc and

contributes significantly to the accumulation of zinc. *Plant Physiology*, 149(2), 938-948.

Thakur, L. S., Varma, A. K. and Mondal, P. (2018). Analysis of thermal behavior and pyrolytic characteristics of vetiver grass after phytoremediation through thermogravimetric analysis. *Journal of Thermal Analysis and Calorimetry*, 131(3), 3053-3064.

Thind, S., Hussain, I., Ali, S., Rasheed, R. and Ashraf, M. A. (2021). Silicon application modulates growth, physio-chemicals, and antioxidants in wheat (*Triticum aestivum* L.) exposed to different cadmium regimes. *Dose-Response*, 19(2), 15593258211014646.

Thomas, J. C., Perron, M., LaRosa, P. C. and Smigocki, A. C. (2005). Cytokinin and the regulation of a tobacco metallothionein-like gene during copper stress. *Physiologia Plantarum*, 123(3), 262-271.

Thomas, N., Stutz, S., Imke, I. H. and Heyer, A. G. (2012). Identification of a metabolic bottleneck for cold acclimation in *Arabidopsis thaliana*. *Plant Journal*, 72 (1), 102-114.

Thor, K. (2019). Calcium - nutrient and messenger. *Frontiers in Plant Science*, 10, 440.

Thounaojam, T. C., Panda, P., Choudhury, S., Patra, H. K. and Panda, S. K. (2014). Zinc ameliorates copper-induced oxidative stress in developing rice (*Oryza sativa* L.) seedlings. *Protoplasma*, 251(1), 61-69.

Tian, Y. L., Zhang, H. Y., Guo, W., Chen, Z. S., Wei, X. F., Zhang, L. Y., Han, L. and Dai, L. M. (2012). Assessment of the phytoremediation potential in the bioenergy crop maize (*Zea mays*) in soil contaminated by cadmium: Morphology, photosynthesis and accumulation. *Fresenius Environmental Bulletin*, 21, 3575-3581.

Tiodar, E. D., Văcar, C. L. and Podar, D. (2021). Phytoremediation and microorganisms-assisted phytoremediation of mercury-contaminated soils:

Challenges and perspectives. *International Journal of Environmental Research and Public Health*, 18(5), 2435.

Todeschini, V., Lingua, G., Agostino, G. D., Carniato, F., Roccotiello, E. and Berta, G. (2011). Effects of high zinc concentration on poplar leaves: A morphological and biochemical study. *Environmental and Experimental Botany*, 71, 50-56.

Tomar, R. S., Sharma, A. and Jajoo, A. (2015). Assessment of phytotoxicity of anthracene in soybean (*Glycine max*) with a quick method of chlorophyll fluorescence. *Plant Biology*, 17(4), 870-876.

Tongra, T., Mehta, P., Mathur, S., Agrawal, D., Bharti, S., Los, D. A., Allakhverdiev, S. I. and Jajoo, A. (2011). Computational analysis of fluorescence induction curves in intact spinach leaves treated at different pH. *Biosystems*, 103, 158-163.

Tóth, G., Hermann, T., da Silva, M. R. and Montanarella, L. (2018). Monitoring soil for sustainable development and land degradation neutrality. *Environmental Monitoring Assessment*, 190, 57.

Tóth, S. Z., Schansker, G. and Strasser, R. J. (2007). A non-invasive assay of the plastoquinone pool redox state based on the OJIP-transient. *Photosynthesis Research*, 93(1-3), 193-203.

Touceda-González, M., Álvarez-López, V., Prieto-Fernández, Á., Rodríguez-Garrido, B., Trasar-Cepeda, C., Mench, M., Puschenreiter, M., Quintela-Sabarís, C. and Kidd, P. S. (2017). Aided phytostabilisation reduces metal toxicity, improves soil fertility and enhances microbial activity in Cu-rich mine tailings. *Journal of Environmental Management*, 186, 301-313.

Tränkner, M., Tavakol, E. and Jákli, B. (2018). Functioning of potassium and magnesium in photosynthesis, photosynthate translocation and photoprotection. *Physiologia Plantarum*, 163(3), 414-431.

Triantaphylidès, C. and Havaux, M. (2009). Singlet oxygen in plants: Production, detoxification and signaling. *Trends in Plant Science*, 14(4), 219-228.

Trigueros, D. and Rossini-Oliva, S. (2021). Tissue distribution and biochemical changes in response to copper accumulation in *Erica australis* L. *Plants*, 10(7), 1428.

Trovato, M., Mattioli, R. and Costantino, P. (2008). Multiple roles of proline in plant stress tolerance and development. *Rendiconti Lincei*, 19(4), 325-346.

Uraguchi, S., Ohshiro, Y., Otsuka, Y., Wada, E., Naruse, F., Sugaya, K., Nagai, K., Wongkaew, A., Nakamura, R., Takanezawa, Y., Clemens, S., Ohkama-Ohtsu, N. and Kiyono, M. (2021). Phytochelatin-mediated metal detoxification pathway is crucial for an organomercurial phenylmercury tolerance in *Arabidopsis*. *Plant Molecular Biology*, 1-15.

Usman, A. R., Alkredaa, R. S. and Al-Wabel, M. I. (2013). Heavy metal contamination in sediments and mangroves from the coast of Red Sea: *Avicennia marina* as potential metal bioaccumulator. *Ecotoxicology and Environmental Safety*, 97, 263-270.

Vamerali, T., Bandiera, M., Coletto, L., Zanetti, F., Dickinson, N. M. and Mosca, G. (2009). Phytoremediation trials on metal-and arsenic-contaminated pyrite wastes (Torviscosa, Italy). *Environmental Pollution*, 157(3), 887-894.

van Hulten, M., Pelser, M., Van Loon, L. C., Pieterse, C. M. and Ton, J. (2006). Costs and benefits of priming for defense in *Arabidopsis*. *Proceedings of the National Academy of Sciences of the United States of America*, 103(14), 5602-5607.

Vangronsveld, J., Herzig, R., Weyens, N., Boulet, J., Adriaensen, K., Ruttens, A., Thewys, T., Vassilev, A., Meers, E., Nehnevajova, E., van der Lelie, D. and Mench, M. (2009). Phytoremediation of contaminated soils and groundwater: Lessons from the field. *Environmental Science and Pollution Research*, 16(7), 765-794.

Venegas-Rioseco, J., Ginocchio, R. and Ortiz-Calderón, C. (2022). Increase in phytoextraction potential by genome editing and transformation: A review. *Plants*, 11(1), 86.

Vezza, M. E., Llanes, A., Travaglia, C., Agostini, E. and Talano, M. A. (2018). Arsenic stress effects on root water absorption in soybean plants: Physiological and morphological aspects. *Plant Physiology and Biochemistry*, 123, 8-17.

Vidal, C., Ruiz, A., Ortiz, J., Larama, G., Perez, R., Santander, C., Ferreira, P. A. A. and Cornejo, P. (2020). Antioxidant responses of phenolic compounds and immobilization of copper in *Imperata cylindrica*, a plant with potential use for bioremediation of Cu contaminated environments. *Plants*, 9(10), 1397.

Viehweger, K. (2014). How plants cope with heavy metals. *Botanical Studies*, 55, 1-12.

Vijayarengan, P. and Jose, M. D. (2014). Changes in growth, pigments and phytoremediating capability of four plant species under copper stress. *International Journal of Environmental Biology*, 4, 119-126.

Wang, C. and Zhang, Q. (2017). Exogenous salicylic acid alleviates the toxicity of chlorpyrifos in wheat plants (*Triticum aestivum*). *Ecotoxicology and Environmental Safety*, 137, 218-224.

Wang, F., Du, C., Chen, J., Shi, L. and Li, H. (2021b). A new method for determination of pectin content using spectrophotometry. *Polymers*, 13(17), 2847.

Wang, H., Dai, B., Shu, X. and Ning, P. (2015b). Effect of kinetin on physiological and biochemical properties of maize seedlings under arsenic stress. *Advances in Materials Science and Engineering*, 2015, 1-7.

Wang, L., Xu, J. Y., Jia, W., Chen, Z. and Xu, Z. C. (2020). Chloride salinity in a chloride-sensitive plant: Focusing on photosynthesis, hormone synthesis and transduction in tobacco. *Plant Physiology and Biochemistry*, 153, 119-130.

Wang, M., Zheng, Q., Shen, Q. and Guo, S. (2013). The critical role of potassium in plant stress response. *International Journal of Molecular Sciences*, 14(4), 7370-7390.

Wang, Q. Y., Liu, J. S. and Hu, B. (2016b). Integration of copper subcellular distribution and chemical forms to understand copper toxicity in apple trees. *Environmental and Experimental Botany*, 123, 125-131.

Wang, R., Lin, K., Chen, H., Qi, Z., Liu, B., Cao, F., Chen, H. and Wu, F. (2021a). Metabolome analysis revealed the mechanism of exogenous glutathione to alleviate cadmium stress in maize (*Zea mays* L.) seedlings. *Plants*, 10(1), 105.

Wang, R., Wang, J., Zhao, L., Yang, S. and Song, Y. (2015a). Impact of heavy metal stresses on the growth and auxin homeostasis of *Arabidopsis* seedlings. *Biometals*, 28(1), 123-132.

Wang, S., Zhao, Y., Guo, J. and Zhou, L. (2016a). Effects of Cd, Cu and Zn on *Ricinus communis* L. Growth in single element or co-contaminated soils: Pot experiments. *Ecological Engineering*, 90, 347-351.

Wang, X., Liu, Y., Zeng, G., Chai, L., Song, X., Min, Z. and Xiao, X. (2008). Subcellular distribution and chemical forms of cadmium in *Bechmeria nivea* (L.) Gaud. *Environmental and Experimental Botany*, 62, 389-395.

Wang, X., Yi, K., Tao, Y., Wang, F., Wu, Z., Jiang, D., Chen, X., Zhu, L. and Wu, P. (2006). Cytokinin represses phosphate-starvation response through increasing of intracellular phosphate level. *Plant, Cell and Environment*, 29(10), 1924-1935.

Wang, Y., Branicky, R., Noë, A. and Hekimi, S. (2018). Superoxide dismutases: Dual roles in controlling ROS damage and regulating ROS signaling. *Journal of Cell Biology*, 217(6), 1915-1928.

Wang, Y., Jiang, X., Li, K., Wu, M., Zhang, R., Zhang, L. and Chen, G. (2014). Photosynthetic responses of *Oryza sativa* L. seedlings to cadmium stress: Physiological, biochemical and ultrastructural analyses. *Biometals*, 27, 389-401.

Wani, S. H., Kumar, V., Shriram, V. and Sah, S. K. (2016). Phytohormones and their metabolic engineering for abiotic stress tolerance in crop plants. *The Crop Journal*, 4(3), 162-176.

Waters, B. M. and Armbrust, L. C. (2013). Optimal copper supply is required for normal plant iron deficiency responses. *Plant Signaling and Behavior*, 8(12), e26611.

Waters, B. M., McInturf, S. A. and Amundsen, K. (2014). Transcriptomic and physiological characterization of the fefe mutant of melon (*Cucumis melo*) reveals new aspects of iron-copper crosstalk. *New Phytologist*, 203(4), 1128-1145.

Weatherley, P. (1950). Studies in the water relations of the cotton plant: I. The field measurement of water deficits in leaves. *New Phytologist*, 49(1), 81-97.

Weigel, H. J. and Jäger, H. J. (1980). Subcellular distribution and chemical form of cadmium in bean plants. *Plant Physiology*, 65(3), 480-482.

Wen, J., Li, P. F., Ran, F., Guo, P. C., Zhu, J. T., Yang, J., Zhang, L. L., Chen, P., Li, J. N. and Du, H. (2020). Genome-wide characterization, expression analyses, and functional prediction of the NPF family in *Brassica napus*. *BMC Genomics*, 21(1), 1-17.

Werner, T., Motyka, V., Strnad, M. and Schmülling, T. (2001) Regulation of plant growth by cytokinin. *Proceedings of the National Academy of Sciences of United States of America*, 98, 10487-10492.

Werner, T., Nehnevajova, E., Köllmer, I., Novák, O., Strnad, M., Krämer, U. and Schmülling, T. (2010). Root-specific reduction of cytokinin causes enhanced root growth, drought tolerance, and leaf mineral enrichment in *Arabidopsis* and tobacco. *The Plant Cell*, 22(12), 3905-3920.

Wu, W., Du, K., Kang, X. and Wei, H. (2021). The diverse roles of cytokinins in regulating leaf development. *Horticulture Research*, 8, 118.

Wu, X., Chen, S., Guo, J. and Gao, G. (2018). Effect of air pollution on the stock yield of heavy pollution enterprises in China's key control cities. *Journal of Cleaner Production*, 170, 399-406.

Wu, X., Zhu, Z., Li, X. and Zha, D. (2012). Effects of cytokinin on photosynthetic gas exchange, chlorophyll fluorescence parameters and antioxidative system in seedlings of eggplant (*Solanum melongena* L.) under salinity stress. *Acta Physiologia Plantarum*, 34, 2105-2114.

Xia, S., Song, Z., Jeyakumar, P., Shaheen, S. M., Rinklebe, J., Ok, Y. S., Bolan, N. and Wang, H. (2019). A critical review on bioremediation technologies for Cr (VI)-contaminated soils and wastewater. *Critical Reviews in Environmental Science and Technology*, 49(12), 1027-1078.

Xiao, S., Xu, T., Wang, Y., Xing, J., Wang, R., Su, A., Wang, S., Song, W. and Zhao, J. (2021). Coordinated effect of ascorbate biosynthesis and recycling in maize seed germination and seedling establishment under low temperature. *Agriculture*, 11(11), 1160.

Xie, H., Zhang, Y., Wu, Z. and Lv, T. (2020). A bibliometric analysis on land degradation: Current status, development, and future directions. *Land*, 9(1), 28.

Xiong, Z. T., Liu, C. and Geng, B. (2006). Phytotoxic effects of copper on nitrogen metabolism and plant growth in *Brassica pekinensis* Rupr. *Ecotoxicology and Environmental Safety*, 64(3), 273-280.

Xu, J., Sun, J., Du, L. and Liu, X. (2012b). Comparative transcriptome analysis of cadmium responses in *Solanum nigrum* and *Solanum torvum*. *New Phytologist*, 196, 110-124.

Xu, J., Zhu, Y., Ge, Q., Li, Y., Sun, J., Zhang, Y. and Liu, X. (2012a). Comparative physiological responses of *Solanum nigrum* and *Solanum torvum* to cadmium stress. *New Phytologist*, 196, 125-138.

Xu, Y. X., Mao, J., Chen, W., Qian, T. T., Liu, S. C., Hao, W. J., Li, C. F. and Chen, L. (2016). Identification and expression profiling of the auxin response

factors (ARFs) in the tea plant (*Camellia sinensis* (L.) O. Kuntze) under various abiotic stresses. *Plant Physiology and Biochemistry*, 98, 46-56.

Xu, Z., Mahmood, K. and Rothstein, S. J. (2017). ROS induces anthocyanin production *via* late biosynthetic genes and anthocyanin deficiency confers the hypersensitivity to ROS-generating stresses in *Arabidopsis*. *Plant and Cell Physiology*, 58, 1364-1377.

Xue, S. G., Huang, Y. H., Wang, J., Tian, S. X., Lei, J. and He, Z. X. (2011). Physiological response of *Polygonum lapathifolium* to manganese stress by FTIR spectroscopy. *Journal of Central South University* (*Science and Technology*), 42(6), 1528-1532.

Xue, Z. C., Gao, H. Y. and Zhang, L.T. (2013). Effects of cadmium on growth, photosynthetic rate, and chlorophyll content in leaves of soybean seedlings. *Biologia Plantarum*, 57, 587-590.

Yadav, S. K. (2010). Heavy metals toxicity in plants: An overview on the role of glutathione and phytochelatins in heavy metal stress tolerance of plants. *South African Journal of Botany*, 76(2), 167-179.

Yadav, S., Elansary, H. O., Mattar, M. A., M Elhindi, K., Alotaibi, M. and Mishra, A. (2021). Differential accumulation of metabolites in *Suaeda*species provides new insights into abiotic stress tolerance in C4-halophytic species in elevated CO_2 conditions. *Agronomy*, 11(1), 131.

Yan, A., Wang, Y., Tan, S. N., Mohd Yusof, M. L., Ghosh, S. and Chen, Z. (2020). Phytoremediation: A promising approach for revegetation of heavy metal-polluted land. *Frontiers in Plant Science*, 11, 359.

Yan, Z. Z., Ke, L. and Tam, N. F. Y. (2010). Lead stress in seedlings of *Avicennia marina*, a common mangrove species in South China, with and without cotyledons. *Aquatic Botany*, 92(2), 112-118.

Yang, F., Tang, C. and Antonietti, M. (2021). Natural and artificial humic substances to manage minerals, ions, water, and soil microorganisms. *Chemical Society Reviews*, 50, 6221-6239.

Yang, Y., Zhang, L., Huang, X., Zhou, Y., Quan, Q., Li, Y. and Zhu, X. (2020). Response of photosynthesis to different concentrations of heavy metals in *Davidiainvolucrata*. *PLoS One*, 15(3), e0228563

Yap, C. K., Tan, W. S., Wong, K. W., Ong, G. H., Cheng, W. H., Nulit, R., Ibrahim, M. H., Chew, W., Edward, F. B., Okamura, H., Al-Mutairi, K. A., Al-Shami, S. A., Sharifinia, M., Mustafa, M., Leong, W. J. and You, C. F. (2021). Antioxidant enzyme activities as biomarkers of Cu and Pb stress in *Centella asiatica*. *Stresses*, 1(4), 253-265.

Yashim Z. I., Agbaji E. B., Gimba C. E. and Idris S. O. (2016). Phytoremediation potential of *Ricinus communis* L. (castor oil plant) in Northern Nigeria. *International Journal of Plant and Soil Science*, 10(5), 1-8.

Yeboah, A., Lu, J., Gu, S., Shi, Y., Amoanimaa-Dede, H., Agyenim-Boateng, K. G. and Yin, X. (2020). The utilization of *Ricinus communis* in the phytomanagement of heavy metal contaminated soils. *Environmental Reviews*, 28(4), 466-477.

Young, S.D. (2013). Chemistry of heavy metals and metalloids in soils. In: *Heavy Metals in Soils*, Alloway, B. J. (Ed.), Springer, Dordrecht, pp. 51-95.

Yruela, I. (2005). Copper in plants. *Brazilian Journal of Plant Physiology*, 17, 145-156.

Yruela, I. (2009). Copper in plants: Acquisition, transport and interactions. *Functional Plant Biology*, 36(5), 409-430.

Yu, Z., Duan, X., Luo, L., Dai, S., Ding, Z. and Xia, G. (2020). How plant hormones mediate salt stress responses. *Trends in Plant Science*, 25(11), 1117-1130.

Zaheer, I. E., Ali, S., Rizwan, M., Farid, M., Shakoor, M. B., Gill, R. A., Najeeb, U., Iqbal, N. and Ahmad, R. (2015). Citric acid assisted phytoremediation of copper by *Brassica napus* L. *Ecotoxicology and Environmental Safety*, 120, 310-317.

Zaynab, M., Al-Yahyai, R., Ameen, A., Sharif, Y., Ali, L., Fatima, M., Khan, K. A. and Li, S. (2022). Health and environmental effects of heavy metals. *Journal of King Saud University-Science*, 34(1), 101653.

Zemanová, V., Pavlík, M. and Pavlíková, D. (2017). Cadmium toxicity induced contrasting patterns of concentrations of free sarcosine, specific amino acids and selected microelements in two *Noccaea* species. *PloS One*, 12, 1-17.

Zemanová, V., Pavlík, M., Pavlíková, D. and Tlustoš, P. (2013). The changes of contents of selected free amino acids associated with cadmium stress in *Noccaeacaerulescens* and *Arabidopsis halleri*. *Plant, Soil and Environment*, 59(9), 417-422.

Zenda, T., Liu, S., Dong, A. and Duan, H. (2021). Revisiting sulphur - the once neglected nutrient: It's roles in plant growth, metabolism, stress tolerance and crop production. *Agriculture*, 11(7), 626.

Zentgraf, U., Andrade-Galan, A. G. and Bieker, S. (2022). Specificity of H_2O_2 signaling in leaf senescence: Is the ratio of H_2O_2 contents in different cellular compartments sensed in *Arabidopsis*plants?. *Cellular and Molecular Biology Letters*, 27(1), 1-19.

Zgorelec, Z., Bilandzija, N., Knez, K., Galic, M. and Zuzul, S. (2020). Cadmium and mercury phytostabilization from soil using *Miscanthus* × *giganteus*. *Scientific Reports*, 10(1), 1-10.

Zhang, H., Chen, X., He, C., Liang, X., Oh, K., Liu, X. and Lei, Y. (2015). Use of energy crop (*Ricinus communis* L.) for phytoextraction of heavy metals assisted with citric acid. *International Journal of Phytoremediation*, 17(7), 632-639.

Zhang, H., Qin, Y., Huang, K., Zhan, F., Li, R. and Chen, J. (2021b). Root metabolite differences in two maize varieties under lead stress. *Frontiers in Plant Science*, 12, 656074.

Zhang, L., Hu, T., Amombo, E., Wang, G., Xie, Y. and Fu, J. (2017b). The alleviation of heat damage to photosystem II and enzymatic antioxidants by exogenous spermidine in tall fescue. *Frontiers in Plant Science*, 8, 1747.

Zhang, W., Peng, K., Cui, F., Wang, D., Zhao, J., Zhang, Y., Yu, N., Wang, Y., Zeng, D., Wang, Y., Cheng, Z. and Zhang, K. (2021a). Cytokinin oxidase/dehydrogenase *OsCKX11* coordinates source and sink relationship in rice by simultaneous regulation of leaf senescence and grain number. *Plant Biotechnology Journal*, 19(2), 335-350.

Zhang, W., Yu, T., Yang, X. and Li, H. (2020). Speciation, transformation, and accumulation of manure-derived Cu and Zn in the soilerice system. *Soil Sediment Contamination*, 29(1), 43-52.

Zhang, X. D., Sun, J. Y., You, Y. Y., Song, J. B., and Yang, Z. M. (2018). Identification of Cd-responsive RNA helicase genes and expression of a putative *BnRH24* mediated by *miR158* in canola (*Brassica napus*). *Ecotoxicology and Environmental Safety*, 157, 159-168.

Zhang, X., Ju, H. W., Chung, M. S., Huang, P., Ahn, S. J. and Kim, C. S. (2011). The RR-type MYB-like transcription factor, *AtMYBL*, is involved in promoting leaf senescence and modulates an abiotic stress response in *Arabidopsis*. *Plant and Cell Physiology*, 52(1), 138-148.

Zhang, X., Wang, X. Q. and Wang, D. F. (2017a). Immobilization of heavy metals in sewage sludge during land application process in China: A review. *Sustainability*, 9, 2020.

Zhang, Y., He, Q., Zhao, S., Huang, L. and Hao, L. (2014). *Arabidopsis* ein2-1 and npr1-1 response to Al stress. *Bulletin of Environmental Contamination and Toxicology*, 93(1), 78-83.

Zhong, C., Cao, X., Hu, J., Zhu, L., Zhang, J., Huang, J. and Jin, Q. (2017). Nitrogen metabolism in adaptation of photosynthesis to water stress in rice grown under different nitrogen levels. *Frontiers in Plant Science*, 8, 1079.

Zhou, J. T., Wan, H. X., He, J. L., Lyu, D. G. and Li, H. F. (2017). Integration of cadmium accumulation, subcellular distribution, and physiological responses to understanding cadmium tolerance in apple rootstocks. *Frontiers in Plant Science*, 8, 966.

Zhou, M., Ghnaya, T., Dailly, H., Cui, G., Vanpee, B., Han, R. and Lutts, S. (2019). The cytokinin trans-zeatine riboside increased resistance to heavy metals in the halophyte plant species *Kosteletzkya pentacarpos* in the absence but not in the presence of NaCl. *Chemosphere* 233, 954-965.

Zornoza, P., Vazquez, S., Esteban, E., Fernandez-Pascual, M. and Carpena R. (2002). Cadmium stress in nodulated white lupin: Strategies to avoid toxicity. *Plant Physiology and Biochemistry*, 40, 1003-1009.

LIST OF PUBLICATIONS AND PRESENTATIONS

Publications in Research Journals

1. **Sameena, P. P**., Kalaji, H. M., Żuk-Gołaszewska, K., Horaczek, T., Sierka, E. and Puthur, J. T. (2021). 6-Benzylaminopurine alleviates the impact of Cu^{2+} toxicity on photosynthetic performance of *Ricinus communis* L. seedlings. *International Journal of Molecular Sciences*, 22, 13349. MDPI (**IF: 5.924**). https://doi.org/10.3390/ijms222413349

2. **Sameena, P. P**. and Puthur, J. T. (2021). Exogenous application of cytokinins confers copper stress tolerance in *Ricinus communis* L. seedlings. *Journal of Plant Growth Regulation*. Springer (**IF: 4.169**). https://doi.org/10.1007/s00344-021-10522-z

3. **Sameena, P. P**. and Puthur, J. T. (2021). Differential modulation of photosynthesis and defense strategies towards copper toxicity in primary and cotyledonary leaves of *Ricinus communis* L. *Journal of Photochemistry and Photobiology*, 8, 100059. Elsevier. https://doi.org/10.1016/j.jpap.2021.100059

4. **Sameena, P. P.** and Puthur, J. T. (2021). Cotyledonary leaves effectively shield the true leaves in *Ricinus communis* L. from copper toxicity. *International Journal of Phytoremediation*, 23(5), 492-504. Taylor and Francis (**IF: 3.212**). https://doi.org/10.1080/15226514.2020.1825331

5. **Sameena, P. P.** and Puthur, J. T. (2021). Heavy metal phytoremediation by bioenergy plants and associated tolerance mechanisms. *Soil and Sediment Contamination: An International*

Journal, 30(3), 253-274. Taylor and Francis (**IF: 2.061**). https://doi.org/10.1080/15320383.2020.1849017

6. Anjitha, K. S., **Sameena, P. P.** and Puthur J. T. (2021). Functional aspects of plant secondary metabolites in metal stress tolerance and their importance in pharmacology. *Plant Stress*, 2, 100038. Elsevier. https://doi.org/10.1016/j.stress.2021.100038

Book chapters

1. **Sameena, P. P**., Sarath, N. G., Noble, L., Amritha, M. S., Dhankher, O. P. and Puthur, J. T. (2022). Bioenergy plants: a sustainable solution for heavy metal phytoremediation. In: *Bioenergy Crops: A Sustainable Means of Phytoremediation*, Puthur, J. T. and Dhankher, O. P. (Eds.), CRC Press, Taylor and Francis Group, pp. 1-17. ISBN: 13-9780367489137.

2. **Sameena, P.P.** and Puthur J. T. Clean energy for environmental protection: an outlook towards phytoremediation. In: *Biotechnological Innovations for Environmental Bioremediation*, Arora, S., Kumar, A., Ogita, S. and Yau, Y. Y. (Eds.). Springer Nature (In Press).

3. **Sameena, P. P.,** Janeeshma, E., Sarath, N. G. and Puthur, J. T. Phytoremediation and phycoremediation: A sustainable solution for wastewater treatment. In: *Recent Trends in Wastewater Treatment*, Madhav, S., Singh, P., Mishra, V., Ahmed, S. and Mishra P. K. (Eds.). Springer Nature (In Press).

4. Janeeshma, E., **Sameena, P. P.,** Sarath, N. G., Veena, M. and Puthur, J. T. Modulation of soil microbiome and related alterations in response to pesticides. In: *Pesticides in Natural Environment: Sources, Health Risks, and Remediation*, Singh, P., Singh, S. and Sillanpää, M. (Eds.), Elsevier, USA, ISBN: 9780323904896 (In Press).

5. Janeeshma, E., **Sameena, P. P.** and Puthur, J. T. Application of microbial nanoparticles in water remediation. In: *Environmental Applications of Microbial Nanotechnology: Emerging trends in Environmental Remediation*, Singh, P., Kumar, V., Bakshi, M., Hussain, C. M. and Sillanpää, M. (Eds.), Elsevier, ISBN: 978-0-323-97255-0 (In Press).

6. Sarath, N. G., **Sameena, P. P.**, Sen, A., Janeeshma, E. and Puthur, J. T.Biosynthesis and distribution of secondary metabolites of medicinal plants as affected by mineral nutrient elements and plant growth regulators in abiotic stress conditions. In: *Medicinal Plants: Their Annoyance due to Abiotic Stress*, Husen, A. and Iqbal, M. (Eds.), Springer (In Press).

Proceedings from Seminars/Conferences

1. **Sameena, P. P.** and Puthur J. T. (2020). Alterations in the antioxidative functions in *Ricinus communis* L. seedlings exposed to increasing levels of copper. In: *Proceedings of Three day International webinar on Plant Functional Biology (Doctrina-11)*. Abdussalam, A. K. and Shackira, A. M. (Eds.), pp. 86-92. ISBN: 978-81-940448-9-5.

Presentations in national/international seminars/conferences:

1. **Sameena, P. P.** and Puthur, J. T. (2020). 'Alterations in the antioxidative functions in *Ricinus communis* L. seedlings exposed to increasing levels of copper' in the International Webinar on Plant Functional Biology – Doctrina-11, organized by the Department of Post Graduate Studies and Research in Botany & IQAC, Sir Syed College, Taliparamba, Kannur, Kerala, In association with Kerala State Higher Education Council, June 05-07, 2020.

2. **Sameena, P. P.** and Puthur, J. T. (2019). 'Effects of copper stress on photosystem II efficiency of cotyledonary and true leaves of *Ricinus communis* L. seedlings' in the National Conference of Plant Physiology - Plant Productivity and Stress Management (NCPP-2019) organized by Kerala Agricultural University, Thrissur, Kerala, December 19-21, 2019.

3. **Sameena, P. P.** and Puthur, J. T. (2019). 'Bioaccumulation pattern of copper and associated physiological changes in cotyledonary and true leaves of *Ricinus communis* seedlings" in XLII All India Botanical Conference of the Indian Botanical Society and National Symposium on 'Innovations and Inventions in Plant Science Research', organized by Department of Botany, University of Calicut, November 06-08, 2019.

4. **Sameena, P. P.** and Puthur, J. T. (2019). 'Photochemical responses of *Ricinus communis* L. towards copper phytotoxicity' in the National Seminar on 'Plant Sciences: Current Challenges and Perspectives' organized by Department of Botany, University of Calicut, Kerala on February 28 to March 02, 2019.

5. **Sameena, P. P.** and Puthur, J. T. (2018). 'Interaction of NaCl with Zinc and Cadmium on stress related metabolism of *Brassica juncea* (L.) Czern.' in International Conference on 'Recent Scenario in Plant Science Research - Climate Change and its Associated Variations' (ICRSPSR - 2018) organized by Department of Botany, Annamalai University, Tamil Nadu on March 23-25, 2018.

International Journal of
Molecular Sciences

MDPI

Article

6-Benzylaminopurine Alleviates the Impact of Cu^{2+} Toxicity on Photosynthetic Performance of *Ricinus communis* L. Seedlings

Puthukkolli P. Sameena [1], Hazem M. Kalaji [2], Krystyna Żuk-Gołaszewska [3], Tomasz Horaczek [4], Edyta Sierka [5] and Jos T. Puthur [1,*]

1 Plant Physiology and Biochemistry Division, Department of Botany, University of Calicut, Calicut University P.O., Malappuram 673635, Kerala, India; sameenapp2017@gmail.com
2 Department of Plant Physiology, Institute of Biology, Warsaw University of Life Sciences SGGW, 02-776 Warsaw, Poland; hazem@kalaji.pl
3 Department of Agrotechnology and Agribusiness, Faculty of Agriculture and Forestry, University of Warmia and Mazury in Olsztyn, ul. Oczapowskiego 8, 10-719 Olsztyn, Poland; kzg@uwm.edu.pl
4 Institute of Technology and Life Sciences—National Research Institute, Falenty, Al. Hrabska 3, 05-090 Raszyn, Poland; t.horaczek@itp.edu.pl
5 Institute of Biology, Biotechnology and Environmental Protection, Faculty of Natural Sciences, University of Silesia in Katowice, 28 Jagiellonska, 40-032 Katowice, Poland; edyta.sierka@us.edu.pl
* Correspondence: jtputhur@yahoo.com; Tel.: +91-94-4750-7845

Abstract: Copper (Cu) is an essential element involved in various metabolic processes in plants, but at concentrations above the threshold level, it becomes a potential stress factor. The effects of two different cytokinins, kinetin (KIN) and 6-benzylaminopurine (BAP), on chlorophyll *a* fluorescence parameters, stomatal responses and antioxidation mechanisms in castor (*Ricinus communis* L.) under Cu^{2+} toxicity was investigated. *Ricinus communis* plants were exposed to 80 and 160 µM $CuSO_4$ added to the growth medium. Foliar spraying of 15 µM KIN and BAP was carried out on these seedlings. The application of these cytokinins enhanced the tissue water status, chlorophyll contents, stomatal opening and photosynthetic efficiency in the castor plants subjected to Cu^{2+} stress. The fluorescence parameters, such as Fm, Fv/Fo, Sm, photochemical and non-photochemical quantum yields, energy absorbed, energy trapped and electron transport per cross-sections, were more efficiently modulated by BAP application than KIN under Cu^{2+} toxicity. There was also effective alleviation of reactive oxygen species by enzymatic and non-enzymatic antioxidation systems, reducing the membrane lipid peroxidation, which brought about a relative enhancement in the membrane stability index. Of the various treatments, 80 µM $CuSO_4$ + BAP recorded the highest increase in photosynthetic efficiency compared to other cytokinin treatments. Therefore, it can be concluded that BAP could effectively alleviate the detrimental effects of Cu^{2+}toxicity in cotyledonary leaves of *R. communis* by effectively modulating stomatal responses and antioxidation mechanisms, thereby enhancing the photosynthetic apparatus' functioning.

Keywords: 6-benzylaminopurine; antioxidation; chlorophyll *a* fluorescence; cytokinin; membrane stability; kinetin; reactive oxygen species

Citation: Sameena, P.P.; Kalaji, H.M.; Żuk-Gołaszewska, K.; Horaczek, T.; Sierka, E.; Puthur, J.T. 6-Benzylaminopurine Alleviates the Impact of Cu^{2+} Toxicity on Photosynthetic Performance of *Ricinus communis* L. Seedlings. *Int. J. Mol. Sci.* **2021**, *22*, 13349. https://doi.org/10.3390/ijms222413349

Academic Editor: Bartolome Sabater

Received: 14 November 2021
Accepted: 10 December 2021
Published: 12 December 2021

1. Introduction

The environmental pollutants released by anthropogenic activities are threatening the existence of biological systems. Among the various pollutants, heavy metals are a serious environmental threat which affects the physiology and metabolism of plants [1]. Heavy metals such as cadmium (Cd), chromium (Cr), copper (Cu), iron (Fe), lead (Pb), nickel (Ni), and zinc (Zn) are common pollutants. The distribution of these metals is influenced by industrial effluents, mining, smelting, and various agricultural activities [2]. Copper (Cu) is an essential element with diverse functions in plant metabolism and development,

Journal of Plant Growth Regulation
https://doi.org/10.1007/s00344-021-10522-z

Exogenous Application of Cytokinins Confers Copper Stress Tolerance in *Ricinus communis* L. Seedlings

P. P. Sameena[1] · **Jos T. Puthur**[1]

Received: 30 April 2021 / Accepted: 22 October 2021

Abstract
As an essential element, copper (Cu) is involved in various metabolic processes in plants. However, this metal becomes a potential stress factor when the concentration reaches the threshold level. A comparative analysis was conducted to investigate the potential role of two cytokinins [kinetin (KIN) and 6-benzylaminopurine (BAP)] in Cu stress alleviation in *Ricinus communis* seedlings by assessing the metal bioaccumulation, antioxidation mechanisms, anatomical changes as well as analysis of various essential elements and bioactive compounds in the cotyledonary leaves. Application of KIN and BAP regulated the Cu toxicity in castor seedlings via modulation of metal uptake and antioxidation mechanisms. The increase in antioxidant enzyme activities during Cu stress was further increased upon exposure to cytokinin treatments, and the enhancement reached up to 25 folds for CAT, 16 folds for POD, and 8 folds for SOD over the control, which helps the plant to alleviate the toxic effects of Cu stress. The FTIR analysis of the cotyledonary leaves revealed that the functional groups associated with cell wall materials contributed to the Cu sequestration in the cell wall, supported by the xylem wall thickening as observed in the SEM analysis. The GCMS analysis revealed that most of the secondary metabolites identified were phenolic and flavonoid compounds with antioxidant properties, which help the castor seedlings withstand the Cu stress, and the presence of these compounds was more prominent in cytokinin-treated seedlings. Findings revealed that BAP was more effective than KIN to withstand the Cu stress effects in castor seedlings.

Keywords 6-Benzylaminopurine · Bioactive compounds · Kinetin · SEM-EDAX · FTIR spectrum · Heavy metal

Introduction

In nature, plants are constantly exposed to various biotic and abiotic stressors. Heavy metals such as As, Cd, Co, Cu, Fe, Hg, Mn, Ni, and Zn are continuously accumulated in the soil by various anthropogenic activities such as mismanaged agricultural and industrial activities (Ghori et al. 2019). Interestingly, plants are regarded as natural metal accumulators, absorbing and concentrating the metal ions from the water and soil (Reeves et al. 2018). These metal ions may or may not be essential for the normal functioning of the plant system. Depending on the type of metal ion, the accumulation rate and tolerance potential vary from plant to plant. The visible symptoms of metal toxicity in plants include stunted growth, chlorosis, root decay, and senescence (Okereafor et al. 2020).

Toxic metal ions induce morphological and metabolic abnormalities in plants, resulting in the generation of reactive oxygen species (ROS) and associated interruption in the cell redox homeostasis, leading to a reduction in plant growth and yield (Amari et al. 2017; Ahmad et al. 2010, 2019; Kohli et al. 2019). Naturally, plants have evolved various defense mechanisms for heavy metal detoxification, including reduced metal ion uptake, metal ion trafficking, enhanced biosynthesis of osmolytes, and antioxidants (Ahmad et al. 2010, 2019; Viehweger 2014; Tiwari and Lata 2018; Kohli et al. 2019). In order to scavenge the ROS and reduce the associated oxidative damage, the plants have developed defense strategies by activating enzymatic antioxidants such as peroxidases, catalases, and superoxide dismutases (Keyster et al. 2020).

Handling Editor: Vaclav Motyka.

✉ Jos T. Puthur
jtputhur@yahoo.com

[1] Plant Physiology and Biochemistry Division, Department of Botany, University of Calicut, Calicut University P.O., Malappuram, Kerala 673635, India

Published online: 01 November 2021

Journal of Photochemistry and Photobiology 8 (2021) 100059

Contents lists available at ScienceDirect

Journal of Photochemistry and Photobiology

journal homepage: www.sciencedirect.com/journal/journal-of-photochemistry-and-photobiology

Differential modulation of photosynthesis and defense strategies towards copper toxicity in primary and cotyledonary leaves of *Ricinus communis* L.

P.P. Sameena, Jos T. Puthur *

Plant Physiology and Biochemistry Division, Department of Botany, University of Calicut, Calicut University P.O., Malappuram, Kerala - 673635, India

ARTICLE INFO

Keywords:
Castor
chlorophyll *a* fluorescence
FT-IR spectrum
Heavy metal
Membrane stability
Photosystem activity

ABSTRACT

Copper (Cu) is an essential element associated with different metabolic processes in plants. However, at concentrations higher than the threshold level, it becomes a potential stress factor. In the present investigation, the Cu-induced photosynthetic changes and prominent Cu detoxification methods were evaluated in *Ricinus communis* seedlings. Exposure of one-month-old seedlings of *R. communis* to 0.2 mM $CuSO_4$ in Hoagland solution for 6 d slightly reduced the plant growth and photosystem activities in the primary leaves. However, these features were significantly reduced in the cotyledonary leaves. The comparative analysis of chlorophyll *a* fluorescence kinetics measured in cotyledonary and primary leaves of castor seedlings subjected to Cu stress indicates that photosynthesis is highly sensitive to Cu-induced stress, and it was predominant in cotyledonary leaves. In order to counteract this metal-induced oxidative damage and to scavenge the reactive oxygen species (ROS), various anti-oxidation processes get enhanced in both the leaves and roots. However, cellular redox homeostasis was better maintained in the primary leaves. The functional groups associated with cell wall materials take part in the sequestration of Cu to the cell wall by forming stable complexes with Cu to reduce the toxicity in the cytoplasm, which was common in both the cotyledonary and primary leaves, observed as structurally similar absorption peaks in FT-IR spectrum.

1. Introduction

Copper (Cu) is an essential trace element, having a significant role in the growth and development of most aerobic organisms. Copper participates in the basic biological processes of plants, including mitochondrial respiration, cellular transportation, antioxidation, and hormone signaling [1]. It has been reported that the concentration of Cu in the soil has surpassed the maximum acceptable level due to industrial incinerators, sewage sludge, use of agrochemicals, and burning of fossil fuels, particularly coal, which releases Cu in both bottom and fly ashes [2]. When accumulated excessively in plants, Cu causes detrimental effects on plant growth, including complications in photosynthesis, defects in cellular respiration, and interferences in peroxidase catalytic cycles [3]. Phytoremediation is a low-cost, eco-friendly green remediation technology, which utilizes metal accumulating plants to minimize the metal concentrations in the soil and water bodies. Therefore this method is widely used to reduce heavy metal toxicity in the environment. The important step in this process is to identify the plants with the potential to flourish and produce higher biomass in metal-contaminated lands [4].

Plants possess innate defense mechanisms for detoxifying heavy metals, which comprises blocking and trafficking of metal ion uptake, osmolyte biosynthesis, and antioxidant enzymes activation [5]. In order to quench the ROS produced as a result of metal toxicity, the plants adopt different defense strategies by the activation of enzymatic antioxidants such as ascorbate peroxidase (APX), catalase (CAT), guaiacol peroxidase (POD), and superoxide dismutase (SOD), and accumulation of non-enzymatic antioxidants such as ascorbate (AsA), and glutathione (GSH) [6,7].

Ricinus communis L. (castor) is a perennial oil-yielding plant with heavy metal accumulation potential. It can grow luxuriously in tropical and subtropical regions and produce high biomass. As this plant can grow in contaminated lands having multiple stresses and can accumulate metal ions in the biomass, it has attracted the attention of

Abbreviations: APX, ascorbate peroxidase; AsA, ascorbate; CAT, catalase; CSI, chlorophyll stability index; Cu, copper; DW, dry weight; EL, electrolyte leakage; FT-IR, Fourier Transform Infrared; FW, fresh weight; GSH, glutathione; MC%, moisture content percentage; MSI, membrane stability index; POD, guaiacol peroxidase; PSI, photosystem I; PSII, photosystem II; ROS, reactive oxygen species; RWC, relative water content; SOD, superoxide dismutase.

* Corresponding author.
E-mail address: jtputhur@yahoo.com (J.T. Puthur).

https://doi.org/10.1016/j.jpap.2021.100059
Received 22 December 2020; Received in revised form 6 July 2021; Accepted 12 August 2021
Available online 14 August 2021

INTERNATIONAL JOURNAL OF PHYTOREMEDIATION
2021, VOL. 23, NO. 5, 492–504
https://doi.org/10.1080/15226514.2020.1825331

Cotyledonary leaves effectively shield the true leaves in *Ricinus communis* L. from copper toxicity

P. P. Sameena and Jos T. Puthur

Plant Physiology and Biochemistry Division, Department of Botany, University of Calicut, Malappuram, India

ABSTRACT

The stress-buffering effects of cotyledonary leaves of *Ricinus communis* and the protection thus offered to the true leaves upon exposure to copper stress was performed by analyzing bioaccumulation of Cu and associated metabolic processes in the presence and absence of cotyledonary leaves. One-month-old seedlings of *R. communis* were treated with various concentrations of $CuSO_4$ for 6 d under hydroponics with quarter strength modified Hoagland medium. Even though the photosynthetic pigments showed a decreasing trend with an increase in $CuSO_4$ concentration and days of exposure in cotyledonary and true leaves, it was significant in true leaves with excised cotyledonary leaves. The results of chlorophyll *a* fluorescence parameters indicated that toxic levels of $CuSO_4$ do not impart any major negative effect on the photochemistry of true leaves along with cotyledonary leaves. The analysis of osmolality, malondialdehyde, and metabolites showed a significantly increasing trend in true leaves with excised cotyledonary leaves. The above observations were strongly supported by higher Cu bioaccumulation in true leaves with excised cotyledonary leaves. The results suggest that the cotyledonary leaves have got the potential to evade Cu toxicity and thereby *R. communis* can be effectively used for the phytoremediation of Cu contaminated lands.

Abbreviations: ANOVA: analysis of variance; Cu: copper; DW: dry weight; FW: fresh weight; MDA: malondialdehyde; PSII: photosystem II; ROS: reactive oxygen species; TF: translocation factor

KEYWORDS

Chlorophyll *a* fluorescence; copper; cotyledonary leaves; heavy metal; metabolites; *Ricinus communis*

Introduction

Copper (Cu) is an essential redox-active transition metal having numerous roles in plant growth and development such as electron transport, cellular transportation, mitochondrial respiration, protein trafficking, hormone signaling, and structural element of regulatory proteins, etc. (Ferreira *et al.* 2015). Even though Cu is an essential element, it has been considered as a heavy metal because of its heavier density ($5\,g\,cm^{-3}$) and it becomes highly toxic to plants at higher concentrations (Singh *et al.* 2011). The major sources of Cu include incineration of municipal wastes and the application of fungicides in the agricultural fields (Mackie *et al.* 2012). Several means are being tried out for the remediation of heavy metals from the environment. Because of the problems in the traditional physical and chemical methods adapted for the remediation of the Cu and other heavy metal contaminated areas, the methods that cause fewer disturbances to the environment are favored. Phytoremediation of the toxic levels of Cu by using hyperaccumulating green plants is one of the best methods for the removal of these elements from the soil (Yan *et al.* 2020). But the main disadvantage of phytoremediation is the penetration of the heavy metals to the food chain via the consumption of these contaminated plants by animals (Farraji *et al.* 2016). This problem could be addressed to a certain extent by the utilization of inedible plants for phytoremediation (Abdelsalam *et al.* 2019).

Ricinus communis, the castor oil plant belonging to the Euphorbiaceae family of the flowering plants, is an inedible, fast-growing, high biomass producing and heavy metal hyperaccumulating plant. Recently, castor has attained popularity as a value-added plant for the phytoremediation of polluted lands along with economic and ecological services because of its ability to grow luxuriously in polluted soils and accumulating toxic metal ions (Gajić *et al.* 2018). It is often found abundantly along disturbed or wastelands and roadsides under harsh environmental conditions. It can be cultivated for phytoremediation as well as bioenergy production, which simultaneously addresses two critical global problems such as remediation of the polluted lands and meeting energy demands (Abdelsalam *et al.* 2019; Palanivel *et al.* 2020). *Ricinus communis* is a heavy metal accumulator plant having different mechanisms for the sequestration of the toxic metal ions. Since the cell wall is the first barrier for the heavy metal entry into the plant system, majority of the metals are sequestered in the cell wall itself and then to other subcellular compartments (He *et al.* 2020). It was

CONTACT Jos T. Puthur jtputhur@yahoo.com Plant Physiology and Biochemistry Division, Department of Botany, University of Calicut, Calicut University P.O., Thenhipalam, Malappuram 673635, Kerala, India.

Supplemental data for this article can be accessed at publisher's website.

SOIL AND SEDIMENT CONTAMINATION: AN INTERNATIONAL JOURNAL
2021, VOL. 30, NO. 3, 253–274
https://doi.org/10.1080/15320383.2020.1849017

Taylor & Francis
Taylor & Francis Group

Heavy Metal Phytoremediation by Bioenergy Plants and Associated Tolerance Mechanisms

Sameena P.P. and Jos T. Puthur

Plant Physiology and Biochemistry Division, Department of Botany, University of Calicut, Calicut University P.O., Malappuram, Kerala, India

ABSTRACT

Bioenergy plants that are better adapted to metal-contaminated lands can be used for phytoremediation purposes and also can be additionally used to produce biofuels such as bioethanol, biodiesel, and biogas. These plants offer the dual advantages of phytoremediation and bioenergy production and majority of them are heavy metal accumulators sequestering exceptionally high amount of the absorbed metals into their biomass. Although diverse heavy metal stress tolerance mechanisms are observed in plants, mainly the metals are effectively immobilized in the roots or if transported to shoots, metal ions are avoided from the sensitive sites and thereby protect the plants from toxicity of the metals. Owing to the fact that most of the reviews published earlier have been focusing on the production of biofuels from the biomass, mostly emphasizing on edible plants, in the present review the heavy metals immobilization mechanisms operational in non-edible bioenergy plants having phytoremediation potential is highlighted. Growing energy plants in heavy metal-contaminated lands is a means of sustainable utilization of the contaminated lands and it also prevents the entry of heavy metals into the food chain. This review, therefore, gives an overview of heavy metal accumulating non-edible bioenergy plants, benefits of using bioenergy plants for phytoremediation, metal tolerance mechanisms in these accumulators, and future perspectives.

KEYWORDS

Bioenergy; biomass; contaminated lands; heavy metal accumulation; phytoextraction; phytostabilization

Introduction

At present, fossil fuels comprise the major part of the global energy supply, but complete dependence on them for energy purposes in the long run will be unsustainable. Therefore, the dependency on fossil fuels should be gradually reduced and the renewable energy sources should be generated and effectively used. One of the main sources of renewable energy is the energy from biological sources particularly plants (Vasudevan et al. 2020). The dependency on plant biomass for the bioenergy extraction requires huge land area which may spread out to arable lands, thus there is a probability for reduction in available land for food production. Under this circumstance, the utilization of degraded/polluted lands for the cultivation of bioenergy crops is considered (Singh et al. 2020).

The degraded/polluted lands are affected by various abiotic stresses including heavy metal toxicity, thereby posing a challenge for the plant growth and biomass production for

CONTACT Jos T. Puthur jtputhur@yahoo.com Plant Physiology and Biochemistry Division, Department of Botany, University of Calicut, Kerala 673635, India.

Plant Stress 2 (2021) 100038

Contents lists available at ScienceDirect

Plant Stress

journal homepage: www.sciencedirect.com/journal/plant-stress

Functional aspects of plant secondary metabolites in metal stress tolerance and their importance in pharmacology

K.S. Anjitha, P.P. Sameena, Jos T. Puthur *

Plant Physiology and Biochemistry Division, Department of Botany, University of Calicut, Calicut University P.O., Malappuram, Kerala - 673635, India

ARTICLE INFO

Keywords:
Abiotic stress
Antioxidation
Elicitors
Metallothioneins
Phenolic compounds
Phytochelatins

ABSTRACT

Toxic trace metals are ecotoxic due to their high bioaccumulation and toxicity, acting as abiotic stress agents, causing oxidative damage to the plant cells. Plants can recognize these threat signals and activate various defense responses. Enhanced production of secondary metabolites is a vital detoxification mechanism evolved in plants to alleviate the detrimental effects caused by toxic metals. Metal stress tolerance in plants can be increased by manipulating the biosynthesis and accumulation of secondary metabolites. The application of elicitors in plant and cell cultures is an efficient method for triggering the large-scale production of secondary metabolites and has significant importance in pharmaceutical and therapeutic industries. This review analyses the role of secondary metabolites as metal precipitators, antioxidants, and metal chelators in plants growing under toxic metal-contaminated environments. Also, this review focuses on the contemporary progression in understanding the machinery of secondary metabolite biosynthetic pathways and discusses the progress and prospects of improving their production through elicitation.

1. Introduction

All living beings on earth are exposed to a wide range of environmental stresses. The unprecedented increase in industrial pollution has resulted in the bioaccumulation and biomagnification of toxic metals in soil and water. Metal toxicity is one of the principal environmental hazards hampering normal functioning and metabolic processes in plants. This has become a significant threat to the natural biogeochemical cycle and food web (Haider et al., 2021). The metals/metalloids at toxic levels can interact with various cellular biomolecules like nuclear proteins and DNA, resulting in the increased production of reactive oxygen species (ROS) such as hydrogen peroxide (H_2O_2), superoxide anion radicals (O_2^-), and hydroxyl radicals (OH^-) (Emamverdian et al., 2015). Under normal growth conditions, there is a balance between the production and detoxification of ROS molecules due to the metabolic processes in plants. However, abiotic stresses such as metal toxicity disrupt the equilibrium between ROS production and removal, resulting in membrane peroxidation, enzyme inhibition, and DNA, RNA, and proteins damage. Plants employ various defense strategies for detoxification of ROS whenever confronted with the stressful concentration of metals (Shahid et al., 2014).

Conventional metal remediation technologies negatively affect soil fertility as well as ecosystem and are also expensive. Phytoremediation is an environment-friendly and cost-effective method in which plants and associated rhizospheric microflora immobilize, degrade or sequester metal pollutants in the soil and water (Ibanez et al. 2016; Sameena and Puthur, 2021a). Different strategies like bioaccumulation, rhizofiltration, biotransformation, biosorption, volatilization, and bioextraction are employed to remove toxic metals (Verma and Sharma, 2017). More than 500 plant species are known to grow luxuriously in metal contaminated soils. Majority of them are obligate metallophytes and some are facultative metallophytes. They can grow on normal, non-metalliferous, and metalliferous soils by hyperaccumulating the metal ions to the shoot system or excluding them in the roots. Concentration and exposure time are important parameters determining the impact of toxic metals on secondary metabolite production in plants. The response of the metabolome and the genes involved in secondary metabolite production in hyperaccumulators can be determined via comparison with non-hyperaccumulators of the same species (Berni et al., 2019).

The organisms with the inherent potential to tolerate metal toxicity can resist the adverse effects of toxic metals imparted on the metabolic and physiological processes and thus can survive in nature (Sameena and Puthur, 2021b). Metal-induced activation of biosynthetic pathways

* Corresponding author.
E-mail address: jtputhur@yahoo.com (J.T. Puthur).

https://doi.org/10.1016/j.stress.2021.100038
Received 14 July 2021; Received in revised form 15 September 2021; Accepted 23 September 2021
Available online 26 September 2021